EMERGING INFECTIOUS DISEASES®

CDC
Centers for Disease Control and Prevention

High-Consequence Pathogens

September 2022

Attributed to the Boreads Painter (active 575–550 BCE), *Black-Figure Kylix with Bellerophon Fighting the Chimaera* (ca. 570 BCE). Terracotta. 14 3/4 in × 7 in × 5 1/2 in/12 cm × 17.8 cm × 14 cm. Public domain image courtesy of The J. Paul Getty Museum, Villa Collection, Malibu, California, USA 85.AE.121.1.

EMERGING INFECTIOUS DISEASES®

Emerging Infectious Diseases is published monthly by the Centers for Disease Control and Prevention, 1600 Clifton Rd NE, Mailstop H16-2, Atlanta, GA 30329-4027, USA. Telephone 404-639-1960; email, eideditor@cdc.gov

EMERGING INFECTIOUS DISEASES®

High-Consequence Pathogens

September 2022

On the Cover

Attributed to the Boreads Painter (active 575–550 BCE), *Black-Figure Kylix with Bellerophon Fighting the Chimaera* (ca. 570 BCE). Terracotta. 14 3/4 in × 7 in × 5 1/2 in/12 cm × 17.8 cm × 14 cmPublic domain image courtesy of The J. Paul Getty Museum, Villa Collection, Malibu, California, USA 85.AE.121.1.

About the Cover p. 1940

Synopsis

Medscape EDUCATION ACTIVITY

Research

Medscape EDUCATION ACTIVITY

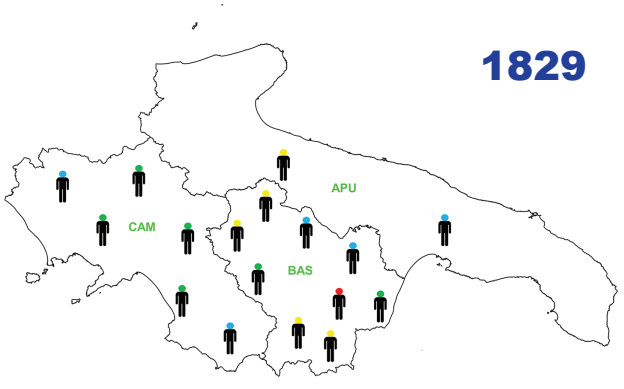

Dispatches

EMERGING INFECTIOUS DISEASES®
September 2022

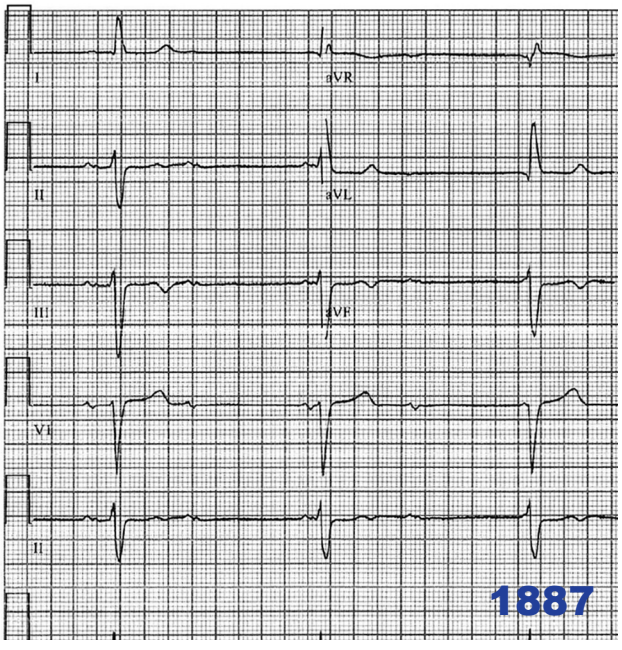

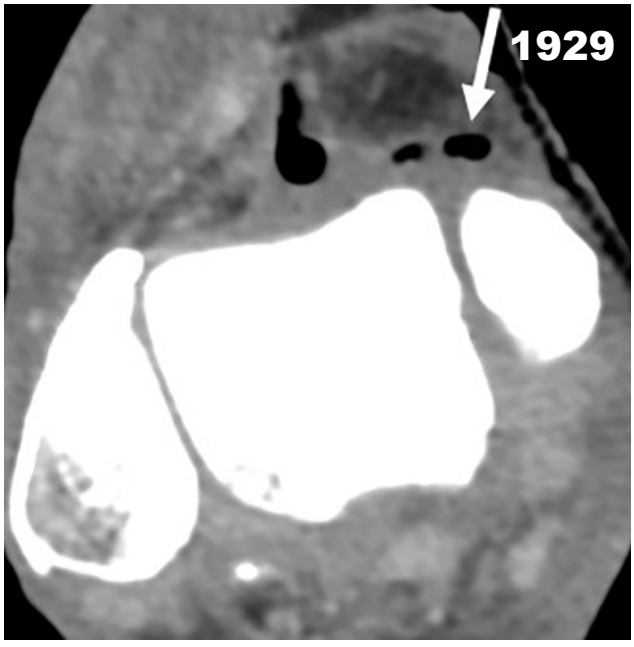

EMERGING INFECTIOUS DISEASES®

September 2022

Research Letters

Books and Media

About the Cover

ICEID Abstracts International Conference on Emerging Infectious Diseases 2022 Poster and Oral Presentation Abstracts

https://bit.ly/3QKbo17

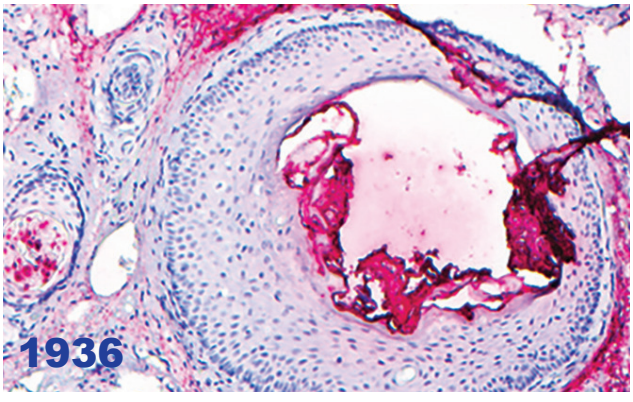

COMING SOON

A special upcoming *EID* supplement highlights CDC's international response to COVID-19, health systems and program adaptation to the pandemic, and lessons learned for future pandemics.

"A World United"
By Vasu Tolia, 69, Bloomfield Hills, Michigan

Fetal Loss and Preterm Birth Caused by Intraamniotic *Haemophilus influenzae* Infection, New Zealand

Thomas Hills, Caitlin Sharpe, Thomas Wong, Tim Cutfield, Arier Lee, Stephen McBride, Matthew Rogers, May Ching Soh, Amanda Taylor, Susan Taylor, Mark Thomas

Medscape ACTIVITY EDUCATION

In support of improving patient care, this activity has been planned and implemented by Medscape, LLC and Emerging Infectious Diseases. Medscape, LLC is jointly accredited by the Accreditation Council for Continuing Medical Education (ACCME), the Accreditation Council for Pharmacy Education (ACPE), and the American Nurses Credentialing Center (ANCC), to provide continuing education for the healthcare team.

Medscape, LLC designates this Journal-based CME activity for a maximum of 1.00 ***AMA PRA Category 1 Credit(s)™***. Physicians should claim only the credit commensurate with the extent of their participation in the activity.

Successful completion of this CME activity, which includes participation in the evaluation component, enables the participant to earn up to 1.0 MOC points in the American Board of Internal Medicine's (ABIM) Maintenance of Certification (MOC) program. Participants will earn MOC points equivalent to the amount of CME credits claimed for the activity. It is the CME activity provider's responsibility to submit participant completion information to ACCME for the purpose of granting ABIM MOC credit.

All other clinicians completing this activity will be issued a certificate of participation. To participate in this journal CME activity: (1) review the learning objectives and author disclosures; (2) study the education content; (3) take the post-test with a 75% minimum passing score and complete the evaluation at http://www.medscape.org/journal/eid; and (4) view/print certificate. For CME questions, see page 1942.

Release date: August 15, 2022; Expiration date: August 15, 2023

Learning Objectives

Upon completion of this activity, participants will be able to:

- Assess the epidemiology of pregnancy-associated invasive *Haemophilus influenzae* disease, based on 10-year surveillance in Auckland, New Zealand
- Evaluate the clinical and microbiological features of pregnancy-associated invasive *Haemophilus influenzae* disease, based on 10-year surveillance in Auckland, New Zealand
- Determine the clinical implications of disease burden and mechanisms of adverse pregnancy outcomes, based on 10-year surveillance of pregnancy-associated invasive *Haemophilus influenzae* infection in Auckland, New Zealand.

CME Editor

Thomas J. Gryczan, MS, Technical Writer/Editor, Emerging Infectious Diseases. *Disclosure: Thomas J. Gryczan, MS, has disclosed no relevant financial relationships.*

CME Author

Laurie Barclay, MD, freelance writer and reviewer, Medscape, LLC. *Disclosure: Laurie Barclay, MD, has the following relevant financial relationships: formerly owned stocks in AbbVie Inc.*

Authors

Thomas Hills, DPhil; Caitlin Sharpe, MBChB; Tim Cutfield, MBChB; Arier Lee, PhD; Stephen McBride, MBChB; Matthew Rogers, MBBS; May Ching Soh, PhD; Amanda Taylor, MBChB; Susan Taylor, MBChB; *and* ***Mark Thomas, MD.***

Author affiliations: Medical Research Institute of New Zealand, Wellington, New Zealand (T. Hills); Auckland District Health Board, Auckland, New Zealand (T. Hills, C. Sharpe, A. Taylor, M. Thomas); Waitematā District Health Board, Auckland (T. Hills, T. Cutfield, M. Rogers); Counties Manukau District Health Board, Auckland (C. Sharpe, T. Wong, S. McBride, M.C. Soh, S. Taylor); University of Auckland, Auckland (A. Lee, M. Thomas)

DOI: https://doi.org/10.3201/eid2809.220313

Invasive *Haemophilus influenzae* infection during pregnancy can cause preterm birth and fetal loss, but the mechanism is unclear. We investigated 54 cases of pregnancy-associated invasive *H. influenzae* disease in 52 unique pregnancies in the Auckland region of New Zealand during October 1, 2008–September 30, 2018. Intraamniotic infection was identified in 36 (66.7%) of 54 cases. Outcome data were available for 48 pregnancies. Adverse pregnancy outcomes, defined as fetal loss, preterm birth, or the birth of an infant requiring intensive/special care unit admission, occurred in 45 (93.8%) of 48 (pregnancies. Fetal loss occurred in 17 (35.4%) of 48 pregnancies, before 24 weeks' gestation in 13 cases, and at ≥24 weeks' gestation in 4 cases. The overall incidence of pregnancy-associated invasive *H. influenzae* disease was 19.9 cases/100,000 births, which exceeded the reported incidence of pregnancy-associated listeriosis in New Zealand. We also observed higher rates in younger women and women of Māori ethnicity.

Haemophilus influenzae serotype B (Hib) causes a range of clinical syndromes, including pneumonia, primary bacteremia, and meningitis (*1*,*2*). Childhood immunization with conjugated Hib vaccines has resulted in dramatic decreases in illness and death attributable to Hib (*2*–*4*). Most invasive *H. influenzae* disease is now caused by nontypeable *H. influenzae* (NTHi) which predominantly affects young children and the elderly (*2*,*5*,*6*). In industrialized countries, deaths caused by NTHi infection are now more common than deaths caused by Hib infection (*6*).

Pregnancy is associated with a 17-fold increase in the incidence of invasive *H. influenzae* infection, largely caused by infection with NTHi (*7*). Invasive *H. influenzae* infection during the first 24 weeks of pregnancy is associated with >90% rate of fetal loss (*7*). Beyond 24 weeks gestation, premature birth occurred in 8 (28.6%) of 28 case-patients and stillbirth in 2 (7.1%) of 28 case-patients (*7*). The burden of NTHi infection extends into the neonatal period, resulting in a high incidence of invasive disease in the first 28 days of life, especially in extremely premature neonate; incidence of invasive NTHi infection is 365-fold higher for neonates at <28 weeks' gestation than for term neonates (>36 weeks' gestation) (*5*,*8*,*9*).

Literature describing the burden of pregnancy-associated invasive *H. influenzae* infection consists largely of case reports and public health surveillance data (*7*,*9*–*11*). Studies have been limited by a paucity of genital tract or postmortem microbiologic data. The mechanisms of preterm birth and fetal loss associated with invasive *H. influenzae* infection are incompletely understood. Historically, *H. influenzae* has not been recognized as a leading cause of intraamniotic infection (IAI) (*12*). However, recent case reports describe IAI that showed histologic evidence of acute necrotizing chorioamnionitis, suggesting that maternal *H. influenzae* infection can involve the amniotic cavity and the fetus (*13*).

We report 10 years of pregnancy-associated invasive *H. influenzae* infection in Auckland, New Zealand. We focus on the overall disease burden and the mechanisms of adverse pregnancy outcomes.

Methods

We identified cases of invasive *H. influenzae* disease during a 10-year period (October 1, 2008–September 30th, 2018) from the hospital laboratory records of Auckland City Hospital, North Shore Hospital, Waitakere Hospital, and Middlemore Hospital, which provide free healthcare to the population of the Auckland region (resident population ≈1.7 million persons in 2018). We searched the computerized records of the 3 microbiology laboratories serving these hospitals to identify all patients who fulfilled the US Centers for Disease Control and Prevention criteria for *H. influenzae* invasive disease: isolation of *H. influenzae* from ≥1 samples collected from a normally sterile site (e.g., blood, cerebrospinal fluid, placental tissue) (*14*). In New Zealand, maternity care is delivered through a network of primary, secondary, and tertiary birthing facilities that, in the Auckland region, are served by these 3 microbiology laboratories. Home births are uncommon, accounting for 3.4% of births (*15*). All neonatal hospital-level care, such as care that would be required for neonates who have *H. influenzae* disease, is delivered in the study hospitals.

We reviewed electronic health records for all cases of invasive disease to identify maternal invasive *H. influenzae* infections, defined as case-patients from whom *H. influenzae* was isolated from samples from pregnant women, and neonatal invasive *H. influenzae* infections, defined as case-patients from whom *H. influenzae* was isolated from samples from infants in the first 28 days of life. Taken together, these case-patients constituted the pregnancy-associated invasive *H. influenzae* study population. Neonatal cases were considered early onset if *H. influenzae* was identified from samples taken within 48 hours of birth.

We extracted prioritized ethnicity, area-level New Zealand deprivation index (NZDep2013; index of socioeconomic deprivation based on maternal location of residence at the time of delivery) (*16*), maternal age, gestation, microbiologic and prespecified clinical outcome data (pregnancy outcome, death at 30 days, and death at 12 months) from the electronic health records. We grouped NZDep2013 index data

into quintiles (1 = least socioeconomic deprivation area, 5 = most socioeconomically deprived area). We defined term birth as delivery at ≥37 weeks' gestation. Whether *H. influenzae* isolates were Hib was determined by testing performed at the Invasive Pathogens Laboratory at the Institute of Environmental Science and Research (Porirua, New Zealand).

Antimicrobial susceptibility testing of all isolates was performed in the hospital laboratories by using accredited methods from the European Committee on Antimicrobial Susceptibility Testing (https://www.eucast.org) or Clinical Laboratory Standards Institute (https://www.clsi.org). We extracted data on susceptibility test results from the laboratory records for each isolate.

We categorized cases as intraamniotic infection when *H. influenzae* was cultured from placental tissue, products of conception, or high vaginal swab specimens for case-patients who had concurrent *H. influenzae* bacteremia. We categorized cases as pneumonia if the clinical diagnosis was pneumonia or if chest radiography during the same hospital admission was reported as demonstrating pneumonia. We categorized cases were as meningitis if the clinical diagnosis was meningitis or if *H. influenzae* was isolated from cerebrospinal fluid. We categorized case-patients who had ≥1 positive blood culture as having primary bacteremia when the documented clinical impression did not specify an alternative clinical syndrome (such as meningitis or pneumonia) and cases could not be otherwise categorized by other microbiologic culture results.

Birth rate and demographic data for the Auckland region during the study period were provided by Statistics New Zealand as a customized data extract to enable calculation of incidence rates. We used relative risk from univariate and multivariate Poisson regression with ethnicity, age, and NZDep2013 in a regression model to look for an association between ethnicity, age, or deprivation and pregnancy-associated invasive *H. influenzae* disease. We performed statistical analyses by using SAS version 9.4 (SAS Institute Inc., https://www.sas.com). The study was approved by the Auckland Health Research Ethics Committee (AHREC 000103).

Results

We identified 54 cases of pregnancy-associated invasive *H. influenzae* disease: 38 (70.4%) maternal cases and 16 (29.6%) neonatal cases. In 2 pregnancies, the mother and the neonate both had invasive *H. influenzae* disease; therefore, the 54 index cases resulted from 52 unique pregnancies.

Case Demographics

Of the 52 women who had maternal *H. influenzae* disease, who gave birth to an infant with neonatal disease, or both, most (77%) were of Māori or Pacific descent (Table 1). All 16 neonatal cases were early-onset *H. influenzae* infection. Socioeconomic deprivation data were available for 48 cases; 26 (54.2%) cases were in women living in areas with the most deprived NZDep2013 quintile score. The median gestation for the neonatal case-patients was 34 weeks (range 26–41 weeks), and the median age of the mother at the time of delivery was 29.5 years (range 18–43 years) (Table 1). Maternal age was unavailable for 2 neonatal case-patients. The median gestation for maternal case-patients was 32 weeks (range 8–40 weeks), and the median age of the women at the time of diagnosis was 25 years (range 15–44 years).

Sites of Infection

We identified IAI in 36 (66.7%) of 54 cases of pregnancy-associated invasive *H. influenzae* infection: 34 (89.5%) of 38 maternal cases and 2 (12.5%) of 16 neonatal cases (Table 1). *H. influenzae* was isolated from placental tissue or products of conception in 33 IAI cases and from maternal or neonatal blood cultures with concurrent isolation from cervical or high vaginal swab specimens in 3 IAI cases (Figure 1).

Microbiologic Characteristics

Typing data were available for 26 isolates, predominantly from cases with bacteremia. Isolates other than those from blood cultures were not routinely sent for typing. Hib was identified in only 1 case. Isolates were not serotypeable for 18/26 cases and confirmed not to be Hib by molecular testing in 7/26 cases (but not further typed by molecular or serologic methods). The proportion of isolates found to be antimicrobial susceptible was 45/53 (84.9% of tested isolates) for amoxicillin, 54/54 (100% of tested isolates) for amoxicillin/clavulanate, 50/52 (96.2% of tested isolates) for cefuroxime, and 33/47 (70.2% of tested isolates) for sulfamethoxazole/trimethoprim.

Pregnancy Outcomes

Pregnancy outcome data were available for 48/52 (92.3%) pregnancies. Fetal loss occurred in 17/48 (35.4%) pregnancies, before 24 weeks' gestation in 13 cases and after 24 weeks' gestation in 4 cases. An additional 21/48 (43.8%) pregnancies resulted in preterm birth. Of those, 20 (95.2%) required admission to a neonatal intensive care unit (NICU) or special care baby unit (SCBU) and 1 died (described earlier). The remaining 10 pregnancies resulted in birth

Table 1. Pregnancy-associated invasive *Haemophilus influenzae* case demographic and clinical data, New Zealand*

Variable	Maternal cases	Neonatal cases	Total pregnancies
Total	38	16	52†
Maternal ethnicity			
European	4 (10.5)	5 (31.3)	8 (15.4)
Māori	17 (44.7)	4 (25)	20 (38.5)
Pacific	14 (36.8)	6 (37.5)	20 (38.5)
Other	3 (7.9)	1 (6.3)	4 (7.7)
Median maternal age, y (range)‡	25 (15–44)	29.5 (18–43)	25 (15–44)
Socioeconomic deprivation‡			
Quintile 5	22 (59.5)	6 (46.1)	26 (54.2)
Quintile 4	10 (27.0)	2 (15.4)	12 (25.0)
Quintile ≤3	5 (13.5)	5 (38.5)	10 (20.8)
Median gestation,‡ wk (range)	32 (8–40)	34 (26–41)	32 (8–41)
Pregnancy outcomes			
Intrauterine death <24 weeks' gestation	13 (34.2)	0	13 (25.0)
Intrauterine death ≥24 weeks' gestation	3 (7.9)	1 (6.3)	4 (7.7)
Live preterm birth	13 (34.2)	10 (62.5)	21 (40.4)
Live birth at term	6 (15.8)	4 (25)	10 (19.2)
Pregnancy outcome unclear	3 (7.9)	1 (6.3)	4 (7.7)
Clinical diagnosis			
Intraamniotic infection§	34 (89.5)	2 (12.5)	36 (69.2)
Primary bacteremia	4 (10.5)	12 (75.0)	14 (26.9)
Pneumonia	0	1 (6.3)	1 (1.9)
Meningitis	0	1 (6.3)	1 (1.9)
Other	0	0	0
Specimens culturing *H. influenzae*¶			
Maternal blood culture	13	1	14
Neonatal blood culture	2	15	17
Placental tissue or products of conception	30	3	33
High vaginal swab specimens§	17	0	17
Cerebrospinal fluid	0	1	1

*Values are no. (%) unless otherwise indicated.
†In 2 pregnancies, invasive *H. influenzae* infection occurred in the mother and the neonate. Thus, the 38 maternal cases and 16 neonatal cases occurred in 52 unique pregnancies.
‡Data for gestational duration were unavailable for 2 neonatal cases and 1 maternal case; maternal age data were unavailable for 2 cases; 2013 area-level New Zealand deprivation index (NZDep2013) data were unavailable for 2 cases. NZDep2013 quintile 5 is the most deprived socioeconomic area, and quintile 1 is the least deprived socioeconomic area.
§Intraamniotic infection was defined as *H. influenzae* isolated from placental samples or products of conception (with or without maternal/neonatal *H. influenzae* bacteremia) or maternal *H. influenzae* bacteremia with *H. influenzae* concurrently isolated from high vaginal swab specimens. Isolation of *H. influenzae* from a high vaginal swab specimen alone, without isolation from another site, was insufficient to meet the case definition for invasive *H. influenzae* disease. Invasive disease was diagnosed in 9 cases with associated maternal bacteremia, 1 case with associated neonatal bacteremia, and 7 cases with documented infection of placental tissue.
¶The total number of positive culture results exceeds the number of cases because in some cases *H. influenzae* was isolated from ≥1 site.

at term, but 7 of those neonates required admission to an NICU or SCBU. Therefore, adverse pregnancy outcomes, defined as fetal loss, preterm birth, or birth of an infant requiring NICU/SCBU care, occurred in 45/48 (93.8%) of the pregnancies for which outcome data were available. Only 3/48 (6.3%) affected pregnancies resulted in a live birth of an infant not requiring NICU/SCBU care.

Mortality Rate Outcomes

One (6.25%) of 16 neonatal case-patients, an infant born at 26 weeks' gestation, had *H. influenzae* bacteremia diagnosed in the first 24 hours of life and died shortly thereafter. None of the 38 maternal case-patients died, although 30-day and 1-year outcome data were unavailable for 1 maternal case-patient (Table 1). Similarly, no mothers of neonatal case-patients died, although 30-day and 1-year outcome data were unavailable for the mother of 1 neonatal case-patient.

Epidemiology

During the study period, there were 241,653 births in the Auckland region. Complete demographic data were available for 48/52 pregnancies, so we used those 48 pregnancies to calculate an overall incidence pregnancy-associated invasive *H. influenzae* disease rate of 19.9 cases/100,000 births. The rate varied greatly by maternal ethnicity; 53.7 cases/100,000 births for Māori women, 33.6 cases/100,000 births for Pacific women, 9.0 cases/100,000 births for women from Europe, and 5.86 cases/100,000 births for women of other ethnicities (Table 2). Incidence was highest in the youngest maternal age group (≤19 years), 65.1 cases/100,000 births, and decreased progressively to 8.8 cases/100,000 births in the oldest maternal age group (≥35 years). Ethnicity, age group, and sociodemographic deprivation were each significantly associated with the incidence of pregnancy-associated invasive *H. influenzae* disease by univariable

analyses (p≤0.0001 for each). In a multivariable regression model (Table 2), ethnicity was significantly associated with the risk for pregnancy-associated invasive *H. influenzae* disease (p = 0.0035), whereas age group (p = 0.1115) and socioeconomic deprivation (0.1015) were not associated. Compared with women from European, the relative risk of infection for Māori women was 3.28 (95% CI 1.32–8.19) and the relative risk for Pacific women was 2.07 (95% CI 0.80–5.37) (Figure 2).

Discussion

H. influenzae has recently been recognized as a rare but major cause of pregnancy-associated invasive disease. In this retrospective study in the Auckland region, accounting for more than one third of the New Zealand population, the overall incidence of pregnancy-associated invasive *H. influenzae* disease was 19.9 cases/100,000 births. Our findings build on those from England and Wales, where the incidence of invasive NTHi infection in pregnant women was 17-fold higher than in nonpregnant women and was strongly associated with preterm birth and a high case-fatality rate (*7*,*9*). However, the mechanism of adverse pregnancy outcomes was unclear; chorioamnionitis was noted in only 7.3% of cases of early-onset neonatal NTHi infection (*9*). Our data indicate that IAI is the probable cause of preterm birth and fetal loss; we found clinical or microbiologic evidence of IAI in 66.7% of our cases. IAI caused by *H. influenzae* has been noted in case reports/series previously (*10*,*11*), but not in a study of this size.

Our data confirm that outcomes of pregnancy-associated invasive *H. influenzae* disease for the fetus or neonate are poor. Adverse pregnancy outcomes (fetal loss, preterm birth, or birth of an infant requiring care in NICU/SCBU) occurred in 94% of pregnancies for which outcome data were available. Only 6% of pregnancies resulted in live birth of an infant not requiring NICU/SCBU care. In contrast, outcomes of pregnancy-associated invasive *H. influenzae* disease for the pregnant woman are generally good. There

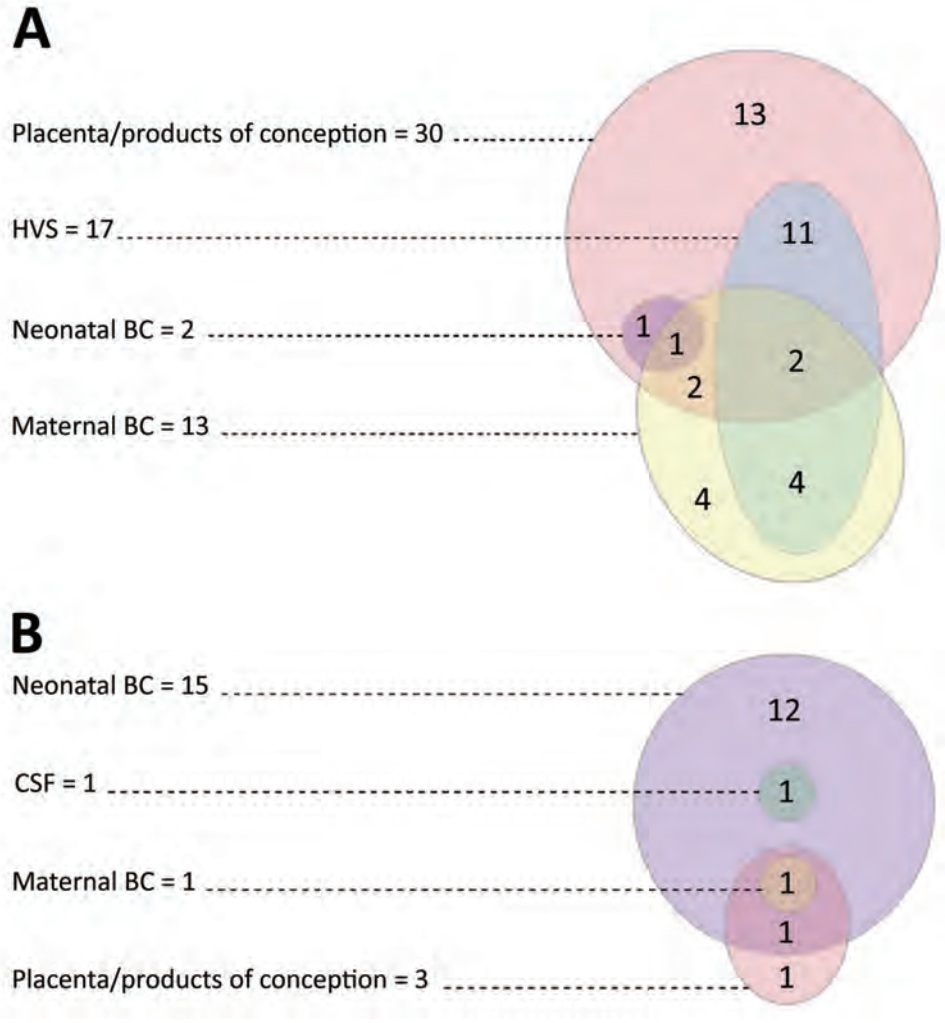

Figure 1. Sites from which *Haemophilus influenzae* was isolated in maternal cases (A) and neonatal cases (B), New Zealand. Overlapping colored circles and ovals indicate multiple types of samples collected from the same cases. BC, blood culture; CSF, cerebrospinal fluid; HVS, high vaginal swab.

Table 2. Pregnancy-associated invasive *Haemophilus influenzae* incidence by maternal ethnicity and age and socioeconomic status, New Zealand*

Variable	Births, no. (%)	Cases, no. (%)	Crude incidence per 100,000 births (95% CI)	Poisson regression relative risk (95% CI)
Maternal ethnicity				
Māori	37,218 (15.4)	20 (42)	53.74 (33.50–80.84)	3.28 (1.32–8.19)
Pacific	47,655 (19.72)	16 (33)	37.58 (19.70–52.81)	2.07 (0.80–5.37)
Other	68,268 (28.25)	4 (8)	5.86 (1.82–13.61)	0.57 (0.17–1.90)
European	88,512 (36.63)	8 (17)	9.04 (4.13–16.82)	Referent
Total	241,653 (100.00)	48 (100.00)	19.86	NA
Maternal age, y				
≤19	10,758 (4.45)	7 (15)	65.07 (27.96–125.80)	3.19 (0.97–10.48)
20–24	36,498 (15.1)	17 (35)	46.58 (27.80–72.35)	2.79 (0.99–7.80)
25–29	61,917 (25.62)	9 (19)	14.54 (6.99–26.20)	1.28 (0.42–3.86)
30–34	75,936 (31.42)	10 (21)	13.17 (6.60–23.10)	1.49 (0.51–4.37)
≥35	56,544 (23.4)	5 (10)	8.84 (3.17–19.01)	Referent
Total	241,653 (100.00)	48 (100.00)	19.86	NA
Socioeconomic deprivation				
Quintile 5	78,822 (32.6)	26 (54.2)	32.99 (21.88–47.34)	1.89 (0.83–4.30)
Quintile 4	40,440 (16.7)	12 (25)	29.67 (15.89–49.76)	2.52 (1.06–6.02)
Quintile ≤3	122,391 (50.7)	10 (20.8)	8.17 (4.09–14.33)	Referent
Total	241,653 (100.00)	48 (100.00)	19.86	NA

*Maternal age data were missing for 2 pregnancies, and 2013 area-level New Zealand deprivation index (NZDep2013) socioeconomic deprivation data were missing for 2 additional pregnancies. Therefore, crude incidence rates and relative risks from a multivariable Poisson regression model with ethnicity, age and NZDep2013 quintile in the model were calculated from the 48 cases where complete demographic data were available. The other ethnicity category comprised 3 Asian women and 1 Middle Eastern woman. p<0.0035 for ethnicity, p<0.1115 for age, and p<0.1015 for socioeconomic deprivation. NZDep2013 quintile 5 is the most deprived socioeconomic area, and quintile 1 is the least deprived socioeconomic area. NA, not applicable.

were no deaths among the 50 women for which data was available, suggesting that this condition can be readily treated by delivery of the fetus and placental tissues, plus administration of antimicrobial drugs.

We found that pregnancy-associated invasive *H. influenzae* infection disproportionately affected Māori persons, who experience a higher burden of many infectious diseases in New Zealand (*17*). Pacific women also had a higher incidence of disease than women of European or other ethnicities, but this difference did not reach statistical significance by multivariable analysis. Potentially relevant to our study are the high rates of sexually transmitted infections in young Māori and Pacific women (*18*). Large ethnic disparities in the incidence of common sexually transmitted infections in New Zealand have persisted, relatively unchanged, in recent years (*19*). In the light of increasing evidence that *H. influenzae* may cause nongonococcal urethritis in men (*20*), one possible hypothesis is that sexually acquired vaginocervical *H. influenzae* infection was the immediate precursor of IAI in the women we studied. A high incidence of sexually transmitted infections (*21*) and a high incidence of pregnancy-associated invasive *H. influenzae* disease (*22*) has also been observed in indigenous women in Australia, supporting this proposed mode of infection.

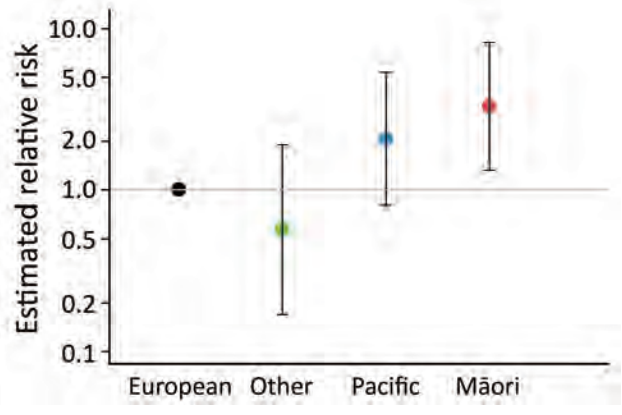

Figure 2. Relative risk for pregnancy-associated invasive *Haemophilus influenzae* infection, by ethnicity, in a multivariable regression model, New Zealand. Error bars indicate 95% CIs.

Our study supports IAI as the mechanism by which *H. influenzae* mediates poor pregnancy outcomes. Our findings suggest that IAI is responsible for the major manifestations of pregnancy-associated invasive *H. influenzae* disease. *H. influenzae* is rarely isolated from the genital tracts of pregnant women, having been found in <0.5% of samples from healthy pregnant women (*23*–*25*). We presume that *H. influenzae* infection of the lower genital tract of pregnant women, perhaps acquired as a sexually transmitted infection, or by some other mode of acquisition, places pregnant women at risk for ascending infection; placental infection would then be the route of infection for the fetus. Alterations in hormonal, metabolic, and immune regulation that occur during pregnancy to enable healthy fetal development might result in spread of *H. influenzae* infection from the vagina to the uterine cavity and increase the risk for placental infection (*26*).

Strengths of this study include the analysis of 10 years of data from 4 hospitals and 3 microbiology laboratories caring for demographically diverse populations, with linked outcomes of neonatal and maternal cases. Weaknesses include the retrospective study design, heterogeneity in the quality of the clinical documentation, and missing data. The true burden of pregnancy-associated *H. influenzae* disease, both in our study and in clinical practice, might be underestimated, given that this diagnosis relies on appropriate collection and testing of microbiologic samples. We applied a strict definition of microbiologically confirmed invasive *H. influenzae* disease. It is likely that some women who have signs and symptoms consistent with pregnancy-associated invasive *H. influenzae* disease during the study period did not have adequate microbiologic sampling to enable this diagnosis to be made. Maternal bacteremia was commonly accompanied by concurrent isolation of *H. influenzae* from genital tract or placental specimens, indicating that clinicians were suspicious of IAI as the cause for bacteremia in these women. In contrast, isolation of *H. influenzae* from maternal specimens was uncommon in cases of neonatal bacteremia, perhaps suggesting that the potential for IAI had not been recognized at the time of delivery, resulting in failure to collect appropriate specimens.

Future work should further examine the epidemiology of pregnancy-associated invasive *H. influenzae* disease, assessing whether incidence varies in specific populations, including other indigenous or socioeconomically deprived populations. Rates of genital tract colonization with *H. influenzae* should be quantified in high-risk populations, particularly Māori and Pacific women in New Zealand and indigenous women in Australia. Larger prospective studies should seek to identify factors that predispose to pregnancy-associated invasive *H. influenzae* disease. This approach might identify associations with other sociodemographic variables that our study lacked power to detect. Invasive *H. influenzae* disease should be also considered for pregnant women with signs of chorioamnionitis. Empiric antimicrobial drug treatment in this setting should be with an agent active against *H. influenzae* and other major maternal/perinatal pathogens. *H. influenzae* bacteremia in pregnancy should prompt clinicians to consider intraamniotic infection.

In our study, the overall incidence of pregnancy-associated *H. influenzae* invasive disease was 19.9 cases/100,000 births, similar to the national rate of early-onset neonatal group B *Streptococcus* sepsis in New Zealand (23 cases/100,000 live births) during 2011–2013 (*27*) and higher than the national rate of pregnancy-associated listeriosis in New Zealand (12.3 cases/100,000 live births) during 1997–2016 (*28*). The rates of early-onset group B *Streptococcus* and of pregnancy-associated listeriosis were not higher in those of Māori descent than in persons of European descent (*27*,*28*).

In conclusion, the rates of adverse outcomes in pregnancy-associated invasive *H. influenzae* disease we found were comparable with those for pregnancy-associated listeriosis; fetal loss occurred in 35.4% of cases in our study and in 34% of pregnancy-associated listeriosis cases in New Zealand (*28*). Comparisons across studies using different methods require caution. Nonetheless, our data indicate that, in New Zealand, the burden of *H. influenzae* in pregnancy might be comparable to, or higher than, that seen for pregnancy-associated listeriosis. In addition, the risk for this condition is particularly high for persons of Māori ethnicity.

Acknowledgments

We thank Jennifer Castle and Sally Roberts for identifying 7 cases during the study from laboratory records at Auckland City Hospital, the Public Health Surveillance Laboratory at the Institute of Environmental Science and Research for typing invasive *H. influenzae* isolates, N.Z. Tatauranga Aotearoa for providing a customized data extract of births data for the study period, and Lynn Sadler for assistance with interpretation of regional births data.

About the Author

Dr. Hills is a registrar in the Clinical Immunology and Infectious Diseases Departments at Auckland City Hospital, Auckland, New Zealand. His primary research interest is infections in the critically ill.

References

1. Agrawal A, Murphy TF. *Haemophilus influenzae* infections in the *H. influenzae* type b conjugate vaccine era. J Clin Microbiol. 2011;49:3728–32. https://doi.org/10.1128/JCM.05476-11
2. Dworkin MS, Park L, Borchardt SM. The changing epidemiology of invasive *Haemophilus influenzae* disease, especially in persons ≥65 years old. Clin Infect Dis. 2007;44:810–6. https://doi.org/10.1086/511861
3. Wahl B, O'Brien KL, Greenbaum A, Majumder A, Liu L, Chu Y, et al. Burden of *Streptococcus pneumoniae* and *Haemophilus influenzae* type b disease in children in the era of conjugate vaccines: global, regional, and national estimates for 2000-15. Lancet Glob Health. 2018;6:e744–57. https://doi.org/10.1016/S2214-109X(18)30247-X
4. Leung B, Taylor S, Drinkovic D, Roberts S, Carter P, Best E. *Haemophilus influenzae* type b disease in Auckland children during the Hib vaccination era: 1995–2009. N Z Med J. 2012;125:21–9.

5. Soeters HM, Blain A, Pondo T, Doman B, Farley MM, Harrison LH, et al. Current epidemiology and trends in invasive *Haemophilus influenzae* disease, United States, 2009–2015. Clin Infect Dis. 2018;67:881–9. https://doi.org/10.1093/cid/ciy187
6. Ladhani S, Slack MPE, Heath PT, von Gottberg A, Chandra M, Ramsay ME; European Union Invasive Bacterial Infection Surveillance participants. Invasive *Haemophilus influenzae* disease, Europe, 1996–2006. Emerg Infect Dis. 2010;16:455–63. https://doi.org/10.3201/eid1603.090290
7. Collins S, Ramsay M, Slack MP, Campbell H, Flynn S, Litt D, et al. Risk of invasive *Haemophilus influenzae* infection during pregnancy and association with adverse fetal outcomes. JAMA. 2014;311:1125–32. https://doi.org/10.1001/jama.2014.1878
8. Wan Sai Cheong J, Smith H, Heney C, Robson J, Schlebusch S, Fu J, et al. Trends in the epidemiology of invasive *Haemophilus influenzae* disease in Queensland, Australia from 2000 to 2013: what is the impact of an increase in invasive non-typable *H. influenzae* (NTHi)? Epidemiol Infect. 2015; 143:2993–3000. https://doi.org/10.1017/S0950268815000345
9. Collins S, Litt DJ, Flynn S, Ramsay ME, Slack MP, Ladhani SN. Neonatal invasive *Haemophilus influenzae* disease in England and Wales: epidemiology, clinical characteristics, and outcome. Clin Infect Dis. 2015;60:1786–92. https://doi.org/10.1093/cid/civ194
10. Cherpes TL, Kusne S, Hillier SL. *Haemophilus influenzae* septic abortion. Infect Dis Obstet Gynecol. 2002;10:161–4. https://doi.org/10.1155/S1064744902000170
11. Roy Chowdhury S, Bharadwaj S, Chandran S. Fatal, fulminant and invasive non-typeable *Haemophilus influenzae* infection in a preterm infant: a re-emerging cause of neonatal sepsis. Trop Med Infect Dis. 2020;5:30. https://doi.org/10.3390/tropicalmed5010030
12. Romero R, Miranda J, Kusanovic JP, Chaiworapongsa T, Chaemsaithong P, Martinez A, et al. Clinical chorioamnionitis at term I: microbiology of the amniotic cavity using cultivation and molecular techniques. J Perinat Med. 2015;43:19–36. https://doi.org/10.1515/jpm-2014-0249
13. Cevik M, Moncayo-Nieto OL, Evans MJ. Non-typeable *Haemophilus influenzae*–associated early pregnancy loss: an emerging neonatal and maternal pathogen. Infection. 2020;48:285–8. https://doi.org/10.1007/s15010-019-01359-6
14. Centers for Disease Control and Prevention. *Haemophilus Influenzae* invasive disease, 2015 case definition, 2015 [cited 2020 Dec 14]. https://wwwn.cdc.gov/nndss/conditions/haemophilus-influenzae-invasive-disease/case-definition/2015
15. New Zealand Ministry of Health. Report on maternity 2017. 2019 [cited 2022 Jun 22] https://www.health.govt.nz/publication/report-maternity-2017
16. Atkinson J, Salmond C, Crampton P. NZDep2013 index of deprivation, 2014 [cited 2022 Jun 22]. https://www.otago.ac.nz/wellington/otago069936.pdf
17. Baker MG, Barnard LT, Kvalsvig A, Verrall A, Zhang J, Keall M, et al. Increasing incidence of serious infectious diseases and inequalities in New Zealand: a national epidemiological study. Lancet. 2012;379:1112–9. https://doi.org/10.1016/S0140-6736(11)61780-7
18. The Institute of Environmental Science and Research Ltd. Sexually transmitted infections in New Zealand: annual surveillance report 2012. Volume 118. 2012 [cited 2022 Jun 22]. https://surv.esr.cri.nz/PDF_surveillance/STISurvRpt/2016/FINAL_2016_STI_AnnualReport.pdf
19. The Institute of Environmental Science and Research Ltd (ESR). Sexually transmitted infections in New Zealand: annual surveillance report 2017/2018/2019, 2022 [cited 2022 Un 22]. https://surv.esr.cri.nz/PDF_surveillance/STISurvRpt/2017/FINALSTIANNUALREPORT17_18_1930032022.pdf
20. Srinivasan S, Chambers LC, Tapia KA, Hoffman NG, Munch MM, Morgan JL, et al. Urethral microbiota in men: association of *Haemophilus influenzae* and *Mycoplasma penetrans* with nongonococcal urethritis. Clin Infect Dis. 2021;73:e1684–93. https://doi.org/10.1093/cid/ciaa1123
21. Kirby Institute. HIV, viral hepatitis and sexually transmissible infections in Australia: annual surveillance report, 2017 [cited 2022 Jun 22]. https://kirby.unsw.edu.au/report/annual-surveillance-report-hiv-viral-hepatitis-and-stis-australia-2017
22. Porter M, Charles AK, Nathan EA, French NP, Dickinson JE, Darragh H, et al. *Haemophilus influenzae*: a potent perinatal pathogen disproportionately isolated from Indigenous women and their neonates. Aust N Z J Obstet Gynaecol. 2016;56:75–81. https://doi.org/10.1111/ajo.12413
23. Albritton WL, Brunton JL, Meier M, Bowman MN, Slaney LA. *Haemophilus influenzae*: comparison of respiratory tract isolates with genitourinary tract isolates. J Clin Microbiol. 1982;16:826–31. https://doi.org/10.1128/jcm.16.5.826-831.1982
24. Schønheyder H, Ebbesen F, Grunnet N, Ejlertsen T. Non-capsulated *Haemophilus influenzae* in the genital flora of pregnant and post-puerperal women. Scand J Infect Dis. 1991;23:183–7. https://doi.org/10.3109/00365549109023398
25. Cardines R, Daprai L, Giufrè M, Torresani E, Garlaschi ML, Cerquetti M. Genital carriage of the genus *Haemophilus* in pregnancy: species distribution and antibiotic susceptibility. J Med Microbiol. 2015;64:724–30. https://doi.org/10.1099/jmm.0.000083
26. Amir M, Brown JA, Rager SL, Sanidad KZ, Ananthanarayanan A, Zeng MY. Maternal microbiome and infections in pregnancy. Microorganisms. 2020;8:1996. https://doi.org/10.3390/microorganisms8121996
27. Darlow BA, Voss L, Lennon DR, Grimwood K. Early-onset neonatal group B streptococcus sepsis following national risk-based prevention guidelines. Aust N Z J Obstet Gynaecol. 2016;56:69–74. https://doi.org/10.1111/ajo.12378
28. Jeffs E, Williman J, Brunton C, Gullam J, Walls T. The epidemiology of listeriosis in pregnant women and children in New Zealand from 1997 to 2016: an observational study. BMC Public Health. 2020;20:116. https://doi.org/10.1186/s12889-020-8221-z

Address for correspondence: Thomas Hills, Department of Infectious Diseases, Auckland City Hospital, Grafton 1023, Auckland, New Zealand; email: thills@adhb.govt.nz

Quantifying Population Burden and Effectiveness of Decentralized Surveillance Strategies for Skin-Presenting Neglected Tropical Diseases, Liberia

Joseph W.S. Timothy, Emerson Rogers, Katherine E. Halliday, Tarnue Mulbah, Michael Marks,[1] Zeela Zaizay, Romeo Giddings, Marie Kempf, Estelle Marion, Stephen L. Walker, Karsor K. Kollie, Rachel L. Pullan[1]

We evaluated programmatic approaches for skin neglected tropical disease (NTD) surveillance and completed a robust estimation of the burden of skin NTDs endemic to West Africa (Buruli ulcer, leprosy, lymphatic filariasis morbidity, and yaws). In Maryland, Liberia, exhaustive case finding by community health workers of 56,285 persons across 92 clusters identified 3,241 suspected cases. A total of 236 skin NTDs (34.0 [95% CI 29.1–38.9]/10,000 persons) were confirmed by midlevel healthcare workers trained to use a tailored program. Cases showed a focal and spatially heterogeneous distribution. This community health worker–led approach showed a higher skin NTD burden than prevailing surveillance mechanisms but also showed high (95.1%) and equitable population coverage. Specialized training and task-shifting of diagnoses to midlevel health workers led to reliable identification of skin NTDs, but reliability of individual diagnoses varied. This multifaceted evaluation of skin NTD surveillance strategies quantifies benefits and limitations of key approaches promoted by the 2030 NTD roadmap of the World Health Organization.

The World Health Organization (WHO) promotes an integrated strategy for neglected tropical diseases that present primarily with skin changes (skin NTDs) (*1*,*2*). These conditions are characterized by debilitating pathology, chronic disability, and stigma (*2*,*3*). Fundamental challenges for skin NTD programs include a lack of epidemiologic data to determine burden at finer spatial scales and limited guidance on how to sustainably and equitably implement resource-intensive case detection and management interventions within primary healthcare services (*4*–*7*). This knowledge is essential for progress toward the WHO 2030 roadmap targets that explicitly outline a 10-fold scale-up of skin NTD programs over the next decade (*8*).

Creating and expanding skin NTD programs requires knowledge about disease distribution, particularly co-occurrence of multiple diseases, and subsequent optimization of integrated surveillance strategies at first-line healthcare providers. However, despite clear programmatic need, there are no standardized approaches for estimating prevalence of skin NTDs. Comprehensive, integrated surveys have not yet been evaluated at scale in West Africa, largely because of the epidemiologic traits that characterize skin NTDs: low prevalence, focal distributions, and inaccessibility of affected communities (*4*,*6*,*7*,*9*). This operational gap creates dependence on routine surveillance reports, often considered unreliable because of variable healthcare-seeking behaviors, inadequate diagnostic tools, and unreliable reporting systems (*10*).

Priorities for improving routine surveillance include integrated community-based case finding and midlevel health worker training programs supporting decentralized detection, diagnosis, and case management. The potential for community-based case finding has been demonstrated in Central and West Africa for some diseases, including Buruli ulcer and lymphatic filariasis morbidity (LFM) (*11*–*14*), and recent

Author affiliations: London School of Hygiene and Tropical Medicine, London, UK (J.W.S. Timothy, K.E. Halliday, M. Marks, S.L. Walker, R.L. Pullan); Ministry of Health, Monrovia, Liberia (E. Rogers, T. Mulbah, Z. Zaizay, R. Giddings, K.K. Kollie); Hospital for Tropical Diseases, London (M. Marks, S.L Walker); Université d'Angers, Angers, France (M. Kempf, E. Marion); Centre Hospitalier Universitaire Angers, Angers (M. Kempf)

DOI: https://doi.org/10.3201/eid2809.212126

[1]These authors contributed equally to this article.

examples of yaws integration with Buruli ulcer in community outreach programs (*15*). Despite promise, these studies have not rigorously evaluated performance or equity indicators, limiting their broader applicability. WHO recently published a skin NTD diagnostic manual for frontline staff to help improve clinical diagnostic capacity among healthcare workers (*16*). However, the feasibility of training this cadre of healthcare workers to accurately diagnose multiple complex skin conditions has yet to be evaluated.

In light of 2030 skin NTD targets, there is a pressing need to bridge these evidence gaps through operational evaluation (*8*). We aimed to estimate the population-level prevalence of 4 endemic skin NTDs, Buruli ulcer, leprosy, LFM, and yaws, within the routine health infrastructure of Maryland County, Liberia. We implemented community-based case finding and clinical training of midlevel health workers within a stratified 1-stage survey design. We present a detailed breakdown of skin NTD epidemiology and evaluation of integrated surveillance strategies within a programmatic setting.

Methods

Study Setting

Maryland County (census population 165,456), a rural county in southeastern Liberia, has the highest levels of absolute poverty (84.0%) in this country (*17*). It is endemic for Buruli ulcer, leprosy, and LFM and borders a yaws-endemic region of Cote d'Ivoire. In March and November 2017, all community health workers (CHWs) and 2 clinicians from each health facility undertook Ministry of Health training modules in recognizing, reporting, and managing skin NTDs, independent from this study.

Study Design and Participants

We conducted a population-based cluster-randomized cross-sectional survey for Buruli ulcer, leprosy, LFM, and yaws in Maryland County during June–October 2018 by using a screen and confirm strategy. All communities in the County Health Department of Maryland were eligible for enrollment, and we selected CHW catchment areas as primary sampling units. We combined contiguous CHW catchments that had <300 persons and divided those that had >1,000 persons before selection. We randomly selected 92 clusters (mean population 618) stratified across all 24 health facilities by using probability proportional to size. All residents of selected clusters were eligible and sought for participation in initial screening.

Ethics

The study protocol was approved by the University of Liberia Institutional Review Board (#18-02-088) and the Ethics Committee of the London School of Hygiene and Tropical Medicine (#14698). Community meetings were held in all study clusters before implementation. We obtained verbal consent from adult residents for household participation in screening, and written consent from adults, or guardians if persons were <18 years of age, for quality control and case verification visits. All skin NTDs and other diagnosed skin conditions were immediately referred for treatment at health facilities in line with national guidelines. This study is registered with ClinicalTrials.gov (https://www.clinicaltrials.gov), no. NCT03683745.

Procedures

We conducted an exhaustive population screening in selected CHW catchment areas (Appendix, https://wwwnc.cdc.gov/EID/article/28/9/21-2126-App1.pdf). CHWs visited all households within their catchment communities over a 5-day period, completed a simple census, and screened residents for suspected skin NTDs on the basis of interviewee report, using photographs of clinical manifestations. The household head or primary caregiver were directly prompted to act as a proxy respondent for absent members. Visited households were provided with quick response–coded study identification cards, and persons who had suspected cases were provided a separate individually identifiable identification card.

One week after community screening, suspected case lists were provided to mobile verification teams for home-based follow-up, diagnosis, and referral. Before survey activities, a team of 7 nationally recruited midlevel health workers (physician assistants) attended a 5-day training course on diagnosis and management of skin NTDs held at a national referral center for Buruli ulcer and leprosy in Ganta, Nimba County, and led by Ministry of Health NTD program (E.R. and T.M.) and UK-based experts, including a consultant tropical dermatologist (M.M., S.L.W, and J.W.S.T.). During household visits, trained skin NTD verifiers performed detailed clinical examination of all suspected persons who had cases before diagnosis.

All survey stages were evaluated through separate quality control (QC) surveys. CHW screening was evaluated by an independent community health services supervisor (CHSS), who randomly visited 10–15 households/cluster during the week after CHW screening activities. At each household,

study identification cards were recaptured and household information was collected. The CHSS performed skin examinations of all consenting household members and recorded all skin lesions comparable to the photographic case definitions used by CHWs. Clinical diagnoses were validated in a purposively selected subpopulation of verified cases by clinically trained members of the national NTD program (E.R., T.M., and R.G). Additional QC was implemented through deployment of global positioning system–enabled electronic data collection devices running open data kit–based data collection platforms across all survey stages.

Outcomes

The primary outcome was prevalence of all skin NTDs diagnosed by trained verification teams. We confirmed clinically suspected Buruli ulcer by using an IS2404 PCR with swab specimens or fine-needle aspirates (*18*). We defined yaws cases as a clinically suspicious lesion plus dual serologic positivity by using a syphilis dual path platform lateral flow assay for both treponemal and nontreponemal antibodies (ChemBio, https://chembio.com). All serologically confirmed yaws cases also underwent PCR confirmation (tp47) of lesion swab specimens. We based LFM and leprosy diagnoses on clinical assessment of signs and symptoms.

We also collected routine program data from Maryland County aggregated by the county health office on all skin NTD outcomes from the year before survey implementation. All diagnoses through the routine program were made on the basis of clinical assessment. We compared the annual new case detection rate to the prevalence of survey cases that we confirmed as being previously unknown to the health system. During verification, a case-patient was determined as unknown to the health system by interviewing the patient and CHSS and by cross-checking all survey cases against county records.

Sample Size and Statistical Analysis

We performed data management and statistical analyses by using R version 4.0.1 (https://www.r-project.org). We assumed a population-level skin NTD prevalence of 5 cases/10,000 persons, absolute precision of 3.5 cases/10,000 persons, a design effect of 3.5, a participation rate of 0.8, and a finite population correction factor. The required sample size was 48,478 by using standard formulas. We estimated prevalence through design-based inference as a stratified 1-stage cluster design with variance estimated by using Jackknife Repeated Replication Survey version 3.36, (https://am.air.org/Manual/Tools/Variance Estimation/Jackknife-Repeated-Replication). We estimated intraclass correlation coefficients (ICC) from intercept-only binomial mixed effects models (lme4 version 1.1–23) (*19*). We analyzed operational factors associated with survey participation by using binomial mixed effect and conditional logistic regression (survival version 3.1–12, https://rdrr.io/cran/survival/man/clogit.html) with model-building approaches (outlined in Appendix). We used the Cohen κ and crude agreement to estimate interrater reliability of all clinical diagnoses (psych version 1.9.12, https://cran.r-project.org/web/packages/psych/psych.pdf).

Results

We visited 10,007 households across 92 clusters (143 refused, 1.4%) and included 56,825 persons (49.8% female, 47.3% <18 years of age) in the sample population (Figure 1). In total, 34,916 persons were present during CHW household screening visits to observe photographs of skin NTDs. The remaining 38.6% were absent at the time of survey, and referrals among this group were based on proxy responses.

Among the sample population, 3,087 persons (5.4%, 95% CI 5.2–5.6) were referred by CHWs because these persons had possible skin NTD symptoms. Median age of referrals was 27 years (35.7% female, increasing to 48.3% when excluding hydrocoele; 102 missing age or sex data). We observed a linear increase in referral rates by age ($p<0.0001$), with an approximate threshold at 35 years, over which referrals increased more than 2-fold from 4.1/100 persons screened (95% CI 3.9–4.3) to 8.6/100 persons screened (95% CI 8.1–9.1). CHW referral rates varied substantially by cluster (range 0.5–23.0/100 persons screened; ICC 0.11) and health district (3.1–7.0/100 persons screened; ICC 0.01). Models exploring associations between referral rates and potential operationally relevant variables indicated only older CHW age to be associated with reduced odds of referral (>35 years of age; odds ratio 0.59, 95% CI 0.43–0.81; $p = 0.001$) (Appendix).

Mobile verification teams successfully followed up with 2,630 case-patients (81.1% of those referred). This group had minor differences in age compared with those who could not be found for follow-up (27.7 years [95% CI 26.1–29.3 years] vs. 30.3 years [95% CI 29.4–31.1]) but no overt difference in sex (35.0% [95% CI 31.0%–39.1%] female patients followed up vs. 36.7% [95% CI 34.8%–38.6%] female patients not followed up) or implementation district of residence ($p = 0.15$). We diagnosed 236 cases of skin NTDs (Table 1), a crude prevalence of 41.5 skin NTDs/10,000 persons and a design-adjusted prevalence of 34.0

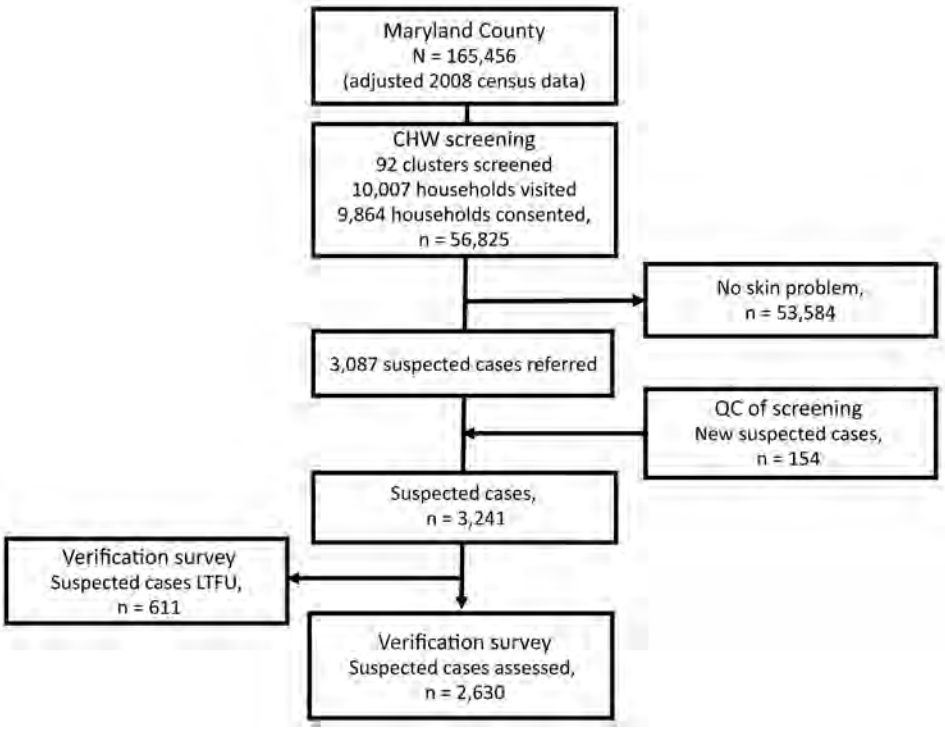

Figure 1. Study population flowchart for study quantify population burden and effectiveness of decentralized surveillance strategies for skin-presenting neglected tropical diseases, Maryland County, Liberia. Consort diagram shows selection, screening, quality control, and verification stages. CHW, community health worker; LFTU, lost to follow-up (did not continue to participate in follow-up contacts); QC, quality control.

(95% CI 29.1–38.9) skin NTDs/10,000 persons (Figure 2). The most prevalent condition was LFM, causing 111 lymphedema (17.5 [95% CI 14.1–21.0] cases/10,000 persons) and 58 hydrocoele cases (8.5 [95% CI 4.8–12.3] cases/10,000 persons). We identified 55 cases of suspected Buruli ulcer on the basis of clinical case definitions, although only 4 were confirmed by PCR (0.9 [95% CI 0–1.9] cases/10,000 persons), establishing PCR-confirmed Buruli ulcer as the rarest outcome (Appendix).

Prevalence of any skin NTD was focally distributed within communities (ICC 0.27), with considerable heterogeneity between clusters (range 0–330 case/10,000 persons) (Figures 3, 4). Analysis of individual skin NTDs showed a greater degree of spatial heterogeneity, with LFM and yaws exhibiting particularly focal distributions (Table 1). Few clusters were co-endemic for more than 1 skin NTD (22 of 92, 23.9%) and only 1 cluster was co-endemic for >2 diseases. Of potential cases identified in screening, 91.0% (2,394/2,630) were diagnosed with conditions not included within the primary outcome, including superficial fungal infections (471 cases, 17.9% of verified cases), scabies (316 cases, 12.0%), scrotal hernia (279 cases, 10.6%) and skin ulcers of unknown etiology (110 cases, 4.2%) (Appendix).

The new case detection rate from existing county-level health records in 2017 was 13.8 cases/10,000 persons compared with our survey point prevalence estimate of 25.4 (95% CI 21.3–29.5) previously unidentified cases/10,000 persons (Figure 5). Overall, there was no evidence of differences in age and sex of case-patients detected through routine reporting. Among leprosy case-patients only, those we detected by using survey methods were older (46.3 vs. 35.2 years; p = 0.02), and there was a greater proportion of

Table 1. Final prevalence estimates of primary and secondary skin NTD outcomes, Liberia*

Disease	Total no. cases	Crude prevalence/10,000 persons (95% CI)	Design-adjusted population prevalence/10,000 persons (95% CI)	Median age, y	Female, %	Cluster prevalence range/10,000 persons	ICC†
All skin NTDs	236	41.5 (36.2–46.8)	34.0 (29.1–38.9)	42	42.3	0–330	0.27
Buruli ulcer	4	0.7 (0.1–1.4)	0.9 (0–1.8)	16.5	50.0	0–39.4	NA
Leprosy	39	6.9 (4.7–9.0)	4.4 (3.3–5.5)	44	42.8	0–74.1	0.18
LF lymphedema	111	19.5 (15.9–23.2)	17.5 (14.1–21.0)	48	67.3	0–209.7	0.41
LF hydrocele	58	10.2 (7.6–12.8)	8.5 (4.8–12.3)	43	0	0–256.4	0.43
Active yaws	24	4.2 (2.5–5.9)	2.6 (1.4–3.9)	10	25.0	0–205	0.93

*Age and sex data were missing for 9 skin NTD cases. ICC, intraclass correlation coefficient; LF, lymphatic filariasis; NA, not available; NTD, neglected tropical disease.
†Not estimated for Buruli ulcer.

paucibacillary leprosy relative to routine data (53.8% vs. 22.9%; p = 0.006).

To assess performance of CHW screening, QC surveys were conducted in 1,382 randomly sampled households (1,379 consented, 99.8%) in 91 clusters before verification of cases took place. Among the QC sample population, 95.1% of households (1,320 of 1,379) reported being visited by the local CHW and shown skin NTD photographs, with no evidence of socioeconomic disparities between households visited or missed (Appendix).

QC teams enumerated 8,021 persons and performed skin examinations on 4,268 household members (53.2%) among 4,409 approached (141 refused, 3.2%). Among persons examined, clinical field officers (trained CHSS cohort) identified 503 cases (11.8 [95% CI 10.8–12.8] cases/100 examined) of skin lesions similar in appearance to photograph-based CHW case definitions. Among the 503 patients who had skin lesions, clinical field officers recaptured patient identification cards from 349 to estimate sensitivity of screening (69.4%; CHSS new case detection rate 3.6 [95% CI 3.1–4.2] cases/100 persons). There was good concordance with CHW referrals for age and proportion of female referrals. We also conducted a sensitivity analysis of the effect of reduced sensitivity on prevalence estimates (Appendix).

We assessed the reliability of clinical diagnoses made by verification teams through separate follow-up QC surveys immediately after case verification activities. We reached 174 of 2,630 verified cases (6.6%) across 16 health facilities and 36 clusters. The crude agreement of all 174 diagnoses as skin NTD was 82.8% (Cohen κ 0.69, 95% CI 0.59–0.79), indicating substantial agreement between raters. Excluding other skin diseases, crude agreement (62.0%) and Cohen κ (0.51, 95% CI 0.39–0.64) were lower for skin NTDs, with a tendency for overdiagnosis among verification teams (Table 2). For individual skin NTDs, we did not estimate Cohen κ because of high prevalence index introduced by our sampling approach (*20*), but crude agreement between raters showed considerable variation between diseases (Table 2).

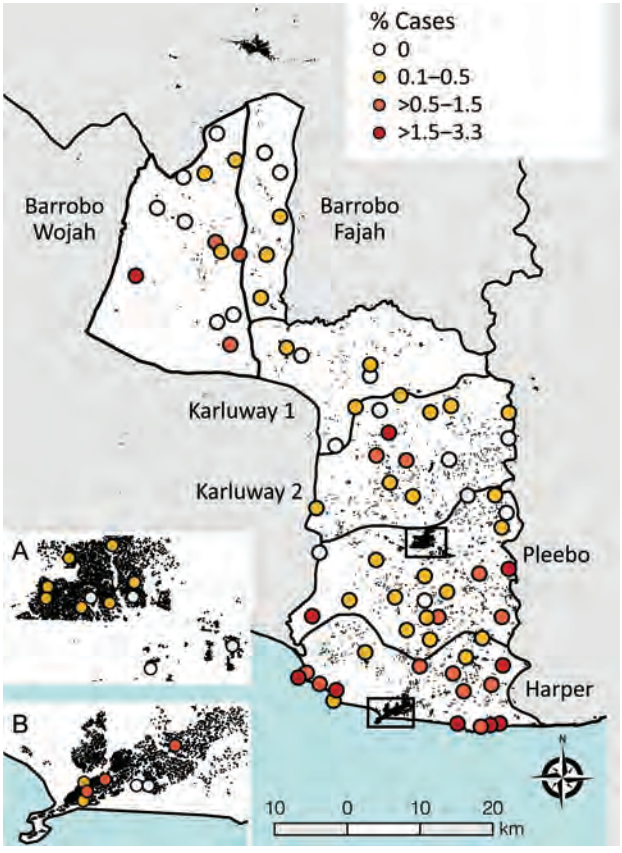

Figure 2. Cluster-level prevalence of all skin-presenting neglected tropical diseases combined, Maryland County, Liberia, June–October 2018. Inset boxes show major urban areas Pleebo (A) and Harper (B). Black features are buildings (OpenStreetMap contributors) to highlight increasing rurality in northern districts.

Discussion

This study was a programmatic-scale integrated skin NTD prevalence survey in West Africa and was conducted entirely within the routine health infrastructure of Maryland County, Liberia. Our results show that skin NTDs in this setting are underreported, spatially heterogeneous, and highly focal, imparting a considerable unmet burden on this largely rural and periurban population.

We concurrently provide new evidence on the effectiveness of surveillance strategies that form the basis of skin NTD program delivery outlined in the WHO 2030 NTD roadmap (*21*). We demonstrate that large-scale screening by CHWs can find unreported cases of stigmatizing diseases while achieving high and equitable coverage among hard-to-reach communities. We also quantified major limitations in sensitivity and specificity from using our chosen approach with this workforce. Integrated clinical training of nonphysician healthcare workers facilitated reliable differentiation between any skin NTD and other skin conditions reported by participants. However, reliability of disease-specific diagnoses of skin NTDs was variable.

The greatest disease burden in Maryland County was attributable to LFM; both BU and yaws showed markedly lower prevalence. Burden across all skin NTDs was higher than reported through routine surveillance systems for the county, as well as those typically reported in surveillance records nationally

and across other co-endemic states in West Africa, although Buruli ulcer remains comparable if limited to PCR-confirmed cases (*5*,*7*,*22*). All diseases appeared spatially heterogeneous in occurrence and prevalence at this implementation scale. The explanatory factors underlying these observations are probably multifaceted, given diverse transmission dynamics, a combination of climatic, ecologic, and sociodemographic (*23*–*26*). However, given highly focal distributions, these observations could be attributable to sampling error.

Population-level skin NTD surveys have previously been undertaken in Ethiopia, Rwanda, and Cameroon (*12*,*27*–*28*), demonstrating a similarly high unmet burden. We believe the additional granularity and operational evaluation in our study provides additional strong justification for integrated approaches to skin NTD surveillance. We demonstrated that at the cluster level, most communities did not have individual skin NTDs, resulting in wasted resources if using nonintegrated surveillance strategies. Although findings indicate that disease-specific interventions could be targeted to smaller implementation units, sampling effort required for accurate delineation might outweigh benefits of microplanning.

The use of CHWs for disease-specific surveillance is common in West Africa, particularly for Buruli

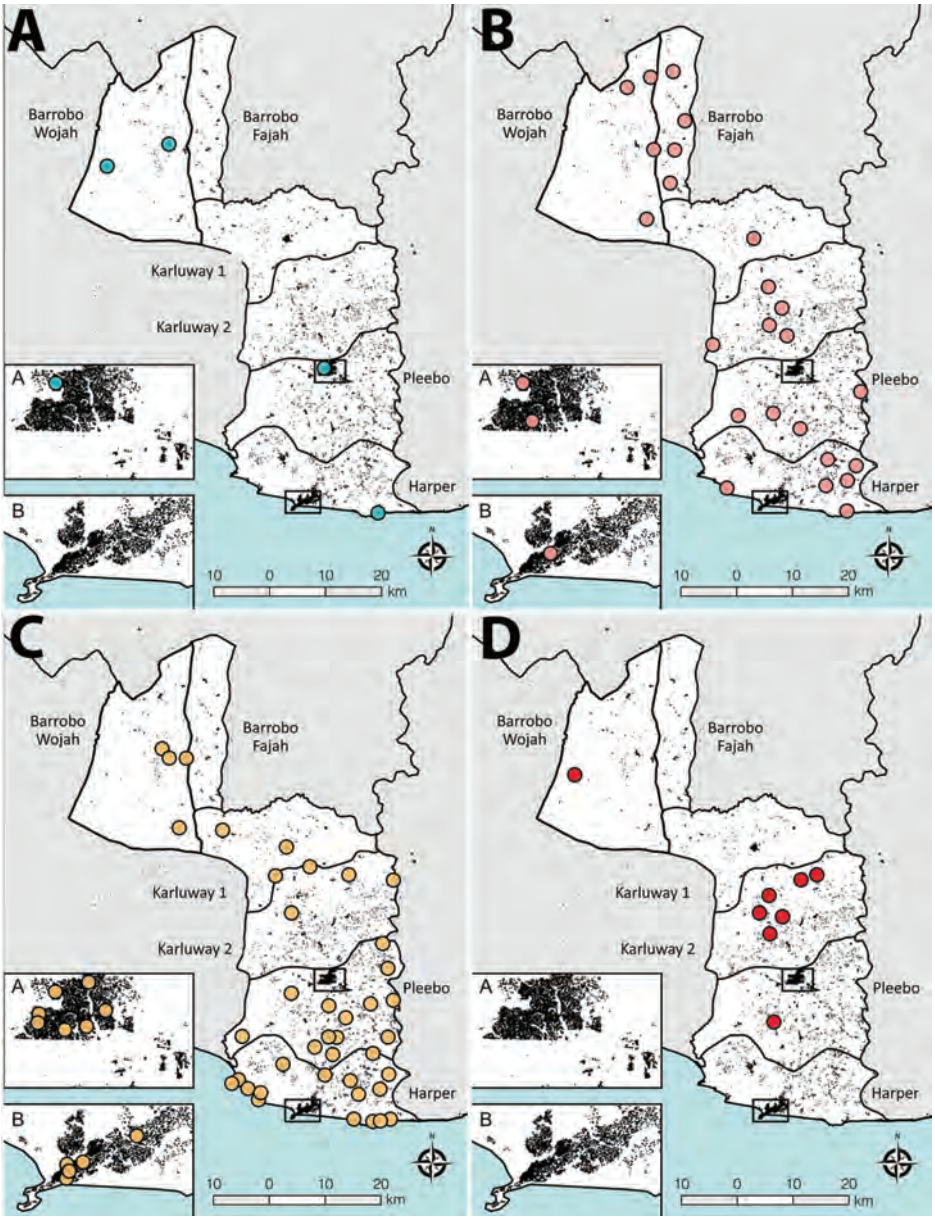

Figure 3. Spatial distribution and occurrence of skin-presenting neglected tropical diseases , Maryland County, Liberia, June–October 2018. A) Buruli ulcer, B) leprosy, C) lymphatic filariasis morbidity; D) yaws. Points represent cluster centroids and not absolute location of cases.

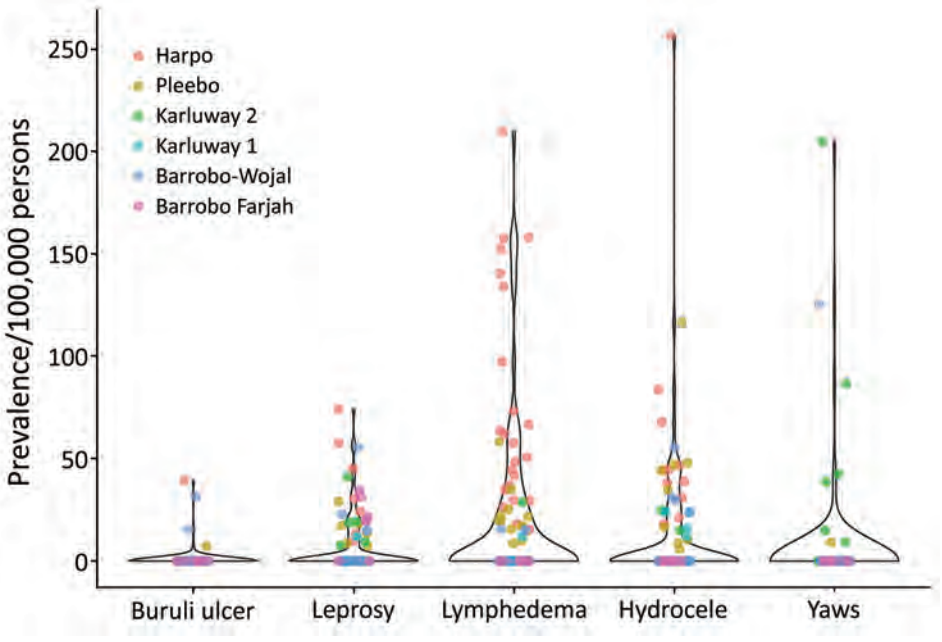

Figure 4. Cluster-level prevalence of skin-presenting neglected tropical diseases, Maryland County, Liberia, June–October 2018. Colors denote health district of cluster.

ulcer, for which increased case numbers or earlier stages of detection have been reported in quasiexperimental studies (*13*,*29*,*30*). Our findings illustrate the feasibility of training a rural community-based workforce with limited smartphone experience to screen for multiple diseases, reliably capture electronic data, and achieve high and equitable population coverage. CHWs identified a large proportion of previously undetected cases, even in a setting with recent previous training of CHWs and formal health workers. We also found no evidence households missed during screening were systematically omitted on the basis of socioeconomic indicators. However, we observed and quantified the probable underestimation of referable skin lesion burden by using our chosen approach. In addition, 91% of persons with verified cases were ultimately diagnosed with non–skin NTD etiology, including a large number of communicable skin diseases (corroborating recent dermatologic surveys in neighboring Côte d'Ivoire [(*31*)]), debilitating ulcers, and scrotal hernias. Given widespread use of CHWs for skin NTD surveillance, our results quantify major considerations with this approach, including management of a potentially large additional burden of disease.

Sustainable skin NTD programs also depend on decentralized diagnosis and case management by mid-level health workers. The performance of integrated skin NTD training programs has not been formally evaluated, despite recent WHO publication of a manual for frontline healthcare workers (*16*). Our findings show that a tailored training program reliably identified skin NTDs but that agreement on specific diagnoses could be inconsistent, particularly in the case of hydrocele and leprosy. Furthermore, confirmation rates of clinically suspected Buruli ulcer and yaws highlight the need for laboratory support for diagnosis. Previous studies in West Africa showed success in developing clinical algorithms for common skin diseases (*32*), and research continues on alternative algorithmic or telemedicine approaches to support decentralized clinical decision-making (*33*,*34*). Our findings support the need for further evaluation of integrated training programs to support frontline healthcare workers, especially in settings in which laboratory support is limited.

The first limitation of our study was that we relied on CHWs to conduct screening, a strategy that might have led to us miss the most marginalized households at higher risk for skin NTDs. Nevertheless, our QC survey suggested high coverage, a finding also supported when cross-comparing household global positioning system points with satellite imagery. Second, screening relied upon self-report and proxy-report of stigmatized conditions. We quantified a degree of loss in sensitivity through QC skin examinations, but inclusion might have been further biased downwards if affected persons were less willing to participate. Third, ascertainment of leprosy and LFM was dependent on clinical diagnosis, with variable reliability potentially biasing estimates from true population prevalence. Finally, we observed a notable percentage (≈19%) of patients who did not continue follow-up

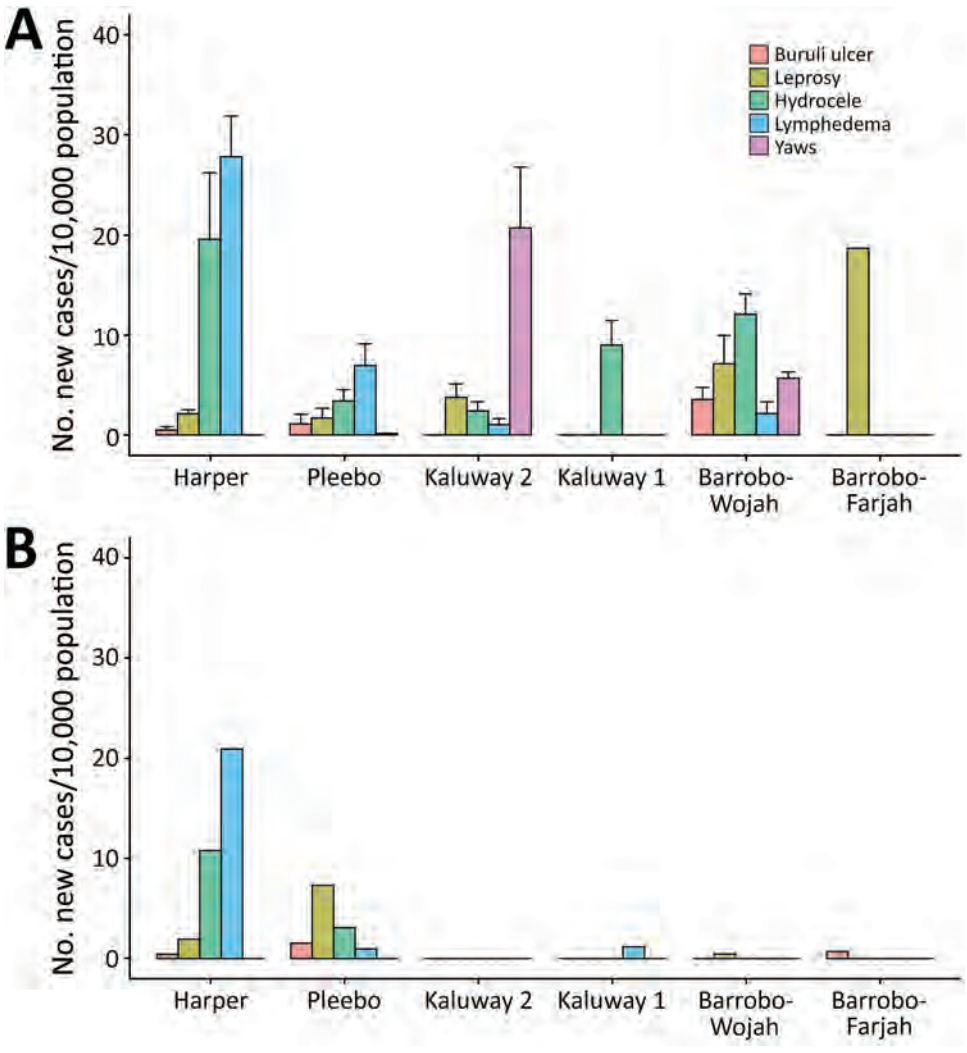

Figure 5. Comparison of cases of skin-presenting neglected tropical diseases before and after survey, Maryland County, Liberia. A) Survey cases previously unknown to the health system; B) annual new case detection rates from routine health system records extracted from the 12 months before survey implementation. Note that plots are comparing point prevalence (A) with annual new case detection rates (B). Routine diagnosis is limited to clinical suspicion for Buruli ulcer. If survey estimates are extended to include all clinically suspected cases of Buruli ulcer, we estimate a countrywide prevalence of 32.4 (95% CI 27.4–37.3) previously unknown cases/10,000 persons.

between screening and verification stages, although we did not see overt differences in the demographics of the censored population. We would expect this aspect to bias final prevalence estimates down, but the magnitude of this effect remains unclear.

With the new WHO 2030 NTD roadmap explicitly mapping out a 10-fold scale-up of skin NTD programs, there is an urgent need to better clarify disease burden and strategies for integrated surveillance to support this global transition (*8*). Our results provide a multifaceted overview of disease epidemiology and operational evaluation of surveillance strategies that can guide countries who are beginning integrated skin NTD programs.

Table 2. Summary of interrater reliability scores of skin NTD clinical diagnoses, Liberia*

Disease	Total survey cases assessed	Total QC clinical diagnoses	Agreement	Verifier-only diagnoses	QC-only diagnosis	Agreement, %	Alternative diagnoses
Suspected Buruli ulcer	15	11	10	5	1	62.5	Traumatic ulcer, tropical ulcer
Leprosy	12	7	7	5	0	58.3	Vitiligo, tinea corporis
LF lymphedema	25	27	24	1	3	85.7	Non-LF edema
LF hydrocele	17	14	8	9	6	34.8	Hernia, non-LF hydrocele
Other skin disease	105	115	95	10	20	76.0	None
Combined skin NTDs	69	59	49	20	10	62.0†	None

*Overall agreement; 82.8%; Cohen κ, all outcomes: 0.69 (95% CI 0.59–0.79). LF, lymphatic filariasis; NTD, neglected tropical disease; QC, quality control.
†Cohen κ: 0.51 (0.39–0.64)

Acknowledgments

We thank Anna Wickenden and Paul Saunderson for their crucial support in conception of the study and implementation; the community health workers, frontline health workers, and Stanley Duwor, William Govergo, Emmanuel Johnson, Tina Hampey, Aloysius Geekor Johnson, Lawrence Kollie for supporting survey implementation; Amos Ballah and Jonathan C. Willie for providing outstanding logistical support; WHO for donation of yaws rapid diagnostic tools; Anthony Solomon and Robin Bailey for providing insightful comments on an earlier draft of the manuscript; and the communities of Maryland County for their participation and support of the study from inception to conclusion.

This study was supported by the Accelerating Integrated Management of the American Leprosy Missions.

About the Author

Dr. Timothy is an epidemiologist at the London School of Hygiene and Tropical Medicine, London, UK, and a member of the UK Public Health Rapid Support Team. His major research interests are the epidemiology and control of neglected tropical diseases and emerging infectious diseases

References

1. Mitjà O, Marks M, Bertran L, Kollie K, Argaw D, Fahal AH, et al. Integrated control and management of neglected tropical skin diseases. PLoS Negl Trop Dis. 2017;11:e0005136. https://doi.org/10.1371/journal.pntd.0005136
2. Engelman D, Fuller LC, Solomon AW, McCarthy JS, Hay RJ, Lammie PJ, et al. Opportunities for integrated control of neglected tropical diseases that affect the skin. Trends Parasitol. 2016;32:843–54. https://doi.org/10.1016/j.pt.2016.08.005
3. Mitra AK, Mawson AR. Neglected tropical diseases: epidemiology and global burden. Trop Med Infect Dis. 2017;2:36. https://doi.org/10.3390/tropicalmed2030036
4. Simpson H, Deribe K, Tabah EN, Peters A, Maman I, Frimpong M, et al. Mapping the global distribution of Buruli ulcer: a systematic review with evidence consensus. Lancet Glob Health. 2019;7:e912–22. https://doi.org/10.1016/S2214-109X(19)30171-8
5. World Health Organization. Global leprosy update, 2016: accelerating reduction of disease burden. Wkly Epidemiol Rec. 2017;92:501–19.
6. World Health Organization. Global programme to eliminate lymphatic filariasis: progress report, 2015. Wkly Epidemiol Rec. 2016;91:441–55.
7. Mitjà O, Marks M, Konan DJP, Ayelo G, Gonzalez-Beiras C, Boua B, et al. Global epidemiology of yaws: a systematic review. Lancet Glob Health. 2015;3:e324–31. https://doi.org/10.1016/S2214-109X(15)00011-X
8. World Health Organization. Ending the neglect to attain the sustainable development goals: a road map for neglected tropical diseases 2021–2030 [cited 2022 Jul 3]. https://www.who.int/publications/i/item/9789240010352
9. Nery JS, Ramond A, Pescarini JM, Alves A, Strina A, Ichihara MY, et al. Socioeconomic determinants of leprosy new case detection in the 100 million Brazilian cohort: a population-based linkage study. Lancet Glob Health. 2019;7:e1226–36. https://doi.org/10.1016/S2214-109X(19)30260-8
10. de Souza DK, Yirenkyi E, Otchere J, Biritwum NK, Ameme DK, Sackey S, et al. Assessing lymphatic filariasis data quality in endemic communities in Ghana, using the neglected tropical diseases data quality assessment tool for preventive chemotherapy. PLoS Negl Trop Dis. 2016;10:e0004590. https://doi.org/10.1371/journal.pntd.0004590
11. Porten K, Sailor K, Comte E, Njikap A, Sobry A, Sihom F, et al. Prevalence of Buruli ulcer in Akonolinga health district, Cameroon: results of a cross sectional survey. PLoS Negl Trop Dis. 2009;3:e466. https://doi.org/10.1371/journal.pntd.0000466
12. Bratschi MW, Bolz M, Minyem JC, Grize L, Wantong FG, Kerber S, et al. Geographic distribution, age pattern and sites of lesions in a cohort of Buruli ulcer patients from the Mapé Basin of Cameroon. PLoS Negl Trop Dis. 2013;7:e2252. https://doi.org/10.1371/journal.pntd.0002252
13. Ahorlu CS, Okyere D, Ampadu E. Implementing active community-based surveillance-response system for Buruli ulcer early case detection and management in Ghana. PLoS Negl Trop Dis. 2018;12:e0006776. https://doi.org/10.1371/journal.pntd.0006776
14. Stanton MC, Mkwanda SZ, Debrah AY, Batsa L, Biritwum NK, Hoerauf A, et al. Developing a community-led SMS reporting tool for the rapid assessment of lymphatic filariasis morbidity burden: case studies from Malawi and Ghana. BMC Infect Dis. 2015;15:214. https://doi.org/10.1186/s12879-015-0946-4
15. Boock AU, Awah PK, Mou F, Nichter M. Yas resurgence in Bankim, Cameroon: the relative effectiveness of different means of detection in rural communities. PLoS Negl Trop Dis. 2017;11:e0005557. https://doi.org/10.1371/journal.pntd.0005557
16. World Health Organization. Control of neglected tropical diseases recognizing neglected tropical diseases through changes on the skin, 2018 [cited 2022 Jul 3]. http://www.who.int/neglected_diseases/en
17. Liberia Institute for Statistics and Geo-Information Services. Household income and expenditure survey 2016 [cited 2022 Jul 3]. https://ekmsliberia.info/document/household-income-and-expenditure-survey-2016
18. Marion E, Ganlonon L, Claco E, Blanchard S, Kempf M, Adeye A, et al. Establishment of quantitative PCR (qPCR) and culture laboratory facilities in a field hospital in Benin: 1-year results. J Clin Microbiol. 2014;52:4398–400. https://doi.org/10.1128/JCM.02131-14
19. Nakagawa S, Johnson PCD, Schielzeth H. The coefficient of determination R^2 and intra-class correlation coefficient from generalized linear mixed-effects models revisited and expanded. J R Soc Interface. 2017;14:20170213. https://doi.org/10.1098/rsif.2017.0213
20. Sim J, Wright CC. The kappa statistic in reliability studies: use, interpretation, and sample size requirements. Phys Ther. 2005;85:257–68. https://doi.org/10.1093/ptj/85.3.257
21. de Vlas SJ, Stolk WA, le Rutte EA, Hontelez JA, Bakker R, Blok DJ, et al. Concerted efforts to control or eliminate neglected tropical diseases: how much health will be gained? PLoS Negl Trop Dis. 2016;10:e0004386. https://doi.org/10.1371/journal.pntd.0004386

22. Omansen TF, Erbowor-Becksen A, Yotsu R, van der Werf TS, Tiendrebeogo A, Grout L, et al. Global epidemiology of Buruli ulcer, 2010–2017, and analysis of 2014 WHO programmatic targets. Emerg Infect Dis. 2019;25:2183–90. https://doi.org/10.3201/eid2512.190427
23. Moraga P, Cano J, Baggaley RF, Gyapong JO, Njenga SM, Nikolay B, et al. Modelling the distribution and transmission intensity of lymphatic filariasis in sub-Saharan Africa prior to scaling up interventions: integrated use of geostatistical and mathematical modelling. Parasit Vectors. 2015;8:560. https://doi.org/10.1186/s13071-015-1166-x
24. Timothy JW, Beale MA, Rogers E, Zaizay Z, Halliday KE, Mulbah T, et al. Epidemiologic and genomic reidentification of yaws, Liberia. Emerg Infect Dis. 2021;27:1123–32. https://doi.org/10.3201/eid2704.204442
25. Simpson H, Tabah EN, Phillips RO, Frimpong M, Maman I, Ampadu E, et al. Mapping suitability for Buruli ulcer at fine spatial scales across Africa: a modelling study. PLoS Negl Trop Dis. 2021;15:e0009157. https://doi.org/10.1371/journal.pntd.0009157
26. Fine PE. Leprosy: the epidemiology of a slow bacterium. Epidemiol Rev. 1982;4:161–88. https://doi.org/10.1093/oxfordjournals.epirev.a036245
27. Deribe K, Mbituyumuremyi A, Cano J, Jean Bosco M, Giorgi E, Ruberanziza E, et al. Geographical distribution and prevalence of podoconiosis in Rwanda: a cross-sectional country-wide survey. Lancet Glob Health. 2019;7:e671–80. https://doi.org/10.1016/S2214-109X(19)30072-5
28. Deribe K, Brooker SJ, Pullan RL, Sime H, Gebretsadik A, Assefa A, et al. Epidemiology and individual, household and geographical risk factors of podoconiosis in Ethiopia: results from the first nationwide mapping. Am J Trop Med Hyg. 2015;92:148–58. https://doi.org/10.4269/ajtmh.14-0446
29. Barogui YT, Sopoh GE, Johnson RC, de Zeeuw J, Dossou AD, Houezo JG, et al. Contribution of the community health volunteers in the control of Buruli ulcer in Bénin. PLoS Negl Trop Dis. 2014;8:e3200. https://doi.org/10.1371/journal.pntd.0003200
30. Abass KM, van der Werf TS, Phillips RO, Sarfo FS, Abotsi J, Mireku SO, et al. Buruli ulcer control in a highly endemic district in Ghana: role of community-based surveillance volunteers. Am J Trop Med Hyg. 2015;92:115–7. https://doi.org/10.4269/ajtmh.14-0405
31. Yotsu RR, Kouadio K, Vagamon B, N'guessan K, Akpa AJ, Yao A, et al. Skin disease prevalence study in schoolchildren in rural Côte d'Ivoire: implications for integration of neglected skin diseases (skin NTDs). PLoS Negl Trop Dis. 2018;12:e0006489. https://doi.org/10.1371/journal.pntd.0006489
32. Mahé A, Faye O, N'Diaye HT, Ly F, Konaré H, Kéita S, et al. Definition of an algorithm for the management of common skin diseases at primary health care level in sub-Saharan Africa. Trans R Soc Trop Med Hyg. 2005;99:39–47. https://doi.org/10.1016/j.trstmh.2004.03.008
33. Mieras LF, Taal AT, Post EB, Ndeve AG, van Hees CL. The development of a mobile application to support peripheral health workers to diagnose and treat people with skin diseases in resource-poor settings. Trop Med Infect Dis. 2018;3:1–7. https://doi.org/10.3390/tropicalmed3030102
34. Messagier AL, Blaizot R, Couppié P, Delaigue S. Teledermatology use in remote areas of French Guiana: experience from a long-running system. Front Public Health. 2019;7:387. https://doi.org/10.3389/fpubh.2019.00387

Address for correspondence: Joseph W.S. Timothy, London School of Hygiene and Tropical Medicine, Keppel St, London WC1E 7HT, UK; email: joseph.timothy@lshtm.ac.uk

Rapid Adaptation of Established High-Throughput Molecular Testing Infrastructure for Monkeypox Virus Detection

Dominik Nörz, Hui Ting Tang, Petra Emmerich, Katja Giersch, Nicole Fischer, Stephan Schmiedel, Marylyn M. Addo, Martin Aepfelbacher, Susanne Pfefferle, Marc Lütgehetmann

Beginning in May 2022, a rising number of monkeypox cases were reported in non–monkeypox-endemic countries in the Northern Hemisphere. We adapted 2 published quantitative PCRs for use as a dual-target monkeypox virus test on widely used automated high-throughput PCR systems. We determined analytic performance by serial dilutions of monkeypox virus reference material, which we quantified by digital PCR. We found the lower limit of detection for the combined assays was 4.795 (95% CI 3.6–8.6) copies/mL. We compared clinical performance against a commercial manual orthopoxvirus research use only PCR kit by using clinical remnant swab samples. Our assay showed 100% positive (n = 11) and 100% negative (n = 56) agreement. Timely and scalable PCR tests are crucial for limiting further spread of monkeypox. The assay we provide streamlines high-throughput molecular testing for monkeypox virus on existing broadly established platforms used for SARS-CoV-2 diagnostic testing.

In May 2022, an unusually high number of monkeypox cases were reported in countries in western Europe and North America; by May 29, 2022, 257 laboratory-confirmed infections were reported from Spain, Portugal, the United Kingdom, Canada, and the United States, sparking fear of another global outbreak on the heels of the continuing SARS-CoV-2 pandemic (*1*–*4*). Endemic transmission of the monkeypox virus (MPXV), a species of the *Orthopoxvirus* genus, is thought to be limited to central and western Africa, where both zoonotic (≈22%–72% of cases) and person-to-person transmission contribute to disease burden (*5*). Previous clusters outside Africa have usually been traceable to animal sources rather than to human-to-human transmission (*6*). In contrast, the 2022 cases seem to have occurred without any links to animal sources and have been concentrated in, but not exclusive to, men who have sex with men (*7*). The sudden appearance of infections in several non–monkeypox-endemic countries suggested that undetected transmission might have taken place for some time but that recent events could have served as a catalyst for spread (*1*).

The ongoing SARS-CoV-2 pandemic has demonstrated the potential and value of highly automated high-throughput molecular testing in outbreak scenarios. We aimed to rapidly adapt existing automated molecular testing infrastructure for SARS-CoV-2 in a large tertiary-care hospital in Hamburg, Germany, for detection of MPXV from clinical samples, thereby creating the capacity for high-throughput testing and quick turnaround times, if needed.

Materials and Methods

Multiplex Assay Setup

On the basis of diagnostic testing during the SARS-CoV-2 pandemic (*8*; C. Manohar et al., unpub. data, https://doi.org/10.1101/2021.10.13.21264919), we chose a dual-target approach, in which 1 assay targets a conserved sequence of the *Orthopoxvirus* genus, not including variola major or minor viruses (*9*), and the other targets a MPXV-specific sequence (*10*) (Table 1). The cobas 5800, 6800, and 8800 systems (Roche Diagnostics, https://diagnostics.roche.com) use a spike-in RNA full process control that is added automatically during extraction. The corresponding

Author affiliations: University Medical Center Hamburg-Eppendorf, Hamburg, Germany (D. Nörz, H.T. Tang, K. Giersch, N. Fischer, S. Schmiedel, M.M. Addo, M. Aepelbacher, S. Pfefferle, M. Lütgehetmann); Bernhard-Nocht Institute for Tropical Medicine, Hamburg (P. Emmerich, M.M. Addo, S. Pfefferle); German Center for Infection Research, Hamburg (M.M. Addo)

DOI: https://doi.org/10.3201/eid2809.220917

Table 1. Primer and probe sequences for a dual-target MPXV assay rapidly adapted from established high-throughput SARS-CoV-2 molecular testing infrastructure*

Oligotype	Oligo name	Sequence, 5′ → 3′	Final concentration, nM
Primers	NVAR fwd	TCA ACT GAA AAG GCC ATC TAT (2'OMe-G)A	400
	NVAR rev	GAG TAT AGA GCA CTA TTT CTA AAT CC(2'OMe-C) A	400
	MPOX fwd	ACG TGT TAA ACA ATG GGT GA(2'OMe-U) G	400
	MPOX rev	AAC ATT TCC ATG AAT CGT AGT (2'OMe-C)C	400
Probes	NVAR P-YAK	YakYellow-CCA TGC AAT (BHQ1)ATA CGT ACA AGA TAG TAG CCA AC-BHQ1	75
	MPOX P-FAM	FAM-TGA ATG AAT (BHQ1)GCG ATA CTG TAT GTG TGG G-BHQ1	75

*Sequences are derived from previously published NVAR assay by Li et al. (*9*) and MPXV assay by Shchelkunov et al. (*10*) and adapted for the cobas omni Utility Channel (Roche Diagnostics, https://diagnostics.roche.com). Oligos were custom made by Ella Biotech GmbH (https://www.ellabiotech.com). Indicated final concentration refers to the final oligo concentrations within the reaction mix. 2′O-methyl-RNA bases are indicated as OMe-X. Internal abasic quenchers are indicated as (BHQ1). NVAR, nonvariola orthopoxvirus; MPXV, monkeypox virus.

internal control assay is preloaded in the open channel reagent for use with cobas omni Utility Channel (Roche Diagnostics) (Table 2). We modified and optimized all assays for use on cobas 5800, 6800, and 8800 systems, including 2'O-methyl-RNA-modified primers and internal quenchers for TaqMan probes, as previously described (*11*).

In Silico Evaluation

As part of a support request for Utility Channel applications, we submitted all sequences of the duplex assay to Roche Diagnostics for evaluation of inclusivity and potential primer-probe interactions. The submitted sequences were aligned to currently available MPXV and orthopoxvirus sequences available in public databases.

Analytical Performance Evaluation

We conducted technical performance evaluations for the assays according to new European Union regulations (Regulation 2017/746 EU IVDR, https://euivdr.com). For reference material, we used inactivated cell culture supernatant containing MPXV recovered from a clinical case in central Africa in 1987 (*12*) and inactivated modified vaccinia virus Ankara (MVA) SARS-CoV-2 vaccine. To obtain a quantitative MPXV standard, we purified nucleic acids by using a MagNA-pure96 extractor and Viral NA Small Volume Kit (Roche Diagnostics) and analyzed on a QIAcuity digital PCR instrument (QIAGEN, https://www.qiagen.com) in conjunction with 3 different previously described quantitative PCRs (qPCRs): 1 for nonvariola (NVAR) orthopoxviruses (*9*); 1 for MPXV (*10*); and the research-use only (RUO) LightMix Modular Orthopoxvirus Assay (TIB MOLBIOL, https://www.tib-molbiol.de).

We determined the lower limit of detection by serial 2-fold dilution of MPXV standard in universal transport medium from 100 to 0.78 copies/mL and 21 repeats per dilution step. Using MedCalc statistical software (https://www.medcalc.org), we determined the limit for 95% probability of detection. We assessed linearity by 10-fold serial dilution of MPXV standard (5 repeats per dilution step) at concentrations of $\approx 10^1$–10^7 copies/mL. We determined linearity and intra-assay variability by using Validation Manager software (Finbiosoft, https://finbiosoft.com). Concentrations represent copies per mL of specimen. For empirical inclusivity and exclusivity testing, we used the assay to test a set of 53 samples, including clinical samples, reference material, and external quality controls from a range of bloodborne and respiratory pathogens (Appendix Table 1, https://wwwnc.cdc.gov/EID/article/28/9/22-0917-App1.pdf). We used an experimental MVA vector-based SARS-CoV-2 vaccine as reference material for a non-MPXV orthopoxvirus.

Clinical Evaluation and Follow-Up Samples

For clinical validation, we used the RUO LightMix Modular Orthopoxvirus assay as reference test,

Table 2. Software settings for run protocol for a dual-target MPXV assay rapidly adapted from established high-throughput molecular testing infrastructure*

Protocol setting	Channel setting, use				
	1, Not used	2, Monkeypox	3, Nonvariola	4, Not used	5, Internal control
Relative fluorescence increase	NA	2	2	NA	2
PCR cycling conditions	UNG incubation	Pre-PCR step	1st measurement	2nd measurement	Cooling
No. cycles	Predefined	1	5	45	Predefined
No. steps	Predefined	3	2	2	Predefined
Temperature	Predefined	55°C; 60°C; 65°C	95°C; 55°C	91°C; 58°C	Predefined
Hold time	Predefined	120 s; 360 s; 240 s	5 s; 30 s	5 s; 25 s	Predefined
Data acquisition	Predefined	None	End of each cycle	End of each cycle	Predefined

*Protocol was run on 400 µL swab samples. Protocol adapted for cobas omni Utility Channel (Roche Diagnostics, https://diagnostics.roche.com). Relative fluorescence increase thresholds were used for automated result calls. NA, not applicable; UNG, uracyl-N-glycosylase.

which we performed according to manufacturer's recommendation by using the MagNA-pure96 system with 200-µL extraction volume. In total, we tested 67 clinical samples consisting of respiratory, skin, and genital swab samples with both assays. Of those samples, 11 were positive for MPXV DNA, which we obtained from 2 confirmed clinical cases in Hamburg, Germany. We analyzed 33 consecutive clinical samples from the same 2 patients and 2 additional cases by using the duplex assay (Appendix Table 2). The clinic provided globalized patient characteristics.

Results

In Silico Analysis

We did not detect any concerning oligo interactions (Appendix Figure 1). Target-1: NVAR was still a 100% match for all but 1 MPXV sequence, which had 1 low-risk mismatch. NVAR also had high sequence similarity with many other orthopoxviruses but might not be optimal for reliable detection of camelpox or cowpox (Appendix Figure 2). Target-2: MPOX is a perfect match for almost all Congo Basin strain MPXV sequences but has a known mismatch for West Africa strain sequences in the probe region. This mismatch is expected to slightly reduce relative fluorescence increase signals, as demonstrated in the clinical sample set. Other orthopoxviruses have extensive sequence mismatches with this assay and are not expected to produce detectable signals (Appendix Figure 3).

Analytical performance

We determined LoD was 9.697 (95% CI 7.424–15.327) copies/mL for the NVAR assay and 6.359 (95% CI 4.908–10.110) copies/mL for the MPOX assay by probability of detection analysis. Overall LoD for both targets combined was 4.795 (95% CI 3.598–8.633) copies/mL. We compiled hit rates (Table 3) and probability of detection plots (Appendix Figure 4) for the assay. The assay showed excellent linearity. Cycle threshold (Ct) values were 37–18, ≈10^1–10^7 copies/mL, and pooled SD and 95% CI were within linear range: Ct 0.194, SD 0.0662% for NVAR; Ct 0.175, SD 0.618% for MPXV (Figure 1).

No false positives occurred within the inclusivity-exclusivity set. The MVA vector vaccine was correctly detected by the NVAR assay, and not by the MPXV assay (Appendix Table 1).

Clinical Evaluation

In total, we tested 67 clinical samples, consisting of respiratory, skin, and genital swab samples, with both assays. Of those, 11 samples obtained from 2 confirmed clinical monkeypox case-patients in Hamburg, Germany, were positive for MPXV DNA. We noted 100% positive (11/11) and 100% negative agreement (56/56) for the 2 assays (Figure 2).

Table 3. Hit rates during limit of detection studies of dual-target MPXV assay rapidly adapted from established high-throughput molecular testing infrastructure*

Concentration, copies/mL	NVAR	MPXV	Overall
100	21/21	21/21	21/21
50	21/21	21/21	21/21
25	21/21	21/21	21/21
12.5	20/21	21/21	21/21
6.25	19/21	20/21	21/21
3.125	11/21	13/21	15/21
1.56	11/21	11/21	17/21
0.78	3/21	6/21	7/21

*Results represent no. positive/no. tested. Limits of detection were determined by serial dilution of a quantified MPXV standard (quantified by digital PCR) as a reference. Concentrations represent copies/mL of specimen. Dilution series were generated automatically using a STARlet Liquid Handler (Hamilton, https://www.hamiltoncompany.com). We calculated 95% probability of detection by using MedCalc statistical software (https://www.medcalc.org). MPXV, monkeypox virus; NVAR, nonvariola orthopoxvirus.

Results from Different Sample Types and Timepoints

Another 33 clinical samples were longitudinally collected from 4 patients, all of whom were male, 20–40 years of age, and had 6–50 skin lesions; 1 patient had known HIV infection under treatment. Lesion swabs generated Ct values of 13.3–16.1, oropharyngeal swabs Ct values of 13.1–33.3, and blood samples Ct values of 30.3–38.4. A small sample set of urine had only low concentrations of viral DNA, Ct 31.1–37.8. A single patient provided seminal fluid, which had Ct values of 32.9 for the NVAR assay and 33.9 for the MPXV assay when diluted in guanidine hydrochloride solution (Appendix Table 2).

Discussion

The trajectory of the ongoing MPXV outbreak in Europe and North America has many uncertainties. However, the World Health Organization acknowledges that known clusters represent a change in transmission pattern and emphasizes the need to limit further spread (*1*). Broad availability of molecular testing with short turnaround times is a crucial prerequisite for reducing monkeypox spread.

We adapted 2 established nonvariola orthopoxvirus and MPXV qPCR assays (*9*,*10*) as a duplex test for the cobas 5800, 6800, and 8800 fully automated sample-to-result platforms, which are widely used for high-throughput SARS-CoV-2 diagnostic testing (*13*). Both assays have been validated extensively against other orthopoxvirus species in previous studies (*9*,*10*) and remain inclusive and highly

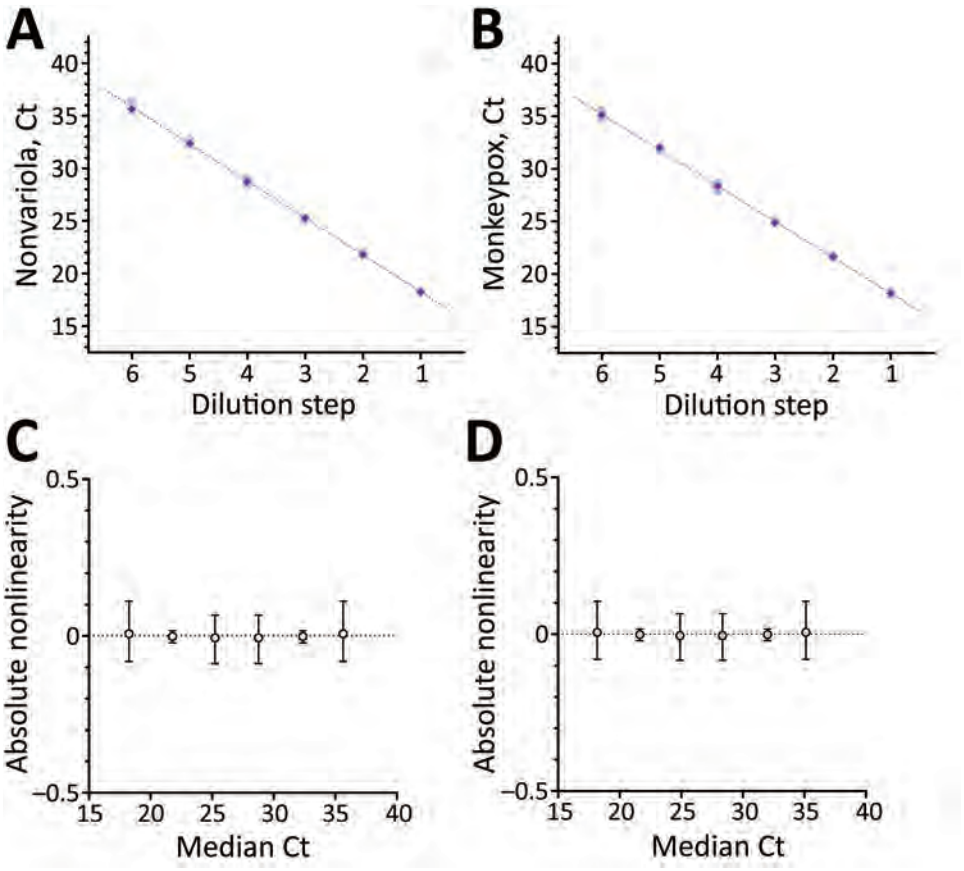

Figure 1. Linearity data for the dual-target monkeypox virus assay rapidly adapted from established high-throughput molecular testing infrastructure. A) Nonvariola orthopoxvirus target; B) monkeypox virus target; C) absolute Ct for nonvariola orthopox virus target; D) absolute Ct for monkeypox virus target. Linearity was determined by serial dilution of monkeypox virus reference material from cell culture supernatant of Congo Basin monkeypox strain collected in 1987. Analysis was performed on Validation Manager software (Finbiosoft, https://finbiosoft.com). Nonvariola orthopoxvirus slope was −3.52, $r^2 = 0.999$; monkeypox virus slope was −3.40, $r^2 = 0.999$. Ct, cycle threshold.

specific for in silico analysis with currently available monkeypox sequences. We demonstrated excellent analytical performance of the duplex assay, showing single-digit detection limits and near-perfect PCR efficiency. A spike-in full-process control assay, similar to commercial in vitro diagnostic assays, already is included in the open channel reagents we used.

Our institution confirmed 4 clinical cases of monkeypox, and we used the initial clinical samples as our clinical positive set. Although the assay was only validated on swab samples, we also detected MPXV DNA in EDTA plasma, urine, and seminal fluid diluted in guanidine hydrochloride solution without any method adaptations. Among all tested clinical samples positive for MPXV DNA, swabs of skin

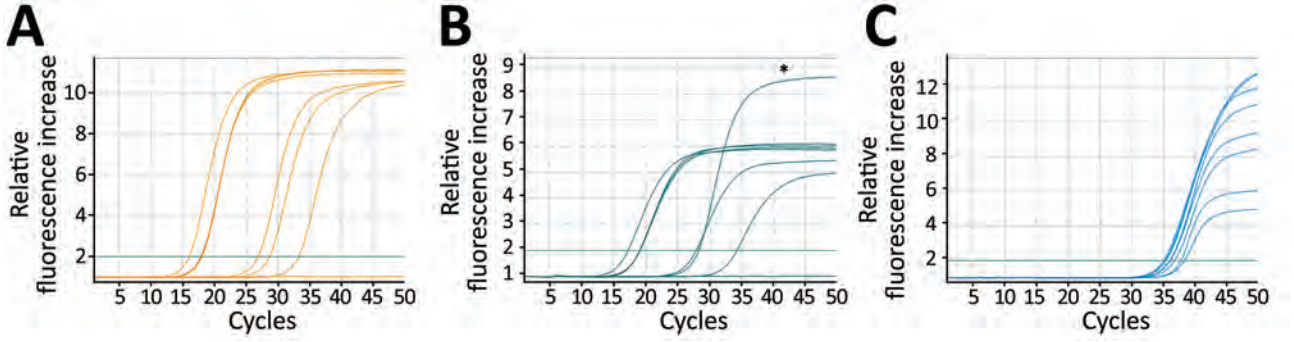

Figure 2. Amplification curves of clinical samples, including internal controls for dual-target monkeypox virus assay rapidly adapted from established high-throughput molecular testing infrastructure. A) Nonvariola orthopoxvirus; B) monkeypox virus; C) internal control. Samples included clinical swab specimens of monkeypox lesions, oropharyngeal swab samples, and EDTA plasma from patients with confirmed monkeypox, Hamburg, Germany. Asterisk (*) in panel B indicates the positive control curve in channel 2, which was the cell culture supernatant of Congo Basin monkeypox strain collected in 1987. West Africa strain samples exhibit a reduction of approximately one third in relative fluorescence increase for monkeypox virus, due to a known mismatch in the probe region (Appendix Figure 1, https://wwwnc.cdc.gov/EID/article/28/9/22-0917-App1.pdf).

lesions consistently yielded early Ct values in the low- to mid-teens, indicating exceedingly high viral DNA loads, which might be a concern for both personnel safety and contamination risks. Viral DNA was readily detectable in oropharyngeal swab samples, as previously reported (*2*,*14*). Likewise, EDTA plasma samples were consistently positive but had later Ct values, mostly around 30. Further studies could evaluate the practical usefulness of plasma or urine for monkeypox diagnostic purposes or longitudinal viral load monitoring. Our data regarding MPXV DNA in different clinical specimen types are well in line with other published studies (*2*,*14*); overall, skin lesion swab samples appeared to be best suited for diagnostic purposes based on our sample set.

In conclusion, we provided technical performance evaluation for a laboratory-developed duplex qPCR assay for MPXV detection for use on the cobas 5800, 6800, and 8800 high-throughput systems. The assay we describe enables laboratories to adapt existing automated SARS-CoV-2 molecular testing infrastructure for a potential large-scale monkeypox outbreak.

M.L. and D.N. received speaker honoraria and related travel expenses from Roche Diagnostics.

M.L., S.P., and D.N. conceptualized and supervised the study. H.T.T., D.N., and P.E. performed the experiments. K.G. performed data analysis. D.N., M.L., S.P., N.F., S.S., M.M.A. and M.A. wrote and edited the manuscript. All authors agreed to the publication of the final manuscript.

About the Author

Dr. Nörz is a fellow in the institute of Medical Microbiology, Virology and Hygiene at University Medical Center Hamburg-Eppendorf, Hamburg, Germany. His research interests include molecular diagnostics for infectious diseases and quantitative PCR assay design.

References

1. World Health Organization. Disease outbreak news: multi-country monkeypox outbreak in non-endemic countries 29 May 2022 [cited 2022 Jun 7]. https://www.who.int/emergencies/disease-outbreak-news/item/2022-DON388
2. Antinori A, Mazzotta V, Vita S, Carletti F, Tacconi D, Lapini LE, et al.; INMI Monkeypox Group. Epidemiological, clinical and virological characteristics of four cases of monkeypox support transmission through sexual contact, Italy, May 2022. Euro Surveill. 2022;27:2200421. https://doi.org/10.2807/1560-7917.ES.2022.27.22.2200421
3. Vivancos R, Anderson C, Blomquist P, Balasegaram S, Bell A, Bishop L, et al.; Monkeypox Incident Management Team. Community transmission of monkeypox in the United Kingdom, April to May 2022. Euro Surveill. 2022;27:2200422. https://doi.org/10.2807/1560-7917.ES.2022.27.22.2200422
4. Perez Duque M, Ribeiro S, Martins JV, Casaca P, Leite PP, Tavares M, et al. Ongoing monkeypox virus outbreak, Portugal, 29 April to 23 May 2022. Euro Surveill. 2022;27:2200424. https://doi.org/10.2807/1560-7917.ES.2022.27.22.2200424
5. Bunge EM, Hoet B, Chen L, Lienert F, Weidenthaler H, Baer LR, et al. The changing epidemiology of human monkeypox-A potential threat? A systematic review. PLoS Negl Trop Dis. 2022;16:e0010141. https://doi.org/10.1371/journal.pntd.0010141
6. Reed KD, Melski JW, Graham MB, Regnery RL, Sotir MJ, Wegner MV, et al. The detection of monkeypox in humans in the Western Hemisphere. N Engl J Med. 2004;350:342–50. https://doi.org/10.1056/NEJMoa032299
7. Adalja A, Inglesby T. A novel international monkeypox outbreak. Ann Intern Med. 2022 May 24 [Epub ahead of print]. https://doi.org/10.7326/M22-1581
8. Corman VM, Landt O, Kaiser M, Molenkamp R, Meijer A, Chu DK, et al. Detection of 2019 novel coronavirus (2019-nCoV) by real-time RT-PCR. Euro Surveill. 2020; 25:25. https://doi.org/10.2807/1560-7917.ES.2020.25.3.2000045
9. Li Y, Olson VA, Laue T, Laker MT, Damon IK. Detection of monkeypox virus with real-time PCR assays. J Clin Virol. 2006;36:194–203. https://doi.org/10.1016/j.jcv.2006.03.012
10. Shchelkunov SN, Shcherbakov DN, Maksyutov RA, Gavrilova EV. Species-specific identification of variola, monkeypox, cowpox, and vaccinia viruses by multiplex real-time PCR assay. J Virol Methods. 2011;175:163–9. https://doi.org/10.1016/j.jviromet.2011.05.002
11. Pfefferle S, Reucher S, Nörz D, Lütgehetmann M. Evaluation of a quantitative RT-PCR assay for the detection of the emerging coronavirus SARS-CoV-2 using a high throughput system. Euro Surveill. 2020;25:2000152. https://doi.org/10.2807/1560-7917.ES.2020.25.9.2000152
12. Müller G, Meyer A, Gras F, Emmerich P, Kolakowski T, Esposito JJ. Monkeypox virus in liver and spleen of child in Gabon. Lancet. 1988;1:769–70. https://doi.org/10.1016/S0140-6736(88)91580-2
13. Poljak M, Korva M, Knap Gašper N, Fujs Komloš K, Sagadin M, Uršič T, et al. Clinical evaluation of the cobas SARS-CoV-2 test and a diagnostic platform switch during 48 hours in the midst of the COVID-19 pandemic. J Clin Microbiol. 2020;58:e00599-20. https://doi.org/10.1128/JCM.00599-20
14. Adler H, Gould S, Hine P, Snell LB, Wong W, Houlihan CF, et al.; NHS England High Consequence Infectious Diseases (Airborne) Network. Clinical features and management of human monkeypox: a retrospective observational study in the UK. Lancet Infect Dis. 2022 May 24 [Epub ahead of print]. https://doi.org/10.1016/S1473-3099(22)00228-6

Address for correspondence: Marc Lütgehetmann, Institute of Medical Microbiology, Virology and Hygiene, Martinistraße 52, D-20246 Hamburg, Germany; email: mluetgeh@uke.de

Tracking Emergence and Spread of SARS-CoV-2 Omicron Variant in Large and Small Communities by Wastewater Monitoring in Alberta, Canada

Casey R.J. Hubert, Nicole Acosta, Barbara J.M. Waddell, Maria E. Hasing, Yuanyuan Qiu, Meghan Fuzzen, Nathanael B.J. Harper, María A. Bautista, Tiejun Gao, Chloe Papparis, Jenn Van Doorn, Kristine Du, Kevin Xiang, Leslie Chan, Laura Vivas, Puja Pradhan, Janine McCalder, Kashtin Low, Whitney E. England, Darina Kuzma, John Conly, M. Cathryn Ryan, Gopal Achari, Jia Hu, Jason L. Cabaj, Chris Sikora, Larry Svenson, Nathan Zelyas, Mark Servos, Jon Meddings, Steve E. Hrudey, Kevin Frankowski, Michael D. Parkins, Xiaoli (Lilly) Pang, Bonita E. Lee

Wastewater monitoring of SARS-CoV-2 enables early detection and monitoring of the COVID-19 disease burden in communities and can track specific variants of concern. We determined proportions of the Omicron and Delta variants across 30 municipalities covering >75% of the province of Alberta (population 4.5 million), Canada, during November 2021–January 2022. Larger cities Calgary and Edmonton exhibited more rapid emergence of Omicron than did smaller and more remote municipalities. Notable exceptions were Banff, a small international resort town, and Fort McMurray, a medium-sized northern community that has many workers who fly in and out regularly. The integrated wastewater signal revealed that the Omicron variant represented close to 100% of SARS-CoV-2 burden by late December, before the peak in newly diagnosed clinical cases throughout Alberta in mid-January. These findings demonstrate that wastewater monitoring offers early and reliable population-level results for establishing the extent and spread of SARS-CoV-2 variants.

The COVID-19 pandemic has led to rapid scientific progress in wastewater-based surveillance of community infections. Measuring levels of RNA from SARS-CoV-2 in sewage samples began to be used as a complementary surveillance tool early in the pandemic, resulting in hundreds of wastewater COVID-19 monitoring groups and online dashboards around the world, including in Alberta (https://covid-tracker.chi-csm.ca), a jurisdiction of 4.5 million persons in western Canada. This strategy is premised on the fecal shedding of SARS-CoV-2 by infected persons (*1*,*2*) and modifies quantitative reverse transcription PCR (qRT-PCR) workflows used for diagnosing patients to quantify viral RNA in sewage sampled at wastewater treatment plants or other nodes within the sewer network (*3*–*5*) at regular intervals. Teams in Alberta and elsewhere demonstrated during pandemic waves that wastewater is a leading indicator of COVID-19; results typically precede clinically diagnosed cases by 4–6 days (*6*–*9*). Sampling, testing, and rapidly reporting wastewater virus RNA levels provides early warning of the populationwide disease burden to policy makers, health officials, and the public, enabling evidence-based decision making for preparedness and disease control.

Author affiliations: University of Calgary, Calgary, Alberta, Canada (C.R.J. Hubert, N. Acosta, B.J.M. Waddell, M.A. Bautista, C. Papparis, J. Van Doorn, K. Du, K. Xiang, L. Chan, L. Vivas, P. Pradhan, J. McCalder, K. Low, W.E. England, D. Kuzma, J. Conly, M.C. Ryan, G. Achari, J. Hu, J.L. Cabaj, J. Meddings, K. Frankowski, M.D. Parkins); University of Alberta, Edmonton, Alberta, Canada (M.E. Hasing, Y. Qiu, T. Gao, C. Sikora, N. Zelyas, S.E. Hrudey, X.[L.] Pang, B.E. Lee); Alberta Health Services, Edmonton (Y. Qiu, C. Sikora, N. Zelyas, X.[L.] Pang); Alberta Health Services, Calgary (J. Conly, J.L. Cabaj, M.D. Parkins); University of Waterloo, Waterloo, Ontario, Canada (M. Fuzzen, N.B.J. Harper, M. Servos); Alberta Health, Government of Alberta, Edmonton (L. Svenson)

DOI: https://doi.org/10.3201/eid2809.220476

On November 24, 2021, South Africa first reported the emergence of a novel SARS-CoV-2 variant associated with rapid community transmission in the Gauteng province (*10*). By November 26, the World Health Organization had labeled Omicron as a new variant of concern (VOC). Omicron was subsequently rapidly identified in countries around the world, including in Canada, where cases were detected in inbound international travelers. The first case of Omicron from clinical specimen testing in Alberta was confirmed on November 30. By December and into January 2022, the virus had spread rapidly throughout large and smaller communities, prompting reintroduction of public health restrictions (*11*,*12*).

Wastewater testing can differentiate changes in disease burden caused by different VOCs in communities (*13*). As soon as viral genomes of VOCs become available within the international scientific community (e.g., by GISAID, https://www.gisaid.org) (*14*), variant-specific PCR primers and probes can be developed and deployed on regularly collected wastewater samples to learn more about the dynamics of community disease burden caused by VOCs (*15*). Although sequencing viral genomes from wastewater is technically feasible, either through targeted amplicon tiling protocols (*16*,*17*) or shotgun metagenomics (*18*,*19*), a rapid and cost-effective alternative is targeted qRT-PCR screening of RNA extracted from wastewater to provide accurate data on VOCs in near-real time (*20*).

For COVID-19 monitoring in Alberta, wastewater has been sampled, processed, and analyzed in university laboratories in Calgary and Edmonton and the results reported to health officials and online to the public, typically 2 days after sample collection. In this study, we used variant-specific PCR assays to assess the emergence and temporal change in prevalence of the Omicron and Delta variants in Alberta by monitoring wastewater in 30 municipalities, ranging from small towns (population <10,000) to large cities (population >1 million), up to 3 times per week. This approach covered >75% of Alberta's population of 4.5 million and demonstrated changes in COVID-19 burden associated with emergence of the new Omicron variant from late November 2021 through mid-January 2022.

Methods

Wastewater was collected from municipal treatment plants across the province as 24-hour composite samples up to 3 times per week. We isolated RNA from wastewater by using either ultrafiltration followed by RNA extraction (*5*), which was used to process 233 samples, or affinity binding columns that purify nucleic acids directly (*21*), used to process 209 samples (Figure 1). We applied the same method consistently at a given sampling site throughout the entire study period. We processed wastewater samples from 3 geographically disparate treatment plants in Calgary, Fort McMurray, and Lethbridge, comprising 11% of all samples in the study, by using both methods for comparison and revealed no significant difference (Mann-Whitney test: $p = 0.46$ [Calgary], $p = 0.39$ [Fort McMurray], and $p = 0.59$ [Lethbridge]) (Appendix Figure 1, https://wwwnc.cdc.gov/EID/article/28/9/22-0476-App1.pdf).

RNA quantification by qRT-PCR incorporated a newly designed set of assays that selectively amplify the BA.1 Omicron variant or the B.1.617.2 Delta variant by targeting mutations R203K/G204R and R203M in the N200 region of the nucleocapsid gene (M. Fuzzen et al., unpub. data, https://www.medrxiv.org/content/10.1101/2022.04.12.2227376 1v1). The R203K/G204R mutation in the BA.1 Omicron variant is also present in the B.1.1.7 Alpha variant. Clinical screening of cases indicated that the Alpha variant was no longer detected in Alberta as of July 2021 (*22*). We confirmed this finding by screening the wastewater samples from this study by using a separate assay that targets a D3L mutation in the nucleocapsid gene of the Alpha variant (*23*). We quantified total SARS-CoV-2 levels separately with widely used universal assays targeting the N1 and N2 regions of the nucleocapsid gene in the wild-type virus (*3*,*4*) and all other VOCs identified to date. We triplexed N200 assays for Omicron, Delta, and total SARS-CoV-2 together so we could estimate an Omicron-to-Delta ratio in each wastewater sample using the Omicron signal (R203K-G204R assay) and the Delta signal (R203M assay) (M. Fuzzen et al., unpub. data). This technique enabled us to track the emergence and prevalence of Omicron at the population level throughout the province.

Wastewater sampling and sample processing followed by identifying and quantifying SARS-CoV-2 is intrinsically more complicated than conducting the same PCR strategy on clinical samples (i.e., nasopharyngeal swabs). Directly comparing results between different treatment plants is not normally recommended because of intrinsic heterogeneities (e.g., physiochemical differences manifesting different PCR inhibition potential; different proportions of urban, industrial, and agricultural inputs to urban wastewater; different flow rates and distances affecting signal degradation) (*24*). Other factors, such as population movement between sewershed catchments, can also influence results. These limitations apply to total SARS-CoV-2 quantification

and have led to evaluating different population normalization markers in wastewater sample analysis (*25*,*26*). However, the approach presented in this study for determining Omicron-to-Delta ratios within the same multiplex qRT-PCR reaction overcomes these issues, because RNA genomes derived from either variant are expected to react similarly to these factors. In this regard, we confirmed that subsets of samples with 100% Omicron showed good correlation between the R203K-G204R (Omicron) and N1 (total SARS-CoV-2) qRT-PCRs (Appendix Figure 1). We collected daily numbers of new cases of COVID-19 clinically diagnosed across the province by positive PCR test from the Data Analytics branch of Alberta Health Services and reported them using a 7-day rolling average (Figure 1).

Results

Omicron variant SARS-CoV-2 was first detected in Alberta community wastewater during late November and early December (corresponding to the displacement of the Delta variant) (Figure 1; Appendix Table). In Calgary, 4 consecutive samples collected during December 5–9 revealed the sustained presence of 3%–9% Omicron (compared with >90% Delta) among infected persons contributing to the sewershed in this cosmopolitan city of 1.3 million. Omicron was first detected in wastewater in the capital city of Edmonton (population 1.1 million) on December 10 (15% Omicron, 85% Delta). The rate of increase of Omicron in the international resort town of Banff was higher than in larger cities such as Calgary and Edmonton (Figure 1, panel A), and Omicron surpassed 80% in samples taken 3 times a week during December 20–23 (Appendix Table). By that time, Calgary and Edmonton had just passed 50% Omicron, and the proportion of Omicron infections was growing in smaller bedroom communities adjacent to these 2 large urban centers (e.g., Okotoks, High River, Strathmore, and especially Airdrie, which are all <70 km from Calgary) (Figure 1; Appendix Figure 2). Communities that experienced the

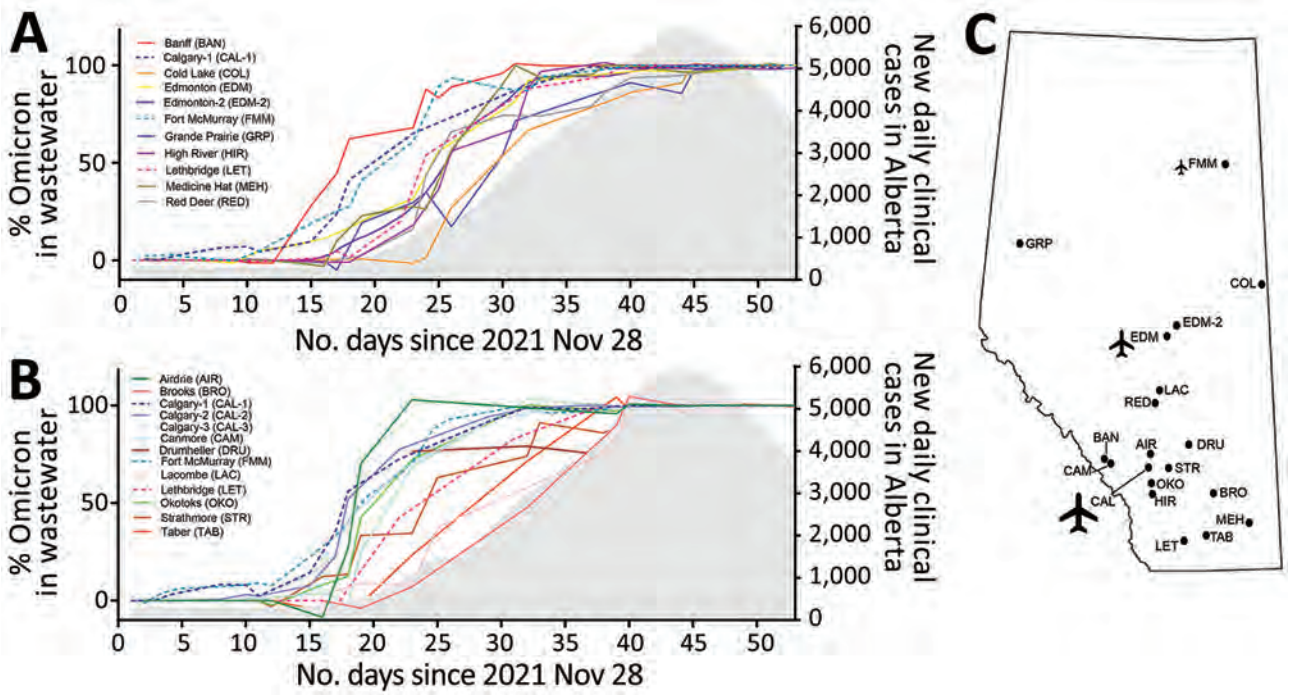

Figure 1. Spread of SARS-CoV-2 Omicron variant in community wastewater samples, Alberta, Canada, November 2021–January 2022. A, B) Percentage of Omicron RNA detected in community wastewater samples (data lines) compared with the 7-day rolling average of new clinical cases reported in Alberta (gray shading). RNA was assessed by using quantitative reverse transcription PCR assays for specific variants following sample processing using ultrafiltration (A) or affinity columns (B). Lines of best fit plotted with second order smoothing are shown for different wastewater treatment plants, including 3 that had samples processed using both ultrafiltration and affinity columns for comparison (Calgary-1, Fort McMurray, and Lethbridge; for details of this comparison, see Appendix Figure 1 [https://wwwnc.cdc.gov/EID/article/28/9/22-0476-App1.pdf]). Monitoring began on November 28, 2021, and lasted for 53 days (plotted as consecutive days on the x-axes). The 7-day rolling average of new cases increased after the Omicron variant was predominant in municipal wastewater from 30 communities sampled. C) Locations of 21 treatment plants (Appendix Table) serving communities throughout the province. Abbreviations are as shown in panels A and B. Calgary and Edmonton are served by 3 and 2 treatment plants, respectively, and some individual treatment plants also serve multiple municipalities (e.g., Edmonton-2 serves >10 others; Red Deer serves 3 others; Calgary's treatment plants serve 3 others).

most delayed emergence of Omicron were smaller and more remote; Brooks (population 14,451, 190 km from Calgary) and Taber (population 19,070, 263 km from Calgary) did not reach high proportions of Omicron until late December (Appendix Table).

The general trend demonstrated by this analysis of objective wastewater evidence is that large cities experienced the emergence of a newly introduced virus before smaller centers farther away from cities, but with notable exceptions. Banff, located 127 kilometers west of Calgary, experienced a more rapid onset of Omicron infection than anywhere else in the province despite its resident population (13,427 persons) being <1% of the Calgary population and the smallest among monitored communities (Appendix Figure 2, panel B). Banff is an international resort community in Banff National Park, Canada's busiest national park, which attracts >4 million visitors annually from around the world (*27*). Early detection of Omicron in Banff might correspond to attracting tourists at the onset of the ski season in November and December. Of note, the nearby and slightly larger mountain town of Canmore (population 27,664), located 105 kilometers west of Calgary (22 km east of Banff and outside the national park), experienced a much later emergence of Omicron infections. This delay is likely related to Canmore hosting fewer international tourists than Banff and featuring less high-density dormitory-style housing, where much of the worker population supporting Banff's tourism industry resides.

More remote communities located a greater distance away from Alberta's large international airports exhibited later emergence of the Omicron variant (Figure 1; Appendix Figure 2). The Calgary International Airport serves 16 million travelers per year with direct flights arriving from 15 countries (*28*), compared with 8 million travelers and 6 countries for Edmonton International Airport (*29*). Plotting Omicron dynamics in Alberta municipalities as a function of distance from Calgary (Appendix Figure 2, panel C) suggests a link to international travel whereby incoming travelers introduce a new virus into a large densely populated urban center, enabling its spread. International travel in and out of Alberta increased sharply in November and December; 22,700 passengers came through Alberta in November and 28,800 in December, compared with only 8,400 travelers during the first 10 months of 2021 combined (*30*).

Fort McMurray offers an interesting example in relation to domestic air travel. Despite being a remote, relatively small (population 79,205) northern community farther from Calgary than any other municipality sampled in this study, Fort McMurray exhibited an Omicron emergence comparable to the rapid onset in Calgary. Fort McMurray has one of the busiest airports in Canada to accommodate shift workers commuting from across the country to work in the oil sands industry (*31*). This high level of contact with other parts of Canada is likely to result in rapid introduction of an emerging virus such as the Omicron variant. Workers traveling to Fort McMurray from other provinces or from major urban centers in Alberta likely contributed to accelerated Omicron emergence relative to other smaller or remotely situated Alberta municipalities.

The rapid emergence of Omicron in Calgary, Edmonton, Banff, and Fort McMurray is especially evident when this variant comprised lower proportions of the SARS-CoV-2 community burden. The time required for these 4 communities to surpass 10% Omicron was on average ($\pm$ SEM) 10.9 $\pm$ 2.0 days faster than the other communities, highlighting the significantly earlier emergence of Omicron in these locations ($p<0.0001$ by unpaired t-test) (Figure 2, panel A). These significant differences are maintained by using Omicron cut-offs of 50% (6.3 $\pm$ 2.7 days faster; $p = 0.0331$), and the trend is similar at 90% (5.0 $\pm$ 2.6 days faster; $p = 0.0686$) (Figure 2, panels B and C). Later emergence of Omicron infections in the less populated outlying communities of Taber, Cold Lake, Lacombe, and Brooks is clearly evident using the 50% cutoff (Figure 2, panel B). In these 4 locations, Omicron surpassed Delta on average 9.8 $\pm$ 1.8 days later than the other communities, highlighting the significantly slower emergence of infection in these smaller, more remote settings ($p<0.0001$). Some evidence suggests lower adherence to COVID-19 public health interventions in rural settings than in urban settings, including in Alberta (*32*,*33*), but less densely populated remote areas can experience slower spread of SARS-CoV-2 (*34*,*35*) because of less frequent interaction events, which could potentially contribute to the patterns we report in this study.

Discussion

Wastewater results demonstrate that the emergence of Omicron was the driver of clinical cases increasing in December and January during Alberta's fifth wave (Figure 1, panels A, B). During this time, COVID-19 public health surveillance shifted to much more focused PCR testing that prioritized essential workers, patients at risk for severe illness and eligible for early treatment, and patients in emergency departments with more serious illness (*36*). This shift resulted in PCR testing dramatically underestimating total disease burden in the population relative to earlier waves. Reported clinical cases still show a steep increase after the emergence and propagation of Omicron revealed

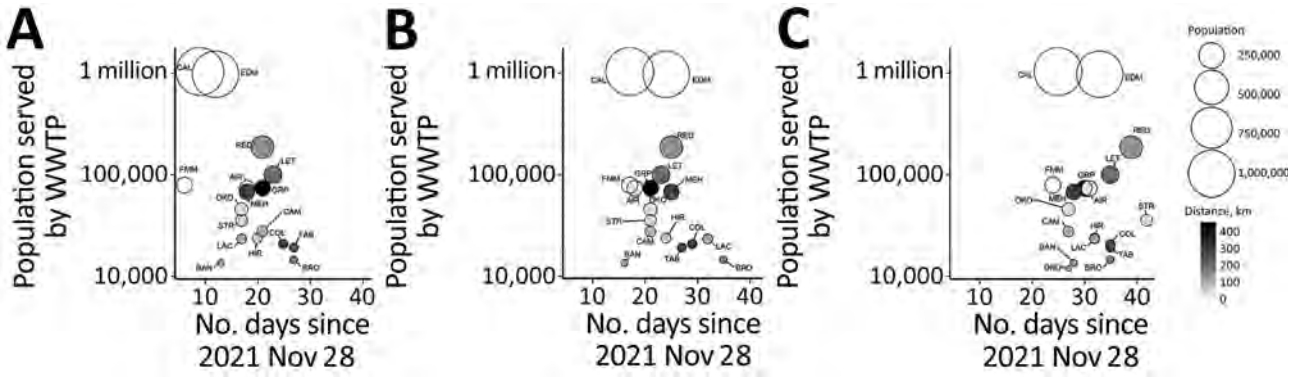

Figure 2. Number of days required for the SARS-CoV-2 Omicron-to-Delta variant ratio to pass thresholds of 10% (A), 50% (B), and 90% (C) of community COVID-19 burden, Alberta, Canada, November 2021–January 2022. General trends of Omicron emergence are shown as a function of decreasing population size and distance from the nearest airport in Calgary, Edmonton, or Fort McMurray. Bubble plots only include data from Calgary-1 and Edmonton-1 wastewater treatment plants (the largest plant from each city), scaled to the population of the corresponding sewershed subcatchment in those cities. AIR, Airdrie; BAN, Banff; BRO, Brooks; CAL, Calgary; CAM, Canmore; COL, Cold Lake; DRU, Drumheller; EDM, Edmonton; FMM, Fort McMurray; GRP, Grande Prairie; HIR, High River; LAC, Lacombe; LET, Lethbridge; MEH, Medicine Hat; OKO, Okotoks; RED, Red Deer; STR, Strathmore; TAB, Taber; WWTP, wastewater treatment plant.

by wastewater testing (Figure 1, panels A, B). These dynamics mirror the shift from Delta to Omicron in Alberta, confirmed clinically by screening subsets of samples using PCR for VOCs and genome sequencing, which revealed levels of Omicron to be >50% by December 16 and >95% by December 28 (*22*). This finding demonstrates that wastewater surveillance reliably provides information vital to public health officials.

VOC information derived from viral genome sequencing of clinical samples in Alberta is nonrandom (which is also the case in many other jurisdictions), placing emphasis on clinical cases of interest (e.g., outbreaks, hospitalizations) or incoming international travelers (*37*). Similarly, clinical PCR testing is susceptible to changes in testing policies, capacity limitations, or persons not getting tested (e.g., by personal choice or when infections are asymptomatic) (*28*). Wastewater testing offers an unbiased representation of disease prevalence, capturing all persons and groups contributing to the sewershed. This comprehensive coverage can be achieved for a tiny fraction of the cost of clinical testing on a per capita basis (*39*). In large cities such as Calgary and Edmonton, which have >1 million residents (Figure 2; Appendix Figure 1), monitoring wastewater for COVID-19 community burden costs only a few cents per person per year (based on testing 3 times per week in Alberta) and can provide objective information about community infection to public health authorities, policy makers, and the public in near-real time. COVID-19 clinical testing strategies and resources are becoming more targeted with jurisdictions such as Alberta turning to self-testing and less frequent public reporting. Wastewater monitoring offers an objective population-based surveillance metric of disease burden that continues to deliver real-time information on COVID-19 and could potentially be adapted for other emerging pathogens.

This article was preprinted at https://www.medrxiv.org/content/10.1101/2022.03.07.22272055v1.

Acknowledgments

We thank Norma Ruecker, Rhonda Clark, Alexander Buchner Beaudet, and Navid Sedaghat for help with sampling and logistics. This work would not have been possible without collaboration from provincial and municipal leaders and WWTP operators in Calgary, Edmonton, Fort McMurray, Grande Prairie, Cold Lake, Edson, Lacombe, Red Deer, Banff, Canmore, Drumheller, Strathmore, Okotoks, High River, Brooks, Medicine Hat, Taber, and Lethbridge.

This work was funded by Alberta Health.

The authors dedicate this work to our colleague and coauthor Larry Svenson, who passed away while the manuscript was under review. Dr. Svenson's career achievements were featured in a 2021 profile in the American Journal of Epidemiology (https://doi.org/10.1093/aje/kwab282).

About the Author

Dr. Hubert is professor of geomicrobiology in the Department of Biological Sciences at the University of Calgary. His primary research interests are molecular microbiology and microbial genomics in complex environmental samples, such as wastewater.

References

1. Cevik M, Tate M, Lloyd O, Maraolo AE, Schafers J, Ho A. SARS-CoV-2, SARS-CoV, and MERS-CoV viral load dynamics, duration of viral shedding, and infectiousness: a systematic review and meta-analysis. Lancet Microbe. 2021; 2:e13–22. https://doi.org/10.1016/S2666-5247(20)30172-5
2. Yuan C, Wang H, Li K, Tang A, Dai Y, Wu B, et al. SARS-CoV-2 viral shedding characteristics and potential evidence for the priority for faecal specimen testing in diagnosis. PLoS One. 2021;16:e0247367. https://doi.org/10.1371/journal.pone.0247367
3. Acosta N, Bautista M, Hollman J, McCalder J, Buchner Beaudet A, Man L, et al. Wastewater monitoring of SARS-CoV-2 from acute care hospitals identifies nosocomial transmission and outbreaks. Water Res. 2021;201:117369. https://doi.org/10.1016/j.watres.2021.117369
4. Acosta N, Bautista MA, Waddell BJ, McCalder J, Beaudet AB, Man L, et al. Longitudinal SARS-CoV-2 RNA wastewater monitoring across a range of scales correlates with total and regional COVID-19 burden in a well-defined urban population. Water Res. 2022;220:118611. https://doi.org/10.1016/j.watres.2022.118611
5. Qiu Y, Yu J, Pabbaraju K, Lee BE, Gao T, Ashbolt NJ, et al. Validating and optimizing the method for molecular detection and quantification of SARS-CoV-2 in wastewater. Sci Total Environ. 2022;812:151434. https://doi.org/10.1016/j.scitotenv.2021.151434
6. D'Aoust PM, Graber TE, Mercier E, Montpetit D, Alexandrov I, Neault N, et al. Catching a resurgence: increase in SARS-CoV-2 viral RNA identified in wastewater 48 h before COVID-19 clinical tests and 96 h before hospitalizations. Sci Total Environ. 2021;770:145319. https://doi.org/10.1016/j.scitotenv.2021.145319
7. Medema G, Heijnen L, Elsinga G, Italiaander R, Brouwer A. Presence of SARS-Coronavirus-2 RNA in sewage and correlation with reported COVID-19 prevalence in the early stage of the epidemic in the Netherlands. Environ Sci Technol Lett. 2020;7:511–6. https://doi.org/10.1021/acs.estlett.0c00357
8. Nemudryi A, Nemudraia A, Wiegand T, Surya K, Buyukyoruk M, Cicha C, et al. Temporal detection and phylogenetic assessment of SARS-CoV-2 in municipal wastewater. Cell Rep Med. 2020;1:100098. https://doi.org/10.1016/j.xcrm.2020.100098
9. Randazzo W, Truchado P, Cuevas-Ferrando E, Simón P, Allende A, Sánchez G. SARS-CoV-2 RNA in wastewater anticipated COVID-19 occurrence in a low prevalence area. Water Res. 2020;181:115942. https://doi.org/10.1016/j.watres.2020.115942
10. World Health Organization. Tracking SARS-CoV-2 variants [cited 2022 Feb 28]. https://www.who.int/en/activities/tracking-SARS-CoV-2-variants
11. Alberta Government. General guidance for COVID-19 and other respiratory infections [cited 2022 Jun 21]. https://open.alberta.ca/publications/general-guidance-for-covid-19-and-other-respiratory-illnesses
12. Sylvester K. Alberta announces new targeted COVID health measures, opens up booster eligibility. 2021 Dec 22 [cited 2022 Jun 21]. https://calgarycitizen.com/article/alberta-covid-omicron
13. Lee WL, Imakaev M, Armas F, McElroy KA, Gu X, Duvallet C, et al. Quantitative SARS-CoV-2 Alpha variant B.1.1.7 tracking in wastewater by allele-specific RT-qPCR. Environ Sci Technol Lett. 2021;8:675–82. https://doi.org/10.1021/acs.estlett.1c00375
14. Elbe S, Buckland-Merrett G. Data, disease and diplomacy: GISAID's innovative contribution to global health. Glob Chall. 2017;1:33–46. https://doi.org/10.1002/gch2.1018
15. Peterson SW, Lidder R, Daigle J, Wonitowy Q, Dueck C, Nagasawa A, et al. RT-qPCR detection of SARS-CoV-2 mutations S 69-70 del, S N501Y and N D3L associated with variants of concern in Canadian wastewater samples. Sci Total Environ. 2022;810:151283. https://doi.org/10.1016/j.scitotenv.2021.151283
16. Rios G, Lacoux C, Leclercq V, Diamant A, Lebrigand K, Lazuka A, et al. Monitoring SARS-CoV-2 variants alternations in Nice neighborhoods by wastewater nanopore sequencing. Lancet Reg Health Eur. 2021;10:100202.
17. Lin X, Glier M, Kuchinski K, Ross-Van Mierlo T, McVea D, Tyson JR, et al. Assessing multiplex tiling PCR sequencing approaches for detecting genomic variants of SARS-CoV-2 in municipal wastewater. mSystems. 2021;6:e0106821. https://doi.org/10.1128/mSystems.01068-21
18. Rothman JA, Loveless TB, Kapcia J III, Adams ED, Steele JA, Zimmer-Faust AG, et al. RNA viromics of southern California wastewater and detection of SARS-CoV-2 single nucleotide variants. Appl Environ Microbiol. 2021;87:e0144821. https://doi.org/10.1128/AEM.01448-21
19. Pérez-Cataluña A, Chiner-Oms Á, Cuevas-Ferrando E, Díaz-Reolid A, Falcó I, Randazzo W, et al. Spatial and temporal distribution of SARS-CoV-2 diversity circulating in wastewater. Water Res. 2022;211:118007. https://doi.org/10.1016/j.watres.2021.118007
20. Safford HR, Shapiro K, Bischel HN. Opinion: wastewater analysis can be a powerful public health tool-if it's done sensibly. Proc Natl Acad Sci U S A. 2022;119:e2119600119. https://doi.org/10.1073/pnas.2119600119
21. Whitney ON, Kennedy LC, Fan VB, Hinkle A, Kantor R, Greenwald H, et al. Sewage, salt, silica, and SARS-CoV-2 (4S): an economical kit-free method for direct capture of SARS-CoV-2 RNA from wastewater. Environ Sci Technol. 2021;55:4880–8. https://doi.org/10.1021/acs.est.0c08129
22. Alberta Health. COVID-19 Alberta statistics [cited 2022 Feb 28]. https://www.alberta.ca/stats/covid-19-alberta-statistics.htm#variants-of-concern
23. Graber TE, Mercier É, Bhatnagar K, Fuzzen M, D'Aoust PM, Hoang HD, et al. Near real-time determination of B.1.1.7 in proportion to total SARS-CoV-2 viral load in wastewater using an allele-specific primer extension PCR strategy. Water Res. 2021;205:117681. https://doi.org/10.1016/j.watres.2021.117681
24. Pecson BM, Darby E, Haas CN, Amha YM, Bartolo M, Danielson R, et al.; SARS-CoV-2 Interlaboratory Consortium. Reproducibility and sensitivity of 36 methods to quantify the SARS-CoV-2 genetic signal in raw wastewater: findings from an interlaboratory methods evaluation in the U.S. Environ Sci (Camb). 2021;7:504–20. https://doi.org/10.1039/D0EW00946F
25. D'Aoust PM, Mercier E, Montpetit D, Jia JJ, Alexandrov I, Neault N, et al. Quantitative analysis of SARS-CoV-2 RNA from wastewater solids in communities with low COVID-19 incidence and prevalence. Water Res. 2021;188:116560. https://doi.org/10.1016/j.watres.2020.116560
26. Feng S, Roguet A, McClary-Gutierrez JS, Newton RJ, Kloczko N, Meiman JG, et al. Evaluation of sampling, analysis, and normalization methods for SARS-CoV-2 concentrations in wastewater to assess COVID burdens in Wisconsin communities. ACS Environmental Science & Technology Water. 2021;1:1955–65. https://doi.org/10.1021/acsestwater.1c00160
27. Town of Banff. Learn about Banff [cited 2022 Feb 28]. https://banff.ca/252/Learn-About-Banff

28. YYC Calgary International Airport [cited 2022 Feb 28]. https://www.yyc.com
29. Edmonton International Airport [cited 2022 Feb 28]. https://flyeia.com
30. Government of Alberta. Alberta tourism market monitor [cited 2022 Apr 29]. https://www.alberta.ca/alberta-tourism-market-monitor.aspx
31. Fort McMurray International Airport. Fort McMurray Airport Authority 2020 annual report [cited 2022 Feb 28]. https://www.flyymm.com/publications
32. Lang R, Benham JL, Atabati O, Hollis A, Tombe T, Shaffer B, et al. Attitudes, behaviours and barriers to public health measures for COVID-19: a survey to inform public health messaging. BMC Public Health. 2021;21:765. https://doi.org/10.1186/s12889-021-10790-0
33. Hudson A, Montelpare WJ. Predictors of vaccine hesitancy: implications for COVID-19 public health messaging. Int J Environ Res Public Health. 2021;18:8054. https://doi.org/10.3390/ijerph18158054
34. Wong DWS, Li Y. Spreading of COVID-19: density matters. PLoS ONE. 2020;15:e0242398.
35. Diao Y, Kodera S, Anzai D, Gomez-Tames J, Rashed EA, Hirata A. Influence of population density, temperature, and absolute humidity on spread and decay durations of COVID-19: a comparative study of scenarios in China, England, Germany, and Japan. One Health. 2020;12:100203. https://doi.org/10.1016/j.onehlt.2020.100203
36. Alberta Health Services. Assessment and testing COVID-19 [cited 2022 Feb 28]. https://www.albertahealthservices.ca/topics/Page17058.aspx
37. Williams GH, Llewelyn A, Brandao R, Chowdhary K, Hardisty KM, Loddo M. SARS-CoV-2 testing and sequencing for international arrivals reveals significant cross border transmission of high risk variants into the United Kingdom. eClinicalMedicine. 2021;38:101021.
38. Green MA, García-Fiñana M, Barr B, Burnside G, Cheyne CP, Hughes D, et al. Evaluating social and spatial inequalities of large scale rapid lateral flow SARS-CoV-2 antigen testing in COVID-19 management: an observational study of Liverpool, UK (November 2020 to January 2021). Lancet Reg Health Eur. 2021;6:100107. https://doi.org/10.1016/j.lanepe.2021.100107
39. World Health Organization. Environmental surveillance for SARS-COV-2 to complement public health surveillance—interim guidance [cited 2022 Apr 29]. https://www.who.int/publications/i/item/WHO-HEP-ECH-WSH-2022.1

Address for correspondence: Casey Hubert, Department of Biological Sciences, University of Calgary, Calgary AB T2N 1N4, Canada; email: chubert@ucalgary.ca

Age-Dependent Effects of COVID-19 Vaccine and of Healthcare Burden on COVID-19 Deaths, Tokyo, Japan

Yura K. Ko, Hiroaki Murayama, Lisa Yamasaki, Ryo Kinoshita, Motoi Suzuki, Hiroshi Nishiura

COVID-19 vaccine effectiveness against death in Japan remains unknown. Furthermore, although evidence indicates that healthcare capacity influences case-fatality risk (CFR), it remains unknown whether this relationship is mediated by age. With a modeling study, we analyzed daily COVID-19 cases and deaths during January–August 2021 by using Tokyo surveillance data to jointly estimate COVID-19 vaccine effectiveness against death and age-specific CFR. We also examined daily healthcare operations to determine the association between healthcare burden and age-specific CFR. Among fully vaccinated patients, vaccine effectiveness against death was 88.6% among patients 60–69 years of age, 83.9% among patients 70–79 years of age, 83.5% among patients 80–89 years of age, and 77.7% among patients ≥90 years of age. A positive association of several indicators of healthcare burden with CFR among patients ≥70 years of age suggested an age-dependent effect of healthcare burden on CFR in Japan.

Since the emergence of SARS-CoV-2 in Japan, COVID-19 has remained a substantial public health concern. As of September 1, 2021, the cumulative number of reported cases in Japan had reached 1,482,000, resulting in >16,000 deaths. Among those, 346,742 cases and 2,500 deaths occurred in Tokyo alone (*1*). Officials at various levels have requested the cooperation of residents in implementing several nonpharmaceutical measures to mitigate disease burden and prevent the collapse of the healthcare system (*2*). In addition, mass vaccination has been publicly available in Japan since April 12, 2021, initially targeting persons ≥65 years of age. Three types of vaccine have been used in Japan: mRNA-1273 (Moderna, https://www.modernatx.com), BNT162b2 vaccine (Pfizer-BioNTech, https://www.pfizer.com), and ChAdOx1 nCoV-19 vaccine (AstraZeneca, https://www.astrazeneca.com). As of September 1, 2021, vaccination coverage in Tokyo reached 58.1%, and 87.9% of persons ≥65 years of age had completed the 2-dose regimen (*3*).

Numerous studies have investigated vaccine effectiveness (VE) against SARS-CoV-2, and most derived their estimates by using test-negative designs or cohort analyses (*4*–*7*). However, attaining a sample size sufficient for such rigorous epidemiologic investigation requires a substantial amount of time, especially in countries like Japan, where COVID-19 mortality rate is low. Nonetheless, the need for valid real-world estimates of VE against death is urgent.

Case-fatality risk (CFR) acts as a proxy for disease virulence and is often used to identify risk factors for death within a population (*8*). A previous study indicated that the CFR for COVID-19 varies substantially with age (*9*). Detailed time-series surveillance data, including incidence and death information as well as background characteristics (e.g., patient age, sex, vaccination status), are critical for elucidating SARS-CoV-2 virulence in real time during the pandemic (*9*). Therefore, we aimed to jointly estimate VE against death and CFR on the date of death according to age by using both local-level and national-level surveillance data from Tokyo during the period when the Alpha or Delta variant was predominant (*10*,*11*). Crude CFR, defined as the ratio of the cumulative number of deaths to the cumulative number of confirmed cases, can underestimate actual CFR when cases are increasing and overestimate it when they are decreasing (*12*). To address this issue, which results from the

Author affiliations: National Institute of Infectious Diseases, Tokyo, Japan (Y.K. Ko, R. Kinoshita, M. Suzuki); Tohoku University, Miyagi, Japan (Y.K.Ko); International University of Health and Welfare, Chiba, Japan (H. Murayama); University of Tokyo, Tokyo (L. Yamasaki); Nagasaki University, Nagasaki, Japan (L. Yamasaki); Kyoto University, Kyoto, Japan (H. Nishiura)

DOI: https://doi.org/10.3201/eid2809.220377

delay from reporting to death and is referred to as right truncation bias, we constructed a mathematical model incorporating the time delay.

Several studies have also demonstrated that healthcare capacity substantially influences CFR (*13*–*15*). As COVID-19 incidence increases, the healthcare burden in the region also increases, and infected persons with severe signs/symptoms may not be able to receive rapid and appropriate treatment (i.e., ventilator support, extracorporeal membrane oxygenation [ECMO]). Thus, CFR may increase, given that a limited number of patients with severe signs/symptoms would be able to receive proper treatment. Therefore, monitoring healthcare capacity along with CFR could be a way to implement appropriate public health interventions tailored to the temporal situation. With this study, we aimed to examine temporal changes in age-specific CFR with respect to the healthcare burden. No ethics approval was required because the data were anonymized and collected in response to the outbreak.

Methods

Data Collection

In this modeling study, we used publicly available local-level data published by the Tokyo Metropolitan Government (*16*) to estimate VE against death and time-varying CFR. The number of positive cases according to the date of diagnosis and the number of deaths at specific time points were evaluated for each age group. We obtained data regarding vaccination status (fully vaccinated, partially vaccinated, and unvaccinated) among SARS-CoV-2–positive persons and deaths in Tokyo during each epidemiologic week by using the national-level Health Center Real-Time Information-Sharing System on COVID-19 (HER-SYS) (*17*).

The government of Japan recognized COVID-19 as a designated infectious disease in January 2020, after which a legal mandate to report all confirmed COVID-19 cases to the Ministry of Health, Labour, and Welfare was issued. In Tokyo, in addition to PCR and antigen testing for symptomatic persons and close contacts, screening testing has been conducted to detect outbreaks at early stages in facilities where clusters are likely to occur (*18*). Since May 2020, incidence reporting to the national government has been conducted through HER-SYS, and all diagnosed COVID-19 cases in the country are registered in this system. Although essential epidemiologic information for case identification (e.g., age, sex, and date of diagnosis) is entered into HER-SYS, details regarding prognosis may be incomplete. Thus, information related to death may not be entered, especially when public health centers are faced with an overwhelming workload. However, as a public health measure, the Tokyo Metropolitan Government has published information related to all COVID-19 deaths in Tokyo, including age, date of diagnosis, and date of death.

To analyze the effect of the healthcare burden on the CFR, we obtained the daily proportion of asymptomatic cases at the time of report in each age group by using HER-SYS. We collected data associated with the following 4 variables from the Tokyo Metropolitan Government website and used them as indicators of the healthcare burden in Tokyo (*19*): the number of persons with severe COVID-19 cases, defined as those requiring a ventilator or ECMO; the number of persons to whom the Tokyo rules apply, defined as persons for whom the care site destination has not been determined within 20 minutes of the emergency medical services team's request for or selection of 5 medical institutions to receive the patient; the proportion of nonhospitalized COVID-19 case-patients among all case-patients reported that day; and the proportion of case-patients for whom coordination of the care site was in progress.

To avoid underestimating the disease burden of COVID-19, we defined COVID-19-related deaths as death within 60 days of diagnosis, not within 28 days. To account for reporting delays, we accessed data as of November 15, 2021, for both HER-SYS and Tokyo Metropolitan Government published data, and we included data up to August 31, 2021.

Handling of Vaccination Data

For case-patients for whom date of vaccination was known, we considered those for whom date of vaccination and date of diagnosis were separated by 14 days to be fully vaccinated. All case-patients for whom date of vaccination was unknown were also considered fully vaccinated.

To avoid underestimating the number of positive cases and deaths among fully vaccinated case-patients, we used logistic regression to impute vaccination status for case-patients with unknown vaccination history in HER-SYS. In this analysis, we considered the month of diagnosis, age, presence of symptoms, and occurrence of death to be associated with vaccination history (Appendix, https://wwwnc.cdc.gov/EID/article/28/9/22-0377-App1.pdf).

Estimating VE Against Death and Time-Varying CFR According to Age Group

To jointly estimate VE against death and CFR by age group, we modeled the process to generate data for

deaths by using data for confirmed case-patients for whom date of diagnosis was available and for deceased case-patients for whom date of death was available. Because a delay between diagnosis and death leads to complexity when using confirmed cases and deaths in a model (Appendix Figure 1), we convoluted the incidence on a specific date of diagnosis with the function representing the age-specific relative frequency of the delay and estimated the number of cases on a provisional date of death as a denominator of CFR. In this setting, we explicitly modeled the binomial process according to vaccination history while incorporating VE and CFR against death for both partially and fully vaccinated case-patients, which were considered unknown parameters. We estimated these unknown parameters by using the Markov chain Monte Carlo method with improper flat priors. In addition, we calculated the probabilities representing the unconditional protection against death for partially and fully vaccinated persons by exploiting the posterior distributions of VE against death and VE against documented infection in Japan, as reported elsewhere (*20*). We conducted all procedures according to age stratification (Appendix).

To determine the effect of COVID-19 vaccination on the burden of the disease, we simulated the daily cumulative incidence of deaths by using the estimated conditional VE against death and CFR in 2 scenarios. The scenarios were if all reported case-patients were fully vaccinated and if all positive case-patients had not been fully vaccinated.

As a sensitivity analysis, we also estimated VE and CFR against death in 2 contexts. First, we excluded all case-patients with unknown vaccination status and definition of death occurring within 28 days of diagnosis as COVID-19–related. In addition, to avoid overestimation, we used the different assumptions of VE against documented infection, setting 40% for partially vaccinated case-patients and 80% for fully vaccinated case-patients on the basis of previous reports, which estimated VE against infection with the Delta variant (*4*).

Effects of Healthcare Burden on CFR, According to Age Group

Next, we explored the effect of the healthcare burden on time-varying age-specific CFR by using data for confirmed case-patients and deaths of unvaccinated case-patients. We constructed a Bayesian multilevel model for the unvaccinated population based on the binomial process, which had already been constructed for the joint estimation of CFR and VE. Assuming that the CFR follows a β distribution in the binomial process, we performed an inverse logit transformation on its mean, in which the explanatory variables were embedded as a regression model. As explanatory variables, we considered the daily empirical asymptomatic rate by age and each of the 4 healthcare burden indicators. The asymptomatic rate was added as an explanatory variable because that rate may be considered to be biologically identical among the infected population; however, the rate among PCR-confirmed case-patients varies because of changes in testing policies and intensity of contact tracing (ascertainment bias) and, therefore, is suitable for adjusting for such bias.

We then selected the best-fit model for the length of lag of each healthcare burden indicator. We estimated the parameters (i.e., coefficients α_1 and α_2, intercept β, and the variance of the β distribution κ) in a Bayesian framework with weakly informative priors (α_1, β_2, and β are normally distributed with mean 0 and variance 100; κ is normally distributed with mean 0 and variance 10). For model selection, we computed the widely applicable information criterion by using the marginalized posterior log-likelihoods (*21*). We used Markov chain Monte Carlo for this analysis (Appendix).

Results

We included in our study all 2,065 COVID-19–associated deaths reported by the Tokyo Metropolitan Government for case-patients ≥30 years of age during January 1–August 31, 2021. We calculated the percentages by vaccination status for each of SARS-CoV-2–positive case-patients and deaths by using HER-SYS data, which required imputation of unknown vaccination status for 10,327 case-patients. On the basis of imputation, we considered 752 case-patients to be partially vaccinated, 390 fully vaccinated, and the rest unvaccinated. The proportions of positive cases and deaths after full vaccination increased over time, starting with older adults (Figure 1).

Among partially vaccinated case-patients, estimates of VE against death in each age group ranged from 34% to 66%. Among fully vaccinated case-patients, VE against death were 38.0% (95% credible interval [CrI] 2.6–82.4), 88.6% (64.3–98.1), 83.9% (68.8–92.9), 83.5% (72.5–91.0), and 77.7% (60.7–89.4) among case-patients who were 30–59, 60–69, 70–79, 80–89, and ≥90 years of age, respectively. Unconditional protection against death was estimated as 93.8% (90.3–98.2) in the 30–59-year age group and >97% in the ≥60-year age groups (Table). The sensitivity analysis revealed similar results for age-specific VE (Appendix Table 1). We also observed temporal changes in CFR according to age group. Minimum estimated

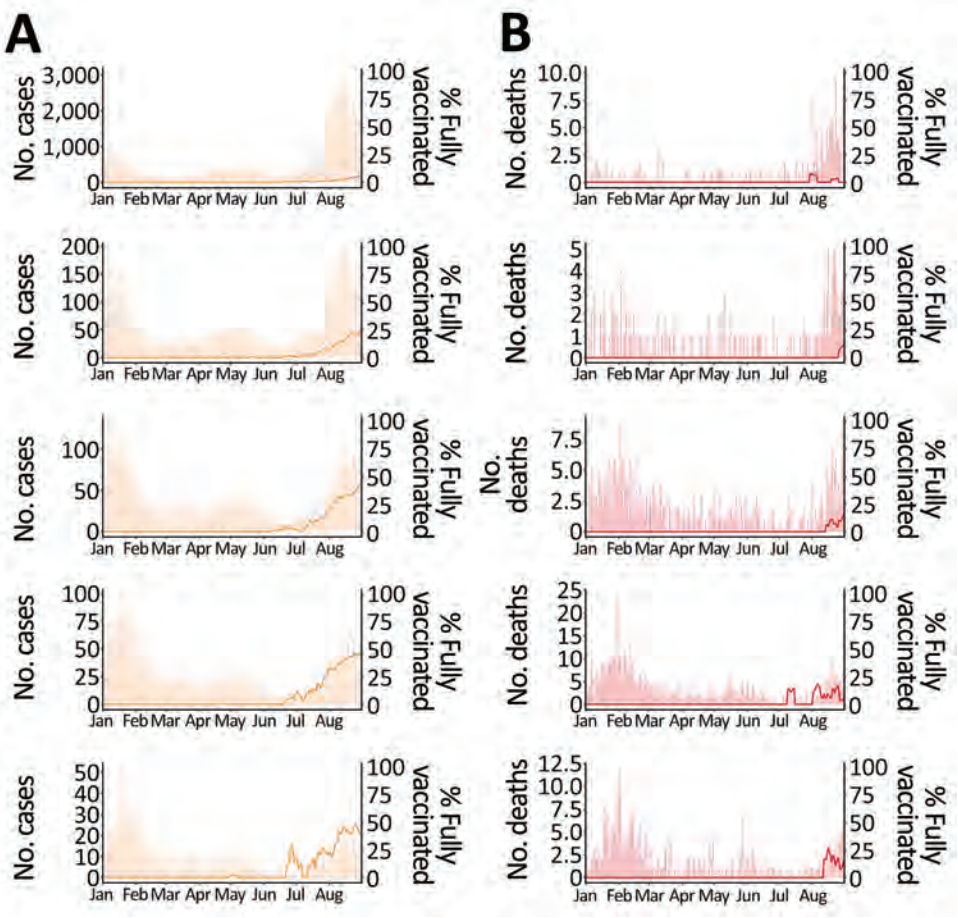

Figure 1. Effects of COVID-19 vaccine on deaths, stratified by age group, Tokyo, Japan, January–August 2021. A) Daily number of SARS-CoV-2–positive case-patients (bar) and proportion of fully vaccinated SARS-CoV-2–positive case-patients (line, 7-day moving average). B) Daily number of deaths (bar) and proportion of deaths among fully vaccinated case-patients (line, 7-day moving average). Ranges indicate years of age. From top to bottom, age groups are 30–59, 60–69, 70–79, 80–89, ≥90 years.

median values were 0.14%, 1.30%, 3.12%, 6.81%, and 8.87% and maximum estimated median values 1.02%, 5.37%, 13.76%, 27.08%, and 41.16% among persons 30–59, 60–69, 70–79, 80–89, and ≥90 years of age, respectively (Appendix Figure 2).

Subsequently, our simple simulation showed that among case-patients ≥60 years of age, if all had been vaccinated, the counterfactual number of deaths would have been less than one third to one fifth of actual deaths. If all case-patients had been unvaccinated, the counterfactual number of deaths would have increased by 100–200 in each age group (Figure 2).

An exploratory analysis of the effect on CFR of each of the 4 Tokyo healthcare burden indicators according to age group revealed that the number of severe cases was positively associated with CFR for persons 70–79, 80–89, and ≥90 years of age. Likewise, the number of cases to which Tokyo rules applied also exhibited a positive association with CFR among those who were 70–79 years of age, and both the proportion of nonhospitalized case-patients and the proportion of case-patients for whom coordination of hospital care was in progress were positively associated with CFR among persons who were 80–89 years of age (Appendix Table 2). When we compared CFR estimated using the best-fit model with CFR estimated jointly with the VE against death, the models in the 70–79-year and 80–89-year age groups captured a part of the variation in the temporal change in CFR (Figure 3). We were not able to capture the time variation in CFR and the healthcare burden indicators for those in the 30–69-year age groups.

Discussion

Our joint estimation of VE against death and age-specific CFR in Japan, using surveillance data, indicated that during the period when the SARS-CoV-2 Alpha or Delta variant was predominant (*10*,*11*), VE against death in fully vaccinated persons ≥60 years of age was as high as 80%; estimates were unstable for those 30–59 years of age because of the small number of deaths in the corresponding age groups. Unconditional protection from death was also estimated to be extremely high (>97%) for persons in all age groups. These results suggest that even if breakthrough infections occur, VE against deaths was sufficiently high

Table. Estimated COVID-19 vaccine effectiveness in terms of protection against death over test-positive and unconditional protection against death, by age group, Tokyo, Japan, January 1–August 31, 2021*

Effect of interest, by age, y	Vaccine effectiveness (95% credible interval)	
	Partially vaccinated*	Fully vaccinated†
Protection against death over documented infection		
30–59 y	34.2 (2.2–71.4)	38.0 (2.6–82.4)
60–69 y	66.1 (33.0–85.4)	88.6 (64.3–98.1)
70–79 y	38.2 (7.3–63.8)	83.9 (68.8–92.9)
80–89 y	46.4 (17.9–68.7)	83.5 (72.5–91.0)
≥90 y	52.7 (19.6–76.6)	77.7 (60.7–89.4)
Unconditional protection against death		
30–59 y	68.7 (53.5–86.4)	93.8 (90.3–98.2)
60–69 y	83.9 (68.1–93.0)	99.2 (97.4–99.9)
70–79y	70.6 (55.9–82.8)	99.3 (98.6–99.7)
80–89 y	74.5 (60.9–85.1)	99.4 (98.9–99.6)
≥90 y	77.5 (61.8–88.8)	98.4 (97.1–99.2)

*14 d after the first vaccination and <14 d after the second vaccination.
†14 d after the second vaccination.

enough to avert most of the risk for COVID-19 death during the predominant periods of Alpha and Delta. Given the length of time required to collect sufficient cases to achieve a plausible estimate of VE against death in test-negative designs or cohort studies, our analysis of surveillance data demonstrates the benefits of vaccine dissemination in the general population. We also believe that the approach used in our study, which jointly estimated CFR and VE against death by using only the number of positive cases and deaths according to vaccination status, is a practical method that can be naturally extended to the effectiveness of booster vaccine and applied in various countries and regions.

Our results suggest that VE against death from COVID-19 declines with age. These results are consistent with the findings of previous reports, which indicated that the decline in VE estimates observed in older adults may be related to age-related immune senescence, which limits the protective effects of vaccines (*22*).

In the exploratory analysis investigating the effect of the healthcare burden on CFR, the regression coefficients with their uncertainty bounds were positive for many indicators among older adults, especially those 80–89 years of age, including the number of patients with severe cases, the proportion of nonhospitalized case-patients, and the proportion of case-patients for whom coordination of the care site was in progress. Among those 70–79 and 80–89 years of age, the healthcare burden indicators and rate of asymptomatic illness captured

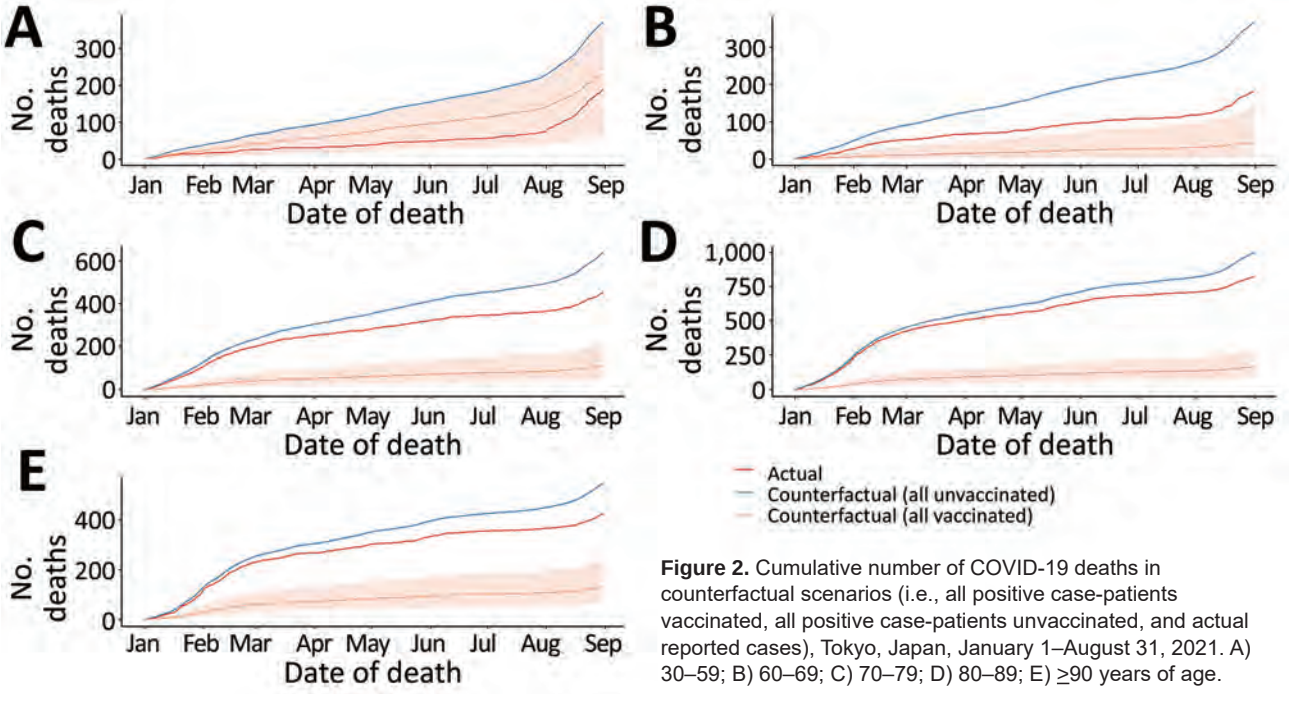

Figure 2. Cumulative number of COVID-19 deaths in counterfactual scenarios (i.e., all positive case-patients vaccinated, all positive case-patients unvaccinated, and actual reported cases), Tokyo, Japan, January 1–August 31, 2021. A) 30–59; B) 60–69; C) 70–79; D) 80–89; E) ≥90 years of age.

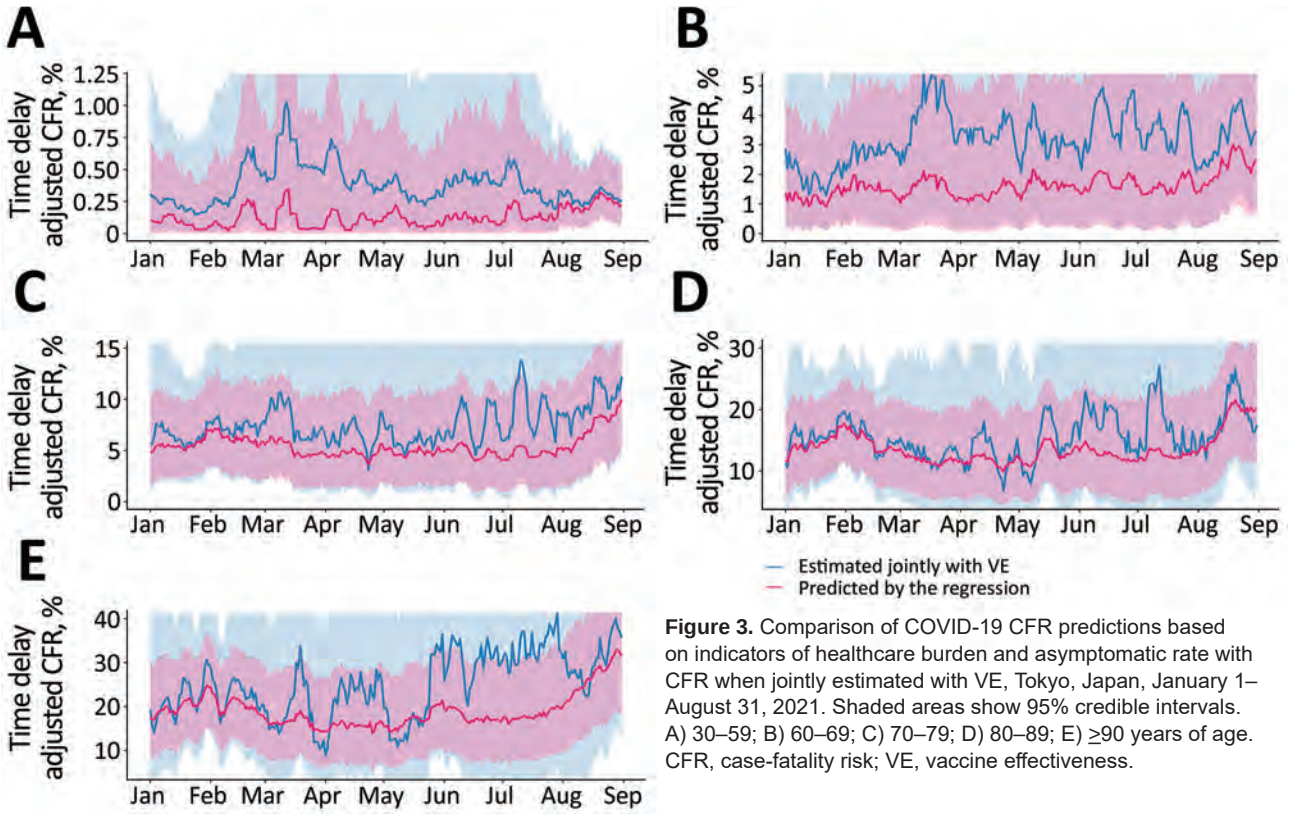

Figure 3. Comparison of COVID-19 CFR predictions based on indicators of healthcare burden and asymptomatic rate with CFR when jointly estimated with VE, Tokyo, Japan, January 1–August 31, 2021. Shaded areas show 95% credible intervals. A) 30–59; B) 60–69; C) 70–79; D) 80–89; E) ≥90 years of age. CFR, case-fatality risk; VE, vaccine effectiveness.

the upward trend in CFR in February and August 2021; among those ≥90 years of age, some of the time-varying trends were captured, although they frequently diverged from the estimated CFR. This finding may be because do-not-resuscitate orders are relatively more common among persons ≥90 years of age, which may have been an unconsidered confounder in our analysis. Furthermore, the temporal change in CFR could not be captured by the healthcare burden indicators for the younger age groups. Although many countries have reported that mortality rate increases with healthcare burden and reduced capacity (*13*–*15*), our results suggest that the effect of healthcare burden on CFR differs according to age group. One explanation is the possibility that medical resources such as ventilators and ECMO were preferentially allocated to young persons with severe cases. As in France in the early stages of the pandemic (*23*), even if not explicitly documented, these triage procedures probably took place, especially during July–August 2021, when the number of infected persons and deaths soared. From a clinical perspective, delays in treatment initiation have been reported to lead to poor outcomes (*24*). It is also possible that frail older case-patients were more affected by delays in treatment initiation because of healthcare burden. Such age-dependent differences may be useful for determining appropriate public health countermeasures. However, as we aimed to propose that vulnerability to healthcare burden varies by age, the effect of healthcare burden may not necessarily be causal. Further studies are required to determine whether this hypothesis can be constructed with causality.

Among the limitations of our study, we obtained information about vaccination status from HER-SYS. During the study period, vaccination status in the HER-SYS was automatically entered as unvaccinated if no input was provided, which may have resulted in underestimation of case-patients with unknown vaccination status. However, the proportion of fully vaccinated case-patients increased over time as the vaccination coverage in the population progressed (Figure 1). Furthermore, the same trend was observed even in August 2021, when the epidemic was most severe and the workload at public health centers and hospitals was considered the greatest, suggesting that the quality of data entered for vaccination status was maintained to some extent. A second limitation is that although other risk factors, such as underlying disease, can contribute to severe outcomes, we were not able to take this into account because of the limited information available

in the surveillance dataset. Differences in the proportions of these risk factors between the vaccinated and unvaccinated groups may have biased estimates of VE. Third, we could not obtain information about reinfection status from the dataset. However, the incidence of reinfection was reported to be very low before the emergence of the Omicron variant (*25*). We believe that the effect of reinfection on our analysis was small. Fourth, when exploring the effect of healthcare burden on CFR, we did not consider the effects of newly emerging variants. In Japan, during the study period, the Alpha variant began to increase in February 2021 and became predominant in June, and the Delta variant surged in the following 2 months (*10*). Fifth, we did not account for the introduction of therapeutic agents (antibody cocktail of casirivimab and imdevimab) in our analysis. Sixth, we used the number of persons with severe cases and the proportion of nonhospitalized case-patients as proxies for healthcare burden but did not take into account the increased provision of bed capacity for hospitalized patients and patients with severe cases during the study period. However, as with the other proxy indicators of healthcare burden used in our study, we believe that they indirectly reflect part of the medical situation because they also peaked during January–February and July–August 2021, when the number of cases increased (Appendix Figure 3). Last, ascertainment bias is always a problem when estimating CFR, and it may not have been fully eliminated in this analysis. Although testing policies (PCR or antigen tests) did not change substantially over the study period, the frequency and scale of screening tests may have been affected by the size of the epidemic. In particular, screening capacity for nursing homes was probably limited in August 2021, when the magnitude of the epidemic was greatest. This possibility is suggested by the fact that the proportion of asymptomatic case-patients among those ≥90 years of age decreased during the same period (Appendix Figure 4). However, we attempted to address this bias as much as possible by including the asymptomatic rate among SARS-CoV-2–positive case-patients in Tokyo as an explanatory variable.

In summary, our study estimated VE against death in Japan based on surveillance data. Our findings highlight the potential effect of the healthcare burden on CFR, especially among older adults. The positive association between several indicators of healthcare burden and CFR among patients ≥70 years of age suggests an age-dependent effect of healthcare burden on CFR in Japan.

Acknowledgments

We thank all the staff at the local and prefectural health centers and people engaged in COVID-19 responses in Japan. We also appreciate the work of the Ministry of Health, Labor, and Welfare and the National Institute of Infectious Diseases in collecting and collating the surveillance data.

Detailed data on COVID-19 cases in Tokyo are freely available online at https://catalog.data.metro.tokyo.lg.jp/dataset/t000010d0000000068/resource/c2d997db-1450-43fa-8037-ebb11ec28d4c. Data on deceased case-patients are reported daily by the Tokyo Metropolitan Government, at https://www.metro.tokyo.lg.jp. HER-SYS data, such as vaccination status and presence of signs/symptoms in SARS-CoV–2 positive case-patients, are not publicly available. All codes for the analysis are available at https://github.com/KoKYura/covid19_cfr_ve_tokyo.

This study was conducted in cooperation with the Tokyo Infectious Disease Control Center. This work was supported by a Research on Emerging and Re-emerging Infectious Diseases and Immunization program grant awarded by the Ministry of Health, Labour, and Welfare (no. JPMH20HA2007).

Y.K.K. and M.S. conceived the study. Y.K.K., H.M., and H.N. designed the research; Y.K.K managed and curated data; Y.K.K. and H.M. analyzed data; Y.K.K., H.M., L.Y., R.K., M.S., and H.N. interpreted data; Y.K.K and H.M. wrote the first draft of the manuscript, which was revised by all authors. All authors approved the final version of the manuscript.

About the Author

Dr. Ko is a research scientist in the Center for Surveillance, Immunization, and Epidemiologic Research, National Institute of Infectious Diseases, Tokyo, Japan, and a PhD student at Tohoku University. His main research interests include public health, epidemiology, and infectious diseases surveillance.

References

1. Ministry of Health, Labour and Welfare. Situation report [cited 2022 Jul 7]. https://www.mhlw.go.jp/stf/covid-19/kokunainohasseijoukyou_00006.html
2. Ministry of Health, Labour and Welfare. Press conference [cited 2022 Jul 7]. https://www.mhlw.go.jp/stf/seisakunitsuite/bunya/newpage_00032.html
3. Government Chief Information Officers' Portal J. COVID-19 vaccine status [in Japanese]. https://info.vrs.digital.go.jp/dashboard/
4. Lopez Bernal J, Andrews N, Gower C, Gallagher E, Simmons R, Thelwall S, et al. Effectiveness of Covid-19 vaccines against the B.1.617.2 (Delta) variant. N Engl J Med. 2021;385:585–94. https://doi.org/10.1056/NEJMoa2108891

5. Young-Xu Y, Korves C, Roberts J, Powell EI, Zwain GM, Smith J, et al. Coverage and estimated effectiveness of mRNA COVID-19 vaccines Among US veterans. JAMA Netw Open. 2021;4:e2128391. https://doi.org/10.1001/jamanetworkopen.2021.28391
6. Sheikh A, Robertson C, Taylor B. BNT162b2 and ChAdOx1 nCoV-19 vaccine effectiveness against death from the Delta variant. N Engl J Med. 2021;385:2195–7. https://doi.org/10.1056/NEJMc2113864
7. Bruxvoort K, Sy LS, Qian L, Ackerson BK, Luo Y, Lee GS, et al. Real-world effectiveness of the mRNA-1273 vaccine against COVID-19: interim results from a prospective observational cohort study. SSRN Electron J. 2021;100134. https://doi.org/10.2139/ssrn.3916094
8. Mizumoto K, Endo A, Chowell G, Miyamatsu Y, Saitoh M, Nishiura H. Real-time characterization of risks of death associated with the Middle East respiratory syndrome (MERS) in the Republic of Korea, 2015. BMC Med. 2015;13:228. https://doi.org/10.1186/s12916-015-0468-3
9. Kayano T, Nishiura H. A comparison of case fatality risk of COVID-19 between Singapore and Japan. J Clin Med. 2020;9:3326. https://doi.org/10.3390/jcm9103326
10. Ito K, Piantham C, Nishiura H. Predicted dominance of variant Delta of SARS-CoV-2 before Tokyo Olympic Games, Japan. July 8, 2021. Euro Surveill. 2021;26. https://doi.org/10.2807/1560-7917.ES.2021.26.27.2100570
11. Murayama H, Kayano T, Nishiura H. Estimating COVID-19 cases infected with the variant Alpha (VOC 202012/01): an analysis of screening data in Tokyo, January-March 2021. Theor Biol Med Model. 2021;18:13. https://doi.org/10.1186/s12976-021-00146-x
12. Nishiura H, Klinkenberg D, Roberts M, Heesterbeek JAP. Early epidemiological assessment of the virulence of emerging infectious diseases: a case study of an influenza pandemic. PLoS One. 2009;4:e6852. https://doi.org/10.1371/journal.pone.0006852
13. Khan JR, Awan N, Islam MM, Muurlink O. Healthcare capacity, health expenditure, and civil society as predictors of COVID-19 case fatalities: a global analysis. Front Public Health. 2020;8:347. https://doi.org/10.3389/fpubh.2020.00347
14. Grosso FM, Presanis AM, Kunzmann K, Jackson C, Corbella A, Grasselli G, et al. Decreasing hospital burden of COVID-19 during the first wave in Regione Lombardia: an emergency measures context. BMC Public Health. 2021;21:1–9. PMID: 34479535
15. Asch DA, Sheils NE, Islam MN, Chen Y, Werner RM, Buresh J, et al. Variation in US hospital mortality rates for patients admitted with COVID-19 during the first 6 months of the pandemic. JAMA Intern Med. 2021;181:471–8. https://doi.org/10.1001/jamainternmed.2020.8193
16. Bureau of Social Welfare and Public Health. Press release [cited 2022 Jul 7]. https://www.fukushihoken.metro.tokyo.lg.jp/hodo/index.html
17. Ministry of Health, Labour and Welfare. Health Center Real-time Information-sharing System on COVID-19 (HER-SYS) [cited 2022 Jul 7]. https://www.mhlw.go.jp/stf/seisakunitsuite/bunya/0000121431_00181.html
18. Bureau of Social Welfare and Public Health, Tokyo Metropolitan Government. Covid-19 medical examination information site [in Japanese] [cited 2022 Jul 7]. https://www.fukushihoken.metro.tokyo.lg.jp/iryo/kansen/kensa/index.html
19. Tokyo Metropolitan Government. Updates on COVID-19 in Tokyo [cited 2022 Jul 7]. https://stopcovid19.metro.tokyo.lg.jp/en
20. National Institute of Infectious Diseases. Estimation of the effectiveness of the new corona vaccine BNT162b2 (Pfizer/BioNTech) by applying a mathematical model to surveillance data (Report 1) [in Japanese] [cited 2022 Jul 7]. https://www.niid.go.jp/niid/ja/2019-ncov/2484-idsc/10618-covid19-56.html
21. Watanabe S. Asymptotic equivalence of Bayes cross validation and widely applicable information criterion in singular learning theory. J Mach Learn Res. 2010;11:3571–94.
22. Nunes B, Rodrigues AP, Kislaya I, Cruz C, Peralta-Santos A, Lima J, et al. mRNA vaccine effectiveness against COVID-19-related hospitalisations and deaths in older adults: a cohort study based on data linkage of national health registries in Portugal, February to August 2021. Euro Surveill. 2021;26:1–7. https://doi.org/10.2807/1560-7917.ES.2021.26.38.2100833
23. Orfali K. What triage issues reveal: ethics in the COVID-19 pandemic in Italy and France. J Bioeth Inq. 2020;17:675–9. https://doi.org/10.1007/s11673-020-10059-y
24. Li X, Hu M, Zheng R, Wang Y, Kang H, Jiang L, et al. Delayed initiation of ECMO is associated with poor outcomes in patients with severe COVID-19: a multicenter retrospective cohort study. Front Med (Lausanne). 2021;8:716086. https://doi.org/10.3389/fmed.2021.716086
25. Ministry of Health, Labour and Welfare. The 68th Meeting of the Advisory Board for COVID-19. 2022 January 20; Tokyo, Japan [in Japanese] [cited 2022 Jun 22]. https://www.mhlw.go.jp/content/10900000/000887662.pdf

Address for correspondence: Yura K. Ko, Center for Surveillance, Immunization, and Epidemiologic Research, National Institute of Infectious Diseases, Toyama 1-23-1, Shinjuku-ku, Tokyo 162-8640, Japan; email: yurako0603@gmail.com

Increasing Incidence of Invasive Group A *Streptococcus* Disease, Idaho, USA, 2008–2019

Eileen M. Dunne, Scott Hutton, Erin Peterson, Anna J. Blackstock, Christine G. Hahn, Kathryn Turner, Kris K. Carter

Medscape ACTIVITY EDUCATION

In support of improving patient care, this activity has been planned and implemented by Medscape, LLC and Emerging Infectious Diseases. Medscape, LLC is jointly accredited by the Accreditation Council for Continuing Medical Education (ACCME), the Accreditation Council for Pharmacy Education (ACPE), and the American Nurses Credentialing Center (ANCC), to provide continuing education for the healthcare team.

Medscape, LLC designates this Journal-based CME activity for a maximum of 1.00 ***AMA PRA Category 1 Credit(s)™***. Physicians should claim only the credit commensurate with the extent of their participation in the activity.

Successful completion of this CME activity, which includes participation in the evaluation component, enables the participant to earn up to 1.0 MOC points in the American Board of Internal Medicine's (ABIM) Maintenance of Certification (MOC) program. Participants will earn MOC points equivalent to the amount of CME credits claimed for the activity. It is the CME activity provider's responsibility to submit participant completion information to ACCME for the purpose of granting ABIM MOC credit.

All other clinicians completing this activity will be issued a certificate of participation. To participate in this journal CME activity: (1) review the learning objectives and author disclosures; (2) study the education content; (3) take the post-test with a 75% minimum passing score and complete the evaluation at http://www.medscape.org/journal/eid; and (4) view/print certificate. For CME questions, see page 1943.

Release date: August 22, 2022; Expiration date: August 22, 2023

Learning Objectives

Upon completion of this activity, participants will be able to:

- Assess the epidemiology and clinical features of invasive group A *Streptococcus* and streptococcal toxic shock syndrome in Idaho during 2008 to 2019, based on a retrospective analytical study using surveillance data and medical record review
- Evaluate *emm* typing results and potential risk factors for increased incidence in invasive group A *Streptococcus*, based on a comparison of cases reported during 2014 to 2019 with those from 2008 to 2013
- Determine the clinical and public health implications of the epidemiology and clinical features of invasive group A *Streptococcus* in Idaho during 2008 to 2019, based on a retrospective analytical study using surveillance data and medical record review

CME Editor

Tony Pearson-Clarke, MS, Technical Writer/Editor, Emerging Infectious Diseases. *Disclosure: Tony Pearson-Clarke, MS, has disclosed no relevant financial relationships.*

CME Author

Laurie Barclay, MD, freelance writer and reviewer, Medscape, LLC. *Disclosure: Laurie Barclay, MD, has the following relevant financial relationships: formerly owned stocks in AbbVie Inc.*

Authors

Eileen M. Dunne, PhD; Scott Hutton, PhD; Erin Peterson, BS; Anna J. Blackstock, PhD; Christine G. Hahn, MD; Kathryn Turner, PhD; *and* ***Kris K. Carter, DVM.***

Author affiliations: Centers for Disease Control and Prevention, Atlanta, Georgia, USA (E.M. Dunne, A.J. Blackstock, K.K. Carter); Idaho Department of Health and Welfare, Boise, Idaho, USA (E.M. Dunne, S. Hutton, E. Peterson, C.G. Hahn, K. Turner, K.K. Carter)

DOI: https://doi.org/10.3201/eid2809.212129

We investigated invasive group A *Streptococcus* epidemiology in Idaho, USA, during 2008–2019 using surveillance data, medical record review, and *emm* (M protein gene) typing results. Incidence increased from 1.04 to 4.76 cases/100,000 persons during 2008–2019. *emm* 1, 12, 28, 11, and 4 were the most common types, and 2 outbreaks were identified. We examined changes in distribution of clinical syndrome, patient demographics, and risk factors by comparing 2008–2013 baseline with 2014–2019 data. Incidence was higher among all age groups during 2014–2019. Streptococcal toxic shock syndrome increased from 0% to 6.4% of cases (p = 0.02). We identified no differences in distribution of demographic or risk factors between periods. Results indicated that invasive group A *Streptococcus* is increasing among the general population of Idaho. Ongoing surveillance of state-level invasive group A *Streptococcus* cases could help identify outbreaks, track regional trends in incidence, and monitor circulating *emm* types.

Invasive group A *Streptococcus* (iGAS) disease is a severe bacterial infection caused by *Streptococcus pyogenes*, sometimes called strep A; ≈25,000 cases occurred in the United States in 2019 (*1*). iGAS disease is defined as illness associated with detection of group A *Streptococcus* in a normally sterile site, such as blood, pleural fluid, joint fluid, or deep tissue. iGAS has different clinical syndromes, including bacteremia without focus, pneumonia, and cellulitis, and severe manifestations, include necrotizing fasciitis and streptococcal toxic shock syndrome (STSS). The highly variable M protein, encoded by *emm* (M protein gene), is essential for virulence and serves as the primary target for epidemiologic typing of GAS (*2*). Most patients with iGAS are hospitalized and the estimated case-fatality rate in the United States is 12% (*3*). Numerous risk factors are associated with iGAS, including older age, diabetes, HIV infection, heart disease, cancer, obesity, injection drug use, long-term care facility (LTCF) residence, homelessness, preceding or concurrent influenza infection, and exposure to children with sore throats (*4*–*9*). No licensed vaccines for GAS exist despite its substantial global disease burden: an estimated 1.78 million new cases of severe GAS (iGAS, acute rheumatic fever, rheumatic heart disease, and poststreptococcal glomerulonephritis) and 517,000 deaths occurring each year (*10*). In 2019, the World Health Organization recognized GAS as a leading cause of infectious disease burden and proposed better characterization of GAS epidemiology as a priority activity for vaccine development (*11*).

During the past decade, iGAS incidence has increased in the United States, Canada, Ireland, Australia, and New Zealand (*1*,*12*–*16*). Reasons for these increases are unclear but could include changing demographics (e.g., an aging population at higher risk for iGAS), rising prevalence of other risk factors associated with iGAS infection, or changes in circulating *emm* types. In some US states, iGAS outbreaks among specific populations (e.g., persons experiencing homelessness or who inject drugs) or the emergence of rarely occurring *emm* types were linked to increases in iGAS incidence (*17*–*21*). In Idaho, a rural, western US state with a 2020 population of ≈1.8 million persons, iGAS is a reportable disease. We conducted a retrospective analytical study using surveillance data, *emm* typing results, and medical record review to describe the epidemiology of iGAS in Idaho during 2008–2019. In addition, we compared cases reported during 2014–2019 with cases from a lower-incidence 2008–2013 baseline period to determine whether clinical syndromes, patient demographics, and risk factors were associated with increased iGAS incidence.

Methods

Case Identification and Data Collection

We defined confirmed iGAS cases as *S. pyogenes* isolated by culture from a normally sterile site (e.g., blood, or cerebrospinal, joint, pleural, or pericardial fluids). Cases of iGAS in Idaho must be reported to the Idaho Division of Public Health or local public health agencies, according to Idaho reportable disease rules (https://publicdocuments.dhw.idaho.gov/WebLink/DocView.aspx?id=6798&dbid=0&repo=PUBLIC-DOCUMENTS). Reportable disease surveillance is a passive surveillance system, and with rare exceptions, reports are submitted by laboratories. After iGAS cases are reported, local public health district epidemiologists collect data and determine whether a given case is associated with a congregate setting or an outbreak. For this retrospective study, we used information about iGAS cases reported during 2008–2019, including patient demographics, laboratory reports, and data obtained from public health investigations, recorded in the Idaho National Electronic Disease Surveillance System Base System (NBS) and from review of medical records to collect additional clinical and risk factor information. We viewed medical records in the Idaho Health Data Exchange or obtained them by faxing medical record requests to hospitals. Because reported iGAS cases increased substantially from 2013 to 2014, we reviewed reporting facilities and submission procedures to determine whether potential changes in reporting methods (for example, an increase in electronic

over manual reporting) might have contributed to the increase in reported cases.

We obtained data concerning hospitalization and death from NBS or medical records; however, the records for fatal cases did not always indicate whether iGAS was considered a cause of or contributing factor to death. Case information encompassed patient demographics (i.e., age, sex, race and ethnicity), type of residence, clinical syndrome (i.e., pneumonia, bacteremia, meningitis, cellulitis), and underlying conditions and behavioral risk factors (i.e., diabetes, skin wound or injury, cancer, chronic obstructive pulmonary disease or emphysema, obesity, dialysis or renal failure, immunosuppression, postpartum status, recent surgery, alcohol abuse, injection drug use, current smoking). We selected variables for data abstraction based on the Centers for Disease Control and Prevention (CDC) Active Bacterial Core surveillance (ABCs) case report form (https://www.cdc.gov/abcs/downloads/abcs-case-rpt-form.pdf). We collected data on other risk factors (e.g., GAS pharyngitis, recent or concurrent influenza infection, household member with GAS infection), when available, from medical records or NBS.

Except for results from 2 isolates from 2012 that underwent *emm* typing at the Boise Veterans Administration Medical Center, *emm* typing results were provided by the Idaho Bureau of Laboratories, which began *emm* typing GAS isolates voluntarily submitted by diagnostic laboratories in 2014. *emm* typing at Idaho Bureau of Laboratories was conducted by PCR amplification and Sanger sequencing of the *emm* gene according to CDC protocols (https://www.cdc.gov/streplab/protocol-emm-type.html). *emm* types were assigned using a CDC M type–specific sequence database library within the bionumerics software platform (ftp://ftp.cdc.gov/pub/infectious_diseases/biotech/tsemm). Sequences were verified using the CDC Blast-*emm* database (https://www2.cdc.gov/vaccines/biotech/strepblast.asp).

Data Analysis

We used Stata software version 14.2 (StataCorp, LLC, https://www.stata.com) to conduct data analysis and compiled categorical data as percentages and continuous data as medians with interquartile ranges (IQRs). We calculated annual incidence per 100,000 persons overall and by age group using annual census data for Idaho population estimates (https://www.census.gov/data.html); we age-standardized incidence rates to the average population distribution for Idaho during 2008–2019 and reported with 95% CIs. We calculated incidence estimates by race and ethnicity using data from the Idaho Bureau of Vital Records and Health Statistics (Appendix, https://wwwnc.cdc.gov/EID/article/28/9/21-2129-App1.pdf).

To investigate the increase in iGAS incidence, we conducted a case-case analysis, comparing cases from the higher incidence period (2014–2019) with cases from the lower incidence baseline period (2008–2013). We used the χ^2 test to compare associations between periods and disease syndromes, deaths, hospitalization status, and predisposing conditions; we used the Mann-Whitney U test to compare median length of hospital stay. We used logistic regression models to compare demographics, underlying conditions, and other risk factors between the 2 periods to identify any factors that might be positively associated with the higher incidence period (Appendix). We included age group, obesity, residence type, and injection drug use as variables in the multivariable logistic regression model. We reported results as odds ratios for the univariable models and adjusted odds ratios for the multivariable model and calculated 95% CIs for all results. Odds ratios >1 indicated higher odds of cases with that risk factor being in the 2014–2019 period, compared with the baseline period. Idaho Division of Public Health and CDC determined this project to be nonresearch (public health practice). We conducted this activity consistent with applicable federal law and CDC policy.

Results

During 2008–2019, a total of 483 cases of iGAS disease were reported among Idaho residents. Annual disease incidence per 100,000 persons increased from 1.04 to 4.76 during 2008–2019 (Figure 1). Case numbers were highest in January and lowest in August with similar patterns across years (Figure 2; Appendix Figure 1). We identified no changes in the surveillance system that might have led to increased case reporting. Overall, 52.8% of cases occurred among men; median age of case-patients was 62 years (Table 1). Data concerning race and ethnicity were available for 444 (91.9%) patients, most of whom were white, non-Hispanic persons (87.8%), followed by Hispanic (5.0%) and American Indian or Alaska Native persons (4.1%). For comparison, the 2018 population of Idaho was estimated to be 83.1% white non-Hispanic, 12.7% Hispanic, and 2.0% American Indian or Alaska Native (22). The average annual incidence per 100,000 persons was 2.39 during 2008–2019; incidence was 2.55 among white non-Hispanic, 1.03 among Hispanic, and 5.19 among American Indian and Alaska Native persons. Data concerning residence type were available for 428 (88.6%) patients; most (349, 81.5%)

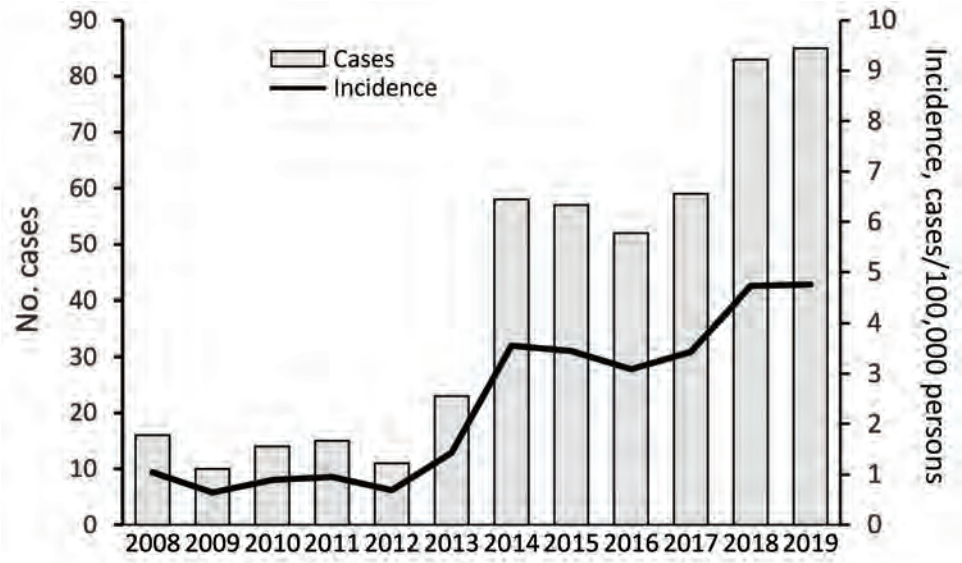

Figure 1. Annual number of reported cases of invasive group A *Streptococcus* (n = 483) and incidence (cases per 100,000 persons) from an investigation in Idaho, USA, comparing cases reported during 2014–2019 with cases from a lower-incidence baseline period, 2008–2013.

resided in a private residence, followed by 63 (14.7%) in a LTCF or nursing home.

Mean annual incidence per 100,000 persons was 0.94 during the 2008–2013 baseline period (n = 89 cases) and 3.84 during 2014–2019 (n = 394 cases). Patient demographics were similar between the periods (Table 1); we included odds ratios in risk factor analysis (Table 2). Disease incidence increased between periods among all age groups (Figure 3). The mean annual age-standardized incidence per 100,000 persons increased from 1.0 (95% CI 0.5–1.5) during 2008–2013 to 3.7 (95% CI 2.8–4.6) for 2014–2019. iGAS incidence increased in all 7 of Idaho's public health districts (Appendix Figure 2).

Medical records were available for 383/483 (79.3%) cases, 62/89 (70%) during the baseline 2008–2013 period and 321/394 (81.5%) during 2014–2019. Information concerning deaths was available for 464 (96.0%) patients, 55 (11.9%) of whom died. The case-fatality rate was 14/84 (16.7%) for the baseline period and 41/380 (10.4%) during 2014–2019 (p = 0.132). Of 471 patients with data on hospitalization status, 441 (93.6%) were hospitalized. The proportion of patients hospitalized was slightly lower during 2008–2013 (88.4%, 76/86) compared with 94.8% (365/385) during 2014–2019 (p = 0.027). Data on length of hospital stay were available for 385 hospitalized patients.

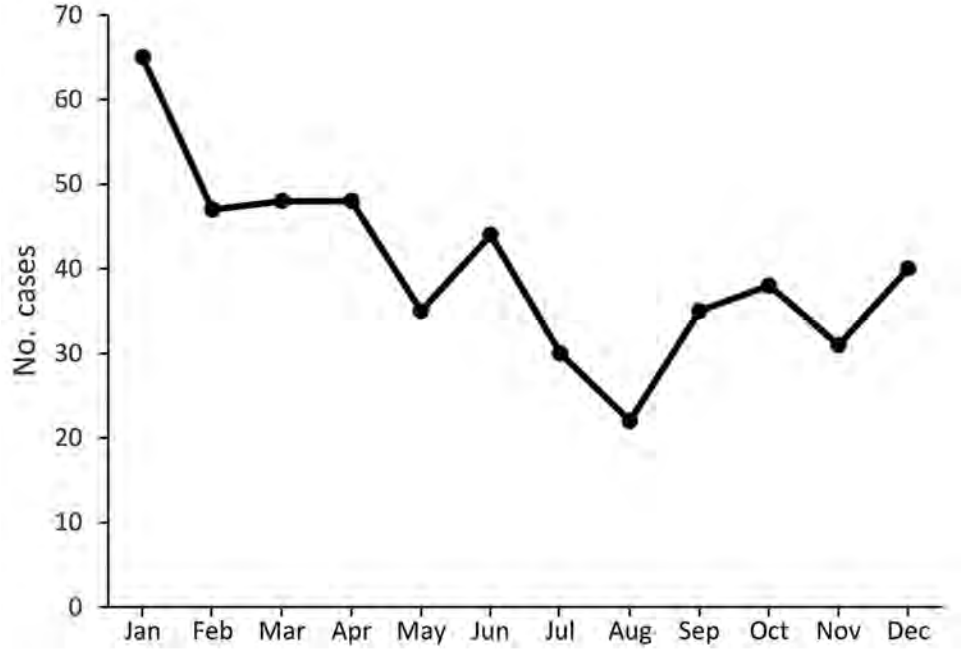

Figure 2. Seasonality of invasive group A *Streptococcus* (n = 483) by month of diagnosis, from an investigation in Idaho, USA, comparing cases reported during 2014–2019 with cases from a lower-incidence baseline period, 2008–2013.

Table 1. Demographics of patients with invasive group A *Streptococcus* disease, overall and by 6-year periods, Idaho, USA, 2008–2019*

Variable	Overall, N = 483	2008–2013, n = 89	2014–2019, n = 394
Sex			
F	228 (47.2)	48 (53.9)	180 (45.7)
M	255 (52.8)	41 (46.1)	214 (54.3)
Age, y, median (interquartile range)	62 (41–75)	60 (37–75)	64 (41–75)
Age group, y			
<5	24 (5.0)	4 (4.5)	20 (5.1)
5–17	43 (4.8)	5 (5.6)	18 (4.6)
18–34	45 (9.3)	12 (13.5)	33 (8.4)
35–49	58 (12.0)	10 (11.2)	48 (12.2)
50–64	104 (21.5)	20 (22.5)	84 (21.3)
65–79	147 (30.4)	21 (23.6)	126 (32.0)
≥80	92 (17.0)	17 (19.1)	65 (16.5)
Race/ethnicity	n = 444†	n = 83†	n = 361†
Hispanic	22 (5.0)	2 (2.4)	20 (5.5)
Non-Hispanic			
White	390 (87.8)	74 (89.2)	316 (87.5)
Black	4 (0.9)	1 (1.2)	3 (0.8)
American Indian/Alaska Native	18 (4.1)	5 (6.0)	13 (3.6)
Asian	5 (1.1)	1 (1.2)	4 (1.1)
Native Hawaiian/Pacific Islander	5 (1.1)	0 (0.0)	5 (1.4)
Residence type	n = 428†	n = 71†	n = 357†
Private residence	349 (81.5)	56 (78.9)	293 (82.1)
Long-term care or nursing facility	63 (14.7)	13 (18.3)	50 (14.1)
Homeless	9 (2.1)	1 (1.4)	8 (2.2)
Correctional facility	7 (1.6)	1 (1.4)	6 (1.7)

*Values are no. (%) patients except as indicated.
†Excludes cases with missing data.

Median stay was 5 days (IQR 4–9) for all hospitalized patients: 5 days (IQR 3–8) for 58 patients hospitalized during 2008–2013 compared with 6 days (IQR 4–9; p = 0.118) for 327 patients hospitalized during 2014–2019.

Cellulitis was the most common clinical syndrome, reported in 41.4% of cases, followed by bacteremia without focus (34.2%) and pneumonia (16.8%) (Table 3). STSS, a rare but severe syndrome caused by GAS infection, was identified in 25 cases, all during 2014–2019 (p = 0.02). Toxic shock syndrome is a reportable disease in Idaho; however, 11 (44%) STSS cases were identified only retrospectively through medical record review. Ages of STSS patients ranged from 10 months to 82 years; 6/22 (27%) died (data missing for 3 patients). We observed no other differences in clinical syndromes between periods. GAS was cultured from blood in 92.9% (442/476) of cases, with no differences over time: 74/82 (90.2%) for the baseline period compared with 368/394 (93.4%; p = 0.31) during 2014–2019. Data on postpartum status were available for 47/50 women 15–44 years of age, 10/47 (21%) of whom were postpartum, with no difference between periods: 2/9 (22%) during the baseline period compared with 8/38 (21%; p = 0.94) during 2014–2019.

emm typing was conducted on bacterial isolates from 194 (40.2%) iGAS cases, 2/89 (2.3%) during 2008–2013 and 192/394 (48.7%) during 2014–2019. In total, we identified 38 different *emm* types; the most common were types 1 (n = 26, 13%), 12 (n = 25, 13%), 28 (n = 23, 12%), 11 (n = 15, 8%), and 4 (n = 15, 8%) (Figure 4; Appendix Table 1). *emm* typing results were available for 14/25 (56%) STSS cases, from which 10 *emm* types were observed; types 1 (n = 3), 12 (n = 2), and 1.25 (n = 2) were identified in >1 patient.

Two outbreaks were previously identified on the basis of epidemiologic information and *emm* types. During July–September 2016, an outbreak of 5 cases of iGAS caused by *emm59* occurred among residents of a single county. During 2014–2016, an outbreak of iGAS occurred among residents of a LTCF; 9 cases were *emm11*, and 4 cases did not have *emm* typing conducted. In addition, a household cluster of 2 cases, both associated with injection drug use, occurred in May 2015, but *emm* typing was not conducted. In total, 16/394 (4.1%) of cases during 2014–2019 were associated with a cluster or outbreak.

Information concerning underlying medical conditions was available for 432 (90.2%) patients, 69/89 (78%) during 2008–2013 and 363/394 (92.1%) during 2014–2019. Of these patients, 73.8% had ≥1 underlying condition; diabetes (41.2%), heart disease (26.9%), and obesity (22.0%) were the most common (Table 4). No patients had HIV infection. Overall, 201/412 (47.8%) patients had skin injuries, and nonsurgical wounds were most frequently reported. Injection drug use was reported for 8/386 (2.1%) and methamphetamine use for 6/386 (1.6%) patients, all during the 2014–2019

period. Data for other risk factors (GAS pharyngitis, household member with GAS infection, influenza infection) were available for 389 patients, and GAS pharyngitis was identified in 8.0% of patients. In regression analyses, we observed no associations between demographic or risk factors and the higher-incidence 2014–2019 period (Table 2). Injection drug use had an adjusted odds ratio of 3.2; however, the limited number of observations yielded wide 95% CIs.

Discussion

Using statewide reportable disease surveillance data supplemented by information from medical record review, we investigated the epidemiology of iGAS in Idaho over a 12-year period, during which incidence increased ≈4-fold. The ABCs program, which does not include data from Idaho, identified a similar increase in nationwide iGAS incidence per 100,000 persons, from 3.69 in 2008 to 7.63 in 2019 (*1*,*12*,*23*). In Canada, incidence per 100,000 persons rose from 4.42 in 2008 to 8.12 in 2019 (https://diseases.canada.ca/notifiable/charts).

In Idaho, average annual iGAS incidence during our study was 2-fold as high among American Indian or Alaska Native persons compared with white non-Hispanic persons. Higher iGAS incidence among indigenous compared with nonindigenous populations has been reported in multiple settings, including the United States, Australia, and New Zealand (*24*). In Alberta, Canada, iGAS incidence was 6-fold as high and increasing more rapidly among First Nation compared with non-First Nation populations, rising to 52.2 cases per 100,000 persons in 2017 (*25*). Neither the proportion of cases occurring among American Indian and Alaska Native persons nor the racial and ethnic distribution of Idaho's population changed substantially during our study period (Appendix Table 2).

Approximately three quarters of iGAS patients had ≥1 underlying medical condition; diabetes, obesity, and skin injuries were common, emphasizing

Table 2. Individual risk factor and multivariable analysis of risk factors comparing invasive group A *Streptococcus* cases during 2014–2019 with cases from the 2008–2013 baseline period, Idaho, USA

Variable	Unadjusted odds ratio* (95% CI)	p value	Adjusted odds ratio† (95% CI)	p value
Sex				
F	Referent			
M	1.4 (0.9–2.2)	0.16		
Age group, y				
0–17	1.2 (0.5–2.8)	0.71	1.3 (0.5–3.3)	0.63
18–49	Referent		Referent	
50–64	1.2 (0.6–2.3)	0.65	1.6 (0.7–3.8)	0.29
65–79	1.7 (0.9–3.2)	0.13	1.7 (0.8–3.8)	0.16
≥80	1.1 (0.5–2.1)	0.90	1.1 (0.5–2.6)	0.84
Ethnicity				
Non-Hispanic	Referent			
Hispanic	2.4 (0.5–10.4)	0.25		
Residence type				
Private	Referent		Referent	
Long-term care or nursing facility	0.7 (0.4–1.4)	0.37	0.7 (0.3–1.5)	0.33
Correctional facility	1.2 (0.1–9.7)	0.90	1.9 (0.1–36.7)	0.67
Homeless	1.5 (0.2–12.5)	0.69	0.7 (0.1–4.8)	0.74
Underlying conditions				
Diabetes	0.9 (0.5–1.5)	0.68		
Heart disease: congestive heart failure or coronary artery disease	1.3 (0.7–2.3)	0.46		
Obesity	1.3 (0.7–2.4)	0.49	1.2 (0.6–2.5)	0.58
Chronic kidney disease or failure	1.6 (0.7–3.6)	0.30		
Chronic obstructive pulmonary disease	0.8 (0.4–1.8)	0.62		
Cancer	2.4 (0.7–7.9)	0.17		
Immunosuppression	2.0 (0.5–8.6)	0.37		
Hepatitis C or chronic liver disease	1.5 (0.4–6.9)	0.57		
Other‡	2.3 (0.3–18.2)	0.42		
Any underlying condition	0.9 (0.5–1.7)	0.75		
Other risk factors				
Skin injury	1.0 (0.6–1.7)	0.97		
Cigarette smoking	0.9 (0.5–1.9)	0.82		
Alcohol abuse	0.9 (0.3–2.3)	0.75		
Injection drug use	3.4 (0.2–60.0)	0.40	3.2 (0.2–63.0)	0.45

*Standard logistic regression analysis performed unless otherwise noted. An odds ratio >1 indicates higher odds of being in the 2014–2019 period.
†Firth logistic regression used to account for separation attributable to limited sample size and highly predictive risk factors. For multivariable analysis, results for residence type and injection drug use represent total effect and results for age group and obesity represent direct effect.
‡Other underlying conditions include paralysis, neurologic conditions, and developmental delay.

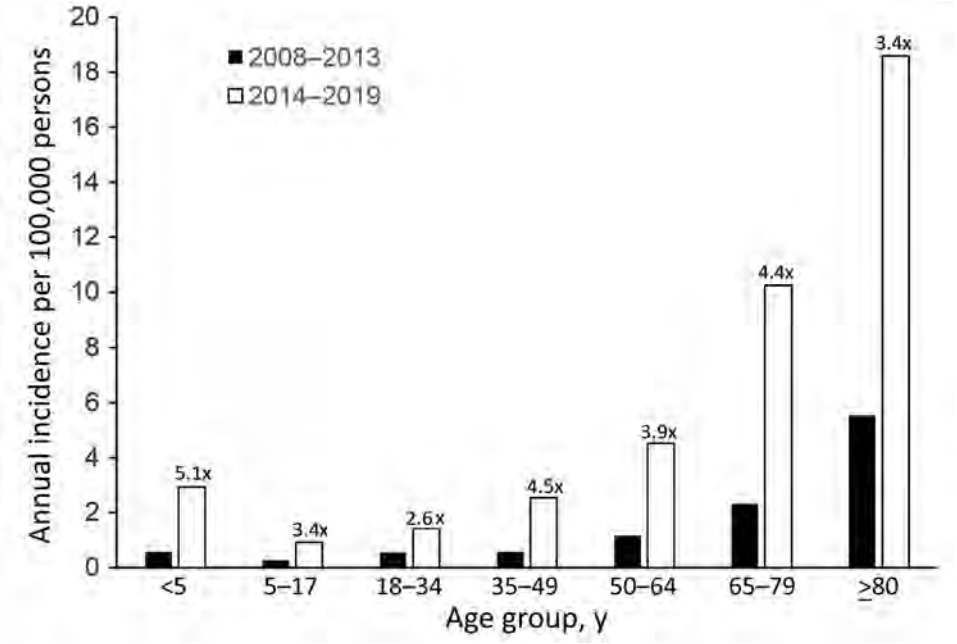

Figure 3. Average annual incidence of invasive group A *Streptococcus* (cases per 100,000 persons) during 2008–2013 (n = 89) and 2014–2019 (n = 394), by age group, Idaho, USA. The fold change for 2014–2019 compared with 2008–2013 is shown for each age group above the paired columns.

the need for diabetes management and wound care to reduce the risk for iGAS associated with these conditions (*4*,*5*). The high proportion of cases associated with skin injury or infection is consistent with national data; in 2019, a total of 44.7% of iGAS case-patients had cellulitis (*1*). Two outbreaks and a household cluster were identified through routine surveillance, all during 2014–2019; *emm* typing made outbreak detection easier. Because the state public health laboratory only began *emm* typing in 2014, earlier outbreaks might not have been detected. We recommend that states with available resources conduct *emm* typing to enhance surveillance and outbreak detection.

The incidence of iGAS in Idaho, 4.76 cases per 100,000 persons in 2019, is lower than the national incidence rate, 7.63 per 100,000 persons in 2019, possibly because Idaho iGAS estimates are based on passive data reporting, whereas national estimates are based on data from the ABCs active surveillance system. Other factors related to demographics or prevalence of risk factors might also contribute to lower Idaho compared with national iGAS incidence estimates. Increased iGAS rates across all age groups and in all geographic regions of Idaho during 2008–2019 present cause for concern. We identified no changes in surveillance procedures that might have led to increased case reporting. However, we did not assess potential changes in clinical practice (e.g., the number of blood cultures ordered by emergency departments), which might have affected case detection.

We identified a rise in STSS incidence: 25 cases occurred during 2014–2019, compared with none during 2008–2013, although these numbers do not

Table 3. Clinical syndromes of invasive group A *Streptococcus* disease, overall and by 6-year periods, Idaho, USA, 2008–2019*

Type of infection or clinical syndrome	No. (%) patients			p value‡
	Overall, N = 476†	2008–2013, n = 82†	2014–2019, n = 394	
Bacteremia without focus§	163 (34.2)	34 (41.5)	129 (32.7)	0.13
Cellulitis	197 (41.4)	30 (36.6)	167 (42.4)	0.33
Pneumonia	80 (16.8)	15 (18.3)	65 (16.5)	0.69
Streptococcal toxic shock syndrome	25 (5.3)	0 (0.0)	25 (6.4)	0.02
Septic arthritis	24 (5.0)	6 (7.3)	18 (4.6)	0.30
Empyema	19 (4.0)	4 (4.9)	15 (3.8)	0.65
Necrotizing fasciitis	12 (2.5)	4 (4.9)	8 (2.0)	0.14
Osteomyelitis	6 (1.3)	0 (0.0)	6 (1.5)	0.26
Meningitis	4 (0.8)	0 (0.0)	4 (1.0)	0.36
Other¶	3 (0.6)	1 (1.2)	2 (0.5)	0.46

*Cases can have >1 type of infection or clinical syndrome.
†Excludes 7 cases with missing data on type of infection or clinical syndrome, all during 2008–2013.
‡By χ^2 test.
§Group A *Streptococcus* isolated from blood, with no other clinical syndrome identified.
¶Other includes abscess, epiglottitis, and pelvic inflammatory disease.

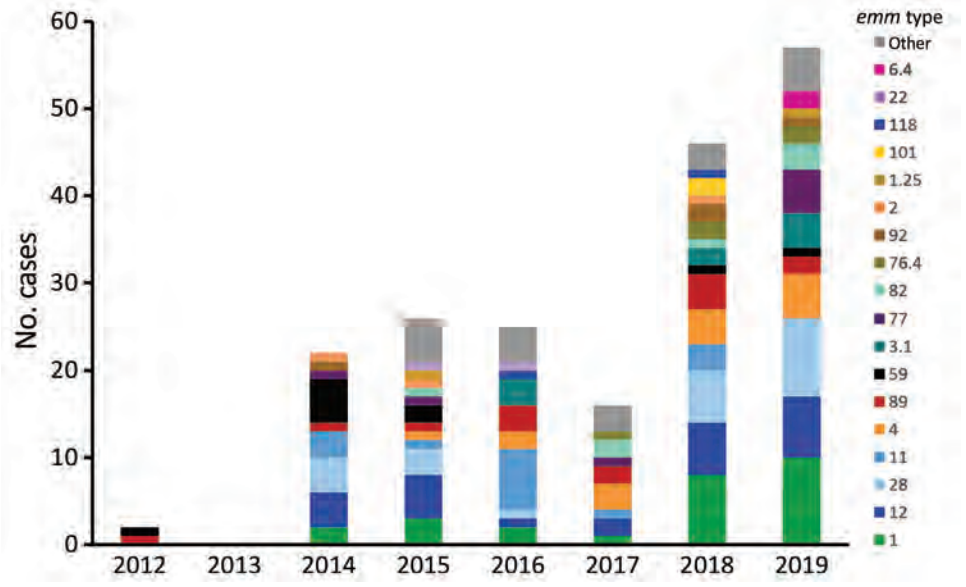

Figure 4. Invasive group A *Streptococcus emm* types (n = 194), Idaho, USA, 2012–2019, from an investigation in Idaho comparing invasive group A *Streptococcus* cases reported during 2014–2019 with cases from a lower-incidence baseline period, 2008–2013. The Idaho Bureau of Laboratories only began *emm* typing in 2014; 2012 data are from the Boise Veterans Administration Medical Center. Data for 2013 were unavailable.

account for the increase in overall iGAS cases. We found evidence of STSS underreporting, as has been reported in other studies (*26*). Cases of STSS from the baseline period might have been missed because medical records were only available for 70% of iGAS patients. We observed 10 different *emm* types among STSS cases that had an isolate submitted for typing, indicating a lack of clonality. Of note, a study in the Netherlands identified a temporal association between STSS and influenza A virus (*27*). However, STSS cases in Idaho occurred throughout the year, without seasonal patterns that might have been associated with influenza.

emm1 was the most common *emm* type identified in Idaho and also the most common cause of iGAS nationally during 2008–2019 (*1*,*12*,*23*). The diversity of *emm* types observed in Idaho was consistent with reports from high-income countries in North America and Europe (*28*–*30*). Although no vaccines targeting GAS are available, the 30-valent M protein–based strep A vaccine, one of the few vaccines under development in phase 1 or 2 clinical trials, would potentially cover 167/194 (86.1%) *emm* types from Idaho iGAS cases, and possibly more through cross-protection within *emm* clusters based on M protein structure (*31*–*33*).

We identified no associations between risk factors and increased incidence during 2014–2019. In New Mexico, increases in iGAS incidence were linked to rises in cases among persons experiencing homelessness and persons injecting drugs (*17*). Similarly, an analysis of ABCs national surveillance data concluded that injection drug use and homelessness likely contribute to increasing iGAS incidence in the United States, noting that particular *emm* types are increasing among this patient population (*7*). Factors responsible for increased incidence of iGAS during 2003–2017 in Alberta, Canada, were not clear, and multiple risk factors likely contributed, particularly alcohol abuse and drug use (*13*). In Idaho, only 8 patients reported injection drug use and 9 experiencing homelessness. Although these conditions might be underreported, homelessness and injection drug use do not appear to be driving the increase in iGAS in Idaho, although they might be contributing factors. We found no evidence that alcohol abuse was contributing to the increase in iGAS in Idaho.

Our results suggest that iGAS is increasing among the general population of Idaho and not limited to a particular age group or associated with an individual risk factor. The reasons for increases in reported incidence in Idaho might be multifactorial and involve factors not assessed in this study, such as expansion of ≥1 *emm* types and improvements in collection of diagnostic specimens by clinicians and passive reporting by laboratories. One limitation of our study is that we did not directly assess whether changes in the distribution of risk factors in the underlying population, such as the proportion of adults with skin injuries, could have led to increases in iGAS. For certain characteristics and risk factors, Idaho population data on estimated prevalence or proportion were unavailable (Appendix Table 2). For most factors, only minor changes over time were observed, and we did not identify any changes considered potentially responsible for the increase in iGAS incidence. Another limitation to the risk factor analysis was the small sample size during the baseline period—only 89 cases, some

missing data. A third key limitation to our study was the lack of *emm* typing data from the 2008–2013 baseline period, because only 2% of cases had *emm* typing conducted, compared with 49% during 2014–2019. Therefore, we could not assess potential shifts in *emm* types, which might have contributed to increasing rates of iGAS. In Ireland, an increase in iGAS during 2012–2015 coincided with an upsurge in *emm3* (*34*). In the United States, expansion over time of select *emm* types, including 11, 77, and 92, was linked to increasing prevalence of antimicrobial drug–resistant iGAS infections (*35*). Factors that contribute to the emergence of *emm* types are not well understood but might include genetic changes in bacteria and acquisition of new virulence factors, as well as variations in population immunity (*30*). *emm59*, which emerged initially in Canada and more recently has been found in the southwestern United States, was the most common *emm* type in Idaho in 2014; all 5 cases were associated with outbreaks, but *emm59* declined during subsequent years (*19*,*36*).

In conclusion, in Idaho, iGAS is an urgent and consequential clinical and public health concern because of its severity, high case-fatality rate, and statewide

Table 4. Underlying conditions and risk factors of patients with invasive group A *Streptococcus* disease, overall and by 6-year periods, Idaho, 2008–2019

Risk factor	No. (%) patients		
	Overall, N = 432*	2008–2013, n = 69*	2014–2019, n = 363*
Any underlying condition			
No	113 (26.2)	17 (24.6)	96 (26.5)
Yes	319 (73.8)	52 (75.4)	267 (73.6)
Condition			
Diabetes	178 (41.2)	30 (43.5)	148 (40.8)
Heart disease: congestive heart failure or coronary artery disease	116 (26.9)	16 (23.2)	100 (27.6)
Obesity	95 (22.0)	13 (18.8)	82 (22.6)
Kidney disease: chronic kidney disease or chronic kidney failure	61 (14.1)	7 (10)	54 (14.9)
Chronic obstructive pulmonary disease or emphysema	43 (10.0)	8 (11.6)	35 (9.6)
Cancer	38 (8.8)	3 (4.3)	35 (9.6)
Immunosuppression	22 (5.1)	2 (2.9)	20 (5.5)
Hepatitis C or chronic liver disease	18 (4.2)	2 (2.9)	16 (4.4)
Other†	13 (3.0)	1 (1.4)	12 (3.3)
Total underlying conditions			
0	115 (26.6)	17 (24.6)	98 (27.0)
1	113 (26.2)	24 (34.8)	89 (24.5)
2	93 (21.5)	10 (14.5)	83 (22.9)
≥3	111 (25.7)	18 (26.1)	93 (25.6)
Skin injury			
Any skin injury	n = 412*	n = 70*	n = 342*
No	211 (51.2)	36 (51.4)	175 (51.2)
Yes	201 (47.8)	34 (48.6)	167 (48.8)
Type of skin injury‡	n = 201	n = 34	n = 167
Nonsurgical wound	127 (63.2)	22 (64.7)	105 (62.9)
Surgical wound	17 (8.5)	3 (8.8)	14 (8.4)
Trauma§	47 (23.4)	8 (23.5)	39 (23.4)
Burn	2 (1.0)	0	2 (1.2)
Skin breakdown	3 (1.5)	1 (2.9)	2 (1.2)
Other	5 (2.5)	0	5 (3.0)
Behavioral risk factors			
Current cigarette smoking¶	n = 375*	n = 60*	n = 315*
No	310 (82.7)	49 (81.6)	261 (82.9)
Yes	65 (17.3)	11 (18.3)	54 (17.1)
Substance abuse	n = 386*	n = 63*	n = 323*
Alcohol abuse	27 (7.0)	5 (7.9)	22 (6.8)
Methamphetamine use	6 (1.6)	0	6 (1.8)
Injection drug use	8 (2.1)	0	8 (2.5)
None of the above	346 (89.6)	58 (92.1)	288 (89.2)
Other risk factors	n = 389*	n = 66*	n = 323*
Group A *Streptococcus* pharyngitis	31 (8.0)	7 (10.6)	24 (7.4)
Household member with Group A *Streptococcus*	8 (2.1)	2 (3.0)	6 (1.9)
Influenza	12 (3.1)	4 (6.1)	8 (2.5)
None of the above	336 (86.4)	54 (81.8)	282 (87.3)

*Excludes missing data.
†Other underlying conditions include paralysis, neurologic conditions, and developmental delay.
‡Data from 201 cases with a skin injury reported.
§Cut, laceration, or puncture wounds.
¶Does not include e-cigarette use or vaping.

increases. The absence of an identified risk factor contributing to increasing iGAS incidence in the general population suggests a potential role for vaccination as a preventive measure. Ongoing surveillance of state-level iGAS cases would help identify outbreaks, track regional trends in incidence, and monitor circulating *emm* types.

Acknowledgments

We thank epidemiologists from Idaho's 7 public health districts for conducting case investigations, the Idaho Bureau of Laboratories for *emm* typing, clinical diagnostic laboratories for submission of isolates for *emm* typing, and hospital medical records staff for providing requested records. We acknowledge Byron Robinson and Bozena Morawski for advice on statistical analysis and Mayra Vasquez-Alvarez for assistance with data entry. We thank Kristine Bisgard for providing feedback on the manuscript, and Dennis Stevens and Amy Bryant for helpful discussions.

About the Author

Dr. Dunne is a microbiologist and epidemiologist whose research interests include streptococcal diseases, respiratory infections, and immunization. She was formerly a CDC Epidemic Intelligence Service officer assigned to the Idaho Department of Health and Welfare and currently works for Pfizer.

References

1. Centers for Disease Control and Prevention. 2019. Active Bacterial Core Surveillance report. Emerging infections program network group A *Streptococcus*, 2019 [cited 2021 Sep 19] https://www.cdc.gov/abcs/downloads/GAS_Surveillance_Report_2019.pdf
2. Bessen DE. Molecular basis of serotyping and the underlying genetic organization of *Streptococcus pyogenes*. 2016 Feb 10 [updated 2016 Mar 25]. In: Ferretti JJ, Stevens DL, Fischetti VA, editors. *Streptococcus pyogenes*: basic biology to clinical manifestations. Oklahoma City, Oklahoma, USA: University of Oklahoma Health Sciences Center; 2016. https://www.ncbi.nlm.nih.gov/books/NBK333428/
3. Nelson GE, Pondo T, Toews KA, Farley MM, Lindegren ML, Lynfield R, et al. Epidemiology of invasive group A streptococcal infections in the United States, 2005–2012. Clin Infect Dis. 2016;63:478–86. https://doi.org/10.1093/cid/ciw248
4. Factor SH, Levine OS, Schwartz B, Harrison LH, Farley MM, McGeer A, et al. Invasive group A streptococcal disease: risk factors for adults. Emerg Infect Dis. 2003;9:970–7. https://doi.org/10.3201/eid0908.020745
5. Langley G, Hao Y, Pondo T, Miller L, Petit S, Thomas A, et al. The impact of obesity and diabetes on the risk of disease and death due to invasive group A *Streptococcus* infections in adults. Clin Infect Dis. 2016;62:845–52. https://doi.org/10.1093/cid/civ1032
6. Steer AC, Lamagni T, Curtis N, Carapetis JR. Invasive group a streptococcal disease: epidemiology, pathogenesis and management. Drugs. 2012;72:1213–27. https://doi.org/10.2165/11634180-000000000-00000
7. Valenciano SJ, Onukwube J, Spiller MW, Thomas A, Como-Sabetti K, Schaffner W, et al. Invasive group A streptococcal infections among people who inject drugs and people experiencing homelessness in the United States, 2010–2017. Clin Infect Dis. 2021;73:e3718–26. https://doi.org/10.1093/cid/ciaa787
8. Factor SH, Levine OS, Harrison LH, Farley MM, McGeer A, Skoff T, et al. Risk factors for pediatric invasive group A streptococcal disease. Emerg Infect Dis. 2005;11:1062–6. https://doi.org/10.3201/eid1107.040900
9. Jordan HT, Richards CL Jr, Burton DC, Thigpen MC, Van Beneden CA. Group A streptococcal disease in long-term care facilities: descriptive epidemiology and potential control measures. Clin Infect Dis. 2007;45:742–52. https://doi.org/10.1086/520992
10. Carapetis JR, Steer AC, Mulholland EK, Weber M. The global burden of group A streptococcal diseases. Lancet Infect Dis. 2005;5:685–94. https://doi.org/10.1016/S1473-3099(05)70267-X
11. Vekemans J, Gouvea-Reis F, Kim JH, Excler JL, Smeesters PR, O'Brien KL, et al. The path to group A *Streptococcus* vaccines: World Health Organization research and development technology roadmap and preferred product characteristics. Clin Infect Dis. 2019;69:877–83. https://doi.org/10.1093/cid/ciy1143
12. Centers for Disease Control and Prevention. ABCs bact facts interactive data dashboard [cited 2022 Feb 21]. https://www.cdc.gov/abcs/bact-facts-interactive-dashboard.html
13. Tyrrell GJ, Fathima S, Kakulphimp J, Bell C. Increasing rates of invasive group A streptococcal disease in Alberta, Canada; 2003–2017. Open Forum Infect Dis. 2018;5:ofy177. https://doi.org/10.1093/ofid/ofy177
14. Meehan M, Murchan S, Bergin S, O'Flanagan D, Cunney R. Increased incidence of invasive group A streptococcal disease in Ireland, 2012 to 2013. Euro Surveill. 2013;18:20556. https://doi.org/10.2807/1560-7917.ES2013.18.33.20556
15. Oliver J, Wilmot M, Strachan J, St George S, Lane CR, Ballard SA, et al. Recent trends in invasive group A *Streptococcus* disease in Victoria. Commun Dis Intell (2018). 2019;43:43. https://doi.org/10.33321/cdi.2019.43.8
16. Williamson DA, Morgan J, Hope V, Fraser JD, Moreland NJ, Proft T, et al. Increasing incidence of invasive group A *streptococcus* disease in New Zealand, 2002-2012: a national population-based study. J Infect. 2015;70:127–34. https://doi.org/10.1016/j.jinf.2014.09.001
17. Valenciano SJ, McMullen C, Torres S, Smelser C, Matanock A, Van Beneden C. Identifying risk behaviors for invasive group A *Streptococcus* infections among persons who inject drugs and persons experiencing homelessness—New Mexico, May 2018. MMWR Morb Mortal Wkly Rep. 2019;68:205–6. https://doi.org/10.15585/mmwr.mm6808a5
18. Mosites E, Frick A, Gounder P, Castrodale L, Li Y, Rudolph K, et al. Outbreak of invasive infections from subtype *emm*26.3 group A *Streptococcus* among homeless adults—Anchorage, Alaska, 2016–2017. Clin Infect Dis. 2018;66:1068–74. https://doi.org/10.1093/cid/cix921
19. Engelthaler DM, Valentine M, Bowers J, Pistole J, Driebe EM, Terriquez J, et al. Hypervirulent *emm*59 clone in invasive group A *Streptococcus* outbreak, southwestern United States. Emerg Infect Dis. 2016;22:734–8. https://doi.org/10.3201/eid2204.151582
20. Chochua S, Metcalf BJ, Li Z, Rivers J, Mathis S, Jackson D, et al. Population and whole genome sequence based

characterization of invasive group A streptococci recovered in the United States during 2015. MBio. 2017;8:e01422–17. https://doi.org/10.1128/mBio.01422-17
21. Li Y, Rivers J, Mathis S, Li Z, Velusamy S, Nanduri SA, et al. Genomic surveillance of *Streptococcus pyogenes* strains causing invasive disease, United States, 2016–2017. Front Microbiol. 2020;11:1547. https://doi.org/10.3389/fmicb.2020.01547
22. Idaho Department of Health and Welfare, Division of Public Health, Bureau of Vital Records and Health Statistics. Idaho vital statistics—population 2018. [cited 2021 Sep 19] https://publicdocuments.dhw.idaho.gov/WebLink/DocView.aspx?id=8151&dbid=0&repo=PUBLIC-DOCUMENTS
23. Centers for Disease Control and Prevention. Active Bacterial Core surveillance report, Emerging Infections Program Network, group A *Streptococcus*, 2008 [cited 2021 Sep 19]. https://www.cdc.gov/abcs/reports-findings/survreports/gas08.html
24. Close RM, McAuley JB. Disparate effects of invasive group A *Streptococcus* on Native Americans. Emerg Infect Dis. 2020;26:1971–7. https://doi.org/10.3201/eid2609.181169
25. Tyrrell GJ, Bell C, Bill L, Fathima S. Increasing incidence of invasive group A *Streptococcus* disease in First Nations population, Alberta, Canada, 2003–2017. Emerg Infect Dis. 2021;27:443–51. https://doi.org/10.3201/eid2702.201945
26. Nanduri SA, Onukwube J, Apostol M, Alden N, Petit S, Farley M, et al. Challenges in surveillance for streptococcal toxic shock syndrome: Active Bacterial Core Surveillance, United States, 2014–2017. Public Health Rep. 2022;137:687–94. https://doi.org/10.1177/00333549211013460
27. de Gier B, Vlaminckx BJM, Woudt SHS, van Sorge NM, van Asten L. Associations between common respiratory viruses and invasive group A streptococcal infection: A time-series analysis. Influenza Other Respir Viruses. 2019;13:453–8. https://doi.org/10.1111/irv.12658
28. Gherardi G, Vitali LA, Creti R. Prevalent *emm* types among invasive GAS in Europe and North America since year 2000. Front Public Health. 2018;6:59. https://doi.org/10.3389/fpubh.2018.00059
29. Steer AC, Law I, Matatolu L, Beall BW, Carapetis JR. Global *emm* type distribution of group A streptococci: systematic review and implications for vaccine development. Lancet Infect Dis. 2009;9:611–6. https://doi.org/10.1016/S1473-3099(09)70178-1
30. Boukthir S, Moullec S, Cariou ME, Meygret A, Morcet J, Faili A, et al. A prospective survey of *Streptococcus pyogenes* infections in French Brittany from 2009 to 2017: Comprehensive dynamic of new emergent *emm* genotypes. PLoS One. 2020;15:e0244063. https://doi.org/10.1371/journal.pone.0244063
31. Pastural É, McNeil SA, MacKinnon-Cameron D, Ye L, Langley JM, Stewart R, et al. Safety and immunogenicity of a 30-valent M protein-based group a streptococcal vaccine in healthy adult volunteers: A randomized, controlled phase I study. Vaccine. 2020;38:1384–92. https://doi.org/10.1016/j.vaccine.2019.12.005
32. Dale JB, Walker MJ. Update on group A streptococcal vaccine development. Curr Opin Infect Dis. 2020;33:244–50. https://doi.org/10.1097/QCO.0000000000000644
33. Shulman ST, Tanz RR, Dale JB, Steer AC, Smeesters PR. Added value of the *emm*-cluster typing system to analyze group A *Streptococcus* epidemiology in high-income settings. Clin Infect Dis. 2014;59:1651–2. https://doi.org/10.1093/cid/ciu649
34. Meehan M, Murchan S, Gavin PJ, Drew RJ, Cunney R. Epidemiology of an upsurge of invasive group A streptococcal infections in Ireland, 2012-2015. J Infect. 2018;77:183–90. https://doi.org/10.1016/j.jinf.2018.05.010
35. Fay K, Onukwube J, Chochua S, Schaffner W, Cieslak P, Lynfield R, et al. Patterns of antibiotic nonsusceptibility among invasive group A *Streptococcus* infections—United States, 2006–2017. Clin Infect Dis. 2021;73:1957–64. https://doi.org/10.1093/cid/ciab575
36. Fittipaldi N, Beres SB, Olsen RJ, Kapur V, Shea PR, Watkins ME, et al. Full-genome dissection of an epidemic of severe invasive disease caused by a hypervirulent, recently emerged clone of group A *Streptococcus*. Am J Pathol. 2012;180:1522–34. https://doi.org/10.1016/j.ajpath.2011.12.037

Address for correspondence: Kris K. Carter, Idaho Department of Health and Welfare, Division of Public Health, 450 W State St, 4th Fl, Boise, ID 83702, USA; email: Kris.Carter@dhw.idaho.gov

Revised Definitions of Tuberculosis Resistance and Treatment Outcomes, France, 2006–2019

Yousra Kherabi, Mathilde Fréchet-Jachym, Christophe Rioux, Yazdan Yazdanpanah, Frédéric Méchaï, Valérie Pourcher, Jérôme Robert, Lorenzo Guglielmetti, for the MDR-TB Management Group

Definitions of resistance in multidrug-resistant tuberculosis (MDR TB) and extensively drug-resistant tuberculosis (XDR TB) have been updated. Pre–XDR TB, defined as MDR TB with additional resistance to fluoroquinolones, and XDR TB, with additional resistance to bedaquiline or linezolid, are frequently associated with treatment failure and toxicity. We retrospectively determined the effects of pre-XDR/XDR TB resistance on outcomes and safety of MDR TB treatment in France. The study included 298 patients treated for MDR TB at 3 reference centers during 2006–2019. Of those, 205 (68.8%) cases were fluoroquinolone-susceptible MDR TB and 93 (31.2%) were pre-XDR/XDR TB. Compared with fluoroquinolone-susceptible MDR TB, pre-XDR/XDR TB was associated with more cavitary lung lesions and bilateral disease and required longer treatment. Overall, 202 patients (67.8%) had favorable treatment outcomes, with no significant difference between pre-XDR/XDR TB (67.7%) and fluoroquinolone-susceptible MDR TB (67.8%; p = 0.99). Pre-XDR/XDR TB was not associated with higher risk for serious adverse events.

Rifampin-resistant tuberculosis (RR TB) and multidrug-resistant tuberculosis (MDR TB), defined as TB resistant to both rifampin and isoniazid, are a global public health threat. In 2019, there were 465,000 incident cases of RR TB, among which 78% were MDR TB (*1*). In France, the yearly incidence of MDR TB cases was stable at ≈50 cases during 2006–2010, dramatically increased in the next 4 years (*2*) to >100 cases in 2014 (*3*), and slightly decreased afterwards to 75 cases in 2019 (*4*).

RR/MDR TB cases are difficult to treat, and patients need prolonged treatment courses, which are burdened by frequent drug-related adverse events. Global treatment success for RR/MDR TB was 59% in 2018 (*1*). At that time, fluoroquinolones were considered the cornerstone of RR/MDR TB treatment. In 2018, the World Health Organization (WHO) published new treatment guidelines, relying on a large-scale meta-analysis (*5*), which revolutionized the traditional hierarchy of anti-TB drugs (*6*). In those guidelines, newer and repurposed drugs, such as bedaquiline and linezolid, were recommended for all MDR TB patients in addition to fluoroquinolones; second-line injectables would be reserved for cases where no other options are available.

Globally, 16.2% of RR/MDR TB isolates have acquired resistance to fluoroquinolones (*1*), indicating the need for an update in resistance definitions. Thus, in January 2021, WHO defined pre–extensively drug-resistant TB (pre-XDR TB) as MDR TB with additional resistance to fluoroquinolones, and XDR TB as pre-XDR TB with additional resistance to ≥1 additional group A drug (bedaquiline and linezolid as of July 2022) (*7*).

Resistance to fluoroquinolones is classically considered a risk factor for treatment failure (*5*,*8*,*9*). However, recent studies from countries with both low (*10*) and high (*11*) TB prevalence did not confirm this finding in high-income settings in which diagnostics and group A drugs are widely available. Furthermore,

Author affiliations: Assistance Publique Hôpitaux de Paris, Hôpital Bichat-Claude Bernard, Paris, France (Y. Kherabi, C. Rioux, Y. Yazdanpanah); Sorbonne Université, INSERM U1135, Paris (Y. Kherabi, J. Robert, L. Guglielmetti); Centre Hospitalier de Bligny, Briis-sous-Forges, France (M. Frechet-Jachym); Assistance Publique—Hopitaux de Paris, Paris (C. Rioux, Y. Yazdanpanah); INSERM U1137, IAME, Université de Paris, Paris (Y. Yazdanpanah); Universite Paris Diderot, Paris (Y. Yazdanpanah); Assistance Publique Hôpitaux de Paris, Hôpital Avicenne, Paris (F. Méchaï); Hopital Avicenne, Bobigny, France (F. Méchaï); Assistance Publique Hôpitaux de Paris, Hôpital Pitié-Salpêtrière, Paris (V. Pourcher); Assistance Publique Hôpitaux de Paris, Sorbonne-Université, Hôpital Pitié-Salpêtrière, Paris (J. Robert, L. Guglielmetti)

DOI: https://doi.org/10.3201/eid2809.220458

evidence on the effect of fluoroquinolone resistance on treatment safety is scarce (*11*).

We assessed whether pre-XDR TB and XDR TB status (i.e., additional resistance to any fluoroquinolone) affected outcomes and safety of MDR TB treatment for TB in France, a high-income, low TB incidence country. The Institutional Review Board of the Bligny Hospital (Briis-sous-Forges, France) granted ethical clearance (CRE 2021 08).

Methods

Study Design and Participants

In this retrospective observational cohort study, we included all consecutive MDR TB patients confirmed at the French National Reference Center for Mycobacteria (NRC; Paris, France) who initiated treatment at 3 referral hospitals (Bligny, in Briis-sous-Forges, and Pitié-Salpêtrière and Bichat-Claude Bernard, both in Paris) during January 1, 2006–December 31, 2019. Patients were followed up for 2 years after the end of treatment. We considered only the first episode of MDR TB within the study period. We retrieved the latest data on December 31, 2021.

We reviewed medical records to retrieve demographic and clinical features, as well as results of laboratory, radiographic, and microbiological tests. We extracted routinely collected data from medical records and anonymized the data; the investigator who extracted data was not involved in patient care. We obtained comprehensive drug susceptibility testing (DST) profiles from the database of the NRC laboratory.

Definitions

We performed phenotypic DST at the NRC using the Löwenstein–Jensen proportion method (*12*). We obtained genotypic DST through commercially available line-probe assays (GenoType MTBDRplus and GenoType MTBDRs; Hain Lifescience, https://www.hain-lifescience.de) or targeted DNA sequencing. We used new definitions of drug-resistant TB (*7*): we defined MDR TB as TB resistant to isoniazid and rifampin, pre-XDR TB as MDR TB with resistance to any fluoroquinolone, and XDR TB as MDR TB with additional resistance to any fluoroquinolone and another WHO group A drug (bedaquiline or linezolid). We classified patients as new or previously treated according to WHO definitions. Sputum smear and cultures were routinely performed at treatment start, every 14 days until culture conversion, and monthly thereafter. We defined sputum culture conversion as 2 consecutive negative cultures collected at least 30 days apart. We defined treatment outcomes using 2020 WHO definitions (*13*). Of note, we defined treatment outcome as not evaluated for patients for whom no treatment outcome was assigned; this definition includes cases transferred out to another treatment unit and those whose treatment outcome was unknown but excludes those who did not attend follow-up appointments and did not respond to attempted contact from clinical staff, which we categorized as lost to follow-up.

Treatment Regimens

Throughout the study period, treatment regimens were designed in accordance with WHO treatment guidelines and in consultation with the French MDR TB Consilium, a multidisciplinary team coordinated by the France NRC (*14*–*17*). Of note, linezolid has been used for MDR TB treatment in France since 2006 and bedaquiline since 2011. Drugs were considered to be part of the treatment regimen if they were administered for ≥30 days.

Outcomes

The primary study outcome was the proportion of treatment success (defined as the sum of cured and treatment completed). Secondary outcomes were time to sputum culture conversion and proportion of treatment-emergent serious adverse events (SAE), as defined by the US Food and Drug Administration (*18*).

Statistical Analysis

Sample Size

Based on NRC surveillance data for the period under review, we estimated that ≈300 MDR TB patients, 200 with fluoroquinolone-susceptible MDR TB and 100 with pre-XDR/XDR TB, could be included. Taking into account the results of a large meta-analysis comparing MDR TB treatment outcomes according to different resistance patterns (*5*), we estimated a relative risk of 1.59 for an unfavorable treatment outcome in pre-XDR/XDR TB compared with fluoroquinolone-susceptible MDR TB cases. With these assumptions, the expected sample size would provide a power of 93% with a 2-sided α risk of 2.5% to detect a difference between the 2 groups.

Statistical Methods

We collected the extracted data on standardized forms, entered them into a database located at the NRC, and ran analyses using Stata version 16 (StataCorp, https://www.stata.com). We performed sensitivity analyses focusing on patients

Table 1. Characteristics and demographics of patients affected by MDR TB, France, 2006–2019*

Characteristic	Total, N = 298	TB resistance status		p value
		MDR, n = 205	Pre-XDR/XDR, n = 93	
Median age, y (IQR)	34 (27–42)	33 (27–42)	36 (28–42)	NS
Sex				
M	202 (67.8)	130 (63.4)	72 (77.4)	0.02
F	96 (32.2)	75 (36.6)	(22.6)	
WHO Region place of birth				<0.001
Europe	162 (54.6)	85 (41.7)	77 (82.8)	
Africa	95 (32.0)	85 (41.7)	10 (10.8)	
South-East Asia	23 (7.7)	20 (9.8)	3 (3.2)	
Others	18 (6.0)	15 (7.3)	3 (3.2)	
Precarious housing or homeless	177 (59.6)	105 (51.5)	72 (77.4)	<0.001
Past imprisonment	22 (7.4)	7 (3.3)	15 (16.1)	<0.001
Comorbidities				
HIV infection	29 (9.8)	20 (9.8)	9 (9.8)	NS
HBV infection	21 (7.1)	13 (6.4)	8 (8.7)	NS
HCV infection	46 (15.5)	17 (8.3)	29 (31.2)	<0.001
Immunosuppressive condition	14 (4.8)	8 (4.0)	6 (6.5)	NS
Immunosuppressive treatment	8 (2.7)	6 (2.9)	2 (2.1)	NS
Diabetes	13 (4.4)	9 (4.4)	4 (4.3)	NS
Psychiatric disorder	23 (7.7)	10 (4.9)	13 (14.0)	<0.001
Albumin, median, g/L (IQR)	34 (31–38)	35 (31–39)	33 (30–37)	NS
BMI, median, kg/m^2 (IQR)	20.1 (18.4–22.2)	20.2 (18.6–22.3)	19.8 (17.9–21.9)	NS
Previous TB treatment	159 (53.5)	90 (44.1)	69 (74.2)	<0.001
Previous TB treatment with second-line drugs	89 (45.2)	35 (28.9)	54 (71.1)	<0.001
Other risk factors				
Alcohol abuse	37 (12.5)	20 (9.8)	17 (18.3)	0.002
Active smoking	103 (34.7)	54 (26.5)	49 (52.7)	<0.001
IVDU	44 (14.8)	17 (8.3)	27 (29.0)	<0.001

*Values are presented as no. (%), unless indicated otherwise. BMI, body-mass index; IQR, interquartile range; IVDU, intravenous drug use; MDR, multidrug resistant (susceptible to all fluoroquinolones); NS, not statistically significant; pre-XDR/XDR = pre–extensively drug resistant/extensively drug resistant, (resistant to ≥1 fluoroquinolone); TB, tuberculosis; WHO, World Health Organization.

treated after 2011, the year bedaquiline was introduced in France.

For descriptive statistics, we reported continuous variables as medians with interquartile range (IQR) and compared them using the Wilcoxon rank-sum test or 2-sample t-test, as appropriate. We reported categorical variables as frequencies with percentages and compared using the Fisher exact test or χ^2 test, as appropriate. A 2-sided $\alpha<0.05$ was considered statistically significant. Because the cohort included few XDR TB patients, we performed most analyses by grouping together pre-XDR TB and XDR TB cases.

To identify risk factors associated to the dependent categorical variables (treatment success and SAE), we fitted unconditional logistic regression models. We included explanatory variables in the initial models if associated with the dependent variable at $p<0.20$ in univariate analysis. We then performed backward analysis: we kept explanatory variables associated with the dependent variable that had $p<0.20$, in addition to the variable of interest (pre-XDR/XDR TB), in the model.

As secondary objectives, we performed survival analyses to describe time from treatment start to sputum culture conversion (for patients with positive sputum cultures at treatment start) and unfavorable treatment outcome (for all patients). We estimated Kaplan-Meier curves and performed log-rank tests to assess the effects of pre-XDR/XDR TB. We fitted multivariable Cox proportional-hazard models to identify predictive factors of sputum culture conversion. We included variables into multivariable Cox proportional hazards models if they predicted the outcome at $p\leq0.20$ in univariate analysis and if they fulfilled the proportional hazards assumption at baseline or, if appropriate, after addition of a time interaction. We reported hazard ratios with 95% CI.

For both logistic regression and Cox models, we performed complete case analyses to identify the variables included in the model and then imputed missing data with multiple imputation using chained equations with 10 imputed datasets. Overall, the proportion of missing observations in the included variables was 0%–9%.

Results

Population Characteristics

The study population was made up of 298 MDR TB patients, including 84 (28.2%) with pre-XDR TB and 9 (3.0%) with XDR TB. Sixty-six patients (22.1%) were treated during 2006–2010 and 232 (77.9%) during 2011–2019. The median age at admission was 34 years (IQR 27–42), and 202 (67.8%) patients were male. Patients were mainly born in the WHO Europe region

(54.6%) (Table 1). Pre-XDR/XDR TB patients were more frequently born in the WHO Europe region; had more frequently precarious housing, past imprisonment history, and active drug abuse (alcohol, smoking, intravenous drugs); and had more severe pulmonary tuberculosis, including cavitary lesions and bilateral disease. Patients with pre-XDR/XDR TB more frequently had additional resistance to cycloserine, second-line injectables, pyrazinamide, and P-aminosalicylic acid.

Treatment and Outcomes

Overall, 94.3% patients were treated with ≥1 group A drug (levofloxacin, moxifloxacin, bedaquiline, or linezolid) and 76.8% with ≥1 group B drug (clofazimine or cycloserine). Linezolid (89.3% vs. 69.8%, p<0.001) and bedaquiline (74.2% vs. 28.3%, p<0.001) were more frequently used in pre-XDR/XDR TB cases. A large part of our study population received second-line injectables (85.2%), including similar proportions in the 2 groups of interest (81.7% vs. 86.8%). Total treatment duration was longer in pre-XDR/XDR TB patients (median 21.2 months vs. 17.3 months; p<0.001) (Table 2).

Overall, 202 patients (67.8%) had treatment success, including cure (62.1%) and treatment completion (5.7%) (Table 3). Ninety-six patients (32.2%) had unfavorable or other outcomes. Of those, 3 patients had treatment failure and 5 died; 54 were lost to follow-up, and 34 did not have treatment outcomes evaluated (Table 3). Of note, 67.9% of patients with pre-XDR TB and 66.7% patients with XDR TB had treatment success. For the 5 patients who died during TB treatment, causes of death were malignancy progression (2 patients), septic shock (urinary tract sepsis for 1 patient and disseminated candidemia for 1 patient), and decompensated cirrhosis (1 patient). Among patients with treatment success, 145 (71.8%) were followed up to 12 months after end of treatment and 129 (63.9%) up to 24 months. Two patients with pre-XDR/XDR TB relapsed in the first year and 1 in the second year of follow-up after end of treatment.

Table 2. Baseline disease characteristics for 298 patients affected by MDR TB, France, 2006–2019*

Characteristic	Total, N = 298	TB resistance status		p value
		MDR, n = 205	Pre-XDR/XDR, n = 93	
TB characteristics				
Pulmonary tuberculosis	272 (91.6)	179 (87.8)	93 (100)	0.002
Bilateral lung involvement, n = 233	174 (74.7)	100 (71.0)	74 (86.0)	0.009
Cavitary lung disease, n = 224	156 (69.6)	82 (59.4)	74 (86.0)	<0.001
Miliary TB	11 (3.8)	8 (4.0)	3 (3.2)	NS
Sputum smear positive†	202 (68.0)	118 (57.8)	84 (90.3)	<0.001
Sputum culture positive†	214 (71.8)	132 (64.4)	82 (88.2)	<0.001
Extrapulmonary TB	83 (28.1)	69 (34.0)	14 (15.2)	0.003
Additional drug resistance				
Any second-line injectable, n = 287‡	83 (28.9)	32 (16.3)	51 (56.0)	<0.001
Linezolid, n = 260	5 (1.9)	1 (0.6)	4 (4.5)	NS
Bedaquiline, n = 101	6 (5.9)	0	6 (19.4)	<0.001
Linezolid and/or bedaquiline, n = 260	10 (3.8)	1 (0.6)	9 (10.1)	<0.001
Pyrazinamide, n = 183	109 (59.6)	65 (49.6)	44 (84.6)	<0.001
Ethambutol, n = 287	177 (61.7)	104 (53.1)	73 (80.2)	<0.001
Ethionamide or prothionamide, n = 276	175 (63.4)	113 (60.1)	62 (70.5)	NS
Cycloserine, n = 279	70 (25.1)	26 (13.6)	44 (50.0)	<0.001
P-aminosalicylic acid, n = 262	33 (20.4)	17 (9.6)	16 (18.8)	0.04
Delamanid, n = 26	2 (7.7)	1 (5.3)	1 (14.3)	NS
Anti-TB treatment				
Treatment regimens				
Fluoroquinolones	218 (73.2)	182 (88.8)	36 (38.7)	<0.001
Levofloxacin	56 (18.8)	43 (21.0)	13 (14.0)	NS
Moxifloxacin 400 mg/day	187 (62.8)	167 (81.5)	20 (21.5)	<0.001
Moxifloxacin 800 mg/day	14 (4.7)	3 (1.4)	11 (11.8)	<0.001
Linezolid	226 (75.8)	143 (69.8)	83 (89.3)	<0.001
Bedaquiline	127 (42.6)	58 (28.3)	69 (74.2)	<0.001
Total treatment duration, mo, median (IQR), n = 228	17.8 (13.4–20.6)	17.3 (13.1–18.1)	21.2 (16.7–24.0)	<0.001
Duration of treatment with second-line injectable, median mo (IQR), n = 220	4.7 (3.0–7.1)	3.9 (3.0–5.5)	7.7 (4.7–14.0)	NS
Lung surgery	27 (9.9)	8 (4.4)	19 (20.9)	<0.001
Good treatment adherence§	232 (78.4)	161 (79.3)	71 (76.3)	NS

*Values are no. (%) except as indicated. IQR, interquartile range; MDR, multidrug resistant (susceptible to all fluoroquinolones); NS, not statistically significant; pre-XDR/XDR, pre–extensively drug resistant/extensively drug resistant, (resistant to ≥1 fluoroquinolone); TB, tuberculosis; WHO, World Health Organization.
†At treatment start.
‡Amikacin, capreomycin, or kanamycin.
§Assessed by treating physician.

Table 3. Tuberculosis treatment outcomes of patients affected by MDR TB, France, 2006–2019*

Characteristic	Total, N = 298	TB resistance status		p value
		MDR, n = 205	Pre-XDR/XDR, n = 93	
Treatment success	202 (67.8)	139 (67.8)	63 (67.7)	NS
Cure	185 (62.1)	126 (61.5)	59 (63.4)	NS
Treatment completed	17 (5.7)	13 (6.3)	4 (4.3)	NS
Sustained treatment success at 12 mo†, n = 145	143 (98.6)	101 (100)	42 (95.5)	NS
Treatment failure	3 (1.0)	1 (0.5)	2 (2.2)	NS
Others	93 (31.2)	65 (31.7)	28 (30.1)	NS
Died	5 (1.7)	2 (1.0)	3 (3.2)	NS
Lost to follow-up‡	54 (18.1)	36 (17.6)	18 (19.4)	NS
Not evaluated	34 (11.4)	27(13.2)	7 (7.5)	NS
Days to sputum culture conversion, n = 198§ (IQR)	60 (38–90)	50 (31–73)	88 (51–108)	<0.001

*Values are no (%) except as indicated. IQR, interquartile range; MDR, multidrug resistant (susceptible to all fluoroquinolones); NS, not statistically significant; pre-XDR/XDR = pre–extensively drug resistant/extensively drug resistant, (resistant to ≥1 fluoroquinolone); TB, tuberculosis.
†Among patients with treatment success at end of treatment.
‡These patients did not attend follow-up appointments and did not respond to attempted contact from clinical staff.
§Among patients with a positive sputum culture at treatment start.

One patient with fluoroquinolone-susceptible MDR TB relapsed in the second year of follow-up.

Predictors of Treatment Outcome

Multivariable analysis showed that pre-XDR/XDR TB status was not independently associated with treatment outcome (adjusted odds ratio [aOR] 0.81, 95% CI 0.47–1.41); conversely, previous anti-TB treatment (aOR 1.80, 95% CI 1.13–2.89) and poor treatment adherence (aOR 1.19, 95% CI 1.07–1.33) were independently associated with unfavorable treatment outcome (Table 4). Multivariable Cox proportional hazard model for unfavorable outcome was consistent with these findings (Appendix Table 2, https://wwwnc.cdc.gov/EID/article/28/9/22-0458-App1.pdf). We confirmed these results by a sensitivity analysis restricting the sample to patients who started treatment during 2011–2019 (Appendix Table 3).

Table 4. Risk factors for unsuccessful outcomes in patients affected by MDR TB, France, 2006–2019*

Characteristic	aOR (95% CI)	p value
TB resistance status		
Fluoroquinolone-susceptible MDR	Referent	
Pre-XDR/XDR	0.81 (0.47–1.41)	0.48
History of anti-TB treatment		
No	Referent	
Yes	2.16 (1.32–3.55)	0.002
Treatment adherence†		
Good	Referent	
Poor	1.21 (1.08–1.35)	0.001
HCV co-infection		
No	Referent	
Yes	0.63 (0.36–1.10)	0.11
Immunosuppression‡		
No	Referent	
Yes	1.56 (0.50–4.89)	0.44
Pulmonary tuberculosis		
No	Referent	
Yes	2.92 (0.90–9.50)	0.07

*We used multivariable logistic regression with multiple imputation for missing data. Results are from the final model. aOR, adjusted odds ratio; MDR, multidrug resistant (susceptible to all fluoroquinolones); NS, not statistically significant; pre-XDR/XDR, pre–extensively drug resistant/extensively drug resistant, (resistant to ≥1 fluoroquinolone); TB, tuberculosis.
†Assessed by treating physician.
‡Immunosuppressive disease and/or immunosuppressive treatment.

Sputum Culture Conversion

Among 214 patients with positive sputum culture at baseline, pre-XDR/XDR TB patients showed longer time to sputum culture conversion than MDR TB patients (median 88 days vs. 50 days; p = 0.001 by log rank test) (Figure 1). Time to sputum culture conversion in XDR TB patients was 114 days (95% CI 60–191 days). In a multivariable Cox proportional hazard model, pre-XDR/XDR TB (adjusted hazard ratio [aHR] 0.59, 95% CI 0.42–0.84) and alcohol abuse (aHR 0.61, 95% CI 0.38–0.99) were independently associated with slower sputum culture conversion (Table 5).

Adverse Drug Reactions

Overall, 152 patients (51.0%) had ≥1 SAE while being treated for MDR TB (Table 6). SAE were more frequent in pre-XDR/XDR TB case-patients than in fluoroquinolone-susceptible MDR TB case-patients (62.4% vs. 45.9%; p = 0.02). Peripheral neuropathy was the most frequent SAE (27.5%), regardless of TB resistance status; in all cases, peripheral neuropathy was attributed to linezolid. Severe ototoxicity occurred more frequently in pre-XDR/XDR TB than in fluoroquinolone-susceptible MDR TB cases (38.7% vs. 20.5%; p = 0.01) (Appendix Table 4); all cases of severe ototoxicity were attributed to amikacin. In multivariable analysis (Table 7), pre-XDR/XDR TB was not independently associated with severe toxicity (aOR 1.31, 95% CI 0.76–2.26; p = 0.34), whereas poor treatment adherence was associated with a higher risk for SAE (aOR 1.24 95% CI 1.04–1.47; p = 0.01).

Discussion

Overall, we did not detect a significant effect of pre-XDR and XDR TB resistance, in accordance with the revised WHO definitions, on treatment outcomes of MDR TB in France during 2006–2019. The global treatment success proportion in MDR TB patients was 67.8%; previous TB treatment and poor treatment adherence were each independently associated with unfavorable outcome. Pre-XDR/XDR TB patients showed longer time to sputum culture conversion compared with fluoroquinolone-susceptible MDR TB. Pre-XDR/XDR TB resistance status was not independently associated with higher risk for SAEs.

In the literature, pre-XDR/XDR TB has been consistently associated with treatment failure (*19*–*22*). Indeed, in a meta-analysis published by Ahmad et al., the pooled successful treatment proportion for fluoroquinolone-susceptible MDR TB was estimated at 62%–73%, whereas that of pre-XDR/XDR TB was 51%–57% during the same period (2009–2016) (*5*). However, MDR/XDR TB treatment outcomes have improved with the introduction of bedaquiline and delamanid (*23*–*25*), together with repurposed TB drugs such as linezolid, clofazimine, and carbapenems (*26*–*29*). In our cohort, treatment success proportions were comparable between fluoroquinolone-susceptible MDR TB, pre-XDR TB, and XDR TB patients. These results are consistent with previous studies from high-income countries such as Italy (*10*) and South Korea (*11*). In those countries, as in France, these results may be explained by the routine availability of rapid molecular testing, therapeutic drug monitoring, newer and repurposed drugs, and treatment design in consultation with a MDR TB consilium (*16*,*17*,*30*).

The finding that fluoroquinolone resistance does not affect treatment outcomes reflects the early access and use of new and repurposed drugs in France. However, the proportion of treatment success in our cohort (67.8%) may appear low compared with clinical trials, which usually achieve >80% success (*31*,*32*). A likely explanation is the high proportion of lost-to-follow-up (18.1%) and nonevaluated (11.4%) outcomes, which account for 92% of all unfavorable outcomes in our real-world cohort. This reasoning is consistent with previous findings showing that even high-income settings have room to improve with respect to supports provided to MDR TB patients (*33*), especially when a high proportion is not locally born and may not be permanent residents.

In our study, pre-XDR/XDR TB was associated with substantially longer time to sputum culture conversion than was fluoroquinolone-susceptible MDR TB. However, the difference did not affect treatment outcomes; this finding is consistent with previous studies in which time to culture conversion was not a good predictor of treatment outcome (*34*,*35*). In our study, the pre-XDR/XDR TB and fluoroquinolone-susceptible MDR TB populations were very different. Indeed, pre-XDR/XDR TB patients had more severe TB pulmonary disease, as previously reported (*10*,*11*). In addition, social indicators of precarity and psychiatric disorders were more frequently observed in the pre-XDR/XDR TB population. Despite these differences in baseline characteristics that we expected to cause worse outcome in pre-XDR/XDR TB patients, fluoroquinolone-resistant MDR TB patients yielded treatment success rate similar to that of fluoroquinolone-susceptible MDR TB patients, and pre-XDR/XDR TB resistance was not independently associated with unfavorable treatment outcomes.

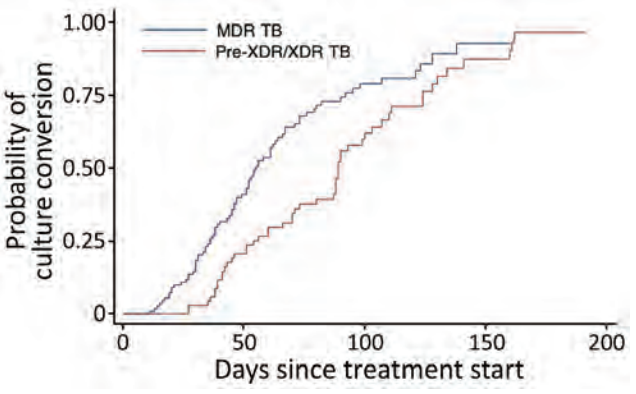

Figure. Kaplan–Meier curves of sputum time to culture conversion in fluoroquinolone-susceptible MDR TB and pre-XDR/XDR TB patients (log rank test p = 0.001). MDR, multidrug resistant (susceptible to all fluoroquinolones); pre-XDR/XDR, pre–extensively drug resistant/extensively drug resistant (resistant to >1 fluoroquinolone); TB, tuberculosis.

Table 5. Multivariable Cox proportional hazard model for sputum conversion in 214 patients affected by MDR TB and with positive sputum culture at baseline, France, 2006–2019*

Characteristic	aHR (95% CI)	p value
TB resistance status		
Fluoroquinolone-susceptible MDR	Referent	
Pre-XDR/XDR	0.59 (0.42–0.84)	0.003
Diabetes		
No	Referent	
Yes	1.54 (0.79–2.97)	0.20
Treatment adherence†		
Good	Referent	
Poor	1.40 (0.88–2.25)	0.16
Addiction to alcohol		
No	Referent	
Yes	0.61 (0.38–0.99)	0.04

*We used multiple imputation for missing data. Results are from the final model. aHR, adjusted hazard ratio.
†Assessed by treating physician.

Table 6: Serious adverse events of 298 patients affected by MDR TB, France, 2006–2019*

Characteristic	Total, N = 298	TB resistance status		p value
		MDR, n = 205	Pre-XDR/XDR, n = 93	
Serious adverse events	152 (51.0)	94 (45.9)	58 (62.4)	0.02
Event type				
Peripheral neuropathy	82 (27.5)	50 (24.4)	32 (34.4)	NS
Ototoxicity	78 (26.2)	42 (20.5)	36 (38.7)	0.001
Gastrointestinal	39 (13.1)	26 (12.7)	16 (17.2)	NS
Hepatotoxicity	35 (11.7)	27 (13.2)	8 (8.6)	NS
Hematologic abnormalities	29 (9.7)	17 (8.3)	12 (13.0)	NS
Anemia	20 (6.7)	12 (5.9)	8 (8.6)	NS
Thrombocytopenia	11 (3.7)	5 (2.4)	6 (6.5)	NS
Neutropenia	6 (2.0)	4 (2.0)	2 (2.2)	NS
Musculoskeletal pain	24 (8.1)	20 (9.8)	4 (4.3)	NS
Tendinopathy	10 (3.4)	9 (4.4)	1 (1.1)	NS
Arthralgia	15 (5.0)	12 (5.9)	3 (3.2)	NS
Psychiatric	18 (6.0)	12 (5.9)	6 (6.5)	NS
Renal toxicity	17 (5.7)	14 (6.8)	3 (3.2)	NS
Optic neuritis	10 (3.4)	5 (2.4)	5 (5.4)	NS
Hypothyroidism	9 (3.0)	6 (2.9)	3 (3.2)	NS
QT prolongation	8 (2.7)	4 (2.0)	4 (4.3)	NS
Other	14 (4.7)	4 (2.0)	10 (10.8)	NS

*Values are no (%) except as indicated. MDR, multidrug resistant (susceptible to all fluoroquinolones); NS, not statistically significant; QT, QT interval on electrocardiogram; pre-XDR/XDR, pre–extensively drug resistant/extensively drug resistant, (resistant to ≥1 fluoroquinolone); TB, tuberculosis.

Our study also highlights that the revised definition of XDR TB concerns a limited number of patients in France, as previously reported (*36*). Indeed, only 9 patients >14 years of age, corresponding to 3% of the total MDR TB patients, could be classified as XDR TB in our cohort. The small number of patients affected by XDR TB prevented us from performing planned subgroup analyses. Overall, treatment outcome and safety in this group seemed comparable with other MDR TB patients, whereas time to sputum culture conversion was longer.

In multivariable logistic regression, previous TB treatment and poor treatment adherence, but not pre-XDR/XDR TB status, were independently associated with treatment failure. In the literature, numerous risk factors were reported for treatment failure, including age, lower body mass index, history of drug abuse, and comorbidities (*10*,*11*,*37*,*38*). We tested and confirmed the absence of interaction between previous TB treatment and poor treatment adherence before including those variables in multivariable models; however, we could hypothesize that previous treatment that led to poor outcome could be associated with lower adherence to medical visits (i.e., a patient's lack of confidence in treatment after failure of a previous TB treatment).

Table 7. Risk factors for serious adverse events in 298 patients affected by MDR TB, France, 2006–2019*

Characteristic	aOR (95% CI)	p value
TB resistance status		
Fluroroquinolone-susceptible MDR	Referent	
Pre-XDR/XDR	1.31 (0.76–2.26)	0.34
Treatment adherence†		
Good	Referent	
Poor	1.24 (1.04–1.47)	0.01
Past imprisonment		
No	Referent	
Yes	1.15 (0.92–1.44)	0.21
Pulmonary tuberculosis		
No	Referent	
Yes	0.71 (0.47–1.09)	0.18

*We used multivariable logistic regression with multiple imputation for missing data. Results are from the final model. aOR, adjusted odds ratio; MDR, multidrug resistant (susceptible to all fluoroquinolones); pre-XDR/XDR, pre–extensively drug resistant/extensively drug resistant, (resistant to ≥1 fluoroquinolone); TB, tuberculosis.
†Assessed by treating physician.

A strength of our study is that it includes a multivariable evaluation of safety of treatment in fluoroquinolone-susceptible MDR TB compared with pre-XDR/XDR TB (*11*). In univariate analysis, serious adverse events were more frequent in pre-XDR/XDR TB cases than in fluoroquinolone-susceptible MDR TB cases, but this difference was not confirmed in multivariable analysis. The higher proportion of SAE in the pre-XDR/XDR group is likely linked to a longer duration of treatment and to a more frequent use of poorly tolerated drugs, such as linezolid, in this group, as described previously (*39*).

Our analysis had the inherent limitations of retrospective studies; one was the issue of missing data, which we managed using multiple imputation. Overall, the rate of loss to-follow-up was high in our cohort, and we were not able to collect data up to 2 years after end-of-treatment outcome for all patients. Furthermore, we focused on retrieving only SAEs, without considering nonserious adverse events that, for instance, might have compromised treatment adherence. In addition, we included 3 referral centers in the metropolitan Paris area. A large part of the more

complex patients from all areas in France are known to be referred to those 3 centers. Hence, we have a potential bias in extrapolating our conclusions to all cases of MDR TB in France.

In summary, in our cohort of MDR TB patients treated in France during 2006–2019, the proportion of treatment success was only 67.8% because of high rates of patients who did not complete follow-up and unevaluated outcomes. We were unable to detect any differences in success rates between fluoroquinolone-susceptible MDR TB and pre-XDR/XDR TB patients; this finding may be linked to the high proportion of pre-XDR/XDR TB patients receiving newly defined group A drugs and to individually tailored treatment regimens through a multidisciplinary consilium. As expected, SAEs were frequent and affected more than half our cohort patients, which underlines the need for better management of the more toxic drugs such as linezolid.

Members of the MDR TB Management Group (in alphabetical order by affiliation): Alexandra Aubry, Isabelle Bonnet, Johannes Eimer, Florence Morel, Nicolas Veziris (Sorbonne Université, INSERM, U1135, Centre d'Immunologie et des Maladies Infectieuses, Cimi-Paris, équipe 2, Paris, France); Emmanuelle Cambau, Emmanuel Lecorché, Faiza Mougari (Centre National de Référence des Mycobactéries et de la Résistance des Mycobactéries aux Antituberculeux, AP-HP, Paris, France); Claire Andrejak, Anne Bourgarit, Elise Klement, Bénédicte Rivoire, Guillaume Thouvenin, Simone Tunesi, Marie Wicky (French MDR TB Consilium) ; Marie Jaspard (Groupe Hospitalier Universitaire Sorbonne Université, Hôpital Pitié-Salpêtrière, Service de Maladies Infectieuses et Tropicales, AP-HP, Paris, France); Corentine Alauzet (Laboratoire de Bactériologie, CHRU de Nancy, Université de Lorraine, Vandoeuvre-Lès-Nancy, France); Lelia Escaut (Service de Maladies Infectieuses et Tropicales, Hôpital Kremlin-Bicêtre, AP-HP, Le Kremlin-Bicêtre, France); Sophie Ellis-Corbet (CLAT des Côtes d'Armor, Saint-Brieuc, France); Anne-Laure Roux (Service de Microbiologie, Hôpital Ambroise Paré, AP-HP, Boulogne, France).

This research did not receive any specific grant from funding agencies in the public, commercial, or not-for-profit sectors.

About the Author

Dr. Kherabi is an infectious diseases specialist particularly interested in drug-resistant tuberculosis management in France. She is also involved in educational affairs through the European Society of Clinical Microbiology and Infectious Diseases.

References

1. World Health Organization. Global tuberculosis report 2021. 2021 [cited 2021 Nov 7]. https://www.who.int/teams/global-tuberculosis-programme/tb-reports/global-tuberculosis-report-2021
2. Bernard C, Brossier F, Sougakoff W, Veziris N, Frechet-Jachym M, Metivier N, et al.; MDR-TB Management group of the NRC. A surge of MDR and XDR tuberculosis in France among patients born in the former Soviet Union. Euro Surveill. 2013;18:20555. https://doi.org/10.2807/1560-7917.ES2013.18.33.20555
3. Guthmann J-P, Comolet T, Trébucq A. EMC [in French]. Pneumologie. 2019;1:1–16.
4. Tuberculosis in France: epidemiological data 2019 [in French]. 2021 [cited 2021 Oct 15]. https://www.santepubliquefrance.fr/les-actualites/2021/tuberculose-en-france-donnees-epidemiologiques-2019
5. Ahmad N, Ahuja SD, Akkerman OW, Alffenaar JC, Anderson LF, Baghaei P, et al.; Collaborative Group for the Meta-Analysis of Individual Patient Data in MDR-TB treatment–2017. Treatment correlates of successful outcomes in pulmonary multidrug-resistant tuberculosis: an individual patient data meta-analysis. Lancet. 2018;392:821–34. https://doi.org/10.1016/S0140-6736(18)31644-1
6. World Health Organization. WHO consolidated guidelines on drug-resistant tuberculosis treatment. Licence: CC BY-NC-SA 3.0 IGO. Geneva: The Organization. 2019.
7. World Health Organization. Meeting report of the WHO expert consultation on the definition of extensively drug-resistant tuberculosis [cited 2021 May 17]. https://www.who.int/publications-detail-redirect/meeting-report-of-the-who-expert-consultation-on-the-definition-of-extensively-drug-resistant-tuberculosis
8. Ahuja SD, Ashkin D, Avendano M, Banerjee R, Bauer M, Bayona JN, et al.; Collaborative Group for Meta-Analysis of Individual Patient Data in MDR-TB. Multidrug resistant pulmonary tuberculosis treatment regimens and patient outcomes: an individual patient data meta-analysis of 9,153 patients. PLoS Med. 2012;9:e1001300. https://doi.org/10.1371/journal.pmed.1001300
9. Roelens M, Battista Migliori G, Rozanova L, Estill J, Campbell JR, Cegielski JP, et al. Evidence-based definition for extensively drug-resistant tuberculosis. Am J Respir Crit Care Med. 2021;204:713–22. https://doi.org/10.1164/rccm.202009-3527OC
10. Riccardi N, Saderi L, Borroni E, Tagliani E, Cirillo DM, Marchese V, et al. Therapeutic strategies and outcomes of MDR and pre-XDR-TB in Italy: a nationwide study. Int J Tuberc Lung Dis. 2021;25:395–9. https://doi.org/10.5588/ijtld.21.0036
11. Lee EH, Yong SH, Leem AY, Lee SH, Kim SY, Chung KS, et al. Improved fluoroquinolone-resistant and extensively drug-resistant tuberculosis treatment outcomes. Open Forum Infect Dis. 2019;6:ofz118. https://doi.org/10.1093/ofid/ofz118
12. World Health Organization. Policy guidance on drug-susceptibility testing (DST) of second-line antituberculosis drugs. 2008 [cited 2020 Aug 4]. https://apps.who.int/iris/handle/10665/70500
13. World Health Organization. Meeting report of the WHO expert consultation on drug-resistant tuberculosis treatment outcome definitions; Geneva, Switzerland; November 17–19, 2020 [cited 2021 Oct 15]. https://www.who.int/publications-detail-redirect/9789240022195
14. World Health Organization. Consolidated guidelines on tuberculosis. Module 4: treatment—drug-resistant tuberculosis treatment [cited 2021 Nov 7]. https://www.who.int/publications-detail-redirect/9789240007048

15. High Council for Public Hygiene. Tuberculosis with resistant bacilli: diagnosis and management. HCSP report [in French]. 2014 Dec [cited 2020 Aug 2]. https://www.hcsp.fr/explore.cgi/avisrapportsdomaine?clefr=483
16. Guglielmetti L, Jaffré J, Bernard C, Brossier F, El Helali N, Chadelat K, et al. Multidisciplinary advisory teams to manage multidrug-resistant tuberculosis: the example of the French Consilium. Int J Tuberc Lung Dis. 2019;23:1050–4.
17. D'Ambrosio L, Bothamley G, Caminero Luna JA, Duarte R, Guglielmetti L, Muñoz Torrico M, et al. Team approach to manage difficult-to-treat TB cases: experiences in Europe and beyond. Pulmonology. 2018;24:132–41. https://doi.org/10.1016/j.rppnen.2017.10.005
18. US Food and Drug Administration. What is a serious adverse event? 2020 Sep 9 [cited 2021 Oct 15]. https://www.fda.gov/safety/reporting-serious-problems-fda/what-serious-adverse-event
19. Kim H-R, Hwang SS, Kim HJ, Lee SM, Yoo C-G, Kim YW, et al. Impact of extensive drug resistance on treatment outcomes in non-HIV-infected patients with multidrug-resistant tuberculosis. Clin Infect Dis. 2007;45:1290–5. https://doi.org/10.1086/522537
20. Kim DH, Kim HJ, Park S-K, Kong S-J, Kim YS, Kim T-H, et al. Treatment outcomes and long-term survival in patients with extensively drug-resistant tuberculosis. Am J Respir Crit Care Med. 2008;178:1075–82. https://doi.org/10.1164/rccm.200801-132OC
21. Kwak N, Kim H-R, Yoo C-G, Kim YW, Han SK, Yim J-J. Changes in treatment outcomes of multidrug-resistant tuberculosis. Int J Tuberc Lung Dis. 2015;19:525–30. https://doi.org/10.5588/ijtld.14.0739
22. Falzon D, Gandhi N, Migliori GB, Sotgiu G, Cox HS, Holtz TH, et al.; Collaborative Group for Meta-Analysis of Individual Patient Data in MDR-TB. Resistance to fluoroquinolones and second-line injectable drugs: impact on multidrug-resistant TB outcomes. Eur Respir J. 2013;42:156–68. https://doi.org/10.1183/09031936.00134712
23. Diacon AH, Pym A, Grobusch MP, de los Rios JM, Gotuzzo E, Vasilyeva I, et al.; TMC207-C208 Study Group. Multidrug-resistant tuberculosis and culture conversion with bedaquiline. N Engl J Med. 2014;371:723–32. https://doi.org/10.1056/NEJMoa1313865
24. Skripconoka V, Danilovits M, Pehme L, Tomson T, Skenders G, Kummik T, et al. Delamanid improves outcomes and reduces mortality in multidrug-resistant tuberculosis.Eur Respir J. 2013;41:1393–400. https://doi.org/10.1183/09031936.00125812
25. Bastard M, Guglielmetti L, Huerga H, Hayrapetyan A, Khachatryan N, Yegiazaryan L, et al. Bedaquiline and repurposed drugs for fluoroquinolone-resistant multidrug-resistant tuberculosis: how much better are they? Am J Respir Crit Care Med. 2018;198:1228–31. https://doi.org/10.1164/rccm.201801-0019LE
26. Lee M, Lee J, Carroll MW, Choi H, Min S, Song T, et al. Linezolid for treatment of chronic extensively drug-resistant tuberculosis. N Engl J Med. 2012;367:1508–18. https://doi.org/10.1056/NEJMoa1201964
27. Lee M, Song T, Kim Y, Jeong I, Cho SN, Barry CE III. Linezolid for XDR-TB—final study outcomes. N Engl J Med. 2015;373:290–1. https://doi.org/10.1056/NEJMc1500286
28. Tang S, Yao L, Hao X, Zhang X, Liu G, Liu X, et al. Efficacy, safety, and tolerability of linezolid for the treatment of XDR-TB: a study in China. Eur Respir J. 2015;45:161–70. https://doi.org/10.1183/09031936.00035114
29. Dooley KE, Sayre P, Borland J, Purdy E, Chen S, Song I, et al. Safety, tolerability, and pharmacokinetics of the HIV integrase inhibitor dolutegravir given twice daily with rifampin or once daily with rifabutin: results of a phase 1 study among healthy subjects. J Acquir Immune Defic Syndr 2013;62:21–7.
30. Guglielmetti L, Le Dû D, Veziris N, Caumes E, Marigot-Outtandy D, Yazdanpanah Y, et al.; MDR-TB Management Group of the French National Reference Center for Mycobacteria and the Physicians of the French MDR-TB Cohort. Is bedaquiline as effective as fluoroquinolones in the treatment of multidrug-resistant tuberculosis? Eur Respir J. 2016;48:582–5. https://doi.org/10.1183/13993003.00411-2016
31. Conradie F, Diacon AH, Ngubane N, Howell P, Everitt D, Crook AM, et al.; Nix-TB Trial Team. Treatment of highly drug-resistant pulmonary tuberculosis. N Engl J Med. 2020;382:893–902. https://doi.org/10.1056/NEJMoa1901814
32. Nunn AJ, Phillips PPJ, Meredith SK, Chiang C-Y, Conradie F, Dalai D, et al.; STREAM Study Collaborators. A trial of a shorter regimen for rifampin-resistant tuberculosis. N Engl J Med. 2019;380:1201–13. https://doi.org/10.1056/NEJMoa1811867
33. Kherabi Y, Mollo B, Gerard S, Lescure F-X, Rioux C, Yazdanpanah Y. Patient-centered approach to the management of drug-resistant tuberculosis in France: How far off the mark are we? PLOS Glob Public Health. 2022;2:e0000313. https://doi.org/10.1371/journal.pgph.0000313
34. Kurbatova EV, Gammino VM, Bayona J, Becerra MC, Danilovitz M, Falzon D, et al. Predictors of sputum culture conversion among patients treated for multidrug-resistant tuberculosis. Int J Tuberc Lung Dis. 2012;16:1335–43. https://doi.org/10.5588/ijtld.11.0811
35. Bastard M, Sanchez-Padilla E, Hayrapetyan A, Kimenye K, Khurkhumal S, Dlamini T, et al. What is the best culture conversion prognostic marker for patients treated for multidrug-resistant tuberculosis? Int J Tuberc Lung Dis. 2019;23:1060–7. https://doi.org/10.5588/ijtld.18.0649
36. Veziris N, Bonnet I, Morel F, Guglielmetti L, Maitre T, Ray LFL, et al. Impact of the revised definition of extensively drug resistant tuberculosis. Eur Respir J. 2021 Jan 1 [cited 2021 Nov 1]. https://erj.ersjournals.com/content/early/2021/04/08/13993003.00641-2021
37. Oliveira O, Gaio R, Correia-Neves M, Rito T, Duarte R. Evaluation of drug-resistant tuberculosis treatment outcome in Portugal, 2000–2016. PLoS One. 2021;16:e0250028. https://doi.org/10.1371/journal.pone.0250028
38. Heyckendorf J, van Leth F, Kalsdorf B, Olaru ID, Günther G, Salzer HJF, et al. Relapse-free cure from multidrug-resistant tuberculosis in Germany. [cited 2021 Nov 27]. Eur Respir J. 2018;51:1702122. https://doi.org/10.1183/13993003.02122-2017
39. Lan Z, Ahmad N, Baghaei P, Barkane L, Benedetti A, Brode SK, et al.; Collaborative Group for the Meta-Analysis of Individual Patient Data in MDR-TB treatment 2017. Drug-associated adverse events in the treatment of multidrug-resistant tuberculosis: an individual patient data meta-analysis. Lancet Respir Med. 2020;8:383–94. https://doi.org/10.1016/S2213-2600(20)30047-3

Address for correspondence: Yousra Kherabi, Sorbonne Université, INSERM U1135, Centre d'Immunologie et des Maladies Infectieuses, Cimi-Paris, Équipe 2, Paris, France; email: yousra.kherabi@aphp.fr

Fulminant Transfusion-Associated Hepatitis E Virus Infection Despite Screening, England, 2016–2020

Heli Harvala, Claire Reynolds, Su Brailsford, Katy Davison

In England, all blood donations are screened in pools of 24 by nucleic acid test (NAT) for hepatitis E virus (HEV) RNA. During 2016–2020, this screening successfully identified and intercepted 1,727 RNA-positive donations. However, review of previous donations from infected platelet donors identified 9 donations in which HEV RNA detection was missed, of which 2 resulted in confirmed transmission: 1 infection resolved with ribavirin treatment, and 1 proceeded to fatal multiorgan failure within a month from infection. Residual risk calculations predict that over the 5-year study period, HEV RNA detection was missed by minipool NAT in 12–23 platelet and 177–354 whole-blood donations, but transmission risk remains undetermined. Although screening has been able to largely eliminate infectious HEV from the blood supply in England, missed detection of low levels of HEV RNA in donated blood can lead to a severe, even fulminant, infection in recipients and could be prevented by more sensitive screening.

Hepatitis E virus (HEV) is a nonenveloped enteric virus, classified in the genus *Orthohepevirus*, family *Hepeviridae* (*1*). HEV is divided into 8 genotypes that differ substantially in their host ranges and zoonotic capacities. Genotypes 1 and 2 typically infect humans and have been associated with large waterborne outbreaks of infections in developing countries. By contrast, genotypes 3 and 4 are endemic among domestic pigs, wild boar, and rabbits; most pigs reared for pork production in Europe have been infected with genotype 3 (*2*), and HEV RNA is detected in 40% of farmed pig fecal samples (*3*). Humans are increasingly exposed to HEV in developed countries through consumption of uncooked processed or cured pork products, typically with genotype 3 in Europe, North America, and Japan and with genotype 4 in China and other parts of Southeast Asia (*2*,*4*–*7*). Seroprevalence of HEV antibodies, indicative of past exposure and infection, are in the range of 5%–13% in the United Kingdom (*8*–*10*) and in the low-to-middle range of incidence estimated for other countries in Europe (*11*–*13*). Recent increases in human infections (*14*) are undoubtedly the direct consequence of increasing circulation of HEV in farmed pigs; 20% of pigs have active infection at time of slaughter, posing universal human exposure risk at time of slaughter (*15*).

Ongoing and increasing HEV endemicity among farmed pigs creates downstream effects for human blood transfusion from infected blood donors. HEV infections are associated with variable periods (3–5 weeks) of often intense viremia (*16*) during acute infections that may transmit infections to blood recipients (*17*,*18*). Measured frequencies of RNA as an indicator of viremia in blood donors are remarkably high, ≈1 detection/2,000 donations tested to 1 detection/3,000 donations according to several studies of blood donors in different countries in western Europe (*17*,*19*,*20*) and as high as 1 detection/762 donations in the Netherlands (*21*) and 1 detection/157 donations in Italy (*13*). Several studies have documented transmission of HEV infections to blood recipients (*16*,*17*,*20*,*22*), typically from donations that have higher viral loads and are seronegative for HEV antibodies and from blood components with higher residual plasma volumes, such as platelets (*2*,*17*). A proposed threshold by which infectious and noninfectious donations could be differentiated was 2×10^4 IU of HEV RNA (*23*).

Although HEV infections are typically mild and self-resolving, those in immunocompromised blood and platelet recipients may persist and induce

Author affiliations: University College of London, London, UK (H. Harvala); NHS Blood and Transplant, London (H. Harvala, C. Reynolds, S. Brailsford, K. Davison); UK Health Security Agency, London (K. Davison)

DOI: https://doi.org/10.3201/eid2809.220487

rapidly progressive liver disease and frequently cause death (*24*–*27*). The potential for severe disease outcomes in recipients of blood components has led to detailed modeling-based investigations of HEV RNA screening for blood and platelet donors (*28*). Only the United Kingdom, Ireland, and the Netherlands now perform universal donor screening; for immunocompromised patients, many blood services in Germany, France, and Switzerland also perform selective screening for components. Many countries, notably the United States, have elected not to screen on the basis of low risk and cost-effectiveness (*29*). Among blood services that do screen for HEV RNA, the lack of international consensus for screening requirements has introduced further variability in the pool sizes used for screening; larger pools reduce costs but also sensitivity. A number of modelling studies have attempted to estimate residual infectivity risk by using different pool sizes and assay formats for HEV RNA testing (*30*–*33*), albeit with conclusions tempered by ongoing uncertainty over the upper limit of viral loads that are noninfectious.

In the United Kingdom, transfusion complications are monitored by the Serious Hazards of Transfusion (SHOT) hemovigilance group (https://www.shotuk.org/shot-reports). However, reported cases of HEV transmission may underestimate their true extent because infections may be unsuspected and underdiagnosed or not linked to blood component transfusion in patients in whom complications may develop.

With this study, we aimed to describe the burden of HEV among blood donors, determine the risk for nondetection of HEV, and reassess the extent and effect of transfusion-transmitted infections in the presence of a national screening programme. Signed consent was obtained from each donor before blood collection, including consent for NHS Blood and Transfusion (NHSBT) to use their data for clinical audit to assess and improve our services, as well as to increase our knowledge of the donor population.

Methods

Study Population

We used surveillance data collected by the joint NHSBT/UK Health Security Agency (UKHSA) Epidemiology Unit from all HEV RNA–positive apheresis and whole-blood donors identified in England from March 1, 2016, through December 31, 2020. We also used the total number of donations tested in both categories within that period.

HEV Testing of Donated Blood

We tested all apheresis donations collected in England during the study period for HEV RNA. On April 10, 2017, testing of whole-blood donations changed from selective to universal, for reasons of operational simplicity and cost-effectiveness. We performed HEV RNA testing in pools of 24 donations (cobas MPX for use on the 6800/8800 systems; Roche Diagnostics, https://www.roche.com). A reported 95% limit of detection was 18.6 IU/mL, translating to 446 IU/mL at the individual donation level when tested in pools of 24. We resolved reactive pools to individual HEV RNA–containing donations by using the same assay and subjected individual samples to confirmatory HEV testing, including serology and molecular investigations at the Microbiology Services Laboratory (NHSBT, Colindale, UK) as described previously (*34*). Donations in which HEV RNA was detected at screening were removed from the clinical supply, and the donors were followed up clinically (informed and advised to contact their general practitioner if unwell) (*34*).

Archived Samples and Testing of Transfusion Recipient when Indicated

NHSBT archived 900 µL plasma from each blood donation for a minimum of 3 years. We requested the archived plasma sample from the most recent HEV RNA–negative donation for individual HEV RNA and antibody testing for all apheresis donors whose subsequent donation was HEV RNA positive. If HEV RNA was detected, we also retrieved the next most recent archive sample for testing. During March 2016–June 2018, hospitals that received the HEV RNA–positive blood components were informed of potential risks and advised to consider appropriate actions. Since July 2018, clinical teams have followed up with transfusion recipients, and testing for HEV RNA and IgG for up to 6 months after transfusion has been recommended.

Transfusion-Transmitted Infections

The NHSBT/UKHSA Epidemiology Unit collated data on all suspected transfusion-transmitted HEV infections reported to, and investigated by, NHSBT during the 5-year study period and reported them to SHOT. The outcomes of the investigations were determined to be confirmed, probable, or not transfusion-transmitted infection. We did not consider transmissions that had occurred before the introduction of HEV screening.

Residual Risk Calculations

To estimate residual risk of not detecting HEV RNA in apheresis and whole-blood donations, we applied

the traditional window period method to HEV testing data. We assume that nondetection resulted from proximity to initial infection in a window period of HEV NAT screening. The number of apheresis and whole-blood donations tested and found positive for HEV RNA were available from NHSBT/UKHSA epidemiology surveillance for March 2016 through December 2020.

We assumed incidence to be equal to the rate of HEV RNA positivity among donors. To estimate risk, we multiplied incidence by the duration of the window period in years for HEV NAT by using 0.019 years (corresponding to 7 days) and 0.038 years (corresponding to 14 days). These parameters were based on expert opinion in the absence of any published values. We calculated risk for apheresis and whole-blood donations by year per million donations tested. To derive an approximate number of undetected HEV RNA-positive donations, we extrapolated risks to the estimated number of apheresis and whole-blood donations each year.

Results

Detection of HEV RNA in Donated Blood

From March 1, 2016, through December 31, 2020, a total of 6,297,904 blood donations, including 350,323 apheresis and 5,947,581 whole-blood donations, were screened for HEV RNA in England. HEV RNA was detected and infection confirmed in all 1,727 initially RNA-reactive blood donations collected from 1,727 blood donors, of which 107 were apheresis and 1,620 whole-blood donors (Table 1). Most blood donors (1,559,517) were screened in 2018, and most HEV RNA-positive donations (470) were identified in 2019. Overall, HEV RNA was detected in 1 of every 2,000 donors (varying from 1/1,258 donors in 2016 to 1/2,591 donors in 2017) and in 1 of every 3,647 donations (varying from 1/1,258 donations in 2016 to 1/2,591 donations in 2017).

Viral loads were available for 1,200 HEV RNA–positive donations. The geometric mean viral load was 998 IU/mL (range 1–8.7 × 10^6 IU/mL); viral load was below the theoretical 95% detection limit of screening assay used in 35.8% of donations. Of note, <100 IU/mL of HEV RNA was detected in 17% of donations (Figure). All donations that were retrospectively shown to contain HEV RNA had a low viral load, below the level of reliable quantification (37 IU/mL).

Residual Risk for HEV Nondetection

The annual HEV incidence and estimated risk for nondetection fluctuated each year for apheresis and whole-blood donors (Table 2). For apheresis donors, estimates were highest in 2020 (incidence 2,052.7 and risk for nondetection 39.34 per 1 million donations tested), whereas estimates for whole-blood donors were highest when screening was first introduced in 2016 (incidence 2,401.9 and risk for nondetection 46.03 per 1 million donations tested). Risk for both groups of donors increased 2-fold if a window period of 14 days instead of 7 days was used. During the study period, the estimated risk, with a 7-day window period, predicted that 12 apheresis and up to 177 whole-blood donations positive for HEV RNA were not detected (Table 3); that prediction increased to 24 apheresis and 354 whole-blood donations positive when a 14-day window period was assumed.

HEV Lookback

During the 5-year study period, a total of 107 HEV RNA–positive apheresis platelet donations were

Table 1. Number of donations and donors tested for hepatitis E virus RNA, number of positive results, detection rate, and incidence rate for apheresis and whole-blood donors, England, March 2016–December 2020

Donation type, year	Donations	Donors	Positive	Detection rate, no. HEV RNA detections/1 million donations	Incidence rate, HEV RNA–positive samples/ 1 million donors
Apheresis					
2016	69,605	14,952	24	344.8	1,966.5
2017	74,422	15,987	20	268.7	1,532.6
2018	70,709	15,189	24	339.4	1,935.8
2019	68,907	15,450	15	217.7	1,241.5
2020	66,680	13,593	24	359.9	2,052.7
Total	350,323	75,170	107	305.4	1,741.9
Whole blood					
2016	413,153	234,141	174	421.2	2,401.9
2017	1,256,503	712,083	261	207.7	1,184.6
2018	1,488,808	843,734	351	235.8	1,344.6
2019	1,450,628	825,363	455	313.7	1,788.8
2020	1,338,489	769,420	379	283.2	1,614.9
Total	5,947,581	3,384,741	1,620	272.4	1,553.4

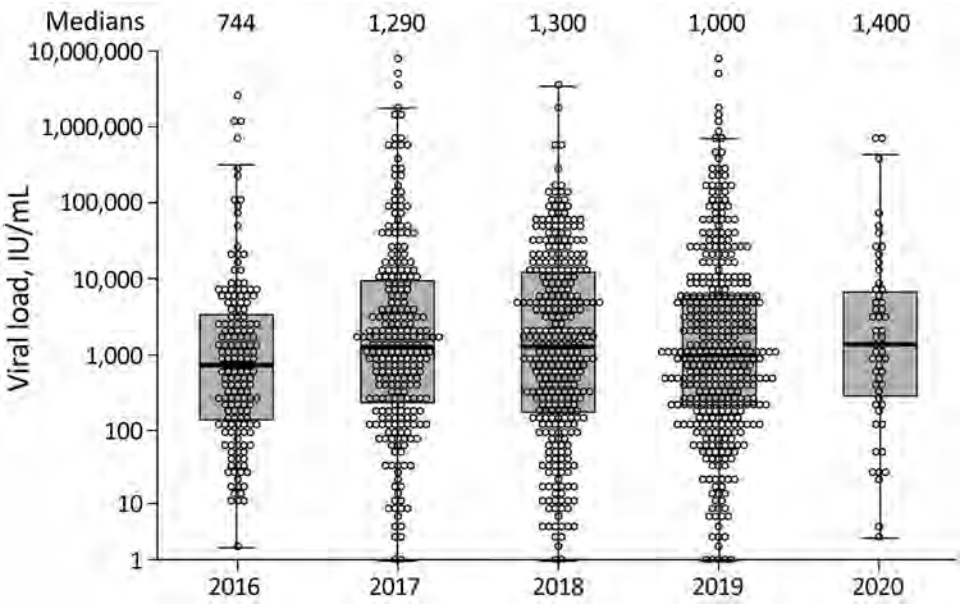

Figure. Hepatitis E virus viral loads in 1,200 individual blood donors in England, 2016–2020. Median viral loads were comparable over the study period. Circles indicate individual donors; horizontal lines within boxes and numbers above plots indicate medians; boxes indicate first and third quartile values; whiskers indicate lowest and highest data points.

identified (Table 4). Retrospective individual HEV RNA testing of donors' 98 previous donations identified 9 HEV RNA–positive donations that were undetected by screening because of low viral loads (≤37 IU/mL) and supplied for clinical use. Retrospective investigations included identification and follow-up of the 18 recipients of the platelet components produced from the indicated donations (Table 5). All components were traced; no data were received back from 8 recipients, 3 had subsequently died, and sufficient follow-up data were received for the remaining 7. Follow-up testing excluded HEV infection in 5 recipients (all were HEV IgG and RNA negative 6 months after transfusion) and confirmed HEV infection in 2 recipients (1 in 2018 and 1 in 2019; both were HEV RNA positive). Further investigations, including sequence analysis, confirmed that both recipients had acquired their infection via transfusion.

Confirmed HEV Transmission in 2018

Retrospective individual PCR testing detected a low level (37 IU/mL) of HEV RNA in a platelet donation. One recipient was a young patient with sepsis, who died of an underlying condition 2 days after transfusion. The other was a hematology patient who had completed treatment for B-cell lymphoma. He became viremic 8 weeks after transfusion and was immediately placed under the care of the hepatology team. He received ribavirin, and ≈6 months later, the HEV infection cleared. Identical HEV sequences obtained from donor and recipient samples confirmed the blood transfusion as a source of this HEV infection.

Confirmed HEV Transmission in 2019

The index apheresis platelet donation contained low levels of HEV RNA (<37 IU/mL). A male patient, 40–50 years of age, with aplastic anemia and portal

Table 2. Incidence of hepatitis E virus RNA positive samples and estimated risk for nondetection, with 7-day window period risk for apheresis and whole blood donors. England, March 2016–December 2020

Donation type, year	Incidence, HEV RNA–positive samples/ 1 million donors	Risk per 1 million if window period 7 days (95% CI)
Apheresis		
2016	1,966.5	37.69 (24.15–56.07)
2017	1,532.6	29.37 (17.94–45.36)
2018	1,935.8	37.10 (23.77–55.20)
2019	1,241.5	23.79 (13.32–39.24)
2020	2,052.7	39.34 (25.21–58.53)
Whole blood		
2016	2,401.9	46.03 (39.45–53.40)
2017	1,184.6	22.70 (20.03–25.63)
2018	1,344.6	25.77 (23.14–28.61)
2019	1,788.8	34.28 (31.21–37.58)
2020	1,614.9	30.95 (27.91–34.23)

Table 3. Estimated number of hepatitis E virus RNA–positive donors not detected, according to 7-day window period risk for apheresis and whole blood donors, England, March 2016–December 2020

Donation type, year	Donations tested	No. not detected if window period 7 days (95% CI)
Apheresis		
2016	69,605	2.62 (1.68–3.90)
2017	74,422	2.19 (1.34–3.38)
2018	70,709	2.62 (1.68–3.90)
2019	68,907	1.64 (0.92–2.70)
2020	66,680	2.62 (1.68–3.90)
Total	350,323	11.70 (7.30–17.79)
Whole blood		
2016	413,153	19.02 (16.30–22.06)
2017	1,256,503	28.53 (25.17–32.21)
2018	1,488,808	38.36 (34.46–42.59)
2019	1,450,628	49.73 (45.27–54.52)
2020	1,338,489	41.42 (37.36–45.81)
Total	5,947,581	177.07 (158.55–197.19)

hypertension received the first unit of apheresis platelets in September 2019. At the time of HEV diagnosis in early November 2019 (sample taken at our advice), he was clinically well. He was monitored carefully and remained stable with unchanged liver function test results until mid-November, when his viral load peaked at 29,200,000 IU/mL and a strong antibody response against HEV developed, coinciding with a sudden increase in bilirubin and aspartate aminotransferase levels. Treatment with ribavirin was initiated, but his liver and renal function continued to deteriorate, leading to acute hepatitis with kidney failure, and he died at the end of November. Transmission was confirmed by sequence identity of the infecting HEV strains and of the subsequent apheresis donation (viral load of 4,900 IU/mL), collected 3 weeks after the index donation.

The other recipient of platelets from this donation had vascular type Ehlers-Danlos syndrome and was followed up for 6 months. HEV infection was excluded by both serology and molecular testing.

Transfusion-Transmitted Infections

In England, all suspected transfusion-transmitted infections investigated by NHSBT are reported to the NHSBT/UKHSA Epidemiology Unit and to SHOT. During 2016–2020, NHSBT investigated and reported 6 cases of possible transfusion-transmitted HEV. Transfusion-transmitted infection was not considered for 3 cases, was confirmed for 2 cases, and was probable for the remaining case, for which a red blood cell transfusion was shown to be the probable source of the recipient's HEV infection. The recipient was a multitransfused young adult with aplastic anemia and Turner syndrome; infection cleared after ribavirin treatment, but the virus in the donor could not be typed because of low levels of viremia.

Discussion

To mitigate the risk for transfusion-transmitted chronic HEV infection in immunocompromised patients in the United Kingdom, blood donation screening for HEV RNA was introduced in March 2016. Since then, through screening of >6.2 million blood donations for HEV RNA in England, 1,727 HEV RNA–positive donations have been removed from the blood supply and only 2 cases of transfusion-transmitted HEV infection have been identified. Although these findings suggest that the pooled screening strategy has been able to largely eliminate the infectious HEV from the blood supply in England, our residual risk calculations argue against that conclusion.

Although individual NAT represents the most effective screening method for identifying HEV RNA in donations, including those with the lowest level of HEV RNA, our data suggest that pooled NAT performs better than the theoretically calculated sensitivity would indicate. Almost one third of identified

Table 4. Nondetection of HEV RNA based on retrospective investigations for apheresis donors, in which indicated donations are individually retested for HEV RNA, England, March 2016 to–December 2020

	Screening		Previous donations		
Year(s)	No. apheresis donations screened	No. HEV RNA–positive donations	No. retrospectively tested	No. HEV RNA–positive donations identified by retesting	No. components produced and supplied for clinical use
2016–2017	144,027	44	35	2	4
2018	70,709	24	24	3	6
2019	68,907	15	14	2	4
2020	66,680	24	*25*	2	4
Total	350,323	107	98	9	18

Table 5. Details of lookback investigations into 9 HEV RNA positive platelet donations supplied for clinical use in England, March 2016 to December 2020*

Donation no.	HEV viral load, IU/mL†	Components	Recipient details	Recipient follow-up testing results
Donation 1	4	Platelet 1 Platelet 2	Hospitals informed, no data back	NA
Donation 2	8	Platelet 1 Platelet 2	Hospitals informed, no data back	NA
Donation 3	<37	Platelet 1 Platelet 2	Hospitals informed, no data back	NA
Donation 4	<37	Platelet 1 Platelet 2	Hospitals responded, no evidence of transmission	NA
Donation 5	37	Platelet 1 Platelet 2	M, 50–60 years, B-cell lymphoma F, 20-30 y, sepsis	Confirmed transmission Deceased
Donation 6	37	Platelet 1 Platelet 2	F, 60–70 y, aplastic anemia M, 50–60 y, lymphoma	Tested negative Tested negative
Donation 7	4.5	Platelet 1 Platelet 2	M, 40–50 y, aplastic anemia F, 50–60 y, vascular syndrome	Confirmed transmission Tested negative
Donation 8	10	Platelet 1 Platelet 2	M, 60–70 y, aplastic anemia M, <10 y, cancer	Tested negative Deceased
Donation 9	3	Platelet 1 Platelet 2	F, 40–50 y, myelodysplastic syndrome M, 40–50 y, acute myeloid leukemia	Tested negative Deceased

*Each donation was tested for HEV RNA and divided into 2 platelet packs.
†Estimated viral loads given where available. HEV, hepatitis E virus; NA, not applicable.

HEV RNA–positive donations had a viral load below the theoretical assay sensitivity of 446 IU/mL calculated for individual donors (430/1,200, 36%), and approximately half of those had a viral load of <100 IU/mL (206/1,200, 17%). These data are comparable to those obtained by individual NAT screening with an increased sensitivity of 7.89 IU/mL (Grifols, https://www.grifols.com) in Ireland, where 37.5% of HEV RNA–containing blood donations had a viral load of <100 IU/mL (*18*).

Consistent with those data, during our 5-year period of pooled screening, missed HEV RNA detection in donations retrospectively identified low levels of HEV RNA (≤37 IU/mL). Although pooled HEV screening is generally effective for identifying donations with low-level viremia, the process repeatedly missed donations with HEV RNA ≤37 IU/mL. Similar findings were obtained in Germany, where all HEV RNA–positive donations exclusively identified by individual NAT screening had viral loads of <25 IU/mL (*32*,*33*).

When we further calculated the residual risk for HEV RNA nondetection on the basis of 7-day and 14-day window periods, the estimated risk predicted that 12–24 apheresis platelet donations and 177–354 whole-blood donations positive for HEV RNA would not have been detected over the 5-year study period. Despite uncertainty in the parameters, this predicted risk is similar to the true risk demonstrated so far for apheresis donations: during 2016–2020, initial pooled screening did not detect HEV RNA positivity in 9 apheresis donations.

Although the model predicted that the screening is missing HEV RNA in a much larger number of whole-blood donations, these missed detections do not directly equate to transmission risk. Infectious HEV is considered to partition into the plasma component of a donation; the residual plasma volume is substantially higher in platelet (180 mL) than in red blood cell (5 mL) donations. The 7-fold lower residual plasma volume in red blood cell donations may therefore reduce transmission risk from this component. Indeed, the estimated maximum dose of HEV RNA in red blood cell donations containing low levels of HEV RNA would probably remain at <1,000 IU of HEV RNA (37 IU/mL × 25 mL = 925 IU), in contrast to the level predicted for platelet donations (37 IU/mL × 180 mL = 6,660 IU).

The minimum infectious dose of HEV RNA leading to an infection in the transfusion recipient remains unknown. Earlier studies suggested that ≈20,000 IU of HEV RNA would be required for efficient transmission (*23*,*35*). Since then, lower amounts of HEV RNA have been occasionally associated with virus transmission (*36*). So far, the lowest amount of HEV RNA leading to transmission is 7,056 IU; transmission occurred via apheresis platelet transfusion and resulted in chronic HEV infection in an immunosuppressed recipient (*20*). Although we could not determine the exact infectious doses linked to the 2 cases of HEV transmission, we can estimate that doses leading to an infection were <6,660 IU of HEV RNA. Both cases were identified in our study via the active lookback investigation in which doctors caring for these recipients were contacted and the importance of HEV RNA testing even without the symptoms was explained. Both recipients were tested 8 weeks after

transfusion and were completely asymptomatic at the time of testing. Even if HEV had been considered as a diagnosis when additional symptoms developed, it is possible that HEV infection would not have been linked to the previous transfusions. Our findings indicate the value of active lookback investigations in cases for which infections may easily be missed or unsuspected clinically. This approach estimates the true minimum infectious dose of HEV RNA required for transmission via blood transfusion.

HEV RNA has traditionally been considered to be largely present in plasma; hence, plasma volume determines the risk for transmission. However, the potential sequestration of HEV virions by platelets should also be considered as contributors to HEV transmission risk from this blood component. Although the main function of platelets is to maintain vascular integrity, they also play roles in viral immune responses. For example, platelets express many receptors, including integrins, that mediate virus attachment and can hence bind to free virus and present it to neutrophils (*37*). Integrins also play a key role for cellular attachment and entry of HEV (*38*). Given the association of HEV transmission with platelet transfusions, whether platelets do indeed bind HEV and contribute to transmission risk independently from HEV circulating in plasma is an additional parameter. Although this platelet-bound virus is probably controlled within an immunocompetent donor host, it could lead to a more severe infection in recipients with suboptimal platelet and neutrophil reservoirs. This consequence could explain the severe outcome in aplastic anemia patients in whom the bone marrow fails to produce enough blood cells because the normal hematopoietic stem cells are replaced by abnormal cells.

HEV genotype 3 can cause a chronic infection and occasionally lead to cirrhosis or even liver failure in immunosuppressed patients and those with underlying chronic liver disease (*24*–*27*). In our study, chronic HEV infection developed in 1 patient with B-cell lymphoma and the HEV infection was successfully treated with ribavirin. However, acute hepatitis with kidney failure developed in the other patient, who had aplastic anemia and died within a month of acquiring the HEV infection via blood transfusion. This outcome was unexpected because aplastic anemia has not previously been considered to be a particular risk factor for HEV infection. Although it might have been a coincidence that the third probable HEV transmission event investigated in England in 2019 was also associated with a recipient with aplastic anemia, those results prompted us to review fulminant cases of transfusion-transmitted HEV infection in patients with aplastic anemia reported in the literature. Of note, 2 patients with aplastic anemia acquired HEV infection via blood transfusion and the cases were reported; both patients died, 1 with sepsis and 1 with cardiac issues (*17*). These data led to the possibility that patients with aplastic anemia might specifically be at higher risk for transfusion-transmitted HEV infection, underlying the value of active surveillance looking for unusual manifestations in blood recipients beyond the typical hepatitis.

In conclusion, the pooled screening strategy has been able to largely eliminate infectious HEV from the blood supply in England because only 2 confirmed transfusion-transmitted HEV infections have been reported since the screening began in 2017. However, 2 cases are probably an underestimate because the analysis of HEV transmissions was based on a small number of donations in which HEV RNA was known to have been missed by pooled screening and even fewer recipients who were available for active follow-up. Further residual risk calculations predict that very low levels of HEV RNA were missed in up to 24 apheresis and 354 whole-blood donations during the study period. This information is especially useful now because our results show that even these low levels of HEV RNA can lead to a severe, even fulminant, infection in the recipient.

Acknowledgments

We thank all staff members with Microbiology Services Teams, including those within Surveillance, Laboratory, Office, and Clinical.

About the Author

Dr. Harvala is a consultant medical virologist and principal investigator at NHSBT. Her main research interests include transfusion-transmitted viral infections and blood safety.

References

1. Purdy MA, Harrison TJ, Jameel S, Meng XJ, Okamoto H, Van der Poel WHM, et al.; ICTV Report Consortium. ICTV virus taxonomy profile: Hepeviridae. J Gen Virol. 2017;98:2645–6. https://doi.org/10.1099/jgv.0.000940
2. Salines M, Andraud M, Rose N. From the epidemiology of hepatitis E virus (HEV) within the swine reservoir to public health risk mitigation strategies: a comprehensive review. Vet Res (Faisalabad). 2017;48:31. https://doi.org/10.1186/s13567-017-0436-3
3. Berto A, Pham HA, Thao TTN, Vy NHT, Caddy SL, Hiraide R, et al.; VIZIONS consortium. Hepatitis E in southern Vietnam: seroepidemiology in humans and molecular epidemiology in pigs. Zoonoses Public Health.

2018;65:43–50. https://doi.org/10.1111/zph.12364
4. Meng XJ. Zoonotic and foodborne transmission of hepatitis E virus. Semin Liver Dis. 2013;33:41–9. https://doi.org/10.1055/s-0033-1338113
5. Ijaz S, Said B, Boxall E, Smit E, Morgan D, Tedder RS. Indigenous hepatitis E in England and Wales from 2003 to 2012: evidence of an emerging novel phylotype of viruses. J Infect Dis. 2014;209:1212–8. https://doi.org/10.1093/infdis/jit652
6. Dalton HR, Izopet J. Transmission and epidemiology of hepatitis E virus genotype 3 and 4 infections. Cold Spring Harb Perspect Med. 2018;8:a032144. https://doi.org/10.1101/cshperspect.a032144
7. Kaba M, Moal V, Gérolami R, Colson P. Epidemiology of mammalian hepatitis E virus infection. Intervirology. 2013;56:67–83. https://doi.org/10.1159/000342301
8. Thom K, Gilhooly P, McGowan K, Malloy K, Jarvis LM, Crossan C, et al. Hepatitis E virus (HEV) in Scotland: evidence of recent increase in viral circulation in humans. Euro Surveill. 2018;23:17–0017423. https://doi.org/10.2807/1560-7917.ES.2018.23.12.17-00174
9. Dalton HR, Stableforth W, Hazeldine S, Thurairajah P, Ramnarace R, Warshow U, et al. Autochthonous hepatitis E in southwest England: a comparison with hepatitis A. Eur J Clin Microbiol Infect Dis. 2008;27:579–85. https://doi.org/10.1007/s10096-008-0480-z
10. Cleland A, Smith L, Crossan C, Blatchford O, Dalton HR, Scobie L, et al. Hepatitis E virus in Scottish blood donors. Vox Sang. 2013;105:283–9. https://doi.org/10.1111/vox.12056
11. O'Riordan J, Boland F, Williams P, Donnellan J, Hogema BM, Ijaz S, et al. Hepatitis E virus infection in the Irish blood donor population. Transfusion. 2016;56:2868–76. https://doi.org/10.1111/trf.13757
12. Mansuy JM, Legrand-Abravanel F, Calot JP, Peron JM, Alric L, Agudo S, et al. High prevalence of anti-hepatitis E virus antibodies in blood donors from south west France. J Med Virol. 2008;80:289–93. https://doi.org/10.1002/jmv.21056
13. Lucarelli C, Spada E, Taliani G, Chionne P, Madonna E, Marcantonio C, et al. High prevalence of anti-hepatitis E virus antibodies among blood donors in central Italy, February to March 2014. Euro Surveill. 2016;21:21. https://doi.org/10.2807/1560-7917.ES.2016.21.30.30299
14. Adlhoch C, Avellon A, Baylis SA, Ciccaglione AR, Couturier E, de Sousa R, et al. Hepatitis E virus: assessment of the epidemiological situation in humans in Europe, 2014/15. J Clin Virol. 2016;82:9–16. https://doi.org/10.1016/j.jcv.2016.06.010
15. Grierson S, Heaney J, Cheney T, Morgan D, Wyllie S, Powell L, et al. Prevalence of hepatitis E virus infection in pigs at the time of slaughter, United Kingdom, 2013. Emerg Infect Dis. 2015;21:1396–401. https://doi.org/10.3201/eid2108.141995
16. Tedder RS, Tettmar KI, Brailsford SR, Said B, Ushiro-Lumb I, Kitchen A, et al. Virology, serology, and demography of hepatitis E viremic blood donors in south east England. Transfusion. 2016;56:1529–36. https://doi.org/10.1111/trf.13498
17. Hewitt PE, Ijaz S, Brailsford SR, Brett R, Dicks S, Haywood B, et al. Hepatitis E virus in blood components: a prevalence and transmission study in southeast England. Lancet. 2014;384:1766–73. https://doi.org/10.1016/S0140-6736(14)61034-5
18. Boland F, Martinez A, Pomeroy L, O'Flaherty N. Blood donor screening for hepatitis E virus in the European Union. Transfus Med Hemother. 2019;46:95–103. https://doi.org/10.1159/000499121
19. Gallian P, Lhomme S, Piquet Y, Sauné K, Abravanel F, Assal A, et al. Hepatitis E virus infections in blood donors, France. Emerg Infect Dis. 2014;20:1914–7. https://doi.org/10.3201/eid2011.140516
20. Huzly D, Umhau M, Bettinger D, Cathomen T, Emmerich F, Hasselblatt P, et al. Transfusion-transmitted hepatitis E in Germany, 2013. Euro Surveill. 2014;19:20812. https://doi.org/10.2807/1560-7917.ES2014.19.21.20812
21. Hogema BM, Molier M, Sjerps M, de Waal M, van Swieten P, van de Laar T, et al. Incidence and duration of hepatitis E virus infection in Dutch blood donors. Transfusion. 2016;56:722–8. https://doi.org/10.1111/trf.13402
22. Colson P, Coze C, Gallian P, Henry M, De Micco P, Tamalet C. Transfusion-associated hepatitis E, France. Emerg Infect Dis. 2007;13:648–9. https://doi.org/10.3201/eid1304.061387
23. Tedder RS, Ijaz S, Kitchen A, Ushiro-Lumb I, Tettmar KI, Hewitt P, et al. Hepatitis E risks: pigs or blood—that is the question. Transfusion. 2017;57:267–72. https://doi.org/10.1111/trf.13976
24. Kamar N, Selves J, Mansuy JM, Ouezzani L, Péron JM, Guitard J, et al. Hepatitis E virus and chronic hepatitis in organ-transplant recipients. N Engl J Med. 2008;358:811–7. https://doi.org/10.1056/NEJMoa0706992
25. Versluis J, Pas SD, Agteresch HJ, de Man RA, Maaskant J, Schipper ME, et al. Hepatitis E virus: an underestimated opportunistic pathogen in recipients of allogeneic hematopoietic stem cell transplantation. Blood. 2013;122:1079–86. https://doi.org/10.1182/blood-2013-03-492363
26. Debes JD, Pisano MB, Lotto M, Re V. Hepatitis E virus infection in the HIV-positive patient. J Clin Virol. 2016;80:102–6. https://doi.org/10.1016/j.jcv.2016.05.006
27. Gauss A, Wenzel JJ, Flechtenmacher C, Navid MH, Eisenbach C, Jilg W, et al. Chronic hepatitis E virus infection in a patient with leukemia and elevated transaminases: a case report. J Med Case Reports. 2012;6:334. https://doi.org/10.1186/1752-1947-6-334
28. Domanović D, Tedder R, Blümel J, Zaaijer H, Gallian P, Niederhauser C, et al. Hepatitis E and blood donation safety in selected European countries: a shift to screening? Euro Surveill. 2017;22:30514. https://doi.org/10.2807/1560-7917.ES.2017.22.16.30514
29. Delage G, Fearon M, Gregoire Y, Hogema BM, Custer B, Scalia V, et al. Hepatitis E virus infection in blood donors and risk to patients in the United States and Canada. Transfus Med Rev. 2019;33:139–45. https://doi.org/10.1016/j.tmrv.2019.05.017
30. de Vos AS, Janssen MP, Zaaijer HL, Hogema BM. Cost-effectiveness of the screening of blood donations for hepatitis E virus in the Netherlands. Transfusion. 2017;57:258–66. https://doi.org/10.1111/trf.13978
31. Kamp C, Blümel J, Baylis SA, Bekeredjian-Ding I, Chudy M, Heiden M, et al. Impact of hepatitis E virus testing on the safety of blood components in Germany - results of a simulation study. Vox Sang. 2018;113:811–3. https://doi.org/10.1111/vox.12719
32. Vollmer T, Diekmann J, Knabbe C, Dreier J. Hepatitis E virus blood donor NAT screening: as much as possible or as much as needed? Transfusion. 2019;59:612–22. https://doi.org/10.1111/trf.15058
33. Cordes AK, Goudeva L, Lütgehetmann M, Wenzel JJ, Behrendt P, Wedemeyer H, et al. Risk of transfusion-transmitted hepatitis E virus infection from pool-tested platelets and plasma. J Hepatol. 2021.

34. Harvala H, Hewitt PE, Reynolds C, Pearson C, Haywood B, Tettmar KI, et al. Hepatitis E virus in blood donors in England, 2016 to 2017: from selective to universal screening. Euro Surveill. 2019;24:1800386. http://doi.org/10.2807/1560-7917.ES.2019.24.10.1800386
35. Gallian P, Pouchol E, Djoudi R, Lhomme S, Mouna L, Gross S, et al. Transfusion-transmitted hepatitis E virus infection in France. Transfus Med Rev. 2019;33:146–53. https://doi.org/10.1016/j.tmrv.2019.06.001
36. Dreier J, Knabbe C, Vollmer T. Transfusion-transmitted hepatitis E: NAT screening of blood donations and infectious dose. Front Med (Lausanne). 2018;5:5. https://doi.org/10.3389/fmed.2018.00005
37. Antoniak S, Mackman N. Platelets and viruses. Platelets. 2021; 32:325–30. https://doi.org/10.1080/09537104.2021.1887842
38. Shiota T, Li TC, Nishimura Y, Yoshizaki S, Sugiyama R, Shimojima M, et al. Integrin α3 is involved in non-enveloped hepatitis E virus infection. Virology. 2019;536:119–24. https://doi.org/10.1016/j.virol.2019.07.025

Address for correspondence: Heli Harvala, Microbiology Services, NHS Blood and Transplant, Colindale, London NW9 5BG, UK; email: heli.harvalasimmonds@nhsbt.nhs.uk

Costs of Tuberculosis at 3 Treatment Centers, Canada, 2010–2016

Jonathon R. Campbell, Placide Nsengiyumva, Leslie Y. Chiang, Frances Jamieson, Hadeel Khadawardi, Henry K.-H. Mah, Olivia Oxlade, Hayden Rasberry, Elizabeth Rea, Kamila Romanowski, Natasha F. Sabur, Beate Sander, Aashna Uppal, James C. Johnston, Kevin Schwartzman, Sarah K. Brode

We estimated costs of managing different forms of tuberculosis (TB) across Canada by conducting a retrospective chart review and cost assessment of patients treated for TB infection, drug-susceptible TB (DS TB), isoniazid-resistant TB, or multidrug-resistant TB (MDR TB) at 3 treatment centers. We included 90 patients each with TB infection and DS TB, 71 with isoniazid-resistant TB, and 62 with MDR TB. Median per-patient costs for TB infection (in 2020 Canadian dollars) were $804 (interquartile range [IQR] $587–$1,205), for DS TB $12,148 (IQR $4,388–$24,842), for isoniazid-resistant TB $19,319 (IQR $7,117–$41,318), and for MDR TB $119,014 (IQR $80,642–$164,015). Compared with costs for managing DS TB, costs were 11.1 (95% CI 9.1–14.3) times lower for TB infection, 1.7 (95% CI 1.3–2.1) times higher for isoniazid-resistant TB, and 8.1 (95% CI 6.1–10.6) times higher for MDR TB. Broadened TB infection treatment could avert high costs associated with managing TB disease.

After marked declines in tuberculosis (TB) incidence in Canada during the second half of the 20th century (*1*), progress toward elimination has stalled (*2*). Although a focus on detection and treatment of TB disease was highly effective in the past, changing epidemiology has limited the impact of this approach in reaching elimination. Additional approaches are needed. These approaches may include more targeted efforts for disproportionately affected populations, such as some Indigenous communities (*2*,*3*) and persons born outside of Canada (*4*).

Yet health resources are scarce (*5*). A fundamental aspect of decision-making in health is understanding the trade-offs associated with potential interventions or programs in comparison to other interventions and programs within the broader health agenda. To achieve the greatest return (improved health) on investment (money spent), policymakers should have accurate cost estimates for the various elements of TB prevention and care. However, costs associated with TB in Canada have not been estimated since 2004 (*6*). With new tests and treatments available for TB infection and disease, updated cost estimates will support informed decision-making for resource allocation around existing and emerging interventions and programs (*7*–*13*).

We sought to estimate the TB-related health system costs associated with managing persons treated for TB infection and different forms of TB disease, and the predictors of these costs, at 3 major TB treatment centers in British Columbia, Ontario, and Quebec, Canada.

Methods

Study Design and Participating TB Treatment Centers

We conducted a retrospective chart review of persons initiating treatment for TB infection, drug-susceptible

Author affiliations: McGill University, Montreal, Quebec, Canada (J.R. Campbell, P. Nsengiyumva, O. Oxlade, A. Uppal, K. Schwartzman); Research Institute of the McGill University Health Centre, Montreal (J.R. Campbell, P. Nsengiyumva, H. Rasberry, A. Uppal, K. Schwartzman); McGill International TB Centre, Montreal (J.R. Campbell, O. Oxlade, K. Schwartzman); British Columbia Centre for Disease Control, Vancouver, British Columbia, Canada (L.Y. Chiang, K. Romanowski, J.C. Johnston); University of Toronto, Toronto, Ontario, Canada (F. Jamieson, E. Rea, B. Sander, S.K. Brode); Public Health Ontario, Toronto (F. Jamieson, B. Sander); West Park Healthcare Centre, Toronto (H. Khadawardi, H.K.-H. Mah, N.F. Sabur, S.K. Brode); Toronto Public Health, Toronto (E. Rea); University of British Columbia, Vancouver (K. Romanowski, J.C. Johnston); St. Michael's Hospital, Toronto (N.F. Sabur); University Health Network, Toronto (B. Sander, S.K. Brode); Montreal Chest Institute, Montreal (K. Schwartzman)

DOI: https://doi.org/10.3201/eid2809.220092

TB (DS TB) disease, isoniazid-resistant TB disease, or multidrug-resistant TB (MDR TB) disease; we defined MDR TB as TB resistant to at least isoniazid and rifampin. We extracted data at 3 TB treatment centers in Canada: the British Columbia Centre for Disease Control (BCCDC), West Park Healthcare Centre (WPHC) in Toronto, Ontario, and the Montreal Chest Institute (MCI) in Quebec. In Canada, healthcare, including TB management, is a provincial and territorial responsibility.

BCCDC operates 2 TB clinics in the greater Vancouver region, treating all persons with TB infection and TB disease in the region. In 2016, BCCDC treated 241 persons for TB disease (all forms) and 676 persons for TB infection. WPHC, a rehabilitation and complex care hospital in Toronto, Ontario, housing a 20-bed dedicated inpatient TB unit and an ambulatory TB clinic, is recognized as a referral center for complex and drug-resistant TB. WPHC treated 119 persons for TB disease (all forms) and 33 persons for TB infection in 2016. MCI is located within the McGill University Health Centre, and is a center for TB screening and surveillance for newly arrived adult migrants to Canada. MCI treated 51 persons for TB disease (all forms) and 488 persons for TB infection in 2016.

Study Inclusion and Exclusion Criteria

We included persons of any age who initiated treatment at any participating site during July 1, 2010–June 30, 2016; we reviewed consecutive patients, working backward from the end date, to permit adequate time to complete treatment and follow-up owing to the approximate 18–20-month duration of MDR TB treatment. All forms of TB disease required microbiologic confirmation (i.e., positive culture or positive nucleic acid amplification test). In addition, DS TB required confirmed susceptibility by phenotypic or genotypic means to all first-line TB drugs (i.e., isoniazid, rifampin, ethambutol, and pyrazinamide); isoniazid-resistant TB required confirmed resistance to isoniazid and susceptibility to rifampin; and MDR TB required confirmed resistance to at least isoniazid and rifampin. We excluded persons who initiated treatment at a participating site but later transferred to another treatment site where we could not access their charts.

For MDR TB disease, all persons meeting inclusion criteria at each site were included because of the low incidence in Canada. For TB infection, DS TB disease, and isoniazid-resistant TB disease, incidence is higher and treatment is more standardized; at each site we included up to 30 consecutive persons meeting inclusion criteria (*14*). This group included patients who had initiated treatment closest to June 30, 2016, for WPHC and MCI, and closest to December 31, 2015, for BCCDC.

Procedures

For each person, we entered data into standardized forms (Appendix Table 1, https://wwwnc.cdc.gov/EID/article/28/9/22-0092-App1.pdf). In brief, for each person we collected detailed information on demographic and clinical characteristics, TB-related diagnostic tests performed, TB-related monitoring tests performed, TB-related inpatient and outpatient visits (including any visits requiring specialists), TB medication dose, frequency, and duration, including adverse events (and, if applicable, reasons for discontinuation), method of treatment administration (directly observed vs. self-administered), adjunct medications administered during treatment, use of interpreters, number of contacts traced (for all groups except those with TB infection), and posttreatment monitoring visits and evaluations. We completed data extraction during August 2018–May 2020.

At each site, we tabulated costs for services, consumables, and overheads (Appendix Table 2). We documented costs from the health system perspective in 2020 Canadian dollars (1.00 CAD ≈ 0.75 USD). When a cost item was unavailable from a given center, we used the mean from the other centers to impute it (Appendix Table 2). To determine drivers of cost, we grouped costs in 5 different categories: diagnosis, treatment, posttreatment follow-up, hospitalization, and public health costs. We did not include costs associated with healthcare seeking before TB diagnosis or for post-TB disease complications. To estimate true resource use, we performed microcosting where possible; in all other cases, we used top-down approaches.

In the diagnosis category, we performed microcosting and considered costs associated with initial physician consultations, nurse and interpreter time, and overheads, as well as costs of diagnostic tests (e.g., tuberculin skin test, chest radiograph, smear microscopy, sputum culture, drug-susceptibility testing, and computed tomography scans) and of routine screening for other related conditions (e.g., HIV infection and viral hepatitis).

In the treatment category, we performed microcosting and considered costs associated with TB and adjunct medications, tests for treatment and adverse event monitoring (e.g., for liver transaminases, complete blood count, therapeutic drug monitoring, and audiometry), tests for treatment response (e.g., sputum culture), and personnel and overhead associated

with follow-up visits with nurses, physicians, and specialists. Bedaquiline and clofazimine are given under compassionate-use programs in Canada and are not associated with costs to programs.

In the posttreatment follow-up category, we performed microcosting and only considered costs associated with surveillance for TB recurrence. These costs included chest imaging and costs of routine follow-up appointments.

In the hospitalization category, we performed microcosting and considered per-diem costs attributed to each day of hospitalization according to setting. We also considered costs associated with visits by physicians during the stay and with investigations and medications.

In the public health category, we considered costs of delivering directly observed therapy (DOT), when performed, and costs associated with contact investigation. For costs of delivering DOT, we performed microcosting at MCI and BCCDC, considering personnel (nurse, pharmacist, or both) and other costs (e.g., travel). We used a top-down approach at WPHC on the basis of data from Toronto Public Health. Because of the varied nature of contact investigations across sites, we used a top-down approach on the basis of data from Toronto Public Health because they had the most systematic and comprehensive data for contact investigation (Appendix).

Data Analysis

We performed descriptive analysis of patient characteristics by TB treatment center and form of TB (TB infection, DS TB, isoniazid-resistant TB, or MDR TB). For persons with TB infection, we also described those receiving different regimens: 9 months of isoniazid, 4 months of rifampin, or other isoniazid-containing regimens. For persons with MDR TB, we further described persons with additional resistance to a fluoroquinolone (ofloxacin, moxifloxacin, or levofloxacin), resistance to a second-line injectable drug (amikacin, kanamycin, or capreomycin), or both.

For each person, we used the itemized costs to estimate the costs associated with each cost category defined previously and summed them to arrive at an overall cost. We estimated median costs and interquartile range (IQR) to illustrate cost variation, but also estimated mean costs, because these data are most useful for policymakers. We estimated costs for each form of TB overall and in different subgroups (as relevant): sex, age at treatment initiation (dichotomous, based on median age in all persons), presence versus absence of adverse events causing drug cessation, duration of hospitalization (dichotomous, based on median hospitalization duration in all persons hospitalized), completion of treatment, acid-fast bacilli smear status, presence of cavities, and location of TB disease.

We performed regression by using linear mixed models to identify predictors of cost for all forms of TB together (using DS TB as the reference category). We conducted a subgroup analysis where we excluded TB infection to assess the impact of clinical characteristics such as radiography and microbiologic findings. We also conducted stratified analyses for each form of TB separately. We treated each site as a random intercept. For each analysis, we log-transformed costs and performed univariable analysis on several predictors (Appendix Table 3). We included age and sex as a priori predictors in all multivariable models and any predictor with a p value <0.2 in univariable analysis. We back-transformed the resultant estimates and 95% CIs, which we interpreted as cost ratios (*15*). Because costs are probably associated with treatment completion or noncompletion, we did a post hoc sensitivity analysis, in which we repeated all analyses but excluded persons who did not complete treatment. We performed all analyses in R version 4.1.0 (*16*) using package lme4 (version 1.1–23) (*17*).

This study was approved by the research ethics boards of the sites where data were collected. These boards were the Research Institute of the McGill University Health Centre (approval no. 2019-4811), the University of British Columbia (approval no. H18-01700), and West Park Healthcare Centre (approval no. 18-017-WP).

Results

Total Population

We included a total of 313 persons in the study: 101 (32%) from BCCDC, 132 (42%) from WPHC, and 80 (26%) from MCI. We tabulated the characteristics of included persons (Table 1) and the estimated costs of their management, stratified by form of TB (Table 2). We also stratified costs by patient characteristics (Appendix Tables 4–7). We determined mean costs for all analyses (Appendix Table 8). Overall, the median cost of TB infection was $804 (IQR $587–$1,205), of DS TB disease was $12,148 (IQR $4,388–$24,842), of isoniazid-resistant TB disease was $19,319 (IQR $7,117–$41,318), and of MDR TB disease was $119,014 (IQR $80,642–$164,015).

We determined the relative contribution of each cost category to the overall cost of management, again stratified by form of TB (Figure). Although diagnosis costs were a substantial contributor to overall costs

in TB infection, their contribution was comparatively smaller for other forms of TB. For TB disease (DS TB, isoniazid-resistant TB, and MDR TB), hospitalization costs accounted for a substantial proportion of all costs (54.4% for DS TB, 61.7% for isoniazid-resistant TB, and 37.2% for MDR TB).

Among the 313 persons, multivariable regression estimated costs of managing TB infection were 11.1 times lower (adjusted cost ratio 0.09 [95% CI 0.07–0.11]) than costs of managing DS TB. Conversely, costs of managing isoniazid-resistant TB were 1.7 times higher (95% CI 1.3–2.1) than DS TB, whereas costs of managing MDR TB were 8.1 times higher (95% CI 6.1–10.6) than DS TB (Table 3; univariable regression results [Appendix Table 9]). When we excluded TB infection from multivariable regression and included clinical characteristics (Appendix Table 10), adjusted cost ratios were reduced for isoniazid-resistant TB (1.3 [95% CI 1.1–1.7]) and MDR TB (3.6 [95% CI 2.6–5.1]). Estimates were not substantially different when we excluded persons who did not complete treatment (Appendix Table 11).

TB Infection

Overall, we included 90 persons treated for TB infection (30 at each center) (Table 1). Of these persons, 53

Table 1. Characteristics of patients initiating treatment for different forms of TB at 3 treatment centers, Canada, July 2010–June 2016*

Characteristic	No. (%)			
	TB infection, n = 90	DS TB, n = 90	INHR TB, n = 71	MDR TB, n = 62
TB treatment center, province				
British Columbia Centre for Disease Control	30 (33)	30 (33)	30 (42)	11 (18)
West Park Healthcare Centre, Ontario	30 (33)	30 (33)	27 (38)	45 (73)
Montreal Chest Institute, Quebec	30 (33)	30 (33)	14 (20)	6 (9)
Year of treatment initiation				
2010–2011	0 (0)	0 (0)	12 (17)	10 (16)
2012–2013	1 (1)	0 (0)	13 (18)	19 (31)
2014	15 (17)	1 (1)	20 (28)	15 (24)
2015	42 (47)	57 (64)	22 (31)	13 (21)
2016	32 (35)	32 (35)	4 (6)	5 (8)
Age				
Median (IQR) age, y	36 (31–49)	43 (30–62)	44 (31–61)	32 (27–47)
Sex				
F	55 (61)	50 (56)	38 (54)	34 (55)
M	35 (39)	40 (44)	33 (46)	28 (45)
Nativity				
Born in Canada	11 (12)	10 (11)	9 (13)	5 (8)
Born outside Canada	79 (88)	80 (89)	62 (87)	57 (92)
HIV status				
Positive	0	1 (1)	0 (0)	1 (2)
Negative	33 (37)	69 (77)	12 (17)	59 (95)
Unknown	57 (63)	20 (22)	59 (83)	2 (3)
Diabetes				
Has diabetes	12 (13)	13 (14)	10 (14)	10 (16)
Does not have diabetes	74 (82)	75 (83)	60 (85)	52 (84)
Unknown	4 (4)	2 (2)	1 (1)	0
Hospitalization Information				
Hospitalized	0	46 (51)	47 (66)	60 (97)
Median (IQR) duration, d	NA	24 (9–36)	23 (17–69)	99 (66–159)
Treatment information				
Median (IQR) duration, mo	5.8 (4.0–9.0)	8.9 (6.1–9.6)	11.7 (9.1–16.7)	21.2 (20.0–24.7)
Had to stop ≥1 drug because of adverse event	7 (8)	38 (42)	29 (41)	52 (84)
Median (IQR) drugs stopped because of adverse event	0 (0–0)	0 (0–1)	0 (0–1)	2 (1–3)
Cure or treatment complete	77 (86)	83 (92)	63 (89)	49 (79)
Incomplete treatment	13 (14)	7 (8)	8 (11)	13 (21)
Clinical characteristics				
Pulmonary TB only	NA	68 (76)	51 (72)	47 (76)
Extrapulmonary TB	NA	22 (24)	20 (28)	15 (24)
AFB smear positive	NA	47 (52)	35 (49)	22 (35)
Cavities on chest x-ray	NA	30 (33)	21 (30)	15 (24)
Public health characteristics				
Used directly observed therapy	NA	32 (36)	33 (46)	54 (86)
Mean (range) no. contacts	NA	4 (0–30)	8 (0–224)	4 (0–97)

*Data are no. (%) except as indicated. AFB, acid-fast bacilli; DS, drug-susceptible; INHR, isoniazid-resistant; IQR, interquartile range; MDR, multidrug-resistant; NA, not applicable; TB, tuberculosis.

Table 2. Total costs and component costs of managing different forms of TB at 3 treatment centers, Canada, July 2010–June 2016*

Characteristic	Cost, in 2020 Canadian dollars			
	TB infection, n = 90	DS TB, n = 90	INHR TB, n = 71	MDR TB, n = 62
Median (IQR) costs†				
Total costs	804 (587–1,205)	12,148 (4,388–24,842)	19,319 (7,117–41,318)	119,014 (80,642–164,015)
Diagnosis	267 (217–376)	701 (526–1,026)	819 (657–1,049)	1,083 (925–1,331)
Treatment	521 (377–771)	2,145 (1,614–3,187)	2,864 (2,263–3,919)	61,426 (29,840–108,703)
Posttreatment monitoring	0 (0–0)	139 (28–283)	130 (39–195)	193 (39–341)
Hospitalization	0 (0–0)	2,600 (0–15,524)	10,400 (0–27,227)	41,216 (35,178–55,766)
Associated with public health interventions	0 (0–0)	3,174 (632–5,232)	2,885 (1,111–6,174)	6,399 (4,657–6,798)
Mean costs‡				
Total costs	917	15,772	32,343	131,780
Diagnosis	308	789	860	1,233
Treatment	587	2,585	4,641	74,709
Posttreatment monitoring	22	181	166	243
Hospitalization	0	8,587	19,963	48,791
Associated with public health interventions	0	3,630	6,713	6,804

*AFB, acid-fast bacilli; DS, drug-susceptible; INHR, isoniazid-resistant; IQR, interquartile range; MDR, multidrug-resistant; TB, tuberculosis.
†Component values may not sum to the total cost value because of use of medians.
‡Component values may not sum to the total cost value because of rounding.

(59%) initiated 9 months of isoniazid, 35 (39%) initiated 4 months of rifampin, and 2 (2%) initiated isoniazid and rifampin (Appendix Tables 12, 13).

Approximately two-thirds of costs for TB infection were associated with treatment (Figure); absolute treatment costs were correlated with duration (Appendix Table 13). Persons initiating an isoniazid-containing regimen had overall costs 1.3-times (95% CI 0.98–1.7) higher than persons initiating a rifampin-only regimen (Table 3).

DS TB Disease

We included 90 persons treated for DS TB disease (30 at each center) (Table 1). Approximately half (46 [51%]) were hospitalized for a median duration of 24 (IQR 9–36) days. The median duration of treatment was 8.9 (IQR 6.1–9.6) months; treatment was shorter for persons who were smear-negative and without cavities (6.6 months [IQR 6.1–9.1]) compared with persons who were smear-positive or had cavities, or both (9.1 months [IQR 6.4–10.0]) (Appendix Table 14).

More than half the cost of DS TB disease management was related to hospitalization, whereas approximately one third reflected contact investigations and DOT administration (Figure). Costs of managing DS TB disease were much lower at MCI (median $4,987) than at WPHC ($13,328) and BCCDC ($15,201), largely because of variation in disease severity and attendant differences in hospitalization among persons treated at these centers (Appendix Table 14). Costs were 3.7 (95% CI 1.9–7.4) times higher for persons hospitalized for ≥2 months compared with persons not hospitalized at all or hospitalized <2 months (Table 3).

Isoniazid-Resistant TB Disease

We included 71 persons treated for isoniazid-resistant TB disease (30 at BCCDC, 27 at WPHC, and 14 at MCI) (Table 1). Of those, 47 (66%) were hospitalized, with median duration 23 (IQR 17–69) days. The

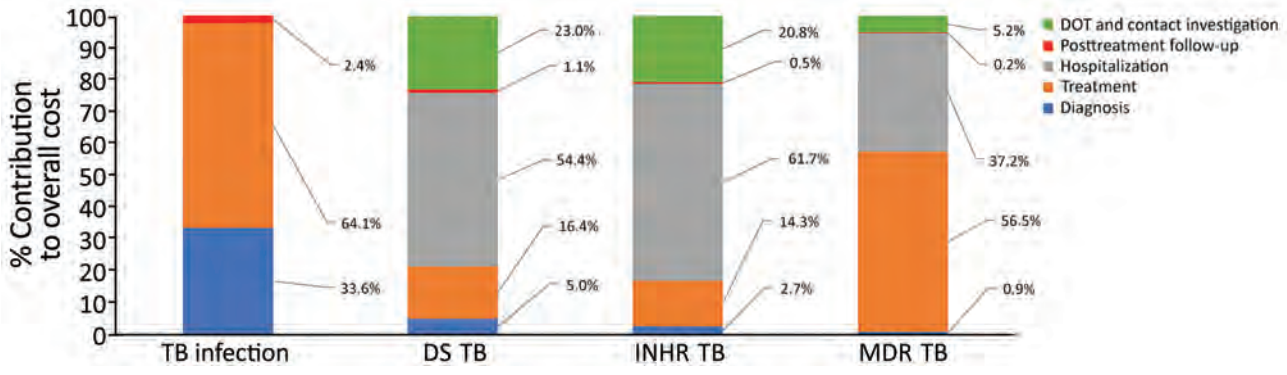

Figure. Relative contribution of each cost category to overall cost of managing different forms of TB at 3 treatment centers, Canada, July 2010–June 2016. DOT, directly observed therapy; DS, drug-susceptible; INHR, isoniazid-resistant; MDR, multidrug-resistant; TB, tuberculosis.

median treatment duration was 11.7 (IQR 9.1–16.7) months and varied substantially by TB treatment center (Appendix Table 15). Fifty-four (76%) persons received regimens containing a fluoroquinolone, and 8 (11%) received a second-line injectable (Appendix Table 15).

Over 60% of costs associated with isoniazid-resistant TB disease were because of hospitalization (Figure). Treatment was shortest and costs lowest at MCI (median duration 8 months; median cost $6,504) and treatment longest and costs highest at WPHC (median duration 17.6 months; median cost $34,400). Costs were 3.2 (95% CI 2.1–4.7) times higher for persons hospitalized ≥2 months compared with patients not hospitalized at all or hospitalized <2 months (Table 3).

MDR TB Disease

We included 62 persons treated for MDR TB disease (11 at BCCDC, 45 at WPHC, and 6 at MCI) (Table 1). Of these, 2 (3%) had additional fluoroquinolone resistance, 6 (10%) had additional resistance to a second-line injectable, and 4 (6%) had both. Nearly all (60 [97%]) were hospitalized for a median duration

Table 3. Multivariable analysis of characteristics associated with increasing or decreasing costs of managing different forms of TB at 3 treatment centers, Canada, July 2010–June 2016*

Characteristic	Cost ratio (95% CI)				
	All patients, n = 313	TB infection, n = 90	DS TB, n = 90	INHR TB, n = 71	MDR TB, n = 62
TB type					
DS TB	Referent	NA	NA	NA	NA
TB infection	0.09 (0.07–0.11)	NA	NA	NA	NA
INHR TB	1.7 (1.3–2.1)	NA	NA	NA	NA
MDR TB	8.1 (6.1–10.6)	NA	NA	NA	NA
Age group, y					
<40	Referent	Referent	Referent	Referent	Referent
≥40	0.97 (0.8–1.2)	1.3 (1.1–1.5)	0.9 (0.6–1.3)	1.2 (0.9–1.6)	0.9 (0.7–1.1)
Sex					
F	Referent	Referent	Referent	Referent	Referent
M	0.9 (0.8–1.1)	0.99 (0.8–1.2)	0.8 (0.6–1.1)	1.01 (0.8–1.4)	0.98 (0.8–1.3)
HIV					
HIV-negative or unknown	Referent	NA†	Referent	NA†	NA‡
HIV-positive	1.8 (0.6–5.4)	NA†	11.9 (2.7–52.0)	NA†	NA‡
Diabetes					
No diabetes or unknown	NA‡	NA‡	NA‡	Referent	NA‡
Has diabetes	NA‡	NA‡	NA‡	1.4 (0.9–2.2)	NA‡
Adverse events causing drug stop					
None	Referent	NA‡	Referent	Referent	NA‡
Because of ≥1 drug	1.4 (1.1–1.7)	NA‡	1.5 (1.03–2.0)	1.2 (0.9–1.7)	NA‡
Hospitalization					
None or <2 mo	NA	NA	Referent	Referent	Referent
≥2 mo	NA	NA	3.7 (1.9–7.4)	3.2 (2.1–4.7)	1.5 (1.1–2.0)
AFB smear					
Negative or unknown	NA	NA	Referent	Referent	Referent
Positive	NA	NA	1.5 (0.98–2.2)	1.3 (0.9–1.7)	1.02 (0.8–1.3)
Cavities on chest radiograph					
No or unknown	NA	NA	Referent	NA‡	Referent
Yes	NA	NA	1.2 (0.8–1.8)	NA‡	1.3 (0.96–1.8)
TB location					
Pulmonary only	NA	NA	Referent	NA‡	NA‡
Extrapulmonary involvement	NA	NA	0.7 (0.5–1.1)	NA‡	NA‡
No. contacts					
Per additional contact	NA	NA	1.05 (1.02–1.08)	1.02 (1.01–1.02)	1.01 (0.99–1.01)
Received DOT					
No	NA	NA	NA‡	Referent	Referent
Yes	NA	NA	NA‡	2.0 (1.2–3.3)	0.8 (0.5–1.3)
TB infection regimen					
Mono-rifampin	NA	Referent	NA	NA	NA
Isoniazid-containing	NA	1.3 (0.97–1.7)	NA	NA	NA
MDR TB resistance pattern					
MDR TB	NA	NA	NA	NA	Referent
Fluoroquinolone-resistance, SLI resistance, or both	NA	NA	NA	NA	1.4 (1.02–2.0)

*AFB, acid-fast bacilli; DOT, directly observed therapy; DS, drug-susceptible; INHR, isoniazid-resistant; IQR, interquartile range; MDR, multidrug-resistant; NA, not applicable; SLI, second-line injectable; TB, tuberculosis.
†No persons living with HIV in patient group.
‡Not retained in multivariable model because p≥0.2 in univariable analysis.

Table 4. Duration and costs of drugs used among patients initiating treatment for MDR-TB disease (n = 62) at 3 treatment centers, Canada, July 2010–June 2016*

Drug	No. (%) patients receiving drug	Median (IQR) duration, mo	Cost, 2020 Canadian dollars	
			Median (IQR) cost per person	Mean cost per person
Amikacin	58 (94)	5.1 (2.6–8.2)	4,024 (2,629–8,479)	7,263
Moxifloxacin	58 (94)	19.9 (8–22.4)	809 (318–985)	698
Ethambutol	56 (90)	8.6 (1.1–15.9)	280 (51–637)	382
Pyrazinamide	53 (85)	3.1 (0.8–8.8)	217 (50–800)	545
Clofazimine	50 (81)	19.7 (6.8–22.6)	Given under compassionate use	
Isoniazid†	47 (76)	0.7 (0.4–1.7)	14 (9–35)	44
Para-amino salicylic acid	47 (76)	13.6 (3.2–20.4)	6,609 (1,917–11,411)	7,036
Rifampin†	46 (74)	0.7 (0.5–1.3)	15 (9–35)	37
Cycloserine	42 (68)	13.4 (7–20.6)	57,658 (28,942–91,935)	61,590
Ethionamide	40 (65)	11.3 (2.8–19.7)	691 (191–1,304)	785
Linezolid	34 (55)	8.4 (3.5–16.2)	10,057 (4,608–19,023)	12,070
Amoxicillin/clavulanate	20 (32)	14.3 (3.9–18.6)	1,144 (286–1,652)	1,524
Imipenem/cilastatin	14 (23)	6.1 (1.8–7.3)	8,459 (3,244–10,267)	7,855
Levofloxacin	13 (21)	11.4 (6.4–18.2)	330 (69–1,328)	1,022
Clarithromycin	10 (16)	16.8 (3.4–21.8)	2,711 (549–3,531)	2,226
Rifabutin	5 (8)	22.9 (22.7–23.7)	13,207 (11,490–13,341)	10,865
Delamanid	4 (6)	3.7 (1.6–6.9)	22,437 (5,616–38,475)	21,654
Azithromycin	3 (5)	9.5 (6.8–13.4)	41 (29–3,850)	2,572
Bedaquiline	3 (5)	5.5 (3.9–5.5)	Given under compassionate use	
Meropenem	3 (5)	2.1 (1.3–10.2)	21,123 (10,766–75,480)	50,456
Streptomycin	2 (3)	0.7 (0.4–1.1)	980 (512–1,448)	980

*IQR, interquartile range.
†Stopped when resistance detected if treatment had been started before MDR TB confirmation.

of 99 (IQR 66–159) days. The median treatment duration was 21.2 (IQR 20.0–24.7) months and was similar across centers (Appendix Table 16). About half (34 [55%]) of the patients received linezolid, whereas few received the newer drugs bedaquiline (3 [5%]) or delamanid (4 [6%]) (Appendix Tables 16, 17).

Costs associated with treatment (56.5%) and hospitalization (37.2%) were the largest cost components for MDR TB management (Figure). In adjusted analyses, resistance to a fluoroquinolone, a second-line injectable, or both were associated with 1.4 (95% CI 1.02–2.0) times higher costs (Table 3).

We analyzed median duration and cost of each medication received (Table 4). Cycloserine was the most expensive drug, costing a median of $57,658 (IQR $28,942–$91,935) per person. New and repurposed drugs (i.e., linezolid, delamanid, and carbapenems) were also expensive (median cost range $8,459–$22,437). Fluoroquinolones and second-line injectables were less expensive (median cost range $330–$4,024). Compassionate-use drugs (clofazimine and bedaquiline) did not contribute to costs to TB programs.

Discussion

At 3 TB treatment centers in Canada, we found costs of managing TB infection were modest compared with costs of managing TB disease. For persons with TB disease, duration of hospitalization and extent of drug resistance were major drivers of cost. Among the 3 TB treatment centers, treatment practices varied with respect to length of hospital stays and composition or duration of treatment regimens, perhaps because of variations in treatment philosophy, isolation practices, patient profiles, or a combination of these factors, which resulted in substantial cost differences between centers.

In 2004, the average health system cost of managing TB disease in Canada was estimated to be $25,986 per person (*6*,*18*). When applying our cost estimates against the distribution of drug-resistant TB disease in Canada (*2*,*19*), we estimate an average cost of $17,506. These differences appear to be influenced by variations in study aims and approaches. The 2004 study aimed to estimate all costs spent on TB services using a top-down approach, whereas our study aimed to estimate costs per patient initiated on treatment, largely by using microcosting approaches. For example, the 2004 study included costs associated with microbiologic testing of all persons tested for TB disease, not only those ultimately treated. In contrast, our study included costs associated with outpatient specialist consultations, additional tests, and adjunctive medications, which were not included in the 2004 study.

Direct costs associated with managing MDR TB disease in Canada appear to be substantially lower than estimates from the United States for 2005–2007 (*20*). When inflated and converted to 2020 Canadian dollars (*21*), direct costs associated with MDR TB disease are ≈$243,000, or 2.0-fold more expensive than comparative estimates from this study, whereas costs

associated with MDR TB with additional resistance to a fluoroquinolone and second-line injectable are ≈$757,000, or 4.5-fold more expensive. These differences appear almost entirely driven by costs associated with hospitalization and inpatient care, as opposed to outpatient care.

This study highlights managing persons with evidence of TB infection is less costly than TB disease, particularly when using 4 months of rifampin (3 months of weekly isoniazid and rifapentine is not widely available in Canada). Hospitalization was a major driver of costs for TB disease; use of community care to prevent hospitalization may reduce overall costs (*22*). From our estimates, the total costs (including diagnosis, treatment, and posttreatment monitoring) of using 4 months of rifampin ($671 per person) for 23 persons with evidence of TB infection are equivalent to the total costs (including diagnosis, treatment, posttreatment monitoring, hospitalization, and public health interventions) of managing 1 person with DS TB disease ($15,771 per person). However, it is important to also consider costs associated with identifying persons who would benefit from TB preventive treatment in specific epidemiologic contexts, because these costs will affect the relative cost-effectiveness of preventive treatment.

Our study focused on persons initiating treatment for TB largely during 2015–2016, but new regimens have since become available. In 2018, the World Health Organization (WHO) recommended that persons with MDR TB disease treated with longer regimens should receive a fluoroquinolone, bedaquiline, linezolid, and ≥1 of clofazimine or cycloserine. Both clofazimine and bedaquiline are given under compassionate-use programs in Canada. However, a course of bedaquiline in Canada could cost $30,000 USD (*23*), whereas a course of clofazimine would cost approximately $600 USD (*24*,*25*). At these prices, the overall costs of treatment are unlikely to change, although regimens should be better tolerated (*26*). Shorter MDR TB regimens recommended by WHO (*27*) are not widely used in Canada. In 2021, the WHO conditionally recommended a moxifloxacin- and rifapentine-based 4-month regimen for DS TB disease (*28*). Despite a shorter treatment duration, costs are unlikely to be reduced in Canada because savings associated with reduced health visits and DOT will probably be outweighed by higher medication costs for rifapentine and moxifloxacin (*29*).

Our study's first limitation is that costs were only considered from the health system perspective and for persons ultimately initiating treatment from the point when persons underwent diagnostic testing for TB. This approach excludes costs associated with prediagnosis healthcare seeking behavior, the long-term financial impacts associated with TB disease, and other patient costs such as lost income, travel, and childcare, which may be substantial (*30*–*32*). The TB treatment centers included in this study were prioritized so as to obtain robust estimates of the costs of treatment for drug-resistant TB disease; the 3 centers treated ≈60% of all MDR TB disease in Canada during the study period (*33*). Other forms of TB managed at the same centers allowed for instructive comparisons. We only could capture information contained in patient charts. Most notably absent were interactions with the health system before diagnosis, which may lead to an underestimation of costs. DOT for TB disease was rarely used at BCCDC and MCI. Costs associated with public health interventions are likely to be higher at centers performing routine, daily DOT. Although we conducted microcosting to estimate true resource use where possible, we had to use top-down approaches for some costs, which may overestimate true resource use. Last, not all costs were available at all centers, and imputed costs for some centers may not be precise, although cost imputation was rare.

A key strength of our study is the comprehensive nature of data collection with respect to healthcare utilization and associated costs, which permitted microcosting of many aspects of TB care and attendant insight into cost drivers and predictors. An additional strength is the separate estimation of costs for drug-resistant TB disease, including isoniazid-resistant and MDR TB, all managed in the same centers, filling a major data gap in Canada.

In summary, costs of managing TB disease increased substantially with drug resistance and were highest among persons hospitalized for ≥2 months; the costs of managing TB infection were comparatively much smaller. Because TB rates remain stagnant in Canada, these data will be useful for policymakers considering TB prevention and care interventions to support the overall goal of TB elimination.

Acknowledgments

We acknowledge Jane McNamee, Monica Avendano, Howard Song, and Peter Derkach for their contributions toward data collection at West Park Healthcare Centre.

This study was funded by a grant (awarded to principal investigator J.C.J) from the Canadian Institutes of Health Research (grant no. PJT-153213). J.C. (award no. 287869) is funded by a postdoctoral fellowship from the Fonds de Recherche du Québec—Santé. H.R. was funded by a summer studentship from the Respiratory Epidemiology and Clinical Research Unit, Research Institute of the

McGill University Health Centre. K.R. is funded by the Canadian Institutes of Health Research Frederick Banting and Charles Best Doctoral Award. B.S. is supported, in part, by a Canada Research Chair in Economics of Infectious Diseases award (grant no. CRC-950-232429). J.C.J. is funded by a Michael Smith Health Research Award.

Author contributions: concept and design (J.R.C., O.O., J.C.J., B.S., K.S., S.K.B.); data collection and curation (J.R.C., P.N., L.C., H.K., H.R., E.R., K.R., N.S., A.U., J.C.J., K.S., S.K.B); data harmonization and analysis (J.R.C., P.N., A.U.); drafting manuscript (J.R.C., K.S., S.K.B.); manuscript revisions and intellectual content (all authors).

About the Author

Dr. Campbell is a postdoctoral fellow at McGill University, Montreal, Quebec, Canada. His primary research interest is in tuberculosis and applying health economic, epidemiologic, and meta-analytical methods in its study.

References

1. Public Health Agency of Canada. Canadian tuberculosis standards. Seventh edition. Ottawa (Ontario): Government of Canada; 2014.
2. LaFreniere M, Hussain H, He N, McGuire M. Tuberculosis in Canada: 2017. Can Commun Dis Rep. 2019;45:67–74.
3. Inuit Tapiriit Kanatami. Inuit Tuberculosis Elimination Framework. 2018 [cited 2021 Jul 29]. https://www.itk.ca/wp-content/uploads/2018/12/FINAL-ElectronicEN-Inuit-TB-Elimination-Framework.pdf
4. Campbell J, Marra F, Cook V, Johnston J. Screening immigrants for latent tuberculosis: do we have the resources? CMAJ. 2014;186:246–7. https://doi.org/10.1503/cmaj.131025
5. Drummond MF, Sculpher MJ, Claxton K, Stoddart GL, Torrance GW. Methods for the economic evaluation of health care programmes. 4th edition. New York: Oxford University Press; 2015.
6. Menzies D, Lewis M, Oxlade O. Costs for tuberculosis care in Canada. Can J Public Health. 2008;99:391–6. https://doi.org/10.1007/BF03405248
7. Menzies D, Adjobimey M, Ruslami R, Trajman A, Sow O, Kim H, et al. Four months of rifampin or nine months of isoniazid for latent tuberculosis in adults. N Engl J Med. 2018;379:440–53. https://doi.org/10.1056/NEJMoa1714283
8. Sterling TR, Villarino ME, Borisov AS, Shang N, Gordin F, Bliven-Sizemore E, et al.; TB Trials Consortium PREVENT TB Study Team. Three months of rifapentine and isoniazid for latent tuberculosis infection. N Engl J Med. 2011;365:2155–66. https://doi.org/10.1056/NEJMoa1104875
9. Diallo T, Adjobimey M, Ruslami R, Trajman A, Sow O, Obeng Baah J, et al. Safety and side effects of rifampin versus isoniazid in children. N Engl J Med. 2018 02;379(5):454–63.
10. Fregonese F, Ahuja SD, Akkerman OW, Arakaki-Sanchez D, Ayakaka I, Baghaei P, et al. Comparison of different treatments for isoniazid-resistant tuberculosis: an individual patient data meta-analysis. Lancet Respir Med. 2018;6:265–75. https://doi.org/10.1016/S2213-2600(18)30078-X
11. Abidi S, Achar J, Neino MMA, Bang D, Benedetti A, Brode S, et al. Standardised shorter regimens versus individualised longer regimens for multidrug-resistant TB. Eur Respir J. 2020;55:1901467.
12. World Health Organization. WHO consolidated guidelines on tuberculosis. Module 4: treatment: drug-resistant tuberculosis treatment. 2020 [cited 2020 Jul 31]. https://www.who.int/publications/i/item/9789240007048
13. Oh CE, Ortiz-Brizuela E, Bastos ML, Menzies D. Comparing the diagnostic performance of QFT-Plus to other tests of latent tuberculosis infection: a systematic review and meta-analysis. Clin Infect Dis. 2021;73:e1116–25. PMID 33289038
14. Kwak SG, Kim JH. Central limit theorem: the cornerstone of modern statistics. Korean J Anesthesiol. 2017;70:144–56. https://doi.org/10.4097/kjae.2017.70.2.144
15. Bastos ML, Campbell JR, Oxlade O, Adjobimey M, Trajman A, Ruslami R, et al. Health system costs of treating latent tuberculosis infection with four months of rifampin versus nine months of isoniazid in different settings. Ann Intern Med. 2020;173:169–78. https://doi.org/10.7326/M19-3741
16. R Core Team. R: a language and environment for statistical computing. 2021 [cited 2021 Jul 27]. https://www.r-project.org
17. Bates D, Mächler M, Bolker B, Walker S. Fitting linear mixed-effects models using lme4. J Stat Softw. 2015;67:1–48. https://doi.org/10.18637/jss.v067.i01
18. Bank of Canada. Inflation calculator. 2021 [cited 2021 Dec 8]. https://www.bankofcanada.ca/rates/related/inflation-calculator
19. LaFreniere M, Hussain H, Vachon J. Tuberculosis drug resistance in Canada: 2017. Can Commun Dis Rep. 2018;44:290–6. https://doi.org/10.14745/ccdr.v44i11a04
20. Marks SM, Flood J, Seaworth B, Hirsch-Moverman Y, Armstrong L, Mase S, et al.; TB Epidemiologic Studies Consortium. Treatment practices, outcomes, and costs of multidrug-resistant and extensively drug-resistant tuberculosis, United States, 2005–2007. Emerg Infect Dis. 2014;20:812–21. https://doi.org/10.3201/eid2005.131037
21. Centers for Disease Control and Prevention. CDC estimates for TB treatment costs (in 2020 U.S. dollars). 2021 [cited 2022 Jan 14]. https://www.cdc.gov/tb/publications/infographic/appendix.htm
22. Sinha P, Shenoi SV, Friedland GH. Opportunities for community health workers to contribute to global efforts to end tuberculosis. Glob Public Health. 2020;15:474–84. https://doi.org/10.1080/17441692.2019.1663361
23. McKenna L. The price of bedaquiline. 2018 [cited 2021 Dec 8]. https://www.treatmentactiongroup.org/wp-content/uploads/2018/10/reality_check_bedaquiline_10_16_18.pdf
24. Stop TB Partnership. Global Drug Facility July 2022 Medicines Catalog. 2022 [cited 2022 Aug 2]. https://www.stoptb.org/sites/default/files/gdfmedicinescatalog_1.pdf
25. Hwang TJ, Dotsenko S, Jafarov A, Weyer K, Falzon D, Lunte K, et al. Safety and availability of clofazimine in the treatment of multidrug and extensively drug-resistant tuberculosis: analysis of published guidance and meta-analysis of cohort studies. BMJ Open. 2014;4:e004143. PMID: 24384902
26. Lan Z, Ahmad N, Baghaei P, Barkane L, Benedetti A, Brode SK, et al.; Collaborative Group for the Meta-Analysis of Individual Patient Data in MDR-TB Treatment 2017. Drug-associated adverse events in the treatment of multidrug-resistant tuberculosis: an individual patient data meta-analysis. Lancet Respir Med. 2020;8:383–94. https://doi.org/10.1016/S2213-2600(20)30047-3
27. World Health Organization. Rapid communication: Key changes to the treatment of drug-resistant tuberculosis. 2022 [cited 2022 May 3]. https://www.who.int/publications/i/item/WHO-UCN-TB-2022-2

28. Dorman SE, Nahid P, Kurbatova EV, Phillips PPJ, Bryant K, Dooley KE, et al.; AIDS Clinical Trials Group; Tuberculosis Trials Consortium. Four-month rifapentine regimens with or without moxifloxacin for tuberculosis. N Engl J Med. 2021;384:1705–18. https://doi.org/10.1056/NEJMoa2033400
29. Pease C, Alvarez G, Mallick R, Patterson M, Finn S, Habis Y, et al. Cost-effectiveness analysis of 3 months of weekly rifapentine and isoniazid compared to isoniazid monotherapy in a Canadian Arctic setting. BMJ Open. 2021;11:e047514. https://doi.org/10.1136/bmjopen-2020-047514
30. Ku CC, Chen CC, Dixon S, Lin HH, Dodd PJ. Patient pathways of tuberculosis care-seeking and treatment: an individual-level analysis of National Health Insurance data in Taiwan. BMJ Glob Health. 2020;5:e002187. https://doi.org/10.1136/bmjgh-2019-002187
31. Meghji J, Gregorius S, Madan J, Chitimbe F, Thomson R, Rylance J, et al. The long term effect of pulmonary tuberculosis on income and employment in a low income, urban setting. Thorax. 2021;76:387–95. https://doi.org/10.1136/thoraxjnl-2020-215338
32. Ghazy RM, El Saeh HM, Abdulaziz S, Hammouda EA, Elzorkany AM, Khidr H, et al. A systematic review and meta-analysis of the catastrophic costs incurred by tuberculosis patients. Sci Rep. 2022;12:558. https://doi.org/10.1038/s41598-021-04345-x
33. Gallant V, Vachon J, Siu W. Tuberculosis drug resistance in Canada: 2006–2016. Can Commun Dis Rep. 2017;43:236–41. https://doi.org/10.14745/ccdr.v43i11a05

Address for corresponding: Kevin Schwartzman, Centre for Outcomes Research and Evaluation, Research Institute of the McGill University Health Centre, 5252 Boulevard de Maisonneuve Ouest, Rm D3.63, Montréal, QC H4A 3S5, Canada; email: kevin.schwartzman@mcgill.ca

Detection of Endosymbiont *Candidatus* Midichloria mitochondrii and Tickborne Pathogens in Humans Exposed to Tick Bites, Italy

Giovanni Sgroi,[1] Roberta Iatta,[1] Piero Lovreglio, Angela Stufano, Younes Laidoudi, Jairo Alfonso Mendoza-Roldan, Marcos Antonio Bezerra-Santos, Vincenzo Veneziano, Francesco Di Gennaro, Annalisa Saracino, Maria Chironna, Claudio Bandi, Domenico Otranto

During 2021, we collected blood and serum samples from 135 persons exposed to tick bites in southern Italy. We serologically and molecularly screened for zoonotic tickborne pathogens and only molecularly screened for *Candidatus* Midichloria mitochondrii. Overall, 62 (45.9%) persons tested positive for tickborne pathogens. *Coxiella burnetii* was detected most frequently (27.4%), along with *Rickettsia* spp. (21.5%) and *Borrelia* spp. (10.4%). We detected *Candidatus* M. mitochondrii DNA in 46 (34.1%) participants who had statistically significant associations to tickborne pathogens (p<0.0001). Phylogenetic analysis of *Candidatus* M. mitochondrii sequences revealed 5 clades and 8 human sequence types that correlated with vertebrates, *Ixodes* spp. ticks, and countries in Europe. These data demonstrated a high circulation of tickborne pathogens and *Candidatus* M. mitochondrii DNA in persons participating in outdoor activities in southern Italy. Our study shows how coordinated surveillance among patients, clinicians, and veterinarians could inform a One Health approach for monitoring and controlling the circulation of tickborne pathogens.

Hard ticks (Acarina: Ixodidae) represent a major public health issue worldwide and are vectors of a broad range of viruses, bacteria, and parasites of human and veterinary concern (*1*). Tickborne diseases are increasing globally (*2*), and several zoonotic tickborne pathogens, such as *Coxiella burnetii*, *Rickettsia* spp., and *Borrelia burgdorferi* sensu lato complex, are emerging or re-emerging in animals and humans (*3*,*4*).

Wild animals are increasingly becoming synanthropic, and urbanization of wildlife could bring them into contact with humans, as recently observed during the COVID-19 lockdown in Chile, when sightings of several animal species not previously seen in cities were reported in urban settlements (*5*). Wildlife movement into areas of human habitation could contribute to higher circulation of ticks, tickborne pathogens, and other zoonotic agents in suburban and rural areas (*6*). However, because of the scant notifications of tickborne diseases, limited data are available on ticks and tickborne pathogens circulating in human populations (*7*).

Because Italy is highly suited to outdoor activities such as camping, gardening, hiking, farming, and forestry work, the risk for tick bites among humans is likely high in suburban and rural environments, especially in southern regions where several species of *Ixodes* ticks have been recorded (*7*,*8*). Indeed, high seroprevalences for *Rickettsia* spp. (8.0%) and *B. burgdorferi* s.l. complex (7.5%) have been reported in forestry workers, farmers, and livestock breeders in the central-southern regions of Italy (*9*). Studies focused on humans exposed to tick bites in southern Italy also reported high seroprevalence for *C. burnetii* (16.0%) and spotted fever group rickettsiae (4.8%) that paralleled molecular detection of the same pathogens in ticks collected from the environment and infested reptiles (*4*). Those data emphasize the importance of wild

Author affiliations: University of Bari Aldo Moro, Bari, Italy (G. Sgroi, R. Iatta, P. Lovreglio, A. Stufano, Y. Laidoudi, J.A. Mendoza-Roldan, M.A. Bezerra-Santos, F. Di Gennaro, A. Saracino, M. Chironna, D. Otranto); University of Naples Federico II, Naples, Italy (V. Veneziano); Osservatorio Faunistico Venatorio, Naples (V. Veneziano); University of Milan Statale, Milan, Italy (C. Bandi); Bu-Ali Sina University, Hamedan, Iran (D. Otranto)

DOI: https://doi.org/10.3201/eid2809.220329

[1]These authors contributed equally to this article.

animals as reservoirs of tickborne pathogens. Among categories of persons at risk for tickborne pathogen infections, hunters are more likely to be infected than hikers or forestry workers (*10*); high seroprevalence for *Rickettsia* spp. was noted in hunters from Germany (9.1%) (*11*) and Brazil (14.7%) (*12*). Also, hunting dogs are considered sentinels and reservoirs of several infectious and parasitic agents, including ticks and tickborne pathogens that can be transmitted to animals and humans (*8*,*13*). Although several epidemiologic studies have reported circulation of tickborne pathogens in animals and humans worldwide, limited data are available on tick endosymbionts and their role in the transmission of pathogens or clinical onset of tickborne diseases in vertebrate hosts.

For instance, *Candidatus* Midichloria mitochondrii is an intracellular bacterial endosymbiont of ticks, which is detected inside mitochondria and has high prevalence in the sheep tick, *Ixodes ricinus* (*14*). This bacterium is vertically transmitted through generations of *I. ricinus* ticks, but strong evidence supports its transmission to vertebrate hosts via a blood meal, which has been experimentally reported in rabbits (*15*). Indeed, high *Candidatus* M. mitochondrii seroprevalence (58%) has been reported in human patients exposed to *I. ricinus* tick bites (*16*) and those affected by Lyme disease (*17*). Although these results support the idea that *Candidatus* M. mitochondrii is inoculated into the vertebrate host during the blood meal of the tick, whether this bacterium is involved in tickborne pathogen transmission remains unclear. However, screening studies for *Candidatus* M. mitochondrii DNA in human blood samples are lacking, even though DNA has been detected in several anthropophilic tick species, such as *Rhipicephalus turanicus*, *Rhipicephalus bursa*, and *Haemaphysalis punctata* (*18*); in domestic dogs, sheep, and horses (*19*); in wild roe deer (*Capreolus capreolus*) (*20*); and in laboratory rabbits (*15*).

We aimed to assess the occurrence of zoonotic tickborne pathogens in persons exposed to tick bites and living in suburban and rural areas of southern Italy. In addition, we investigated the presence and the potential involvement of *Candidatus* M. mitochondrii in tickborne pathogen infections.

Methods

Study Area

The study was conducted in 3 regions of southern Italy, Apulia, Basilicata, and Campania, which are surrounded by the Adriatic, Ionian, and Tyrrhenian Seas. These regions are characterized by a typical Mediterranean temperate climate and have progressively continental features including inland and mountainous landscapes.

Sampling

During February–December 2021, we collected blood and serum samples from 135 persons exposed to tick bites by using 10 mL BD Vacutainer EDTA Blood Collection Tubes and 5 mL BD Vacutainer Serum-separating Tubes (Beckton Dickenson, https://www.bd.com). For each participant, we used a detailed anamnestic form to collect data on patient age, sex, participation in outdoor activities (i.e., hiking, hunting, camping, gardening, farming, or forestry work), geographic origin of tick bite, and post-bite clinical findings ascribable to tickborne diseases. All samples were kept at ±4°C in portable refrigerators and delivered to the Departments of Biomedical Science and Human Oncology and Veterinary Medicine, University of Bari (Bari, Italy), for serologic and molecular analyses.

This study was conducted in accordance with ethical principles of the Declaration of Helsinki. Patients provided written informed consent after they were fully informed about the research aims and features. The research was approved by the ethics committee of the University Hospital of Bari Aldo Moro (Italy) (approval no. 6394, protocol no. 0044469-23062020).

Serologic Assays

We screened all serum samples for pathogen-specific IgG by using indirect chemiluminescent immunoassays, *Coxiella burnetii* VirCLIA IgG, *Rickettsia conorii* VirCLIA IgG, and *Borrelia* VirCLIA IgG (Vircell, https://en.vircell.com). Results were expressed by antibody concentration index, which we calculated as the ratio between the sample and calibrator relative light units and interpreted according to the manufacturer's instructions.

The *C. burnetii* IgG test showed a sensitivity of 90%, specificity of 100%, positive predictive value of 100%, and negative predictive value of 96%. The *R. conorii* IgG test showed sensitivity of 100%, specificity of 100%, positive predictive value of 100%, and negative predictive value of 100%. The *Borrelia* IgG test showed sensitivity of 89%, specificity of 98%, positive predictive value of 97%, and negative predictive value of 92%.

DNA Extraction, PCR, and Phylogenetic Analysis

We used the QIAampDNA Blood & Tissue Kit (QIAGEN, https://www.qiagen.com) to extract DNA from blood samples, according to the manufacturer's instructions, and tested for tickborne pathogens and

Candidatus M. mitochondrii. In all PCR runs, we used sterile water as the negative control and used the following as positive controls: *Anaplasma phagocytophilum* and *Candidatus* M. mitochondrii for PCR targeting 16S rRNA gene; *C. burnetii* for IS1111a and *Borrelia lusitaniae* for Flagellin from *I. ricinus* ticks; and *Rickettsia raoultii* for *gltA* from a *Dermacentor marginatus* tick specimen (Table 1) (*21*–*24*). All ticks used were previously collected from animals or humans in the same study area.

We placed PCR products on 2% agarose gel stained with GelRed Nucleic Acid Gel Stain (Biotium-VWR International, https://us.vwr.com) and visualized products on a Gel Logic 100 Digital Imaging System (Kodak, https://www.kodak.com). We then purified amplicons and sequenced in both directions by using the same primers we used for PCR and by using the BigDye Terminator v3.1 Cycle Sequencing Kit (Thermo Fisher Scientific, https://www.thermofisher.com) in a 3130 Genetic Analyzer (Applied Biosystems/Thermo Fisher Scientific). We edited and analyzed sequences by using Geneious version 9.0 (https://www.geneious.com) and compared the obtained sequences with available sequences in the GenBank database by using BLAST (http://blast.ncbi.nlm.nih.gov/Blast.cgi).

We used MAFFT version 7.490 (*25*) to align the 16S rRNA gene sequences obtained from human blood samples against 123 available *Midichloria* genus entries in GenBank, including a sequence type from *I. ricinus* (accession no. MZ954838) previously found in the study area (*8*). We then trimmed sequences by using TrimAL version 1.4 revision 15 (*26*). We split the multisequence alignment (MSA) file into 2 partitions: a reference sequence alignment (RefMSA) containing 1 reference sequence for each sequence type (38 sequences with 202 nucleotide sites) and a query sequence alignment containing the remaining 115 sequences. We created a maximum-likelihood phylogeny on the RefMSA by using IQ-TREE multicore version 1.6.12 (*27*) under 1,000 ultrafast bootstrap replications (*28*). We selected the Kimura 3-parameter model with empirical frequencies plus regression (TPM3+F+R2) model in ModelFinder (*29*), which we implemented as function in the IQ-TREE computation. We used the DNA sequence of *Lariskella* endosymbiont of *Curculio okumai* beetles (GenBank accession no. AB746416) as an outgroup. To assess the species diversity among the genus *Midichloria*, we performed a multi-rate Poisson tree processes on the maximum-likelihood tree by using mPTP version 0.2.4_osx_x86_64 (*30*). We used an accurate phylogenetic placement based on the least squares method (*31*) to place the query sequences on the maximum-likelihood tree. In brief, we subjected the maximum-likelihood tree generated by IQ-TREE to branch length correction using FastTree 2 software (http://www.microbesonline.org/fasttree). We then used the corrected tree backbone, the RefMSA, and query sequence alignments to generate the phylogenetic placement by using APPLES version 2.0.6 (*31*). Finally, we used the result of species delimitation and informative alignment to annotate the final tree by using iTOL version 5 (*32*). We performed Pearson correlation to assess the relationship between phylogenetic clades of *Midichloria* sequences and their host or isolation source and geographic origin. We performed all analyses on RStudio software (*33*).

Statistical Analysis

We established exact binomial 95% CI for the prevalence values found. We used a χ^2 test to assess statistical differences of prevalence of tickborne pathogens with age, sex, outdoor activity, and geographic origin of tick bite of the enrolled patients. We considered $p<0.05$ statistically significant. We calculated the odds ratio (OR) to assess the infection risk according to several participant variables. We used a κ value formula to compare serologic and molecular methods and considered risk agreement poor at 0–20%, fair at 21%–40%, moderate at 41%–60%, strong at 61%–80%, and perfect at 81%–100%.

We used Epitools Epidemiologic Calculators software (*34*) to calculate 95% CI, χ^2, p value, OR, and κ values. We used QGIS3 version 3.10.2 with GRASS

Table 1. Bacteria investigated by molecular methods in a study on the relationship between endosymbiont *Candidatus* Midichloria mitochondrii and tickborne pathogens in humans exposed to tick bites, Italy, 2021

Tickborne bacteria	Target gene	Primers	Sequence, 5′ → 3′	Base pairs	Reference
Coxiella burnetii	IS1111a	Trans1	TATGTATCCACCGTAGCCAGT	687	(*21*)
		Trans2	CCCAACAACACCTCCTTATTC		
Rickettsia spp.	*gltA*	CS 78F	GCAAGTATCGGTGAGGATGTAAT	401	(*22*)
		CS 323R	GCTTCCTTAAAATTCAATAAATCAGGAT		
Borrelia burgdorferi sensu lato complex	Flagellin	FLA1	AGAGCAACTTACAGACGAAATTAAT	482	(*23*)
		FLA2	CAAGTCTATTTTGGAAAGCACCTAA		
Anaplasmataceae	16S rRNA	EHR 16SD	GGTACCYACAGAAGAAGTCC	345	(*24*)
		EHR 16SR	TAGCACTCATCGTTTACAGC		

7.8.2 (QGIS Project, https://www.qgis.org) to map the distribution of participants who were positive for tickborne pathogens and *Candidatus* M. mitochondrii in the administrative boundaries of the regional study area.

Results

Among 135 participants, 47.4% (64/135) reported having been bitten by ticks in the last year, and 62 (45.9%, 95% CI 37.7%–54.3%) tested positive for ≥1 tickborne pathogen, 54 (40.0%, 95% CI 32.1%–48.4%) by serologic methods and 20 (14.8%, 95% CI 9.8%–21.8%) by molecular methods. We identified *C. burnetii* from 37 (27.4%) participants, *Rickettsia* spp. from 29 (21.5%), and *Borrelia* spp. from 14 (10.4%). We serologically detected tickborne pathogen co-infections in 14 (10.4%) participants, most of whom had *C. burnetii*–*Rickettsia* spp. coinfection. We detected co-infection by molecular methods in 1 (0.7%) case-patient who had *R. raoultii*–*B. lusitaniae* coinfection.

Nine persons were positive for the same pathogen by both diagnostic tools; 4 were positive for *C. burnetii*, 4 for *R. raoultii*, and 1 for *B. lusitaniae*. We noted strong agreement between serologic and molecular results (κ = 63.0%) (Table 2).

Among the 62 participants who tested positive for tickborne pathogens, 31 (50.0%) reported a localized reaction (i.e., edema and redness) at the tick bite site, among whom 13 (20.6%) displayed ≥1 clinical sign ascribable to tickborne pathogen infections (Table 3). We noted a statistically significant association between the occurrence of tickborne pathogens and administrative region among patients living in Basilicata, suggesting this area could have higher levels of tickborne pathogens (Table 4).

We detected *Candidatus* M. mitochondrii DNA in 46 (34.1%, 95% CI 26.6%–42.4%) participants, among whom 11 tested negative for tickborne pathogens and 35 tested positive for ≥1 tickborne pathogen. The 35 participants who tested positive for tickborne infections and *Candidatus* M. mitochondrii DNA represented 18/54 (33.3%, 95% CI 22.2%–46.6%) of participants whose infections were detected serologically and 17/20 (85.0%, 95% CI 63.9%–94.7%) of participants whose infections were detected molecularly. *Candidatus* M. mitochondrii was statistically associated with each pathogen found (i.e., *C. burnetii*, *R. raoultii*, and *B. lusitaniae*) (Table 5; Figure 1). No clinical signs were reported in persons infected by *Candidatus* M. mitochondrii and we saw no statistically significant difference in the clinical signs between subjects who tested positive for tickborne pathogens and those who were positive for both tickborne pathogens and *Candidatus* M. mitochondrii (χ^2 = 0.9, p = 0.342). A single case of *Candidatus* Wolbachia inokumae was molecularly detected in a participant infected by *B. lusitaniae*.

Consensus sequences of all bacteria species we detected displayed 99%–100% nucleotide identity with sequences available in the literature. We submitted sequences to GenBank under the following accession numbers: ON227500 for *C. burnetii*, ON228179 for *R. raoultii*, ON237925 for *B. lusitaniae*, OM982495–2502 for *M. mitochondrii*, and OM983334 for *W. inokumae*.

Phylogenetic analysis of the partial 16S rRNA gene revealed 8 sequence types and the existence of 5 distinct clades (clades A–E); the *Candidatus* M. mitochondrii sequence types we obtained belonged clade A (Figure 2). Pearson correlation (*r*) showed that *Candidatus* M. mitochondrii clade A was significantly correlated with vertebrate hosts (*r* = 0.32), *Ixodes* spp. ticks (*r* = 0.21), and countries in Europe (*r* = 0.46); clade B with *Hyalomma* ticks (*r* = 0.4) and Argasidae ticks (*Ornithodoros* spp.) (*r* = 0.36) and Africa (*r* = 0.48); clade C with *Ixodes* spp. ticks (*r* = 0.46); and clades D and E with marine sources (*r* = 0.57) (Appendix Figure, https://wwwnc.cdc.gov/EID/article/28/9/22-0329-App1.pdf).

Discussion

We report a high serologic and molecular prevalence of infection by zoonotic tickborne bacteria in humans exposed to tick bites in rural areas of southern Italy.

Table 2. Serologic and PCR findings for tickborne pathogens in humans exposed to tick bites, Italy, 2021*

	Serology		PCR	
Tickborne pathogens	No. patients	% Patients (95% CI)†	No. patients (%)	% Patients (95% CI)†
Single infections				
Coxiella burnetii	21	15.6 (10.4–22.6)	7	5.2 (2.5–10.3)
Rickettsia raoultii	14	10.4 (6.3–16.7)	6	4.4 (2.0–9.4)
Borrelia lusitaniae	5	5 (1.6–8.4)	6	4.4 (2.0–9.4)
Co-infections				
Coxiella burnetii, *Rickettsia* spp.	11	11 (4.6–14.0)	NA	NA
Coxiella burnetii, *Borrelia* spp.	2	2 (0.4–5.2)	NA	NA
Rickettsia raoultii, *Borrelia lusitaniae*	1	1 (0.1–4.1)	1	0.7 (0.1–4.1)
Total	54	54 (32.1–48.4)	20	14.8 (9.8–21.8)

*Based on 135 persons tested. NA, not applicable
†Exact binomial 95% CI.

Table 3. Clinical findings in 13 patients tested positive for tickborne pathogens, Italy, 2021*

Patient no.	Tickborne pathogens detected	Clinical findings				
		Rash	Axillary lymphadenomegaly	Fever	Myalgia	Headache
1	*Rickettsia raoultii**	N	Y	N	N	N
2	*Rickettsia* spp.†	N	N	N	N	Y
3	*Coxiella burnetii*†	N	Y	Y	Y	N
4	*Borrelia lusitaniae**	N	N	Y	Y	N
5	*Borrelia* spp.†	N	N	Y	Y	N
6	*Rickettsia* spp.†	N	Y	Y	Y	N
7	*Rickettsia* spp.†	N	N	Y	N	N
8	*B. lusitaniae**	N	N	Y	Y	N
9	*Rickettsia* spp.†	N	N	Y	Y	Y
10	*Rickettsia* spp.†	N	N	Y	Y	N
11	*C. burnetii*†	N	Y	N	N	N
12	*Borrelia* spp.†, *Rickettsia* spp.†, *B. lusitaniae**	Y‡	N	Y	N	N
13	*R. raoultii**	Y§	N	N	N	N

*Pathogen detected by PCR.
†Pathogen detected by serology.
‡Maculopapular rash.
§Erythematous macular rash.

In addition, we noted an association between *Candidatus* M. mitochondrii and tickborne pathogens in humans, suggesting that this tick endosymbiont might be involved in these infections.

The finding of *C. burnetii* as the most representative tickborne pathogen in humans from southern Italy is a public health concern because prevalence of this bacterium in hard ticks is much higher in the Mediterranean Basin than in other areas of Europe (*35*). However, the high (27.4%) overall serologic and molecular prevalence we obtained contrasts with the low (0.5%) rate of molecular detection of the bacterium in ticks collected on citizens in the same study area (*8*). This finding suggests inhalation of contaminated aerosols, not tick bites, might be the main route of pathogen transmission among the study participants (*36*).

Detection of *R. raoultii* is relevant because this pathogen is considered an emerging spotted fever group rickettsiae among humans (*37*,*38*). Although no patient in our study showed the scalp eschar and neck lymphadenopathy that are typical clinical signs for differential diagnosis (*39*), the difference in clinical features might be dependent on the site of the tick bite on a person's body (*40*).

Detection of *B. lusitaniae* in persons frequenting rural environments of southern Italy confirms the circulation of this zoonotic genospecies, which previously was reported in different hosts, such as the Italian wall lizard (*Podarcis siculus*) (*41*) and red foxes (*Vulpes vulpes*) (*42*), and in *I. ricinus* ticks collected on humans from the same study area (*8*). The human pathogenic role of *B. lusitaniae* has not been completely clarified, but the finding of erythematous macules from positive patients examined in this study is of clinical relevance because these skin lesions could cause chronic or long-lasting injuries associated with infiltration of the local subcutaneous tissues (*43*). In addition, co-infections

Table 4. Characteristics of persons tested by serology and PCR for tickborne pathogens in humans exposed to tick bites, Italy, 2021*

Characteristics	Serology†				PCR†			
	No. positive/no. tested	% Positive (95% CI)	p value	X^2	No. positive/no. tested	% Positive (95% CI)	p value	X^2
Age range, y			0.396	0.7			0.614	0.2
25–49	22/61	36.1 (25.2–48.6)			8/61	13.1 (6.8–23.8)		
50–68	32/74	43.2 (32.6–54.6)			12/74	16.2 (9.5–26.2)		
Sex			0.396	0.7			0.120	2.4
M	43/112	38.4 (29.9–47.6)			19/112	17.0 (11.1–25.0)		
F	11/23	47.8 (29.2–67.0)			1/23	4.3 (0.7–21.0)		
Outdoor activity			0.990	0.1			0.190	4.7
Farming	7/18	38.4 (20.3–61.4)			1/18	5.6 (1.0–25.7)		
Hunting	26/65	40.0 (29.0–52.1)			9/65	13.8 (7.5–24.3)		
Camping, gardening	12/31	38.7 (23.7–56.2)			8/31	25.8 (13.7–3.2)		
Hiking, forestry work	9/21	42.9 (24.5–63.4)			2/21	9.5 (2.6–28.9)		
Administrative region			0.030	6.9			0.002	12.3
Apulia	8/36	22.2 (11.7–38.1)			2/36	5.6 (1.5–18.1)		
Basilicata	17/33	51.5 (35.2–67.5)			11/33	33.3 (19.7–50.4)		
Campania	29/66	43.9 (32.6–55.9)			7/66	10.6 (5.2–20.3)		
Total	54/135	40.0 (32.1–48.4)			20/135	14.8 (9.8–21.8)		

*Number and percentage of patients testing positive out of the total number examined for each category.
†Exact binomial 95% CI is given; X^2 and p values are given for each category.

Table 5. Tickborne pathogens and *Candidatus* Midichloria mitochondrii detected in humans exposed to tick bites, Italy, 2021*

Tickborne pathogens	No. patients	*Candidatus* M. mitochondrii, no.†	% Patients (95% CI)‡	X^2	p value	OR
Coxiella burnetii	7	6	85.7 (48.7–97.4)	8.8	0.003	13.2
Rickettsia raoultii	6	5	83.3 (43.6–97.0)	6.9	0.008	11.0
Borrelia lusitaniae	6	5	83.3 (43.6–97.0)	6.9	0.008	11.0
R. raoultii–B. lusitaniae	1	1	NA	NA	NA	NA
Total	20	17	85.0 (63.9–94.7)	26.0	.001	16.1

*NA, not applicable; OR, odds ratio.
†Number and percentage of patients positive for tickborne pathogens and *Candidatus* M. mitochondrii.
‡Exact binomial 95% CI.

in this human population and in ticks previously collected from citizens of the same study area (*8*), indicate that multiple pathogens could be transmitted by the same tick specimen and develop in the same host, complicating the clinical manifestation (*7*).

Despite the strong agreement (κ = 63.0%) in the comparison between serology and PCR, use of both serologic and molecular methods is crucial for identifying all cases of infection (*44*). Indeed, combining PCR and serology can be useful for detecting recent and old infections because PCR is sensitive ≤2 weeks of infection and serology is sensitive ≥2 weeks after illness onset (*17*).

The high molecular prevalence (34.1%) of *Candidatus* M. mitochondrii in participants exposed to tick bites is in accordance with the serologic rate (47.3%) previously outlined for this endosymbiont in humans (*16*), and confirms its role as a candidate tick-bite marker (*17*). Thus, because *Candidatus* M. mitochondrii is known to subsist in several hard tick species (*18*), its detection in human blood could be a useful tool for determining exposure to tick bites and to define tick populations circulating in a certain area. The statistical association between molecular positivity for tickborne pathogens and *Candidatus* M. mitochondrii demonstrated here suggests a link between endosymbiont and tickborne pathogen infections in humans, which was previously established through serologic methods (*16*). However, absence of clinical signs or symptoms in humans testing positive for *Candidatus* M. mitochondrii and the statistically significant difference in the clinical picture between participants who tested positive only for tickborne pathogens and those who tested positive for both tickborne pathogens and *Candidatus* M. mitochondrii, suggests that this bacterium might be not involved in the onset or overt pathogenesis of primary infections. Conversely, the hypothesis of a potential *Candidatus* M. mitochondrii–tickborne pathogen interaction within tick hosts needs further investigation, as previously demonstrated for this endosymbiont in regulating the growth of *R. parkeri* in its competent vector *Amblyomma maculatum* ticks (*45*).

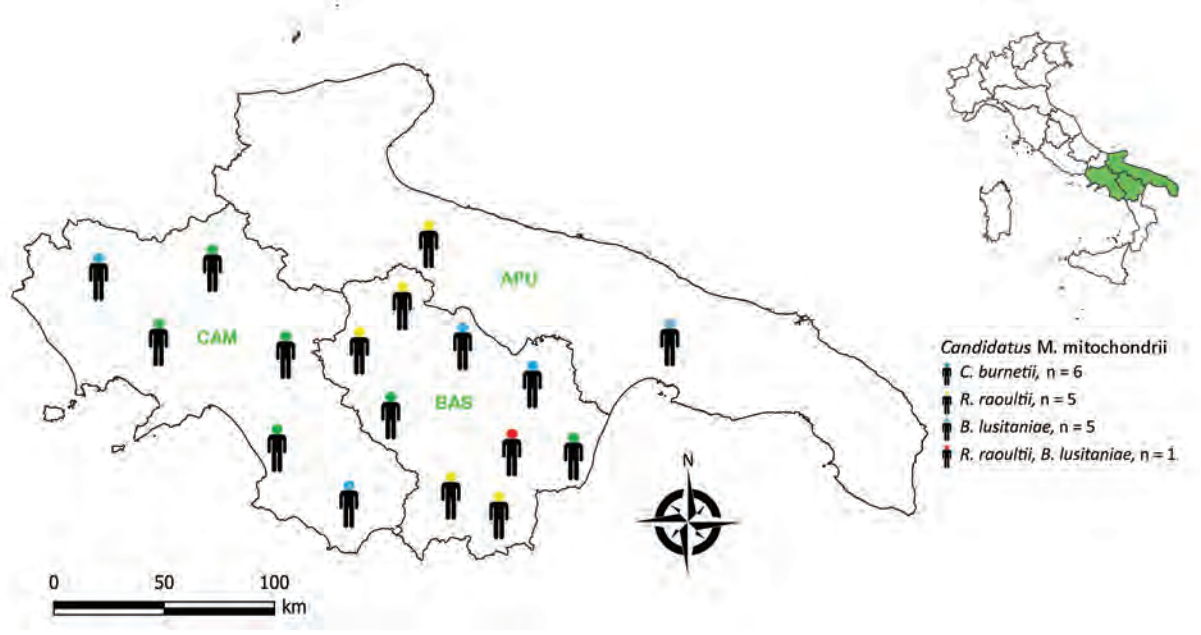

Figure 1. Distribution of 17 persons in whom *Candidatus* Midichloria mitochondrii and tickborne pathogens were detected, Italy, 2021. Inset shows region of interest in southern Italy (green shading). APU, Apulia; BAS, Basilicata; *B. lusitaniae*, *Borrelia lusitaniae*; CAM, Campania; *C. burnetii*, *Coxiella burnetii*; *R. raoultii*, *Rickettsia raoultii*.

Our results also highlight the occurrence of 8 *Candidatus* M. mitochondrii sequence types, suggesting patients were exposed to different tick species, which reinforces the hypothesis that *Candidatus* M. mitochondrii could be used as candidate marker to define the composition of the tick population biting humans in a certain area (*4*). In addition, the clustering of all sequence types into clade A, as we noted, is relevant for public health because this clade encompasses endosymbionts associated with vertebrate hosts, rather than to *Ixodes* spp. ticks, and geographic areas of Europe. On the other hand, the presence of the same *Midichloria* genotype within several tick species indicates that vertebrates might act as ecological arenas for intraspecies and interspecies–specific transmission of endosymbionts among hard ticks, which was previously suggested by similar 16S rRNA sequences in genetically distant tick species (*46*). Another phylogenetic study analyzed concatenated loci of 16S rRNA, and *groEL* and *dnaK* gene sequences, and reported 3 distinct clades (I, II, and III) of *Candidatus* M. mitochondrii associated with ticks, indicating the existence of 2 lineages including different tick species and 1 *Ixodes* genus (*47*).

Detection of *W. inokumae* DNA in humans might be a consequence of exposure to a blood meal by selected phlebotomine sandflies. In fact, *W. inokumae* has only been identified in *Phlebotomus perniciosus* sand fly specimens from France and Tunisia (*48*,*49*), where it has been indicated as endosymbiont of this arthropod species in the Mediterranean Basin.

Our data demonstrate a high circulation of tickborne pathogens and *Candidatus* M. mitochondrii in persons frequenting suburban and rural areas of southern Italy. Further experimental studies could clarify the biologic interaction between tickborne pathogens and *Candidatus* M. mitochondrii and the potential role of *Candidatus* M. mitochondrii in tickborne pathogen transmission to mammalian hosts. The set of 16S rRNA sequences and their cladogenetic classification we generated could be a useful template for future studies, especially for futher description of new *Candidatus* M. mitochondrii clades.

In conclusion, the survey we describe relies on cooperation between different stakeholders, including

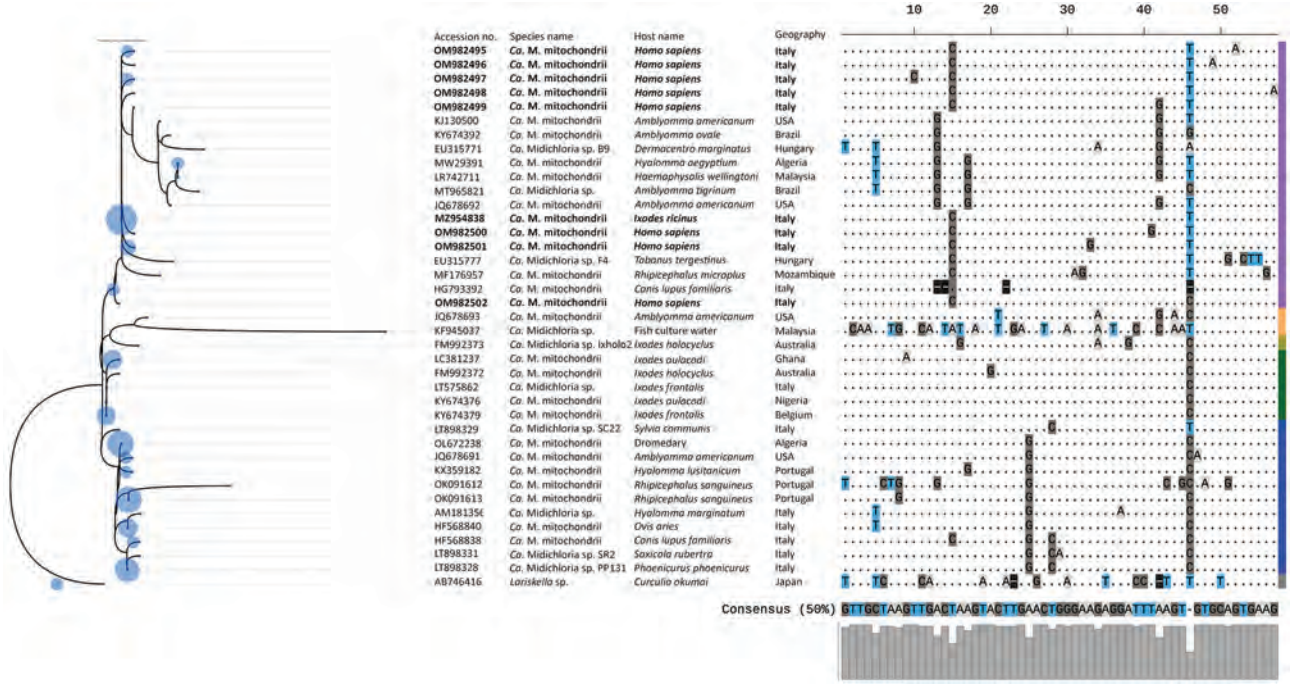

Figure 2. Maximum-likelihood phylogenic tree of endosymbiont *Candidatus* Midichloria mitochondrii clades detected with tickborne pathogens in humans exposed to tick bites, Italy, 2021. The tree corresponds to the IQ-TREE (http://www.iqtree.org) inferred from 38 partial (202 bp) DNA sequences with 28.7% of informative sites by using the Kimura 3-parameter model with empirical frequencies plus regression (TPM3+F+R2) model under 1,000 bootstrap replicates and maximum-likelihood method. Accession numbers and species name are indicated at the tip of each branch. Bold blue text indicates sequences amplified in the study area. The tree includes 123 query sequences representing all 16S rRNA entries from GenBank (blue circles on left) placed at the branch and leaf nodes by using the APPLES algorithm (https://github.com/balabanmetin/apples). The ClustalX (http://www.clustal.org/clustal2) sequence alignment viewer of the informative sites from the 16S rRNA alignment and their 50% consensus are shown. Colored column at far right denotes taxonomic annotation; purple indicates clade A, blue indicates clade B, green indicates clade C, yellow indicates clade D, green indicates clade E, gray indicates outgroup. *Ca*., *Candidatus*.

patients, clinicians, and veterinarians. This type of surveillance could be a small step toward a One Health approach for monitoring and controlling the circulation of tickborne pathogens in suburban and rural areas (*50*).

Acknowledgments

We thank all participants, physicians, and veterinary practitioners involved in the field activities, and we thank Chris Arme for his useful suggestions to the text and English language revisions.

About the Author

Mr. Sgroi is a PhD candidate at the University of Bari Aldo Moro, Bari, Italy. His main research interests focus on biology, epidemiology, and control of vector-borne pathogens of zoonotic concern.

References

1. Dantas-Torres F, Chomel BB, Otranto D. Ticks and tick-borne diseases: a One Health perspective. Trends Parasitol. 2012;28:437–46. https://doi.org/10.1016/j.pt.2012.07.003
2. Kuehn B. Tickborne diseases increasing. JAMA. 2019;321:138.
3. Madison-Antenucci S, Kramer LD, Gebhardt LL, Kauffman E. Emerging tick-borne diseases. Clin Microbiol Rev. 2020;33:e00083-18. https://doi.org/10.1128/CMR.00083-18
4. Mendoza-Roldan JA, Ravindran Santhakumari Manoj R, Latrofa MS, Iatta R, Annoscia G, Lovreglio P, et al. Role of reptiles and associated arthropods in the epidemiology of rickettsioses: A One Health paradigm. PLoS Negl Trop Dis. 2021;15:e0009090. https://doi.org/10.1371/journal.pntd.0009090
5. Silva-Rodríguez EA, Gálvez N, Swan GJF, Cusack JJ, Moreira-Arce D. Urban wildlife in times of COVID-19: what can we infer from novel carnivore records in urban areas? Sci Total Environ. 2021;765:142713. https://doi.org/10.1016/j.scitotenv.2020.142713
6. Sgroi G, Iatta R, Lia RP, D'Alessio N, Manoj RRS, Veneziano V, et al. Spotted fever group rickettsiae in *Dermacentor marginatus* from wild boars in Italy. Transbound Emerg Dis. 2021;68:2111–20. https://doi.org/10.1111/tbed.13859
7. Otranto D, Dantas-Torres F, Giannelli A, Latrofa MS, Cascio A, Cazzin S, et al. Ticks infesting humans in Italy and associated pathogens. Parasit Vectors. 2014;7:328. https://doi.org/10.1186/1756-3305-7-328
8. Sgroi G, Iatta R, Lia RP, Napoli E, Buono F, Bezerra-Santos MA, et al. Tick exposure and risk of tick-borne pathogens infection in hunters and hunting dogs: a citizen science approach. Transbound Emerg Dis. 2022;69:e386–93. https://doi.org/10.1111/tbed.14314
9. Santino I, Cammarata E, Franco S, Galdiero F, Oliva B, Sessa R, et al. Multicentric study of seroprevalence of *Borrelia burgdorferi* and *Anaplasma phagocytophila* in high-risk groups in regions of central and southern Italy. Int J Immunopathol Pharmacol. 2004;17:219–23. https://doi.org/10.1177/039463200401700214
10. Toepp AJ, Willardson K, Larson M, Scott BD, Johannes A, Senesac R, et al. Frequent exposure to many hunting dogs significantly increases tick exposure. Vector Borne Zoonotic Dis. 2018;18:519–23. https://doi.org/10.1089/vbz.2017.2238
11. Jansen A, La Scola B, Raoult D, Lierz M, Wichmann O, Stark K, et al. Antibodies against *Rickettsia* spp. in hunters, Germany. Emerg Infect Dis. 2008;14:1961–3. https://doi.org/10.3201/eid1412.080229
12. Kmetiuk LB, Krawczak FS, Machado FP, Paploski IAD, Martins TF, Teider-Junior PI, et al. Ticks and serosurvey of anti-*Rickettsia* spp. antibodies in wild boars (*Sus scrofa*), hunting dogs and hunters of Brazil. PLoS Negl Trop Dis. 2019;13:e0007405. https://doi.org/10.1371/journal.pntd.0007405
13. Sgroi G, Varcasia A, Dessì G, D'Alessio N, Pacifico L, Buono F, et al. Massive *Taenia hydatigena* cysticercosis in a wild boar (*Sus scrofa*) from Italy. Acta Parasitol. 2019;64:938–41. https://doi.org/10.2478/s11686-019-00110-3
14. Stavru F, Riemer J, Jex A, Sassera D. When bacteria meet mitochondria: the strange case of the tick symbiont *Midichloria mitochondrii*. Cell Microbiol. 2020;22:e13189. https://doi.org/10.1111/cmi.13189
15. Cafiso A, Sassera D, Romeo C, Serra V, Hervet C, Bandi C, et al. *Midichloria mitochondrii*, endosymbiont of *Ixodes ricinus*: evidence for the transmission to the vertebrate host during the tick blood meal. Ticks Tick Borne Dis. 2019;10:5–12. https://doi.org/10.1016/j.ttbdis.2018.08.008
16. Mariconti M, Epis S, Gaibani P, Dalla Valle C, Sassera D, Tomao P, et al. Humans parasitized by the hard tick *Ixodes ricinus* are seropositive to *Midichloria mitochondrii*: is *Midichloria* a novel pathogen, or just a marker of tick bite? Pathog Glob Health. 2012;106:391–6. https://doi.org/10.1179/2047773212Y.0000000050
17. Serra V, Krey V, Daschkin C, Cafiso A, Sassera D, Maxeiner HG, et al. Seropositivity to *Midichloria mitochondrii* (order Rickettsiales) as a marker to determine the exposure of humans to tick bite. Pathog Glob Health. 2019;113:167–72. https://doi.org/10.1080/20477724.2019.1651568
18. Epis S, Sassera D, Beninati T, Lo N, Beati L, Piesman J, et al. *Midichloria mitochondrii* is widespread in hard ticks (Ixodidae) and resides in the mitochondria of phylogenetically diverse species. Parasitology. 2008;135:485–94. https://doi.org/10.1017/S0031182007004052
19. Bazzocchi C, Mariconti M, Sassera D, Rinaldi L, Martin E, Cringoli G, et al. Molecular and serological evidence for the circulation of the tick symbiont *Midichloria* (Rickettsiales: Midichloriaceae) in different mammalian species. Parasit Vectors. 2013;6:350. https://doi.org/10.1186/1756-3305-6-350
20. Serra V, Cafiso A, Formenti N, Verheyden H, Plantard O, Bazzocchi C, et al. Molecular and serological evidence of the presence of *Midichloria mitochondrii* in roe deer (*Capreolus capreolus*) in France. J Wildl Dis. 2018;54:597–600. https://doi.org/10.7589/2017-09-241
21. Berri M, Laroucau K, Rodolakis A. The detection of *Coxiella burnetii* from ovine genital swabs, milk and fecal samples by the use of a single touchdown polymerase chain reaction. Vet Microbiol. 2000;72:285–93. https://doi.org/10.1016/S0378-1135(99)00178-9
22. Labruna MB, Whitworth T, Horta MC, Bouyer DH, McBride JW, Pinter A, et al. *Rickettsia* species infecting *Amblyomma cooperi* ticks from an area in the state of São Paulo, Brazil, where Brazilian spotted fever is endemic. J Clin Microbiol. 2004;42:90–8. https://doi.org/10.1128/JCM.42.1.90-98.2004
23. Wójcik-Fatla A, Szymańska J, Wdowiak L, Buczek A, Dutkiewicz J. Coincidence of three pathogens (*Borrelia burgdorferi* sensu lato, *Anaplasma phagocytophilum* and *Babesia*

microti) in *Ixodes ricinus* ticks in the Lublin macroregion. Ann Agric Environ Med. 2009;16:151–8.
24. Parola P, Roux V, Camicas JL, Baradji I, Brouqui P, Raoult D. Detection of *Ehrlichiae* in African ticks by polymerase chain reaction. Trans R Soc Trop Med Hyg. 2000;94:707–8. https://doi.org/10.1016/S0035-9203(00)90243-8
25. Nakamura T, Yamada KD, Tomii K, Katoh K. Parallelization of MAFFT for large-scale multiple sequence alignments. Bioinformatics. 2018;34:2490–2. https://doi.org/10.1093/bioinformatics/bty121
26. Capella-Gutiérrez S, Silla-Martínez JM, Gabaldón T. trimAl: a tool for automated alignment trimming in large-scale phylogenetic analyses. Bioinformatics. 2009;25:1972–3. https://doi.org/10.1093/bioinformatics/btp348
27. Minh BQ, Schmidt HA, Chernomor O, Schrempf D, Woodhams MD, von Haeseler A, et al. IQ-TREE 2: new models and efficient methods for phylogenetic inference in the genomic era. Mol Biol Evol. 2020;37:1530–4. https://doi.org/10.1093/molbev/msaa015
28. Hoang DT, Chernomor O, von Haeseler A, Minh BQ, Vinh LS. UFBoot2: improving the ultrafast bootstrap approximation. Mol Biol Evol. 2018;35:518–22. https://doi.org/10.1093/molbev/msx281
29. Kalyaanamoorthy S, Minh BQ, Wong TKF, von Haeseler A, Jermiin LS. ModelFinder: fast model selection for accurate phylogenetic estimates. Nat Methods. 2017;14:587–9. https://doi.org/10.1038/nmeth.4285
30. Zhang J, Kapli P, Pavlidis P, Stamatakis A. A general species delimitation method with applications to phylogenetic placements. Bioinformatics. 2013;29:2869–76. https://doi.org/10.1093/bioinformatics/btt499
31. Balaban M, Sarmashghi S, Mirarab S. APPLES: scalable distance-based phylogenetic placement with or without alignments. Syst Biol. 2020;69:566–78. https://doi.org/10.1093/sysbio/syz063
32. Letunic I, Bork P. Interactive Tree Of Life (iTOL) v5: an online tool for phylogenetic tree display and annotation. Nucleic Acids Res. 2021;49(W1):W293–6. https://doi.org/10.1093/nar/gkab301
33. RStudio Team. RStudio: integrated development for R [cited 2022 Jan 12]. https://www.rstudio.com
34. Sergeant ESG. Epitools epidemiological calculators. Ausvet. 2018 [cited 2022 Jan 14]. http://epitools.ausvet.com.au
35. Körner S, Makert GR, Ulbert S, Pfeffer M, Mertens-Scholz K. The prevalence of *Coxiella burnetii* in hard ticks in Europe and their role in Q fever transmission revisited—a systematic review. Front Vet Sci. 2021;8:655715. https://doi.org/10.3389/fvets.2021.655715
36. Gürtler L, Bauerfeind U, Blümel J, Burger R, Drosten C, Gröner A, et al. *Coxiella burnetii* – pathogenic agent of Q (query) fever. Transfus Med Hemother. 2014;41:60–72.
37. Mediannikov O, Matsumoto K, Samoylenko I, Drancourt M, Roux V, Rydkina E, et al. *Rickettsia raoultii* sp. nov., a spotted fever group rickettsia associated with *Dermacentor* ticks in Europe and Russia. Int J Syst Evol Microbiol. 2008;58:1635–9. https://doi.org/10.1099/ijs.0.64952-0
38. Parola P, Rovery C, Rolain JM, Brouqui P, Davoust B, Raoult D. *Rickettsia slovaca* and *R. raoultii* in tick-borne rickettsioses. Emerg Infect Dis. 2009;15:1105–8. https://doi.org/10.3201/eid1507.081449
39. Li H, Zhang PH, Huang Y, Du J, Cui N, Yang ZD, et al. Isolation and identification of *Rickettsia raoultii* in human cases: a surveillance study in 3 medical centers in China. Clin Infect Dis. 2018;66:1109–15. https://doi.org/10.1093/cid/cix917
40. Jia N, Zheng YC, Ma L, Huo QB, Ni XB, Jiang BG, et al. Human infections with *Rickettsia raoultii*, China. Emerg Infect Dis. 2014;20:866–8. https://doi.org/10.3201/eid2005.130995
41. Mendoza-Roldan JA, Colella V, Lia RP, Nguyen VL, Barros-Battesti DM, Iatta R, et al. *Borrelia burgdorferi* (sensu lato) in ectoparasites and reptiles in southern Italy. Parasit Vectors. 2019;12:35. https://doi.org/10.1186/s13071-019-3286-1
42. Sgroi G, Iatta R, Veneziano V, Bezerra-Santos MA, Lesiczka P, Hrazdilová K, et al. Molecular survey on tick-borne pathogens and *Leishmania infantum* in red foxes (*Vulpes vulpes*) from southern Italy. Ticks Tick Borne Dis. 2021;12:101669. https://doi.org/10.1016/j.ttbdis.2021.101669
43. Collares-Pereira M, Couceiro S, Franca I, Kurtenbach K, Schäfer SM, Vitorino L, et al. First isolation of *Borrelia lusitaniae* from a human patient. J Clin Microbiol. 2004;42:1316–8. https://doi.org/10.1128/JCM.42.3.1316-1318.2004
44. Aguero-Rosenfeld ME, Wormser GP. Lyme disease: diagnostic issues and controversies. Expert Rev Mol Diagn. 2015;15:1–4. https://doi.org/10.1586/14737159.2015.989837
45. Budachetri K, Kumar D, Crispell G, Beck C, Dasch G, Karim S. The tick endosymbiont *Candidatus* Midichloria mitochondrii and selenoproteins are essential for the growth of *Rickettsia parkeri* in the Gulf Coast tick vector. Microbiome. 2018;6:141. https://doi.org/10.1186/s40168-018-0524-2
46. Cafiso A, Bazzocchi C, De Marco L, Opara MN, Sassera D, Plantard O. Molecular screening for *Midichloria* in hard and soft ticks reveals variable prevalence levels and bacterial loads in different tick species. Ticks Tick Borne Dis. 2016;7:1186–92. https://doi.org/10.1016/j.ttbdis.2016.07.017
47. Buysse M, Duron O. Multi-locus phylogenetics of the *Midichloria* endosymbionts reveals variable specificity of association with ticks. Parasitology. 2018;145:1969–78. https://doi.org/10.1017/S0031182018000793
48. Matsumoto K, Izri A, Dumon H, Raoult D, Parola P. First detection of *Wolbachia* spp., including a new genotype, in sand flies collected in Marseille, France. J Med Entomol. 2008;45:466–9. https://doi.org/10.1093/jmedent/45.3.466
49. Fraihi W, Fares W, Perrin P, Dorkeld F, Sereno D, Barhoumi W, et al. An integrated overview of the midgut bacterial flora composition of *Phlebotomus perniciosus*, a vector of zoonotic visceral leishmaniasis in the Western Mediterranean Basin. PLoS Negl Trop Dis. 2017;11:e0005484. https://doi.org/10.1371/journal.pntd.0005484
50. Dantas-Torres F, Otranto D. Best practices for preventing vector-borne diseases in dogs and humans. Trends Parasitol. 2016;32:43–55. https://doi.org/10.1016/j.pt.2015.09.004

Address for correspondence: Domenico Otranto, University of Bari Aldo Moro, Strada Provinciale per Casamassima km3, Valenzano 70010, Bari, Italy; domenico.otranto@uniba.it

Detecting *Mycobacterium tuberculosis* Infection in Children Migrating to Australia

Ingrid Laemmle-Ruff, Stephen M. Graham, Bridget Williams, Danielle Horyniak, Suman S. Majumdar, Georgia A. Paxton, Lila V. Soares Caplice, Margaret E. Hellard, James M. Trauer

In 2015, Australia updated premigration screening for tuberculosis (TB) disease in children 2–10 years of age to include testing for infection with *Mycobacterium tuberculosis* and enable detection of latent TB infection (LTBI). We analyzed TB screening results in children <15 years of age during November 2015–June 2017. We found 45,060 child applicants were tested with interferon-gamma release assay (IGRA) (57.7% of tests) or tuberculin skin test (TST) (42.3% of tests). A total of 21 cases of TB were diagnosed: 4 without IGRA or TST, 10 with positive IGRA or TST, and 7 with negative results. LTBI was detected in 3.3% (1,473/44,709) of children, for 30 applicants screened per LTBI case detected. LTBI-associated factors included increasing age, TB contact, origin from a higher TB prevalence region, and testing by TST. Detection of TB and LTBI benefit children, but the updated screening program's effect on TB in Australia is likely to be limited.

Tuberculosis (TB) is a leading contributor to the burden of infectious disease worldwide, causing >1.2 million deaths in 2019 (*1*,*2*). Latent tuberculosis infection (LTBI), defined as infection with *Mycobacterium tuberculosis* without clinical or radiologic evidence of disease, can be diagnosed with interferon-gamma release assay (IGRA) or tuberculin skin test (TST). Estimates suggest one quarter of the global population have LTBI, including 97 million children (<15 years of age) (*3*). Young children (<5 years of age) are at particular risk for TB if infected and have a higher risk for disseminated or severe disease associated with severe illness and death. TB preventive treatment can reduce progression to disease by >90% in children with infection, but effectiveness is greatest if preventive treatment is initiated in the months immediately after infection, emphasizing the importance of early detection and treatment (*4*,*5*). Preventive treatment for children usually involves 6 months of isoniazid monotherapy or, less commonly in Australia, 3 months of rifampin/isoniazid combination therapy (*4*).

Treating LTBI is increasingly recognized as a crucial component of global TB elimination efforts (*6*). Reactivation of overseas-acquired LTBI in adult migrants is the main source of TB in low-burden countries such as Australia (*7*,*8*). Decreasing LTBI in migrants is a key means to further reduce TB incidence (*9*,*10*). LTBI is not notifiable in Australia, and local prevalence estimates vary (*11*). Recent modeling estimates that 17.1% of all overseas-born residents of Australia, 2.1% of overseas-born children <15 years of age, and 0.1% of Australia-born children <15 years of age have LTBI (*12*).

Clinical assessment and chest radiography have long been part of premigration TB screening in Australia and other high-resource settings (*13*–*15*). However, the systematic inclusion of IGRA and TST in premigration health assessments is uncommon internationally and relatively novel in children (*16*,*17*). After the United States and Norway, Australia introduced TB screening using IGRA or TST for children 2–10 years of age on November 20, 2015 (*13*,*18*,*19*). The intention was "to strengthen screening for active TB to improve detection of this disease," which would "also identify children with LTBI" (*20*). Previously, premigration screening of children <11 years of age

Author affiliations: Burnet Institute, Melbourne, Victoria, Australia (I. Laemmle-Ruff, S.M. Graham, B. Williams, D. Horyniak, S.S. Majumdar, M.E. Hellard, J.M. Trauer); Royal Children's Hospital, Melbourne (I. Laemmle-Ruff, S.M. Graham, G.A. Paxton); University of Melbourne, Melbourne (S.M. Graham, S.S. Majumdar, G.A. Paxton, M.E. Hellard, J.M. Trauer); Monash University, Melbourne (D. Horyniak, S.S. Majumdar, M.E. Hellard, J.M. Trauer); The Alfred Hospital, Melbourne (S.S. Majumdar, M.E. Hellard, J.M. Trauer); Department of Home Affairs, Australian Government, Canberra, Australian Capital Territory, Australia (L.V.S. Caplice)

DOI: https://doi.org/10.3201/eid2809.212426

had been limited to medical history and examination and included chest radiography only in those with TB contact or where TB was suspected. More broadly, the updated screening program was "designed to improve public health protections in Australia but also contribute to global efforts to eliminate TB" (*19*), reflecting an emerging recognition of the public health potential of premigration health screening (*21*).

In this cross-sectional study, we aimed to assess the first 20 months of Australia's updated premigration TB screening for children. In particular, we sought to assess the scope of implementation, yield in detecting TB and LTBI, and impacts on follow-up requirements after migration. We present numbers and proportions of children screened, screening results (TB and LTBI), factors associated with LTBI, further investigation, and requirements for linkage to care in Australia.

Methods

The following sections summarize Australia's premigration health screening program and the dataset. Further detail is available elsewhere (*22*).

Screening Program

Migration legislation in Australia requires all permanent, provisional, and humanitarian visa applicants, as well as some temporary visa applicants, to undergo an Immigration Medical Examination (IME) and meet a health requirement before being granted a visa (*23*,*24*). Premigration health screening is intended to protect the Australian community from public health threats, control public expenditure on healthcare and services, and safeguard the access of Australian citizens and permanent residents to healthcare and services in short supply (*20*,*24*). Applicants cannot be granted a visa if they have TB, but the health requirement can be met and a visa granted once TB treatment is complete and the person is free of TB. An IME involves a medical history, examination by a physician, and criteria-based investigations (*20*,*22*,*23*), including criteria for performing IGRA or TST (Table 1). Applicants applying offshore can be assigned a health undertaking, which is an agreement requiring follow-up care in Australia. TB health undertakings (TBHUs) are allocated to applicants with risk factors for TB, including previously treated TB, abnormal chest radiography, and positive IGRA or TST results, and reflect a requirement for linkage to care in Australia in our analysis. Onshore applicants (with their IME conducted in Australia) are referred for care if required without a TBHU.

Study Population

The source study population was all permanent and humanitarian visa applicants to Australia and temporary applicants intending to stay for ≥6 months who completed an IME (onshore or offshore) and met the health requirement or were granted a waiver during July 1, 2014–June 30, 2017. Our analysis is restricted to child applicants (<15 years of age) who completed an IME during November 2015–June 2017, reflecting when new screening commenced. Age was available for analysis in 5-year brackets (0–4, 5–9, and 10–14 years) for privacy reasons. Thus the analysis includes all children 2–10 years of age but also includes children <2 years and 11–14 years who did not meet age-based screening criteria. Deidentified IME data were provided by the Australian Department of Home Affairs. The Alfred Hospital Ethics Committee provided ethics approval (project 320/17).

Variables

Variables were applicant demographics, visa stream, medical history and examination findings, investigation type and results, physician-recorded diagnoses, and allocation of TBHUs. We defined TB as a recorded diagnosis of TB by the assessing physician. We defined IGRA or TST positivity as having any IGRA or TST result recorded as positive in the IME (from options of positive, negative, and indeterminate). LTBI was defined as IGRA or TST positivity without a diagnosis of TB or previous history of TB.

Bacillus Calmette-Guérin (BCG) vaccination status was not available. Data were supplied as categorical variables, based on the menu option selected by the physician. Because country of birth was not available for all applicants, a country of origin variable was derived hierarchically, using (in order, if available) country of birth, country of travel document, or country of residence (*22*).

Statistical Analysis

We described results as absolute numbers and proportions. We used the Fisher exact test to compare proportions. We noted missing and indeterminate IGRA and TST results then excluded them from further analysis.

We used univariate and multivariable-logistic regression to identify demographic and clinical factors associated with LTBI among permanent and humanitarian visa applicants. Temporary applicants were excluded from regression analyses because they were not included in screening criteria unless clinical risk factors were present. We included variables with previous evidence of association with LTBI in the

regression. Exploratory forward regression methods did not reveal additional variables that substantially altered results. Specifically, relevant comorbidity variables were examined but not included because of negligible prevalence (e.g., among children screened, 14 had diabetes and <5 had HIV). Applicants who had previously been treated for TB were excluded because we assumed this history would result in a positive IGRA or TST without reflecting LTBI. Screened applicants with missing or inadequate country of origin were also excluded from regression analyses. We also performed a sensitivity analysis restricted to applicants 5–9 years of age (i.e., all within the age range of new screening criteria).

Results

Participants

During November 2015–June 2017, a total of 134,759 children <15 years of age completed an IME and met the health requirement (Table 2). Of these, 48.6% were girls, 46.5% were 0–4 years of age, and 53.9% were permanent applicants.

Screening Completion

IGRA or TST was completed in 45,060 applicants, representing 33.4% of all child applicants (Table 2); 330 children had multiple tests within an application (reasons not available). Of 45,345 tests conducted, IGRA was the most common testing method (57.7%) in all age groups: children 0–4 years of age (11,121/18,573 [59.9%]), 5–9 years of age (12,871/22,792 [56.5%]), and 10–14 years of age (2,179/3,980 [54.7%]). A higher proportion of children 5–9 years of age completed testing than did those in other age groups (p<0.001), consistent with screening criteria targeting the ages of 2–10 years. A higher proportion of humanitarian applicants completed testing compared with other visa streams (p<0.001); for humanitarian applicants 5–9 years of age (all of whom met criteria), IGRA or TST was completed for 5,403/5,734 (94.2%) persons.

The largest number of children in whom IGRA or TST was performed came from Southern and Central Asia, which had 15,046 applicants tested (12,288 permanent, 1,854 temporary, and 904 humanitarian), reflecting the most common region of origin in the largest visa stream (permanent visa applicants). The North Africa and Middle East region had the highest proportion of applicants tested (48.8%), reflecting a predominantly humanitarian applicant population (819 permanent, 57 temporary, and 6,105 humanitarian).

Table 1. Australia premigration TB screening criteria within the Immigration Medical Examination*

All children completing an IME have a medical history and physical examination
Either IGRA or TST is required for:
Children 2–10 years of age who are:
Applying for a humanitarian visa
Applying for a permanent visa and from a setting placing them at higher risk for TB†
Asylum seekers within Australia
Applicants declaring close contact with TB, with signs or symptoms of TB, or who are immunocompromised (any age or migration stream)
Applicants with positive IGRA or TST results are required to have:
Posteroanterior chest radiograph (and lateral in children <11 years of age)
If abnormalities on chest radiograph, or other indication for further investigation:
Sputum testing and specialist review
Exemptions from IGRA and TST screening:
Written evidence of prior bacteriologically confirmed TB (i.e., positive smear or culture from sputum or other specimen) or a previously positive TST (>10 mm) or IGRA

*Chest radiograph screening for TB is required for all migrants >11 years applying for permanent or humanitarian visas and for temporary visas if from high-risk TB countries and staying for >6 months. TB, tuberculosis disease; IME, Immigration Medical Examination; IGRA, interferon-gamma release assay; TST, tuberculin skin test.
†Prevalence >40 per 100,000 cases of TB based on 2013 World Health Organization estimates.

LTBI Results

Excluding missing and indeterminate results, 1,513/45,060 (3.4%) applicants returned a positive IGRA or TST result (Table 2). In children without TB or a history of treatment for TB, 1,473/44,709 (3.3%) had a positive result, which equates to 3,295 cases of LTBI per 100,000 applicants tested, or 30 applicants screened per LTBI case detected. The proportion of positive results was higher for TST (5.4%) than IGRA (2.0%; p<0.001). Two thirds (1,001/1,513 [66.2%]) of children who tested positive were identified through TST and the remainder were identified through IGRA (512/1,513 [33.8%]; p<0.001). The prevalence of TST positivity increased with age, from 4.6% in children 0–4 years of age to 8.4% in those 10–14 years of age.

The proportion of positive IGRA/TST tests was highest in permanent applicants (3.8%; p<0.001) and applicants 10–14 years of age (5.4%; p<0.001). Applicants from India, China, and the Philippines comprised more than one third of children tested (17,797/45,060 [39.5%]) and more than half of all positive results (867/1,513 [57.3%]).

Factors associated with LTBI (Table 3) included being 10–14 years of age, originating from Southeast Asia or Southern and Eastern Europe, testing by TST, and past close TB contact. Factors negatively associated with LTBI included originating from Oceania, age of 0–4 years, and being a humanitarian applicant.

Sensitivity analyses restricted to children 5–9 years of age did not significantly alter these findings.

Further Investigation and Linkage to Care

Almost all applicants (1,495/1,513 [98.8%]) with positive IGRA or TST completed posteroanterior chest radiography; a lateral film was also performed in 97.1% (1,469/1,513) applicants. Only 2.7% (41/1,495) of radiographs demonstrated any findings consistent with new or old TB; 10 of those children received a TB diagnosis.

During November 2015–June 2017, a total of 21 cases of TB were diagnosed among 134,759 children, of which 1 was bacteriologically confirmed, for a prevalence of 15.6 cases/100,000 child applicants. Of these 21 TB-positive children, 4 did not undergo IGRA or TST, 10 had positive results (8 TST, 2 IGRA), and 7 had negative results (all IGRA). All TB cases had clinical abnormalities, radiological abnormalities, or both on IME.

During November 2015–June 2017, among offshore applicants, 1,640 children were allocated TB-HUs; the greatest number was in those 5–9 years of age (792/1,640 [48.3%]; p<0.001) and permanent applicants (1,113/1,640 [67.9%]; p<0.001). TBHUs increased significantly after new screening introduction. Comparing the time periods July 2014–October 2015 and

Table 2. IGRA and TST testing and positivity in visa applicants <15 years of age migrating to Australia, November 2015–June 2017*

Characteristic	All applicants	Applicants tested by IGRA or TST	Applicants tested, excluding missing/indeterminate results†	IGRA or TST positivity in applicants tested
Total	134,759 (100)	45,060 (33.4)	44,841	1,513 (3.4)
Sex				
F	65,462 (48.6)	22,133 (33.8)	22,028	763 (3.5)
M	69,284 (51.4)	22,925 (33.1)	22,811	750 (3.3)
Age group, y				
≤4	62,646 (46.5)	18,503 (29.5)	18,410	505 (2.7)
5–9	40,357 (30.0)	22,615 (56.0)	22,509	796 (3.5)
10–14	31,756 (23.6)	3,942 (12.4)	3,922	212 (5.4)
Visa stream				
Permanent	72,610 (53.9)	30,474 (42.0)	30,349	1,144 (3.8)
Temporary	45,490 (33.8)	4,466 (9.8)	4,430	160 (3.6)
Humanitarian	16,659 (12.36)	10,120 (60.8)	10,062	209 (2.1)
Region of origin				
Oceania‡	10,704 (7.9)	2,512 (23.5)	2,490	32 (1.3)
Northwest Europe	7,339 (5.5)	255 (3.5)	255	7 (2.8)
Southern and Eastern Europe	2,153 (1.6)	419 (19.5)	417	36 (8.6)
North Africa and Middle East	14,316 (10.6)	6,981 (48.8)	6,950	128 (1.8)
Southeast Asia	21,993 (16.3)	7,597 (34.5)	7,562	574 (7.6)
Northeast Asia	19,667 (14.6)	5,788 (29.4)	5,755	134 (2.3)
Southern and Central Asia	37,741 (28.0)	15,046 (39.9)	15,009	435 (2.9)
Americas	4,363 (3.2)	503 (11.5)	498	11 (2.2)
Sub-Saharan Africa	8,556 (6.4)	3,557 (41.6)	3,522	97 (2.8)
Missing/Inadequately described	7,927 (5.9)	2,402 (30.0)	2,383	59 (2.5)
Top 5 countries of origin, excluding Australia				
India	25,208	9,860 (39.1)	9,831	317 (3.2)
China	14,013	4,703 (33.6)	4,680	114 (2.4)
Philippines	8,684	3,234 (37.2)	3,222	436 (13.5)
United Kingdom	5,562	170 (3.1)	170	5 (2.9)
Pakistan	5,175	2,472 (47.8)	2,471	24 (1.0)
Reported risk factors				
Reported contact with TB	748	310 (41.4)	306	46 (15)
Previous treatment for TB	402	121 (30.1)	121	31 (25.6)
Test type		No. (%) tests completed§	No. tests, excluding indeterminate	No. (%) positive tests
All		45,345	45,171	1,563 (3.5)
IGRA		26,171 (57.7)	25,997	532 (2.0)
TST		19,174 (42.3)	19,174	1,031 (5.4)

*Values are no. (%) except as indicated. Missing results across all applicants (excluded from corresponding demographic denominators): age not recorded for 7 applicants, none of whom were screened (excluded from entire analysis); gender not recorded for 13 applicants, reported TB contact not recorded for 7,645 applicants, previous treatment for TB not recorded for 13,484 applicants. Humanitarian visa holders, while considered as a separate visa application stream by the Department of Home Affairs, have permanent residency in Australia. IGRA, interferon-gamma release assay; TST, tuberculin skin test; TB, tuberculosis disease.

†Applicants who had IGRA or TST but with an indeterminate (IGRA, n = 174) or missing result (n = 45) excluded from column.

‡Oceania region includes 8,358 applicants with country of origin as Australia (8,018 born in Australia). This reflects children born in Australia of families applying for migration. No further information regarding parental country of origin available.

§Total of 45,345 IGRAs and TSTs conducted with 330 applicants with ≥1 test in an application (227 with 2 tests and 3 with 3 tests).

Table 3. Factors associated with LTBI in visa applicants <15 years of age migrating to Australia, November 2015–June 2017*

Characteristic	Univariate regression analysis		Multivariate regression analysis	
	Odds ratio (95% CI)	p value	Odds ratio (95% CI)	p value
Sex				
M	Referent	0.449	Referent	0.481
F	1.04 (0.93–1.17)		1.04 (0.93–1.17)	
Age group, y				
0–4	0.78 (0.69–0.88)	<0.001	0.84 (0.74–0.95)	0.007
5–9	Referent		Referent	
10–14	1.55 (1.31–1.83)	<0.001	1.40 (1.17–1.65)	<0.001
Region of origin				
Northeast Asia	Referent		Referent	
Oceania	0.48 (0.31–0.75)	0.001	0.53 (0.35–0.83)	0.005
Northwest Europe	0.68 (0.21–2.16)	0.515	0.55 (0.17–1.77)	0.318
Southern and Eastern Europe	3.35 (2.15–5.20)	<0.001	2.17 (1.38–3.41)	0.001
North Africa and Middle East	0.77 (0.59–1.00)	0.047	1.01 (0.75–1.38)	0.928
Southeast Asia	3.35 (2.72–4.12)	<0.001	2.65 (2.15–3.28)	<0.001
Southern and Central Asia	1.19 (0.96–1.47)	0.120	0.84 (0.67–1.05)	0.124
Americas	0.96 (0.48–1.90)	0.900	0.79 (0.40–1.57)	0.498
Sub-Saharan Africa	1.28 (0.96–1.69)	0.088	0.84 (0.63–1.12)	0.224
Visa stream				
Permanent	Referent	<0.001	Referent	<0.001
Humanitarian	0.59 (0.51–0.70)		0.47 (0.38–0.58)	
Risk factors				
Past close contact with TB	3.48 (2.15–5.61)	<0.001	2.80 (1.70–4.61)	<0.001
Test type				
IGRA	Referent	<0.001	Referent	<0.001
TST	2.72 (2.41–3.06)		3.01 (2.66–3.42)	

*Indeterminate IGRA results excluded. Temporary applicants excluded as not included in screening unless clinical features or risk factors. Applicants with TB and history of TB excluded, because likely to result in positive IGRA or TST without reflecting LTBI. Screened applicants without country of origin data not included in the regression analysis (n = 2,383); the LTBI prevalence in this group was 2.5% (Table 2). IGRA, interferon-gamma release assay; LTBI, latent tuberculosis infection; TB, tuberculosis disease; TST, tuberculin skin test.

November 2015–June 2017, TBHUs increased from 417 (279/66,887) to 1,751 (1,640/93,650) per 100,000 offshore child applicants (p<0.001). Among offshore applicants with positive IGRA or TST results, 1,245/1,327 (93.8%) were allocated TBHUs. Of note, 183 onshore applicants had positive IGRA or TST results and were likely referred to care in Australia. Thus, 1,428/1,513 (94.4%) of all applicants with positive IGRA or TST results were likely referred for further care.

Discussion

Given the primary aim of the new screening program, we found a low yield in detecting TB. TB is rare in children migrating to Australia; 15.6 cases per 100,000 child applicants were diagnosed over the study period, and annual Australia TB notifications in overseas-born children ranged from 4.5 to 8.8 cases per 100,000 children during 2015–2018 (*7*). Further, the effect of including IGRA and TST in screening on case detection is uncertain. Of the 17 TB-positive children in whom IGRA or TST was performed, 7 had a negative test for infection (all IGRA), and in the other 10 children, it cannot be assumed that the positive IGRA or TST result led to the diagnosis of TB. Although a test for infection is often included in the approach to TB diagnosis in children, the results do not confirm or exclude active disease and so cannot be interpreted in isolation (*25*,*26*).

IGRA and TST detect LTBI in children, who might benefit from TB preventive treatment (*4*). We found that 3.3% of children screened had LTBI, equating to 30 applicants screened per LTBI case detected. Factors associated with LTBI matched well-established risk factors, namely increasing age, history of TB contact, and coming from a region with high TB prevalence (acknowledging variability within regions). These findings support previous evidence showing greater yield from migrant TB screening targeting higher-risk groups (*14*). Increased positivity with TST versus IGRA also reflects known test characteristics; IGRA has greater specificity in BCG-vaccinated children (*26*).

Although the LTBI prevalence of 3.3% found in this population was low, that prevalence was higher than the recently modeled estimate of 2.1% for overseas-born children (0–14 years of age) in Australia (*12*), likely reflecting targeted screening criteria. LTBI prevalence might have been higher if children 11–14 years of age had also been screened, given LTBI prevalence increases with age in TB-endemic settings. LTBI prevalence was much lower than in some other international migrant screening programs. An analysis of premigration LTBI screening in 67,334 children 2–14 years of age bound for the United States (from countries with TB incidence rate

≥20 cases per 100,000 children) found a higher LTBI prevalence of 12% (*27*).

Characteristics of those screened largely reflected screening criteria. Although overall screening completeness could not be determined, screening was nearly universal among humanitarian applicants 5–9 years of age, who all met criteria. Although complete assessment of the risk factors prompting testing in temporary applicants was not possible, a surprisingly high proportion (9.8%) of temporary applicants underwent IGRA or TST; the proportion testing positive (3.6%) was similar to the proportion in permanent applicants (3.8%). In contrast, humanitarian applicants had significantly lower odds of LTBI than permanent applicants despite the presumption of high LTBI risk and mandated testing. This difference is likely because permanent applicants were only screened if they were from a high-burden setting, and the humanitarian intake at the time was predominantly from countries with relatively low TB prevalence (largely refugee applicants from Syria and Iraq) (*28*). Nevertheless, the proportion of positivity (2.1%) in humanitarian applicants was lower than previous LTBI prevalence estimates in refugee-background children tested in Australia, including from the Middle East (*11*,*29*).

Almost all children with positive screening results had further investigation for TB, including chest radiography, as per guidelines. Most were allocated a TBHU requiring linkage to follow-up care in Australia. The updated screening was associated with a marked increase in children with TBHUs. These additional TBHUs might have enabled TB preventative treatment that might not otherwise have occurred, for potential substantial benefit for these children. However, TBHUs require use of services and resources both for families and the health system in Australia. Time from visa application to follow up after migration is often months to years. This delay from a positive test to commencement of TB preventative treatment (in addition to the unknown time between infection and positive test) risks missing the period when disease is more likely to develop in children with LTBI (*5*), which might reduce both the individual and public health benefit of preventative treatment.

After migration, Australia guidelines recommend testing migrants <35 years of age from high-burden TB settings for LTBI (*30*). In practice, this testing occurs infrequently unless migrants are assigned a TBHU, linked with specific services (e.g., refugee health clinics), or there is another specific requirement (e.g., occupational screening) (*31*,*32*). Systematic premigration LTBI testing linked to appropriate follow-up care theoretically offers several advantages, including broader testing within mandated IMEs, targeting migrants from high-risk settings, supporting source country TB infrastructure, and detecting infection promptly, given LTBI reactivation risk is highest early after migration (*21*,*33*–*35*). Some migrant groups have also reported a preference for premigration LTBI testing over postmigration testing (*36*). Researchers analyzing premigration TB screening (with chest radiography) suggest considering expansion to include LTBI, citing reactivation of overseas-acquired LTBI as the primary driver of TB in low-burden countries (*13*,*33*,*37*,*38*). Some reviews and modeling estimates have supported the potential effectiveness and cost-effectiveness of premigration LTBI screening, particularly when targeted to migrants from high-burden settings (*16*,*33*). Others have found limited cost-effectiveness, particularly if screening costs are included in cost-effectiveness calculations (rather than being borne by migrants), and have highlighted the limited likely contribution of migrant screening to TB elimination in low-burden settings (*39*). However, observational data from premigration health screening programs detecting LTBI, particularly in children, remain limited, underscoring the importance of analyses such as this one (*33*,*40*).

Ideally, assessment of the overall effectiveness of the new screening program would consider the full cascade of care, from premigration LTBI detection to postmigration TB preventative treatment uptake and completion, as well as TB incidence (*33*). Losses over the cascade of care are common: of 8,231 children in whom LTBI was detected before migration to the United States, 70% were followed after migration but rates of diagnosis revision and low treatment completion were substantial (*27*). However, given that TB will not develop in most children with LTBI even without TB preventive treatment, the low LTBI prevalence in our analysis implies a large number of children would need to be screened to prevent 1 case of TB.

The first limitation of our analysis is that the study population represents visa applications rather than persons, meaning repeat applicants are not accounted for (*22*). No data were available regarding BCG immunization. Of note, BCG vaccine is included in the immunization schedule of many applicant source countries (e.g., India, China, and the Philippines), and a large proportion of screened applicants likely received the BCG vaccine in infancy. However, in TB-endemic countries, a positive TST indicates infection with *M. tuberculosis* regardless of BCG status, and false positivity decreases with increasing age (*41*,*42*). Further, in children, a positive TST requires clinical follow up regardless of BCG status.

We were unable to assess screening completeness directly against criteria because of privacy limitations on data format. Our denominator for the proportion of children screened was inflated by including children <2 years and 11–14 years of age, whose age placed them outside of screening criteria. Because of these factors, the cohort represents a mix of children screened based on age, visa stream, and clinical risk criteria. Nevertheless, the demographics of the cohort broadly align with screening criteria, and sensitivity analyses restricted to children 5–9 years of age did not alter our conclusions, suggesting our group largely reflects children meeting screening criteria. Further, our results reflect real-world implementation of the updated screening program. Finally, no data were available regarding care linkage in Australia or clinical outcomes.

Our analysis provides the results of Australia's systematic premigration TB screening in children, one of few such programs globally. Notwithstanding inherent delays between infection, screening, and TB preventative treatment, the individual benefit for children with LTBI detected by premigration health screening could be considerable, with potential future reductions in TB incidence in overseas-born children in Australia. However, the low proportion of LTBI found in our analysis, despite the program targeting higher-risk children, suggests a modest yield from the current program toward substantial reductions in TB after migration.

TB elimination in Australia is unlikely to be achieved through migrant screening alone, and strategies such as investment in TB programs in high-burden settings, alongside strong local public health measures, might have greater impact (*10*,*39*,*40*). Key questions remain unanswered that will influence whether, and how, migrant screening can best contribute to TB and LTBI detection. These questions include the effects of changing migration patterns on screening yield, trade-offs between screening older migrants (with higher infection prevalence) versus children (with greater individual benefit for those with LTBI), acceptability and cost for migrants, health resourcing implications, and ultimately, effectiveness for reducing TB burden, toward the overarching goal of TB elimination.

In conclusion, in low-burden settings, additional interventions to prevent TB are inherently likely to have lower yield and be less cost-effective because of already low TB incidence. Shifting screening costs onto migrants might improve apparent cost-effectiveness but has implications for equitable access to screening. Given TB epidemiology in Australia, targeted migrant screening might still make a valuable contribution toward TB elimination even if absolute yield is low.

Acknowledgments

We thank the Australian Government Department of Home Affairs (DHA) for their support in providing data and assisting with data interpretation.

No specific funding was received for this project. I.L.-R. and B.W. were funded through the Australian Government's Specialist Training Program. D.H. and J.M.T. are supported by National Health and Medical Research Council (NHMRC) Early Career Fellowships. S.S.M. is a recipient of a NHMRC Postgraduate Scholarship. M.E.H. is a recipient of a NHMRC Investigator Fellowship.

G.A.P. has provided advice to DHA as an independent medical advisor. L.V.S.C. is senior director of the Immigration Health Policy and Assurance Branch, on behalf of the Health Services Division of DHA. M.E.H. has received grants from Gilead Sciences and Abbvie, unrelated to this work.

About the Author

Dr. Laemmle-Ruff is a pediatrician and public health physician in Melbourne who began analyzing premigration health screening data at the Burnet Institute during her public health training. Her research interests include immigrant health, child health, and use of surveillance and screening data to further public health.

References

1. World Health Organization. Global tuberculosis report 2020 [cited 2021 May 14]. https://www.who.int/publications/i/item/9789240013131
2. World Health Organization. Global health estimates 2020: deaths by cause, age, sex, by country and by region, 2000–2019 [cited 2021 May 14]. https://www.who.int/data/gho/data/themes/mortality-and-global-health-estimates/ghe-leading-causes-of-death
3. Houben RM, Dodd PJ. The global burden of latent tuberculosis infection: a re-estimation using mathematical modelling. PLoS Med. 2016;13:e1002152. https://doi.org/10.1371/journal.pmed.1002152
4. World Health Organization. Consolidated guidelines on tuberculosis. Module 1: prevention – tuberculosis preventive treatment [cited 2021 Jun 7]. https://www.who.int/publications/i/item/9789240001503
5. Martinez L, Cords O, Horsburgh CR, Andrews JR, Pediatric TB; Pediatric TB Contact Studies Consortium. The risk of tuberculosis in children after close exposure: a systematic review and individual-participant meta-analysis. Lancet. 2020; 395:973–84. https://doi.org/10.1016/S0140-6736(20)30166-5
6. World Health Organization Regional Office for Africa. Implementing the end TB strategy: the Essentials [cited 2021 Jun 7]. https://apps.who.int/iris/handle/10665/206499
7. Bright A, Denholm J, Coulter C, Waring J, Stapledon R. Tuberculosis notifications in Australia, 2015–2018.Commun Dis Intell (2018). 2020;44:44. https://doi.org/10.33321/cdi.2020.44.88

8. Globan M, Lavender C, Leslie D, Brown L, Denholm J, Raios K, et al. Molecular epidemiology of tuberculosis in Victoria, Australia, reveals low level of transmission. Int J Tuberc Lung Dis. 2016;20:652–8. https://doi.org/10.5588/ijtld.15.0437
9. Lönnroth K, Migliori GB, Abubakar I, D'Ambrosio L, de Vries G, Diel R, et al. Towards tuberculosis elimination: an action framework for low-incidence countries. Eur Respir J. 2015;45:928–52. https://doi.org/10.1183/09031936.00214014
10. The National Tuberculosis Advisory Committee for the Communicable Diseases Network of Australia. The strategic plan for control of tuberculosis in Australia, 2016–2020: towards disease elimination. Commun Dis Intell (2018). 2019;43.
11. Chaves NJ, Paxton G, Biggs BA, Thambiran A, Smith M, Williams J, et al. Recommendations for comprehensive post-arrival health assessment for people from refugee-like backgrounds. Surry Hills (Australia): Australasian Society for Infectious Diseases; 2016.
12. Dale KD, Trauer JM, Dodd PJ, Houben RMGJ, Denholm JT. Estimating the prevalence of latent tuberculosis in a low-incidence setting: Australia. Eur Respir J. 2018; 52:1801218. https://doi.org/10.1183/13993003.01218-2018
13. Dobler CC, Fox GJ, Douglas P, Viney KA, Ahmad Khan F, Temesgen Z, et al. Screening for tuberculosis in migrants and visitors from high-incidence settings: present and future perspectives. Eur Respir J. 2018;52:1800591. https://doi.org/10.1183/13993003.00591-2018
14. Aldridge RW, Yates TA, Zenner D, White PJ, Abubakar I, Hayward AC. Pre-entry screening programmes for tuberculosis in migrants to low-incidence countries: a systematic review and meta-analysis. Lancet Infect Dis. 2014; 14:1240–9. https://doi.org/10.1016/S1473-3099(14)70966-1
15. Alvarez GG, Gushulak B, Abu Rumman K, Altpeter E, Chemtob D, Douglas P, et al. A comparative examination of tuberculosis immigration medical screening programs from selected countries with high immigration and low tuberculosis incidence rates. BMC Infect Dis. 2011;11:3. https://doi.org/10.1186/1471-2334-11-3
16. Campbell JR, Johnston JC, Cook VJ, Sadatsafavi M, Elwood RK, Marra F. Cost-effectiveness of latent tuberculosis infection screening before immigration to low-incidence countries. Emerg Infect Dis. 2019;25:661–71. https://doi.org/10.3201/eid2504.171630
17. Alvarez GG, Clark M, Altpeter E, Douglas P, Jones J, Paty MC, et al. Pediatric tuberculosis immigration screening in high-immigration, low-incidence countries. Int J Tuberc Lung Dis. 2010;14:1530–7.
18. Scandurra G, Degeling C, Douglas P, Dobler CC, Marais B. Tuberculosis in migrants—screening, surveillance and ethics. Pneumonia (Nathan). 2020;12:9. https://doi.org/10.1186/s41479-020-00072-5
19. Australian Government, Department of Home Affairs. Understanding immigration health changes for 20 November 2015 [cited 2018 Aug 11]. www.homeaffairs.gov.au/Visasupport/Pages/br3-health-client.aspx.
20. Australian Government, Department of Immigration and Border Protection. Panel member instructions: Australian immigration medical examinations July 2016. Canberra (Australia): Australian Government; 2016.
21. Douglas P, Posey DL, Zenner D, Robson J, Abubakar I, Giovinazzo G. Capacity strengthening through pre-migration tuberculosis screening programmes: IRHWG experiences. Int J Tuberc Lung Dis. 2017;21:737–45. https://doi.org/10.5588/ijtld.17.0019
22. Trauer JM, Williams B, Laemmle-Ruff I, Horyniak D, Caplice LVS, McBryde ES, et al. Tuberculosis in migrants to Australia: outcomes of a national screening program. Lancet Reg Health West Pac. 2021;10:100135. https://doi.org/10.1016/j.lanwpc.2021.100135
23. Australian Government, Department of Home Affairs. What health examinations you need. 2020 [cited 2021 Apr 23]. https://immi.homeaffairs.gov.au/help-support/meeting-our-requirements/health/what-health-examinations-you-need
24. Australian Government, Department of Home Affairs. Meeting Our Requirements - Health. 2021 [cited 2021 Apr 23]. https://immi.homeaffairs.gov.au/help-support/meeting-our-requirements/health
25. World Health Organization. Guidance for national tuberculosis programmes on the management of tuberculosis in children, 2nd ed. Geneva: The Organization; 2014.
26. Lewinsohn DM, Leonard MK, LoBue PA, Cohn DL, Daley CL, Desmond E, et al. Official American Thoracic Society/Infectious Diseases Society of America/Centers for Disease Control and Prevention clinical practice guidelines: diagnosis of tuberculosis in adults and children. Clin Infect Dis. 2017;64:111–5. https://doi.org/10.1093/cid/ciw778
27. Taylor EM, Painter J, Posey DL, Zhou W, Shetty S. Latent tuberculosis infection among immigrant and refugee children arriving in the United States: 2010. J Immigr Minor Health. 2016;18:966–70. https://doi.org/10.1007/s10903-015-0273-2
28. Australian Government, Department of Immigration and Border Protection. Department of Immigration and Border Protection Annual Report 2016–2017 [cited 2021 Jun 25]. https://www.homeaffairs.gov.au/reports-and-pubs/Annualreports/2016-17/Complete.pdf
29. Heenan RC, Volkman T, Stokes S, Tosif S, Graham H, Smith A, et al. 'I think we've had a health screen': new offshore screening, new refugee health guidelines, new Syrian and Iraqi cohorts: recommendations, reality, results and review. J Paediatr Child Health. 2019;55:95–103. https://doi.org/10.1111/jpc.14142
30. Stock D; National Tuberculosis Advisory Committee. National position statement for the management of latent tuberculosis infection. Commun Dis Intell Q Rep. 2017; 41:E204–8.
31. Waring J, Waring J; National Tuberculosis Advisory Committee. National Tuberculosis Advisory Committee Guideline: management of tuberculosis risk in healthcare workers in Australia. Commun Dis Intell Q Rep. 2017; 41:E199–203.
32. Flynn MG, Brown LK. Treatment of latent tuberculosis in migrants to Victoria. Commun Dis Intell Q Rep. 2015; 39:E578–83.
33. Zenner D, Hafezi H, Potter J, Capone S, Matteelli A. Effectiveness and cost-effectiveness of screening migrants for active tuberculosis and latent tuberculous infection. Int J Tuberc Lung Dis. 2017;21:965–76. https://doi.org/10.5588/ijtld.16.0935
34. Dale KD, Trauer JM, Dodd PJ, Houben RMGJ, Denholm JT. Estimating long-term tuberculosis reactivation rates in Australian migrants. Clin Infect Dis. 2020;70:2111–8. https://doi.org/10.1093/cid/ciz569
35. Lönnroth K, Mor Z, Erkens C, Bruchfeld J, Nathavitharana RR, van der Werf MJ, et al. Tuberculosis in migrants in low-incidence countries: epidemiology and intervention entry points. Int J Tuberc Lung Dis. 2017;21:624–37. https://doi.org/10.5588/ijtld.16.0845
36. Degeling C, Carter SM, Dale K, Singh K, Watts K, Hall J, et al. Perspectives of Vietnamese, Sudanese and South Sudanese

immigrants on targeting migrant communities for latent tuberculosis screening and treatment in low-incidence settings: a report on two Victorian community panels. Health Expect. 2020;23:1431–40. https://doi.org/10.1111/hex.13121
37. Aldridge RW, Zenner D, White PJ, Muzyamba MC, Loutet M, Dhavan P, et al. Prevalence of and risk factors for active tuberculosis in migrants screened before entry to the UK: a population-based cross-sectional study. Lancet Infect Dis. 2016;16:962–70. https://doi.org/10.1016/S1473-3099(16)00072-4
38. Chan IHY, Kaushik N, Dobler CC. Post-migration follow-up of migrants identified to be at increased risk of developing tuberculosis at pre-migration screening: a systematic review and meta-analysis. Lancet Infect Dis. 2017;17:770–9. https://doi.org/10.1016/S1473-3099(17)30194-9
39. Dale KD, Abayawardana MJ, McBryde ES, Trauer JM, Carvalho N. Modelling the cost-effectiveness of latent tuberculosis screening and treatment strategies in recent migrants to a low incidence setting. Am J Epidemiol. 2022;191:255–70.
40. Campbell JR, Schwartzman K. Invited commentary: the role of tuberculosis screening among migrants to low-incidence settings in (not) achieving elimination. Am J Epidemiol. 2022;191:271–4.
41. Farhat M, Greenaway C, Pai M, Menzies D. False-positive tuberculin skin tests: what is the absolute effect of BCG and non-tuberculous mycobacteria? Int J Tuberc Lung Dis. 2006;10:1192–204.
42. Seddon JA, Paton J, Nademi Z, Keane D, Williams B, Williams A, et al. The impact of BCG vaccination on tuberculin skin test responses in children is age dependent: evidence to be considered when screening children for tuberculosis infection. Thorax. 2016;71:932–9. https://doi.org/10.1136/thoraxjnl-2015-207687

Address for correspondence: Ingrid Laemmle-Ruff, Burnet Institute, 85 Commercial Rd, Melbourne, VIC 3004, Australia; email: ingrid.laemmle-ruff@burnet.edu.au

Coccidioidomycosis Seroincidence and Risk among Military Personnel, Naval Air Station Lemoore, San Joaquin Valley, California, USA[1]

Graham C. Ellis, Charlotte A. Lanteri, Hsing-Chuan Hsieh, Paul C.F. Graf, Gabriel Pineda, Nancy F. Crum-Cianflone, Catherine M. Berjohn, Terrel Sanders, Ryan C. Maves, Robert Deiss

We conducted a retrospective cohort study that tested 2,000 US military personnel for *Coccidioides* antibodies in a disease-endemic region. The overall incidence of seroconversion was 0.5 cases/100 person-years; 12.5% of persons who seroconverted had illnesses requiring medical care. No significant association was found between demographic characteristics and seroconversion or disease.

Coccidioidomycosis is an endemic mycosis caused by inhalation of *Coccidioides immitis* or *C. posadasii* spores (*1*). Severe disease is infrequent, and extrapulmonary dissemination occurs in only 1% of diagnosed cases (*2*,*3*). Mild disease and varied clinical awareness of this pathogen contribute to underestimates of incidence (*4*).

The US military maintains facilities in coccidioidomycosis-endemic regions where nonimmune persons are routinely assigned. We sought to investigate the seroincidence of *Coccidioides* infection in persons stationed at a naval air station (NAS) in the San Joaquin Valley of California, USA, an area to which coccidioidomycosis is endemic (*5*). The study was approved by the Institutional Review Boards of the Uniformed Services University and Naval Health Research Center

The Study

We used samples collected during 2011–2017 from the Department of Defense Serum Repository (DoDSR), a program that stores serum from US service members collected during routine health screenings. We conducted a retrospective cohort study of 2,000 military service members newly transferred to NAS Lemoore, a military base in the San Joaquin Valley that employs 6,400 military personnel (*6*). Our primary objectives were to define the incidence of and risks for seroconversion at NAS Lemoore. Secondary objectives included determining the proportion of seropositive cases associated with the development of clinical disease. We queried the Armed Forces Health Services Division database to identify service members who were newly transferred to NAS Lemoore from a non-*Coccidioides*–endemic region, as determined by postal code associated with the serum sample.

The population consisted of service members for whom the DoDSR had 1 serum sample drawn before arrival at NAS Lemoore (pretransfer) and 1 sample drawn after ≥12 months at NAS Lemoore (posttransfer) during 2011–2017. Posttransfer serum samples (2 mL) from eligible persons were obtained and tested for *Coccidioides* IgG and IgM by the Naval Health Research Center (San Diego, CA, USA) by using the Omega Cocci Antibody Enzyme Immunoassay (EIA) on the automated DS2 instrument (Dynex Technologies, https://www.dynextechnologies.com). Samples seropositive by EIA underwent confirmatory

Author affiliations: Explosive Ordnance Disposal Expeditionary Support Unit TWO, Virginia Beach, Virginia, USA (G.C. Ellis); Naval Medical Center San Diego, San Diego, California, USA (G.C. Ellis, C.M. Berjohn, T. Sanders, R.C. Maves, R. Deiss); Uniformed Services University, Bethesda, Maryland, USA (C.A. Lanteri, H.-C. Hsieh, C.M. Berjohn, R.C. Maves, R. Deiss); The Henry M. Jackson Foundation for the Advancement of Military Medicine, Inc., Bethesda (H.-C. Hsieh, R. Deiss); US Naval Medical Research Unit SIX, Lima, Peru (P.C.F. Graf); US Naval Health Research Center, San Diego (P.C.F. Graf, G. Pineda); Scripps Mercy Hospital, San Diego (N.F. Crum-Cianflone); US Naval Medical Research Unit THREE, Accra, Ghana (T. Sanders); Wake Forest University School of Medicine, Winston-Salem, North Carolina, USA (R.C. Maves); University of California, San Diego (R. Deiss)

DOI: https://doi.org/10.3201/eid2809.220652

[1]This study was presented in part at the Virtual IDWeek 2020 Conference; October 21–25, 2020.

immunodiffusion testing at the University of California Davis Coccidioidomycosis Reference Laboratory (Davis, CA, USA). For positive or equivocal samples, we obtained pretransfer samples from the DoDSR and tested them for *Coccidioides* antibodies by EIA to determine the presence of seroreactivity (seropositive or equivocal) before the service member's transfer to a *Coccidioides*-endemicregion(Appendix,https://wwwnc.cdc.gov/EID/article/28/9/22-0652-App1.pdf).

We defined seroconversion as IgG or IgM detected in a posttransfer sample by EIA, confirmed by immunodiffusion if performed, with a seronegative pretransfer EIA result. IgG seroreactivity in a pretransfer sample was considered evidence of previous *Coccidioides* exposure. Isolated IgM seroreactivity in a pretransfer sample was considered false positive if there was IgM seroreactivity in the posttransfer sample. Cases that could not be confirmed by immunodiffusion because of testing limitations but that otherwise met the above definition were included as cases of seroconversion in our analysis.

We obtained deidentified demographic and clinical data from the Armed Forces Health Services Division. Demographics included branch of service, military rank, and occupational specialty code (Appendix). We obtained clinical diagnosis by query of the International Classification of Diseases 9th and 10th Revisions (Appendix). Case-patients who had coccidioidomycosis were considered if cases occurred while they were stationed at NAS Lemoore, within 90 days after transfer, or within 2 years if disseminated.

We calculated prevalence and incidence with 95% CI based on binomial and Poisson distributions. Prevalence was the number of positive screens divided by the number of seronaive persons on transfer. Incidence was calculated by using person-years at NAS Lemoore. We determined bivariate associations by using the Mann-Whitney U/Wilcoxon rank tests for continuous variables and the χ^2 or Fischer exact test for categorical variables. We used a simple logistical regression model to determine predictors of seroconversion or disease and considered a 2-sided p value <0.05 statistically significant. We performed all statistical calculations by using SAS version 9.4 (https://www.sas.com).

We obtained serum and clinical data for 2,000 participants (Table 1); participants were predominately male and <27 years of age. *Coccidioides* IgG or IgM were detected (positive or equivocal) by EIA in 415 (21%) of 2,000 samples (Appendix); of those, 252 (61%) were equivocal for IgM alone and were

Table 1. Cohort demographics by seroconversion status for incidence of *Coccidioides* seroconversion among military personnel, Naval Air Station Lemoore, San Joaquin Valley, California, USA*

Variables	Seroconversion		Total	p value
	No	Yes		
Total	1,976	24	2,000	
Mean age, y (range)	23.0 (20.0–27.0)	22.5 (19.0–26.5)	23.0 (20.0–27.0)	0.5358
Sex				>0.999
M	1,657 (83.86)	20 (83.33)	1,677 (83.85)	
F	319 (16.14)	4 (16.67)	323 (16.15)	
Race/ethnicity				0.1098
Caucasian	910 (46.05)	6 (25.00)	916 (45.80)	
African American	298 (15.08)	5 (20.83)	303 (15.15)	
Asian/Pacific Islander	120 (6.07)	2 (8.33)	122 (6.10)	
American Indian/Alaskan Native	53 (2.68)	0	53 (2.65)	
Hispanic	338 (17.11)	4 (16.67)	342 (17.10)	
Other	233 (11.79)	6 (25.00)	239 (11.95)	
Unknown	24 (1.21)	1 (4.17)	25 (1.25)	
Education				0.8220
No high school	10 (0.51)	0	10 (0.50)	
High school	1,562 (79.05)	20 (83.33)	1,582 (79.10)	
Bachelor's degree or <4 y of college degree	273 (13.82)	4 (16.67)	277 (13.85)	
Master's degree or higher	32 (1.62)	0	32 (1.60)	
Unknown	99 (5.01)	0	99 (4.95)	
Service				>0.999
Navy	1,965 (99.44)	24 (100.00)	1,989 (99.45)	
Other	11 (0.56)	0	11 (0.55)	
Grade				0.1999
Enlisted	1,791 (90.64)	24 (100.00)	1,815 (90.75)	
Warrant	4 (0.20)	0	4 (0.20)	
Officer	181 (9.16)	0	181 (9.05)	
Outdoor occupations				0.2975
Yes	1,193 (60.37)	17 (70.83)	1,210 (60.50)	
No	783 (39.63)	7 (29.17)	790 (39.50)	

*Values are no. (%) unless indicated otherwise.

excluded as false positives. Confirmatory testing was performed on 144 of the remaining 163 seropositive/seroequivocal samples by EIA (88.3%). Overall, 19 were positive for IgG alone, 1 positive for IgG and IgM, and 2 equivocal for IgM alone. For these 22 samples and the 19 samples that were not sent for confirmatory testing by immunodiffusion, a pretransfer sample was obtained from the DoDSR and tested for *Coccidioides* antibodies by EIA to determine previous seroreactivity. Five persons had serologic evidence of previous *Coccidioides* exposure by pretransfer EIA. Twelve participants were IgG–/IgM+ for pretransfer and posttransfer samples and were considered false positives.

A total of 24 (1.2%) participants met our definition for seroconversion and were included in our analysis (Table 1). Of those, 20 (83.3%) had positive immunodiffusion results by confirmatory testing. Four (16.7%) showed evidence of seroconversion on posttransfer EIAs (one IgG+/IgM–, 1 IgG/IgM equivocal, and 2 IgG equivocal/IgM–) and negative pretransfer EIA results but lacked sufficient posttransfer sample volume for confirmation; they were included as seroconversion cases.

Annual incidence ranged from 0 to 1.32 cases/100 person-years; overall seroconversion incidence was 0.5 cases/100 person-years (Figure; Appendix). Three (12.5%) of the 24 newly seropositive persons were given a diagnosis of coccidioidomycosis or pneumonia after seroconversion. No disseminated infections were diagnosed. No disease was documented in persons who had *Coccidioides* antibodies before arrival. Two coccidioidomycosis diagnoses were for seronegative persons.

We found by bivariate and regression analyses no statistically significant associations between any demographic variable and seropositivity or disease (Tables 1, 2). We did not observe statistically significant differences in seropositivity between racial/ethnic groups or by occupation. Seropositivity was significantly associated with disease (p = 0.027) (Table 2).

Conclusions

Our observed incidence of 0.5 cases/100 person-years is lower than published observations of asymptomatic infection (*7*–*12*). We found no statistically significant association between seropositivity and any demographic variable but were limited by low rates of seroconversion and disease. Prospective *Coccidioides* skin testing at 4 military airfields in southern California, including Lemoore, during 1941–1945 found annual conversion rates as high as 12.43%, decreasing to 1.43% and 2.86% in the 2 years after environmental controls were put in place (*7*). Our incidence rates appear lower than those previously reported and might better represent seroconversion in persons with average dust exposure in the modern era.

The first limitation of our study is that performance of serologic analysis for *Coccidioides* infection depends on time from exposure and varies by method (*13*), which might explain the discordance between coccidioidomycosis diagnoses identified in service members who showed negative test results. High rates of seroreactivity and funding constraints complicated serologic definitions that were limited by discordance between EIA and immunodiffusion results. However, we confirmed

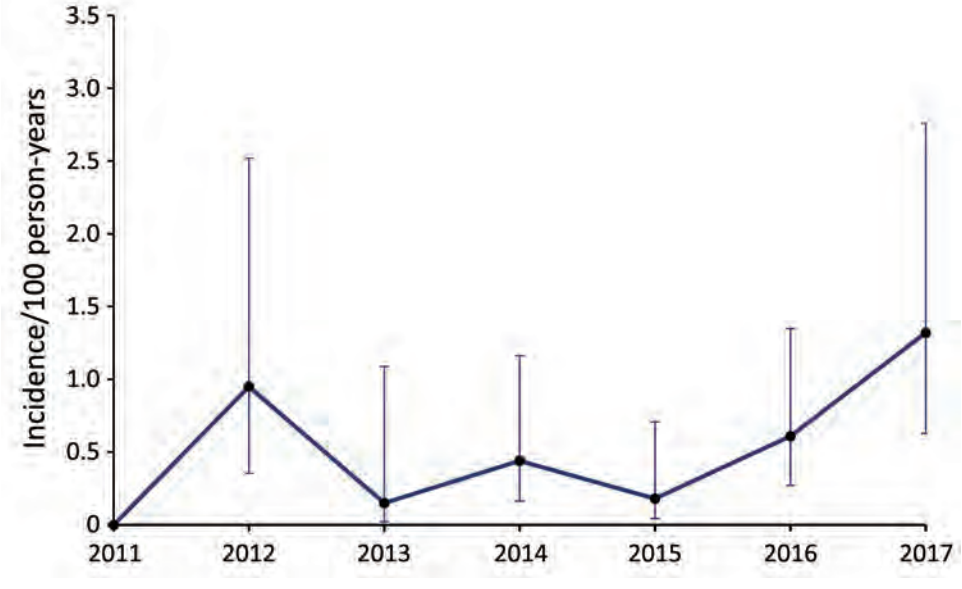

Figure. Incidence of *Coccidioides* seroconversion among military personnel, Naval Air Station Lemoore, San Joaquin Valley, California, USA. Error bars indicate 95% CIs.

Table 2. Cohort demographics by coccidioidomycosis-like diagnosis for incidence of *Coccidioides* seroconversion among military personnel, Naval Air Station Lemoore, San Joaquin Valley, California, USA*

Variables	Diagnosis		Total	p value
	No	Yes		
Seroconversion				0.0267
Yes†	27 (1.38)	3 (6.82)	30 (1.50)	
No	1,929 (98.62)	41 (93.18)	1,970 (98.50)	
Mean age, y (range)	24.0 (20.0–27.0)	21.0 (19.5–25.0)	23.0 (20.0–27.0)	0.0572
Sex				0.1067
M	1,644 (84.05)	33 (75.00)	1,677 (83.85)	
F	312 (15.95)	11 (25.00)	323 (16.15)	
Race/ethnicity				0.5885
Caucasian	892 (45.60)	24 (54.55)	916 (45.80)	
African American	299 (15.29)	4 (9.09)	303 (15.15)	
Asian/Pacific Islander	118 (6.03)	4 (9.09)	122 (6.10)	
Hispanic	335 (17.13)	7 (15.91)	342 (17.10)	
Other	287 (14.67)	5 (11.36)	292 (14.60)	
Unknown	25 (1.28)	0	25 (1.25)	
Education				>0.999
No high school	10 (0.51)	0	10 (0.50)	
High school	1,545 (78.99)	37 (84.09)	1,582 (79.10)	
Bachelor's degree or less	271 (13.85)	6 (13.64)	277 (13.85)	
Master's degree or higher	32 (1.64)	0	32 (1.60)	
Unknown	98 (5.01)	1 (2.27)	99 (4.95)	
Service				>0.999
Navy	1,945 (99.44)	44 (100.00)	1,989 (99.45)	
Other	11 (0.56)	0	11 (0.55)	
Grade				0.1799
Enlisted	1,772 (90.59)	43 (97.73)	1,815 (90.75)	
Warrant/officer	184 (9.41)	1 (2.27)	185 (9.25)	
Outdoor occupation	1,186 (60.63)	20 (45.45)	1,210 (60.50)	0.4139
Total	1,956	44	2,000	

*Values are no. (%) unless indicated otherwise.
†Includes previous seroconversion.

seronegativity by immunodiffusion in more than half of the 252 posttransfer IgG/IgM-equivocal samples, instilling confidence in classifying these results as negatives. Our sample size and cohort homogeneity limited our ability to detect significant risk factors for infection. The retrospective nature of our study could miss mild disease cases. Furthermore, military personnel are often healthy and have few underlying illnesses, potentially explaining the low rate of symptomatic illness in the cohort.

In summary, we found that coccidioidomycosis was uncommon in a military population newly transferred to a disease-endemic region, and progression to clinically apparent disease was infrequent. Longitudinal prospective studies are needed to monitor epidemiologic trends over time and to determine disease risks in diverse populations. Although these low rates of seroincidence and disease are reassuring, caution is warranted when considering this pathogen with complex disease ecology.

Acknowledgments

We thank the Naval Health Research Center for conducting all enzyme immunoassays and the Armed Forces Health Surveillance Division for providing samples and clinical/demographic data.

This study (protocol IDCRP-110) was supported by the National Institute of Allergy and Infectious Diseases, National Institutes of Health, under Inter-Agency Agreement Y1-AI-5072; the Defense Health Program, US DoD, under award HU0001190002; the Armed Forces Health Services Division Global Emerging Infectious Surveillance Branch (ProMIS P0049_17_US); the Infectious Disease Clinical Research Program; and the Henry M. Jackson Foundation.

About the Author

Dr. Ellis is a physician and Undersea Medical Officer in the US Navy. He completed this work while assigned to an operational tour with Explosive Ordnance Disposal Expeditionary Support Unit TWO in Virginia Beach, VA,

and will return to postgraduate training in internal medicine in 2022. His primary research interests are mycotic infections, noncommunicable diseases in low- and middle-income countries, and the Department of Defense's Global Health Engagement.

References

1. Galgiani JN, Ampel NM, Blair JE, Catanzaro A, Geertsma F, Hoover SE, et al. 2016 Infectious Diseases Society of America (IDSA) Clinical practice guideline for the treatment of coccidioidomycosis. Clin Infect Dis. 2016;63:e112–46. https://doi.org/10.1093/cid/ciw360
2. Bays DJ, Thompson GR III. Coccidioidomycosis. Infect Dis Clin North Am. 2021;35:453–69. https://doi.org/10.1016/j.idc.2021.03.010
3. Tsang CA, Anderson SM, Imholte SB, Erhart LM, Chen S, Park BJ, et al. Enhanced surveillance of coccidioidomycosis, Arizona, USA, 2007–2008. Emerg Infect Dis. 2010;16:1738–44. https://doi.org/10.3201/eid1611.100475
4. Freedman M, Anderson S, Benedict K, McCotter O, Derado G, Hockstra R, et al. Preliminary estimates of annual burden of coccidioidomycosis in the United States, 2010–2014. In: Abstracts of the Coccidioidomycosis Study Group. 61st Annual Meeting in collaboration with the 7th International Coccidioidomycosis Symposium; Aug 10–13, 2017; Palo Alto (CA). Standform (CA): Coccidioidomycosis Study Group; 2017. p. 32.
5. McCotter OZ, Benedict K, Engelthaler DM, Komatsu K, Lucas KD, Mohle-Boetani JC, et al. Update on the epidemiology of coccidioidomycosis in the United States. Med Mycol. 2019;57(Supplement_1):S30–40. https://doi.org/10.1093/mmy/myy095
6. Lemoore Installation Guide NAS. Nashville, TN: MyBaseGuide; 2020 [cited 2021 Mar 4]. https://mybaseguide.com/installation/nas-lemoore/relocation-guide
7. Smith CE, Beard RR, Rosenberger HG, Whiting EG. Effect of season and dust control on coccidioidomycosis. JAMA. 1946;132:833–8. https://doi.org/10.1001/jama.1946.02870490011003
8. Wheeler C, Lucas KD, Mohle-Boetani JC. Rates and risk factors for coccidioidomycosis among prison inmates, California, USA, 2011. Emerg Infect Dis. 2015;21:70–5. https://doi.org/10.3201/eid2101.140836
9. Drips W Jr, Smith CE. Epidemiology of coccidioidomycosis: a contemporary military experience. JAMA. 1964;190:1010–2. https://doi.org/10.1001/jama.1964.03070240056021
10. Hooper R, Poppell G, Curley R, Husted S, Schillaci R. Coccidioidomycosis among military personnel in southern California. Mil Med. 1980;145:620–3. https://doi.org/10.1093/milmed/145.9.620
11. Crum-Cianflone NF. Coccidioidomycosis in the U.S. military: a review. Ann N Y Acad Sci. 2007;1111:112–21. https://doi.org/10.1196/annals.1406.001
12. Crum NF, Potter M, Pappagianis D. Seroincidence of coccidioidomycosis during military desert training exercises. J Clin Microbiol. 2004;42:4552–5. https://doi.org/10.1128/JCM.42.10.4552-4555.2004
13 Saubolle MA, McKellar PP, Sussland D. Epidemiologic, clinical, and diagnostic aspects of coccidioidomycosis. J Clin Microbiol. 2007;45:26–30. https://doi.org/10.1128/JCM.02230-06

Address for correspondence: Graham C. Ellis, Explosive Ordnance Disposal Expeditionary Support Unit TWO, 2520 Midway Rd, Ste 300, Norfolk, VA 23459, USA; email: gcellis87@gmail.com

Epidemiologic Features and Control Measures during Monkeypox Outbreak, Spain, June 2022

Berta Suárez Rodríguez,[1] Bernardo R. Guzmán Herrador,[1] Asunción Díaz Franco, María Paz Sánchez-Seco Fariñas, Julia del Amo Valero, Adrián Hugo Aginagalde Llorente, Juan Pablo Alonso Pérez de Agreda, Rosa Carbó Malonda, Daniel Castrillejo, María Dolores Chirlaque López, Eduardo Javier Chong Chong, Sonia Fernández Balbuena, Virtudes Gallardo García, Manuel García-Cenoz, Laura García Hernández, Elisa Gil Montalbán, Fernando González Carril, Teresa González Cortijo, Susana Jiménez Bueno, Aurora Limia Sánchez, Juan Antonio Linares Dópido, Nicola Lorusso, Mario Margolles Martins, Eva María Martínez Ochoa, Ana Martínez Mateo, Jacobo Mendioroz Peña, Ana Isabel Negredo Antón, María Teresa Otero Barrós, Maria del Carmen Pacheco Martinez, Pilar Peces Jiménez, Oscar-Guillermo Pérez Martín, Ana Isabel Rivas Pérez, María Sastre García, National Monkeypox Response Group,[2] Fernando Simón Soria,[3] María José Sierra Moros[3]

During June 2022, Spain was one of the countries most affected worldwide by a multicountry monkeypox outbreak with chains of transmission without identified links to disease-endemic countries. We provide epidemiologic features of cases reported in Spain and the coordinated measures taken to respond to this outbreak.

During May–June 2022, after an alert notification initiated by the United Kingdom (*1*,*2*), >4,500 monkeypox cases had been confirmed worldwide, mainly in the European region (*3*–*6*). Chains of transmission without links to disease-endemic countries have been identified, and cases have occurred mainly

Author affiliations: Coordinating Centre for Health Alerts and Emergencies, Directorate General of Public Health, Ministry of Health, Madrid, Spain (B. Suarez Rodriguez, B.R. Guzmán Herrador, E.J. Chong Chong, S. Fernández Balbuena, F. Simón Soria, M.J. Sierra Moros); National Centre of Epidemiology, Carlos III Health Institute, Madrid (A. Díaz Franco, M. Sastre García); National Centre for Microbiology, Instituto de Salud Carlos III, Madrid (M.P. Sánchez-Seco Fariñas, A. I. Negredo Antón), Division for HIV Control, STI, Viral Hepatitis and Tuberculosis, Ministry of Health, Madrid (J. del Amo Valero); Public Health Observatory of Cantabria, Cantabria, Spain (A.H. Aginagalde Llorente); Dirección General de Salud Pública, Aragón, Spain (J.P. Alonso Pérez de Agreda); Subdirecció General d'Epidemiologia, Vigilància de la Salut i Sanitat Ambiental, Comunidad Valenciana, Spain (R. Carbó Malonda); Consejería de Políticas Sociales, Salud Pública y Bienestar Animal, Melilla, Spain (D. Castrillejo); Regional Health Council, IMIB-Arrixaca, Murcia University, Murcia, Spain (M.D. Chirlaque López); Ministry of Health and Families of Andalusia, Andalusia, Spain (V. Gallardo García, N Lorusso); Instituto de Salud Pública de Navarra, Spain and Navarre Institute for Health Research (IdiSNA), Pamplona, Spain (M. García-Cenoz); Dirección General de Salud Pública del Servicio Canario de la Salud, Tenerife, Spain (L. García Hernández, O.-G. Pérez Martín); Dirección General de Salud Pública de la Comunidad de Madrid, Madrid (E. Gil Montalbán, S. Jiménez Bueno); Departamento de Salud del País, Vasco, Spain (F. González Carril); Dirección General de Salud Pública, Islas Baleares, Spain (T. González Cortijo); Immunization Programme Area, Directorate General of Public Health, Ministry of Health, Madrid (A. Limia Sánchez); Dirección General de Salud Pública. Servicio Extremeño de Salud, Merida, Spain (J.A. Linares Dópido); Dirección General de Salud Pública. Gobierno de Asturias, Oviedo, Spain (M. Margolles Martins); Dirección General de Salud Pública, Consumo y Cuidados de la Consejería de Salud de La Rioja, Logroño, Spain (E.M. Martínez Ochoa); Public Health Agency of Catalonia, Barcelona, Spain (A. Martinez Mateo, J. Mendioroz Peña); Dirección Xeral de Saúde Pública, Consellería de Sanidade, Xunta de Galicia, Santiago, Spain (M.T. Otero Barrós); Dirección General de Salud Pública, Castilla y León, Valladolid, Spain (M.C. Pacheco Martinez); Servicio de Epidemiología, Castilla-La Mancha, Toledo, Spain (P. Peces Jiménez); Consejería de Sanidad, Consumo y Gobernación. Ciudad Autónoma de Ceuta, Ceuta, Spain (A.I. Rivas Pérez); CIBER in Infectious Diseases, Madrid, CIBERINFEC (M.P. Sánchez-Seco Fariñas, A.I. Negredo Antón, M.J. Sierra Moros, A. Díaz Franco); CIBER in Epidemiology and Public Health, Madrid, CIBERESP (M.D. Chirlaque López, M. García-Cenoz, A. Martinez Mateo, M. Sastre García, F. Simón Soria)

DOI: https://doi.org/10.3201/eid2809.221051

[1]These first authors contributed equally to this article.
[2]Members of this group are listed at the end of this article.
[3]These senior authors contributed equally to this article.

among men who have had sex with men (MSM) in high-risk sexual contexts (*5*,*6*).

During June 2022, Spain was one of the countries most affected by monkeypox. We provide epidemiologic features of monkeypox cases reported to the National Surveillance Network through July 4, 2022 (*7*), complemented with information obtained from bilateral consultations with the Spanish Autonomous Regions, and the measures taken to respond to this alert. No ethics approval was sought because this study describes cases and public health actions in Spain linked to the ongoing multicounty outbreak during June 2022. No personal identifiable data for case-patients or any contacts are included in this report.

The Study

Suspected monkeypox cases in Spain were initially reported on May 17. By July 4, of the 19 Autonomous Regions in Spain, 16 had reported 1,256 cases, of which 61.1% (n = 768) were reported by the Region of Madrid. A total of 1,242 cases were in men and 14 in women. The median age of case-patients was 37 years; all but 1 case-patients were adults (Table).

Date of symptom onset was known for 1,182 (89.5%) case-patients . An epidemic plot showed a sustained increasing trend during May and June (Figure). The decreasing numbers during the second half of June might be caused by a delay in reporting.

We obtained information from 4 different series from 4 regions involving 45 patients who self-referred a clear exposure date (range 4–22 patients/region). This information showed average incubation periods of 7–9.6 days.

The most frequent symptoms reported (n = 530) were rash (mainly anogenital), fever, asthenia, and lymphadenopathy (Table). Most patients had ≥1 general symptom plus disseminated and anogenital rash (126 case-patients), ≥1 general symptom plus anogenital rash (exclusively) (105 case-patients), or ≥1 general symptom plus diseminated rash (without anogenital or oro/peribuccal location) (76 case-patients). Of the 216 case-patients who had localized lymphadenopathy, 191 had general symptoms. The median number of days from symptom onset to rash was <1 day (IQR 0–2 days; information was available for 427 case-patients). A total of 30 of the 530 case-patients were hospitalized (median admission 2 days); 33 reported complications, mainly secondary bacterial infections (n = 15) oral ulcers (n = 11), proctitis (n = 2), and pharyngotonsillitis (n = 2). No deaths were reported.

Of 440 case-patients who had available information, 62 had traveled to countries that had reported monkeypox cases during the incubation period. A total of 101 case-patients were reported to be close contacts of confirmed or probable case-patients.

The most likely mechanism of transmission reported by 332 (85.8%) of the 387 case-patients who had available information was intimate and prolonged contact during sex. A total of 31 case-patients reported close contacts unrelated to sex; for 24 case-patients, this information was pending. Of those 332

Table. Characteristics of 1,256 monkeypox case-patients, Spain, July 4, 2022

Characteristic	No. (%) case-patients
Sex	
M	1,242 (98.9)
F	14 (1.10
Age group, y	
<20	6 (0.5)
20–39	238 (18.9)
30–39	511 (40.7)
40–49	361 (28.7)
50–59	126 (10.0)
≥60	13 (1.0)
Unknown	1 (0.1)
General symptoms, n = 530*	
General	
Fever	302 (56.9)
Asthenia	224 (42.3)
Muscle pain	167 (31.5)
Throat pain	136 (25.7)
Headache	140 (26.4)
Specific	
Anogenital rash	355 (66.9)
Disseminated rash in locations other than anogenital or oro/peribuccal	293 (55.3)
Localized lymphadenopathy	216 (40.7)
Oro/peribuccal rash	92 (17.4)
General lymphadenopathy	45 (8.5)

*Exclusive, patients could report >1 symptom.

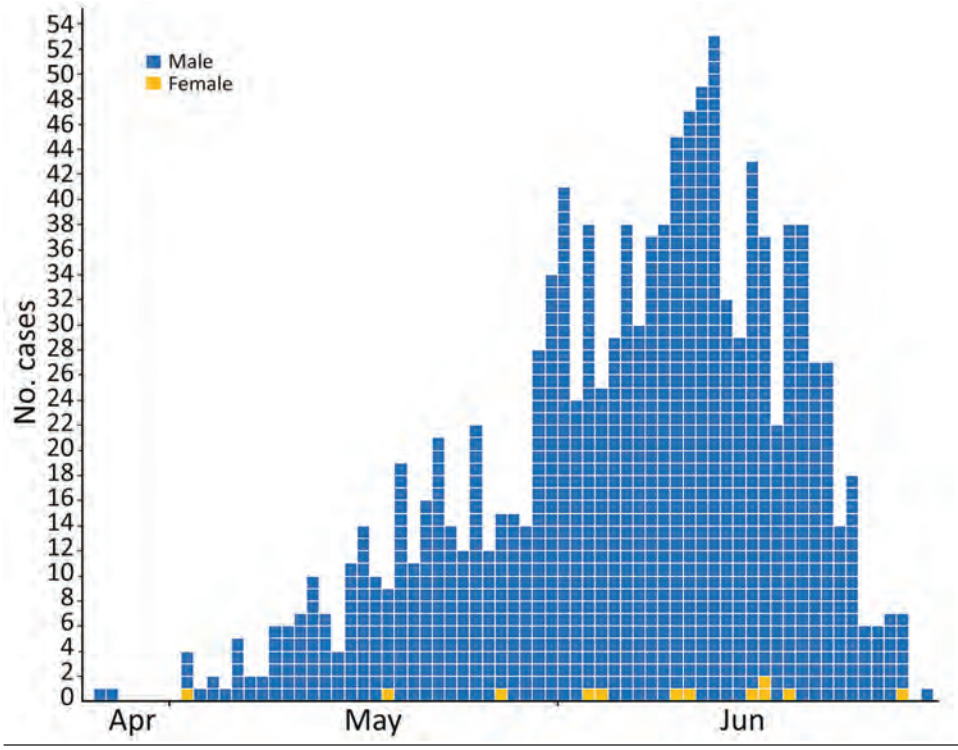

Figure. Epidemic plot of 1,182 confirmed cases of monkeypox according to date of onset of symptoms for late April, May, and June 2022, Spain. April cases were reported during April 25–30. Cases without date of symptom onset were not included (for 72 male case-patients and 2 female case-patients).

case-patients, 290 were MSM; 6 reported heterosexual contact, and information was pending for the remaining 36. Of 413 case-patients who had available information, 163 had attended a mass gathering before symptom onset; 101 attended Pride events in different cities in Spain. Regarding the 14 women, 7 reported intimate contact during sex with men and 2 had close contacts within the family environment; for 5 women, this information was pending.

A total of 11 regions representing 73% of the case-patients reported provided additional details on contact tracing. It was not feasible to identify or obtain any information regarding potential contacts for a substantial number of patients. Most regions reported an average of <3 identifiable contacts/case-patient. Only 4 regions reported case-patients that had >5 identifiable contacts.

The case definition for monkeypox in Spain considers a confirmed case-patient as a person who had monkeypox genome identified by PCR or who had a positive result in a generic PCR for *Orthopoxvirus* in a clinical sample. However, the first confirmation of monkeypox cases was conducted by using sequencing (*8*).

The National Centre for Microbiology conducted partial sequencing of 23 patients and the complete sequencing in samples from 24 cases. This testing identified the West African clade of monkeypox virus.

Following the procedures of the National Early Warning and Rapid Response System, all key stakeholders were alerted to pursue a rapid and coordinated response. A national protocol for early detection and case and contact management was approved and made available by the National Alert Board (*8*) and coordinated by the Ministry of Health 3 days after detection of suspected cases. A rapid risk assessment for Spain has been reported (*9*), and situation reports are updated regularly (*3*). Early consultation and exchange with relevant scientific societies led to publication of an atlas that contained differential diagnoses for monkeypox skin lesions (*10*).

Partnership with the lesbian, gay, transgender, bisexual, intersex, and queer (LGTBIQ) community was seen as pivotal, and the Ministry of Health involved its Advisory and Counselling Board of nongovernmental organizations in the response to promote the engagement of the LGTBIQ community. In this context, several materials, with key health messages developed, are publicly available (*11*), building on previous experience on safe sex campaigns, during summer events and following the general principles of the World Health Organization and European Centre for Disease Prevention and Control (*12*).

Recommendations to offer monkeypox vaccine as postexposure prophylaxis to close contacts, especially those at high risk of developing severe disease and healthcare workers experiencing incidences with the personal protective equipment when in contact with patients, have been proposed by the National Board

for Vaccines (*13*), and ≥80 contacts (information available from 12 regions) have already been vaccinated. Use of vaccination as preexposure prophylaxis for high-risk groups and healthcare workers with occupational risk is now under discussion as the availability of vaccine increases.

Conclusions

Monkeypox transmission is currently centered, but not exclusively, in MSM who have close physical contact in high-risk sexual contexts. However, without optimal control, there is a risk for transmission to other population groups. Early detection, which requires useful information for the differential diagnosis of clinical manifestations, is crucial to control transmission, as is timely case reporting. It is also essential to continue characterizing the dynamics of the outbreak to identify potential changes to tailor and adapt recommendations.

One of the main challenges encountered in the response to this alert is identifying and tracking contacts: case-patients might be hesitant to provide the identities of their contacts or might not be able to do so because risk exposures had occurred anonymously with previously unknown persons. In certain occasions, it was also difficult to ascertain during the epidemiologic interview the exact date in which transmission might had occurred.

The way the ongoing monkeypox outbreak will evolve is still uncertain and will be influenced by how successfully advice reaches the population at risk. Effective risk communication and community engagement strategies are paramount to delivering information to the general population and to most at-risk persons, including summer mass-gathering event organizers. These features should include clear and contrasted information in partnership with the LGTBIQ community to minimize risk behaviors and maximize awareness about the importance of following public health control measures. Explicit warnings to avoid any form of stigmatizing the LGTBIQ community should frame all interventions.

Authors in the National Monkeypox Response Group: Coordinating Centre for Health Alerts and Emergencies, Directorate General of Public Health, Ministry of Health: Andrés Mauricio Brandini Romersi, Cristina Giménez Lozano, Alberto Vallejo-Plaza, Gabriela Saravia Campelli, Patricia Santágueda Balader, Lucía García San Miguel, Esteban Aznar Cano; National Centre of Epidemiology, Carlos III Health Institute: Marta Ruiz-Algueró (second affiliation: CIBER in Infectious Diseases, CIBERINFEC), Lorena Simón, Pedro Arias; National Centre for Microbiology, Instituto de Salud Carlos III: Ana Vázquez (second affiliation: CIBER Epidemiologia y Salud Pública, CIBERESP), Patricia Sánchez (second affiliation: CIBER in Infectious Diseases, CIBERINFEC), Laura Herrero, Francisca Molero, Montserrat Torres; Immunization Programme Area, Directorate General of Public Health, Ministry of Health, Madrid, Spain: Laura Sánchez Cambronero Cejudo; División de control de VIH, ITS, Hepatitis Virales y Tuberculosis Ministerio de Sanidad, Madrid, Spain: Rosa Polo, Javier Gómez Castellá, Ana Koerting; Andalucía: Ministry of Health and Families of Andalusia: Isabel Maria Vazquez Rincon; Aragón: Dirección General de Salud Pública: Alberto Vergara Ugarriza, Carmen Montaño Remacha; Asturias: Dirección General de Salud Pública; Gobierno de Asturias: An Lieve Boone, Marta Huerta Huerta; Islas Baleares: Dirección General de Salud Pública. Antonio Nicolau Riutort; Canarias: Dirección General de Salud Pública, Servicio Canario de la Salud: Álvaro Luis Torres Lana, Araceli Alemán Herrera, Isabel Falcón García; Cataluña: Public Health Agency of Catalonia: Manuel Valdivia Guijarro, Gemma Rosell Duran; Ceuta: Consejería de Sanidad, Consumo y Gobernación: Violeta Ramos Marín; Castilla la Mancha: Servicio de Epidemiología de Castilla la Mancha: M. Remedios Rodolfo Saavedra; Castilla y León: Dirección General de Salud Pública: Socorro Fernández Arribas, Henar Marcos Rodríguez, Nuria Rincón Calvo, Virginia Alvarez Rio, Natalia Gutierrez Garzón, Isabel Martínez-Pino (second affiliation: CIBER in Epidemiology and Public Health, CIBERESP, Madrid, Spain), M. Jesús Rodríguez Recio; Comunidad Valenciana: Subdirección General de Epidemiología; Vigilancia de la Salud y Sanidad Ambiental: Francisco Javier Roig Sena; Extremadura: Dirección General de Salud Pública, Servicio Extremeño de Salud: María del Mar López-Tercero Torvisco; Galicia: Sección de Epidemioloxía; Xefatura Territorial de Sanidade, A Coruña: M. del Carmen García Bañobre, Sección de Epidemioloxía. Xefatura Territorial de Sanidade, Pontevedra: M. del Pilar Sánchez Castro, Sección de Epidemioloxía. Xefatura Territorial de Sanidade, Ourense: Miriam Rebeca Martínez Soto; Madrid: Dirección General de Salud Pública. Marcos Alonso García, Fernando Martin Martínez, M Jose Domínguez Rodríguez, Laura Montero Morales, Ana Humanes Navarro, Esther Cordoba Deorador, Antonio Nunziata Forte, Alba Nieto Julia, Noelia Cenamor Largo, Carmen Sanz Ortíz, Natividad García Marín, Jesús Sánchez Díaz, Mercedes Belen Rumayor Zarzuelo, Nelva Mata Pariente, Jose Francisco Barbas del Buey, Manuel Jose Velasco Rodríguez, Andrés Aragón Peña, Elena Rodríguez Baena, Angel Miguel Benito, Ana Perez Meixeira, Jesus Iñigo Martinez, María Ordobas, Araceli Arce; Murcia: Department of

Epidemiology, Regional Health Council, IMIB-Arrixaca: Alonso Sánchez-Migallón Naranjo; Navarra: Instituto de Salud Pública de Navarra, Pamplona, Spain, Navarre Institute for Health Research (IdiSNA): Jesús Castilla (third affiliation: CIBER Epidemiologia y Salud Pública, CIBERESP), Itziar Casado (third affiliation: CIBER Epidemiologia y Salud Pública, CIBERESP), Cristina Burgui (third affiliation: CIBER Epidemiologia y Salud Pública, CIBERESP), Nerea Egües, Guillermo Ezpeleta; País Vasco: Departamento de Salud del Gobierno Vasco; Subdirección de Salud Pública y Adicciones de Gipuzkoa: Olatz Mokoroa Carollo (second affiliation: Instituto de investigación Sanitaria Biodonostia); Departamento de Salud del País Vasco, Subdirección de Salud Pública y Adicciones de Araba; Vitoria-Gasteiz: Etxebarriarteun Aranzabal, Larraitz; Departamento de Salud del País Vasco Subdirección de Salud Pública y Adicciones de Bizkaia; Esther Hernandez Arricibita; La Rioja: Dirección General de Salud Pública, Consumo y Cuidados: Ana Carmen Ibáñez Pérez.

Acknowledgments

We thank all involved scientific societies in Spain for providing consultations, the advisory and counselling boards of nongovernmental organizations for involvement in the alert response, and the Health Centre Sandoval of the Madrid Health Service for collaboration.

About the Author

Dr. Suarez Rodríguez is a Public Health officer at the Coordinating Centre for Health Alerts and Emergencies at the Ministry of Health and head of the Unit on Preparedness and Response, Madrid, Spain. Her primary research interests are epidemiology, surveillance, and public health preparedness and response.

References

1. UK Health Security Agency. Monkeypox cases confirmed in England: latest updates [cited 2022 Jul 9]. https://www.gov.uk/government/news/monkeypox-cases-confirmed-in-england-latest-updates
2. Vivancos R, Anderson C, Blomquist P, Balasegaram S, Bell A, Bishop L, et al.; UKHSA Monkeypox Incident Management team. Community transmission of monkeypox in the United Kingdom, April to May 2022. Euro Surveill. 2022;27:2200422. https://doi.org/10.2807/1560-7917.ES.2022.27.22.2200422
3. Ministry of Health. Situation report. MPX in Spain and other non-endemic countries, June 28, 2022 [in Spanish] [cited 2022 Jul 9]. https://www.sanidad.gob.es/profesionales/saludPublica/ccayes/alertasActual/alertaMonkeypox/docs/Informe_de_situacion_MPX_20220610.pdf
4. World Health Organization. Multi-country monkeypox outbreak: situation update. June 27, 2022 [cited 2022 Jul 9]. https://www.who.int/emergencies/disease-outbreak-news/item/2022-DON396
5. Joint European Center for Disease Prevention and Control and World Health Organization. Regional Office for Europe Monkepox Surveillance Bulletin, June 29, 2022 [cited 2022 Jun 9]. https://monkeypoxreport.ecdc.europa.eu
6. European Centre for Disease Prevention and Control. Monkeypox multi-country outbreak, May 23, 2022. Stockholm; The Centre; 2022 [cited 2022 Jul 9]. https://www.ecdc.europa.eu/sites/default/files/documents/Monkeypox-multi-country-outbreak.pdf
7. Carlos III Institute. Information technologies applied to the surveillance of diseases in Spain [in Spanish] [cited 2022 Jul 9]. https://administracionelectronica.gob.es/pae_Home/dam/jcr:35d6af28-9efc-4ae0-81a8-c8ae00cbb52f/48eficiencia.pdf
8. Ministry of Health and Carlos III Institute. Protocol for early detection and case management in the context of the MPX alert in Spain, June 10, 2022 [in Spanish] [cited 2022 Jul 9]. https://www.sanidad.gob.es/profesionales/saludPublica/ccayes/alertasActual/alertaMonkeypox/docs/20220610_ProtocoloMPX.pdf
9. Ministry of Health. Rapid Risk Assessment. Authoctonous cases of monkeypox in Spain and other non-endemic countries [in Spanish] [cited 2022 Jul 9]. https://www.sanidad.gob.es/profesionales/saludPublica/ccayes/alertasActual/alertaMonkeypox/docs/ERR_Monkeypox_10062022.pdf
10. Spanish Federation of Scientific Medical Associations. Differential diagnosis of monkeypox cutaneous lesions [cited 2022 Jul 9]. https://facme.es/wp-content/uploads/2022/06/01062022-DIAGNOSTICO-DIFERENCIAL-LESIONES-CUTANEAS-.pdf
11. Ministry of Health. This year the party is healthy [in Spanish] [cited 2022 Jujl 9]. https://www.sanidad.gob.es/ciudadanos/enfLesiones/enfTransmisibles/sida/VIRUELADELMONO/esteveranolafiesta.htm
12. European Centre for Disease Prevention and Control/World Health Organization Regional Office for Europe. Interim advice for public health authorities on summer events during the monkeypox outbreak in Europe, June 14, 2022 [cited 2022 Jul 9]. https://www.ecdc.europa.eu/sites/default/files/documents/Interim-advice-for-public-health-authorities-on-summer-events-mpx.pdf
13. Ministry of Health. Vaccine recommendations in the MPX outbreak [in Spanish] [cited 2022 Jul 9]. https://www.sanidad.gob.es/profesionales/saludPublica/prevPromocion/vacunaciones/MonkeyPox/docs/Propuesta_vacunacion_Monkeypox.pdf

Address for correspondence: Bernardo R. Guzmán Herrador, Coordinating Centre for Health Alerts and Emergencies, Directorate General of Public Health, Ministry of Health, Madrid, Spain; email: bguzman@sanidad.gob.es

Susceptibility of Wild Canids to SARS-CoV-2

Stephanie M. Porter, Airn E. Hartwig, Helle Bielefeldt-Ohmann, Angela M. Bosco-Lauth,[1] J. Jeffrey Root[1]

We assessed 2 wild canid species, red foxes (*Vulpes vulpes*) and coyotes (*Canis latrans*), for susceptibility to SARS-CoV-2. After experimental inoculation, red foxes became infected and shed infectious virus. Conversely, experimentally challenged coyotes did not become infected; therefore, coyotes are unlikely to be competent hosts for SARS-CoV-2.

Throughout the COVID-19 pandemic, multiple instances of natural infections with SARS-CoV-2 have been reported in pet dogs, likely after exposure to an infected human (*1*–*3*). Domestic dogs appear to be minimally susceptible to SARS-CoV-2, as indicated by experimental inoculations resulting in reverse transcription PCR–positive samples and low titer antibody responses but no clinical disease nor shedding of infectious virus (*4*,*5*).

The ability of SARS-CoV-2 to infect domestic dogs, in addition to several other species of carnivores, suggests that additional members of the canid family might be susceptible to infection. Wild canids, such as red foxes (*Vulpes vulpes*) and coyotes (*Canis latrans*), are of particular interest given how widely distributed these animals are, their frequent proximity to humans, and that they prey, scavenge upon, or otherwise interact with species demonstrated to be susceptible to SARS-CoV-2, including felids, skunks, rodents, and white-tailed deer (*6*,*7*). Foxes (species not specified) have been included in modeling efforts and serosurveillance studies aiming to predict animal hosts of SARS-CoV-2, but their ability to serve as hosts for SARS-CoV-2 remains unclear.

Structural analysis of the ACE2 receptor in various animal species predicted that red fox ACE2 have the ability to bind to SARS-CoV-2; different models have predicted low-, medium-, or high-affinity binding (*8*–*10*). Two surveillance studies have sampled wild foxes and failed to detect antibodies against SARS-CoV-2; however, both studies were conducted early in the COVID-19 pandemic and did not exclude the possibility that foxes might become infected with and develop an immune response to SARS-CoV-2, only that spillover had not occurred in the examined animals in those locations at that time (*11*,*12*).

Because numerous carnivore species have proven to be susceptible to SARS-CoV-2, ascertaining the susceptibility of other wild carnivores to the virus, especially those species that are closely associated with humans, is a crucial step in understanding the role that wildlife might play in maintaining and transmitting SARS-CoV-2. The objective of this study was to assess 2 species of wild canids—red foxes and coyotes—for susceptibility to infection with SARS-CoV-2.

The Study

We evaluated captive-reared, juvenile (3–5-month-old), mixed sex red foxes (3 female, 3 male) and coyotes (3 female, 1 male) for susceptibility to SARS-CoV-2. After approval by Colorado State University and National Wildlife Research Center Institutional Animal Care and Use Committees, we individually housed animals in an Animal Biosafety Level 3 (ABSL-3) facility at Colorado State University. Before inoculation, all animals were seronegative against SARS-CoV-2.

We diluted SARS-CoV-2 strain WA1/2020WY96 (obtained from BEI Resources, https://www.beiresources.org) in phosphate-buffered saline and instilled the solution into the nares of each animal. We immediately performed virus back-titration on Vero cells to confirm each animal received 5.1–6.0 $\log_{10}$ plaque-forming units of SARS-CoV-2.

We assessed all animals daily for attitude and signs of clinical disease, including lethargy, anorexia, ocular discharge, nasal discharge, sneezing, coughing, and dyspnea. We did not observe weight loss

Author affiliations: US Department of Agriculture, Fort Collins, Colorado, USA (S.M. Porter, J.J. Root); Colorado State University, Fort Collins (A.E. Hartwig, A.M. Bosco-Lauth); University of Queensland, St Lucia, Queensland, Australia (H. Bielefeldt-Ohmann)

DOI: https://doi.org/10.3201/eid2809.220223

[1]These senior authors contributed equally to this article.

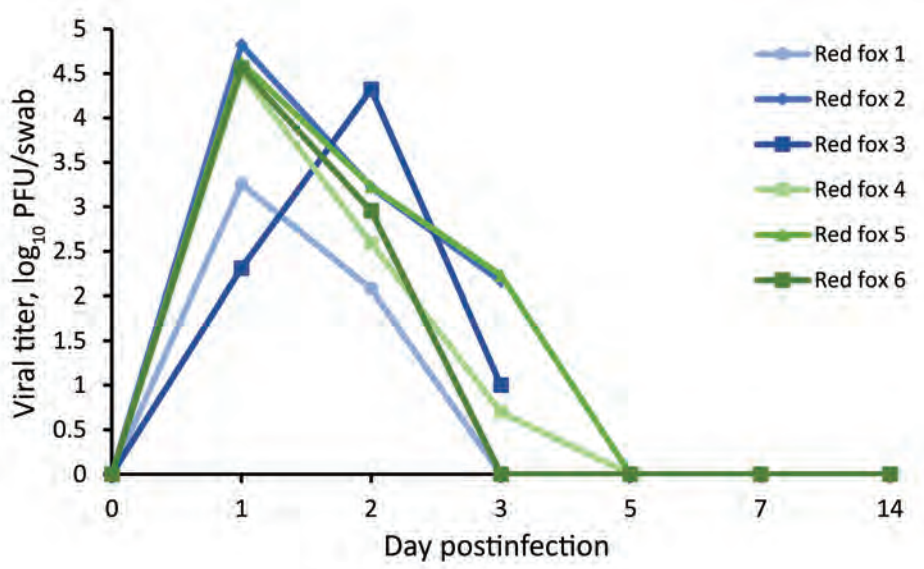

Figure 1. Oropharyngeal shedding of SARS-CoV-2 by red foxes (*Vulpes vulpes*) experimentally infected with SARS-CoV-2 as detected by plaque assay. Red foxes 1, 2, and 3 were euthanized at 3 days postinfection. PFU, plaque-forming unit.

or elevated temperatures in any animals during the study. On 4 days postinfection (dpi), 1 red fox was observed to be lethargic, and all 3 red foxes remaining at 6 dpi were lethargic and sneezing. No other behavioral changes or clinical signs of disease were seen in any of the animals at any other time point.

We collected oral swab and nasal flush samples from each animal on 1, 2, 3, and 5 dpi and obtained additional oral swab samples on 7 and 14 dpi. Plaque assay revealed that all 6 of the red foxes shed infectious virus both orally (Figure 1) and nasally (Figure 2) starting at 1 dpi. Most of the red foxes were still shedding virus at 3 dpi (4/6 oral, 5/6 nasal); all shedding resolved by 5 dpi. We did not isolate infectious virus from any of the oral swabs or nasal flushes collected from any of the coyotes. Reverse transcription PCR confirmed the SARS-CoV-2 shedding profile of the red foxes and revealed that viral RNA was detected beyond the period that infectious virus was detectable (Table 1). The 2 dpi oral swab samples from all 4 coyotes were positive for SARS-CoV-2 RNA, albeit with high cycle threshold values (range 32–35) (Table 1). All other coyote oral swab samples were negative for SARS-CoV-2.

We euthanized and necropsied one half of the animals (3 red foxes, 2 coyotes) at 3 dpi to evaluate tissues for acute viral burden and pathological changes. Infectious virus was isolated from the nasal turbinates of 2 of 3 red fox but not from any other tissues. None of the coyote tissues contained any infectious virus.

We collected blood for serologic testing weekly from the remaining animals until 28 dpi (red fox) or 30

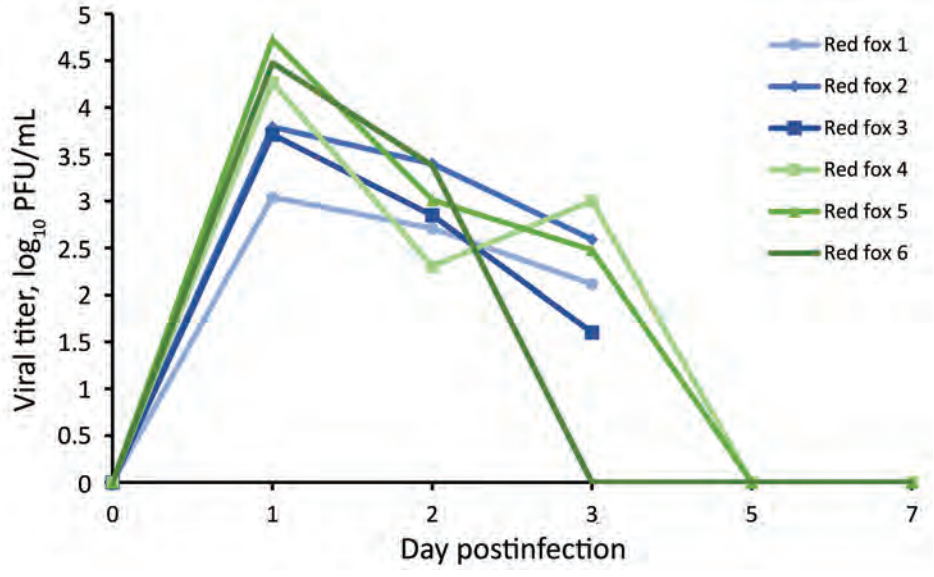

Figure 2. Nasal shedding of SARS-CoV-2 by red foxes (*Vulpes vulpes*) experimentally infected with SARS-CoV-2 as detected by plaque assay. Red foxes 1, 2, and 3 were euthanized at 3 days postinfection. PFU, plaque-forming unit.

Table 1. Cycle threshold values by RT-PCR of oral swab samples from red foxes (*Vulpes vulpes*) and coyotes (*Canis latrans*) experimentally infected with SARS-CoV-2*

	Cycle threshold value					
Animal	1 dpi	2 dpi	3 dpi	5 dpi	7 dpi	14 dpi
Red fox 1	21.2	33.2	31.4			
Red fox 2	18.2	21.4	28.9			
Red fox 3	22.3	16.7	33.7			
Red fox 4	18.4	21.7	28.2	34.8	Undetected	Undetected
Red fox 5	17.9	18.3	28.4	Undetected	25.7	Undetected
Red fox 6	16.9	20.8	31.3	24.3	28.3	Undetected
Coyote 1	Undetected	35.0	Undetected			
Coyote 2	Undetected	32.6	Undetected			
Coyote 3	Undetected	34.0	Undetected	Undetected	Undetected	Undetected
Coyote 4	Undetected	33.1	Undetected	Undetected	Undetected	Undetected

*Red foxes 1, 2, and 3 and coyotes 1 and 2 were euthanized at 3 dpi. dpi, days postinfection; RT-PCR, revere transcription PCR.

dpi (coyote), at which point the animals were euthanized and necropsied. All of the red foxes held until 28 dpi showed a neutralizing antibody response beginning at 7 dpi; peak titers (1:80 or higher) were reached at 14 dpi (Table 2). None of the coyotes seroconverted.

On necropsy, we did not observe gross lesions in any animal. None of the fox tissues evaluated had histopathologic lesions attributable to SARS-CoV-2. We did not assess tissues from the coyotes histologically.

Conclusions

The COVID-19 pandemic has been driven by human-to-human transmission of SARS-CoV-2, but animal species that are susceptible to infection with the virus represent a niche for viral maintenance and could potentially serve as a source for viral spillback into the human population, as has already been the case on mink farms (*13*). Peridomestic species are of particular interest because they presumably run the greatest risk for contracting the virus from humans.

We demonstrated that red foxes are susceptible to infection with SARS-CoV-2. All red foxes in this study shed infectious virus both orally and nasally for ≥3 days. Each of the red foxes held for 28 days displayed mild, self-resolving, clinical signs including lethargy and sneezing and developed neutralizing antibody responses beginning 7 dpi that persisted for the duration of the study. The antibody titers from red foxes were similar to what has been seen in experimentally infected domestic dogs (*4*). Conversely, coyotes appear not to be susceptible to infection with SARS-CoV-2; none of the animals in the study shed detectable virus nor seroconverted after challenge. Coyote oral swabs were positive for viral RNA on 2 dpi, but this result was not associated with isolation of infectious virus and likely represents either residual inoculum or an infection below the limit of detection. Hence, coyotes are unlikely to be competent hosts for SARS-CoV-2.

The animals thus far found to be susceptible to natural infection with SARS-CoV-2 have reflected results from experimental challenge studies, so it is reasonable to assume that our results can be extrapolated. Therefore, attention should be paid to red foxes when considering wildlife species that might serve as reservoir hosts for SARS-CoV-2. We demonstrated that SARS-CoV-2–infected red foxes shed infectious virus for multiple days in both oral and nasal secretions; consequently, the ability of red foxes to transmit SARS-CoV-2 to other susceptible animals should be investigated. Because red foxes commonly consume other species that are susceptible to infection with SARS-CoV-2, predator–prey interactions and scavenging might serve as avenues for interspecies transmission. Should wildlife species such as red foxes become established maintenance hosts of SARS-CoV-2, consequences could include effects on animal health, development of novel viral variants, and spillback into the human population.

This article was preprinted at https://www.biorxiv.org/content/10.1101/2022.01.27.478082v1.

Table 2. Antibody titers for red foxes (*Vulpes vulpes*) experimentally infected with SARS-CoV-2*

	Antibody titer, $PRNT_{80}$				
Animal	Preinfection	7 dpi	14 dpi	21 dpi	28 dpi
Red fox 4	0	20	160	80	80
Red fox 5	0	20	80	80	80
Red fox 6	0	20	320	160	320

*dpi, days postinfection; $PRNT_{80}$, 80% plaque reduction neutralization test.

Acknowledgments

We are very grateful to Julie Young and Stacey Brummer for providing training and the captive-bred coyotes used in this study and to USDA-APHIS-WS-NWRC animal care staff for assistance with husbandry. Special thanks to Jeremy Ellis for invaluable technical assistance and to Richard Bowen for guidance, consulting, and facilities support.

This work was supported by internal funding from Colorado State University and the US Department of Agriculture, Animal and Plant Health Inspection Service.

About the Author

Dr. Porter is an APHIS Science Fellow with the National Wildlife Research Center at the United States Department of Agriculture. Her research interests include the pathogenesis and transmission of infectious disease.

References

1. Decaro N, Vaccari G, Lorusso A, Lorusso E, De Sabato L, Patterson EI, et al. Possible human-to-dog transmission of SARS-CoV-2, Italy, 2020. Emerg Infect Dis. 2021;27:1981–4. https://doi.org/10.3201/eid2707.204959
2. Medkour H, Catheland S, Boucraut-Baralon C, Laidoudi Y, Sereme Y, Pingret JL, et al. First evidence of human-to-dog transmission of SARS-CoV-2 B.1.160 variant in France. Transbound Emerg Dis. 2021 Oct 27 [Epub ahead of print]. https://doi.org/10.1111/tbed.14359
3. Yaglom HD, Hecht G, Goedderz A, Jasso-Selles D, Ely JL, Ruberto I, et al. Genomic investigation of a household SARS-CoV-2 disease cluster in Arizona involving a cat, dog, and pet owner. One Health. 2021;13:100333. https://doi.org/10.1016/j.onehlt.2021.100333
4. Bosco-Lauth AM, Hartwig AE, Porter SM, Gordy PW, Nehring M, Byas AD, et al. Experimental infection of domestic dogs and cats with SARS-CoV-2: pathogenesis, transmission, and response to reexposure in cats. Proc Natl Acad Sci U S A. 2020;117:26382–8. https://doi.org/10.1073/pnas.2013102117
5. Shi J, Wen Z, Zhong G, Yang H, Wang C, Huang B, et al. Susceptibility of ferrets, cats, dogs, and other domesticated animals to SARS-coronavirus 2. Science. 2020;368:1016–20. https://doi.org/10.1126/science.abb7015
6. Palmer MV, Martins M, Falkenberg S, Buckley A, Caserta LC, Mitchell PK, et al. Susceptibility of white-tailed deer (*Odocoileus virginianus*) to SARS-CoV-2. J Virol. 2021;95:e00083–21. https://doi.org/10.1128/JVI.00083-21
7. Peterson M, Baglieri M, Mahon K, Sarno RJ, Ries L, Burman P, et al. The diet of coyotes and red foxes in southern New York. Urban Ecosyst. 2021;24:1–10. https://doi.org/10.1007/s11252-020-01010-5
8. Damas J, Hughes GM, Keough KC, Painter CA, Persky NS, Corbo M, et al. Broad host range of SARS-CoV-2 predicted by comparative and structural analysis of ACE2 in vertebrates. Proc Natl Acad Sci U S A. 2020;117:22311–22. https://doi.org/10.1073/pnas.2010146117
9. Fischhoff IR, Castellanos AA, Rodrigues JPGLM, Varsani A, Han BA. Predicting the zoonotic capacity of mammals to transmit SARS-CoV-2. Proc Biol Sci. 2021;288:20211651.
10. Luan J, Lu Y, Jin X, Zhang L. Spike protein recognition of mammalian ACE2 predicts the host range and an optimized ACE2 for SARS-CoV-2 infection. Biochem Biophys Res Commun. 2020;526:165–9. https://doi.org/10.1016/j.bbrc.2020.03.047
11. Deng J, Jin Y, Liu Y, Sun J, Hao L, Bai J, et al. Serological survey of SARS-CoV-2 for experimental, domestic, companion and wild animals excludes intermediate hosts of 35 different species of animals. Transbound Emerg Dis. 2020;67:1745–9. https://doi.org/10.1111/tbed.13577
12. Jemeršić L, Lojkić I, Krešić N, Keros T, Zelenika TA, Jurinović L, et al. Investigating the presence of SARS CoV-2 in free-living and captive animals. Pathogens. 2021;10:635. https://doi.org/10.3390/pathogens10060635
13. Hammer AS, Quaade ML, Rasmussen TB, Fonager J, Rasmussen M, Mundbjerg K, et al. SARS-CoV-2 transmission between mink (*Neovison vison*) and humans, Denmark. Emerg Infect Dis. 2021;27:547–51. https://doi.org/10.3201/eid2702.203794

Address for correspondence: Jeff Root, USDA/APHIS/WS National Wildlife Research Center, 4101 Laporte Ave, Fort Collins, CO 80521-2154, USA; email: jeff.root@usda.gov

Epidemiology of Infections with SARS-CoV-2 Omicron BA.2 Variant, Hong Kong, January–March 2022

Yonatan M. Mefsin, Dongxuan Chen, Helen S. Bond, Yun Lin, Justin K. Cheung, Jessica Y. Wong, Sheikh Taslim Ali, Eric H.Y. Lau, Peng Wu, Gabriel M. Leung, Benjamin J. Cowling

Our analysis of data collected from multiple epidemics in Hong Kong indicated a shorter serial interval and generation time of infections with the SARS-CoV-2 Omicron variant. The age-specific case-fatality risk for Omicron BA.2.2 case-patients without complete primary vaccination was comparable to that of persons infected with ancestral strains in earlier waves.

Several SARS-CoV-2 variants of concern have caused large outbreaks of infection, including deaths, after the emergence of the ancestral strain in late 2019. First detected in South Africa in November 2021, the Omicron variants quickly became dominant across the world, even in countries with high SARS-CoV-2 vaccination coverage (*1*), probably attributable to enhanced immune escape and increased transmissibility (*2*).

Hong Kong (population 7.4 million), a special administrative region of China, applied intensive public health and social measures to control 4 epidemic waves during 2020–2021, in which 9,403 locally infected (non-imported) cases (1.3 cases/1,000 population) and 207 fatalities occurred. During December 31, 2021–May 21, 2022, a total of 9,148 deaths and >1 million cases largely caused by Omicron were reported in the fifth pandemic wave (Figure 1, panel A, B, https://wwwnc.cdc.gov/EID/article/28/9/22-0613-F1.htm). The COVID-19 vaccination program in Hong Kong began in late February 2021 and uses the mRNA vaccine BNT162b2 (Pfizer-BioNTech, https://www.pfizer.com) and the inactivated vaccine CoronaVac (Sinovac, https://www.sinovac.com). Approximately 10% of the population had been vaccinated with 1 dose by late April 2021, and coverage slowly increased thereafter. The Omicron variant (BA.1) was first detected in Hong Kong among 2 travelers in hotel quarantine in November 2021 (*3*), and a small community outbreak occurred in early January 2022, linked to 2 aircrew members infected overseas (*4*). Subsequently, Omicron BA.2.2 cases were reported in another quarantine hotel in mid-January in an arriving traveler who was reaching the end of a 21-day quarantine (*5*). Ultimately, a large fifth wave dominated by BA.2.2 peaked in early March 2022 after rising exponentially for ≥1 month, with a doubling time of 3.1 days (Figure 1, panel C). Virus sequencing conducted throughout the epidemic indicated that the last local BA.1 cases were detected in mid-January and 1 sporadic local Delta detection occurred in late March (Leo Poon, University of Hong Kong, pers. comm., email, May 28, 2022).

Author affiliations: World Health Organization Collaborating Centre for Infectious Disease Epidemiology and Control, School of Public Health, Li Ka Shing Faculty of Medicine, The University of Hong Kong, Hong Kong, China (Y.M. Mefsin, D. Chen, H.S. Bond, Y. Lin, J.K. Cheung, J.Y. Wong, S.T. Ali, E.H.Y. Lau, P. Wu, G.M. Leung, B.J. Cowling); Laboratory of Data Discovery for Health, Hong Kong Science and Technology Park, Hong Kong (D. Chen, S.T. Ali, E.H.Y. Lau, P. Wu, G.M. Leung, B.J. Cowling)

DOI: https://doi.org/10.3201/eid2809.220613

The Study

We analyzed contact-tracing data on reverse transcription PCR–confirmed COVID-19 cases reported during December 31, 2021–January 22, 2022, to estimate the serial interval and generation time for Omicron (Appendix, https://wwwnc.cdc.gov/EID/article/28/9/22-0613-App1.pdf). Given the 207 deaths that occurred in 9,403 locally infected case-patients in the first 4 epidemic waves and 106 deaths among 4,604 case-patients discharged from hospital isolation in the early period of wave 5, we estimated the age-specific case-fatality risk (CFR) for case-patients infected with ancestral strains compared with Omicron-infected case-patients.

By using information on 80 case-patients (57 infected with BA.1 and 23 with BA.2) with known

exposure and symptom onset information, we estimated the mean (±SD) incubation periods to be 4.58 (±1.72) days for Omicron BA.1 and 4.42 (±1.42) days for Omicron BA.2 (Appendix Table 1). For 43 symptomatic infector–infectee pairs, we estimated the mean (±SD) serial interval for BA.1 infections (n = 30) as 3.30 (±1.95) days; median was 3.17 days. For BA.2 (n = 13), the estimated mean (±SD) serial interval was 2.72 (±1.51) days; median was 2.52 days. We used gamma distribution for estimates of BA.2 accounting for the potential for epidemic phase bias (*6*) with a growth rate of 0.25, because data were collected during the early growth phase of the BA.2 epidemic.

In the early period of the fifth wave (on or before February 15, 2022), all reported COVID-19 cases were only confirmed through reverse transcription PCR conducted by Hong Kong's Public Health Laboratory Services, as in earlier waves (Figure 1; Appendix Figure 1). After accounting for unresolved outcomes in some persons, we estimated that the age-specific CFR for case-patients without completion of a primary series of vaccination in wave 5 was comparable to that of case-patients confirmed in waves 1–4 across all age groups (Figure 2; Appendix Table 2). The highest fatality risk observed in waves 1–4 for patients ≥80 years of age (24.9% [95% CI 20.9%–29.3%]) was similar to that for unvaccinated persons at the same age from wave 5 (21.7% [95% CI 17.1%–26.8%]) (Figure 2). The CFR for persons ≥80 years of age who had not completed a primary series of vaccination in wave 5 was approximately double the risk for persons in the same age group who had completed a primary series (11.1% [95% CI 4.2–22.6]). Among case-patients 65–79 years of age, the CFR was 5.2% (95% CI 4.1%–6.5%) in waves 1–4, 6.7% (4.3%–9.8%) in wave 5 with incomplete primary series, and 0.7% (0.1%–2.4) with complete primary series (Figure 2; Appendix Table 2). The 8 deaths that occurred in adults ≥65 years of age with a complete primary series of vaccination were all in persons who had received 2 or 3 doses of CoronaVac vaccine.

Conclusions

Our study estimated a relatively shorter serial interval and generation time of the Omicron BA.2 subvariant in Hong Kong compared with earlier variants (*7*), which would have contributed to faster spread in the population along with the higher intrinsic transmissibility. Our analysis was conducted on a relatively small number of case pairs in the fifth wave. Similar studies conducted in South Korea and the Netherlands reported shorter mean incubation periods as low as 3.2 days (*8*) and serial intervals of 2.8–3.0 days (*8*,*9*). The peak of the fifth epidemic in Hong Kong in early March despite no major change in social distancing measures probably indicates sufficient infections to create herd immunity, at least temporarily, with subsequent infections overshooting that threshold (*11*).

Among all the deaths in persons whose age was recorded through May 21 in Hong Kong, 92.7% (8,482/9,146) occurred in persons ≥65 years of age and 71.1% (6,500/9,146) in persons ≥80 years of age. We found a generally similar fatality risk for unvaccinated case-patients across age groups in the early period of the fifth wave compared with earlier waves, although the CFR for Omicron cases in person ≥80 years of age without complete primary vaccination series might be slightly lower than persons infected with ancestral strains. This finding indicates that the intrinsic severity of BA.2 may not be much lower than the ancestral strain. Nonetheless, only 106 fatal cases that occurred in the fifth wave were applied in the analysis. Infections with the Omicron variant were reported to have milder severity in South Africa (*12*) and elsewhere (*13*,*14*), where most of the population were either exposed to previous infections or had been vaccinated. However, our estimates might slightly overestimate the fatality risk of Omicron in

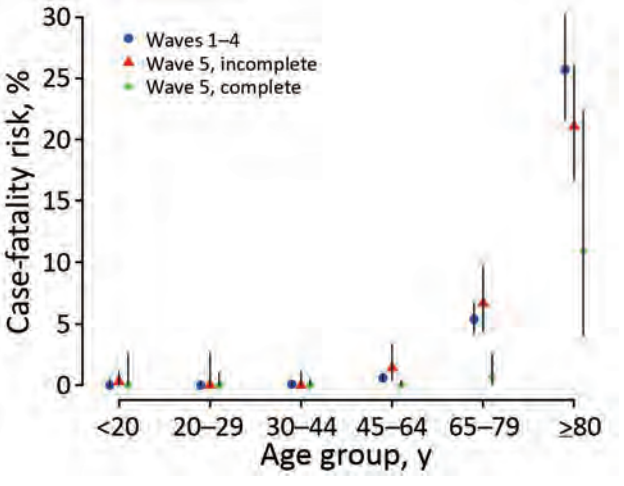

Figure 2. Age-stratified estimates of the case-fatality risk for COVID-19 in epidemic waves 1–4 and wave 5 in Hong Kong by vaccination status. Case-patients were classified as having a complete primary series if they had received ≥2 doses of COVID-19 vaccines ≥2 weeks before symptom onset (for symptomatic case-patients) or ≥3 weeks before laboratory confirmation of the infection (for symptomatic case-patients with a missing onset date or asymptomatic case-patients), otherwise as having an incomplete primary series. The COVID-19 vaccines available in Hong Kong included BNT162b2 (Pfizer-BioNTech, https://www.pfizer.com) and CoronaVac (Sinovac, https://www.sinovac.com) vaccines.

Hong Kong because a small number of cases of Delta infection, including fatal cases, might have been included in the analysis and some milder COVID-19 cases might not have been diagnosed and isolated yet during the early period of the fifth wave.

The relatively high number of deaths in Hong Kong's fifth wave can be attributed to the high incidence of infections within a short period and the low level of vaccination coverage in older adults. Although the overall vaccination coverage was 70% at the start of the fifth wave, only 50% of persons ≥65 years of age and 20% of persons ≥80 years of age had completed a primary series of vaccination. Vaccine hesitancy in older adults in Hong Kong appeared to be associated with low confidence in the government and the concern about the risk for adverse events after vaccination among persons with underlying medical conditions (*15*). Overall, our findings highlight the importance of achieving high vaccination coverage, especially in older adults, and the need to reassess public health and social measures in response to any more transmissible SARS-CoV-2 variant in the future.

Acknowledgments

We thank Julie Au, Chloe Chui, Caitriona Murphy, Faith Ho, and Dillon Adam for technical support.

This project was supported by a commissioned grant from the Health and Medical Research Fund of the Hong Kong SAR Government (grant no. CID-HKU2), the Collaborative Research Scheme (project no. C7123-20G) of the Research Grants Council of the Hong Kong SAR Government, and AIR@InnoHK administered by Innovation and Technology Commission. B.J.C. is supported by a RGC Senior Research Fellow Scheme grant (HKU SRFS2021-7S03) from the Research Grants Council of the Hong Kong SAR, China.

B.J.C. consults for AstraZeneca, Fosun Pharma, GSK, Moderna, Pfizer, Roche, and Sanofi Pasteur. The authors report no other potential conflicts of interest.

Y.M.M., P.W., and B.J.C. conceived the study. Y.M., D.C., H.B., Y.L., J.K.C., J.Y.W., S.T.A., and E.H.Y. collected the data and conducted the analysis. Y.M. and P.W. drafted the manuscript. All authors critically reviewed and revised the manuscript and approved the final version.

References

1. World Health Organization. Statement on Omicron sublineage BA.2 2022. 2022 Feb 22 [cited 2022 Apr 20]. https://www.who.int/news/item/22-02-2022-statement-on-omicron-sublineage-ba.2
2. Hu J, Peng P, Cao X, Wu K, Chen J, Wang K, et al. Increased immune escape of the new SARS-CoV-2 variant of concern Omicron. Cell Mol Immunol. 2022;19:293–5. https://doi.org/10.1038/s41423-021-00836-z
3. Gu H, Krishnan P, Ng DYM, Chang LDJ, Liu GYZ, Cheng SSM, et al. Probable transmission of SARS-CoV-2 Omicron variant in quarantine hotel, Hong Kong, China, November 2021. Emerg Infect Dis. 2022;28:460–2. https://doi.org/10.3201/eid2802.212422
4. Government of the Hong Kong Special Administrative Region. The Centre for Health Protection of the Department of Health investigates three COVID-19 preliminary positive cases [press release]. 2021 Dec 30 [cited 2022 May 28]. https://www.info.gov.hk/gia/general/202112/30/P2021123000898.htm
5. Government of Hong Kong Special Administrative Region. The latest epidemic situation of COVID-19 [press release]. 2022 Jan 16 [cited 2022 May 28]. https://www.info.gov.hk/gia/general/202201/16/P2022011600537.htm
6. Britton T, Scalia Tomba G. Estimation in emerging epidemics: biases and remedies. J R Soc Interface. 2019;16:20180670. https://doi.org/10.1098/rsif.2018.0670
7. Griffin J, Casey M, Collins Á, Hunt K, McEvoy D, Byrne A, et al. Rapid review of available evidence on the serial interval and generation time of COVID-19. BMJ Open. 2020;10:e040263. https://doi.org/10.1136/bmjopen-2020-040263
8. Backer JA, Eggink D, Andeweg SP, Veldhuijzen IK, van Maarseveen N, Vermaas K, et al. Shorter serial intervals in SARS-CoV-2 cases with Omicron BA.1 variant compared with Delta variant, the Netherlands, 13 to 26 December 2021. Euro Surveill. 2022;27:2200042. https://doi.org/10.2807/1560-7917.ES.2022.27.6.2200042
9. Lee JJ, Choe YJ, Jeong H, Kim M, Kim S, Yoo H, et al. Importation and transmission of SARS-CoV-2 B. 1.1. 529 (Omicron) variant of concern in Korea, November 2021. J Korean Med Sci. 2021;36:e346. https://doi.org/10.3346/jkms.2021.36.e346
10. Yang B, Tsang TK, Gao H, Lau EH, Lin Y, Ho F, et al. Universal community nucleic acid testing for COVID-19 in Hong Kong reveals insights into transmission dynamics: a cross-sectional and modelling study. Clin Infect Dis. 2021 Oct 28 [Epub ahead of print].
11. Handel A, Longini IM Jr, Antia R. What is the best control strategy for multiple infectious disease outbreaks? Proc Biol Sci. 2007;274:833–7. https://doi.org/10.1098/rspb.2006.0015
12. Wolter N, Jassat W, Walaza S, Welch R, Moultrie H, Groome M, et al. Early assessment of the clinical severity of the SARS-CoV-2 omicron variant in South Africa: a data linkage study. Lancet. 2022;399:437–46. https://doi.org/10.1016/S0140-6736(22)00017-4
13. Dinh A, Dahmane L, Dahoumane M, Masingue X, Jourdain P, Lescure F-X. Impact of Omicron surge in community setting in greater Paris area. Clin Microbiol Infect. 2022;28:897–9.
14. Nyberg T, Ferguson NM, Nash SG, Webster HH, Flaxman S, Andrews N, et al. Comparative analysis of the risks of hospitalisation and death associated with SARS-CoV-2 Omicron (B. 1.1. 529) and Delta (B. 1.617. 2) variants in England: a cohort study. Lancet. 2022;399:1303–12.
15. Xiao J, Cheung JK, Wu P, Ni MY, Cowling BJ, Liao Q. Temporal changes in factors associated with COVID-19 vaccine hesitancy and uptake among adults in Hong Kong: serial cross-sectional surveys. Lancet Reg Health West Pac. 2022;23:100441. https://doi.org/10.1016/j.lanwpc.2022.100441

Address for correspondence: Peng Wu, School of Public Health, Li Ka Shing Faculty of Medicine, The University of Hong Kong, 7 Sassoon Rd, Pokfulam, Hong Kong, China; email: pengwu@hku.hk

Longitudinal SARS-CoV-2 Nucleocapsid Antibody Kinetics, Seroreversion, and Implications for Seroepidemiologic Studies

Michael Loesche,[1] Elizabeth W. Karlson,[1] Opeyemi Talabi, Guohai Zhou, Natalie Boutin, Rachel Atchley, Gideon Loevinsohn, Jun Bai Park Chang, Mohammad A. Hasdianda, Adetoun Okenla, Elizabeth Sampson, Haley Schram, Karen Magsipoc, Kirsten Goodman, Lauren Donahue, Maureen MacGowan, Lewis A. Novack, Petr Jarolim, Lindsey R. Baden,[2] Eric J. Nilles[2]

Given widespread use of spike antibody in generating coronavirus disease vaccines, SARS-CoV-2 nucleocapsid antibodies are increasingly used to indicate previous infection in serologic surveys. However, longitudinal kinetics and seroreversion are poorly defined. We found substantial seroreversion of nucleocapsid total immunoglobulin, underscoring the need to account for seroreversion in seroepidemiologic studies.

Estimating the incidence of infections caused by SARS-CoV-2 that are frequently asymptomatic is challenging when using routine passive surveillance methods. Antibodies can provide a record of previous infection, whether symptomatic or asymptomatic, and serologic surveys that measure antibodies across populations are routinely used for a variety of pathogens and are believed to provide key insights into the epidemiology and transmission of SARS-CoV-2 (*1*–*3*). However, antibody contraction and seroreversion (loss of previously documented antibodies) may lead to false-negative results, a potential issue as we move into the third year of the SARS-CoV-2 pandemic (*4*). Seroepidemiologic studies can adjust for seroreversion when kinetics are well characterized, but limited data are available from >1 year after infection. To characterize seroreversion and ease interpretation of seroepidemiologic studies, we measured SARS-CoV-2 nucleocapsid antibodies, a marker of previous infection even among populations vaccinated with spike-based COVID-19 vaccines, in a longitudinal study of healthcare workers in the United States.

The Study

The Mass General Brigham Institutional Review Board approved the study protocol (2020P000849). Participants provided written consent to participate in the study.

During April 28–September 30, 2020, a total of 2,358 employees of the Brigham and Women's Hospital (Boston, MA, USA) were enrolled in a longitudinal SARS-CoV-2 cohort study. Blood samples were collected at baseline, monthly for 3 months, and then every 3 months through February 2022, up to 21 months after enrollment. Sociodemographic characteristics (Appendix, https://wwwnc.cdc.gov/EID/article/28/9/22-0729-App1.pdf) were collected on electronic questionnaires.

We tested serum samples by using the Diagnostics Elecsys SARS-CoV-2 N Immunoassay (Roche, https://www.roche.com), a double-antigen sandwich electrochemiluminescence total immunoglobulin immunoassay that detects antibodies against viral nucleocapsid protein. We performed assays based on a cutoff index (≥1.0) defined according

Author affiliations: Brigham and Womens Hospital, Boston, Massachusetts, USA (M. Loesche, E.W. Karlson, O. Talabi, G. Zhou, N. Boutin, R. Atchley, G. Loevinsohn, J.B.P. Chang, M.A. Hasdianda, A. Okenla, E. Sampson, H. Schram, K. Magsipoc, K. Goodman, L. Donahue, M. MacGowan, L.A. Novak, P. Jarolim, L.R. Baden, E.J. Nilles); Massachusetts General Hospital, Boston (M. Loesche, G. Loevinsohn); Harvard Medical School, Boston (E.W. Karlson, G. Zhou, M.A. Hasdianda, P. Jarolim, L.R. Baden, E.J. Nilles); Harvard Humanitarian Initiative, Cambridge, Massachusetts, USA (E.J. Nilles)

DOI: https://doi.org/10.3201/eid2809.220729

[1]These first authors contributed equally to this article.

[2]These senior authors contributed equally to this article.

to manufacturer's guidance. An independent in-house assay performance study that included 832 prepandemic negative controls and 251 PCR-positive samples showed a specificity of 99.6% (95% CI 98.9%–100%) and a sensitivity of 90.8% (95% CI 81.3%–95.7%) for samples collected >14 (range 15–68) days after symptom onset (*5*).

We extracted SARS-CoV-2 PCR test results and dates from the Brigham Health electronic medical record. PCR-positive date was defined as the date of the first registered SARS-CoV-2 PCR-positive test result. For 4 employees who had a positive SARS-CoV-2 PCR test result outside the Brigham Health system, the date of the COVID-19–positive result, generated for all SARS-CoV-2–positive employees in the Brigham Health electronic medical record, was used as the PCR-positive date. To assess antibody kinetics, we used a generalized additive mixed-effect model (GAMM) with the natural logarithm of antibody levels modeled as a function of time from first positive PCR test result. To estimate the half-life, we used a linear mixed-effects model (LMM) and assumed constant exponential decay after the peak level (Appendix).

A total of 125 (5.3%) of 2,358 study participants enrolled in the healthcare worker cohort study were positive for nucleocapsid antibodies during April 2020–January 2021, during predominantly wild-type SARS-CoV-2 circulation (*6*). Of these participants, 110 (88%) had ≥1 samples collected after an index seropositive sample and were included in the analyses. A total of 687 unique samples were collected from the 110 participants (mean 6.3 samples/participant). The median age of participants was 33 (range 20–71) years; 94 (86%) were female, 97 (88%) White, and 6 (5%) Hispanic. The median body mass index was 24 kg/mm^2 (range 19–42 kg/mm^2).

A total of 74 (67%) of 110 participants had a positive SARS-CoV-2 RT-PCR test in the Mass General Brigham electronic health record before the first seropositive sample; 96% were symptomatic (Appendix) and 1 required hospitalization. Symptomatic status was not assessed for study participants who did not have a positive PCR test result because timing of infections was unknown.

The mean peak cutoff index level for nucleocapsid antibodies among PCR-positive participants was 37 (95% CI 27–50) and occurred 72 days after the index PCR-positive test result (Figure 1). Assuming constant linear antibody contraction with the LMM approach, antibody half-life was estimated at 128 (95% CI 114–146) days and mean time to seroreversion as 737 (95% CI 680–793) days. Antibody contraction and seroreversion kinetics diverged between the LMM and GAMM models; the nonlinear GAMM model suggested more rapid contraction up to 1 year postinfection, followed by slower contraction and seroreversion thereafter (Table; Figures 1, 2). We observed a stepwise but nonsignificant trend toward a slower relative decrease in concentration of nucleocapsid antibodies among older age groups but not across body mass index or sex (Appendix).

Conclusions

We report on the kinetics of SARS-CoV-2 nucleocapsid antibodies (total immunoglobulin) up to 21 months after infection and estimate peak antibody

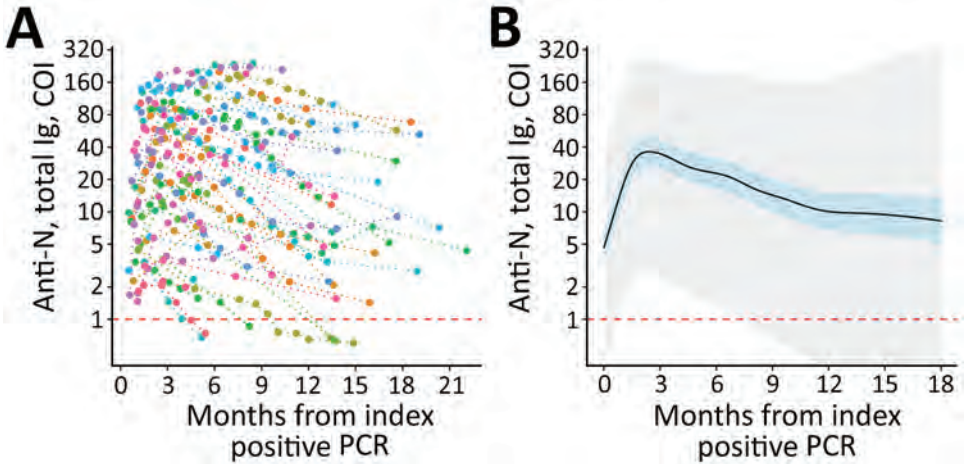

Figure 1. Longitudinal SARS-CoV-2 anti-N total immunoglobulin kinetics among SARS-CoV-2 PCR-positive participants in a study of healthcare workers in Boston, Massachusetts, USA, 2020). A) Individual study participant (n = 74) total anti-N levels from time of index PCR-positive test result. Individual levels are indicated by colored points connected by a dotted line. B) Fitted generalized additive mixed-effect model depicting estimate (solid black line), 95% CI (blue shaded area), and 95% prediction interval (gray shaded area). Estimates are truncated at 18 months given sparsity of later data points. Horizontal dashed red lines indicate the COI for seropositive (above) and seronegative (below) results. The lower limits of detection (COI 0.07) are outside the figure frame. Anti-N, nucleocapsid antibodies; COI, cutoff index.

levels, kinetics, and rates of seroreversion by using 2 modeling methods. Both models suggest substantial seroreversion by 18 months postinfection, and half-life–based estimates suggest seroreversion of ≈50% at 2 years.

Half-life–based approaches that assume constant exponential contraction might underestimate seroreversion through the first year postinfection and overestimate seroreversion at later timepoints (Table). Using a GAMM model that tolerates variable antibody contraction over time, we estimated that seroreversion was 1.4%/month during 4–12 months after infection, but 95% CIs were wide. Assuming contraction remains relatively constant after an initial rapid decrease, an assumption supported by previous studies on SARS-CoV-2 and other common human coronaviruses (*4*), seroreversion would be 19% at 2 years and 35% at 4 years.

These findings suggested that serologic surveys conducted >1 year after widespread SARS-CoV-2 transmission will be markedly affected by seroreversion. The total immunoglobulin immunoassay used for this study shows more durable detection of nucleocapsid antibodies than other formats, particularly single isotope assays, and rates of seroreversion might be higher across other assay designs (*5*,*7*). Total immunoglobulin immunoassays specific for spike antibodies versus nucleocapsid antibodies appear to provide improved durability of antibody detection, and single isotype antispike assays provide similar or lower durability than total nucleocapsid immunoglobulin assays (*7*). However, given the widespread use of spike-based COVID-19 vaccines, the utility of spike antibodies for detection of previous infection in population-level surveys is limited.

Table. SARS-CoV-2 nucleocapsid total immunoglobulin seroreversion by GAMM and half-life methods, by months from infection, among healthcare workers in Boston, Massachusetts, USA, 2020*

Months	GAMM, % (95% CI)	Half-life, % (95% CI)
4	0 (0–4.9)	0.6 (0.6–0.6)
6	2.7 (3.0–9.5)	1.2 (1.0–1.3)
8	5.5 (1.5–13.4)	2.1 (1.8–2.6)
10	9.6 (3.9–18.8)	3.8 (2.9- 4.8)
12	11 (4.9–20.5)	6.2 (4.7–8.3)
14	12.3 (5.8–22.1)	9.8 (7.2–13.3)
16	13.7 (6.8–23.8)	14.8 (10.6–20.1)
18	15.1 (7.8–25.4)	21.1 (15.0–28.7)
24	NC	48.9 (36.1–62.1)

*The GAMM method estimates are restricted to observational data and therefore not calculated more than 18 months postinfection. Half-life method represents constant log linear antibody contraction with an estimated peak total nucleocapsid antibody level that had a cutoff index of 37 and a half-life of 128 days. GAMM, generalized additive mixed model; NC, not calculated.

This study has several strengths, including a mean of 6.3 unique sample time points/participant that enables more precise demarcation of antibody dynamics and a long study interval that includes samples collected up to 21 months postinfection. However, our cohort was based in the United Sates, enrolled only adults, and overrepresented women and White participants. Therefore, our findings might not be generalizable. Peak antibody levels were estimated for PCR-positive persons; lower peak levels might be observed among seropositive persons who do not provide a PCR-positive test result, which would cause more rapid seroreversion than that we report. Data points >18 months

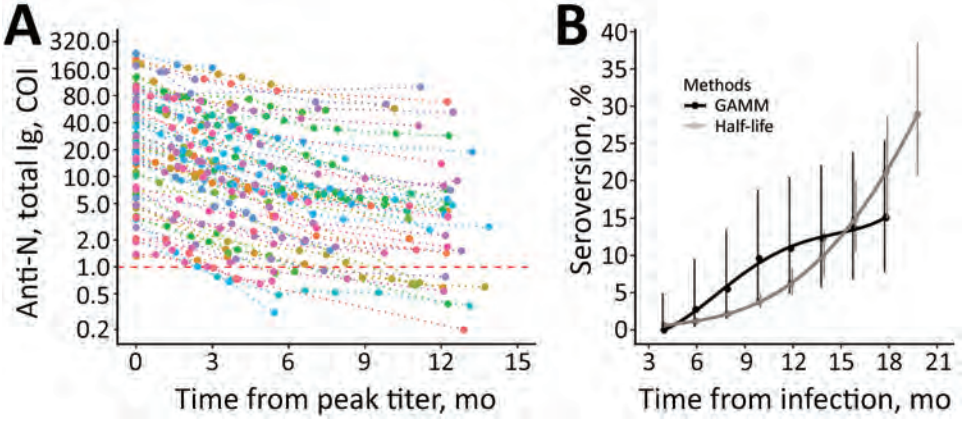

Figure 2. Longitudinal SARS-CoV-2 total anti-N immunoglobulin contraction and estimated seroreversion over time in a study of healthcare workers in Boston, Massachusetts, USA, 2020. A) Consistency in contraction of individual-level total anti-N immunoglobulin levels over time when indexed against participants' highest recorded sample value. Includes seropositive participants with and without registered SARS-CoV-2 PCR-positive test results and with ≥1 sampling time points after peak level (n = 90). Individual levels are indicated by colored points connected by a dotted line. Horizontal dashed red line indicates the cutoff index for seropositive (above) and seronegative (below) results. The lower limit of detection (COI 0.07) is outside the figure frame. B) Points indicating estimated rates of seroreversion from total anti-N immunoglobulin seropositive to seronegative by 2-month intervals. The half-life estimate is based on peak total anti-N immunoglobulin level of 37 COI and half-life of 128 days. Solid lines indicate quadratic polynomial trend; error bars indicate 95% CIs. Anti-N, nucleocapsid antibodies; COI, cutoff index; GAMM, generalized additive mixed-effect model.

postinfection are sparse, and antibody dynamics might differ outside our measurement window. Infections accrued during wild-type predominance, in the prevaccination setting, are assumed to reflect a single infection. Antibody kinetics might differ for infections caused by other SARS-CoV-2 strains or after vaccine breakthrough or repeat infections (H.J. Whitaker et al., unpub. data, https://www.medrxiv.org/content/10.1101/2021.10.25.21264964v1.full-text; D. Follman et al., unpub. data, https://www.medrxiv.org/content/10.1101/2022.04.18.22271936v1.full).

In summary, antibody seroreversion and the global rollout of vaccines are increasingly useful considerations when planning and interpreting SARS-CoV-2 seroepidemiologic studies. Immunoassays targeting the nucleocapsid protein can detect previous infection among populations vaccinated with spike protein vaccines, but antibody contraction and seroreversion are likely to be substantial as we move into the third year of the pandemic. By characterizing seroreversion after SARS-CoV-2 infection, this study provides provisional format-specific considerations for interpreting and adjusting estimates of previous infection for seroepidemiologic purposes.

Acknowledgments

We thank all Brigham Health cohort study participants for their commitment and time.

About the Author

Dr. Loesche is an emergency medicine resident at Brigham and Womens Hospital and Massachusetts General Hospital, Boston, MA. His primary research interests are microbiology, epidemiology, and bioinformatics.

References

1. Kleynhans J, Tempia S, Wolter N, von Gottberg A, Bhiman JN, Buys A, et al.; PHIRST-C Group. SARS-CoV-2 seroprevalence in a rural and urban household cohort during first and second waves of infections, South Africa, July 2020–March 2021. Emerg Infect Dis. 2021;27:3020–9. https://doi.org/10.3201/eid2712.211465
2. O'Driscoll M, Ribeiro Dos Santos G, Wang L, Cummings DA, Azman AS, Paireau J, et al. Age-specific mortality and immunity patterns of SARS-CoV-2. Nature. 2021;590:140–5. https://doi.org/10.1038/s41586-020-2918-0
3. Clarke KE, Jones JM, Deng Y, Nycz E, Lee A, Iachan R, et al. Seroprevalence of infection-induced SARS-CoV-2 antibodies—United States, September 2021–February 2022. MMWR Morb Mortal Wkly Rep. 2022;71:606–8. https://doi.org/10.15585/mmwr.mm7117e3
4. Harris RJ, Whitaker HJ, Andrews NJ, Aiano F, Amin-Chowdhury Z, Flood J, et al. Serological surveillance of SARS-CoV-2: six-month trends and antibody response in a cohort of public health workers. J Infect. 2021;82:162–9. https://doi.org/10.1016/j.jinf.2021.03.015
5. Nilles EJ, Karlson EW, Norman M, Gilboa T, Fischinger S, Atyeo C, et al. Evaluation of three commercial and two non-commercial immunoassays for the detection of prior infection to SARS-CoV-2. J Appl Lab Med. 2021;6:1561–70. https://doi.org/10.1093/jalm/jfab072
6. Brown C, Doucette M, Fink T, Gallagher G, Lang A, Madoff L, et al. Detection of a large cluster and multiple introductions of the P.1 SARS-CoV-2 variant of concern in Massachusetts: SARS-CoV-2 coronavirus/nCoV-2019 genomic epidemiology, virological, 2021 [cited 2022 Jun 9]. https://virological.org/t/detection-of-a-large-cluster-and-multiple-introductions-of-the-p-1-sars-cov-2-variant-of-concern-in-massachusetts/671
7. Stone M, Grebe E, Sulaeman H, Di Germanio C, Dave H, Kelly K, et al. Evaluation of commercially available high-troughput SARS-CoV-2 serologic assays for serosurveillance and related applications. Emerg Infect Dis. 2022;28:672–83. https://doi.org/10.3201/eid2803.211885

Address for correspondence: Eric J. Nilles, Brigham and Womens Hospital, 75 Francis St, Boston, MA 02115, USA; email: enilles@bwh.harvard.edu

Creutzfeldt-Jakob Disease Incidence, South Korea, 2001–2019

Yong-Chan Kim, Byung-Hoon Jeong

We found increasing trends of Creutzfeldt-Jakob disease (CJD) cases and annual incidence in South Korea during 2001–2019. We noted relatively low (5.7%) distribution of familial CJD. An unusually high percentage (≈1%) of patients were in the 30–39 age group, which should prompt a preemptive CJD control system.

Prion diseases are fatal, irreversible, and transmissible brain proteinopathies caused by abnormal aggregated prion protein (PrP^{Sc}) converted from normal prion protein (PrP^{C}), which is encoded by the prion protein gene (*PRNP*) (*1*–*3*). The major type of human prion disease is Creutzfeldt-Jakob disease (CJD), and several countries have reported increasing trends in CJD cases and incidence (*4*).

CJD is subdivided into 3 types: sporadic, familial, and iatrogenic (*5*–*7*). The most common type is sporadic CJD, which accounts for >85% of all CJD cases. Familial CJD accounts for 10%–15% of all cases and is caused by germline mutations of the human *PRNP* gene, including D178N-M129V, V180I, E200K, V203I, and M232R. Iatrogenic CJD accounts for <1% of all CJD cases and includes variant CJD, which is caused by ingestion of beef products from bovine spongiform encephalopathy–affected cattle (*7*–*9*).

In South Korea, the Korea Centers for Disease Control and Prevention (KCDC) has operated the CJD surveillance system and issued epidemiologic reports since 2001. In addition, except for variant CJD, the surveillance system has reported all 3 types of CJD. Furthermore, CJD has been reported annually and has exhibited increasing trends in case numbers. However, no long-term estimation of the various characteristics of CJD patients, including onset age, sex, germline mutations of familial CJD, or overall CJD incidence are available for South Korea. We conducted a study on CJD cases in South Korea from 2001–2019 to assess case count and incidence trends.

Authors affiliation: Jeonbuk National University, Jeonju, South Korea

DOI: https://doi.org/10.3201/eid2809.212050

The Study

We collected data on CJD patients from Statistics Korea (KOSTAT) (https://kostat.go.kr) and epidemiologic reports issued by the KCDC (https://www.kdca.go.kr). We analyzed the characteristics of CJD patients in South Korea. In addition, we obtained the global incidence of sporadic CJD from previous studies and compared these with the incidence in South Korea (*4*).

CJD diagnosis was performed according to guidelines from the World Health Organization in South Korea (*10*). During 2001–November 2010, CJD was controlled through a sample monitoring system centered in medical institutions in the country and KCDC collected the CJD-related data. Beginning December 2010, CJD was designated as a statutory infectious disease, and KCDC conducts a complete epidemiologic investigation and monitors suspected patients. CJD death rates in South Korea have not been available.

The number of possible, probable, and definite CJD diagnoses was not available during 2001–2015. Among all cases during 2016–2019, KCDC reported 6 (3.2%) possible CJD cases, 179 (95.2%) probable cases, and 3 (1.6%) definite cases. Genetic testing was performed on all patients with diagnosed CJD.

We obtained population data stratified by age, region, sex, and year from KOSTAT. We used χ^2 test to determine statistically significant differences and performed calculations in SAS version 9.4 (SAS Institute Inc., https://www.sas.com).

During 2001–2019, a total of 579 CJD cases were reported in South Korea (Table). Of note, the annual number of cases and CJD incidence in South Korea exhibited an upward trend (Figure 1, Table). Among 579 cases, 545 (94.13%) were sporadic, 33 (5.7%) were familial, and 1 (0.17%) was iatrogenic. Variant CJD was not reported in Korea during 2001–2019 (Table). During 2008–2019, a total of 31 familial CJD cases were reported, as were 5 types of germline mutations of the *PRNP* gene, including D178N-M129V, V180I, E200K, V203I and M232R (Appendix Table 1,

Table. Annual cases and incidence of CJD, Korea, 2001–2019*

Year	Patients, no. (%)	Sex, no. (%)		p value	Subtypes, no. (%)				Total population	Incidence‡
		M	F		Sporadic	Iatrogenic†	Variant	Familial		
2001	5 (0.86)	2 (40)	3 (60)	0.7498	5 (100)	0	0	0	47,370,164	0.11
2002	9 (1.55)	5 (55.56)	4 (44.44)	0.6162	9 (100)	0	0	0	47,644,736	0.19
2003	19 (3.28)	7 (36.84)	12 (63.16)	0.3756	19 (100)	0	0	0	47,892,330	0.40
2004	13 (2.25)	8 (61.54)	5 (38.46)	0.3042	12 (92.31)	0	0	1 (7.69)	48,082,519	0.27
2005	15 (2.59)	7 (46.67)	8 (53.33)	0.9705	14 (93.33)	0	0	1 (6.67)	48,184,561	0.31
2006	19 (3.28)	11 (57.89)	8 (42.11)	0.3561	19 (100)	0	0	0	48,438,292	0.39
2007	18 (3.11)	13 (72.22)	5 (27.78)	**0.0360**	18 (100)	0	0	0	48,683,638	0.37
2008	28 (4.84)	15 (53.57)	13 (46.43)	0.5063	25 (89.29)	0	0	3 (10.71)	49,054,708	0.57
2009	30 (5.18)	13 (43.33)	17 (56.67)	0.6829	29 (96.67)	0	0	1 (3.33)	49,307,835	0.61
2010	29 (5.01)	14 (48.28)	15 (51.72)	0.9057	28 (96.55)	1 (3.45)	0	0	49,554,112	0.59
2011	29 (5.01)	15 (51.72)	14 (48.28)	0.6302	26 (89.66)	0	0	3 (10.34)	49,936,638	0.58
2012	45 (7.77)	23 (51.11)	22 (48.89)	0.6083	42 (93.33)	0	0	3 (6.67)	50,199,853	0.90
2013	34 (5.87)	13 (38.24)	21 (61.76)	0.3112	31 (91.18)	0	0	3 (8.82)	50,428,893	0.67
2014	65 (11.23)	31 (47.69)	34 (52.31)	0.9338	62 (95.38)	0	0	3 (4.62)	50,746,659	1.28
2015	33 (5.70)	17 (51.52)	16 (48.48)	0.6252	33 (100)	0	0	0	51,014,947	0.65
2016	43 (7.43)	16 (37.21)	27 (62.79)	0.2073	173 (92.02)§	0	0	15 (7.98)	51,217,803	0.84
2017	38 (6.56)	13 (34.21)	25 (65.79)	0.1213	NA	NA	NA	NA	51,361,911	0.74
2018	54 (9.33)	26 (48.15)	28 (51.85)	0.8883	NA	NA	NA	NA	51,606,633	1.05
2019	53 (9.15)	24 (45.28)	29 (54.72)	0.7943	NA	NA	NA	NA	51,709,098	1.02
Total	579 (100)	273 (47.15)	306 (52.85)	NA	545 (94.13)	1 (0.17)	0	33 (5.70)	NA	NA

*CJD includes possible, probable, and definite CJD diagnoses. Bold indicates statistical significance (p<0.05). CJD, Creutzfeldt-Jakob disease; NA, not applicable.
†The source of transmission for the iatrogenic CJD case is dura mater graft.
‡Cases per 1 million population.
§Reported cases and subtypes of CJD in South Korea, 2016–2019.

Figure 1, https://wwwnc.cdc.gov/EID/article/28/9/21-2050-App1.pdf).

During 2011–2019, a total of 394 cases of CJD were reported in South Korea; 162 (41.12%) among persons ≥70 years of age, 129 (32.74%) among persons 60–69 years of age, 75 (19.04%) among persons 50–59 years of age, 23 (5.84%) among persons 40–49 years of age, and 5 (1.27%) among persons 30–39 years of age (Appendix Table 2, Figure 2). Of note, the distribution of CJD cases by age in South Korea was significantly different in 2011 compared with 2011–2019 (p<0.05). In particular, the distribution of CJD in the 40–49 year age group in 2011 (17.24%) was ≈2.9 times higher than that of the 40–49 age group during 2011–2019 (5.84%).

Overall, Gyeonggi Province had the highest number of CJD cases (88, 22.34%), along with the cities of Seoul (83 cases, 21.07%), Busan (25 cases, 6.35%), and Daegu (25 cases, 6.35%). Sejong (2 cases, 0.51%) and Jeju (2 cases, 0.51%) had the fewest CJD cases, and Ulsan (7 cases, 1.78%) and Gwanju (8 cases, 2.03%) also had fewer cases than other cities (Appendix Table 3). Chungnam Province had the highest CJD incidence (1.21 cases per million population), along with the cities of Sejong (1.19 cases per million population) and Daegu (1.13 cases per million population). The city of Jeju had the lowest CJD incidence (0.37 cases per million population), and Gwangju (0.59 cases per million population) and Incheon (0.62 cases per million population) also had low incidence (Figure 2, panel A).

We compared the incidence of sporadic CJD in South Korea with the global incidence. Switzerland had the highest incidence (1.73 cases per million

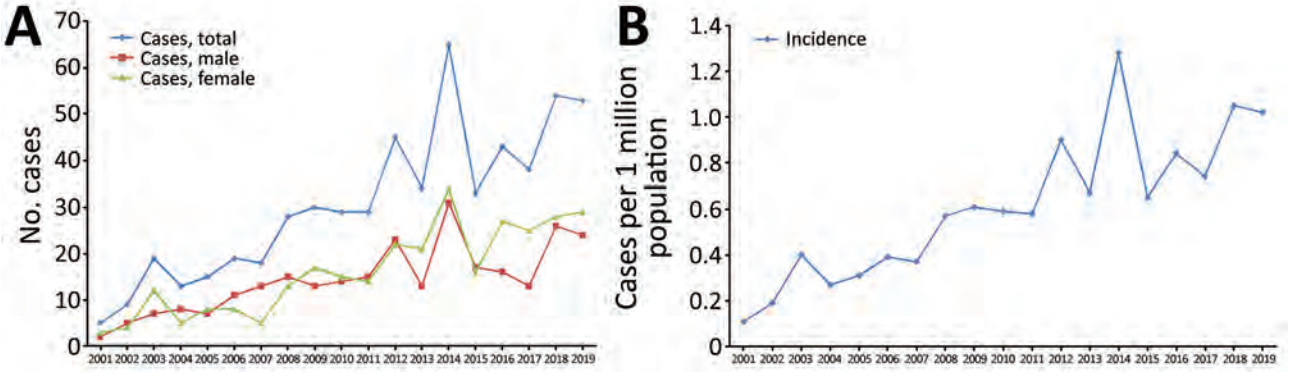

Figure 1. Annual incidence of Creutzfeldt-Jakob disease, South Korea, 2001–2019. A) Total number of reported cases per year and sex. B) Annual incidence per million population.

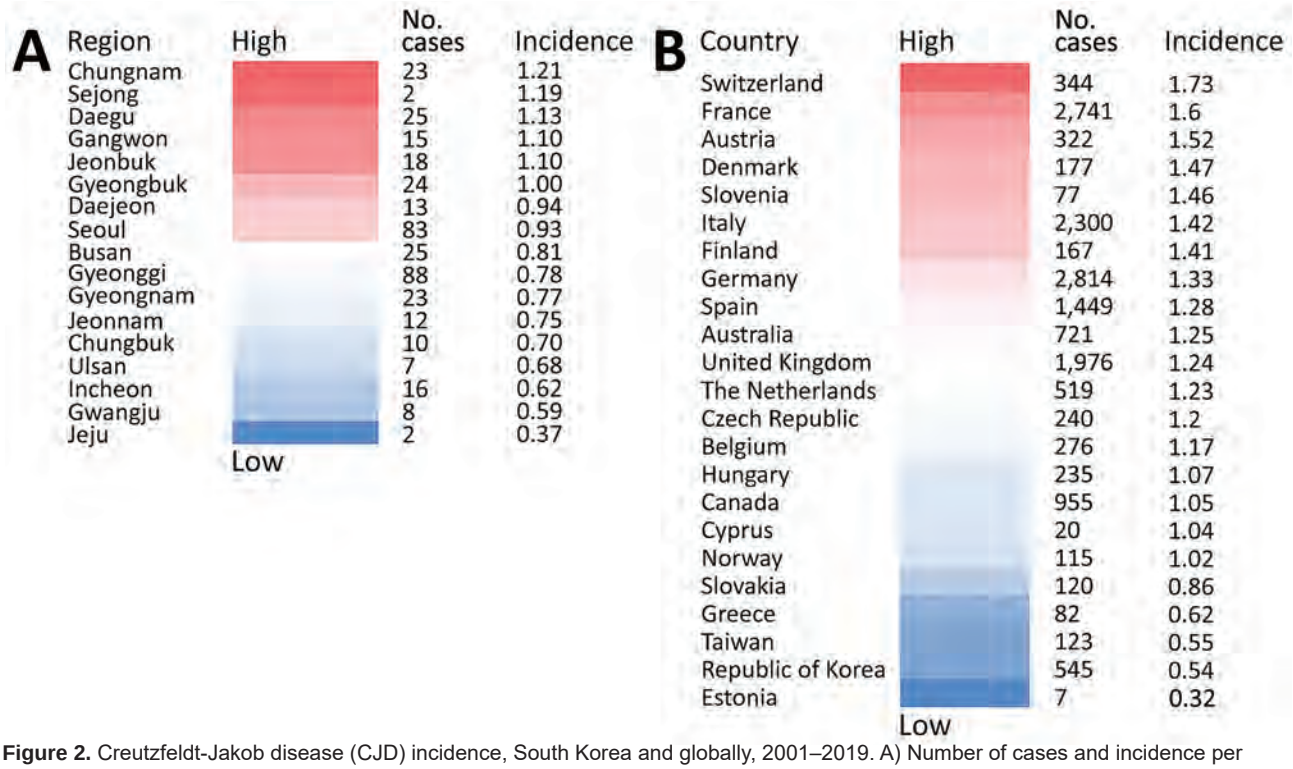

Figure 2. Creutzfeldt-Jakob disease (CJD) incidence, South Korea and globally, 2001–2019. A) Number of cases and incidence per million persons in cities and provinces of South Korea, including probable, possible, and definite CJD diagnoses. B) Global number of sporadic CJD cases and incidence per million population by country (*4*). Sporadic CJD incidence for South Korea is from this study.

population), but incidence was also high in France (1.6 cases per million population) and Austria (1.52 cases per million population). Estonia had the lowest incidence of sporadic CJD at 0.32 cases per million population. By comparison, incidence of sporadic CJD in South Korea was extremely low, 0.54 cases per million population (Figure 2, panel B).

Conclusions

In this study, we found increasing trends in CJD rates in South Korea during 2001–2019. These increasing trends might be the result of advanced diagnostic technology and capacity, more neurologic specialists, an increase in the average age of the population, or a combination of these factors. In addition, designation of CJD as a statutory infectious disease might have affected increased reporting. Nonetheless, further research could investigate the CJD incidence trend through the country's high-level surveillance system.

In addition, we observed that ≈1% of CJD patients in South Korea were in the 30–39-year age group (Appendix Figure 2). Because the average age of onset of familial CJD is over 50, younger CJD patients in the 30–39-year age group are extremely unusual (*11*,*12*). However, the exact subtypes of CJD (sporadic or variant) for each CJD patient in this age group were not available. Previous studies have reported variant CJD occurring at a relatively younger age than familial and sporadic CJD (*7*–*9*). Thus, further in-depth investigation of the subtypes of CJD among younger age groups is essential to determine causes of CJD in this age group and devise prevention strategies.

In conclusion, we identified increasing trends of CJD cases and incidence in South Korea during 2001–2019. We investigated CJD cases by subtype and found a relatively low (5.7%) distribution of familial CJD. Of note, sporadic CJD incidence was only 0.54 cases per million persons. In addition, we investigated the distribution of CJD patients by sex, age group, and region and found the highest incidence in the Chungnam region. A comprehensive long-term investigation could shed light on the characteristics of CJD in South Korea and help KCDC construct a preemptive control system.

Acknowledgments

This work was supported by the National Research Foundation of Korea (NRF) through a grant funded by the Korea government (grant no. 2021R1A2C1013213); NRF grant NRF-2019-Fostering Core Leaders of the Future Basic Science Program/Global Ph.D. Fellowship

Program); and the Basic Science Research Program through NRF funded by the Ministry of Education (grant nos. 2017R1A6A1A03015876, 2021R1A6A3A010864, 2022R1C1C2004792). Y.-C.K. was supported by the BK21 Plus Program in the Department of Bioactive Material Sciences, Jeonbuk National University.

About the Authors

Dr. Kim is research professor in the Korea Zoonosis Research Institute, Jeonbuk National University, Jeonbuk, South Korea. His research interests include prion diseases.

Dr. Jeong is associate professor in the Korea Zoonosis Research Institute, Jeonbuk National University. His research interests include prion diseases.

References

1. Prusiner SB. The prion diseases. Brain Pathol. 1998;8:499–513. https://doi.org/10.1111/j.1750-3639.1998.tb00171.x
2. Prusiner SB. Prions. Proc Natl Acad Sci U S A. 1998;95:13363–83. https://doi.org/10.1073/pnas.95.23.13363
3. Kim YC, Won SY, Jeong BH. Altered expression of glymphatic system-related proteins in prion diseases: implications for the role of the glymphatic system in prion diseases. Cell Mol Immunol. 2021;18:2281–3. https://doi.org/10.1038/s41423-021-00747-z
4. Uttley L, Carroll C, Wong R, Hilton DA, Stevenson M. Creutzfeldt-Jakob disease: a systematic review of global incidence, prevalence, infectivity, and incubation. Lancet Infect Dis. 2020;20:e2–10. https://doi.org/10.1016/S1473-3099(19)30615-2
5. Asante EA, Linehan JM, Desbruslais M, Joiner S, Gowland I, Wood AL, et al. BSE prions propagate as either variant CJD-like or sporadic CJD-like prion strains in transgenic mice expressing human prion protein. EMBO J. 2002;21:6358–66. https://doi.org/10.1093/emboj/cdf653
6. Mastrianni JA. The genetics of prion diseases. Genet Med.|2010;12:187–95. https://doi.org/10.1097/GIM.0b013e3181cd7374
7. Collinge J, Palmer MS, Dryden AJ. Genetic predisposition to iatrogenic Creutzfeldt-Jakob disease. Lancet. 1991;337:1441–2. https://doi.org/10.1016/0140-6736(91)93128-V
8. Kovács GG, Puopolo M, Ladogana A, Pocchiari M, Budka H, van Duijn C, et al.; EUROCJD. Genetic prion disease: the EUROCJD experience. Hum Genet. 2005;118:|166–74. https://doi.org/10.1007/s00439-005-0020-1
9. Jeong BH, Kim YS. Genetic studies in human prion diseases. J Korean Med Sci. 2014;29:623–32. https://doi.org/10.3346/jkms.2014.29.5.623
10. World Health Organization. WHO infection control guidelines for transmissible spongiform encephalopathies. Geneva: The Organization; 2000.
11. Chandra S, Mahadevan A, Shankar SK. Familial CJD—brief commentary. Ann Indian Acad Neurol. 2019;22:462–3.
12. Arata H, Takashima H. Familial prion disease (GSS, familial CJD, FFI). Nihon Rinsho. 2007;65:1433–7.

Address for correspondence: Byung-Hoon Jeong, Korea Zoonosis Research Institute, Jeonbuk National University, 820-120 Hana-ro, Iksan, Jeonbuk, South Korea; email: bhjeong@jbnu.ac.kr

Zoonotic *Ancylostoma ceylanicum* Hookworm Infections, Ecuador

William J. Sears,[1] Jorge Cardenas,[1] Joseph Kubofcik, Thomas B. Nutman, Philip J. Cooper

Ancylostoma ceylanicum hookworms are zoonotic parasites that can infect humans. To detect autochthonous transmission, we analyzed human fecal samples collected in 2000. Multiparallel quantitative PCR detected infection in persons who had never traveled outside Ecuador. These data indicate human transmission of *A. ceylanicum* in the Americas, although endemicity remains unknown.

Ancylostoma ceylanicum hookworms can infect humans and have been increasingly recognized as endemic among humans living or traveling to the Asia–Pacific region (*1*). Although *A. ceylanicum* hookworms are known to infect dogs and cats globally, locally acquired human infections have not been reported by persons who have never traveled outside of North or South America. Previous evidence for the potential presence of *A. ceylanicum* hookworms in humans in the Americas is derived from 3 observations: 1) a 1922 autopsy study from northern Brazil identified zoonotic *Ancylostoma* spp. adult hookworms in human intestines when morphologic differentiation of *A. ceylanicum* from *A. braziliense* was still a matter of debate (*2*); 2) a molecular analysis of fecal samples from patients at hospitals in France identified *A. ceylanicum* hookworms in 2 samples, one in a migrant from Colombia and the other in a traveler returning from French Guiana (*3*); and 3) diffuse subacute unilateral neuroretinitis in a child adopted from Colombia and living in Germany was molecularly identified as *A. ceylanicum* infection (*4*). One report describes *A. ceylanicum* identified morphologically in domestic animal populations in South America that originated in Surinam, but no molecular methods were used (*5*).

Author affiliations: National Institutes of Health, Bethesda, Maryland, USA (W.J. Sears, J. Kubofcik, T.B. Nutman); University of Miami Miller School of Medicine, Miami, Florida, USA (J. Cardenas); Fundación Ecuatoriana Para Investigación en Salud, Quito, Ecuador (P.J. Cooper); Universidad Internacional del Ecuador, Quito (P.J. Cooper); St George's University of London, London, UK (P.J. Cooper)

DOI: https://doi.org/10.3201/eid2809.220248

Such reports, although suggestive, do not provide definitive evidence for autochthonous transmission of *A. ceylanicum* hookworms to humans in the Americas. We used molecular methods to identify autochthonous infections with *A. ceylanicum* in humans who had no history of travel outside Ecuador and who lived in a region of the country where soil-transmitted helminths are endemic. The study protocol was approved by the ethics committees of St George's Hospital Medical School, London, United Kingdom, and the Foundation Salud y Desarollo Andino, Quito, Ecuador. Informed written consent was obtained from adult participants or from the parents or legal representatives of child participants.

The Study

In 2000, we collected fecal samples from a convenience subsample of preschool children, schoolchildren, and daycare staff in a larger cross-sectional study of the relationship between soil-transmitted helminth infections and allergy among urban and rural populations living in the Provinces of Pichincha and Esmeraldas, Ecuador. The subsamples represented settings considered to be at high risk for helminth infection (*6*). (Appendix Figure 1, https://wwwnc.cdc.gov/EID/article/28/9/22-0248-App1.pdf). We analyzed single frozen samples from 230 participants with a median age of 9 years (mean age 11, range <1 to 63 years); 40.4% were male and 69.6% were living in an urban setting (town of San Lorenzo). None of the study participants had a history of travel outside Ecuador.

The samples were thawed and ≈250 mg was transferred into collection microtubes in a 96-well format (QIAGEN, https://www.qiagen.com). We performed initial sample lysis by using a TissueLyzer II bead mill (QIAGEN) with 5-mm stainless steel beads. We performed high-throughput DNA extraction on a QiaSymphony (QIAGEN) instrument by using a PowerFecal Pro Kit (QIAGEN), following the manufacturer's instructions with minor modifications (i.e., samples

[1]These authors contributed equally to this article.

were pretreated with only the proprietary buffer CD1, and steps involving pretreatment with buffer CD2 were omitted to expedite the high-throughput protocol). All samples were extracted after an internal control was added as reported previously (*7*).

We prepared high-throughput, multiparallel quantitative PCR (qPCR) reactions by using 3.5 µL of Taqman Fast Advanced Master Mix (QIAGEN), 2 µL water, and 1 µL of a PrimeTime qPCR Probe Assay (Integrated DNA Technologies, https://www.idtdna.com) with forward primer, reverse primer, and probe at a final reaction concentrations of 500 nmol/L, 500 nmol/L, and 250 nmol/L, respectively. A 96-well qPCR master plate was prepared for each respective target (*Ascaris lumbricoides/suum* [*8*], *A. ceylanicum* [*9*], *Strongyloides stercoralis* [*10*], *Trichuris trichiura* [*11*], *Necator americanus* [*11*], and *Ancylostoma duodenale* [*11*]), and 6.5 µL of the qPCR solution was transferred to a 384-well plate with a Beckman Coulter liquid handler (Beckman Coulter, https://www.beckmancoulter.com) and subsequently frozen at –80°C until use. After DNA elution, we used the liquid handler to transfer 2 µL of eluted DNA into a 384-well plate preloaded with the qPCR reagents. After brief centrifugation, the sample reactions were run on a ViiaA7 Real Time PCR System (Thermo Fisher Scientific, https://www.thermofisher.com). Genomic DNA or plasmids served as positive reaction controls.

We first amplified the hookworm internal transcribed spacer (ITS) 1, 5.8s, and ITS2 regions by using primers and cycling conditions as described previously (*12*). After PCR amplification, we prepared the amplicon library for sequencing by using the Nanopore Ligation Sequencing Kit (SQK-LSK109; Oxford Nanopore Technologies, https://nanoporetech.com) according to the manufacturer's instructions. The prepped library was loaded into an R9.4 flow cell and sequenced on a MinION device (Oxford Nanopore Technologies). We base called sequences by using Guppy Software, version 4.5.4 (Oxford Nanopore Technologies), and we determined consensus sequences by using NGSpeciesID with the following parameters: -ont -sample size 300 -m 330 -s 50 -consensus -medaka (*13*). We performed alignment to reference analysis by using Geneious Prime 2021.02 (Biomatters, Ltd, https://www.geneious.com). In addition, the cyclooxygenase 1 region was PCR amplified by using previously reported primers and then Sanger sequenced (Quintara Biosciences, https://quintarabio.com) (*14*). We produced a phylogenetic tree of ITS and *cox1* sequences by using the maximum-likelihood method performed in Geneious Prime 2021.02 with bootstrapping × 1,000 (*15*).

Of samples tested, hookworm infection was detected in 88 (38.3%) samples, of which 85 were infected with *N. americanus* (37.0%), 6 with *A. ceylanicum* (2.6%), and none with *A. duodenale* hookworms. Prevalence rates for other soil-transmitted helminth infections were *Ascaris lumbricoides* (63.9%) *T. trichiura* (69.7%), and *S. stercoralis* (15.2%). Cycle threshold values for *A. ceylanicum*–positive fecal samples detected by qPCR ranged from 25.2 to 37.6. We stratified distributions of sociodemographic factors and soil-transmitted helminth co-infections according to presence versus absence of *A. ceylanicum* or *N. americanus* hookworm infections (Table).

Table. Sociodemographic and soil-transmitted helminth co-infection characteristics of 230 persons for whom fecal samples were examined, Ecuador*

Variable	*Ancylostoma ceylanicum*		*Necator americanus*	
	Uninfected, n = 224	Infected, n = 6	Uninfected, n = 145	Infected, n = 85
Median age, y (range)	9 (<1–53)	4 (1–12)	10 (<1–63)	9 (<1–48)
Sex				
M, n = 93	89 (39.7)	4 (66.7)	54 (37.2)	46 (54.1)
F, n = 137	135 (60.3)	2 (33.3)	91 (62.8)	39 (45.9)
Residence				
Rural, n = 70	70 (31.2)	0	25 (17.2)	45 (52.9)
Urban, n = 160	154 (68.8)	6 (100)	120 (82.8)	40 (47.1)
STH co-infections				
Ascaris lumbricoides, n = 147	142 (63.4)	5 (83.3)	74 (51.0)	73 (85.8)
Trichuris trichiura, n = 160	154 (68.8)	6 (100)	94 (64.8)	66 (77.7)
Strongyloides stercoralis, n = 35	32 (14.3)	50.0 (3)	29 (20.0)	6 (7.1)
N. americanus, n = 85	82 (36.8)	50.0 (3)	NA	NA
A. ceylanicum, n = 6	NA	NA	3 (2.1)	6 (7.1)
No. co-infecting species				
0, n = 22	22 (9.8)	0	22 (15.2)	0
1, n = 62	62 (27.7)	0	59 (40.7)	3 (3.5)
≥2, n = 146	140 (62.5)	6 (100)	64 (44.1)	82 (96.5)

*Values are no. (%) except as indicated. Data are stratified according to presence versus absence of *A. ceylanicum* or *N. americanus* hookworm infections. STH, soil-transmitted infection; NA, not applicable.

We successfully performed hookworm ITS1, 5.8S, ITS2 PCR amplification and amplicon sequencing on 2 of 6 *A. ceylanicum*–positive samples. The consensus sequences (GenBank accession nos. ON773142, ON773142) obtained from these 2 samples were >99% identical to the corresponding unique *A. ceylanicum* sequence targeted by the qPCR (Appendix Figure 2). We prepared a phylogenetic tree comparing known ITS1 sequences of *A. ceylanicum*, *A. duodenale*, *Ancylostoma braziliense*, and *Ancylostoma caninum* hookworms, including the consensus sequences from these 2 positive samples (referred to as being from subjects A and B; Appendix Figure 3). We also compared the phylogeny of *cox1* gene sequences for *A. ceylanicum* hookworms from this study (*A. ceylanicum* accession nos. ON773158) with isolates of the parasite from Asia (Appendix Figure 4).

Conclusions

We identified *A. ceylanicum* hookworm infection in 6 study participants who lived in an urban setting in Esmeraldas Province and had not traveled outside of Ecuador. All infections were detected in children in a marginalized urban setting where overcrowding is typical and hygiene standards are poor. Although the study was limited by small sample size and geographic restriction, the data provide evidence for autochthonous transmission of *A. ceylanicum* hookworm to humans in the Americas.

Funding for this study was provided by the National Institute of Allergy and Infectious Diseases, National Institutes of Health, Bethesda, MD, USA, and Wellcome Trust, London, UK.

About the Author

Dr. Sears is an infectious disease physician-scientist in the Laboratory of Parasitic Disease at the US National Institute of Allergy and Infectious Disease, National Institutes of Health. His research interests include development of novel diagnostics and application of "omics" approaches to describe underlying mechanisms of parasitic phenomena.

References

1. Traub RJ, Zendejas-Heredia PA, Massetti L, Colella V. Zoonotic hookworms of dogs and cats - lessons from the past to inform current knowledge and future directions of research. Int J Parasitol. 2021;51:1233–41. https://doi.org/10.1016/j.ijpara.2021.10.005
2. Gordon RM. Ancylostomes recorded from sixty-seven post-mortems performed in Amazonas. Ann Trop Med Parasitol. 1922;16:223–8. https://doi.org/10.1080/00034983.1922.11684313
3. Gerber V, Le Govic Y, Ramade C, Chemla C, Hamane S, Desoubeaux G, et al. *Ancylostoma ceylanicum* as the second most frequent hookworm species isolated in France in travellers returning from tropical areas. J Travel Med. 2021;28:taab014.
4. Poppert S, Heideking M, Agostini H, Fritzenwanker M, Wüppenhorst N, Muntau B, et al. Diffuse unilateral subacute neuroretinitis caused by *Ancylostoma* hookworm. Emerg Infect Dis. 2017;23:343–4. https://doi.org/10.3201/eid2302.142064
5. Rep BH, Heinemann DW. Changes in hookworm distribution in Surinam. Trop Geogr Med. 1976;28:104–10.
6. Chico ME, Vaca MG, Rodriguez A, Cooper PJ. Soil-transmitted helminth parasites and allergy: Observations from Ecuador. Parasite Immunol. 2019;41:e12590. https://doi.org/10.1111/pim.12590
7. Deer DM, Lampel KA, González-Escalona N. A versatile internal control for use as DNA in real-time PCR and as RNA in real-time reverse transcription PCR assays. Lett Appl Microbiol. 2010;50:366–72. https://doi.org/10.1111/j.1472-765X.2010.02804.x
8. Pilotte N, Maasch JRMA, Easton AV, Dahlstrom E, Nutman TB, Williams SA. Targeting a highly repeated germline DNA sequence for improved real-time PCR-based detection of *Ascaris* infection in human stool. PLoS Negl Trop Dis. 2019;13:e0007593. https://doi.org/10.1371/journal.pntd.0007593
9. Papaiakovou M, Pilotte N, Grant JR, Traub RJ, Llewellyn S, McCarthy JS, et al. A novel, species-specific, real-time PCR assay for the detection of the emerging zoonotic parasite *Ancylostoma ceylanicum* in human stool. PLoS Negl Trop Dis. 2017;11:e0005734. https://doi.org/10.1371/journal.pntd.0005734
10. Basuni M, Muhi J, Othman N, Verweij JJ, Ahmad M, Miswan N, et al. A pentaplex real-time polymerase chain reaction assay for detection of four species of soil-transmitted helminths. Am J Trop Med Hyg. 2011;84:338–43. https://doi.org/10.4269/ajtmh.2011.10-0499
11. Pilotte N, Papaiakovou M, Grant JR, Bierwert LA, Llewellyn S, McCarthy JS, et al. Improved PCR-based detection of soil transmitted helminth infections using a next-generation sequencing approach to assay design. PLoS Negl Trop Dis. 2016;10:e0004578. https://doi.org/10.1371/journal.pntd.0004578
12. Traub RJ, Inpankaew T, Sutthikornchai C, Sukthana Y, Thompson RC. PCR-based coprodiagnostic tools reveal dogs as reservoirs of zoonotic ancylostomiasis caused by *Ancylostoma ceyla*nicum in temple communities in Bangkok. Vet Parasitol. 2008;155:67–73. https://doi.org/10.1016/j.vetpar.2008.05.001
13. Sahlin K, Lim MCW, Prost S. NGSpeciesID: DNA barcode and amplicon consensus generation from long-read sequencing data. Ecol Evol. 2021;11:1392–8. https://doi.org/10.1002/ece3.7146
14. Inpankaew T, Schär F, Dalsgaard A, Khieu V, Chimnoi W, Chhoun C, et al. High prevalence of *Ancylostoma ceylanicum* hookworm infections in humans, Cambodia, 2012. Emerg Infect Dis. 2014;20:976–82. https://doi.org/10.3201/eid2006.131770
15. Stamatakis A. RAxML-VI-HPC: maximum likelihood-based phylogenetic analyses with thousands of taxa and mixed models. Bioinformatics. 2006;22:2688–90. https://doi.org/10.1093/bioinformatics/btl446

Address for correspondence: William Sears, Bldg 4, Rm 211B, 4 Center Dr, National Institutes of Health, Bethesda, MD 20892-0425, USA; email: william.sears@nih.gov

Ancylostoma ceylanicum Hookworms in Dogs, Grenada, West Indies

Patsy A. Zendejas-Heredia,[1] Vito Colella,[1] Maxine L. A. Macpherson, Wayne Sylvester, Robin B. Gasser, Calum N. L. Macpherson, Rebecca J. Traub

Ancylostoma ceylanicum hookworms are recognized agents of human infection in the Asia–Pacific region. We investigated prevalence of zoonotic hookworm infections in dogs in Grenada in 2021; 40.8% were infected by hookworms, including *Ancylostoma ceylanicum*. Surveillance of this parasite in dogs and humans is needed in tropical/subtropical countries in the Americas.

Hookworms are blood-feeding enteric parasites that infect >700 million persons worldwide and cause detrimental health outcomes such as iron deficiency anemia, protein malnutrition, and impaired growth, particularly in children (*1*). Although most infections are attributed to anthroponotic species of hookworm, dogs serve as a reservoir for transmission of zoonotic species to humans (*1*,*2*). Of those hookworm species, only *Ancylostoma ceylanicum* can complete its life cycle in humans and dogs; both species of mammals contribute to environmental contamination with eggs (*1*).

Traditionally, the diagnosis of hookworm infection has relied on detectiing eggs in fecal samples (*3*). Because of the morphologic similarity of hookworm eggs, it is not possible to definitively differentiate these parasites at the species level by light microscopy alone (*1*,*3*). In the past decade, copromolecular tools, such as multiplex quantitative real-time PCR (M-qPCR), have enabled molecular differentiation of hookworm species in fecal samples from dogs and humans (*1*). These molecular tools are contributing to knowledge of the distribution of these parasites, particularly *A. ceylanicum*, which is now recognized as the second most common species infecting humans in the Asia–Pacific region (*2*). Despite early reports of *A. ceylanicum* hookworms in humans in Brazil, in dogs in Suriname in the early 1900s (*1*,*4*), and recently in a child living in Germany who most likely acquired the infection while in Colombia (*5*), endemicity of this parasite in dogs in the Americas has not been molecularly confirmed.

Grenada is a tropical small island developing state located in the West Indies and comprises 3 main islands (Grenada, Carriacou, and Petite Martinique) and many smaller uninhabited islands (*6*). Grenada has a population of ≈112,579 persons, 23.2% of whom are children <14 years of age (*6*) and of ≈35,000 dogs, a high proportion of which are pothounds (strays, mongrels) that roam freely; few receive veterinary care or anthelmintic treatment (*7*).

We applied molecular tools to investigate the presence of zoonotic hookworms in 220 dogs from 6 parishes in Grenada. The Institutional Animal Care and Use Committee of the St. George's University, Grenada, approved the study (approval no.: IACUC-21001-R).

The Study

Fecal samples collected from the rectal ampulla of 220 dogs were preserved in 70% ethanol for molecular analysis. We isolated genomic DNA from the samples (≈200 mg each) by using the QIAmp PowerFecal Pro DNA Kit (QIAGEN, https://www.qiagen.com), eluted into 50 µL (instead of 100 µL) of solution C6, and then stored the samples at –20°C. To differentiate the hookworm species, we subjected individual DNA samples to M-qPCR (*3*) and analyzed and displayed the data by using GraphPad Prism version 8.0 (GraphPad, https://www.graphpad.com). Samples positive for *A. ceylanicum* hookworm DNA by quantitative

Author affiliations: The University of Melbourne, Parkville, Victoria, Australia (P.A. Zendejas-Heredia, V. Colella, R.B. Gasser, R.J. Traub); St. George's University, St. George's, Grenada (M.L.A. Macpherson, W. Sylvester, C.N.L. Macpherson)

DOI: https://doi.org/10.3201/eid2809.220634

[1]These authors contributed equally to this article.

PCR underwent conventional PCR and Sanger sequencing targeting a partial region of the cytochrome oxidase subunit 1 (*cox*1) gene as previously described (*8*). To analyze sequences, we used Geneious prime 2021, version 2.2 (https://www.geneious.com).

Overall, of the 211 samples for which DNA isolation was successful, 40.8% (95% CI 34.1%–47.3%) were positive for >1 hookworm species: 27.5% (95% CI 21.4%–33.5%) *A. caninum*, 4.7% (95% CI 1.87%–7.61%) *A. ceylanicum*, and 8.5% (95% CI 4.76%–12.3%) both parasites. Neither *A. braziliense* nor *Uncinaria stenocephala* DNA was detected (Figure). BLAST (https://blast.ncbi.nlm.nih.gov) analyses of *cox*1 sequences showed 100% nt identity with sequences of *A. ceylanicum* hookworms isolated from humans (GenBank accession nos. MK7928230-35) and dogs (GenBank accession no. LC533320). A representative *cox*1 sequence of *A. ceylanicum* hookworms found in this study was deposited in GenBank under accession no. OP077312.

Conclusions

Molecular analysis identified *A. ceylanicum* hookworms in dogs in the Americas. In the past decade, unexpectedly high prevalence and distribution of *A. ceylanicum* hookworms in dogs, wildlife, and humans has been reported mainly in the Asia–Pacific region but also in Africa (*1*,*2*,*9*). *A. ceylanicum* was erroneously considered synonymous with *A. braziliense*, until the 2 hookworm species were differentiated on the basis of configuration of the lateral bursal rays of the male (*1*). Hence, the "emergence" of *A. ceylanicum* hookworms may be associated with the increased use of molecular tools to specifically identify and differentiate these parasites in areas where multiple species of hookworm co-exist (*1*,*2*).

In the Americas, *A. ceylanicum* hookworms have not been considered etiologic agents of human infection, despite isolation of adult worms in 4 of 64 human cadavers in the Amazonas, Brazil, in the early 1920s and, more recently, reported detection of this parasite in travelers returning from countries in Latin America (e.g., Colombia and French Guiana) to France (*1*,*5*,*10*). Of note, the geographic distribution of *A. ceylanicum* hookworms in dogs strongly mirrors that in humans in the Asia–Pacific region (*2*). To date, only a few coproscopic studies of hookworms in dogs in Grenada have been undertaken (*11*), but absence of molecular investigation raises questions as to the specific identity of the hookworms on the island.

In humans, other species of hookworms of canids can cause hookworm-related cutaneous larva migrans. *A. braziliense* hookworms cause severe serpiginous "creeping eruptions," and *A. caninum* hookworms cause peripheral eosinophilia and aphthous ileitis (*1*). Although recent cases of long-lasting hookworm-related cutaneous larva migrans have been reported in the Caribbean, including Grenada (*11*,*12*), Martinique, Jamaica, and Brazil (*1*), we did not detect *A. braziliense* hookworm infection in our canine cohort. Nonetheless, cases of hookworm-related cutaneous larva migrans in some countries in Latin America have been attributed to hookworms of canids, despite lack of molecular evidence. For instance, 4 cases were detected in 1983 during a hookworm outbreak among US military soldiers returning from Grenada, but the etiology of these infections was not established (*11*). Furthermore, although some circumstantial evidence indicates that *A. caninum* hookworms cause patent infections in humans (*9*,*13*), molecular evidence is lacking, which is particularly pertinent given the close genetic relatedness of *A. caninum* and *A. duodenale* hookworms (*1*,*13*). Thus, use of molecular methods to specifically detect, identify, and differentiate is crucial for surveillance of hookworm infections/disease in dogs and humans and for monitoring the success of control campaigns in hookworm-endemic areas (*14*).

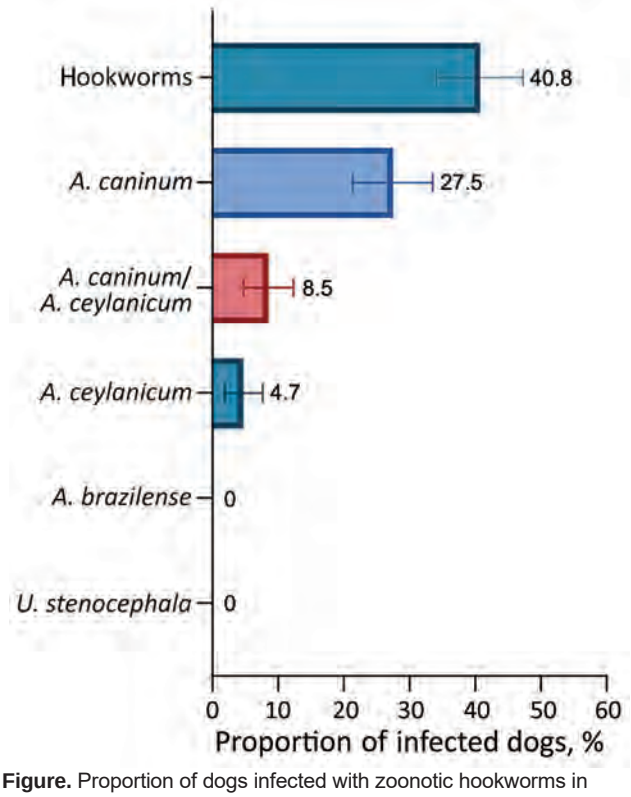

Figure. Proportion of dogs infected with zoonotic hookworms in Grenada, 2021, determined by using multiplex quantitative real-time PCR. Error bars indicate 95% CI. *A.*, *Ancylostoma*; *U.*, *Uncinaria*.

Molecular detection of *A. ceylanicum* and *A. caninum* and the absence of *A. braziliense* hookworms in dogs in Grenada demonstrates the value of using molecular techniques to accurately identify hookworm species in dogs and humans living in the Americas. The climate in Grenada is similar to that in other countries where prevalence of zoonotic hookworms is high (*1*,*6*,*15*). According to the World Bank in Grenada, 34.3% of its population still live in households considered multidimensionally poor, where solid waste management and public sewer systems remain inadequate (*6*). Those factors, together with lack of appropriate veterinary care for dogs and closeness of human–dog interactions, favor transmission of zoonotic pathogens to humans. Given the significance of *A. ceylanicum* hookworms as agents of human hookworm infection in the Asia–Pacific region (*1*,*2*), we advocate for active surveillance of this zoonotic parasite in dogs and humans living in tropical and subtropical countries in the Americas by using reliable molecular diagnostic tools targeting appropriate genetic markers.

Collection of samples for this study was funded by a grant from the Windward Islands Research and Education Foundation.

About the Author

Ms. Zendejas-Heredia is undertaking a PhD program and receives a scholarship from The University of Melbourne. Her research focuses on elucidating the transmission dynamics of zoonotic soil-transmitted helminths in the Asia–Pacific region.

References

1. Traub RJ, Zendejas-Heredia PA, Massetti L, Colella V. Zoonotic hookworms of dogs and cats - lessons from the past to inform current knowledge and future directions of research. Int J Parasitol. 2021;51:1233–41. https://doi.org/10.1016/j.ijpara.2021.10.005
2. Colella V, Bradbury R, Traub R. *Ancylostoma ceylanicum*. Trends Parasitol. 2021;37:844–5. https://doi.org/10.1016/j.pt.2021.04.013
3. Massetti L, Colella V, Zendejas PA, Ng-Nguyen D, Harriott L, Marwedel L, et al. High-throughput multiplex qPCRs for the surveillance of zoonotic species of canine hookworms. PLoS Negl Trop Dis. 2020;14:e0008392. https://doi.org/10.1371/journal.pntd.0008392
4. Rep BH, Heinemann DW. Changes in hookworm distribution in Surinam. Trop Geogr Med. 1976;28:104–10.
5. Poppert S, Heideking M, Agostini H, Fritzenwanker M, Wüppenhorst N, Muntau B, et al. Diffuse unilateral subacute neuroretinitis caused by *Ancylostoma* hookworm. Emerg Infect Dis. 2017;23:343–4. https://doi.org/10.3201/eid2302.142064
6. The World Bank. Living conditions in Grenada: poverty and equity update. Washington (DC): The Bank; 2021.
7. Schwartz R, Bidaisee S, Fields PJ, Macpherson MLA, Macpherson CNL. The epidemiology and control of *Toxocara canis* in puppies. Parasite Epidemiol Control. 2021;16:e00232. https://doi.org/10.1016/j.parepi.2021.e00232
8. Inpankaew T, Schär F, Dalsgaard A, Khieu V, Chimnoi W, Chhoun C, et al. High prevalence of *Ancylostoma ceylanicum* hookworm infections in humans, Cambodia, 2012. Emerg Infect Dis. 2014;20:976–82. https://doi.org/10.3201/eid2006.131770
9. Ngcamphalala PI, Lamb J, Mukaratirwa S. Molecular identification of hookworm isolates from stray dogs, humans and selected wildlife from South Africa. J Helminthol. 2019;94:e39. https://doi.org/10.1017/S0022149X19000130
10. Gerber V, Le Govic Y, Ramade C, Chemla C, Hamane S, Desoubeaux G, et al. *Ancylostoma ceylanicum* as the second most frequent hookworm species isolated in France in travellers returning from tropical areas. J Travel Med. 2021;28(6):taab014.
11. Kelley PW, Takafuji ET, Wiener H, Milhous W, Miller R, Thompson NJ, et al. An outbreak of hookworm infection associated with military operations in Grenada. Mil Med. 1989;154:55–9. https://doi.org/10.1093/milmed/154.2.55
12. Chris RB, Keystone JS. Prolonged incubation period of hookworm-related cutaneous larva migrans. J Travel Med. 2016;23:tav021. https://doi.org/10.1093/jtm/tav021
13. Furtado LFV, Dias LTO, Rodrigues TO, Silva VJD, Oliveira VNGM, Rabelo ÉML. Egg genotyping reveals the possibility of patent *Ancylostoma caninum* infection in human intestine. Sci Rep. 2020;10:3006. https://doi.org/10.1038/s41598-020-59874-8
14. Colella V, Khieu V, Worsley A. Senevirathna D, Muth S, Huy R, et al. Risk profiling and efficacy of albendazole against the hookworms *Necator americanus* and *Ancylostoma ceylanicum* in Cambodia to support control programs in Southeast Asia and the Western Pacific. Lancet Reg Health West Pac. 2021;16:100258.
15. Zendejas-Heredia PA, Crawley A, Byrnes H, Traub RJ, Colella V. Zoonotic soil-transmitted helminths in free-roaming dogs, Kiribati. Emerg Infect Dis. 2021;27:2163–5. https://doi.org/10.3201/eid2708.204900

Address for correspondence: Vito Colella, The University of Melbourne, Faculty of Veterinary and Agricultural Sciences, Corner of Park Dr and Flemington Rd, Parkville, Victoria, Australia; email: vito.colella@unimelb.edu.au

Evaluation of Effectiveness of Global COVID-19 Vaccination Campaign

Daihai He,[1] Sheikh Taslim Ali,[1] Guihong Fan, Daozhou Gao, Haitao Song, Yijun Lou, Shi Zhao, Benjamin J. Cowling, Lewi Stone

To model estimated deaths averted by COVID-19 vaccines, we used state-of-the-art mathematical modeling, likelihood-based inference, and reported COVID-19 death and vaccination data. We estimated that >1.5 million deaths were averted in 12 countries. Our model can help assess effectiveness of the vaccination program, which is crucial for curbing the COVID-19 pandemic.

The real-time evaluation of the effectiveness of vaccination campaigns at the population level is essential for public health policy makers and scientists working toward successful mitigation of the COVID-19 pandemic. Vaccination coverage against SARS-CoV-2 has increased globally and become even more crucial because of the emergence of variants of concern that have increased transmissibility and lethality (*1*). We assessed population-level effects of the COVID-19 vaccination campaign in 12 countries worldwide before November 14, 2021. Our modeling framework enabled us to disentangle the effects of vaccination and a time-varying transmission rate. We also fit the model to multiple waves of death in these countries before the Omicron variant was detected.

Author affiliations: The Hong Kong Polytechnic University, Hong Kong, China (D. He, Y. Lou); The University of Hong Kong, Hong Konga (S.T. Ali, B.J. Cowling); The Laboratory of Data Discovery for Health, Hong Kong Science and Technology Park, Hong Kong (S.T. Ali, B.J. Cowling); Columbus State University, Columbus, Georgia, USA (G. Fan); Shanghai Normal University, Shanghai, China (D. Gao); Shanxi University, Taiyuan, China (H. Song); Chinese University of Hong Kong, Hong Kong, China (S. Zhao); RMIT University, Melbourne, Victoria, Australia and Tel Aviv University, Tel Aviv, Israel (L. Stone)

DOI: https://doi.org/10.3201/eid2809.212226

The Study

We developed a transmission modeling approach to analyze diverse spatiotemporal datasets from different countries and attempted to evaluate the COVID-19 vaccination campaign in real time by adapting our related earlier work (*2*). The COVID-19 pandemic continues to be complex because of various short-term enforcements of public health and social measures (e.g., lockdowns), emergence of new virus variants, shifts in age profiles of infected persons, availability of multiple vaccines with different effectiveness, reinfection, and other factors. However, many of these factors are reflected in the key measure, the time-varying transmission rate, $\beta(t)$, which characterizes the changes in contact pattern in the population over time. Vaccination is intended to reduce the susceptibility of the population to the disease. Disentangling real-time variation in $\beta(t)$ and the effectiveness of vaccination is crucial for assessing the vaccination program and might only be achievable through mathematical modeling.

Country-specific mortality data generally provide a more reliable characterization of the key epidemic dynamics than data on reported confirmed COVID-19 cases, which rely on widely different testing and reporting systems that can vary temporally and spatially and be subject to various ascertainment rates. For our analysis, we obtained data from the World Health Organization, including daily confirmed COVID-19 death numbers (*3*,*4*) and the proportion of the population fully vaccinated (2 doses) for 12 countries: the United Kingdom, Italy, the United States, Spain, Russia, France, India, Brazil, Colombia, Mexico, Germany, and Canada (*5*). We used a partially observed Markov process (*6*) model and maximum-likelihood–based iterative filtering technique to fit and make predictions on the mortality

[1]These authors contributed equally to this work.

data by susceptible-exposed-infectious-recovered–type models (Appendix, https://wwwnc.cdc.gov/EID/article/28/9/21-2226-App1.pdf).

We estimated the transmission rate, $\beta(t)$, which reflects the simultaneous effect of all possible interventions, excluding vaccination, over the study period. The model assumed a 14-day delay between the 2 vaccine doses and the time for the vaccine to take effect. We set the unified vaccine efficacy (VE; represented by η) at 85% and examined vaccine effectiveness from 75% to 95% (Appendix). The COVID-19 surveillance data we used were originally collected from public domains; thus, neither ethical approval nor patient consent was applicable.

To evaluate effectiveness of vaccination and the lives saved, we compared the final model fit and simulations of the baseline scenario of vaccination to the counterfactual scenario of without vaccination by setting VE to $\eta = 0$. Vaccination coverage was defined as the proportion of the country's population that was fully vaccinated (i.e., either receiving 2 vaccine doses or receiving 1 vaccine dose after infection). We plotted vaccination coverage as a function of time for the 12 countries (Appendix Figure 1).

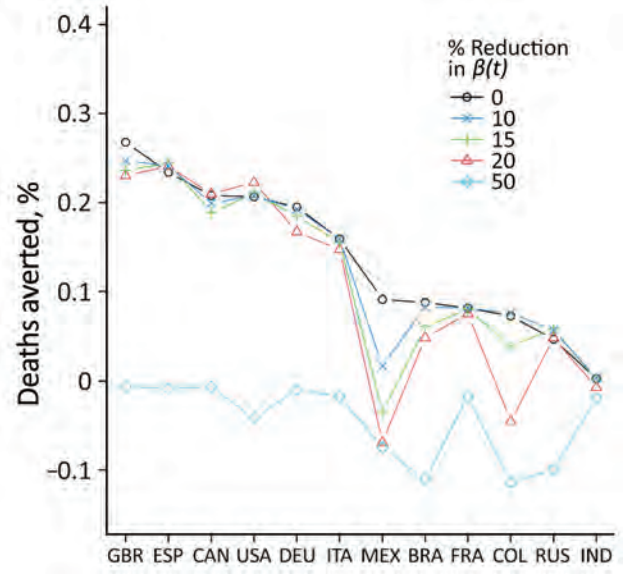

Figure. Deaths averted because of vaccination according to a model used to evaluate effectiveness of global COVID-19 vaccination campaign. The graph represents the difference in total deaths under the counterfactual scenario (without vaccination) and under the baseline scenario (with vaccination) as a percentage of the population. We compared 5 counterfactual scenarios under without-vaccination in which we set the transmission rates after April 16, 2021, to reduce by 0, 10%, 15%, 20%, and 50% compared with the baseline scenario. The y-axis 0.3% means 3 persons per 1,000 population were saved from COVID-19–related death because of vaccination. The absolute value of negative deaths averted results from substantial reduction in transmission rate, rather than vaccination. $\beta(t)$, time-varying transmission rate; BRA, Brazil; CAN, Canada; COL, Colombia; DEU, Germany; ESP, Spain; FRA, France; GBR, Great Britain (United Kingdom); IND, India; ITA, Italy; MEX, Mexico; RUS, Russia; USA, United States.

We compared and fitted the model to data on weekly confirmed waves of COVID-19 deaths in the 12 countries during 2020–2021 and reconstructed transmission rates (Appendix Figure 1, panels A–I). We then used the model to reconstruct COVID-19 deaths that would have occurred in these countries in the hypothetical without-vaccination counterfactual scenario (i.e., in complete absence of vaccination). Thus, we could compare the observed mortality rate against that of the model's without-vaccination scenario (Appendix Figure 1).

We found that vaccination campaigns saved the lives of up to 1,822,670 (0.069% of the total population) persons in these 12 countries (Appendix Table 2). For instance, the United States reported 416,842 confirmed deaths during January 1–November 14, 2021 (Appendix Figure 1, panel E). According to the model's without-vaccination predictions, had the United States not initiated a vaccination program, 1,102,958 deaths would have occurred there during the same time frame. Thus, vaccination saved 686,115 lives (0.2% of the population) in the United States during the study period. The model estimated that vaccination averted 182,464 (0.27% of the population) deaths in the United Kingdom; 109,367 (0.23% of the population) deaths in Spain; 78,969 (0.2% of the population) deaths in Canada; and 96,008 (0.16% of the population) deaths in Italy. Vaccination coverage in each of these countries was >60% (Appendix Table 2).

Vaccination seems to have prevented severe Delta waves in Italy, France, Germany, and Canada during the second half of 2021 (Appendix Figure 1). For Russia, India, Brazil, Colombia, and Mexico, where vaccine coverage was relatively low or delayed, vaccination had only a mild effect on the epidemic dynamics and mortality rates (Appendix Table 2).

Widely available vaccines might encourage risky behavioral practices among the population, which might be less prevalent in the absence of a countrywide vaccination campaign. Our idealized reconstruction method ignores this possibility and might have led to overestimation of both the transmission rate in the without-vaccination scenario and the number of deaths averted (*7*). To examine this possibility further, we plotted the changes in deaths averted by vaccination as a percentage of the population as calculated for 5 levels of transmission rate reduction (Figure). The reductions are intended to compensate for risky behaviors persons might engage in when vaccinated. We considered these as

5 counterfactual without-vaccination scenarios in which transmission rates after April 16, 2021, were reduced to 0 (scenario 1), 10% (scenario 2), 15% (scenario 3), 20% (scenario 4), and 50% (scenario 5) of the level of transmissibility in the baseline scenario. These counterfactual scenarios were intended to show that any overestimation of deaths averted based on the idealized counterfactual scenario 1 (0 reduction) was generally minimal unless the transmission rate was reduced by >25% (Appendix).

We conducted additional sensitivity analyses on the model performance and counterfactual scenarios to explore parameter ranges and several different model structures, constructing more complex models of imperfect vaccination (Appendix Tables 1–3, Figures 2, 3). Our estimates of deaths averted show reasonable robustness to changes in the model structure and parameters.

Conclusions

We used a disease transmission model and likelihood-based inference approach to evaluate effectiveness of COVID-19 vaccination in 12 countries. Our analysis indicated that vaccination averted >1.5 million deaths in the studied countries until November 14, 2021, or at least precluded the need to reintroduce more stringent public health and social measures to control transmission.

Of our several assumptions for this evaluation, we first assumed the infection fatality ratio was roughly constant over time (*1*,*8*,*9*). We evaluated a second model in which we allowed the infection fatality ratio to decrease because of vaccination (Appendix). In addition, we used a unified constant VE although VE differs across countries, demographic characteristics (*10*), and type of vaccine and its coverage (*11*). Nonetheless, our modeling framework enabled us to assess the effect of vaccination on a time-varying transmission rate. Our model can help assess effectiveness of the COVID-19 vaccination program, which is crucial for curbing the COVID-19 pandemic.

This study was supported by the Collaborative Research Fund (grant no. HKU C7123-20G) of the Research Grants Council of Hong Kong, China. D.G. was partially supported by the National Science Foundation of Shanghai (grant no. 20ZR1440600). H.S. was partially supported by the National Natural Science Foundation of China (grant no. 12171291), the Fund Program for the Scientific Activities of Selected Returned Overseas Professionals in Shanxi Province (grant no. 20200001), and the Fundamental Research Program of Shanxi Province (grant no. 20210302124018). B.J.C. is supported by the AIR@innoHK program of the Innovation and Technology Commission of the Hong Kong Special Administrative Region Government.

The funding agencies had no role in the design and conduct of the study; collection, management, analysis, and interpretation of the data; preparation, review, or approval of the manuscript; or decision to submit the manuscript for publication.

D.H., S.T.A., and L.S. conceived the study and conducted the analysis. All authors discussed the results, drafted the manuscript, revised the manuscript, read the manuscript, and approved it for publishing.

B.J.C. has consulted for AstraZeneca, GlaxoSmithKline, Moderna, Pfizer, Roche, and Sanofi Pasteur.

About the Author

Dr. He is an associate professor in the Department of Mathematics, The Hong Kong Polytechnic University, Hong Kong Special Administrative Region, China. His primary areas of research are infectious disease modeling and mathematical epidemiology, with a focus on understanding mechanisms of virus transmission dynamic and control measures.

References

1. Yang W, Shaman J. Development of a model-inference system for estimating epidemiological characteristics of SARS-CoV-2 variants of concern. Nat Commun. 2021;12:5773. PubMed https://doi.org/10.1038/s41467-021-27703-9
2. Zhao S, Stone L, Gao D, He D. Modelling the large-scale yellow fever outbreak in Luanda, Angola, and the impact of vaccination. PLoS Negl Trop Dis. 2018;12:e0006158. https://doi.org/10.1371/journal.pntd.0006158
3. Ritchie H, Mathieu E, Rodés-Guirao L, Appel C, Giattino C, Ortiz-Ospina E, et al. Coronavirus pandemic (COVID-19) [cited 2022 May 1]. https://ourworldindata.org/coronavirus
4. World Health Organization. COVID-19 deaths [cited 2021 Aug 20]. https://covid19.who.int/info
5. Mathieu E, Ritchie H, Ortiz-Ospina E, Roser M, Hasell J, Appel C, et al. A global database of COVID-19 vaccinations. Nat Hum Behav. 2021;5:947–53. https://doi.org/10.1038/s41562-021-01122-8
6. Ionides EL, Bretó C, King AA. Inference for nonlinear dynamical systems. Proc Natl Acad Sci U S A. 2006; 103:18438–43. https://doi.org/10.1073/pnas.0603181103
7. Leung K, Wu JT, Leung GM. Effects of adjusting public health, travel, and social measures during the roll-out of COVID-19 vaccination: a modelling study. Lancet Public Health. 2021;6:e674–82. https://doi.org/10.1016/S2468-2667(21)00167-5
8. Twohig KA, Nyberg T, Zaidi A, Thelwall S, Sinnathamby MA, Aliabadi S, et al.; COVID-19 Genomics UK (COG-UK) Consortium. Hospital admission and emergency care attendance risk for SARS-CoV-2 delta (B.1.617.2) compared with alpha (B.1.1.7) variants of concern: a cohort study. Lancet Infect Dis. 2022;22:35–42. https://doi.org/10.1016/S1473-3099(21)00475-8

9. COVID-19 Forecasting Team. Variation in the COVID-19 infection-fatality ratio by age, time, and geography during the pre-vaccine era: a systematic analysis. Lancet. 2022;399:1469–88. https://doi.org/10.1016/S0140-6736(21)02867-1
10. Goldstein JR, Cassidy T, Wachter KW. Vaccinating the oldest against COVID-19 saves both the most lives and most years of life. Proc Natl Acad Sci U S A. 2021;118:e2026322118. https://doi.org/10.1073/pnas.2026322118
11. Mallapaty S, Callaway E, Kozlov M, Ledford H, Pickrell J, Van Noorden R. How COVID vaccines shaped 2021 in eight powerful charts. Nature. 2021;600:580–3. https://doi.org/10.1038/d41586-021-03686-x

Address for correspondence: Lewi Stone, RMIT University, 124 La Trobe St., Melbourne, Victoria 3000 Australia; email: lewistone100@gmail.com

Laboratory Misidentifications Resulting from Taxonomic Changes to *Bacillus cereus* Group Species, 2018–2022

Laura M. Carroll, Itumeleng Matle, Jasna Kovac, Rachel A. Cheng, Martin Wiedmann

Whole-genome sequencing (WGS) is being applied increasingly to *Bacillus cereus* group species; however, misinterpretation of WGS results may have severe consequences. We report 3 cases, 1 of which was an outbreak, in which misinterpretation of *B. cereus* group WGS results hindered communication within public health and industrial laboratories.

The *Bacillus cereus* group of bacteria is a complex of closely related species with varying pathogenic potential (*1*). Notable members, as defined in the US Food and Drug Administration's Bacteriological Analytical Manual, include *B. anthracis*, an etiologic agent of anthrax, and *B. cereus*, which has been associated with numerous illnesses, including foodborne emetic intoxication, diarrheal toxicoinfection, anthrax-like illness, and nongastrointestinal infections (*1*–*5*).

Whole-genome sequencing (WGS) is used increasingly in clinical and industrial microbiology laboratories to characterize *B. cereus* group strains (*6*). However, interpreting WGS results from these organisms is challenging; insights derived from WGS may conflict with information provided by traditional microbiologic assays (*6*–*8*). Previously, we hypothesized that results from some WGS-based species classification methods can be easily misinterpreted when applied to the *B. cereus* group (*7*). Here, we show that this scenario is not hypothetical: we report 3 recent cases among public health and industrial laboratories in which misinterpretation of WGS results directly hindered public health and food safety investigations or responses.

Author affiliations: EMBL, Heidelberg, Germany (L.M. Carroll); Onderstepoort Veterinary Research, Pretoria, South Africa (I. Matle); The Pennsylvania State University, University Park, Pennsylvania, USA (J. Kovac); Cornell University, Ithaca, New York, USA (R.A. Cheng, M. Wiedmann)

DOI: https://doi.org/10.3201/eid2809.220293

The Study

We report 3 cases of WGS-based *B. cereus* group species assignment misinterpretations in 3 continents: Europe, North America, and Africa (Table 1; Appendix, https://wwwnc.cdc.gov/EID/article/28/9/22-0293-App1.pdf). Two cases (cases 2 and 3) occurred within the last 6 months and involved regional and national public health laboratories; 1 case (case 1) involved an industrial laboratory (Table 1). All cases involved strains known colloquially as group III *B. cereus*, a phylogenetic lineage within the *B. cereus* group that was identified using pantoate-β-alanine ligase gene (*panC*) sequencing (*9*).

Case 1 occurred in November 2018 at an industrial microbiology laboratory in Europe (Table 1). The inquiring party isolated *B. cereus* group strains from a food processing facility, then characterized them by WGS (protocols unknown). Each *B. cereus* group strain was assigned to a species by comparing its genome to the genomes of all *B. cereus* group species type strains and identifying the most similar species type strain by average nucleotide identity (*7*). Two strains were classified as *B. anthracis* using this approach (Table 1), and the inquiring party was concerned that the strains represented a potential anthrax threat (because of their *B. anthracis* label). However, subsequent investigation by M.W. and L.M.C. revealed that, although the strains most closely resembled *B. anthracis*, neither strain belonged to the historical, clonal *B. anthracis* lineage typically associated with anthrax toxin production (*6*), and neither strain possessed anthrax toxin- or capsule-encoding genes (Table 1; Figure 1). Thus, the strains were deemed incapable of causing anthrax, despite being assigned to *B. anthracis* by WGS. The authors noted that historically, these strains would be known colloquially as group III *B. cereus*, using microbiologic methods and *panC* phylogenetic group assignment (Figure 2, panel A).

Table 1. Summary of cases of laboratory misidentifications caused by taxonomic changes to *Bacillus cereus* group species, 2018–2022*

Case	Date	Location	Inquiring party	WGS-assigned species of inquiry	Case summary†
1	November 2018	Europe	Industrial laboratory	*B. anthracis*	Two *B. cereus* strains isolated from a food processing facility were assigned to the *B. anthracis* species but were not closely related to the *B. anthracis* lineage most commonly responsible for anthrax illness and did not possess anthrax encoding genes or represent an anthrax threat. They would historically be referred to as *B. cereus* or group III *B. cereus*.
2	October 2021	North America (USA)	Government laboratory	*B. paranthracis*	A *B. cereus* strain isolated from a food product responsible for a foodborne outbreak was assigned to the *B. paranthracis* species using WGS-based methods. *B. paranthracis* was historically referred to as *B. cereus* or group III *B. cereus* and encompasses *B. cereus* group strains capable of causing emetic and/or diarrheal foodborne illness.
3	January 2022	Africa (South Africa)	Government laboratory	*B. anthracis*	Two *B. cereus* strains isolated during routine surveillance of meat products were classified using multiple WGS-based methods; they were assigned to the *B. anthracis* species but did not represent an anthrax threat. They would historically be referred to as *B. cereus* or group III *B. cereus*.

*WGS, whole genome sequencing; ANI, average nucleotide identity; MLST, multilocus sequence typing; ST, sequence type; Group III, *panC* phylogenetic Group III; PubMLST, https://pubmlst.org; GTDB, Genome Taxonomy Database Releases R95 and R202, https://gtdb.ecogenomic.org.
†*B. cereus* refers to the historical and/or colloquial species definition assigned using traditional microbiological methods, as outlined in the US Food and Drug Administration's Bacteriological Analytical Manual (FDA BAM) (*5*).

Case 2 occurred in October 2021 at a regional public health microbiology laboratory in the United States (Table 1). The inquiring party was responding to a foodborne outbreak that occurred at a correctional facility in Maryland in mid-September 2021. During the outbreak investigation, a *B. cereus* group strain was isolated from rehydrated dehydrated potatoes using standard protocols (*5*). The strain underwent WGS and was classified as *B. paranthracis* (protocols unknown) (Table 1). The inquiring party had never heard of *B. paranthracis* before and conducted a literature search, noting that the species was first

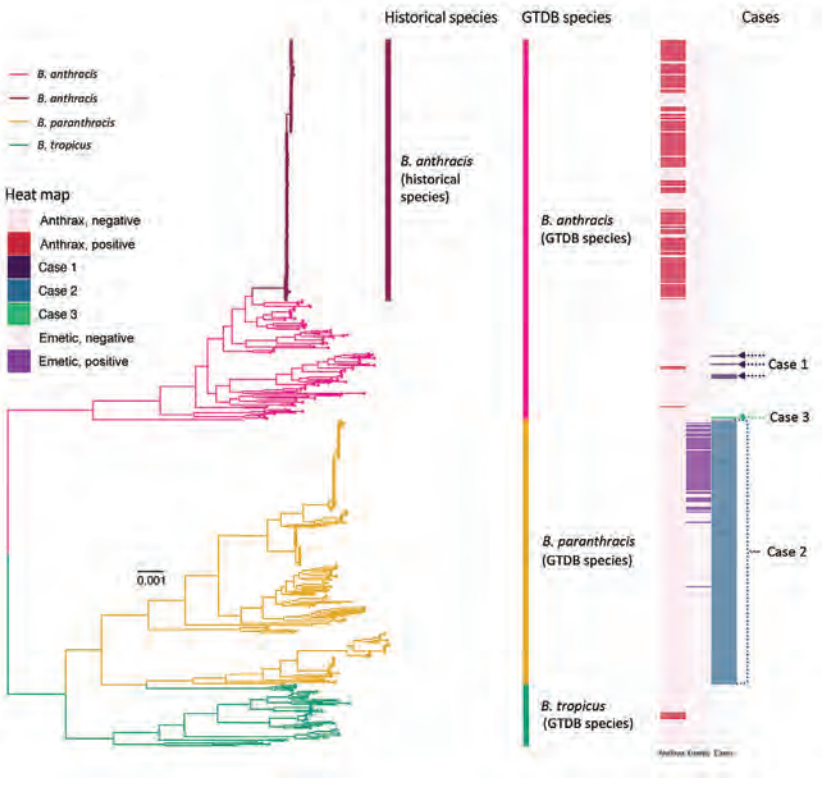

Figure 1. Maximum-likelihood phylogeny constructed using core genes detected among 605 genomes assigned to the (GTDB) *B. anthracis*, *B. paranthracis*, and *B. tropicus* species. Branch colors and clade labels denote GTDB species assignments or, for *B. anthracis*, historical species assignments. The heatmap to the right of the phylogeny shows whether a strain possessed anthrax toxin-encoding genes or not (anthrax); whether a strain possessed cereulide synthetase (emetic toxin)-encoding genes or not (emetic); and the strains or lineages discussed in the cases we detailed here (cases) (Table 1). For case 1, the actual genomes were not publicly available; thus, genomes assigned to the same sequence types (STs, via 7-gene multilocus sequence typing) are highlighted. For case 2, the only information provided to the authors was that the genome in question belonged to species *B. paranthracis*; thus, all genomes assigned to GTDB's *B. paranthracis* species are highlighted. For case 3, the actual strain genomes associated with the case are highlighted. The phylogeny was rooted using *panC* Group II *B. cereus* group strain FSL W8-0169 as an outgroup (National Center for Biotechnology Information RefSeq Assembly accession no. GCF_001583695.1; omitted for readability). Branch lengths are reported in substitutions per site. GTDB, Genome Taxonomy Database.

described in 2017 (*10*); because of limited documented history of *B. paranthracis*, the inquiring party contacted M.W., J.K., and L.M.C. for assistance. We informed the inquiring party that *B. paranthracis* has historically been identified as group III *B. cereus* on the basis of microbiologic methods and *panC* phylogenetic group assignment. We also noted that *B. paranthracis* encompasses all strains known colloquially as emetic *B. cereus* (for their ability to produce cereulide, an emetic toxin) and some group III *B. cereus* strains capable of causing diarrheal foodborne illness (Figure 2, panel A) (*11*). We suggested that the inquiring party use multilocus sequence typing and virulence factor detection to determine if the strain belonged to a lineage previously associated with foodborne illness.

Case 3 occurred in January 2022 at a national veterinary public health microbiology laboratory in South Africa (Table 1). I.M. and collaborators isolated *B. cereus* group strains during routine surveillance of meat products (*12*). WGS was conducted on some strains (*13*). I.M. and L.M.C. assigned *B. cereus* group strains to species using multiple WGS-based methods (*13*); one method relied on the Genome Taxonomy Database (GTDB), a popular contemporary microbial species classification framework (*14*). GTDB releases R95 and R202 classified 2 strains as *B. anthracis* (Table 1); however, neither strain belonged to the historical, clonal *B. anthracis* lineage (*6*), and neither possessed anthrax toxin- or capsule-encoding genes (Table 1; Figure 1). Nevertheless, an inquiring party was concerned that the strains represented an anthrax threat because of the GTDB *B. anthracis* label (Table 1). We informed the inquiring party that neither possessed anthrax toxin-encoding genes. We noted that historically these strains would be known as group III *B. cereus*, using microbiologic methods and *panC* phylogenetic group assignment (Figure 2, panel A).

Conclusions

The growing popularity of WGS offers tremendous potential for improving *B. cereus* group surveillance, source tracking, and outbreak investigations. However, taxonomic issues in the *B. cereus* group have become more pronounced as researchers grapple with historical and WGS-based species definitions.

Here, we detailed 3 cases in which misinterpretation of *B. cereus* group WGS results directly hindered public health and food safety efforts. Two cases (cases 1 and 3) represented false-positive scenarios, in which group III *B. cereus* strains incapable of causing anthrax were incorrectly assumed to be anthrax-causing agents (Table 1). As noted previously, strains that lack anthrax toxin-encoding genes but are assigned to *B. anthracis* using WGS-based methods are not uncommon (Table 2); these strains have been isolated from diverse environments (e.g., meat, milk, spices, egg whites, baby wipes) on 6 continents and the International Space Station, and although some may cause illness, they cannot cause anthrax (*6*). One way of denoting that a *B. cereus* group strain may produce anthrax toxin is to append the term "biovar Anthracis" to the genus/species name (Figure 2, panel B) (*2*).

The remaining case (case 2) represented a worst-case, false-negative scenario, in which a WGS-assigned species label with limited clinical interpretability or previous associations to foodborne illness

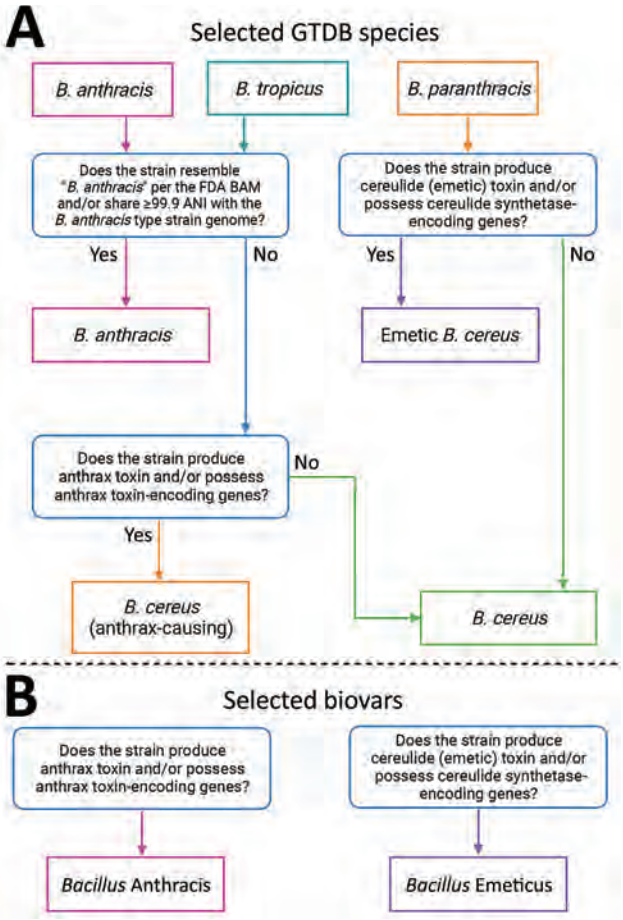

Figure 2. Flowcharts of *Bacillus* species and biovar name assignments. A) Flowchart depicting how 3 *Bacillus* species names assigned using GTDB releases R95 and R202 can be translated to historically important or colloquial names for *B. cereus* group species, as outlined in the US FDA's BAM (*5*). B) Chart depicting how anthrax and cereulide (emetic) toxin-producing strains can be referred to using a previously proposed standardized collection of *B. cereus* group biovar terms (*6*). Figure was created using BioRender.com. ANI, average nucleotide identity; BAM, Bacteriological Analytical Manual; FDA, Food and Drug Administration; GTDB, Genome Taxonomy Database.

Table 2. Selected GTDB *Bacillus* species names and the clinically important strains they encompass*

GTDB species name	Encompasses strains which: Can cause anthrax illness	Can cause emetic illness	Cannot cause anthrax or emetic illness	Notes†
B. anthracis	Yes	No	Yes	Encompasses all anthrax-causing *B. anthracis* strains, some anthrax-causing *B. cereus* strains, and many *B. cereus* strains that are incapable of causing anthrax illness but are commonly isolated from environmental and food sources (*6*,*7*).
B. paranthracis	No	Yes	Yes	Encompasses all cereulide-producing *B. cereus* strains known colloquially as emetic *B. cereus*, including the high-risk ST26 lineage; also encompasses many environmental and food isolates that are incapable of causing emetic illness (*7*,*11*).
B. tropicus	Yes	No	Yes	Encompasses some anthrax-causing *B. cereus* strains, as well as *B. cereus* strains that are incapable of causing anthrax illness (*6*,*7*).

*Obtained using GTDB Releases R95 and R202, but is applicable to any taxonomic framework, in which species names are assigned relative to *B. cereus* group species type strain genomes, e.g., by a species threshold of 95–96 average nucleotide identity or species threshold of 70% *in silico* DNA-DNA hybridization (*7*). GTDB, Genome Taxonomy Database; ST, sequence type assigned using the PubMLST 7-gene multilocus sequence typing scheme for *B. cereus* (https://pubmlst.org).
†*B. anthracis* and *B. cereus* refer to historical and/or colloquial species definitions assigned using traditional microbiological methods, as outlined in the US Food and Drug Administration's Bacteriological Analytical Manual (*5*).

(*B. paranthracis*) was assigned to an established pathogen (group III *B. cereus*) and directly hindered an outbreak investigation (Table 1). We anticipate that similar problems may arise with anthrax-causing *B. cereus*, because WGS-based methods assign some of these strains to *B. tropicus*, a species proposed in 2017 (Table 2) (*7*).We encourage readers to be mindful of this potential issue (Table 2). Overall, we hope that the cases we described can serve as cautionary tales for those who are transitioning to WGS for *B. cereus* group strain characterization.

This work was supported by United States Department of Agriculture National Institute of Food and Agriculture (USDA NIFA) Hatch Appropriations (project no. PEN04646; accession no. 1015787) and USDA NIFA grants (no. GRANT12686965 and 2019-67017-29591).

About the Author

Dr. Carroll is a computational biologist at the European Molecular Biology Laboratory in Heidelberg, Germany. Her research focuses on developing and utilizing bioinformatic approaches to study the evolution and transmission dynamics of foodborne and zoonotic pathogens. She has specific expertise in the genomics and taxonomy of the *Bacillus cereus* group.

References

1. Stenfors Arnesen LP, Fagerlund A, Granum PE. From soil to gut: *Bacillus cereus* and its food poisoning toxins. FEMS Microbiol Rev. 2008;32:579–606. https://doi.org/10.1111/j.1574-6976.2008.00112.x
2. Baldwin VM. You can't *B. cereus*—a review of *Bacillus cereus* strains that cause anthrax-like disease. Front Microbiol. 2020;11:1731. https://doi.org/10.3389/fmicb.2020.01731
3. Bottone EJ. *Bacillus cereus*, a volatile human pathogen. Clin Microbiol Rev. 2010;23:382–98. https://doi.org/10.1128/CMR.00073-09
4. Jovanovic J, Ornelis VFM, Madder A, Rajkovic A. *Bacillus cereus* food intoxication and toxicoinfection. Compr Rev Food Sci Food Saf. 2021;20:3719–61. https://doi.org/10.1111/1541-4337.12785
5. Tallent SM, Knolhoff A, Rhodehamel EJ, Harmon SM, Bennett RW. *Bacillus cereus*. In: Bacteriological analytical manual (BAM). 8th ed. Silver Spring (MD): Food and Drug Administration; 2019.
6. Carroll LM, Wiedmann M, Kovac J. Proposal of a taxonomic nomenclature for the *Bacillus cereus* group which reconciles genomic definitions of bacterial species with clinical and industrial phenotypes. MBio. 2020;11:e00034–20. https://doi.org/10.1128/mBio.00034-20
7. Carroll LM, Cheng RA, Wiedmann M, Kovac J. Keeping up with the *Bacillus cereus* group: taxonomy through the genomics era and beyond. Crit Rev Food Sci Nutr. 2021:1–26. https://doi.org/10.1080/10408398.2021.1916735
8. Balloux F, Brønstad Brynildsrud O, van Dorp L, Shaw LP, Chen H, Harris KA, et al. From theory to practice: translating whole-genome sequencing (WGS) into the clinic. Trends Microbiol. 2018;26:1035–48. https://doi.org/10.1016/j.tim.2018.08.004
9. Guinebretière MH, Velge P, Couvert O, Carlin F, Debuyser ML, Nguyen-The C. Ability of *Bacillus cereus* group strains to cause food poisoning varies according to phylogenetic affiliation (groups I to VII) rather than species affiliation. J Clin Microbiol. 2010;48:3388–91. https://doi.org/10.1128/JCM.00921-10
10. Liu Y, Du J, Lai Q, Zeng R, Ye D, Xu J, et al. Proposal of nine novel species of the *Bacillus cereus* group. Int J Syst Evol Microbiol. 2017;67:2499–508. https://doi.org/10.1099/ijsem.0.001821
11. Carroll LM, Wiedmann M. Cereulide synthetase acquisition and loss events within the evolutionary history of group III *Bacillus cereus sensu lato* facilitate the transition between emetic and diarrheal foodborne pathogens. MBio. 2020;11:e01263-20. https://doi.org/10.1128/mBio.01263-20
12. Madoroba E, Magwedere K, Chaora NS, Matle I, Muchadeyi F, Mathole MA, et al. Microbial communities of meat and meat products: an exploratory analysis of the

product quality and safety at selected enterprises in South Africa. Microorganisms. 2021;9:507. https://doi.org/10.3390/microorganisms9030507

13. Carroll LM, Pierneef R, Mathole A, Atanda A, Matle I. Genomic surveillance of *Bacillus cereus sensu lato* strains isolated from meat and poultry products in South Africa enables inter- and intra-national surveillance and source tracking. Microbiology Spectrum. 2022;10:e00700--22. https://doi.org/10.1128/spectrum.00700-22

14. Chaumeil PA, Mussig AJ, Hugenholtz P, Parks DH. GTDB-Tk: a toolkit to classify genomes with the Genome Taxonomy Database. Bioinformatics. 2019;btz848. https://doi.org/10.1093/bioinformatics/btz848

Address for correspondence: Laura M. Carroll, EMBL, Meyerhofstraße 1, 69117 Heidelberg, Germany; email: lmc297@cornell.edu

Experimental Infection of *Peromyscus* Species Rodents with Sin Nombre Virus

Kaye Quizon, Kimberly Holloway, Mahmood Iranpour, Bryce M. Warner, Yvon Deschambault, Geoff Soule, Kevin Tierney, Darwyn Kobasa, Angela Sloan, David Safronetz

We demonstrate that 6 distinct *Peromyscus* rodent species are permissive to experimental infection with Sin Nombre orthohantavirus (SNV). Viral RNA and SNV antibodies were detected in members of all 6 species. *P. leucopus* mice demonstrated markedly higher viral and antibody titers than *P. maniculatus* mice, the established primary hosts for SNV.

Orthohantaviruses, a genus of enveloped, segmented, negative-sense, single-stranded RNA viruses, are the cause of hantavirus cardiopulmonary syndrome. Hantavirus species are primarily associated and coevolve with specific rodent host species (*1*,*2*). In North America, Sin Nombre virus (SNV) causes most confirmed cases of hantavirus cardiopulmonary syndrome (*3*) and is primarily maintained in *Peromyscus maniculatus* deer mice (*4*). *P. maniculatus* mice are widely distributed in North America (Figure) and are a complex of subspecies that diverge according to geographic location (*2*,*7*). Likewise, SNV and its related viruses are found to diverge in association with their rodent reservoirs (*1*). Although host switching is thought to be uncommon in SNV (*1*,*2*), other rodent species sharing a geographic site were recently found to carry the virus, potentially acting as additional reservoirs and sources of human infection (*8*). We evaluated the permissiveness of 6 colony-bred *Peromyscus* mouse species, whose founders originated from locations across North America, to infection by SNV originating from New Mexico.

Author affiliations: Public Health Agency of Canada, Winnipeg, Manitoba, Canada (K. Quizon, K. Holloway, M. Iranpour, B.M. Warner, Y. Deschambault, G. Soule, K. Tierney, D. Kobasa, A. Sloan, D. Safronetz); University of Manitoba, Winnipeg (D. Kobasa, D. Safronetz)

DOI: https://doi.org/10.3201/eid2809.220509

The Study

We obtained geographically distinct peromyscine mice (of both sexes and ≥6 weeks of age) from breeding colonies maintained by the *Peromyscus* Genomic Stock Center, University of South Carolina (Columbia, SC, USA) (*P. maniculatus bairdii* prairie deer mouse, *P. maniculatus sonoriensis* Sonoran deer mouse, *P. polionotus subgriseus* Oldfield mouse, *P. leucopus* white-footed or wood mouse, *P. californicus insignis* California mouse), and the University of Manitoba (Winnipeg, Manitoba, Canada) (*P. maniculatus rufinus* deer mouse) (Figure) (*9*). We experimentally infected the mice with SNV strain no. 77734, which had been exclusively passaged in *P. maniculatus rufinus* mice (both the virus and the host used to propagate it originating from New Mexico) as previously described (*9*–*11*). At no point postinoculation did we note any deleterious effects of infection in rodents. We collected tissue samples (lung, heart, spleen, kidney) and either blood (days 7 and 14) or serum (days 21 and 42) samples from mice at 7, 14, 21, and 42 days postinfection (dpi) and evaluated them for the presence of viral (small-segment) RNA (*10*). We performed ELISA on serum samples, as previously described (*12*), to assess seroconversion.

We detected SNV RNA in all 6 species to varying degrees; peak median levels occurred at 21 dpi (Figure 2). The lowest levels of viral RNA (a surrogate metric for permissiveness and viral infection or replication) were in *P. maniculatus sonoriensis*, *P. polionotus*, and *P. californicus* mice. These results align with expectations of *P. californicus* mice, which differ genetically and geographically from *P. maniculatus* mice (Figure). However, patterns of viral detection can vary between *P. maniculatus* mice subspecies. For instance, patterns of viral RNA positivity in *P. maniculatus bairdii* mice were markedly similar to those in *P. maniculatus rufinus* mice, despite the distance between their original

trapping locations. Median viral RNA peaked at 21 dpi and were sustained through 42 dpi; however, only serum was positive at 42 dpi in *P. maniculatus rufinus* mice. *P. maniculatus bairdii* mice founders were trapped in southeastern Michigan (Figure), whereas *P. maniculatus rufinus* mice descended from founders from central and northwestern New Mexico (Figure). *P. leucopus* mice appear to be highly permissive to SNV based on detection of SNV RNA. We observed high levels of viral RNA in serum, heart, kidney, lung, and spleen samples at 21 dpi and 42 dpi. Further studies are required to confirm whether this finding translates to persistent infection, viral shedding, and possible transmission between animals.

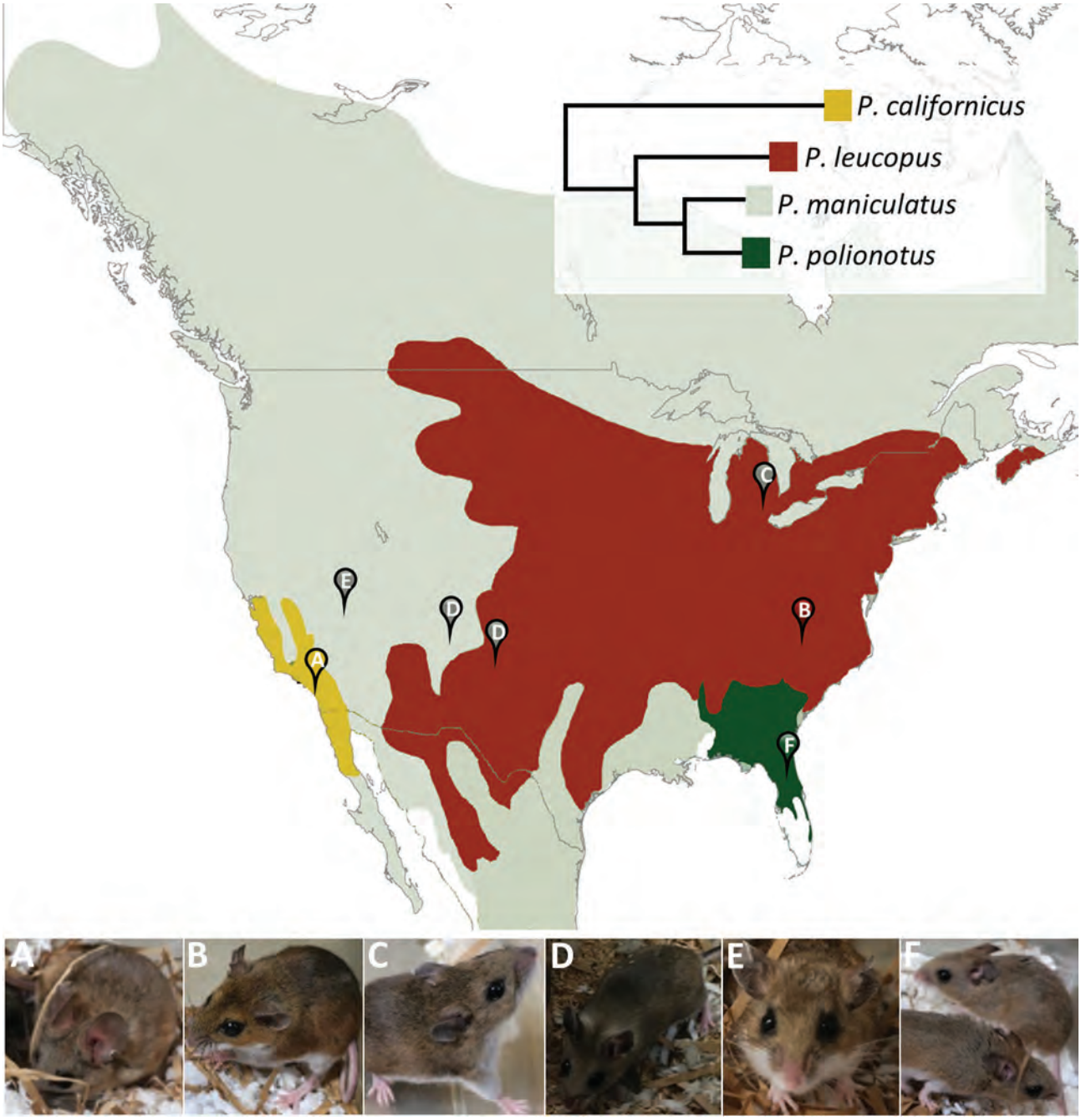

Figure. Geographic distribution of *Peromyscus* mouse species represented in a serologic analysis of serum samples from experimentally infected peromyscine rodents. Pins indicate collection sites of colony founders: *P. californicus* (A), *P. leucopus* (B), *P. maniculatus bairdii* (C), *P. maniculatus rufinus* (D), *P. maniculatus sonoriensis* (E), and *P. polionotus* (F). Inset shows phylogenetic relationships with evolutionary distances estimated by Miller and Engstrom (*5*). Map adapted from Bedford and Hoekstra (*6*).

Table. Summary of serologic analysis of serum samples from peromyscine rodents experimentally infected with Sin Nombre virus*

Day	Sex	*Peromyscus maniculatus rufinus*	*P. m. bairdii*	*P. m. sonoriensis*	*P. leucopus*	*P. polionotus*	*P. californicus*
Day 21	M	2/3	0/3	1/3	3/4	3/3	0/3
	F	3/3	3/3	3/3	3/3	3/3	0/3
	Total	5/6	3/6	4/6	7/7	6/6	0/6
Day 42	M	3/3	3/3	3/3	3/3	4/4	1/3
	F	3/3	3/3	3/3	2/3	3/3	0/3
	Total	6/6	6/6	6/6	5/6	7/7	1/6

*Results shown are the number of seropositive animals per timepoint. Serum samples were tested by using a recombinant Sin Nombre orthohantavirus nucleocapsid-based ELISA for reactive antibodies that used a *P. leucopus* IgG heavy- and light-chain secondary antibody. Titers of ≥100 were considered positive.

Although sex differences have been noted to have little effect on SNV infection in *P. maniculatus rufinus* mice (*10*), differences may exist in other rodent species. The numbers in our study are small; however, the data suggest sex-related differences might occur according to species. For example, male *P. maniculatus bairdii* mice have higher viral RNA titers at 42 dpi, whereas in *P. maniculatus sonoriensis* mice at 21 dpi, almost all positive animals are female. Meanwhile, *P. leucopus* mice showed indiscriminate viral RNA detection between sexes across all timepoints (Appendix Figure, https://wwwnc.cdc.gov/EID/article/28/9/22-0509-App1.pdf). Future studies are required to shed light on this aspect.

P. maniculatus mice were established early on as the primary reservoir for SNV (*4*). However, studies of this virus–host relationship rarely report the host taxon beyond the species level. Moreover, although levels of viral RNA tended to be negligible in the early stages of infection, an observation consistent with previous studies in susceptible animals (*9*,*10*,*13*), the detection of viral RNA at later timepoints probably means members of these species are nonetheless susceptible to SNV infection. That animals were positive at 42 dpi hints at the possibility of persistent infection, although longer-term studies would be needed to confirm.

Antibodies against the SNV nucleoprotein were detected in most serum samples collected from days 21 and 42 from the peromyscine rodents (Table). The lone exception was *P. californicus* mice, for which only a single animal had detectable SNV antibodies. Rates of seroconversion broadly mirrored the rates of detection by quantitative reverse transcription PCR. The development of antibodies reactive to the SNV nucleoprotein appeared to be delayed in male mice from 2 species (*P. maniculatus bairdii* and *P. maniculatus sonoriensis*), and only 1 of 6 of these rodents demonstrated positive serum samples at 21 dpi.

Conclusions

Overall, our data support recent observations from Goodfellow et al. (*8*) that rodents other than *P. maniculatus* mice are capable of carrying SNV without showing signs of disease. In that study, wild-caught members of *P. boylii* mice, *Mus musculus* mice, and *Tamias minimus* chipmunks trapped at 2 sites had detectable SNV RNA in their lung tissues. SNV sequences from these rodents were more similar to each other than to previously reported sequences, suggesting circulation of the virus within these rodent populations.

In our study, we experimentally infected 6 *Peromyscus* mouse species, including 3 that fall under the *P. maniculatus* species complex, and whose founders originate from locations across North America, with a strain of SNV originating from a single wild-caught animal. Although replicating SNV was detected in animals of all 6 species, permissiveness of each species to SNV infection varied. Susceptibility to SNV infection appears to be multifactorial and is not fully explained by characteristics relating to geographic proximity or genetic relatedness. Given the variability in the patterns of infection between subspecies within *P. maniculatus*, future studies should consider reporting the subspecies when studying this virus–host relationship. Furthermore, other *Peromyscus* mouse species may play an important role in the molecular evolution and transmission of SNV. Host-switching events are thought to give rise to SNV variants and even new hantaviral species (*1*,*2*,*14*). That SNV was capable of replicating to high levels in *P. leucopus* mice for sustained periods is notable. The geographic distributions of *P. maniculatus* and *P. leucopus* mice overlap greatly, presenting opportunities for these 2 populations and their respective viruses to come into contact. Together, these regions cover most of North America, including nearly the entirety of the contiguous United States.

These findings demonstrate the importance of broadening our understanding of the SNV–*P. maniculatus* virus–host relationship and highlight the benefit of identifying infected and infectious rodent reservoirs at the subspecies level to help elucidate epizootics and spillover events to humans. Furthermore,

although distinct eastern and western patterns of genetic evolution have been documented in *P. maniculatus* rodents and associated strains of SNV in North America (*1*,*2*), our study suggests that these patterns might not necessarily prevent western lineages of SNV from emerging into eastern populations of peromyscine rodents.

Acknowledgments

We thank Hippokratis Kiaris and Vimala Kaza for assistance with obtaining the mice from the *Peromyscus* Genetic Stock Center.

This work was funded by the Public Health Agency of Canada.

Animal studies were conducted in accordance with the Canadian Council of Animal Care guidelines and an animal use document approved by the Canadian Science Centre for Human and Animal Health's institutional animal care and use committee. Work involving infectious SNV was performed in a Biosafety Level 4 laboratory of the Public Health Agency of Canada. When required, materials were inactivated according to approved procedures for subsequent analysis.

All authors declare no conflict of interest.

About the Author

Ms. Quizon is a laboratory biologist at the Public Health Agency of Canada in Winnipeg. Her primary research interests are zoonoses and the development of diagnostic methods for infectious diseases.

References

1. Drebot MA, Gavrilovskaya I, Mackow ER, Chen Z, Lindsay R, Sanchez AJ, et al. Genetic and serotypic characterization of Sin Nombre–like viruses in Canadian *Peromyscus maniculatus* mice. Virus Res. 2001;75:75–86. https://doi.org/10.1016/S0168-1702(01)00227-1
2. Dragoo JW, Lackey JA, Moore KE, Lessa EP, Cook JA, Yates TL. Phylogeography of the deer mouse (*Peromyscus maniculatus*) provides a predictive framework for research on hantaviruses. J Gen Virol. 2006;87:1997–2003. https://doi.org/10.1099/vir.0.81576-0
3. Warner BM, Dowhanik S, Audet J, Grolla A, Dick D, Strong JE, et al. Hantavirus cardiopulmonary syndrome in Canada. Emerg Infect Dis. 2020;26:3020–4. https://doi.org/10.3201/eid2612.202808
4. Childs JE, Ksiazek TG, Spiropoulou CF, Krebs JW, Morzunov S, Maupin GO, et al. Serologic and genetic identification of *Peromyscus maniculatus* as the primary rodent reservoir for a new hantavirus in the southwestern United States. J Infect Dis. 1994;169:1271–80. https://doi.org/10.1093/infdis/169.6.1271
5. Miller JR, Engstrom MD. The relationships of major lineages within peromyscine rodents: a molecular phylogenetic hypothesis and systematic reappraisal. J Mammal. 2008;89:1279–95. https://doi.org/10.1644/07-MAMM-A-195.1
6. Bedford NL, Hoekstra HE. *Peromyscus* mice as a model for studying natural variation. eLife. 2015;4:e06813. https://doi.org/10.7554/eLife.06813
7. Kalkvik HM, Stout IJ, Doonan TJ, Parkinson CL. Investigating niche and lineage diversification in widely distributed taxa: phylogeography and ecological niche modeling of the *Peromyscus maniculatus* species group. Ecography. 2012;35:54–64. https://doi.org/10.1111/j.1600-0587.2011.06994.x
8. Goodfellow SM, Nofchissey RA, Schwalm KC, Cook JA, Dunnum JL, Guo Y, et al. Tracing transmission of Sin Nombre virus and discovery of infection in multiple rodent species. J Virol. 2021;95:e0153421. https://doi.org/10.1128/JVI.01534-21
9. Botten J, Mirowsky K, Kusewitt D, Bharadwaj M, Yee J, Ricci R, et al. Experimental infection model for Sin Nombre hantavirus in the deer mouse (*Peromyscus maniculatus*). Proc Natl Acad Sci U S A. 2000;97:10578–83. https://doi.org/10.1073/pnas.180197197
10. Warner BM, Stein DR, Griffin BD, Tierney K, Leung A, Sloan A, et al. Development and characterization of a Sin Nombre virus transmission model in *Peromyscus maniculatus*. Viruses. 2019;11:E183. https://doi.org/10.3390/v11020183
11. Safronetz D, Prescott J, Feldmann F, Haddock E, Rosenke R, Okumura A, et al. Pathophysiology of hantavirus pulmonary syndrome in rhesus macaques. Proc Natl Acad Sci U S A. 2014;111:7114–9. https://doi.org/10.1073/pnas.1401998111
12. Warner BM, Sloan A, Deschambault Y, Dowhanik S, Tierney K, Audet J, et al. Differential pathogenesis between Andes virus strains CHI-7913 and Chile-9717869 in Syrian Hamsters. J Virol. 2021;95:108–29. https://doi.org/10.1128/JVI.00108-21
13. Botten J, Mirowsky K, Kusewitt D, Ye C, Gottlieb K, Prescott J, et al. Persistent Sin Nombre virus infection in the deer mouse (*Peromyscus maniculatus*) model: sites of replication and strand-specific expression. J Virol. 2003;77:1540–50. https://doi.org/10.1128/JVI.77.2.1540-1550.2002
14. Black WC IV, Doty JB, Hughes MT, Beaty BJ, Calisher CH. Temporal and geographic evidence for evolution of Sin Nombre virus using molecular analyses of viral RNA from Colorado, New Mexico and Montana. Virol J. 2009;6:102. https://doi.org/10.1186/1743-422X-6-102

Address for correspondence: David Safronetz, Special Pathogens Program, National Microbiology Laboratory Branch, Public Health Agency of Canada, 1015 Arlington St, Winnipeg, MB R3E 3R2, Canada; email: david.safronetz@phac-aspc.gc.ca

Acute Q Fever with Atrioventricular Block, Israel

Karawan Badarni, Miry Blich, Yafit Atiya-Nasagi, Nesrin Ghanem-zoabi

Cardiac involvement in acute Q fever is rare. We report 2 cases of an advanced atrioventricular block in young adult patients in Israel who sought care for acute Q fever without evidence of myocarditis. Q fever should be suspected in unexplained conduction abnormalities, especially in febrile young patients residing in disease-endemic areas.

Q fever is a zoonosis caused by *Coxiella burnetii* bacteria; the main route of infection is through inhalation of infected aerosols (*1*). Acute Q fever is mainly a self-limited influenza-like illness but may manifest as pneumonia or hepatitis. Less common manifestations involve different organs of the nervous, cardiovascular, skin, gastrointestinal, and hematopoietic systems (*2*). Cardiac involvement in Q fever is usually observed in the chronic form and manifests as endocarditis, aortitis, and vascular aneurysm infection. Less common cardiovascular manifestations in acute Q fever include myocarditis, pericarditis, and acute endocarditis (*2*). We report 2 patients in Israel who had acute Q fever and advanced atrioventricular block as the cardiac manifestation.

Patient 1 was a 48-year-old man was admitted to an intensive cardiac care unit (ICCU) for dizziness and electrocardiogram (EKG) abnormalities. He had type 2 diabetes mellitus and hypertension. Ten days before admission, he had fever and myalgia; his symptoms lasted for 1 week and resolved spontaneously. Three days later, he experienced dizziness; he sought care, and an EKG showed a new atrioventricular block.

At admission, the patient's vital signs were within reference ranges except for bradycardia (37 bpm); results of a physical examination was unremarkable. Complete blood count showed decreased hemoglobin (12.5 g/dL) and elevated C-reactive protein. Liver enzyme, cardiac troponin, and coagulation test results were all within reference ranges, and blood cultures were negative. Serology testing for brucellosis was negative. Chest radiograph showed no pathology. His EKG showed a complete atrioventricular block with a ventricular escape rate of 35 bpm and a QRS wave duration of 140 ms (Figure 1). A cardiac evaluation including resting EKG with standard and high leads, 12-lead Holter EKG, and echocardiogram all excluded a channelopathy or cardiomyopathy; cardiac stress testing excluded ischemia. Fluorodeoxyglucose positron emission computed tomography (FDG/PET-CT) showed no pathological uptake in the myocardium or elsewhere in the body. Because of his symptomatic atrioventricular block, a permanent pacemaker was implanted.

The patient had no familial history of cardiac conduction defects or cardiomyopathy. We suspected infectious etiology because of his history of a febrile illness preceding the atrioventricular block occurrence. This patient lived in northern Israel, where Q fever is endemic, and worked in a slaughterhouse. Serology testing for *C. burnetii* demonstrated positive phase II IgM, phase II IgG with a titer of 1:100, and negative phase I IgG. PCR testing for *C. burnetii* (targeting insertion sequence 1111) in serum returned negative results. Repeated serologic testing 4 weeks later demonstrated titers of phase II IgG had increased to 3,200. We used an in-house indirect immunofluorescence assay with a cutoff of 1:100 to diagnose definitive acute Q fever and treated the patient with doxycycline (100 mg 2×/d for 2 weeks). Pacemaker testing 5 months and 12 months later showed no restoration of normal conduction. Repeated serologic testing showed no evidence for progression to chronic disease, and repeated echocardiography and FDG/PET-CT showed no focal infection.

Patient 2 was an otherwise healthy 23-year-old man referred to the ICCU for recurrent episodes of

Author affiliations: Rambam Health Care Campus, Haifa, Israel (K. Badarni, M. Blich, N. Ghanem-zoabi); The Ruth and Bruce Rappaport Faculty of Medicine of Technion, Haifa (M. Blich, N. Ghanem-zoabi); Israel Institute for Biological Research, Ness-Ziona, Israel (Y. Atiya-Nasagi)

DOI: https://doi.org/10.3201/eid2809.212565

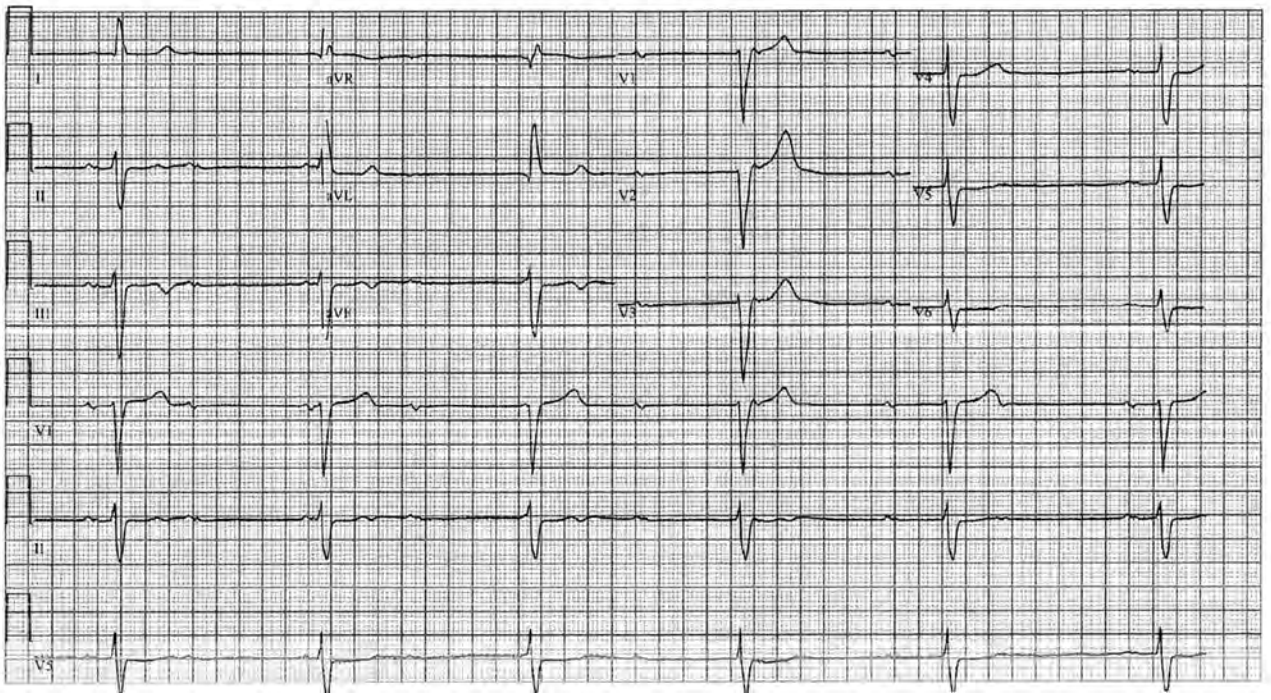

Figure 1. Electrocardiogram of a a 48-year-old patient in Israel with Q fever, showing a complete atrioventricular block with ventricular escape rate of 35 bpm and a QRS duration of 140 ms.

syncope and EKG abnormalities. At admission, his vital signs were within reference ranges except for bradycardia (35 bpm). Results of a physical examination were unremarkable. Results of blood tests including complete blood count, coagulation tests, liver enzymes, C-reactive protein, and cardiac troponin were all within reference ranges. Chest radiograph showed no pathology, but EKG showed a left bundle branch block with sinus bradycardia 35 bpm (Figure 2). Electrophysiologic study demonstrated an infranodal dysfunction. Echocardiography showed a normal heart function; cardiac stress testing excluded ischemia. Cardiac magnetic resonance imaging results ruled out myocardial inflammation or infiltration process. FDG/PET-CT revealed no pathological reuptake. The patient's family history was unremarkable for premature sudden cardiac death, cardiomyopathy, and inherited arrythmias. Other systemic causes for atrioventricular block–like hypothyroidism and hemochromatosis were ruled out. Serologic test results for syphilis and toxoplasmosis were negative.

The patient, who lived in northern Israel, denied direct contact with livestock animals; however, he raised and bred horses. Serologic testing for *C. burnetii* was positive for phase II IgM and IgG, with titers of 1:400 and 1:800 taken at admission and 4 weeks later. Results of testing for phase I IgM and IgG and *C. burnetii* PCR in serum were all negative.

We treated the patient with doxycycline (100 mg 2×/d for 2 weeks). After 10 days of observation, his heart returned to normal sinus rhythm, and no permanent pacing was indicated. The patient was discharged, but no follow-up was completed.

The diagnosis of acute Q fever in patient 1 was considered definitive on the basis of a 4-fold increase in antibody titer in 2 consecutive serum samples (*3*). Patient 2 did not have classic symptoms of Q fever, but his serology profile was consistent with probable acute infection (3). The high titer of phase II IgG in the presence of positive phase II IgM titer is highly suggestive of a recent acute infection (*4*). PCR testing for *C. burnetti* was negative, consistent with the acute setting in which the bacteremia is short and usually precedes antibody formation (*5*). After thorough cardiac evaluation of each patient, we found no alternative diagnosis explaining an advanced atrioventricular block at their young ages.

Conclusions

Myocardial involvement in acute Q fever is rare and reported among 0.5%–1% of cases (*2*,*6*). Cardiac complications include myocarditis, pericarditis, and acute endocarditis (*2*). Patients with myocarditis often seek care for shortness of breath, chest

pain, or heart failure. Cardiac enzymes are usually elevated with or without EKG changes; ST-T segment abnormalities and T-wave inversion are the most frequent. None of these features existed in these patients. The reported course of Q fever myocarditis is prolonged and linked with high mortality rates (*6*).

Acute Q fever endocarditis was suggested as an autoimmune complication in 9/759 patients (1.2%) infected with *C. burnetii*; these patients had valve vegetations detected by echocardiography and positive anticardiolipin antibodies (*7*). The presence of antiphospholipid autoantibodies is known to lead to cardiac damage causing different manifestations, such as coronary artery disease, valve abnormalities, and myocardial dysfunction (*8*). Although rarely described, atrioventricular block can be complicated by these antibodies (*9*). This complication was described in other autoimmune disease, such as systemic lupus erythematosus (*10*). We did not perform evaluation of these patients for anticardiolipin antibodies. However, imaging results showed no vegetations or valve thickening.

Few infectious diseases have a predilection for the conduction system; the most well-recognized one is Lyme disease, in which the atrioventricular block is transient and can be the only cardiac manifestation, as we observed in patient 2. Animal studies in mice infected with *Borrelia burgdorferi*, the causative bacterium of Lyme disease, have demonstrated a higher burden of infection within the heart connective tissue (*11*). Chagas disease, a parasitic tropical disease caused by infection with the parasite *Trypanosoma cruzi*, may manifest with various conduction abnormalities usually accompanying myocarditis (*12*).

The pathophysiology in which the cardiac abnormality was persistent in patient 1 and transient in patient 2 is not fully understood. We hypothesize that either a direct damage of *C. burnetii* to the conduction system or, more likely, an indirect damage through an inflammatory process with or without autoantibodies may have occurred in both patients. This damage was theoretically more critical in patient 1, whose disease course was more severe than that of patient 2 and led to an irreversible atrioventricular block. In areas to which Q fever is endemic, *C. burnetii* should be considered a possible etiology for unexplained conduction disorders in young adults.

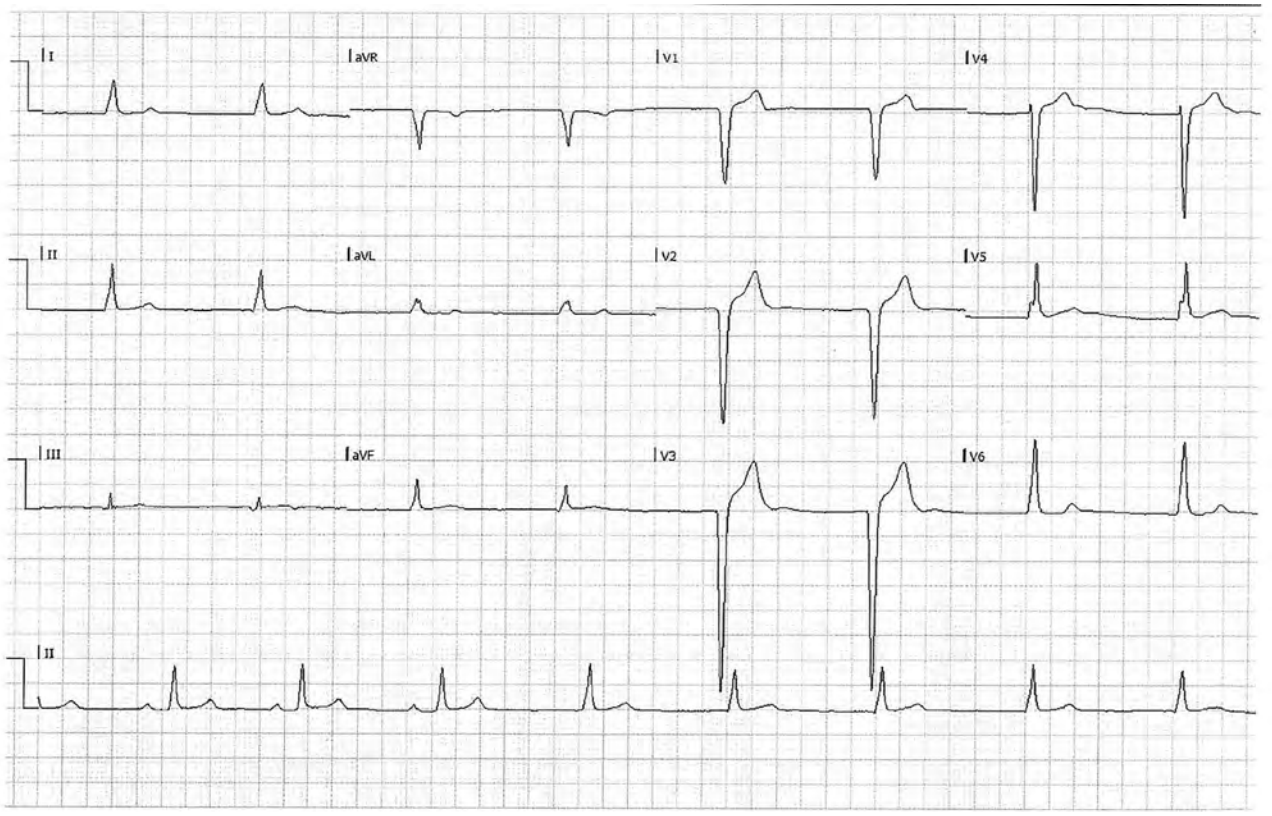

Figure 2. Electrocardiogram of a 23-year-old patient in Israel with Q fever, showing a left bundle branch block with sinus bradycardia of 35 bpm.

About the Author

Dr. Badarni is an internal medicine specialist and fellow in the intensive care division, Rambam Health Care Campus, Haifa, Israel. She works in cooperation with the infectious diseases unit. Her primary research interest is infectious diseases affecting patients in the intensive care unit.

References

1. Georgiev M, Afonso A, Neubauer H, Needham H, Thiery R, Rodolakis A, et al. Q fever in humans and farm animals in four European countries, 1982 to 2010. Euro Surveill. 2013;18:20407. https://doi.org/10.2807/ese.18.08.20407-en
2. Eldin C, Mélenotte C, Mediannikov O, Ghigo E, Million M, Edouard S, et al. From Q fever to *Coxiella burnetii* infection: a paradigm change. Clin Microbiol Rev. 2017;30:115–90. https://doi.org/10.1128/CMR.00045-16
3. Anderson A, Bijlmer H, Fournier P-E, Graves S, Hartzell J, Kersh GJ, et al. Diagnosis and management of Q fever—United States, 2013: recommendations from CDC and the Q Fever Working Group. MMWR Recomm Rep. 2013; 62(RR-03):1–30.
4. Dupont HT, Thirion X, Raoult D. Q fever serology: cutoff determination for microimmunofluorescence. Clin Diagn Lab Immunol. 1994;1:189–96. https://doi.org/10.1128/cdli.1.2.189-196.1994
5. Schneeberger PM, Hermans MHA, van Hannen EJ, Schellekens JJA, Leenders ACAP, Wever PC. Real-time PCR with serum samples is indispensable for early diagnosis of acute Q fever. Clin Vaccine Immunol. 2010;17:286–90. https://doi.org/10.1128/CVI.00454-09
6. Fournier PE, Etienne J, Harle JR, Habib G, Raoult D. Myocarditis, a rare but severe manifestation of Q fever: report of 8 cases and review of the literature. Clin Infect Dis. 2001;32:1440–7. https://doi.org/10.1086/320159
7. Million M, Thuny F, Bardin N, Angelakis E, Edouard S, Bessis S, et al. Antiphospholipid antibody syndrome with valvular vegetations in acute Q fever. Clin Infect Dis. 2016;62:537–44. https://doi.org/10.1093/cid/civ956
8. Kolitz T, Shiber S, Sharabi I, Winder A, Zandman-Goddard G. Cardiac manifestations of antiphospholipid syndrome with focus on its primary form. Front Immunol. 2019;10:941. https://doi.org/10.3389/fimmu.2019.00941
9. Soubrier M, Prudat M, Marcaggi X, Lamaison D, Dubost JJ, Sauvezie B. [Antiphospholipid antibodies revealed by an atrioventricular conduction disorder] [in French]. Presse Med. 1991;20:1626–8.
10. Tincani A, Biasini-Rebaioli C, Cattaneo R, Riboldi P. Nonorgan specific autoantibodies and heart damage. Lupus.2005;14:656–9. https://doi.org/10.1191/0961203305lu2194oa
11. Armstrong AL, Barthold SW, Persing DH, Beck DS. Carditis in Lyme disease susceptible and resistant strains of laboratory mice infected with *Borrelia burgdorferi*. Am J Trop Med Hyg. 1992;47:249–58. https://doi.org/10.4269/ajtmh.1992.47.249
12. Elizari MV, Chiale PA. Cardiac arrhythmias in Chagas heart disease. J Cardiovasc Electrophysiol. 1993;4:596–608. https://doi.org/10.1111/j.1540-8167.1993.tb01247.x

Address for correspondence: Karawan Badarni, Intensive Care Division, Rambam Health Care Campus, HaAliya HaShniya St 8, PO Box 9602 Haifa 31096, Israel; email: karawanb@gmail.com

Sporadic Occurrence of Enteroaggregative Shiga Toxin–Producing *Escherichia coli* O104:H4 Similar to 2011 Outbreak Strain

Claudia E. Coipan, Ingrid H. Friesema, Maaike J.C. van den Beld, Thijs Bosch, Sabine Schlager, Menno van der Voort, Christina Frank, Christina Lang, Angelika Fruth, Eelco Franz

We describe the recent detection of 3 Shiga toxin–producing enteroaggregative *Escherichia coli* O104:H4 isolates from patients and 1 from pork in the Netherlands that were genetically highly similar to isolates from the 2011 large-scale outbreak in Europe. Our findings stress the importance of safeguarding food supply production chains to prevent future outbreaks.

Shiga toxin–producing *Escherichia coli* (STEC) is a zoonotic pathogen that causes illness ranging from mild diarrhea to hemolytic uremic syndrome and death. During 2011, an exceptionally large outbreak caused by serotype O104:H4 STEC occurred in Europe, mainly in Germany and France, that was associated with sprouts grown from imported fenugreek seeds (*1*). Besides the ability to produce Shiga toxin, specifically *stx2a*, the strain had the genetic characteristics and phylogenetic backbone of an enteroaggregative *E. coli* (EAEC) pathotype (*2*) but lacked other classical STEC virulence markers *eae* and *hlyA* (*3*). In addition, the outbreak strain carried plasmid-borne $bla_{\text{CTX-M-15}}$ and $bla_{\text{TEM-1}}$ genes. The epidemiologic investigation revealed that a contaminated batch of fenugreek seeds imported into the European Union from Egypt was the most probable source of the pathogen causing the outbreak (*4*).

After the 2011 outbreak in Germany and France, only a few sporadic cases of infection with Shiga toxin–producing EAEC O104:H4 were reported, most related to travel to Turkey or North Africa (*5*–*8*). We describe the sporadic occurrence of Shiga toxin–producing EAEC O104:H4 isolates in the Netherlands, originating from 2 clinical cases from 2019 and 2020 and 1 food isolate from 2017. In addition, we report a clinical case from Austria in 2021.

The Study

Surveillance of Shiga toxin–producing *E. coli* (STEC) in the Netherlands is performed in 1 or both of 2 ways: by mandatory case notification from medical laboratories or physicians to regional public health services, which then report the cases to the Netherlands National Institute for Public Health and the Environment (RIVM), or by microbiological surveillance, when medical laboratories send suspected STEC isolates to RIVM for confirmation and further molecular characterization. Since 2016, STEC isolates have been subjected to whole-genome sequencing for high-resolution detection of clusters and outbreaks nationwide. During detailed retrospective analysis of the whole-genome sequencing data, we identified isolates from 2 clinical cases of STEC infection from 2019 and 2020 and characterized them as *stx2a*-encoding EAEC O104:H4 (isolates NL1981 and NL2076). Both cases involved middle-aged nonhospitalized women with abdominal cramps and bloody diarrhea. Neither of the 2 case-patients reported recent travel. The 2019 case-patient reported consuming cooked minced beef, and the 2020 case-patient reported consuming beef, hamburger meat, and vegetables and fruits from her own garden. In 2021, the Austrian Agency for Health and Food Safety obtained a sample of similar *stx2a*-encoding EAEC O104:H4 from a 10-year-old girl with hemolytic uremic syndrome. This case-patient also reported no recent travel, but she had consumed raw

Author affiliations: National Institute for Public Health and the Environment (RIVM), Bilthoven, the Netherlands (C.E. Coipan, I.H. Friesema, M.J.C. van den Beld, T. Bosch, E. Franz); Agency for Health and Food Safety (AGES), Graz, Austria (S. Schlager); Wageningen Food Safety Research, Wageningen, the Netherlands (M. van der Voort); Robert Koch Institute, Berlin, Germany (C. Frank); Robert Koch Institute, Wernigerode, Germany (C. Lang, A. Fruth)

DOI: https://doi.org/10.3201/eid2809.220037

veal. Finally, we retrospectively identified *stx2a*-encoding EAEC O104:H4 in a sample obtained from pig meat (pork) in 2017 in the Netherlands.

We performed a genomic comparison among the recently identified isolates, 2 Shiga toxin–producing EAEC O104:H4 isolates in cases from the Netherlands from 2013 described elsewhere (*8*), and a set of representative isolates from a 2011 outbreak in Germany and France, including isolates from case-patients in Germany who shed the outbreak strain well into 2012 (long-term shedders). To achieve our full set of isolates (Table), we supplemented the dataset with O104:H4 isolates retrieved from public repositories to gain more insights into the relatedness among investigated isolates and track possible evolutionary events. We assessed genomic relations between isolates by core- and accessory-genome multilocus sequence typing using the Enterobase STEC schema implemented in Ridom Seqsphere version 8.0.1 (https://www.ridom.de). The resulting dendrogram was rooted with strain 1060_13, a Clermont type A isolate. The 2020 patient isolate from the Netherlands (NL2076) and the pork isolate (ESBL3427) clearly clustered with the representative outbreak isolates (Figures 1, 2). Conversely, patient isolates NL1981 from the Netherlands in 2019 and MRV-21-00239 from Austria in 2021 appeared more similar to each other and the 2 patient isolates (338 and 381_1) from the Netherlands in 2013 than to isolates from the outbreak cluster (Figures 1, 2).

We determined the content of the plasmid, virulence, and antimicrobial resistance genes using the PlasmidFinder, VirulenceFinder, and ResFinder databases (http://www.genomicepidemiology.org). Within the outbreak cluster, including the patient (NL2076) and pork (ESBL3427) strains from the

Table. Overview of strains used in study of enteroaggregative Shiga toxin–producing *Escherichia coli* O104:H4 from the Netherlands*

Strain	Country	Source	Year	Reference/source
11-4632-C2	France	Patient	2011	(*13*)
11-3798	Germany	Patient	2011	(*13*)
11-02030	Germany	Patient	2011	(*13*)
11-02033	Germany	Patient	2011	(*13*)
11-02092	Germany	Patient	2011	(*13*)
11-02093	Germany	Patient	2011	(*13*)
11-02281	Germany	Patient	2011	(*13*)
11-06811	Germany	Patient	2011	(*14*)
F338	Netherlands	Patient	2013	(*8*)
381-1	Netherlands	Patient	2013	(*8*)
12-01621	Germany	Long-term shedder	2012	†
12-02462	Germany	Long-term shedder	2012	†
12-05378	Germany	Long-term shedder	2012	†
ESBL3427	Netherlands	Pork	2017	†
NL1981	Netherlands	Patient	2019	†
NL2076	Netherlands	Patient	2020	†
MRV-21-00239	Austria	Patient	2021	†
2015EL-1494M1	United States	Human	NA	Enterobase
TIAC1951	Belgium	NA	2003	Enterobase
09-7901	France	NA	2009	Enterobase
2012C-3196	United States	NA	2012	Enterobase
FORC_069	South Korea	Human	2016	Enterobase
PSU-0479	South Korea	NA	2000	Enterobase
NCCP15648	South Korea	Human	2001	Enterobase
1060_13	United Kingdom	Human	2014	Enterobase
55989	Central African Republic	Human	2002	Enterobase
201909204	France	Human	2019	Enterobase
216_13	United Kingdom	Human	2014	Enterobase
SCPM-O-B-9428	Russia	Human	2018	Enterobase
SCPM-O-B-9427	Russia	Human	2018	Enterobase
201600757	France	Human	2016	Enterobase
2011C-3907	United States	NA	2011	Enterobase
2012C-3808	United States	Human	2012	Enterobase
2014C-3008	United States	NA	2013	Enterobase
E90/11	Germany	Human	2011	Enterobase
GOS1	NA	Human	2011	NCBI
H112180541	United Kingdom	Human	2011	NCBI
H112180283	United Kingdom	Human	NA	NCBI
H112180540	United Kingdom	Human	NA	NCBI
11-02913	Germany	Human	2011	Enterobase

*NA, not available; NCBI, National Center for Biotechnology Information.
†Genome sequence raw data files are available from the European Nucleotide Archive (projects PRJNA174138 and PRJEB49642).

Netherlands, isolates showed virulence profiles typical of the 2011 outbreak strain, including STEC virulence markers *stx2a, lpfA,* and *iha*; the EAEC pAA plasmid (with *aggR*, *aar*, *aap*, *sepA*, the *aatPABCD* operon, and the *aggABCD* operon); and some chromosomal EAEC markers such as *pic* and *sigA*, but they lacked the STEC hallmark intimin *eae*. In addition, the isolates within the outbreak cluster showed similar antimicrobial resistance profiles, including $bla_{\text{CTX-M-15}}$ and $bla_{\text{TEM-1B}}$. Exceptions were the 2012 isolates from long-term shedders in Germany, which lost the pAA plasmid but belong to the outbreak cluster on the basis of their core genome (*9*) (Figure 1). Ancestral trait reconstruction as implemented in the R package ape v.5.5 (*10*), indicated a high likelihood that the most recent common ancestor of the isolates identified in this study were lysogenized with an *stx*-encoding phage. Among the isolates in the outbreak cluster, the core-genome allelic distance was 0–15 alleles (Figure 2).

Conclusions

After the 2011 outbreak in Europe, only a few sporadic cases of infection with *stx*-producing EAEC O104:H4 strains, most related to travel to Turkey or North Africa (*8*,*11*), were reported. The fact that the particular EAEC O104:H4 strains have never convincingly been isolated from food, animal, or environmental sources, and that EAEC in general are primarily human-adapted (*12*), support the hypothesis of a human reservoir and potential multiple events of import by travelers from an area where this pathogen is endemic. On the other hand, the loss of essential virulence markers in

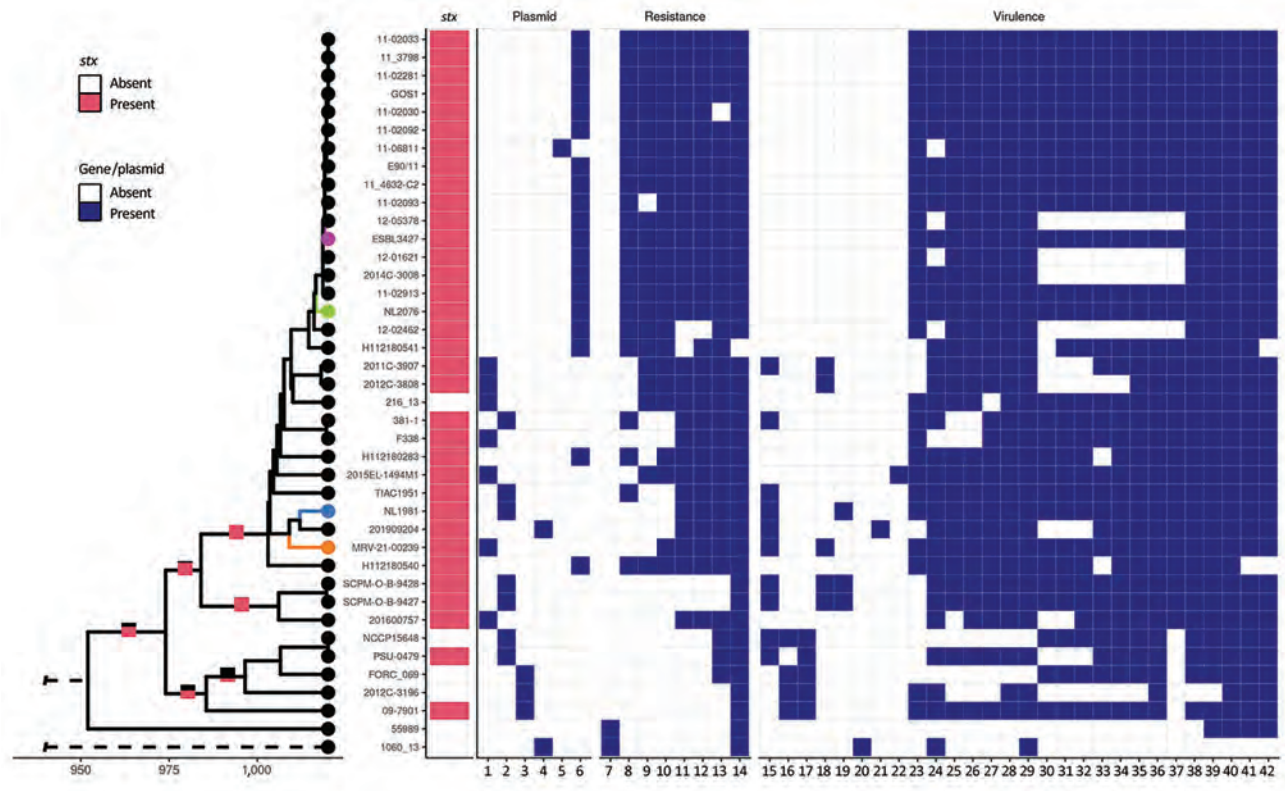

Figure 1. Single-linkage hierarchical clustering tree of enteroaggregative Shiga toxin–producing *Escherichia coli* O104:H4 from the Netherlands and reference sequences. Tree results from core- and accessory-genome multilocus sequence typing with a heatmap indicating presence or absence of *stx*-encoding bacteriophage, plasmids, resistance, and virulence genes. Only genes present in at least 1 isolate are depicted. Colored isolates are those added during this study: green indicates the patient isolate from the Netherlands in 2020, purple the pork isolate from the Netherlands in 2017, blue the patient isolate from the Netherlands in 2019, orange the patient isolate from Austria in 2021. The stacked bar plots on a few selected branches in the tree indicate the likelihood at the downstream nodes of having contained an *stx*-encoding phage (black: absence, pink: presence). Lane 1, IncFII(prSB107); lane 2, IncB/O/K/Z; lane 3, IncFIB(AP001918); lane 4, IncFII; lane 5, Col(BS512); lane 6, IncI1-I(Alpha); lane 7, *tet(B)*; lane 8, $bla_{\text{CTM-M-15}}$; 9, *tet(A)*; lane 10, *aph*(3″)-Ib, *aph*(6)-Id, *sul2*; lane 11, *dfrA7*; lane 12, *qacE*, *sul1*; lane 13, $bla_{\text{TEM-1B}}$; lane 14, *formA*, mdf(A); lane 15, *traT*; lane 16, *agg3A*, *agg3D*; lane 17, *agg3B*, *agg3C*, *astA*; lane 18, *iss*; lane 19, *celb*; lane 20, *aadA1*, *aadA2b*, *ant*(3″)-Ia, $bla_{\text{OXA-1}}$, *catA1*, *eatA*; lane 21, *ireA*; lane 22, *hra*; lane 23, *neuC*; lane 24, *gad*; lane 25, *mchB*; lane 26, *mchC*; lane 27, *stx2A*, *stx2B*; lane 28, *aaiC*, *capU*, *iucC*, *lpfA*; lane 29, *terC*; lane 30, *aatA*; lane 31, ORF3; lane 32, ORF4; lane 33, *aap*; lane 34, *aggR*; lane 35, *aar*; lane 36, *afaD*; lane 37, *aggA*, *aggB*, *aggC*, *aggD*, *sepA*; lane 38, *mchF*; lane 39, *iha*; lane 40, *iutA*, *pic*, *sigA*; lane 41, *fyuA*; lane 42, *irp2*. ESBL, extended spectrum β-lactamase; ORF, open reading frame.

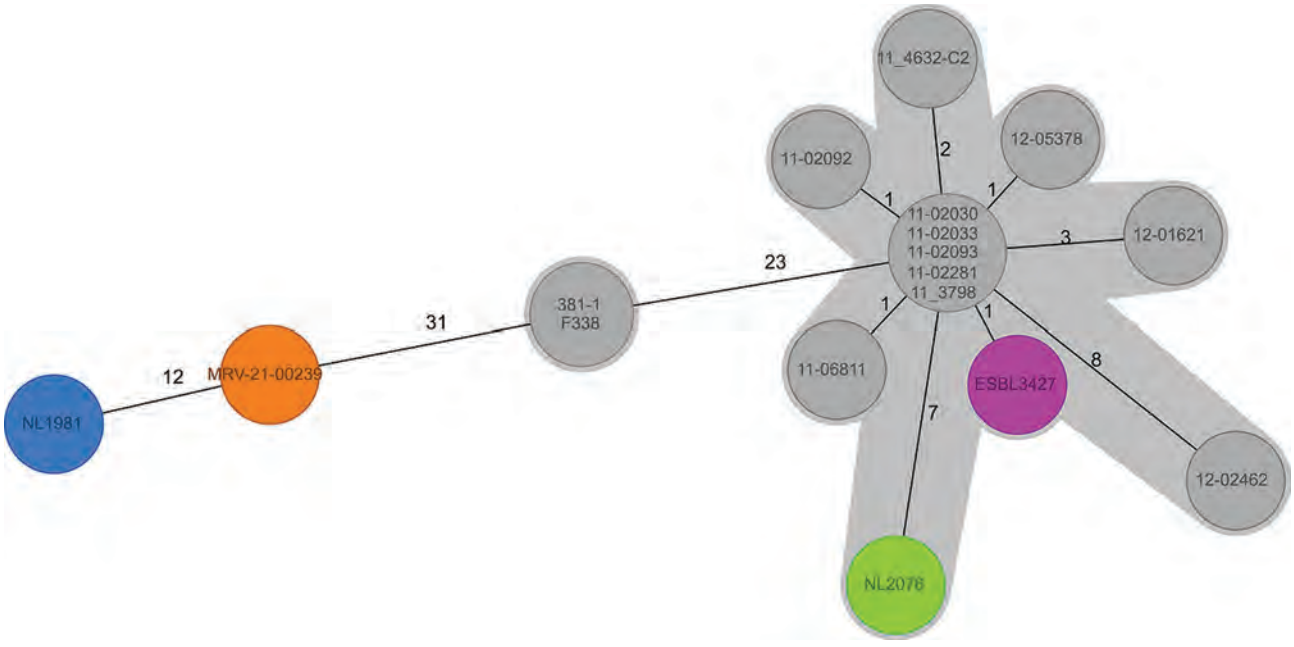

Figure 2. Minimum-spanning tree from cgMLST (Enterobase STEC scheme) of enteroaggregative Shiga toxin–producing *Escherichia coli* O104:H4 from the Netherlands and reference sequences. Colored isolates are those added during this study: green indicates the patient isolate from the Netherlands in 2020, purple the pork isolate from the Netherlands in 2017, blue the patient isolate from the Netherlands in 2019, orange the patient isolate from Austria in 2021. The gray-shaded area connects strains that have an allelic distance <10. ESBL, extended spectrum β-lactamase.

long-term shedders might be a preview of common trends of bacterial genome reduction in long-term carriage in humans which, in turn, might indicate that the newly signaled isolates are maintained in niches other than the human one. Genomic analysis of several post-outbreak EAEC O104:H4 isolates suggests that they are not derived from the 2011 outbreak but share a recent common ancestor (*13*). Our analysis indicates that distinct more- or less-distant variants of Shiga toxin–producing EAEC O104:H4 are circulating worldwide. These variants are more likely to represent independent evolutionary events than continuous diversification of a single clade established and circulating in Europe after the large 2011 outbreak (*14*). In the absence of any previous indication of Shiga toxin–producing EAEC O104:H4 in animals, it was surprising to retrieve such an isolate from a pork product. However, this finding does not necessarily imply that pigs are a reservoir, because the contamination could also have originated from a food handler or contaminated feed rather than the pigs.

In conclusion, we show that Shiga toxin–producing EAEC O104:H4 isolates highly related to the 2011 outbreak strain are sporadically occurring in Europe. We emphasize the need to optimize safeguarding vulnerable chains of food production to prevent future outbreaks.

Acknowledgments

The authors thank GGD, the Dutch municipal health services, for interviewing the STEC case-patients and the MML medical laboratories for submitting STEC isolates for additional typing. We thank Kees Veldman for his assistance in tracking the food strain history, reculturing the strain for whole genome sequencing, and reviewing the manuscript.

About the Author

Dr. Coipan is a genomic epidemiologist in the department of epidemiology and surveillance of enteric infections and zoonoses. Her primary research focus is the integration of bioinformatics, microbial ecology, population genetics, and classical epidemiology to understand origins and spread of pathogens.

References

1. Buchholz U, Bernard H, Werber D, Böhmer MM, Remschmidt C, Wilking H, et al. German outbreak of *Escherichia coli* O104:H4 associated with sprouts. N Engl J Med. 2011;365:1763–70. https://doi.org/10.1056/NEJMoa1106482
2. Scheutz F, Nielsen EM, Frimodt-Møller J, Boisen N, Morabito S, Tozzoli R, et al. Characteristics of the enteroaggregative Shiga toxin/verotoxin-producing *Escherichia coli* O104:H4 strain causing the outbreak of haemolytic uraemic syndrome in Germany, May to June 2011. Euro Surveill. 2011;16:19889. https://doi.org/10.2807/ese.16.24.19889-en

3. Bielaszewska M, Mellmann A, Zhang W, Köck R, Fruth A, Bauwens A, et al. Characterisation of the *Escherichia coli* strain associated with an outbreak of haemolytic uraemic syndrome in Germany, 2011: a microbiological study. Lancet Infect Dis. 2011;11:671–6. https://doi.org/10.1016/S1473-3099(11)70165-7
4. EFSA. Shiga toxin-producing *E. coli* (STEC) O104:H4 2011 outbreaks in Europe: taking stock. EFSA J. 2011;9:2390. https://doi.org/10.2903/j.efsa.2011.2390
5. Jourdan-da Silva N, Watrin M, Weill FX, King LA, Gouali M, Mailles A, et al. Outbreak of haemolytic uraemic syndrome due to Shiga toxin-producing *Escherichia coli* O104:H4 among French tourists returning from Turkey, September 2011. Euro Surveill. 2012;17:20065. https://doi.org/10.2807/ese.17.04.20065-en
6. Frank C, Milde-Busch A, Werber D. Results of surveillance for infections with Shiga toxin-producing *Escherichia coli* (STEC) of serotype O104:H4 after the large outbreak in Germany, July to December 2011. Euro Surveill. 2014;19:20760. https://doi.org/10.2807/1560-7917.ES2014.19.14.20760
7. Guy L, Jernberg C, Arvén Norling J, Ivarsson S, Hedenström I, Melefors Ö, et al. Adaptive mutations and replacements of virulence traits in the *Escherichia coli* O104:H4 outbreak population. PLoS One. 2013;8:e63027. https://doi.org/10.1371/journal.pone.0063027
8. Ferdous M, Zhou K, de Boer RF, Friedrich AW, Kooistra-Smid AM, Rossen JW. Comprehensive characterization of *Escherichia coli* O104:H4 isolated from patients in the Netherlands. Front Microbiol. 2015;6:1348. https://doi.org/10.3389/fmicb.2015.01348
9. Zhang W, Bielaszewska M, Kunsmann L, Mellmann A, Bauwens A, Köck R, et al. Lability of the pAA virulence plasmid in *Escherichia coli* O104:H4: implications for virulence in humans. PLoS One. 2013;8:e66717. https://doi.org/10.1371/journal.pone.0066717
10. Paradis E, Schliep K. ape 5.0: an environment for modern phylogenetics and evolutionary analyses in R. Bioinformatics. 2019;35:526–8. https://doi.org/10.1093/bioinformatics/bty633
11. Grad YH, Godfrey P, Cerquiera GC, Mariani-Kurkdjian P, Gouali M, Bingen E, et al. Comparative genomics of recent Shiga toxin–producing Escherichia coli O104:H4: short-term evolution of an emerging pathogen. MBio. 2013;4:e00452–12. https://doi.org/10.1128/mBio.00452-12
12. Okeke IN, Wallace-Gadsden F, Simons HR, Matthews N, Labar AS, Hwang J, et al. Multi-locus sequence typing of enteroaggregative *Escherichia coli* isolates from Nigerian children uncovers multiple lineages. PLoS One. 2010;5:e14093. https://doi.org/10.1371/journal.pone.0014093
13. Grad YH, Lipsitch M, Feldgarden M, Arachchi HM, Cerqueira GC, Fitzgerald M, et al. Genomic epidemiology of the *Escherichia coli* O104:H4 outbreaks in Europe, 2011. Proc Natl Acad Sci U S A. 2012;109:3065–70. https://doi.org/10.1073/pnas.1121491109
14. Tietze E, Dabrowski PW, Prager R, Radonic A, Fruth A, Auraß P, et al. Comparative genomic analysis of two novel sporadic Shiga toxin–producing *Escherichia coli* O104:H4 strains isolated 2011 in Germany. PLoS One. 2015;10:e0122074. https://doi.org/10.1371/journal.pone.0122074

Address for correspondence: Eelco Franz, Antonie van Leeuwenhoeklaan 9, 3721 MA Bilthoven, Netherlands; email: eelco.franz@rivm.nl

Sequestration and Destruction of Rinderpest Virus–Containing Material 10 Years after Eradication

Christine M. Budke, Dirk U. Pfeiffer, Bryony A. Jones, Guillaume Fournié, Younjung Kim, Mariana Marrana, Heather L. Simmons

In 2021, the world marked 10 years free from rinderpest. The United Nations Food and Agriculture Organization and World Organisation for Animal Health have since made great strides in consolidating, sequencing, and destroying stocks of rinderpest virus–containing material, currently kept by only 14 known institutions. This progress must continue.

In 2011, ten years after the last confirmed outbreak, the Food and Agriculture Organization of the United Nations (FAO) and the World Organisation for Animal Health (WOAH, formerly OIE) jointly declared global freedom from rinderpest. Rinderpest, also known as cattle plague, is only the second infectious disease eradicated from the world, smallpox being the first. Over the 10 years since eradication, the main goal of the Rinderpest Post-Eradication Programme (https://www.woah.org/en/disease/rinderpest) has been to track and reduce global stocks of rinderpest virus–containing material (RVCM).

RVCM comprises field and laboratory strains of rinderpest virus; vaccine strains of rinderpest virus, including valid and expired vaccine stocks; tissues, serum, and other clinical material from infected or suspect animals; diagnostic material containing or encoding live virus; recombinant morbilliviruses (segmented or nonsegmented) containing unique rinderpest virus nucleic acid or amino acid sequences; and full-length genomic material, including from virus RNA and cDNA copies of virus RNA. Subgenomic fragments of morbillivirus nucleic acid not capable of incorporation into a replicating morbillivirus or morbillivirus-like viruses are not considered RVCM.

Accounting for remaining RVCM is critical to limit the risk for reintroducing the pathogen by intentional or inadvertent release from a laboratory (*1*). In support of this effort, in 2015, FAO and WOAH started the Sequence and Destroy project, which enabled whole-genome sequencing of rinderpest virus (RPV) isolates before their destruction. Participating institutes were expected to deposit the genome sequences into publicly accessible databases. In addition, FAO has provided hands-on assistance and remote support to destroy viral stocks in Africa and Asia and led organization of >5 global and regional advocacy meetings. During June–October 2021, a review was conducted to mark progress towards RVCM sequestration and destruction 10 years after eradication. We report the main findings of this review.

The Study

In 2011, a total of 150 countries were surveyed regarding their RVCM stocks (*2*). At that time, 35 countries (44 laboratories) reported keeping RVCM. In 2013, WOAH began annual surveys of institutes keeping RVCM. In 2013, a total of 23 countries reported keeping RVCM; 13 kept live virulent virus and 19 live-attenuated virus in the form of vaccine (n = 17) or seedstock (n = 17), and 9 countries kept both virulent virus and vaccine. Because FAO and WOAH worked with members to eliminate or transfer RVCM stocks, the number of countries keeping RVCM had decreased to 12 (14 institutes) as of 2021 (Figure). In addition, FAO/WOAH designated some of these institutes either

Author affiliations: Texas A&M University, College Station, Texas, USA (C.M. Budke); Texas A&M AgriLife Research, College Station (C.M. Budke, H.L. Simmons); Royal Veterinary College, London, UK (D.U. Pfeiffer, G. Fournié); City University of Hong Kong, Hong Kong (D.U. Pfeiffer, Y. Kim); Animal and Plant Health Agency, Weybridge, UK (B.A. Jones); University of Sussex, Brighton, UK (Y. Kim); World Organisation for Animal Health, Paris, France (M. Marrana)

DOI: https://doi.org/10.3201/eid2809.220297

category A or B or dual-category rinderpest-holding facilities (RHFs) (https://www.oie.int/en/disease/rinderpest/#ui-id-3). Category A RHFs are designated for storing RVCM, excluding vaccine stocks; category B RHFs are approved for storing only manufactured vaccines and materials for their production.

To confirm that no relevant findings unknown to WOAH had been published by research groups or laboratories, we reviewed the scientific literature to identify any publications about rinderpest virus research undertaken since 2011. A search of 21 databases identified 623 unique publications of which we evaluated 17 at the full-text level (Appendix Table 1, https://wwwnc.cdc.gov/EID/article/28/9/22-0297-App1.pdf). The search identified no institutes conducting work with RVCM not already known to WOAH. Nine (53%) of 17 reviewed studies were conducted in facilities that are FAO/WOAH-designated RHFs; 4/17 were published in 2011. Besides genome sequencing data, the main finding from recent research was that vaccination of cattle with peste des petits ruminants virus (PPRV) does not provide protective immunity against RPV (*3*), leading to the decision to maintain and even expand global contingency stocks of RPV vaccine (Appendix Table2).

Members of the study team contacted a representative from each institute known by WOAH to keep RVCM as of August 2021 to arrange an interview to discuss current and historic RVCM stocks and laboratory biosecurity. Interviews were conducted remotely and accompanied by completion of a structured questionnaire. All institutes keeping RVCM, except for 1 located in the Middle East, responded to the request for an interview. Because of logistical difficulties and COVID-19–related challenges, interviews were not conducted with institutes in 2 countries in Europe. Therefore, during August 8–September 17, 2021, interviews proceeded with 11 of the 14 institutes known to keep RVCM. Several of the institute directors contacted were not familiar with the specific content of their RVCM stocks and indicated that these materials were simply in

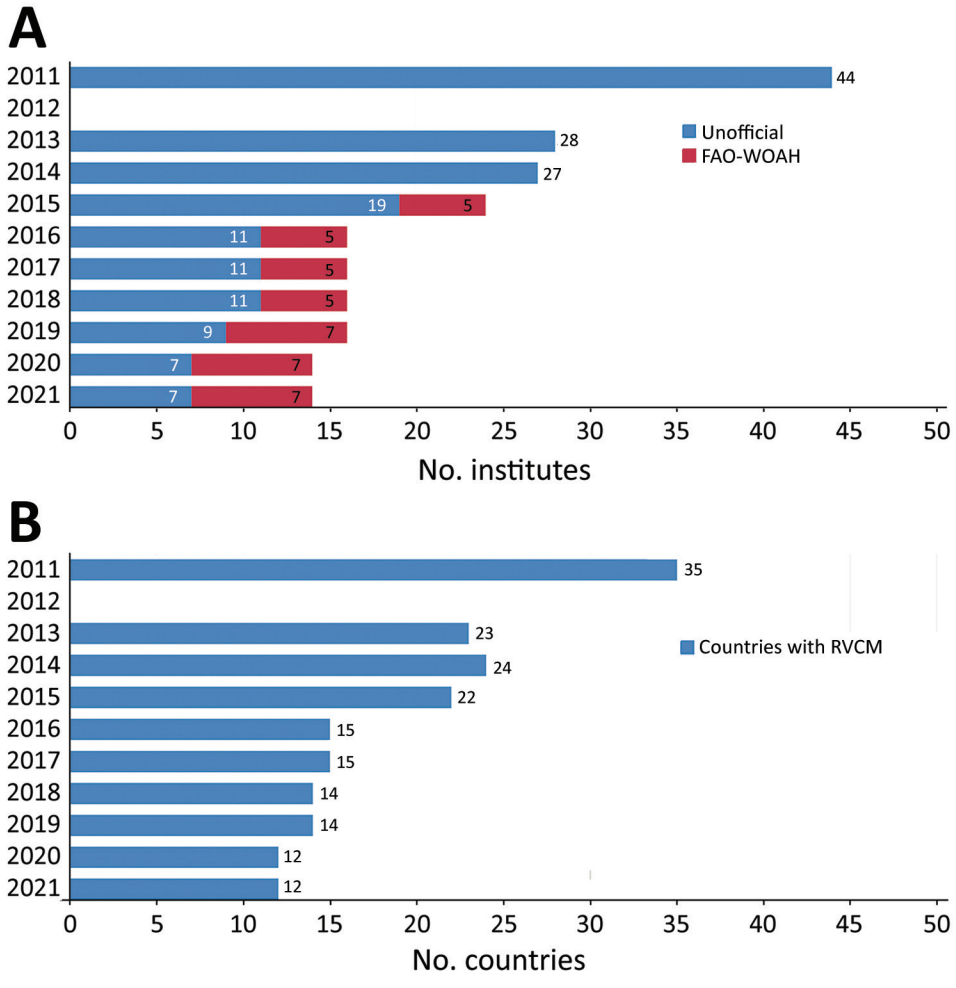

Figure. Number of institutes (A) and countries (B) keeping RVCM, by year, 2011 and 2013–2021. Data from 2011 are based on a single study, whereas data for 2013–2021 are based on WOAH country reports and institute director interviews (2021). FAO, Food and Agriculture Organization of the United Nations; RVCM, rinderpest virus–containing material; WOAH, World Organisation for Animal Health.

Table. Regional institutes with rinderpest virus–containing material, by biosafety level and type, for 2013 and 2021*

Category	Africa	Asia, Far East, and Oceania	Europe	Middle East	The Americas	World
Biologic safety level						
2	3/0	1/2	0/0	1/1	1/0	6/3
2+	0/0	0/1	0/0	0/0	0/0	0/1
3	4/1	9/3	3/3	0/0	2/1	18/8
3+	0/0	0/0	1/1	0/0	0/0	1/1
4	0/1	0/0	2/0	0/0	0/0	2/1
Unknown	1/0	0/0	0/0	0/0	0/0	1/0
Type						
A	0/0	0/1	0/1	0/0	0/1	0/3
B	0/0	0/1	0/0	0/0	0/0	0/1
A/B	0/1	0/1	0/1	0/0	0/0	0/3
Unofficial	8/1	10/3	6/2	1/1	3/0	28/7
Overall	8/2	10/6	6/4	1/1	3/1	28/14

*Values are given as 2013/2021 numbers.

storage, which is concerning because of the critical nature of these materials. At present, Africa is the only region actively attempting to consolidate its RVCM into a single facility.

According to Resolution 18, passed in 2011 during the 79th general session of the World Assembly of WOAH Delegates: "Rinderpest virus-containing material that is not in an approved BSL3 [Biosecurity Level 3] facility shall be destroyed by a validated process or transferred to an approved BSL3 facility." Biosecurity levels for institutes keeping RVCM during 2011–2021 ranged from BSL2 to BSL4 (Table) meaning some institutes still do not meet this requirement; continued efforts are therefore needed. Three category B RHFs have actively contributed to the global rinderpest vaccine reserve. One institute in Europe keeps a rinderpest RBOK (Muguga-modification of the Kabate-0-strain) vaccine seed bank sufficient to produce ≈800,000 doses. One institute in the WOAH Asia and the Pacific region biannually produces a total reserve of ≈772,000 doses of LA-AKO (master seed virus) strain vaccine. One institute in Africa has a historic reserve of ≈959,000 doses of RBOK vaccine. Three RHFs have participated in sequence and destroy projects, and 2 more have initiated the approval process for sequence and destroy projects from the FAO/WOAH rinderpest secretariat.

During recent genomic analysis of PPRV isolates held at an FAO/WOAH–designated RHF, 1 sample was found to contain a sequence that aligned with RPV in addition to PPRV sequences. A traceback investigation found that this sample, obtained from the field by another institute in the early 1970s, appears to have been destroyed. All materials derived from the original stock before the contaminated sample was identified were uncontaminated, but those derived from the contaminated stock were RPV-contaminated, so contamination appears to have occurred inside the institute, from an unknown source, but likely during a period in the late 1990s when both RPV and PPRV were being manipulated concurrently at the institute. All contaminated samples were destroyed. After examining all other samples being manipulated during the same period, the institute concluded that no others were contaminated. Records indicated that the institute had not shared this sample with other facilities and that it would thereafter screen all PPRV samples by PCR for RPV before sharing them. No contaminated samples had escaped containment and all processes to secure stocks appeared to be working well. Risks associated with remaining global stocks are being evaluated and will be presented in a future publication.

Conclusions

We document discovery of RPV-contaminated PPRV samples; our findings suggest that because of risk for cross-contamination, other laboratories should take precautions with samples manipulated alongside RPV, especially PPRV. Although progress is being made in consolidating RVCM stocks, 2 of 6 nonapproved institutes known to keep RVCM stockpiles have indicated no plans to destroy or transfer them to an FAO/WOAH RHF. Therefore, in spite of the progress, much work remains. Current FAO/WOAH strategy is to continue removing RVCM from nonapproved laboratories and advocating for reduced RVCM stocks in FAO/WOAH-designated RHFs. Ultimately, the only remaining RCVM materials should be manufactured vaccines and materials for vaccine production and diagnostics.

Acknowledgments

The authors thank the members of the Rinderpest Holding Facility Network and other laboratories interviewed during this process and recognize the contribution of the Food and Agriculture Organization of the United Nations. We thank Heather Moberly for assistance with the literature review and Sarah Manning for assistance creating the figures.

The project or effort depicted was or is sponsored by the United States Department of Defense, Defense Threat Reduction Agency. The content of the information does not necessarily reflect the position or the policy of the Federal Government of the United States, and no official endorsement should be inferred.

About the Author

Dr. Budke is a professor of epidemiology at Texas A&M University and a senior lead scientist in risk prevention for the Institute for Infectious Animal Diseases (IIAD). Her research interests include epidemiology, burden of disease indicators, zoonotic diseases, and international veterinary medicine and public health.

References

1. Fournié G, Jones BA, Beauvais W, Lubroth J, Njeumi F, Cameron A, et al. The risk of rinderpest re-introduction in post-eradication era. Prev Vet Med. 2014;113:175–84. https://doi.org/10.1016/j.prevetmed.2013.11.001
2. Fournié G, Beauvais W, Jones BA, Lubroth J, Ambrosini F, Njeumi F, et al. Rinderpest virus sequestration and use in posteradication era. Emerg Infect Dis. 2013;19:151–3. https://doi.org/10.3201/eid1901.120967
3. Holzer B, Hodgson S, Logan N, Willett B, Baron MD. Protection of cattle against rinderpest by vaccination with wild-type but not attenuated strains of peste des petits ruminants virus. J Virol. 2016;90:5152–62. https://doi.org/10.1128/JVI.00040-16

Address for correspondence: Christine M. Budke, Texas A&M University, 4458 TAMU, College Station, TX 77843-4458, USA; email: CBudke@cvm.tamu.edu

International Spread of Multidrug-Resistant *Rhodococcus equi*

Jorge Val-Calvo, Jane Darcy, James Gibbons, Alan Creighton, Claire Egan, Thomas Buckley, Achim Schmalenberger, Ursula Fogarty, Mariela Scortti, José A. Vázquez-Boland

A multidrug-resistant clone of the animal and human pathogen *Rhodococcus equi*, MDR-RE 2287, has been circulating among equine farms in the United States since the 2000s. We report the detection of MDR-RE 2287 outside the United States. Our finding highlights the risk for MDR-RE spreading internationally with horse movements.

Rhodococcus equi is a soilborne aerobic actinomycete bacterium that infects animals and humans. Human infections are opportunistic, zoonotic in origin, and considered to be linked to exposure to farm environments (*1*–*3*). Although clinical *R. equi* infections are relatively rare in most animal species, foals are commonly affected, and incidence is often high in horse farms in equine breeding countries (*4*). Long courses of rifampin and a macrolide is the mainstay therapy for foal rhodococcosis. This treatment has been systematically used since the 1980s and no significant resistance was detected until the early 2000s, after mass prophylactic application at *R. equi*–endemic farms in the United States (*5*,*6*).

The emerging dual macrolide–rifampin resistance is attributable to a multidrug-resistant *R. equi* (MDR-RE) clone, named 2287, which has spread among horse farms across the United States. MDR-RE 2287 arose by co-acquisition of the conjugative plasmid pRErm46 and a specific *rpoB*^{S531F} (TCG to TTC) mutation conferring high-level rifampin resistance (*7*,*8*). pRErm46 specifies resistance to macrolides, lincosamides, and streptogramins via the *erm*(46) gene carried on Tn*RErm46,* a highly mobile transposon, and to sulfonamides, streptomycin, spectinomycin, tetracycline, and doxycycline via a class 1 integron (C1I) and associated *tetRA*(33) determinant (*9*). Although it has so far been found only in the United States, we predicted MDR-RE could spread to other countries with the movement of equids (*10*).

Author affiliations: University of Edinburgh, Edinburgh, Scotland, UK (J. Val-Calvo, M. Scortti, J.A. Vazquez-Boland); University of Limerick, Limerick, Ireland (J. Darcy, A. Schmalenberger); Irish Equine Centre, Naas, Ireland (J. Gibbons, A. Creighton, C. Egan, T. Buckley, U. Fogarty)

DOI: https://doi.org/10.3201/eid2809.220222

The Study

After MDR-RE was characterized in 2019 (*8*), we established an informal surveillance network with colleagues in North and South America, Europe, the United Kingdom, Africa, Asia, and Australia. We asked collaborating laboratories to review their retrospective *R. equi* collections and prospectively identify isolates with erythromycin MIC ≥4 μg/mL, potentially denoting *erm*(46)-mediated macrolide resistance. Two equine clinical strains from necropsied foals in Ireland met the criterion: PAM2528, recovered in 2016, and PAM2578, recovered in 2021 (henceforth designated as 2528 and 2578). Both strains originated from the same farm and had MICs ≥32 μg/mL for erythromycin and >256 μg/mL for rifampin, consistent with MDR-RE's resistance phenotype (*7*–*10*).

We confirmed that both isolates were *erm*(46) positive by PCR and carried the *rpoB*^{S531F} mutation unique to the MDR-RE 2287 clone using previously described methods (*9*). A PCR using primers 5′-CCGAGATGTGTCGGACTTC-3′ (forward) and 5′-CGCCGAAGAACAACCCGAGGATG-3′ (reverse) showed the pRErm46 resistance plasmid carried the ΔC1I-*tetRA* deletion, observed in some recent MDR-RE isolates (*9*,*10*). Accordingly, 2528 and 2578 were susceptible to trimethoprim/sulfamethoxazole, streptomycin, spectinomycin, and tetracycline, to which the C1I-*tetRA*(33) determinant confers resistance (*9*). We used paired-end Illumina sequencing (Illumina, https://www.illumina.com) to obtain genomic libraries of the isolates. Reads were quality-checked using FastQC version 0.11.9 (https://www.bioinformatics.babraham.ac.uk/projects/fastqc), trimmed with TrimmomaticPE version 0.39 (*11*), and assembled using SPAdes v3.15.2 (*12*). For 2528 sequences, average

forward/reverse Phred score was 38/38, coverage depth 79×, and number of contigs (≥1 kb) 117. For 2578, average Phred score was 36/36; coverage depth, 243×; and number of contigs, 26. BlastN searches (https://blast.ncbi.nlm.nih.gov/Blast.cgi) confirmed presence of pRErm46 sequences in the draft genomes. We used ParSNP version 1.5.6 (*13*) and FastTree version 2.1.11 (http://www.microbesonline.org/fasttree) to build approximate maximum-likelihood trees based on core single-nucleotide polymorphisms (SNPs) to determine the position of the isolates in the *R. equi* population structure. The output *R. equi* tree showed that the 2 resistant isolates from Ireland belonged to the MDR-RE 2287 clone (Figure 1).

Because the short genetic distances compressed the branching of the MDR-RE 2287 isolates, we repeated the phylogenetic analysis with only the clonal genomes to explore their relationships in

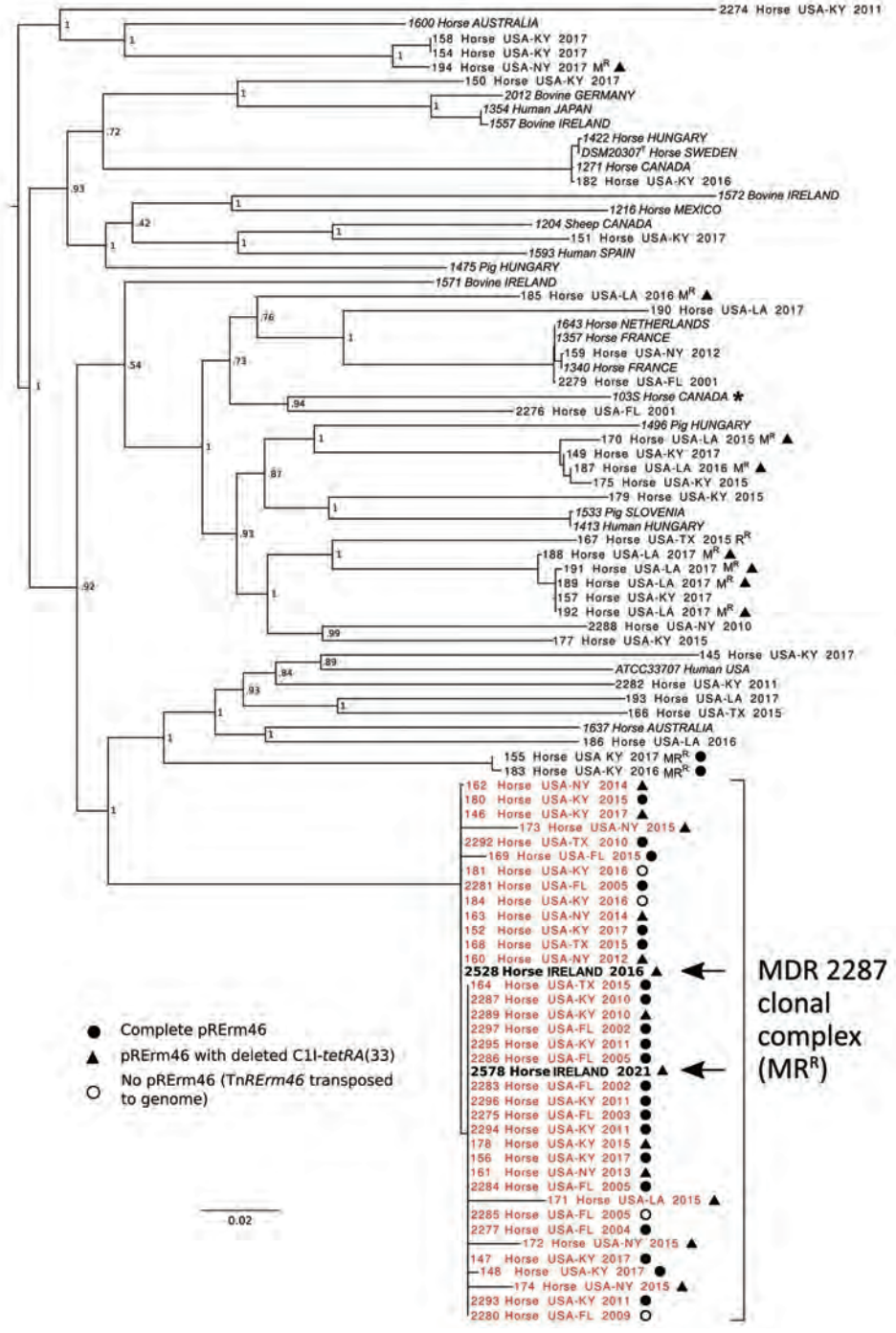

Figure 1. Whole-genome phylogenetic analysis of *Rhodococcus equi* and its multidrug-resistant 2287 clone. Asterisk indicates strain 103S used as reference genome (GenBank accession no. FN563149). For analysis we used 92 *R. equi* genome sequences including 68 macrolide-resistant and -susceptible equine isolates from the United States and 22 global strains from a previously reported *R. equi* diversity set (*14*) (italics). Macrolide-resistant isolates include 36 members of the MDR-RE 2287 clonal complex (red text) as well as isolates representing spillages of the pRErm46 plasmid to other *R. equi* genotypes (*8*,*10*). Arrows indicate the 2 MDR-RE 2287 isolates from Ireland. Labels indicate geographic origin, year of isolation, and resistance phenotype when applicable (MR^R, macrolide and rifampin resistance; M^R, macrolide resistance; R^R, rifampin resistance). Symbols indicate pRErm46 carriage in macrolide-resistant isolates, described in the key; open circles indicate MDR-RE isolates where pRErm46 has been lost after transposition of the Tn*RErm46* element to the host genome (*8*). Numbers at nodes indicate bootstrap values for 1,000 replicates. Tree was drawn with FigTree (http://tree.bio.ed.ac.uk/software/figtree).

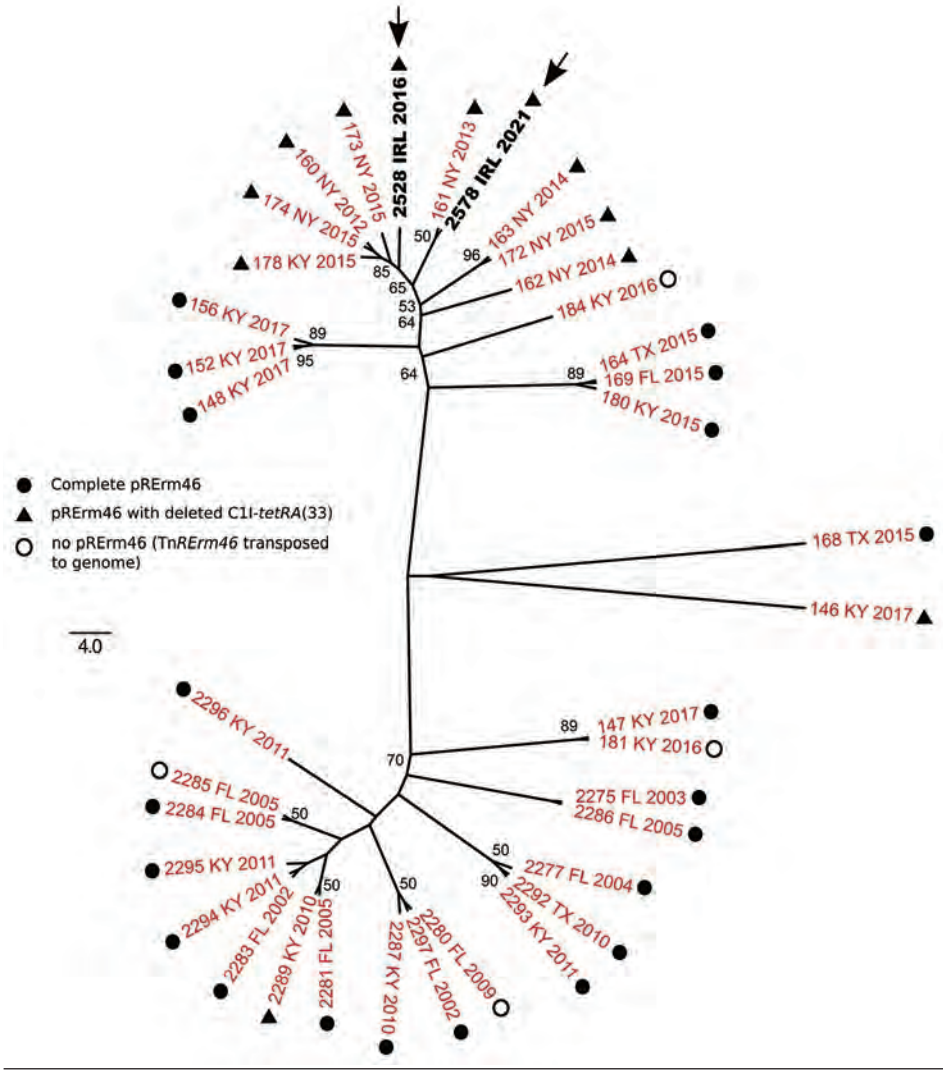

Figure 2. Unrooted maximum-likelihood tree of multidrug-resistant *Rhodococcus equi* 2287 clonal complex showing the relationships of the isolates from Ireland (arrows). Whole-genome phylogeny inferred from 45 parsimony informative sites using SNIPPY (https://github.com/tseemann/snippy) and IQ-tree (http://www.iqtree.org) for tree reconstruction. Best-fit model was selected by IQ-tree's ModelFinder module. Bootstrap values ≥50 are shown. The genome of the prototype MDR-RE 2287 isolate PAM2287 (National Center for Biotechnology Information assembly accession no. GCA_002094405.1) was used as a reference for SNP calling. Labels indicate isolate name, geographic origin (FL, Florida; IRL, Ireland, KY, Kentucky; NY, New York; TX, Texas), and year of isolation. Symbols indicate pRErm46 plasmid type. Tree was drawn with FigTree (http://tree.bio.ed.ac.uk/software/figtree).

more detail (Figure 2). For this analysis, we detected core SNPs using SNIPPY version 4.6.0 (https://github.com/tseemann/snippy), which avoided genome alignment errors observed with ParSNP that distort the phylogenetic reconstruction of virtually identical isolates.

The consensus maximum-likelihood tree subdivided the MDR-RE 2287 clonal complex in 2 main sublineages, one comprising older isolates from 2002–2011 and the other isolates from 2015 and later. *R. equi* 2528 and 2578 were located in 2 adjacent top branches within the younger sublineage, together with all (n = 7) isolates from New York. Because the analyzed MDR-RE 2287 collection comprised isolates from different US locations, the clustering with the New York isolates suggested a common origin. The New York isolates were recovered over a period of several years since 2012, pointing to a locally circulating MDR-RE 2287 subpopulation as the likely source of the isolates later found in Ireland. This possibility was further supported by the finding that both the 2528 and 2578 genomes possessed ΔC1I-*tetRA* pRErm46 variants, also carried by the New York subpopulation but only exceptionally by other MDR-RE 2287 complex members (Figures 1, 2).

Conclusions

We document the international spread of the MDR-RE 2287 clone that has been circulating in the United States since the 2000s (*8*,*10*). MDR-RE 2287 appears to be following the same pattern of the pandemic multidrug-resistant clones of human bacterial pathogens, which within a few years after emergence and initial local expansion become globally disseminated (*15*). For MDR-RE, the process is slower, likely because of fewer opportunities for transmission afforded by horse trade and contacts compared with the scale of human interactions and travel.

The positioning of the Ireland isolates in 2 separate subbranches of the New York radiation (Figure 2) may indicate they represent independent, temporally distinct import events that took place around 2016 and 2021, involving different MDR-RE 2287 subclones. That MDR-RE 2287 was not detected again in Ireland until 5 years later indicates that it might not have persisted after its first appearance in the country in 2016. This scenario may be explained by the different *R. equi*–targeted equine farm management in Ireland compared with that in the United States, where the emergence, maintenance, and spread of MDR-RE was favored by the application of mass antibioprophylaxis at *R. equi*-endemic farms (*6*,*8*). This practice was not implemented on the affected farm, nor is it applied in Ireland in general. However, the genetic distance between the 2528 and 2578 strains is comparable to that for the 7 New York isolates, recovered during 2012–2015. It cannot therefore be excluded that the 2 Ireland strains represent successive isolations of a locally evolving single imported MDR-RE 2287 subclone (21 SNPs difference over 5M bp, ≈1 × 10^{-6} substitutions/site/year, consistent with normal genetic drift values).

A Kentucky isolate of the ΔC1I-*tetRA* type was also located in a terminal branch of the New York cluster, whereas Kentucky isolates with complete pRErm46 plasmids were positioned at basal bifurcations of the radiation (e.g., the 148, 152, and 153 clusters) (Figure 2). These observations suggest a transmission history in which a relatively recent MDR-RE 2287 subclone that acquired a pRErm46 ΔC1I-*tetRA* deletion, possibly originating from Kentucky where MDR-RE emerged and is prevalent (*8*,*9*), became endemic in a New York farm and was transferred, directly or indirectly, to Ireland. International trade in thoroughbred horses is frequent, and the affected farm in Ireland received horses from the United States, Europe, and the United Kingdom on a regular basis. Previous phylogenomic studies provided evidence of global circulation of *R. equi* genomotypes, probably linked to livestock trade (*14*). Our findings reinforce this notion and warn about the risk for MDR-RE becoming globally disseminated over time with horse movements.

Our study is not comprehensive but based on the voluntary collaboration of a small number of international colleagues, and thus MDR-RE may have also spread to other countries. We recommend actively monitoring the occurrence of the emerging MDR-RE 2287 clone for which, as our data highlight, *erm*(46) and the *rpoB*^{S531F} (TCG→TTC) mutation can be used as molecular markers, eventually complemented with pRErm46/ΔC1I-*tetRA*(33) variant detection.

Acknowledgments

We thank the network of international collaborators for their participation in macrolide- and rifampin-resistant *R. equi* monitoring.

New *R. equi* genome assemblies were deposited in GenBank under accession nos. JAJNNF000000000 (PAM2528) and JAJNNG000000000 (PAM2578).

Work on multidrug-resistant *R. equi* at J.V.-B.'s laboratory is supported by HBLB (grant no. prj-796).

About the Author

Dr. Val-Calvo is a postdoctoral fellow at the Laboratory of Microbial Pathogenesis, Medical School of the University of Edinburgh. His primary research interests include molecular microbiology, plasmid biology, bacterial genomics and evolution, and antimicrobial resistance.

References

1. Prescott JF. *Rhodococcus equi*: an animal and human pathogen. Clin Microbiol Rev. 1991;4:20–34. https://doi.org/10.1128/CMR.4.1.20
2. Yamshchikov AV, Schuetz A, Lyon GM. *Rhodococcus equi* infection. Lancet Infect Dis. 2010;10:350–9. https://doi.org/10.1016/S1473-3099(10)70068-2
3. Vázquez-Boland JA, Meijer WG. The pathogenic actinobacterium *Rhodococcus equi*: what's in a name? Mol Microbiol. 2019;112:1–15. https://doi.org/10.1111/mmi.14267
4. Muscatello G, Leadon DP, Klayt M, Ocampo-Sosa A, Lewis DA, Fogarty U, et al. *Rhodococcus equi* infection in foals: the science of 'rattles'. Equine Vet J. 2007;39:470–8. https://doi.org/10.2746/042516407X209217
5. Giguère S. Treatment of infections caused by *Rhodococcus equi*. Vet Clin North Am Equine Pract. 2017;33:67–85. https://doi.org/10.1016/j.cveq.2016.11.002
6. Burton AJ, Giguère S, Sturgill TL, Berghaus LJ, Slovis NM, Whitman JL, et al. Macrolide- and rifampin-resistant *Rhodococcus equi* on a horse breeding farm, Kentucky, USA. Emerg Infect Dis. 2013;19:282–5. https://doi.org/10.3201/eid1902.121210
7. Anastasi E, Giguère S, Berghaus LJ, Hondalus MK, Willingham-Lane JM, MacArthur I, et al. Novel transferable *erm*(46) determinant responsible for emerging macrolide resistance in Rhodococcus equi. J Antimicrob Chemother. 2015;70:3184–90.
8. Álvarez-Narváez S, Giguère S, Anastasi E, Hearn J, Scortti M, Vázquez-Boland JA. Clonal confinement of a highly mobile resistance element driven by combination therapy in *Rhodococcus equi*. MBio. 2019;10:e02260–19. https://doi.org/10.1128/mBio.02260-19
9. Erol E, Scortti M, Fortner J, Patel M, Vázquez-Boland JA. Antimicrobial resistance spectrum conferred by pRErm46 of emerging macrolide (multidrug)-resistant *Rhodococcus equi*. J Clin Microbiol. 2021;59:e01149-21. https://doi.org/10.1128/JCM.01149-21
10. Álvarez-Narváez S, Giguère S, Cohen N, Slovis N, Vázquez-Boland JA. Spread of multidrug-resistant *Rhodococcus equi*, United States. Emerg Infect Dis. 2021;27:529–37. https://doi.org/10.3201/eid2702.203030

11. Bolger AM, Lohse M, Usadel B. Trimmomatic: a flexible trimmer for Illumina sequence data. Bioinformatics. 2014; 30:2114–20. https://doi.org/10.1093/bioinformatics/btu170
12. Bankevich A, Nurk S, Antipov D, Gurevich AA, Dvorkin M, Kulikov AS, et al. SPAdes: a new genome assembly algorithm and its applications to single-cell sequencing. J Comput Biol. 2012;19:455–77. https://doi.org/10.1089/cmb.2012.0021
13. Treangen TJ, Ondov BD, Koren S, Phillippy AM. The Harvest suite for rapid core-genome alignment and visualization of thousands of intraspecific microbial genomes. Genome Biol. 2014;15:524. https://doi.org/10.1186/s13059-014-0524-x
14. Anastasi E, MacArthur I, Scortti M, Alvarez S, Giguère S, Vázquez-Boland JA. Pangenome and phylogenomic analysis of the pathogenic actinobacterium *Rhodococcus equi*. Genome Biol Evol. 2016;8:3140–8. https://doi.org/10.1093/gbe/evw222
15. Baker S, Thomson N, Weill FX, Holt KE. Genomic insights into the emergence and spread of antimicrobial-resistant bacterial pathogens. Science. 2018;360:733–8. https://doi.org/10.1126/science.aar3777

Address for correspondence: José A. Vázquez-Boland, Microbial Pathogenesis Laboratory, University of Edinburgh Medical School (Biomedical Sciences—Infection Medicine), Edinburgh BioQuarter, Chancellor's Building, 49 Little France Crescent, Edinburgh, UK EH16 4SB, UK; email: v.boland@ed.ac.uk

Fatal Fungicide-Associated Triazole-Resistant *Aspergillus fumigatus* Infection, Pennsylvania, USA

Kennedy Bradley,[1] Audrey Le-Mahajan,[1] Beth Morris, Tiina Peritz, Tom Chiller, Kaitlin Forsberg, Natalie S. Nunnally, Shawn R. Lockhart, Jeremy A.W. Gold,[2] Jane M. Gould[2]

Author affiliations: Department of Public Health, Philadelphia, Pennsylvania, USA (K. Bradley, B. Morris, T. Peritz, J.M. Gould); Hospital of the University of Pennsylvania, Philadelphia (A. Le-Mahajan); Centers for Disease Control and Prevention, Atlanta, Georgia, USA (T. Chiller, K. Forsberg, N.S. Nunnally, S.R. Lockhart, J.A.W. Gold)

DOI: https://doi.org/10.3201/eid2809.220517

We report a fatal infection in a 65-year-old immunocompromised male patient caused by pan-triazole–resistant *Aspergillus fumigatus* containing a TR_{34}/L98H genetic mutation linked to agricultural fungicide use. Clinical and environmental surveillance of triazole-resistant *A. fumigatus* is needed in the United States to prevent spread and guide healthcare and agricultural practices.

Aspergillus fumigatus is the most common cause of invasive aspergillosis, a life-threatening fungal infection that primarily affects immunocompromised persons, including those with hematologic malignancies or stem cell or solid organ transplants or those receiving immunosuppressive medications (*1*). Patients are infected by inhaling *A. fumigatus* spores found in the environment. Each year, invasive aspergillosis accounts for >14,000 hospitalizations and imposes >$1.2 billion in direct costs on the US healthcare system (*2*).

Voriconazole belongs to the triazole class of antifungal drugs and is a first-line treatment for invasive aspergillosis (*1*). Triazole drugs have improved patient survival; however, the emergence of triazole-resistant *A. fumigatus* threatens the effectiveness of triazoles in clinical practice (*3*). Patients with invasive aspergillosis caused by voriconazole-resistant *A. fumigatus* had a mortality rate of ≈60%, which was ≈2 times the mortality rate associated with voriconazole-susceptible infection (*4*). Patients can acquire triazole-resistant *A. fumigatus* infections because of exposure to long-term triazole therapy for chronic aspergillosis or by directly inhaling environmental spores that are already triazole-resistant (*3*). The agricultural use of triazole fungicides, a practice that recently increased 4-fold in the United States, can select for *A. fumigatus* strains harboring unique *CYP51A* gene mutations, such as TR_{34}/L98H and TR_{46}/Y121F/T289A, that can cause pan-triazole resistance in patients (*5*,*6*).

Reports of environmentally acquired triazole-resistant *A. fumigatus* infections are increasing worldwide; however, data on these infections and their clinical implications are lacking in the United States (*3*). We report a patient who died from an invasive infection caused by a pan-triazole–resistant *A. fumigatus* strain containing an environmentally acquired TR_{34}/L98H mutation in *CYP51A*.

The male patient was 65 years of age and previously underwent chimeric antigen receptor T-cell therapy for acute myeloid leukemia. One month before hospital admission, the patient received an allogeneic stem cell transplant that was complicated by cutaneous graft-versus-host disease. Despite topical therapy, he was admitted to the hospital because of worsening rashes, fever, and lethargy. The patient received broad-spectrum antibacterial drugs and systemic corticosteroid therapy for progressive graft-versus-host disease involving the gastrointestinal tract and eyes and continued receiving transplant-related fluconazole prophylaxis.

On hospital day 3, the patient was transferred to the intensive care unit for wound management and treated for hypovolemic shock; his antifungal prophylaxis was changed from fluconazole to posaconazole. After 6 days, posaconazole was replaced with caspofungin because the posaconazole was potentially exacerbating the patient's rash. The patient improved and remained hemodynamically stable for ≈2 weeks, after which clinicians deescalated antibacterial therapy.

On hospital day 23, acute-onset shock and hypoxemic respiratory failure developed in the patient; he was intubated and placed on mechanical ventilation. Chest computed tomography imaging showed multifocal pneumonia; bronchial cultures were positive for *A. fumigatus*. Clinicians initiated voriconazole therapy for probable invasive aspergillosis and continued caspofungin. On hospital day 27, progressive acidemia, refractory hypotension, and focal neurologic deficits developed in the patient. *Rhizopus* spp. was identified from the patient's skin culture, but the patient was not treated for this pathogen because his family had decided to focus on comfort care. The patient died on hospital day 28. An autopsy determined that the cause of death was sepsis from disseminated *A. fumigatus* and *Rhizopus* spp. infections.

Although most US clinical laboratories do not perform antifungal susceptibility testing, triazole

[1]These first authors contributed equally to this article.

[2]These senior authors contributed equally to this article.

susceptibility testing for *A. fumigatus* isolates is available through the Centers for Disease Control and Prevention (CDC) Antibiotic Resistance Laboratory Network (https://www.cdc.gov/drugresistance/laboratories.html). Clinicians sent an isolate from the patient's bronchial washings to CDC as part of an ongoing passive surveillance for triazole-resistant *A. fumigatus*. Using previously described methods (*7*), CDC performed broth microdilution to determine the MICs of itraconazole (>16 μg/mL) and voriconazole (2 μg/mL) for the isolate. The isolate was classified as voriconazole-resistant in accordance with Clinical and Laboratory Standards Institute MIC breakpoints (*8*). The MIC of itraconazole for the isolate was considered non–wild-type on the basis of proposed epidemiologic cutoff values (*9*). CDC performed DNA sequence analysis of the *CYP51A* gene and determined that the isolate contained the TR_{34}/L98H mutation (*7*).

In summary, we report a fatal disseminated fungal infection in an immunocompromised patient in the United States involving pan-triazole–resistant *A. fumigatus* with an environmentally acquired TR_{34}/L98H mutation. This report underscores the potential severity of triazole-resistant *A. fumigatus* infections in immunocompromised persons. Furthermore, clinicians should consider the possible presence of drug-resistant *A. fumigatus* in patients with invasive aspergillosis who do not improve with first-line therapy. In Europe, the emergence of environmentally acquired triazole resistance is well documented, and voriconazole monotherapy is no longer recommended as a first-line invasive aspergillosis treatment for patients in regions with environmental resistance rates of ≥10% (*10*). In the United States, systematic clinical and environmental surveillance for triazole-resistant *A. fumigatus* is needed to determine the spread of this fungus and guide clinical and agricultural practices.

Acknowledgments

We thank Elizabeth Berkow for establishing laboratory surveillance protocols for *A fumigatus* infections; Brendan Jackson, Megan Lyman, and Mitsuru Toda for assistance with manuscript editing; laboratory staff from the Mycotic Diseases Branch, Division of Foodborne, Waterborne, and Environmental Diseases, National Center for Emerging and Zoonotic Infectious Diseases, CDC; and the Medical Examiner's Office, Philadelphia, Pennsylvania, USA, for performing the autopsy.

This activity was reviewed by CDC and conducted consistently with applicable federal laws and CDC policy (see e.g., 45 C.F.R. part 46.102(l)(2); 21 C.F.R. part 56; 42 U.S.C. §241(d); 5 U.S.C. §552a; 44 U.S.C. §3501 et seq).

About the Author

Ms. Bradley is an epidemiology fellow in the Healthcare Associated Infections and Antimicrobial Resistance Program of the Department of Public Health, Philadelphia, Pennsylvania. Her primary research interests are the epidemiology of infectious diseases and antimicrobial stewardship.

References

1. Patterson TF, Thompson GR III, Denning DW, Fishman JA, Hadley S, Herbrecht R, et al. Practice guidelines for the diagnosis and management of aspergillosis: 2016 update by the Infectious Diseases Society of America. Clin Infect Dis. 2016;63:e1–60. https://doi.org/10.1093/cid/ciw326
2. Benedict K, Jackson BR, Chiller T, Beer KD. Estimation of direct healthcare costs of fungal diseases in the United States. Clin Infect Dis. 2019;68:1791–7. https://doi.org/10.1093/cid/ciy776
3. Beer KD, Farnon EC, Jain S, Jamerson C, Lineberger S, Miller J, et al. Multidrug-resistant *Aspergillus fumigatus* carrying mutations linked to environmental fungicide exposure—three states, 2010–2017. MMWR Morb Mortal Wkly Rep. 2018;67:1064–7. https://doi.org/10.15585/mmwr.mm6738a5
4. Lestrade PP, Bentvelsen RG, Schauwvlieghe AFAD, Schalekamp S, van der Velden WJFM, Kuiper EJ, et al. Voriconazole resistance and mortality in invasive aspergillosis: a multicenter retrospective cohort study. Clin Infect Dis. 2019;68:1463–71. https://doi.org/10.1093/cid/ciy859
5. Toda M, Beer KD, Kuivila KM, Chiller TM, Jackson BR. Trends in agricultural triazole fungicide use in the United States, 1992–2016 and possible implications for antifungal-resistant fungi in human disease. Environ Health Perspect. 2021;129:55001. https://doi.org/10.1289/EHP7484
6. Kang SE, Sumabat LG, Melie T, Mangum B, Momany M, Brewer MT. Evidence for the agricultural origin of resistance to multiple antimicrobials in *Aspergillus fumigatus*, a fungal pathogen of humans. G3 (Bethesda). 2022;12:jkab427. https://doi.org/10.1093/g3journal/jkab427
7. Berkow EL, Nunnally NS, Bandea A, Kuykendall R, Beer K, Lockhart SR. Detection of TR_{34}/L98H *CYP51A* mutation through passive surveillance for azole-resistant *Aspergillus fumigatus* in the United States from 2015 to 2017. Antimicrob Agents Chemother. 2018;62:e02240-17. https://doi.org/10.1128/AAC.02240-17
8. Clinical and Laboratory Standards Institute. Performance standards for antifungal susceptibility testing of filamentous fungi, 2nd ed. (document M61). Wayne (PA): The Institute; 2020.
9. Espinel-Ingroff A, Diekema DJ, Fothergill A, Johnson E, Pelaez T, Pfaller MA, et al. Wild-type MIC distributions and epidemiological cutoff values for the triazoles and six *Aspergillus* spp. for the CLSI broth microdilution method (document M38-A2). J Clin Microbiol. 2010;48:3251–7. https://doi.org/10.1128/JCM.00536-10
10. Verweij PE, Ananda-Rajah M, Andes D, Arendrup MC, Brüggemann RJ, Chowdhary A, et al. International expert opinion on the management of infection caused by azole-resistant *Aspergillus fumigatus*. Drug Resist Updat. 2015;21-22:30–40. https://doi.org/10.1016/j.drup.2015.08.001

Address for correspondence: Kennedy Bradley, Department of Public Health, 1101 Market St, Philadelphia, PA 19107, USA; email: kennedy.bradley@phila.gov

Correlation between Clinical and Wastewater SARS-CoV-2 Genomic Surveillance, Oregon, USA

Devrim Kaya, Rebecca Falender, Tyler Radniecki, Matthew Geniza, Paul Cieslak, Christine Kelly, Noah Lininger, Melissa Sutton

Author affiliations: Oregon State University, Corvallis, Oregon, USA (D. Kaya, T. Radniecki, M. Geniza, C. Kelly); Oregon Health Authority, Portland, Oregon, USA (R. Falender, P. Cieslak, N. Lininger, M. Sutton)

DOI: https://doi.org/10.3201/eid2809.220938

SARS-CoV-2 variant proportions in a population can be estimated through genomic sequencing of clinical specimens or wastewater samples. We demonstrate strong pairwise correlation between statewide variant estimates in Oregon, USA, derived from both methods (correlation coefficient 0.97). Our results provide crucial evidence of the effectiveness of community-level genomic surveillance.

Genomic surveillance to detect SARS-CoV-2 variants has become a critical component of monitoring the virus over time. Both patient- and community-level surveillance through the sequencing of clinical specimens and wastewater samples can detect variants and estimate their proportions in a population. Sequencing wastewater for SARS-CoV-2 variants is an emerging science that offers several advantages over patient-level surveillance, including reduced cost and tracking of cases regardless of symptoms or testing access (*1*,*2*), but few data have demonstrated comparable effectiveness in estimating variant proportions over time (*3*–*5*). We describe the correlation between SARS-CoV-2 variant proportions detected through sequencing of wastewater samples and clinical specimens in Oregon, USA, during February 7, 2021–February 26, 2022.

In brief, 24-hour composite samples were collected ≥1 time each week from wastewater treatment facility influents for sequencing. We quantified SARS-CoV-2 RNA concentrations via droplet digital reverse transcription PCR and sequenced positive samples on a HiSeq 3000 or NextSeq 2000 sequencer (Illumina, https://www.illumina.com) by using the Swift Amplicon SARS-CoV-2 Panel and Swift Amplicon Combinatorial Dual indexed adapters (Integrated DNA Technologies [IDT] Swift Biosciences, https://www.idtdna.com), according to the manufacturers' protocols, as previously described (*6*).

During each surveillance week of the study period, we used clinical specimen and wastewater sample data to estimate the proportion of SARS-CoV-2 variants according to US Centers for Disease Control and Prevention variant of concern (VOC) designations (*7*). We defined the circulation period of each variant by its earliest and latest detections in either wastewater or clinical specimens; we included estimated proportions of 0 that fell within a variant's circulation period in all analyses. To estimate variant proportions using clinical data, we divided the number of specimens for each variant by the total number of SARS-CoV-2–positive specimens from Oregon submitted to the GISAID database (https://www.gisaid.org) by surveillance week (*8*). To estimate variant proportions using wastewater data, we divided the statewide gene copies of each variant by the total gene copies of all variants by surveillance week. To derive the denominator, we normalized the SARS-CoV-2 concentration to wastewater influent flow at each facility and summed the values for all facilities by surveillance week. To derive the numerator, we multiplied the normalized SARS-CoV-2 concentration by the proportion of sequence reads for each SARS-CoV-2 variant detected at each facility and summed the values for all facilities by surveillance week.

We used the Pearson correlation coefficient (*r*) to assess the relationship between the statewide weekly estimated proportions of each VOC detected in clinical specimens and wastewater samples. We used simple linear regression with a least-squares regression line to assess goodness of fit (R^2) and considered $p<0.05$ statistically significant. We used Stata version 17.0 (StataCorp LLC, https://www.stata.com) for all analyses.

Of 488,308 confirmed COVID-19 cases in Oregon during the study period, 38,386 (7.9%) clinical samples were sequenced and submitted to the GISAID database. Of 2,948 wastewater samples collected from 42 communities, 2,852 (97%) tested positive for SARS-CoV-2 and 2,749 (96%) were sequenced. We included 233 pairs of estimated proportions in the correlation analysis and rounded all estimates to 0.001.

Overall, statewide weekly estimated percentages of each SARS-CoV-2 variant detected in clinical specimens were strongly associated with those from wastewater samples; *r* was 0.97 for all variants ($p<0.0001$) (Figure). However, *r* fluctuated by SARS-CoV-2 variant, from 0.61 for Beta to 0.98 for Delta,

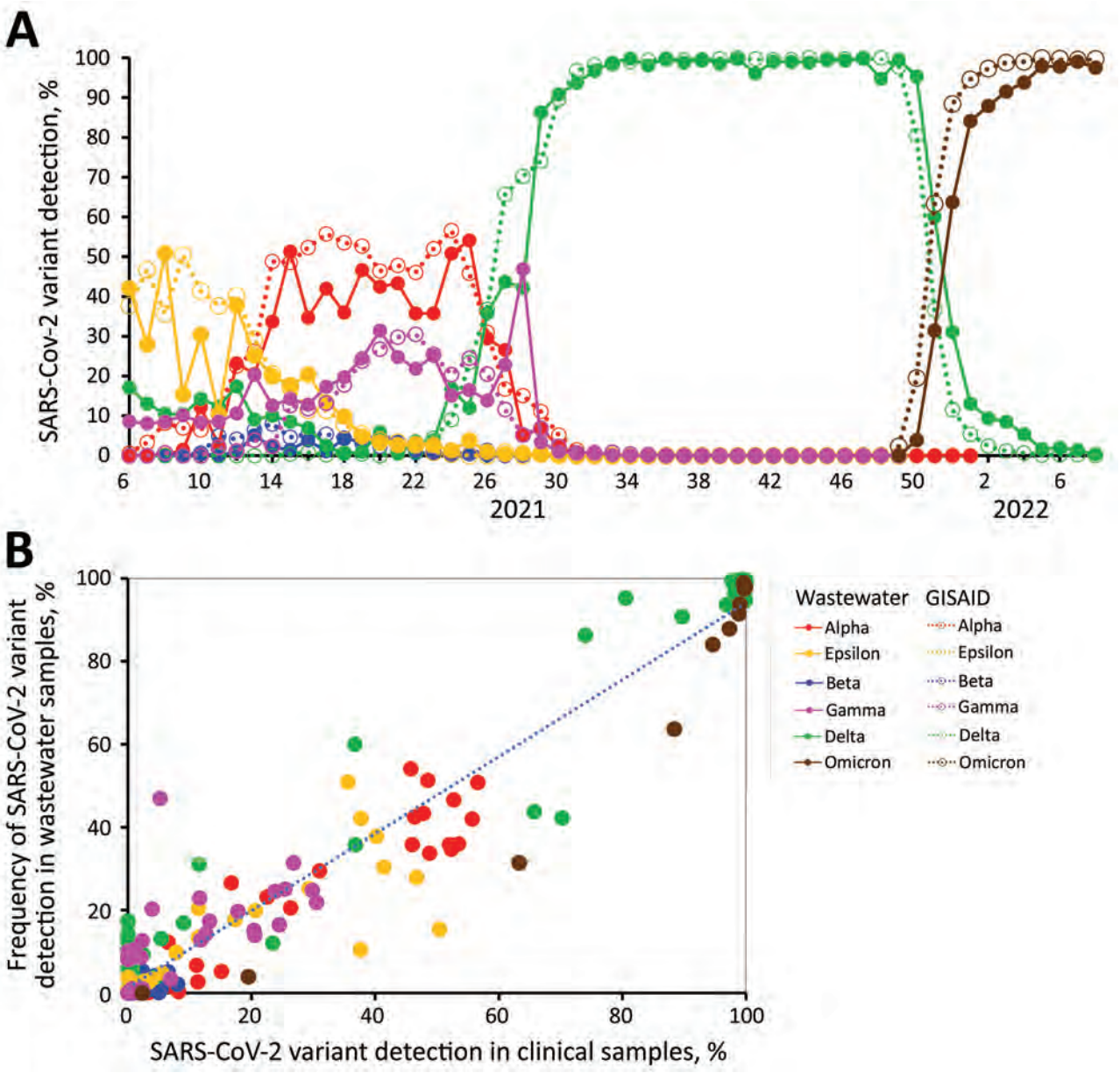

Figure. Comparison of SARS-CoV-2 genomic sequence data from confirmed COVID-19 case clinical specimens and wastewater samples collected in Oregon, USA, February 6, 2021–February 26, 2022. A) Percentages of different SARS-CoV-2 variants detected during each epidemiologic week. B) Scatter plot comparing variant detection frequency by sample type. Clinical specimens were retrieved from the GISAID database (https://www.gisaid.org).

and we noted a general increasing trend in *r* as total variant proportions increased (Table). A scatter plot demonstrated a linear relationship between estimated percentages of each variant derived from clinical specimens and wastewater samples (Figure, panel B). The conditional SD was greatest for proportion estimates of 0.2–0.6. Simple linear regression demonstrated a strong linear relationship between estimated proportions derived from both genomic surveillance data sources ($R^2 = 0.94$; $p<0.0001$).

Our pairwise correlation analysis demonstrates the effectiveness of wastewater sequencing for estimating SARS-CoV-2 variant proportions at the statewide level over time and at varying prevalences. Overall, the association between estimates of variant proportions produced from clinical specimens and wastewater samples was strong. However, correlations varied by VOC and were weakest for the least prevalent variants.

A limitation of wastewater surveillance is that it excludes populations without access to municipal

Table. Correlation between estimated SARS-CoV-2 variant proportions detected in clinical specimens and wastewater samples, Oregon, USA, February 7, 2021–February 26, 2022*

Variant	*r*	R^2	p value	No. (%) pairwise observations included in correlation
All	0.97	0.94	<0.0001	233 (100)
Alpha B.1.1.7†	0.96	0.93	<0.0001	48 (20.6)
Beta B.1.351	0.61	0.38	0.0003	30 (12.9)
Delta B.1.617.2‡	0.98	0.97	<0.0001	55 (23.6)
Epsilon B.1.427/429	0.86	0.74	<0.0001	44 (18.9)
Gamma P.1§	0.71	0.50	<0.0001	44 (18.9)
Omicron B.1.1.529¶	0.97	0.93	<0.0001	12 (5.2)

*Sequence data for clinical samples were retrieved from GISAID (https://www.gisaid.org). *r*, Pearson correlation coefficient; R^2, simple linear regression with a least-squares regression line to assess model fit.
†B.1.1.7 includes all Q sublineages.
‡B.1.617.2 includes all AY sublineages.
§P.1 includes all P.1 sublineages.
¶B.1.1.529 includes all BA sublineages.

sewer service (i.e., those with septic systems); therefore, it might not be generalizable to all populations within a state. However, for other areas, leveraging wastewater surveillance for SARS-CoV-2 genomic surveillance offers several advantages over estimating variant proportions from clinical specimens. Because wastewater surveillance does not rely on healthcare access, testing acceptance, and molecular testing availability, it likely provides more robust and less biased estimates than sequencing of clinical specimens. Thus, wastewater genomic surveillance could prove valuable in surveillance for many other pathogens of public health concern.

Acknowledgments

We thank all the Oregon wastewater utilities that participated in the statewide wastewater SARS-CoV-2 surveillance program and all Oregon State University staff and students involved in this program for their help and assistance in the management and logistics of the sample collection and analysis.

About the Author

Dr. Kaya is a faculty research associate in the School of Chemical, Biological and Environmental Engineering at Oregon State University. Her primary research interests include wastewater surveillance for communicable diseases and environmental surveillance and bioremediation of emerging contaminant of concerns.

References

1. Hart OE, Halden RU. Computational analysis of SARS-CoV-2/COVID-19 surveillance by wastewater-based epidemiology locally and globally: feasibility, economy, opportunities and challenges. Sci Total Environ. 2020; 730:138875. https://doi.org/10.1016/j.scitotenv.2020.138875
2. Daughton CG. Wastewater surveillance for population-wide COVID-19: the present and future. Sci Total Environ. 2020; 736:139631. https://doi.org/10.1016/j.scitotenv.2020.139631
3. Crits-Christoph A, Kantor RS, Olm MR, Whitney ON, Al-Shayeb B, Lou YC, et al. Genome sequencing of sewage detects regionally prevalent SARS-CoV-2 variants. MBio. 2021;12:e02703-20. https://doi.org/10.1128/mBio.02703-20
4. Agrawal S, Orschler L, Schubert S, Zachmann K, Heijnen L, Tavazzi S, et al. Prevalence and circulation patterns of SARS-CoV-2 variants in European sewage mirror clinical data of 54 European cities. Water Res. 2022; 214:118162. https://doi.org/10.1016/j.watres.2022.118162
5. Rios G, Lacoux C, Leclercq V, Diamant A, Lebrigand K, Lazuka A, et al. Monitoring SARS-CoV-2 variants alterations in Nice neighborhoods by wastewater nanopore sequencing. Lancet Reg Health Eur. 2021;10:100202. https://doi.org/10.1016/j.lanepe.2021.100202
6. Sutton M, Radniecki TS, Kaya D, Alegre D, Geniza M, Girard A-M, et al. Detection of SARS-CoV-2 B.1.351 (Beta) variant through wastewater surveillance before case detection in a community, Oregon, USA. Emerg Infect Dis. 2022;28:1101–9. https://doi.org/10.3201/eid2806.211821
7. Centers for Disease Control and Prevention. SARS-CoV-2 variant classifications and definitions 2022 Apr 26 [cited 2022 Apr 29]. https://www.cdc.gov/coronavirus/2019-ncov/variants/variant-classifications.html
8. Elbe S, Buckland-Merrett G. Data, disease and diplomacy: GISAID's innovative contribution to global health. Glob Chall. 2017;1:33–46. https://doi.org/10.1002/gch2.1018

Address for correspondence: Melissa Sutton, Public Health Division, Oregon Health Authority, 800 NE Oregon St, Ste 772, Portland, OR 97232, USA; email: melissa.sutton@dhsoha.state.or.us

Social and Behavioral Factors Associated with Lack of Intent to Receive COVID-19 Vaccine, Japan

Takeshi Arashiro, Yuzo Arima, Ashley Stucky, Chris Smith, Martin Hibberd, Koya Ariyoshi, Motoi Suzuki

Author affiliations: National Institute of Infectious Diseases, Tokyo, Japan (T. Arashiro, Y. Arima, A. Stucky, M. Suzuki); London School of Hygiene and Tropical Medicine, London, UK (T. Arashiro, C. Smith, M. Hibberd); Nagasaki University, Nagasaki, Japan (T. Arashiro, C. Smith, M. Hibberd, K. Ariyoshi, M. Suzuki)

DOI: https://doi.org/10.3201/eid2809.220300

Persons in Japan who did not intend to receive COVID-19 vaccines after widespread rollout were less likely than others to engage in preventive measures or to be afraid of getting infected or infecting others. They were also not less likely to engage in potentially high-risk behaviors, suggesting similar or higher exposure risks.

COVID-19 vaccines have become a critical tool in pandemic control (*1*). In Japan, BNT162b2 (Pfizer-BioNTech, https://www.pfizer.com), mRNA-1273 (Moderna, https://www.modernatx.com), and ChAdOx1 nCoV-19 (AZD1222; Oxford/AstraZeneca, https://www.astrazeneca.com) have been approved, but use of ChAdOx1 nCoV-19 has been minimal. For the Omicron variant, 2 doses of mRNA vaccines might not be highly protective against symptomatic infection, but early data suggest they are still highly protective against severe disease and that a booster dose provides further protection (*2*–*4*). Addressing persons at highest risk for severe or fatal COVID-19 who do not intend to be vaccinated has become paramount as we transition to the endemic phase, which is especially true in Japan because most persons are not protected by natural infection (*5*). Several studies have addressed reasons behind this hesitancy at the early stage of vaccine rollout (*6*–*9*), but evidence on attitudes toward risk for infection and prevention and risk behaviors is scarce.

We retrospectively analyzed an online survey about life during the COVID-19 pandemic conducted by a marketing research company in Japan during November 26–28, 2021, after the vaccine rollout had stabilized and 70% of the population had received 2 doses. The total number of survey participants was 2,500 (250 participants for each sex and 10-year age group, 20–60 years of age) (Appendix, https://wwwnc.cdc.gov/EID/article/28/9/22-0300-App1.pdf). We extracted sociodemographic information, vaccination status (choices included vaccinated once, vaccinated twice, unvaccinated with intention to be vaccinated, unvaccinated without intention to be vaccinated, and prefer not to answer), attitudes toward COVID-19-related issues (e.g., whether participants were afraid of getting infected), and behaviors in the previous week (e.g., preventive measures such as mask-wearing and potentially high-risk behaviors such as visiting bars or restaurants) (*10*). For vaccination status, we categorized the first 3 options into vaccinated or intend to be vaccinated and the last 2 choices into no intention to be vaccinated, because persons who preferred not to answer likely did not intend to be vaccinated but were unwilling to disclose this information. Depending on the social or behavioral factor, we adjusted for potential confounders that were determined a priori (*6*–*9*). This study was reviewed and exempt from ethics approval by the Institutional Review Board of the National Institute of Infectious Diseases, Japan.

Overall, 2,069 (82.8%) participants had received 2 doses, 35 (1.4%) had received 1 dose, 95 (3.8%) were not vaccinated but intended to be, 203 (8.1%) had no intention of being vaccinated, and 98 (3.9%) preferred not to answer. By age group, proportions of vaccinated persons were similar to those in the general population of Japan (Appendix). The proportions of participants residing in each geographic region were also similar to the national distribution (Appendix). Compared with men 60–69 years of age, men 20–39 years of age, as well as women 20–40 years of age, were ≥2-fold more likely to have no intention of being vaccinated (Appendix Table 1). Persons who did not intend to be vaccinated were less likely to be afraid of getting infected (adjusted odds ratio [aOR] 2.32, 95% CI 1.53–3.53), family members getting infected (aOR 2.50, 95% CI 1.68–3.71), infecting others (aOR 2.58, 95% CI 1.73–3.84), and bed shortages caused by a surge in severe COVID-19 cases (aOR 1.89, 95% CI 1.25–2.87). Persons who did not intend to be vaccinated also did not plan to receive a third (booster) dose, but 74% of persons who had received or intended to receive vaccines also intended to receive a booster dose. Persons without intention to be vaccinated were more likely to report not wearing a mask (aOR 2.01, 95% CI 1.52–2.65) and not using hand sanitizer (aOR 1.90, 95% CI 1.47–2.47) in the previous week. These persons were less likely to have gone shopping for nonessential goods in the past week (aOR 0.70, 95% CI 0.51–0.97), but no association was seen between vaccination intent and refraining from meeting with others (aOR

1.20, 95% CI 0.87–1.65) or going to crowded places or traveling (aOR 1.11, 95% CI 0.83–1.47). We also saw no association between vaccination intent and meeting noncohabitating friends, acquaintances, or family members (aOR 0.73, 0.47–1.12); dining out (aOR 0.92, 0.65–1.30); going out socially (aOR 0.87, 0.59–1.27); traveling (aOR 0.51, 0.22–1.22); or going to a gym (aOR 1.08, 0.64–1.83). We obtained similar results when we excluded persons who preferred not to answer regarding their vaccination status.

Persons who did not intend to receive COVID-19 vaccines were less likely to engage in preventive measures or be afraid of getting infected or infecting others, but we observed no association between vaccine intention and engaging in potentially high-risk behaviors. These results suggest that these nonintenders have similar or higher exposure risks compared with vaccinees and intenders. Similar surveys might be considered in other countries to understand vaccine denial and inform policies and risk communication.

Limitations of our study include selection bias and recall bias. Social desirability bias might be an issue, but this survey about life during the pandemic was not administered as an assessment about COVID-19 vaccination intent.

Acknowledgment

We thank the marketing research company for providing the original survey data.

This work was supported in part by a grant from the Japan Agency for Medical Research and Development (AMED) (grant no. JP21fk0108612) and the Nagasaki University WISE Programme.

About the Author

Dr. Arashiro is a research scientist in the Center for Surveillance, Immunization, and Epidemiologic Research at the National Institute of Infectious Diseases, Tokyo, Japan (joint appointment with the Department of Pathology), and a student in the joint PhD program at the London School of Hygiene and Tropical Medicine and Nagasaki University. His research interests include infectious diseases (especially emerging and reemerging infectious diseases) and global health.

References

1. World Health Organization. Coronavirus disease (COVID-19) pandemic [cited 2022 Jun 5]. https://www.who.int/emergencies/diseases/novel-coronavirus-2019
2. Andrews N, Stowe J, Kirsebom F, Toffa S, Rickeard T, Gallagher E, et al. Covid-19 vaccine effectiveness against the Omicron (B.1.1.529) variant. N Engl J Med. 2022;386:1532–46. https://doi.org/10.1056/NEJMoa2119451
3. Tseng HF, Ackerson BK, Luo Y, Sy LS, Talarico CA, Tian Y, et al. Effectiveness of mRNA-1273 against SARS-CoV-2 Omicron and Delta variants [Erratum in: Nat Med. 2022;28:1095]. Nat Med. 2022;28:1063–71. https://doi.org/10.1038/s41591-022-01753-y
4. United Kingdom Health Security Agency. COVID-19 vaccine surveillance reports [cited 2022 Jun 5]. https://www.gov.uk/government/publications/covid-19-vaccine-weekly-surveillance-reports
5. Dong E, Du H, Gardner L. An interactive web-based dashboard to track COVID-19 in real time. Lancet Infect Dis. 2020;20:533–4. https://doi.org/10.1016/S1473-3099(20)30120-1
6. Nomura S, Eguchi A, Yoneoka D, Kawashima T, Tanoue Y, Murakami M, et al. Reasons for being unsure or unwilling regarding intention to take COVID-19 vaccine among Japanese people: a large cross-sectional national survey. Lancet Reg Health West Pac. 2021;14:100223. https://doi.org/10.1016/j.lanwpc.2021.100223
7. Yoda T, Katsuyama H. Willingness to receive COVID-19 vaccination in Japan. Vaccines (Basel). 2021;9:48. https://doi.org/10.3390/vaccines9010048
8. Machida M, Nakamura I, Kojima T, Saito R, Nakaya T, Hanibuchi T, et al. Acceptance of a COVID-19 vaccine in Japan during the COVID-19 pandemic. Vaccines (Basel). 2021;9:210. https://doi.org/10.3390/vaccines9030210
9. Okubo R, Yoshioka T, Ohfuji S, Matsuo T, Tabuchi T. COVID-19 vaccine hesitancy and its associated factors in Japan. Vaccines (Basel). 2021;9:662. https://doi.org/10.3390/vaccines9060662
10. Arashiro T, Arima Y, Muraoka H, Sato A, Oba K, Uehara Y, et al. Behavioral factors associated with SARS-CoV-2 infection in Japan. Influenza Other Respir Viruses. 2022; 16:952–61. https://doi.org/10.1111/irv.12992

Address for correspondence: Takeshi Arashiro, Center for Surveillance, Immunization, and Epidemiologic Research, National Institute of Infectious Diseases, Toyama 1-23-1, Shinjuku, Tokyo 162-8640, Japan; email: arashirot@niid.go.jp

Infection with SARS-CoV-2 Omicron Variant 24 Days after Non-Omicron Infection, Pennsylvania, USA

Arlene G. Seid, Tigist Yirko, Sameera Sayeed, Nottasorn Plipat

Author affiliations: Pennsylvania Department of Health, Bureau of Epidemiology, Harrisburg, Pennsylvania, USA (A.G. Seid, N. Plipat); Bureau of Epidemiology, Lancaster, Pennsylvania, USA (T. Yirko); Bureau of Laboratories, Exton, Pennsylvania, USA (S. Sayeed

DOI: http://doi.org/10.3201/eid2809.220539

A 42-year-old man, with up-to-date COVID-19 vaccination, experienced symptomatic SARS-CoV-2 infection in December 2021. Mutation tests suggested a non-Omicron variant. After his recovery, and 24 days after the first positive SARS-CoV-2 test, he had onset of symptomatic infection with the BA.1.1 (Omicron) variant, which was confirmed by whole-genome sequencing.

Repeated positive findings for SARS-CoV-2 infection within 90 days pose diagnostic challenges for public health professionals. Such results imply persistent viral shedding, reinfection, or coinfection, and each determination requires a different isolation and quarantine approach. When genetic sequencing resources are limited, healthcare professionals must base risk assessment decisions on such criteria as exposure history and community transmission levels. We describe a vaccinated healthcare worker who had positive SARS-CoV-2 tests 24 days apart. Each positive test was associated with a separate symptomatic illness.

On December 20, 2021, a 42-year-old otherwise healthy man, employed in a nursing home, had onset of nausea and emesis. He was up to date with COVID-19 vaccinations, having received the 2 initial doses of the Pfizer-BioNTech vaccine (https://www.pfizer.com), as well as a booster dose on October 11, 2021. He tested positive for SARS-CoV-2 by real-time reverse transcription PCR (RT-PCR) using Taqman assays (Thermo Fisher Scientific, https://www.thermofisher.com). The PCR test detected nucleocapsid 1 protein (cycle threshold [Ct] 33), nucleocapsid 2 protein (Ct 28), and spike protein (Ct 33) genes and did not detect the open reading frame 1ab gene. Further mutation tests by TaqMan Mutation Detection Assays (Thermo Fisher Scientific) showed the absence of delH69V70, suggesting the patient's infection was probably not caused by the Omicron BA.1 variant. The patient recovered within 1 week.

On January 12, 2022, the patient had new onset of fever, chills, myalgia, and cough. Four of his 6 household members were also sick and received positive results after administration of SARS-CoV-2 at-home antigen tests (Figure). The patient was tested at an urgent care clinic. The Quidel QuickVue SARS antigen test (Quidel, https://www.quidel.com) showed a positive result, and the BD Veritor influenza A/B antigen test (Thermo Fisher Scientific) showed a negative result. Negative findings from a multiplex RT-PCR for respiratory pathogens eliminated consideration of alternative diagnoses. The patient's specimen was sent to the Pennsylvania Department of Health Bureau of Laboratories (BOL) and tested by the CDC Influenza SARS-CoV-2 (FluSC2) Multiplex RT-PCR Assay. The test result was negative for Influenza A and B, but positive for SARS-CoV-2 (Ct 19). The whole-genome sequencing (Illumina, https://www.illumina.com) yielded Omicron variant BA.1.1. The patient tested negative by RT-PCR 1 week later.

Reinfection with a different virus variant is the most likely explanation for the positive antigen and PCR tests 24 days after this patient's initial SARS-CoV-2 infection diagnosis. We base this assumption on 3 facts: the symptomatic illnesses were separated by a full, albeit brief, recovery period; tests uncovered 2 genotypically distinct variants; and household exposure presented a likely route of transmission for the second infection during an Omicron surge.

Studies have described co-infections with 2 SARS-CoV-2 variants; however, those co-infections were noted either as contributors to a singular illness or as co-detected events in the same samples (*1*,*2*). Although persistent positive test results may follow an asymptomatic period, the onset of new symptoms and subsequent confirmation of a different variant by whole-genome sequencing makes that explanation unlikely for the patient we studied.

The frequency of coronavirus reinfection has been shown to depend on many variables: the studied population, the SARS-CoV-2 variants, time and place, and the defined duration between the initial and subsequent infections. The interval between infections of the same seasonal coronavirus could be <12 months (*3*). For SARS-CoV-2, the interval between reported infections of genetically distinct variants has ranged from 23 to >90 days (*4*).

Although this case appears to lend support to prior studies demonstrating the capacity of the Omicron variant to evade immunity, our findings also suggest that a fully protective humoral and cell-mediated immunity might take longer than 24 days to

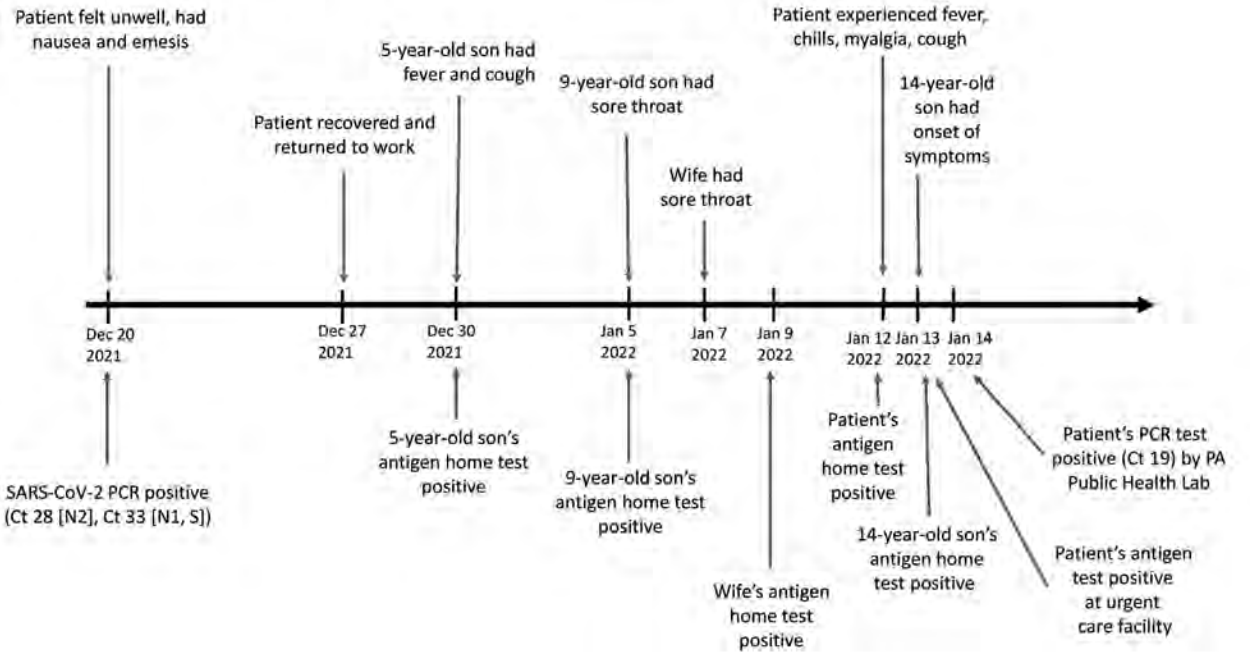

Figure. Timeline of a vaccinated healthcare worker who had positive viral tests for SARS-CoV-2 infection 24 days apart (December 20, 2021, and January 12, 2022), Pennsylvania, USA. Image shows symptoms and test results for the patient and household members. The patient and his wife were up to date with Pfizer-BioNTech (https://www.pfizer.com) SARS-CoV-2 vaccines (2 doses of primary series and 1 booster dose). Both eligible children (9-year-old and 14-year-old sons) were fully vaccinated against SARS-CoV-2. Ct, cycle threshold; N1, nucleocapsid 1 protein; N2, nucleocapsid 2 protein; PA, Pennsylvania; S, spike protein.

develop (*5*,*6*). Antibodies to SARS-CoV-2 infection may be present as early as 10 days postinfection, but the presence of antibodies alone is an incomplete predictor of protection (*7*). Cross-reactive immunity after COVID-19 illness and SARS-CoV-2 vaccination has been shown to confer broad protection against heterologous coronaviruses. This protection, however, might be variable depending on variants (*8*). When compared with ancestor and other variants, the Omicron variant has been shown to demonstrate reduced neutralization (*9*). Convalescent serum from infected patients largely did not neutralize the Omicron variant; conversely, serum from infected patients who were subsequently vaccinated and from patients who were vaccinated and had breakthrough infections did neutralize the Omicron variant, but to a lesser degree than for the Delta variant (*9*). In the patient we describe, immune response from 3 mRNA vaccines and COVID-19 infection did not prevent reinfection.

As documented in another study, household secondary attack rate by Omicron is higher (25%) than for the Delta variant (11%), even among booster-vaccinated persons (F.P. Lyngse et al., unpub. data, https://doi.org/10.1101/2021.12.27.21268278). In the patient we describe, it is more likely that household exposure led to the second infection. Still, given the short interval (24 days) between the 2 infections and the unavailable genetic sequencing data, we cannot rule out that this patient's initial infection might have been the source of the subsequent infections among members of the household. Full assessment of the clinical context, individual risk exposure, and community transmission level is essential in determining diagnosis and appropriate health intervention in patients who test positive again shortly after an initial positive viral test for SARS-CoV-2 infection.

Acknowledgments

We thank David White for helpful collaboration and Lisa Dettinger for assistance in confirmatory laboratory diagnosis.

About the Author

Dr. Seid is a public health physician at the Pennsylvania Department of Health. Her research interests include vaccine-preventable diseases.

References

1 Francisco Junior RS, Almeida LGPd, Lamarca AP, Cavalcante L, Martins Y, Gerber AL, et al. Emergence of within-host SARS-CoV-2 recombinant genome after coinfection by Gamma and Delta variants: a case

report. Front Public Health. 2022;10:849978. https://doi.org/10.3389/fpubh.2022.849978
2. Samoilov AE, Kaptelova VV, Bukharina AY, Shipulina OY, Korneenko EV, Saenko SS, et al. Case report: change of dominant strain during dual SARS-CoV-2 infection. BMC Infect Dis. 2021;21:959. https://doi.org/10.1186/s12879-021-06664-w
3. Galanti M, Shaman J. Direct observation of repeated infections with endemic coronaviruses. J Infect Dis. 2021; 223:409–15. https://doi.org/10.1093/infdis/jiaa392
4. Roskosky M, Borah BF, DeJonge PM, Donovan CV, Blevins LZ, Lafferty AG, et al. Notes from the field: SARS-CoV-2 omicron variant infection in 10 persons within 90 days of previous SARS-CoV-2 delta variant infection—four states, October 2021–January 2022. MMWR Morb Mortal Wkly Rep. 2022;71:524–6. https://doi.org/10.15585/mmwr.mm7114a2
5. Pulliam JRC, van Schalkwyk C, Govender N, von Gottberg A, Cohen C, Groome MJ, et al. Increased risk of SARS-CoV-2 reinfection associated with emergence of the omicron variant in South Africa. Science. 2022;376:eabn4947. https://doi.org/10.1126/science.abn4947
6. Soleimanian S, Alyasin S, Sepahi N, Ghahramani Z, Kanannejad Z, Yaghobi R, et al. An update on protective effectiveness of immune responses after recovery from COVID-19. Front Immunol. 2022;13:884879. https://doi.org/10.3389/fimmu.2022.884879
7. Hueston L, Kok J, Guibone A, McDonald D, Hone G, Goodwin J, et al. The antibody response to SARS-CoV-2 infection. Open Forum Infect Dis. 2020;7:ofaa387.
8. Dangi T, Palacio N, Sanchez S, Park M, Class J, Visvabharathy L, et al. Cross-protective immunity following coronavirus vaccination and coronavirus infection. J Clin Invest. 2021;131:e151969. https://doi.org/10.1172/JCI151969
9. Rössler A, Riepler L, Bante D, von Laer D, Kimpel J. SARS-CoV-2 omicron variant neutralization in serum from vaccinated and convalescent persons. N Engl J Med. 2022;386:698–700. https://doi.org/10.1056/NEJMc2119236

Address for correspondence: Nottasorn Plipat, Division of Infectious Diseases Epidemiology, Pennsylvania Department of Health, 625 Forster St, Harrisburg, PA 17120, USA; email: nplipat@pa.gov

Pathogenesis and Transmissibility of North American Highly Pathogenic Avian Influenza A(H5N1) Virus in Ferrets

Joanna A. Pulit-Penaloza, Jessica A. Belser, Nicole Brock, Poulami Basu Thakur, Terrence M. Tumpey, Taronna R. Maines

Author affiliation: Centers for Disease Control and Prevention, Atlanta, Georgia, USA

DOI: https://doi.org/10.3201/eid2809.220879

Highly pathogenic avian influenza A(H5N1) viruses have spread rapidly throughout North American flyways in recent months, affecting wild birds in over 40 states. We evaluated the pathogenicity and transmissibility of a representative virus using a ferret model and examined replication kinetics of this virus in human respiratory tract cells.

Highly pathogenic avian influenza (HPAI) A(H5Nx) viruses (clade 2.3.4.4, primarily H5N2 and H5N8 subtypes) were first detected along the Pacific flyway in 2014, resulting in outbreaks in wild bird and domestic poultry populations in North America (*1*). No human cases were associated with these outbreaks in the United States, but sporadic HPAI H5Nx virus human infections have been documented in other geographic locations, highlighting the potential of these viruses to jump species barriers during culling or sampling of infected birds (*2*). Despite reduced detection of H5Nx viruses in North America in recent years, clade 2.3.4.4b H5N1 virus, which emerged and displaced other H5Nx virus in Europe, Asia, and Africa, was detected in wild birds in North America in late 2021. Since then, the virus has been introduced into all 4 flyways of North America (*3*). The detection and spread of this virus in US commercial and backyard poultry pose substantial economic implications and concerns for human health, as evidenced by the first confirmed HPAI H5N1 human case, documented in the United States in April 2022 (*4*), underscoring the pandemic potential presented by continued circulation of viruses at the animal–human interface. To investigate the relative risk posed by these viruses, we examined the pathogenicity and transmissibility of a representative HPAI H5N1 virus, A/American Wigeon/SC/22-000345-001/2021 (aw/SC) by using a ferret model and assessed the capacity of this virus to replicate in a human respiratory cell line compared with seasonal H1N1 viruses.

Table. Results of ferrets inoculated with influenza A(H5N1) virus isolate A/American Wigeon/SC/22–000345–001/2021*

Parameter	Value
Weight loss, %†	4.7
Temperature increase, °C‡	1.1
Nasal wash titer (peak titer days)§	4.6 (1–5)
Virus titer at day 3 postinoculation¶	
Nasal wash	2.4 (3/3)
Nasal turbinates	3.5 (3/3)
Soft palate	2.9 (3/3)
Trachea	ND
Lung	2.2 (1/3)

*Six ferrets were inoculated with 6 $\log_{10}$ EID_{50} of A/American Wigeon/SC/22-000345-001/2021 (GISAID identical virus sequence accession no. EPI_ISL_9869760), https://www.gisaid.org; in a 1-mL volume. Three additional ferrets were inoculated and then euthanized and tested for virus titer at day 3 postinoculation. EID_{50}, 50% egg infectious dose; ND, not detected
†Percentage mean maximum weight loss within 9 days postinoculation.
‡Mean maximum rise in body temperature from baseline (37.6°C–39.4°C).
§Mean maximum virus titer in nasal washes, expressed as $\log_{10}$ EID_{50}/mL.
¶Viral titers are expressed as $\log_{10}$ EID_{50}/mL, except for lung titer, which is expressed as $\log_{10}$ EID_{50}/g of tissue. Number of ferrets with detectable virus is specified in parentheses. Limit of virus detection was 1.5 $\log_{10}$ EID_{50}/mL or g.

We inoculated 6 ferrets with 6 $\log_{10}$ 50% egg infectious dose (EID_{50}) of aw/SC virus (GISAID accession no. EPI_ISL_9869760; https://www.gisaid.org) and observed them for 9 days. The animals became productively infected, but the disease was generally mild; ferrets exhibited <5% weight loss and transient fever (elevated by 1.1°C) (Table). We observed no sneezing or nasal discharge during infection. Virus replication in tissues collected on day 3 postinoculation from 3 additional ferrets was limited to the upper respiratory tract except for 1 animal that had low-level virus in the lungs. We did not detect infectious virus in blood, intestines, olfactory bulb, brain, kidneys, spleen, or liver (data not shown). That finding indicates less extensive tissue dissemination of the aw/SC virus compared with previously evaluated clade 2.3.4.4 North America H5Nx viruses, which we observed throughout the ferret respiratory tract and in some olfactory bulb and intestinal samples (*5*).

Next, we evaluated transmissibility of the aw/SC H5N1 virus. We detected infectious virus in nasal wash specimens among all inoculated ferrets up to day 7 postinoculation (Figure, panels A, B). Mean peak nasal wash titers (4.6 $\log_{10}$ EID_{50}/mL) were comparable to those observed for the 2014 North America H5Nx isolates that did not transmit between ferrets

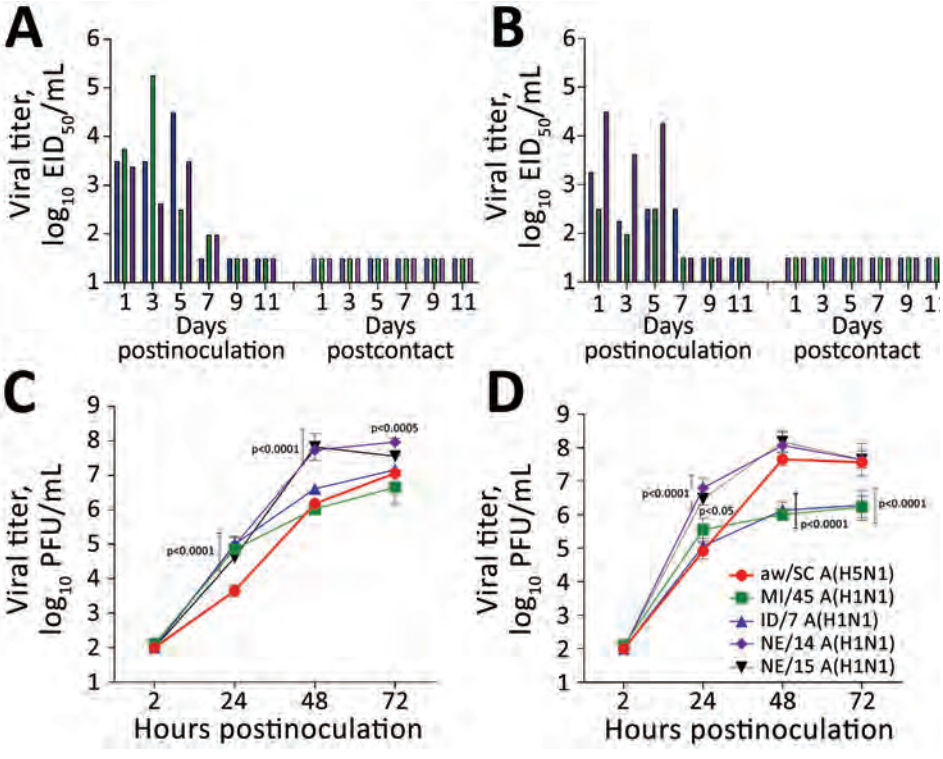

Figure. Evaluating influenza A(H5N1) virus isolate aw/SC using in vivo and in vitro models. A, B) Ferrets were intranasally inoculated with 6 $\log_{10}$ EID_{50} of aw/SC virus in 1 mL of phosphate-buffered saline and direct contact (A) and respiratory droplet (B) transmission models were established with naive ferrets (1:1 ratio) the following day as described previously (*9*). Nasal wash samples were collected from inoculated and contact ferrets every other day, and virus titers were determined in eggs (*10*). As shown, infectious virus was detected in nasal wash specimens from all inoculated ferrets up to day 7 (left side of each panel); however, ferrets exposed only by direct contact (panel A, right) or through the air (panel B, right) did not show infectious virus. C, D) Replication kinetics of aw/SC virus were evaluated in human respiratory tract cells and compared with the H1N1 viruses, A/Michigan/45/2015 (MI/45), A/Idaho/7/2018 (ID/7), A/Nebraska/14/2019 (NE/14), and A/Nebraska/15/2018 (NE/15). Calu-3 cells (ATCC, https://www.atcc.org) were grown to confluence under submerged conditions in 12-mm diameter transwell inserts (Corning, https://www.corning.com). The cells were infected apically at a multiplicity of infection of 0.01 for 1 h and then washed and incubated at 33°C (C) or 37°C (D) as previously described (*6*). Virus titers in triplicate cell-supernatant samples were determined by standard plaque assay in MDCK cells (*10*). The limit of virus detection was 1.5 $\log_{10}$ EID_{50}/mL or 2 $\log_{10}$ PFU/mL. Error bars indicate SDs. p values provided for avian H5N1 versus human seasonal H1N1 viruses were calculated by 2-way analysis of variance with a Tukey posttest. aw/SC, A/American Wigeon/SC/22-000345-001/2021; EID_{50}, 50% egg infectious dose.

($\leq$4.2 $\log_{10}$ EID_{50}/mL) (*5*). However, the aw/SC virus did not transmit in a direct-contact setting (cohoused inoculated and naive ferret pairs) or through the air (ferret pairs in separate cages with perforated cage walls), as evidenced by lack of virus detection in nasal washes and lack of seroconversion of the contact ferrets to homologous virus.

Prior evaluations of North America HPAI H5N2 and H5N8 isolates in human airway cells demonstrated that these viruses were capable of productive replication, albeit at reduced titers compared with virulent H5N1 and seasonal H1N1 viruses (*5*). To assess whether human bronchial epithelial cells support replication of the aw/SC H5N1 virus, we compared growth kinetics of this virus with contemporary H1N1 strains at 33°C and 37°C in Calu-3 cells (ATCC, https://www.atcc.org), a cell line that permits concurrent evaluation of human and zoonotic influenza viruses for risk assessment evaluations (Figure, panels C, D) (*6*). At 37°C, aw/SC H5N1 virus reached comparable peak mean titer to all H1N1 viruses tested by 48 hours postinoculation. However, at 33°C, aw/SC showed a substantial delay in virus replication at 24 hours postinoculation compared with all tested H1N1 strains ($p<0.0001$). This delay could, in part, be explained by the lack of E627K and D701N substitutions in the polymerase basic protein 2 sequence of the aw/SC virus, substitutions that are considered critical for the mammalian adaptation of avian influenza viruses (*7*). Although we noted strain-specific differences between all viruses, the data indicate that aw/SC virus can replicate efficiently in the types of cells that make up the human respiratory tract.

The introduction of HPAI H5N1 viruses into multiple North America flyways represents a substantial concern for human health. Continued circulation of viruses in wild bird populations and repeated introduction of these viruses into gallinaceous poultry confer a multitude of opportunities for these viruses to acquire molecular features associated with enhanced mammalian fitness and human infection. Our data support the Influenza Risk Assessment Tool determination that HPAI H5N1 viruses do not pose a substantial risk to public health at this time (*8*). However, close surveillance of circulating strains and continued assessment of new viruses are crucial to ensure strains with enhanced mammalian fitness are quickly identified.

Acknowledgments

We thank the CDC Comparative Medicine Branch (Division of Scientific Resources, National Center for Emerging and Zoonotic Infectious Diseases) for providing excellent animal care and Mia Torchetti, Mary Lea Killian, Kristina Lantz, and staff of the Diagnostic Virology Laboratory, National Veterinary Services Laboratories, Animal and Plant Health Inspection Service, US Department of Agriculture, for access to the virus.

All animal procedures were approved by the Institutional Animal Care and Use Committee of the Centers for Disease Control and Prevention and were conducted in an Association for Assessment and Accreditation of Laboratory Animal Care International–accredited facility.

About the Author

Dr. Pulit-Penaloza is a biologist at the Centers for Disease Control and Prevention in Atlanta. Her research interests include the pathogenicity and transmissibility of newly emerging influenza viruses with pandemic potential.

References

1. Lee DH, Torchetti MK, Winker K, Ip HS, Song CS, Swayne DE. Intercontinental spread of Asian-origin H5N8 to North America through Beringia by migratory birds. J Virol. 2015;89:6521–4. https://doi.org/10.1128/JVI.00728-15
2. Wille M, Barr IG. Resurgence of avian influenza virus. Science. 2022;376:459–60. https://doi.org/10.1126/science.abo1232
3. Bevins SN, Shriner SA, Cumbee JC Jr, Dilione KE, Douglass KE, Ellis JW, et al. Intercontinental movement of highly pathogenic avian influenza A(H5N1) clade 2.3.4.4 virus to the United States, 2021. Emerg Infect Dis. 2022;28:1006–11. https://doi.org/10.3201/eid2805.220318
4. Centers for Disease Control and Prevention. US case of human avian influenza A(H5) virus reported. 2022 Apr 28 [cited 2022 Apr 28]. https://www.cdc.gov/media/releases/2022/s0428-avian-flu.html
5. Pulit-Penaloza JA, Sun X, Creager HM, Zeng H, Belser JA, Maines TR, et al. Pathogenesis and transmission of novel highly pathogenic avian influenza H5N2 and H5N8 viruses in ferrets and mice. J Virol. 2015;89:10286–93. https://doi.org/10.1128/JVI.01438-15
6. Zeng H, Goldsmith C, Thawatsupha P, Chittaganpitch M, Waicharoen S, Zaki S, et al. Highly pathogenic avian influenza H5N1 viruses elicit an attenuated type I interferon response in polarized human bronchial epithelial cells. J Virol. 2007;81:12439–49. https://doi.org/10.1128/JVI.01134-07
7. Nuñez IA, Ross TM. A review of H5Nx avian influenza viruses. Ther Adv Vaccines Immunother. 2019;7:2515135518821625. https://doi.org/10.1177/2515135518821625
8. Centers for Disease Control and Prevention. Summary of Influenza Risk Assessment Tool (IRAT). H5N1 clade 2.3.4.4b [A/American wigeon/South Carolina/AH0195145/2021] [cited 2022 Mar 31]. https://www.cdc.gov/flu/pandemic-resources/monitoring/irat-virus-summaries.htm#H5N122
9. Maines TR, Chen LM, Matsuoka Y, Chen H, Rowe T, Ortin J, et al. Lack of transmission of H5N1 avian-human reassortant influenza viruses in a ferret model. Proc Natl Acad Sci U S A. 2006;103:12121–6. https://doi.org/10.1073/pnas.0605134103
10. Szretter KJ, Balish AL, Katz JM. Influenza: propagation, quantification, and storage. Curr Protoc Microbiol. 2006;15:15G.1.1–1.22.

Address for correspondence: Taronna R. Maines, Centers for Disease Control and Prevention, 1600 Clifton Rd NE, Mailstop H17-5, Atlanta, GA 30329-4027, USA; email: zay9@cdc.gov

Antibodies against SARS-CoV-2 Suggestive of Single Events of Spillover to Cattle, Germany

Kerstin Wernike, Jens Böttcher, Silke Amelung, Kerstin Albrecht, Tanja Gärtner, Karsten Donat, Martin Beer

Author affiliations: Friedrich-Loeffler-Institut, Greifswald–Insel Riems, Germany (K. Wernike, M. Beer); Bavarian Animal Health Service, Poing, Germany (J. Böttcher); LUFA Nord-West, Oldenburg, Germany (S. Amelung); State Institute for Consumer Protection of Saxony-Anhalt, Stendal, Germany (K. Albrecht); Thuringian Animal Diseases Fund, Animal Health Service, Jena, Germany (T. Gärtner, K. Donat)

DOI: https://doi.org/10.3201/eid2809.220125

Human infection with SARS-CoV-2 poses a risk for transmission to animals. To characterize the risk for cattle, we serologically investigated 1,000 samples collected from cattle in Germany in late 2021. Eleven antibody-positive samples indicated that cattle may be occasionally infected by contact with SARS-CoV-2–positive keepers, but we found no indication of further spread.

Since its first detection at the end of 2019, SARS-CoV-2, which induces COVID-19 in humans, very rapidly spread around the world, causing a massive global pandemic that resulted in >5 million deaths in <2 years of virus circulation (*1*). Since the beginning of the pandemic, researchers have discussed the role of livestock and wildlife species at the human–animal interface, with a special focus on the identification of susceptible species and potential intermediate or reservoir hosts.

Under experimental conditions, various animal species could be infected with SARS-CoV-2, including nonhuman primates, felids, canids, mustelids, white-tailed deer, and several species of *Cricetidae* rodents; poultry or swine were not susceptible (*2*). For domestic ruminants such as cattle, sheep, or goats, susceptibility after experimental inoculation was low; only a small proportion of animals could be infected without animal-to-animal transmission (*3*–*5*). Furthermore, 26 cattle exposed in the field to SARS-CoV-2 by contact with their infected keepers tested negative by reverse transcription PCR (*6*). However, given the very short time at which cattle test positive by reverse transcription PCR after experimental infection (1–2 days) (*3*,*7*), serologic screening could be more beneficial for identifying previously infected animals and estimating the rate of spillover infections in the field.

We analyzed 1,000 serum or plasma samples from cattle at 83 farms in 4 federal states in Ger-

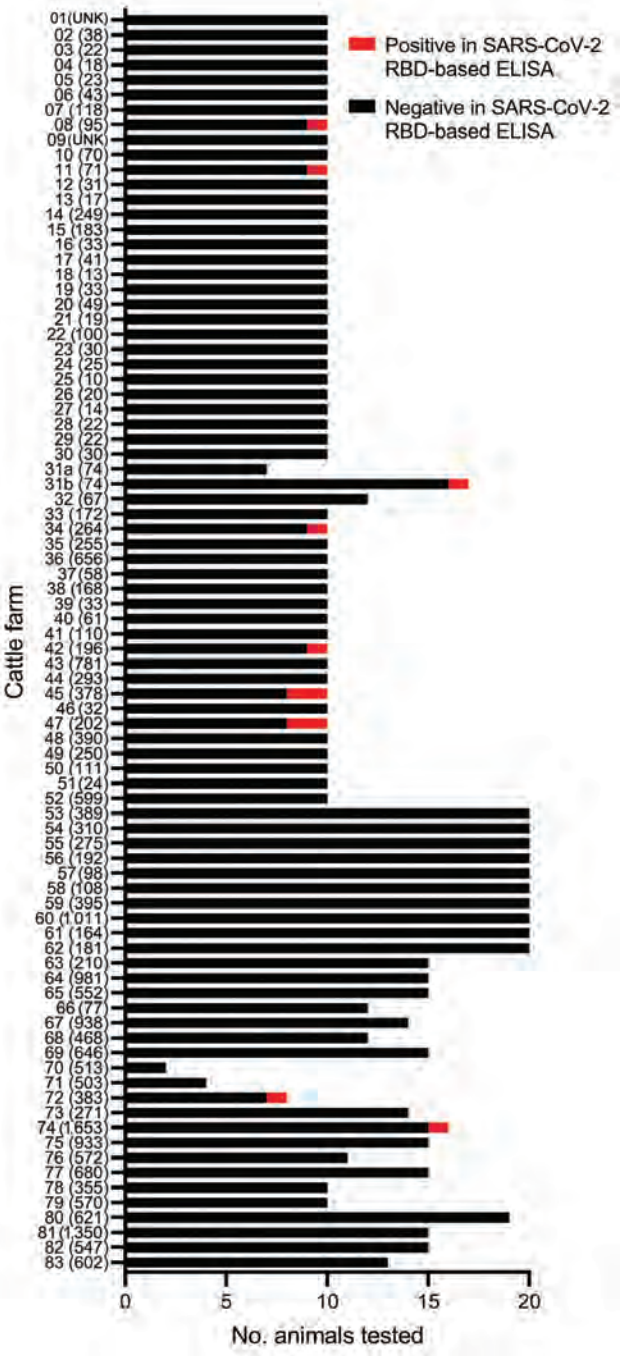

Figure. Number of cattle per farm tested for antibodies against SARS-CoV-2, Germany, 2021. Numbers in parentheses indicate herd size. Black bar sections indicate samples with negative reaction in the RBD-based ELISA; red bar sections indicate positive samples. Farm 31 was sampled twice (indicated as 31a and 31b), before and after animal owner quarantine. RBD, receptor-binding domain; UNK, unknown.

Table. Results of samples that tested positive by a multispecies SARS-CoV-2 RBD-based ELISA, Germany, 2021*

Cattle farm/animal number (federal state)	RBD-ELISA, corrected OD	Indirect IFA, titer	sVNT, % inhibition
8/1 (Bavaria)	**0.35**	<1:8	6.1
11/1 (Bavaria)	**0.70**	**1:32**	**36.4**
31/1 (Bavaria)	**1.00**	**1:512**	**57.8**
34/1 (Lower Saxony)	**0.50**	**1:32**	11.7
42/1 (Lower Saxony)	**0.65**	**1:16**	5.5
45/1 (Lower Saxony)	**0.67**	**1:8**	10.6
45/2 (Lower Saxony)	**0.33**	**1:16**	9.0
47/1 (Lower Saxony)	**0.48**	**1:8**	**37.1**
47/2 (Lower Saxony)	**0.67**	**1:8**	0.6
72/1 (Thuringia)	**0.52**	**1:16**	4.7
74/1 (Thuringia)	**0.76**	**1:32**	**54.2**

*Boldface indicates positive results. IFA, immunofluorescence assay; OD, optical density; RBD, receptor-binding domain; sVNT, surrogate virus neutralization test (cPass SARS-CoV-2 Surrogate Virus Neutralization Test Kit; GenScript, https://www.genscript.com; cutoff ≥30% positive and <30% negative).

many (Bavaria, Lower Saxony, Saxony-Anhalt, and Thuringia). Because the samples represented superfluous material from routine diagnostic submissions by the responsible veterinarians in the context of the health monitoring of the respective cattle farm, no permissions were needed to collect these specimens. Sampling dates were autumn 2021 and early winter 2021–22, during a massive wave of infections in the human population driven by the SARS-CoV-2 Delta variant of concern. We analyzed 2–20 randomly selected serum or plasma samples per farm (Figure). Farm 31 was sampled twice; between farm samplings, the animal owner was quarantined. We do not know whether this quarantine resulted from contact with an infected person or whether the owner himself tested SARS-CoV-2 positive. All bovine samples were tested by a receptor-binding domain (RBD)–based multispecies ELISA (diagnostic sensitivity 98.31% and specificity 100%) performed as described previously (*8*). Initial test validation and an experimental SARS-CoV-2 infection study in cattle have demonstrated that the ELISA does not cross-react with the bovine coronavirus (BCoV) (*3*,*8*). We investigated an additional 100 cattle control samples randomly collected across Germany in 2016, and all tested negative.

Of the cattle sampled in 2021, eleven animals from 9 farms tested positive by the RBD ELISA; among them was 1 animal on farm 31, sampled after the owner was quarantined (Figure). Positive ELISA results for all but 1 sample (farm 8) could be confirmed by an indirect immunofluorescence assay that used Vero cells infected with the SARS-CoV-2 strain 2019_nCoV Muc-IMB-1 (multiplicity of infection of 0.1) as antigen matrix (*3*). Titers ranged from 1:8 through 1:512, and the highest titer was from the seropositive animal on farm 31 (Table). To further confirm the reactivity toward SARS-CoV-2, we additionally tested the 11 samples that reacted positive in the RBD-ELISA by using a surrogate virus neutralization test (cPass SARS-CoV-2 Surrogate Virus Neutralization Test [sVNT]; Kit; GenScript, https://www.genscript.com). This test enables detection of neutralizing antibodies by mimicking the interaction between SARS-CoV-2 and host cell membrane receptor protein ACE2; it is reportedly highly specific but only moderately sensitive for animal samples because it does not detect low antibody titers (*9*). sVNT produced positive results for 4 cattle (farms 11, 31, 47, and 74; Table).

Our findings of a low number of individual seropositive cattle on several farms demonstrate that cattle might be occasionally infected and seroconvert after contact with infected humans. However, in keeping with experimental infection studies (*3*), intraspecies transmission seems likewise to not occur in the field. Nevertheless, cattle farms should be included in future monitoring programs, especially because another coronavirus (i.e., BCoV) is highly prevalent in the cattle population and a BCoV infection did not prevent a SARS-CoV-2 infection in a previous study (*3*). Furthermore, we do not know the susceptibility of animal hosts for the Omicron variant. Double infections of individual animals could potentially lead to recombination between both viruses, a phenomenon described for other coronaviruses (*10*). Although emergence is highly unlikely because of the low susceptibility of cattle for SARS-CoV-2, a conceivable chimera between SARS-CoV-2 and BCoV could represent an additional threat. Hence, ruminants should be included in outbreak investigations, and regular screenings should be performed to exclude any spread of new variants in the livestock population.

This article was originally a preprint (https://www.biorxiv.org/content/10.1101/2022.01.17.476608v1).

Acknowledgments

We thank Bianka Hillmann and Mareen Lange for excellent technical assistance.

The study was supported by intramural funding by the German Federal Ministry of Food and Agriculture provided to the Friedrich-Loeffler-Institut.

About the Author

PD Dr. Wernike is a veterinarian and senior scientist at the Friedrich-Loeffler-Institut, Greifswald-Insel Riems, Germany. Her research interests include emerging viruses, host–virus interactions, and immunoprophylaxis.

References

1. Dong E, Du H, Gardner L. An interactive web-based dashboard to track COVID-19 in real time. Lancet Infect Dis. 2020;20:533–4. https://doi.org/10.1016/S1473-3099(20)30120-1
2. Michelitsch A, Wernike K, Ulrich L, Mettenleiter TC, Beer M. SARS-CoV-2 in animals: from potential hosts to animal models. Adv Virus Res. 2021;110:59–102. https://doi.org/10.1016/bs.aivir.2021.03.004
3. Ulrich L, Wernike K, Hoffmann D, Mettenleiter TC, Beer M. Experimental infection of cattle with SARS-CoV-2. Emerg Infect Dis. 2020;26:2979–81. https://doi.org/10.3201/eid2612.203799
4. Gaudreault NN, Cool K, Trujillo JD, Morozov I, Meekins DA, McDowell C, et al. Susceptibility of sheep to experimental co-infection with the ancestral lineage of SARS-CoV-2 and its alpha variant. Emerg Microbes Infect. 2022;11:662–75.
5. Bosco-Lauth AM, Walker A, Guilbert L, Porter S, Hartwig A, McVicker E, et al. Susceptibility of livestock to SARS-CoV-2 infection. Emerg Microbes Infect. 2021;10:2199–201. https://doi.org/10.1080/22221751.2021.2003724
6. Cerino P, Buonerba C, Brambilla G, Atripaldi L, Tafuro M, Concilio DD, et al. No detection of SARS-CoV-2 in animals exposed to infected keepers: results of a COVID-19 surveillance program. Future Sci OA. 2021;7:FSO711. https://doi.org/10.2144/fsoa-2021-0038
7. Falkenberg S, Buckley A, Laverack M, Martins M, Palmer MV, Lager K, et al. Experimental inoculation of young calves with SARS-CoV-2. Viruses. 2021;13:441. https://doi.org/10.3390/v13030441
8. Wernike K, Aebischer A, Michelitsch A, Hoffmann D, Freuling C, Balkema-Buschmann A, et al. Multi-species ELISA for the detection of antibodies against SARS-CoV-2 in animals. Transbound Emerg Dis. 2021;68:1779–85. https://doi.org/10.1111/tbed.13926
9. Embregts CWE, Verstrepen B, Langermans JAM, Böszörményi KP, Sikkema RS, de Vries RD, et al. Evaluation of a multi-species SARS-CoV-2 surrogate virus neutralization test. One Health. 2021;13:100313. https://doi.org/10.1016/j.onehlt.2021.100313
10. Forni D, Cagliani R, Clerici M, Sironi M. Molecular evolution of human coronavirus genomes. Trends Microbiol. 2017;25:35–48. https://doi.org/10.1016/j.tim.2016.09.001

Address for correspondence: Kerstin Wernike and Martin Beer, Institute of Diagnostic Virology, Friedrich-Loeffler-Institut, Südufer 10, 17493 Greifswald–Insel Riems, Germany; email: kerstin.wernike@fli.de and martin.beer@fli.de

Effect of Frequent SARS-CoV-2 Testing on Weekly Case Rates in Long-Term Care Facilities, Florida, USA

Lao-Tzu Allan-Blitz, Belal Aboabdo, Isaac Turner, Jeffrey D. Klausner

Author affiliations: Brigham and Women's Hospital Department of Medicine, Boston, Massachusetts, USA (L.-T. Allan-Blitz); Curative Inc., San Dimas, California, USA (B. Aboabdo, I. Turner); University of Southern California Keck School of Medicine, Los Angeles, California, USA (J.D. Klausner)

DOI: https://doi.org/10.3201/eid2809.212577

We analyzed 1,292,165 SARS-CoV-2 test results from residents and employees of 361 long-term care facilities in Florida, USA. A 1% increase in testing resulted in a 0.08% reduction in cases 3 weeks after testing began. Increasing SARS-CoV-2 testing frequency is a viable tool for reducing virus transmission in these facilities.

Residents of long-term care facilities (LTCFs) in the United States have suffered a disproportionate number of deaths from SARS-CoV-2 (*1*). Testing frequency and result turnaround times may be more relevant than test sensitivity for infection control (*2*,*3*), information that might be used to guide infection control efforts in congregate living facilities (*4*). Semimonthly testing for SARS-CoV-2 was mandated in Florida, USA, for all employees and residents of skilled nursing, elder care, and assisted living facilities beginning June 7, 2020 (*5*). Comparing data from before and after the mandate took effect, we evaluated the effect of testing frequency on weekly SARS-CoV-2 case rates in a real-world setting.

We analyzed deidentified test results from Florida LTCFs during June 2020–April 2021, aggregated with the Nursing Home Provider Information dataset (*6*), which includes the number of facility beds and staff and average aid hours per resident. We further combined our dataset with Johns Hopkins University SARS-CoV-2 time-series data on rates of hospitalization and death (*7*). For the duration of the study period, only care facility staff were permitted entry to the facilities to limit potential sources of infection.

We used a generalized linear mixed regression model with weekly cases as a negative binomial random count variable to assess how the independent variables affected test positivity. We created a naive

Table. Estimated change in weekly SARS-CoV-2 cases because of increased testing frequency for residents of long-term care facilities, Florida, USA, June 2020–April 2021

Characteristics	Percent change in weekly cases	p value
Time-point of increased testing*		
One week preceding	0.10 (0.03–0.16)	0.003
Two weeks preceding	–0.02 (–0.09 to 0.04)	0.53
Three weeks preceding	–0.08 (–0.14 to –0.02)	0.01
Four weeks preceding	–0.03 (–0.09 to 0.03)	0.34
Nursing home size and quality		
Certified beds per facility	0.006 (0.004–0.008)	<0.001
Aid hours per resident per facility	–0.07 (–0.17 to 0.03)	0.16
Virus conditions		
Cases among long-term care facilities in preceding week	0.09 (0.09–0.10)	<0.001
New county-level cases per 100,000 persons	0.002 (0.001–0.002)	<0.001
Tested after January 2021†	–0.70 (–0.82 to –0.58)	<0.001

*Based on number of tests per occupied bed.
†Used as a surrogate for SARS-CoV-2 vaccination.

model based on frequency of SARS-CoV-2 on the day before the start of semimonthly testing to establish a baseline from which to forecast change. We then regressed weekly positive cases from the date semimonthly testing began (given heterogeneity in compliance, modeled as percentage increase in number of tests above baseline), cases from the preceding week, new cases per 100,000 persons in the county, total tests per occupied bed (a surrogate for compliance with semimonthly testing), number of certified beds in the facility, total nurse staffing hours per resident per day (as a surrogate for quality of care), and whether the date of infection was after January 1, 2021, to control for vaccination effects. We analyzed the date that semimonthly testing began as distinct weeks preceding any change in average weekly SARS-CoV-2 cases to investigate a potential time-delay between onset of testing and any potential reduction in case rate. We log transformed all variables except number of cases in the preceding week. We applied a random effect for each nursing home. We performed all analyses using R statistical software (http://www.r-project.org). Review of deidentified data was deemed exempt from institutional review.

We analyzed 1,292,165 SARS-CoV-2 RNA test results from residents and employees among 361 facilities located across 247 Florida postal codes. The average age (±SD) of the study population was 49 years (±31). The average number of new cases among all LTCFs in Florida was 187.9 per week (±148.7), an estimated 0.7 tests/week/occupied bed (±16.2). The average test turnaround time from laboratory receipt was 17.1 hours (±10.4). The average number of tests completed per week was 31,454 (±10,926).

In multivariable analysis, a 1% increase in testing frequency resulted in a 0.08% reduction in SARS-CoV-2 cases (Table). On the basis of the coefficients from the multivariable model, we predicted that a 10% increase in testing frequency would result in a 1% reduction in the weekly long-term care facility case rate among residents. Assuming generalizability on the basis of similar characteristics between LTCFs in our dataset and those reported by the Nursing Home Provider Information dataset (*6*), that reduction would result in 126 fewer cases per week, or 6,552 fewer cases per year, among LTCF residents across the United States.

Our findings suggest that even a 1% increase in testing might be an effective strategy for combating the SARS-CoV-2 pandemic among LTCF residents, although results likely would not emerge until ≈3 weeks after the increase. In the initial 1–2 weeks after semimonthly testing began, isolation and contact tracing interventions likely had not had sufficient time to substantially reduce viral transmission. Conversely, increased testing frequency >3 weeks before data collection was likely too remote to affect case estimates for a given week. A similar finding has been reported; a SARS-CoV-2 infection outbreak in a 135-bed facility was contained predominantly through serial testing of all residents and staff every 3–5 days (*8*). Routine testing is furthermore necessary to identify presymptomatic and asymptomatic cases, which could account for up to 40% of new infections (*9*) and contribute substantially to transmission. Additional studies should evaluate the cost per case prevented of strategies employing varying frequencies of testing to guide use of testing programs among LTCFs.

Our study was limited by the absence of details on interventions started in response to positive tests or whether test samples were from employees or residents. We also were unable to account for concomitant local or statewide interventions such as mask mandates, resident spacing, or indoor ventilation, which might have confounded the effects of testing frequency. Thus, our findings cannot definitively

attribute the reduction in case rates to increased testing frequency. However, the large sample size and number of LTCFs included in the analysis, which controlled for several notable confounders, lend credibility to our findings. We advocate increasing SARS-CoV-2 testing frequency as a viable tool for reducing transmission in LTCFs.

Acknowledgments

The authors acknowledge Mitchel Roznik and the state of Florida government for contributions to the project.

This research was supported in part by a gift to the Keck School of Medicine of the University of Southern California by the W.M. Keck Foundation.

L.-T.A.-B. served as a consultant for and Belal Aboabdo is an employee of Curative Inc. I.T. is chief technology officer and cofounder of Curative Inc. J.D.K. served as an independent medical director for Curative Inc.

About the Author

Dr. Allan-Blitz is a resident physician in internal medicine and pediatrics at Brigham and Women's Hospital and Boston Children's Hospital. His research focuses on infectious diseases and health equity, specifically in resource-limited settings.

References

1. Thomas KS, Zhang W, Dosa DM, Carder P, Sloane P, Zimmerman S. Estimation of excess mortality rates among us assisted living residents during the COVID-19 pandemic. JAMA Netw Open. 2021;4:e2113411. https://doi.org/10.1001/jamanetworkopen.2021.13411
2. Larremore DB, Wilder B, Lester E, Shehata S, Burke JM, Hay JA, et al. Test sensitivity is secondary to frequency and turnaround time for COVID-19 surveillance. Sci Adv. 2021;7:eabd5393.
3. Mina MJ, Parker R, Larremore DB. Rethinking Covid-19 test sensitivity—a strategy for containment. N Engl J Med. 2020;383:e120. https://doi.org/10.1056/NEJMp2025631
4. Holmdahl I, Kahn R, Hay JA, Buckee CO, Mina MJ. Estimation of transmission of COVID-19 in simulated nursing homes with frequent testing and immunity-based staffing. JAMA Netw Open. 2021;4:e2110071. https://doi.org/10.1001/jamanetworkopen.2021.10071
5. Agency for Health Care Administration. Florida. Rule 59AER20–5 mandatory testing for nursing home staff [cited 2021 Jun 22]. https://ahca.myflorida.com/docs/59AER20-5_Mandatory_Testing_for_Nursing_Home_Staff.pdf
6. Centers for Medicare Services. COVID-19 nursing home data [cited 2021 Jun 1]. https://data.cms.gov/stories/s/COVID-19-Nursing-Home-Data/bkwz-xpvg
7. Dong E, Du H, Gardner L. An interactive web-based dashboard to track COVID-19 in real time. Lancet Infect Dis. 2020;20:533–4. https://doi.org/10.1016/S1473-3099(20)30120-1
8. Escobar DJ, Lanzi M, Saberi P, Love R, Linkin DR, Kelly JJ, et al. Mitigation of a COVID-19 outbreak in a nursing home through serial testing of residents and staff. Clin Infect Dis. 2021;72:e394–6. PubMed https://doi.org/10.1093/cid/ciaa1021
9. Louie JK, Scott HM, DuBois A, Sturtz N, Lu W, Stoltey J, et al.; San Francisco Department of Public Health COVID-19 Skilled Nursing Facility Outbreak Response Team. Lessons From mass-testing for coronavirus disease 2019 in long-term care facilities for the elderly in San Francisco. Clin Infect Dis. 2021;72:2018–20. https://doi.org/10.1093/cid/ciaa1020

Address for correspondence: Lao-Tzu Allan-Blitz, Department of Medicine, Brigham and Women's Hospital, 75 Francis St, Boston, MA 02115, USA; email: lallan-blitz@partners.org; Jeffrey D. Klausner, Department of Population and Public Health Sciences, Keck School of Medicine, University of Southern California, 1845 N Soto Ave, Los Angeles, CA 90033, USA; email: jdklausner@med.usc.edu

Highly Divergent SARS-CoV-2 Alpha Variant in Chronically Infected Immunocompromised Person

Bas B. Oude Munnink, Roel H.T. Nijhuis, Nathalie Worp, Marjan Boter, Babette Weller, Babs E. Verstrepen, Corine GeurtsvanKessel, Maarten F. Corsten, Anne Russcher, Marion Koopmans

Author affiliations: Erasmus Medical Center, Rotterdam, the Netherlands (B.B. Oude Munnink, N. Worp, M. Boter, B. Weller, B.E. Verstrepen, C. GeurtsvanKessel, M. Koopmans); Meander Medical Center, Amersfoort, the Netherlands (R.H.T. Nijhuis, M.F. Corsten, A. Russcher)

DOI: https://doi.org/10.3201/eid2809.220875

We detected a highly divergent SARS-CoV-2 Alpha variant in an immunocompromised person several months after the latest detection of the Alpha variant in the Netherlands. The patient was infected for 42 weeks despite several treatment regimens and disappearance of most clinical symptoms. We identified several potential immune escape mutations in the spike protein.

Persons with an immune deficiency can be infected with viral pathogens for a prolonged period. This occurrence has been reported for noroviruses (*1*) but also has been documented for SARS-CoV-2 (*2*). We report a patient with type 2 diabetes mellitus and chronic lymphocytic leukemia who had been infected for 42 weeks with SARS-CoV-2. The patient was hospitalized on April 23, 2021, and received optiflow treatment with dexamethasone, tocilizumab, and remdesivir. After May 11, 2021, the patient recovered and experienced no residual symptoms. Almost 9 months later, on February 3, 2022, the patient was readmitted to the hospital for leukemia-related anemia and tested positive for SARS-CoV-2 once again. A month later, the patient died of causes unrelated to SARS-CoV-2.

In all, the patient tested positive for SARS-CoV-2 in 6 nasal or pharyngeal swab specimens. We performed whole-genome sequencing on all specimens by using an amplicon-based sequencing approach, as previously described, with the updated ARTIC primers version 4.1 (ARTIC Network, https://artic.network/mcov-2019) (*3*). The sequencing was successful for 2 specimens from mid-2021 and 2 specimens from early 2022 (Table). Pangolin version 4.0.6 PLEARN-v1.8 classification using default settings demonstrated that all sequenced viruses belonged to the Alpha (B.1.1.7) variant of concern (VOC) (*5*), Nextclade version 1.14.1 strain 20I (*6*). The samples were run on flow-cells containing 96 samples, including a positive and negative control (pangolin lineage B.1.77.50) to exclude potential contamination. GISAID's EpiCoV database (https://www.gisaid.org) showed that the latest isolate identified as Alpha in the Netherlands was collected on October 13, 2021, suggesting that the variant had not been circulating in the Netherlands since that time. Phylogenetic analysis by IQ-TREE (*7*) using all unique downsampled Alpha sequences available in GISAID (*8*) from the Netherlands showed that the viruses detected on January 31 and February 3, 2022, were identical but distinct from previously observed Alpha lineages in the Netherlands (Figure). A zoom-in of the phylogenetic tree showed that all sequences of the virus in the patient cluster together in a separate branch, suggesting that the patient was chronically infected with this specific variant of SARS-CoV-2 (Appendix Figure 1, https://wwwnc.cdc.gov/EID/article/28/9/22-0875-App1.pdf).

Over time, we identified 24 nucleotide mutations when we compared sequences from the earliest and latest timepoints. Of these mutations, 19 mutations were nonsynonymous, resulting in 13 amino acid mutations in open reading frame 1ab and 6 amino acid mutations in the spike protein (Table; Appendix Figure 2). Of the 6 mutations in the spike protein, 3 are located in the receptor-binding domain (G339D, N439K, and V483F), 2 are located in the N-terminal domain (W64R and

Table. Mutations detected over time by WGS in an immunocompromised person chronically infected with a highly divergent SARS-CoV-2 Alpha variant in the Netherlands, using the nucleotide coordinate system of Wuhan-Hu-1*

Collection date	GISAID (ENA) accession no.	Ct value†	ORF1ab mutations	Spike mutations	E gene mutations	N gene mutations
2021 Apr 13	EPI_ISL_10688798 (ERS1216848)	20.3				
2021 Apr 28	NA	17.9	NS	NS	NS	NS
2021 May 5	NA	22.3	NS	NS	NS	NS
2021 May 26	EPI_ISL_2887843 (ERS7202253)	22.1	C5178A, G5880T, C12852T, C17555A	NM	NM	NM
2022 Jan 31	EPI_ISL_10072285 (ERS10975083)	NA‡	A570T, G713T, G4232T, C5178A, G5880T, C11653T, C11665T, C12528T, A12555G, C12624T, G12761T, C12774T, C12852T, C17555A, T18340C, G20578T	T21752A, G21987T, G22578A, C22879A, G23009T, C25282T, C25350T	T26418C	NM
2022 Feb 3	EPI_ISL_13133128 (ERS11204596)	23.6	A570T, G713T, G4232T, C5178A, G5880T, C11653T, C11665T, C12528T, A12555G, C12624T, G12761T, C12774T, C12852T, C17555A, T18340C, G20578T	T21752A, G21987T, G22578A, C22879A, G23009T, C25282T, C25350T	T26418C	NM

*Wuhan-Hu-1 strain, GenBank accession no. NC_045512.2. Ct, cycle threshold; E, envelope; ENA, European Nucleotide Association (https://www.ebi.ac.uk/ena/browser); GISAID, https://www.gisaid.org; ORF1ab, open reading frame 1ab; N, nucleocapsid; NA, not applicable; NM, no mutations compared with the sequence from the earliest timepoint; NS, whole-genome sequencing not successful; WGS, whole-genome sequencing.
†Real-time PCR as described previously was performed (*4*) to test for the E gene and the RNA-dependent RNA polymerase gene. The lowest Ct value is reported.
‡This specimen was tested using the Aptima SARS-CoV-2 assay (Hologic, https://www.hologic.com) using the Panther system. This system does not provide Ct values.

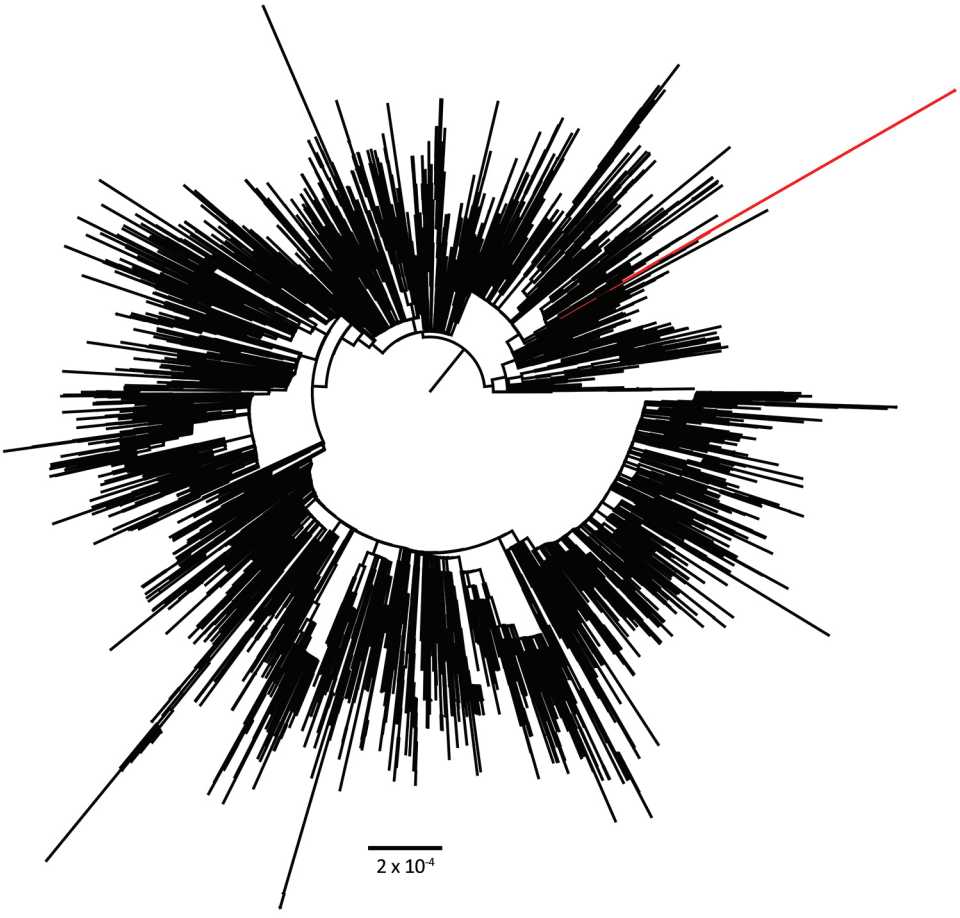

Figure. Phylogenetic analysis of all downsampled SARS-CoV-2 Alpha variants (B.1.1.7) in the Netherlands. Scale bar indicates number of substitutions per site.

G142V), and 1 is located in the transmembrane domain (P1263L). The mutation G339D can also be found in all Omicron VOCs. G142V has coevolved independently in ≥1 immunocompromised person with a long-term Alpha variant infection (S.A.J. Wilkinson et al., unpub. data, https://doi.org/10.1101/2022.03.02.22271697), and a mutation in the same position (G142D) has also been described in the Delta (B.1.617.2) and in all Omicron variants.

Our data imply that, despite receiving treatment with dexamethasone, tocilizumab, and remdesivir and being discharged without residual symptoms, the patient had not cleared the infection. Unfortunately, ex vivo rescuing of the viruses from the swabs to assess potential immune escape from circulating neutralizing antibodies was not successful, but some of the mutations we observed in this immunocompromised person with long-term SARS-CoV-2 infection could be linked to immune escape. Previous studies suggest that the G339D mutation affects neutralization in a subset of neutralizing antibodies (*9*) and that the N439K mutation causes immune escape and enhances binding affinity for human angiotensin-converting enzyme 2 (*10*,*11*). In addition, the V483F mutation has been shown previously to cause immune escape (*12*).

The constellation of this particular set of mutations has not been found elsewhere yet despite active ongoing genomic surveillance, which indicates the virus did not spread in the population (Appendix Table). Nonetheless, the detection of an Alpha variant infection in an immunocompromised person in a time when Omicron was the primary circulating variant indicates that reinfection is unlikely, which is also supported by phylogenetic analysis. This occurrence illustrates that this VOC did not completely disappear although it was last detected on October 13, 2021, in the Netherlands. In addition, several mutations were found that are also present in other VOCs, suggesting that VOCs might have emerged in long-term infected immunocompromised persons as suggested previously (*13*).

Our findings illustrate that in previously unidentified reservoirs, such as immunocompromised persons, virus variants might still be present even

when these variants are regarded as extinct and are no longer circulating among the population. In addition, we show that several mutations associated with immune escape that maintain virulence and fitness can accumulate in such an immunocompromised person. Continuous genomic surveillance in long-term infected persons is essential to elucidate their potential role in the emergence of future VOCs.

Acknowledgments

We thank the originating laboratories, where specimens were first obtained, and the submitting laboratories, where sequence data were generated and submitted to GISAID's EpiCoV Database, on which this research is based. All contributors of data may be contacted directly through the GISAID website (http://platform.gisaid.org).

This work is supported by European Union's Horizon 2020 research and innovation program under grant nos. 874735 (VEO) and 101003589 (RECoVER), as well as by ZonMW under grant no. 10150062010005.

About the Author

Dr. Oude Munnink is a researcher at the Erasmus Medical Center. His research interests include genomic surveillance of pathogens and viral zoonoses.

References

1. van Beek J, de Graaf M, Smits S, Schapendonk CME, Verjans GMGM, Vennema H, et al. Whole-genome next-generation sequencing to study within-host evolution of norovirus (NoV) among immunocompromised patients with chronic NoV infection. J Infect Dis. 2017;216:1513–24. https://doi.org/10.1093/infdis/jix520
2. Corey L, Beyrer C, Cohen MS, Michael NL, Bedford T, Rolland M. SARS-CoV-2 variants in patients with immunosuppression. N Engl J Med. 2021;385:562–6. https://doi.org/10.1056/NEJMsb2104756
3. Oude Munnink BB, Nieuwenhuijse DF, Stein M, O'Toole Á, Haverkate M, Mollers M, et al.; Dutch-Covid-19 response team. Rapid SARS-CoV-2 whole-genome sequencing and analysis for informed public health decision-making in the Netherlands. Nat Med. 2020;26:1405–10. https://doi.org/10.1038/s41591-020-0997-y
4. Corman VM, Landt O, Kaiser M, Molenkamp R, Meijer A, Chu DK, et al. Detection of 2019 novel coronavirus (2019-nCoV) by real-time RT-PCR. Euro Surveill. 2020;25:2000045. https://doi.org/10.2807/1560-7917.ES.2020.25.3.2000045
5. Rambaut A, Holmes EC, O'Toole Á, Hill V, McCrone JT, Ruis C, et al. A dynamic nomenclature proposal for SARS-CoV-2 lineages to assist genomic epidemiology. Nat Microbiol. 2020;5:1403–7. https://doi.org/10.1038/s41564-020-0770-5
6. Aksamentov I, Roemer C, Hodcroft EB, Neher RA. Nextclade: clade assignment, mutation calling and quality control for viral genomes. J Open Source Softw. 2021;6:3773. https://doi.org/10.21105/joss.03773
7. Minh BQ, Schmidt HA, Chernomor O, Schrempf D, Woodhams MD, von Haeseler A, et al. IQ-TREE 2: new models and efficient methods for phylogenetic inference in the genomic era. Mol Biol Evol. 2020;37:1530–4. https://doi.org/10.1093/molbev/msaa015
8. Shu Y, McCauley J. GISAID: Global initiative on sharing all influenza data—from vision to reality. Euro Surveill. 2017 ;22:30494. https://doi.org/10.2807/1560-7917.ES.2017.22.13.30494
9. Cao Y, Wang J, Jian F, Xiao T, Song W, Yisimayi A, et al. Omicron escapes the majority of existing SARS-CoV-2 neutralizing antibodies. Nature. 2022;602:657–63. https://doi.org/10.1038/s41586-021-04385-3
10. Thomson EC, Rosen LE, Shepherd JG, Spreafico R, da Silva Filipe A, Wojcechowskyj JA, et al.; ISARIC4C Investigators; COVID-19 Genomics UK (COG-UK) Consortium. Circulating SARS-CoV-2 spike N439K variants maintain fitness while evading antibody-mediated immunity. Cell. 2021;184:1171–87.e20. https://doi.org/10.1016/j.cell.2021.01.037
11. Starr TN, Greaney AJ, Hannon WW, Loes AN, Hauser K, Dillen JR, et al. Shifting mutational constraints in the SARS-CoV-2 receptor-binding domain during viral evolution. Science. 2022;377;420–4. https://doi.org/10.1126/science.abo7896
12. Weisblum Y, Schmidt F, Zhang F, DaSilva J, Poston D, Lorenzi JCC, et al. Escape from neutralizing antibodies by SARS-CoV-2 spike protein variants. Elife. 2020;9:1. https://doi.org/10.7554/eLife.61312
13. Oude Munnink BB, Worp N, Nieuwenhuijse DF, Sikkema RS, Haagmans B, Fouchier RAM, et al. The next phase of SARS-CoV-2 surveillance: real-time molecular epidemiology. Nat Med. 2021;27:1518–24. https://doi.org/10.1038/s41591-021-01472-w

Address for correspondence: Bas Oude Munnink, Erasmus Medical Center, Department of Viroscience, Doctor Molewaterplein 40, 3015GD Rotterdam, The Netherlands; email: b.oudemunnink@erasmusmc.nl

Molecular Epidemiology of *Blastomyces gilchristii* Clusters, Minnesota, USA

Ujwal R. Bagal, Malia Ireland, Annastasia Gross, Jill Fischer, Meghan Bentz, Elizabeth L. Berkow, Anastasia P. Litvintseva, Nancy A. Chow

Author affiliations: Centers for Disease Control and Prevention, Atlanta, Georgia, USA (U.R. Bagal, M. Bentz, E.L. Berkow, A.P. Litvintseva, N.A. Chow); Minnesota Department of Health, St. Paul, Minnesota, USA (M. Ireland, A. Gross, J. Fischer)

DOI: https://doi.org/10.3201/eid2809.220392

We characterized 2 clusters of blastomycosis cases in Minnesota, USA, using whole-genome sequencing and single-nucleotide polymorphism analyses. *Blastomyces gilchristii* was confirmed as the cause of infection. Genomic analyses corresponded with epidemiologic findings for cases of *B. gilchristii* infections, demonstrating the utility of genomic methods for future blastomycosis outbreak investigations.

Three pathogenic *Blastomyces* species, *B. dermatitidis, B. gilchristii, and B. helicus*, have been identified in North America. In the United States, *B. dermatitidis* has been found throughout areas surrounding the Great Lakes, the Ohio and Mississippi River valleys, and the St. Lawrence River (*1*). In contrast, *B. gilchristii* has a smaller geographic range in Canada and the northern United States (*2*), and *B. helicus* has been found in the northwestern United States (*3*). No differences in clinical manifestations have been reported among these *Blastomyces* species.

In the United States, previous case reports have linked blastomycosis infections to outdoor activities, especially those involving moist soil and proximity to waterways (*4*,*5*). One of the largest reported outbreaks of blastomycosis occurred in 2015 among persons who had recreated along the Little Wolf River in Wisconsin (*6*). In Minnesota, blastomycosis is a reportable disease; epidemiologists at the Minnesota Department of Health (MDH) routinely collect demographic and clinical information for blastomycosis cases and attempt interviews to characterize illness and exposure history. The MDH Public Health Laboratory provides fungal identification services and stores isolates submitted by clinical laboratories.

Although whole-genome sequencing has been used to investigate outbreaks involving various fungal pathogens, such as *Candida auris* and *Coccidioides* spp. (*7*,*8*), this molecular technology has not been used to investigate *Blastomyces* spp. outbreaks in the United States. We performed whole-genome sequencing to determine the genetic diversity and phylogenetic relationships of 2 familial clusters of *B. gilchristii* infections identified in Minnesota.

In August 2020, five cases of blastomycosis were identified as cluster A, which comprised a family of 2 White Hispanic parents and 3 children (Table). Four of the 5 patients were hospitalized, of which 3 had sputum cultures that were positive for *Blastomyces* sp. All 5 patients recovered from illness. The mother reported that the family had visited rivers in St. Croix County, Wisconsin, numerous times during the summer. No other likely exposure locations or activities were reported.

In addition, 2 cases of blastomycosis were identified in White non-Hispanic sisters. Only 1 sister was hospitalized and had a positive culture for *Blastomyces* sp. from a bronchoalveolar lavage specimen. MDH learned that their father had blastomycosis in 2014, which was attributed to *B. dermatitidis* (*9*). The 2 patients with isolates (1 sister and the father) were classified as cluster B (Table). The family owned a cabin in Hubbard County, Minnesota, which is highly endemic for blastomycosis and was likely the exposure location for the three cases. All 3 patients recovered from illness.

Blastomyces identification is routinely performed by MDH only at the genus level. Therefore, the Centers for Disease Control and Prevention (CDC) determined the species in 4 isolates from the 2 blastomycosis clusters and performed Illumina (https://www.illumina.com) short-read sequencing (National Center

Table. Demographic and clinical data used for molecular epidemiology of 2 *Blastomyces gilchristii* clusters, Minnesota, USA*

Sample no.	Age, y/sex	Race/ethnicity	Cluster	Family relationship	Diagnosis location	Exposure location†	Clinical specimen	Specimen collection date
B19405	15/F	White Hispanic	A	Sister	MN	WI	Sputum	2020 Aug 23
B19406	27/M	White Hispanic	A	Brother	MN	WI	Sputum	2020 Aug 19
B19407	3/F	White non-Hispanic	B	Daughter	MN	MN	Bronchial washing	2020 Jul 25
B19408	38/M	White non-Hispanic	B	Father	MN	MN	Subcutaneous abscess	2014 Dec 16

*Data for 2 isolates per cluster that underwent whole-genome sequencing and single-nucleotide polymorphism analyses.
†Likely exposure location on the basis of interviews with family members.

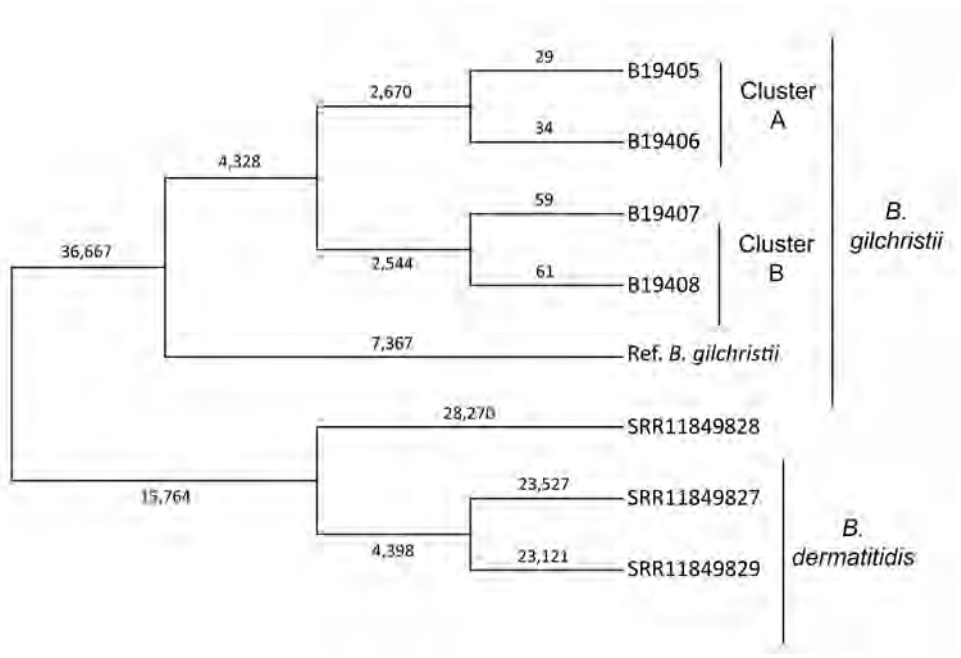

Figure. Genetic relationships and molecular epidemiology of *Blastomyces gilchristii* clusters, Minnesota, USA. We performed whole-genome sequencing of isolates from 4 patients in Minnesota who had *Blastomyces gilchristii* infections and compared the sequences with 3 publicly available *B. dermatitidis* isolates (National Center for Biotechnology Information run nos. SRR11849827, SRR11849828, SRR11849829). We analyzed single-nucleotide polymorphisms (SNPs) using the MycoSNP version 0.19 analytical workflow (https://github.com/CDCgov/mycosnp). We used the genome assembly data for *B. gilchristii* strain SLH14081 from GenBank (accession no. GCA_000003855.2) as a reference. Neighbor-joining tree shows the genetic relationships between cluster A and B, which each comprised isolates from 2 patients, the *B. gilchristii* reference strain, and *B. dermatitidis* isolates. Numbers represent the SNPs for each strain. Ref., reference.

for Biotechnology Information BioProject accession no. PRJNA786864). To investigate genetic diversity between strains, we performed whole-genome single-nucleotide polymorphism (SNP) analysis using the MycoSNP version 0.19 analytical workflow (https://github.com/CDCgov/mycosnp). We used publicly available sequences from *B. dermatitidis* isolates (NCBI run nos. SRR11849827, SRR11849828, SRR11849829) for comparison and genome assembly data for *B. gilchristii* strain SLH14081 from GenBank (accession no. GCA_000003855.2) as a reference. We constructed a neighbor-joining tree showing SNP differences and maximum-likelihood tree showing bootstrap values using MEGA software version 7.0, (https://www.megasoftware.net) and FastTree 2 (*10*).

All the isolates were *B. gilchristii* rather than *B. dermatitidis*. Phylogenetic tree analysis showed *B. dermatitidis* and *B. gilchristii* grouped into distinct clades, which were separated by 52,431 SNPs (Figure). Sequences from all 4 *B. gilchristii* isolates clustered with the reference genome SLH14081 and were separated by a minimum of 11,695 SNPs. Each familial cluster formed a subclade within the *B. gilchristii* clade; the subclades were separated by 5,214 SNPs. In cluster A, where all family members were infected at the same time and location, we found 63 SNPs separated the 2 cases. In cluster B, where exposures occurred in the same location but infections were 6 years apart, the cases differed by 120 SNPs (Figure).

Both *B. dermatitidis* and *B. gilchristii* have been reported in Minnesota (*2*). We used whole-genome sequencing and SNP analysis to evaluate clusters of blastomycosis infections caused by *B. gilchristii* in Minnesota. The genomic data showed that cases within cluster A or B were closely related genetically, whereas clusters A and B were genetically distinct. *B. gilchristii* is likely responsible for a higher proportion of blastomycosis clusters than is currently known. Therefore, pairing genomic data with clinical information and geographic location can be used to monitor blastomycosis infections and determine whether they are clusters, outbreaks, or sporadic occurrences. Our findings demonstrate the utility of genomic analyses for investigating blastomycosis outbreaks, determining genetic diversity of *B. dermatitidis* and *B. gilchristii*, and identifying common sources of environmental exposures among cases.

Acknowledgments

We thank the Office of Advanced Molecular Detection, National Center for Emerging and Zoonotic Infectious Diseases, CDC, for supporting fungal disease molecular epidemiology; the MDH graduate students who conducted patient interviews; Mitsuru Toda for reviewing and providing feedback, and Suzanne Gibbons-Burgener for providing feedback.

MDH fungal disease epidemiology is supported by the Epidemiology and Laboratory Capacity for Infectious Diseases cooperative agreement with CDC.

About the Author

Dr. Bagal is a bioinformatician with the Mycotic Diseases Branch, Division of Foodborne, Waterborne, and Environmental Diseases, National Center for Emerging and Zoonotic Infectious Diseases, Centers for Disease Control and Prevention, Atlanta, GA, USA. Her research interests are genomics and evolutionary biology, metagenomics, and data science.

References

1. Furcolow ML, Busey JF, Menges RW, Chick EW. Prevalence and incidence studies of human and canine blastomycosis. II. Yearly incidence studies in three selected states, 1960–1967. Am J Epidemiol. 1970;92:121–31. https://doi.org/10.1093/oxfordjournals.aje.a121184
2. McTaggart LR, Brown EM, Richardson SE. Phylogeographic analysis of *Blastomyces dermatitidis* and *Blastomyces gilchristii* reveals an association with North American freshwater drainage basins. PLoS One. 2016;11:e0159396. https://doi.org/10.1371/journal.pone.0159396
3. Schwartz IS, Wiederhold NP, Hanson KE, Patterson TF, Sigler L. *Blastomyces helicus*, a new dimorphic fungus causing fatal pulmonary and systemic disease in humans and animals in western Canada and the United States. Clin Infect Dis. 2019;68:188–95. https://doi.org/10.1093/cid/ciy483
4. Klein BS, Vergeront JM, DiSalvo AF, Kaufman L, Davis JP. Two outbreaks of blastomycosis along rivers in Wisconsin. Isolation of *Blastomyces dermatitidis* from riverbank soil and evidence of its transmission along waterways. Am Rev Respir Dis. 1987;136:1333–8. https://doi.org/10.1164/ajrccm/136.6.1333
5. Reed KD, Meece JK, Archer JR, Peterson AT. Ecologic niche modeling of *Blastomyces dermatitidis* in Wisconsin. PLoS One. 2008;3:e2034. https://doi.org/10.1371/journal.pone.0002034
6. Thompson K, Sterkel AK, Brooks EG. Blastomycosis in Wisconsin: beyond the outbreaks. Acad Forensic Pathol. 2017;7:119–29. https://doi.org/10.23907/2017.014
7. Chow NA, Gade L, Tsay SV, Forsberg K, Greenko JA, Southwick KL, et al.; US Candida auris Investigation Team. Multiple introductions and subsequent transmission of multidrug-resistant *Candida auris* in the USA: a molecular epidemiological survey. Lancet Infect Dis. 2018;18:1377–84. https://doi.org/10.1016/S1473-3099(18)30597-8
8. Oltean HN, Etienne KA, Roe CC, Gade L, McCotter OZ, Engelthaler DM, et al. Utility of whole-genome sequencing to ascertain locally acquired cases of coccidioidomycosis, Washington, USA. Emerg Infect Dis. 2019;25:501–6. https://doi.org/10.3201/eid2503.181155
9. Kaka AS, Sarosi GA. Disseminated blastomycosis. N Engl J Med. 2017;376:e9. https://doi.org/10.1056/NEJMicm1606811
10. Price MN, Dehal PS, Arkin AP. FastTree 2—approximately maximum-likelihood trees for large alignments. PLoS One. 2010;5:e9490. https://doi.org/10.1371/journal.pone.0009490

Address for correspondence: Nancy A. Chow, Centers for Disease Control and Prevention, 1600 Clifton Rd NE, Mailstop H17-2, Atlanta, GA 30329-4027, USA; email: nchow@cdc.gov

Tropheryma whipplei Intestinal Colonization in Migrant Children, Greece

Sofia Makka, Ioanna Papadogiannaki, Androniki Voulgari-Kokota, Theano Georgakopoulou, Myrto Koutantou, Emmanouil Angelakis

Author affiliations: Hellenic Pasteur Institute, Athens, Greece (S. Makka, I. Papadogiannaki, A. Voulgari-Kokota, M. Koutantou, E. Angelakis); National Public Health Organization, Marousi, Greece (T. Georgakopoulou)

DOI: http://doi.org/10.3201/eid2809.220068

We obtained fecal samples from migrant children ≤12 years of age throughout hotspots in Greece and tested them for *Tropheryma whipplei* by using a quantitative PCR assay. We identified 6 genotypes of *T. whipplei*, 4 of which are newly described. Our findings suggest a high prevalence of *T. whipplei* in these regions.

Tropheryma whipplei is an intracellular bacterium recognized as the causative agent of enteric infection Whipple disease (*1*). *T. whipplei* intestinal colonization prevalence in humans depends on geographic area, age, and method of exposure (*2*). In Europe, *T. whipplei* has been detected in stool specimens in 2%–11% of healthy persons (*1*). The prevalence of *T. whipplei* intestinal colonization has been reported to be higher in children than in adults, suggesting an age-dependent presence (*3*). In developing countries, the rates are especially high, probably because of poor sanitary conditions (*3*). The prevalence of *T. whipplei* was shown to be high among children in Senegal (West Africa), reaching 75%; in contrast, the prevalence rate for children in France was 15% (*1*,*4*). *T. whipplei* has been associated with diarrhea in young children, suggesting a causative link between the bacterium and that symptom (*5*). Because migrants often live without resources that enable appropriate personal hygiene, and because they have limited access to healthcare, they are exposed to many communicable infections. As a result, migrant populations have a poorer standard of overall physical health compared with the general population, and they suffer from a disproportionate burden of communicable diseases, including those caused by parasites, enteroviruses, and *Mycobacterium tuberculosis* (*6*). In Greece, in collaboration with the Hellenic National Public Health Organization, we routinely test stool samples of persons classified as migrants, with the intent of determining the

presence of *T. whipplei* and identifying genotypes circulating among migrant children.

We obtained stool specimens from children 0–12 years of age living in different hotspots throughout Greece and tested them for *T. whipplei*. We screened all samples by using a quantitative PCR that targeted 155-bp and 150-bp repeated sequences (*4*). For positive samples, we performed genotyping by using a multispacer system that targeted 4 highly variable genomic sequences (HVGSs) as previously described (*4*). The 4 HVGSs obtained from each specimen were compared with those available in the GenBank database and those listed on the Institut Hospitalo-Universitaire Méditerranée Infection website (Multispacer Typing—*T. whipplei*, https://ifr48.timone.univ-mrs.fr/mst/tropheryma_whipplei) to determine the corresponding genotype. We added all of the HVGSs we discovered to the Institut Hospitalo-Universitaire

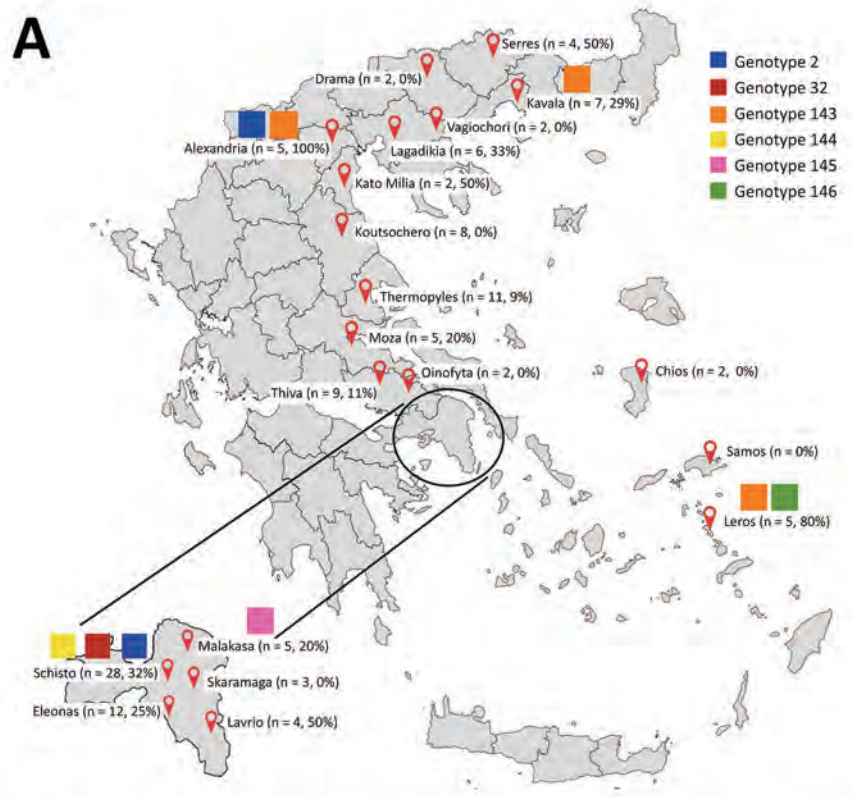

B

	HVGS-1	HVGS-2	HVGS-3	HVGS-4	Country				
Genotype 2	1	7	1	1	France	Germany	Laos	Greece (2)	
Genotype 11	1	7	3	1	France				
Genotype 36	2	7	3	1	France	Switzerland			
Genotype 37	2	7	12	1	France				
Genotype 32	1	8	1	2	France	Greece (1)			
Genotype 145	2	8	3	2	Greece (1)				
Genotype 3	1	6	1	1	France	Italy	Switzerland		
Genotype 29	4	6	1	1	France				
Genotype 28	1	1	9	6	France				
Genotype 1	1	1	1	3	France	Germany	Switzerland	Austria	Belgium
Genotype 143	1	28	1	3	Greece (4)				
Genotype 17	2	1	1	3	Switzerland				
Genotype 8	6	1	5	3	France	Switzerland			
Genotype 4	9	4	8	3	France				
Genotype 19	8	1	8	3	France	Switzerland			
Genotype 85	1	6	6	1	France				
Genotype 27	10	6	6	1	France				
Genotype 144	10	29	6	1	Greece (1)				
Genotype 48	16	6	22	1	Senegal				
Genotype 49	16	14	21	14	Senegal				
Genotype 119	8	7	2	2	France				
Genotype 52	18	6	20	1	Senegal				
Genotype 53	18	14	20	14	Senegal				
Genotype 81	18	14	20	1	Senegal				
Genotype 16	6	7	5	1	France	Switzerland	Germany		
Genotype 39	6	6	5	1	France				
Genotype 146	37	8	6	2	Greece (1)				

Figure. Results of stool sample tests for *Tropheryma whipplei* from migrant children 0–12 years of age from 20 hotspots throughout Greece. A) Defined hotspots throughout Greece, showing numbers and percentages of *T. whipplei* recovered from each location and distribution of different genotypes. B) Phylogenetic diversity of 6 genotypes of *T. whipplei* obtained from migrants (red boxes). Phylogenetic tree was constructed by using the maximum-likelihood method based on the Tamura 3-parameter substitution model. Sequences from the 4 HVGSs were concatenated. Noted next to the genotypes are the countries in which they have been previously detected. Numbers in parentheses note positive test results for children based on each genotype found in Greece. HVGS, highly variable genomic sequence.

Méditerranée Infection website and performed Student *t* or χ^2 tests by using Epi Info 6.0 (https://www.cdc.gov/epiinfo); we considered differences with a p value <0.05 to be significant.

We tested 128 stool samples obtained from 20 hotspots throughout Greece and identified 35 (27%) samples positive for *T. whipplei*. We found positive samples in 13 (65%) of the 20 hotspots we investigated, and we noted the highest presence of *T. whipplei* in the Alexandria hotspot, where all samples were positive, followed by the hotspot of Leros (Figure, panel A). The study population was 53% boys, and median age (±SD) was 5 (±3.8) years); the median age (±SD) of children whose stool samples tested positive was 4 (±3.6) years, and 19 (54%) of them were boys. Stool samples from boys tended to have increased bacterial loads (p =0.06), and stool samples from children 0–4 years of age had significantly higher bacterial loads (74%) compared with samples from children 5–12 years of age (33%) (p = 0.004).

Because of insufficient DNA loads, we obtained genotypes by reverse transcription PCR for only 10 of the 35 samples that tested positive for *T. whipplei*. We classified *T. whipplei* strains into 6 unique HVGS genotypes (Figure, panel B); most of them belonged to genotype 143, identified in 3 hotspots, followed by genotype 2, observed in 2 hostspots. We found 2 children from the same family in the Kavala hotspot who exhibited the same genotype, 143 (*7*). Our quantitative PCR has been previously evaluated (*8*), as has the HVGSs we used for genotyping (*4*).

Our identification of a high percentage of *T. whipplei* in stool samples from migrant children living in different hotspots throughout Greece supports prior data showing that persons living under poor hygienic conditions, particularly children, have increased rates of *T. whipplei* infection compared with the general adult population (*3*). A high percentage of *T. whipplei* infection was observed also in Ghana (*9*), and an upward tendency of *T. whipplei* was noted in Laos, Gabon, and Senegal (*3*,*9*).

We identified 6 genotypes of *T. whipplei*, including 4 newly described genotypes, in fecal samples from migrant children in Greece. The presence of genotype 143 in 3 hotspots suggests that this clone is possibly epidemic, and our results support the highly contagious nature of *T. whipplei*. To date, no specific genotypes have been associated with disease versus asymptomatic carriage, and the same genotype can be observed in acute infections, chronic infections, and asymptomatic carriage (*3*). The fact that 2 children from the same family exhibited the same genotype supports the hypothesis that *T. whipplei* can be transmitted between humans through saliva or feces, depending on hygiene conditions (*7*,*10*).

In conclusion, we provide evidence of a high prevalence of *T. whipplei* in migrant children throughout Greece. Because *T. whipplei* is associated with acute diarrhea in children (*5*), we emphasize the need for systematic surveillance in tracking this bacterium in immigrant populations.

About the Author

Miss Makka is a researcher at the Hellenic Pasteur Institute in Athens, Greece. Her research interests are emerging pathogens.

References

1. Lagier JC, Fenollar F, Raoult D. Acute infections caused by *Tropheryma whipplei*. Future Microbiol. 2017;12:247–54. https://doi.org/10.2217/fmb-2017-0178
2. Fenollar F, Marth T, Lagier JC, Angelakis E, Raoult D. Sewage workers with low antibody responses may be colonized successively by several *Tropheryma whipplei* strains. Int J Infect Dis. 2015;35:51–5. https://doi.org/10.1016/j.ijid.2015.04.009
3. Beltrame A, Ragusa A, Perandin F, Formenti F, Fenollar F, Edouard S, et al. *Tropheryma whipplei* intestinal colonization in Italian and migrant population: a retrospective observational study. Future Microbiol. 2019;14:283–92. https://doi.org/10.2217/fmb-2018-0347
4. Bassene H, Mediannikov O, Socolovschi C, Ratmanov P, Keita AK, Sokhna C, et al. *Tropheryma whipplei* as a cause of epidemic fever, Senegal, 2010–2012. Emerg Infect Dis. 2016;22:1229–334. https://doi.org/10.3201/eid2207.150441
5. Fenollar F, Minodier P, Boutin A, Laporte R, Brémond V, Noël G, et al. *Tropheryma whipplei* associated with diarrhoea in young children. Clin Microbiol Infect. 2016;22:869–74. https://doi.org/10.1016/j.cmi.2016.07.005
6. Stauffer WM, Kamat D, Walker PF. Screening of international immigrants, refugees, and adoptees. Prim Care. 2002;29:879–905. https://doi.org/10.1016/S0095-4543(02)00035-0
7. Fenollar F, Keita AK, Buffet S, Raoult D. Intrafamilial circulation of *Tropheryma whipplei*, France. Emerg Infect Dis. 2012;18:949–55. https://doi.org/10.3201/eid1806.111038
8. Angelakis E, Fenollar F, Lepidi H, Birg ML, Raoult D. *Tropheryma whipplei* in the skin of patients with classic Whipple's disease. J Infect. 2010;61:266–9. https://doi.org/10.1016/j.jinf.2010.06.007
9. Vinnemeier CD, Klupp EM, Krumkamp R, Rolling T, Fischer N, Owusu-Dabo E, et al. *Tropheryma whipplei* in children with diarrhoea in rural Ghana. Clin Microbiol Infect. 2016;22:65.e1–3. https://doi.org/10.1016/j.cmi.2015.09.022
10. Keita AK, Dubot-Pérès A, Phommasone K, Sibounheuang B, Vongsouvath M, Mayxay M, et al. High prevalence of *Tropheryma whipplei* in Lao kindergarten children. PLoS Negl Trop Dis. 2015;9:e0003538. https://doi.org/10.1371/journal.pntd.0003538

Address for correspondence: Emmanouil Angelakis, Diagnostic Department and Public Health Laboratories, Hellenic Pasteur Institute, Athens, Greece; email: E.angelakis@hotmail.com

Arthritis Caused by *Nannizziopsis obscura*, France

Hélène Mascitti, Valérie Sivadon-Tardy, Marie-Elisabeth Bougnoux, Clara Duran, Mickael Tordjman, Marie-Alice Colombier, Isabelle Bourgault-Villada, Aurélien Dinh

Author affiliations: Raymond-Poincaré University Hospital, Public Assistance–Paris Hospitals, Paris Saclay University, Garches, France (H. Mascitti, C. Duran, A. Dinh); Ambroise-Paré University Hospital, Public Assistance–Paris Hospitals, Paris Saclay University, Boulogne-Billancourt, France (V. Sivadon-Tardy, M. Tordjman, I. Bourgault-Villada); Necker University Hospital, Public Assistance–Hospitals of Paris, University of Paris, Paris, France (M.-E. Bougnoux); Foch Hospital, Suresnes, France (M.-A. Colombier)

DOI: http://doi.org/10.3201/eid2809.220375

Nannizziopsis spp., fungi responsible for emerging diseases, are rarely involved in human bone and joint infections. We present a rare case of septic arthritis with necrotizing cellulitis caused by *N. obscura* in a patient in France who had undergone kidney transplant. Rapid, aggressive medical and surgical management led to a favorable outcome.

Nannizziopsis spp. are keratinophilic fungi that can cause aggressive pyogranulomatous lesions affecting the skin, integument, and musculoskeletal systems of reptiles. The ecology of these fungi is not well known, and human infections are rarely. We report a case of septic arthritis caused by *N. obscura*.

In April 2019, a 56-year-old man, originally from Senegal and a former taxi driver in France, was hospitalized in the intensive care unit of Ambroise-Paré Hospital, Boulogne-Billancourt, France, for renal failure and sepsis. He had a prior diagnosis of diabetes mellitus, had undergone kidney transplant 6 years earlier for interstitial kidney disease, and had been undergoing dialysis during the prior year. His usual medication regimen included tacrolimus (4 mg 2×/d), prednisolone (5 mg 2×/d), and mycophenolate mofetil (250 mg 4×/d; stopped at admission).

At admission, the patient was hypothermic (34.9°C) and had moderate impaired consciousness. Blood pressure was 152/85 mm Hg and heart rate 95 bpm. No septic shock was observed. The patient's right leg showed swelling, redness, and tenderness. Testing revealed creatinine level of 333 μmol/L, leukocyte count of 5.6 G/L, neutrophil count of 4.77 G/L, and creatine phosphokinase level of 26 IU/L. A computed tomography scan of the right lower limb revealed ankle joint effusion associated with gas, compatible with septic arthritis (Figure). On the basis of these findings and the observance of concomitant necrotizing cellulitis, the patient underwent immediate surgery, which involved debridement of the skin and subcutaneous tissues of the dorsal face of the right foot and the medial face of the distal tibia, including excision of necrotic tissue (fascia and muscle). Abundant purulent discharge was observed during surgery.

Because direct histologic examination of intraoperative samples revealed several septate and arthrosporous mycelial filaments, we prescribed empiric treatment that included liposomal amphotericin B and broad-spectrum antibiotics. Because no bacteria were isolated, we stopped antibiotic therapy 5 days after surgery. The patient underwent additional surgeries 48 and 96 hours after initial surgery based on a diminishing clinical course and persistence of the previously observed fluid collections and air pockets on computed tomography scan, revealing effusion of the right tibio-talar joint and arthritis.

A subculture on Sabouraud dextrose agar with chloramphenicol yielded white, cottony colonies after 3–5 days. Using molecular identification by PCR amplification and sequencing of internal

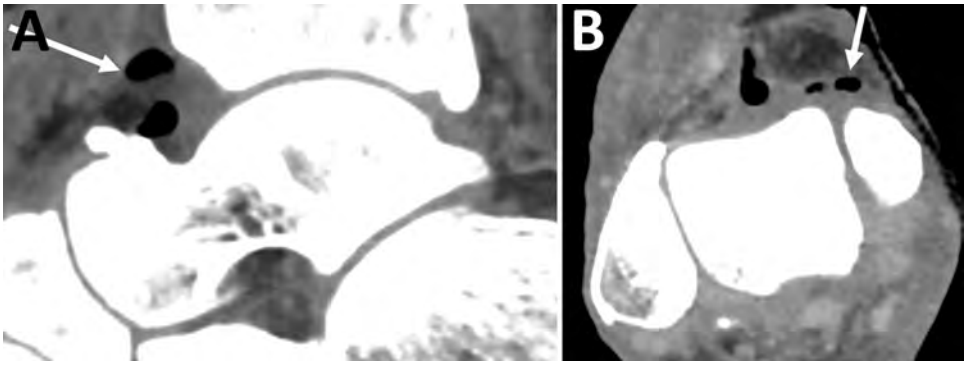

Figure. Sagittal (left) and axial (right) contrast-enhanced computed tomography images demonstrating ankle joint effusion associated with gas (arrows) in an immunocompromised man in France who had septic arthritis and soft tissue infection caused by *Nannizziopsis obscura*.

transcribed spacer (ITS) regions (ITS1–5,8S -ITS2), the clinical isolate was identified as *N. obscura,* confirmed by matrix-assisted laser desorption/ionization time-of-flight mass spectrometry. An antifongigram revealed a strain sensitive to azole antifungals (itraconazole [MIC 0.380 μg/mL], isavuconazole [MIC 0.064 μg/mL], voriconazole [MIC 0.008 μg/mL], and posaconazole [MIC 0.190 μg/mL]), micafungin (MIC 0.023 μg/mL), and amphotericin B (MIC 0.125 μg/mL). Serum β-D-glucan level was elevated (>500 pg/mL).

Because the *Nannizziopsis* strain was sensitive to voriconazole, we prescribed an initial oral regimen of the drug (3 mg/kg 2×/d) on day 6 of the initial intervention, without a loading dose. Drug monitoring revealed a plasma drug concentration of 0.7 mg/L, which was below the therapeutic threshold (1–2 mg/L), due to an ultra-rapid metabolizer profile after the genotyping of CYP2C19*17/*17. Voriconazole was then stopped and replaced by a regimen of posaconazole (loading dose, 300 mg 2×/d; maintenance dose, 300 mg/d) for a 1-year period. The patient's plasma drug concentration was 0.6 mg/L, above the therapeutic threshold (0.5 mg/L).

Computed tomography scans of the head, chest, abdomen, and pelvis and transesophageal cardiac ultrasound performed 2 months after admission revealed no lesion. The patient resumed immunosuppressive therapy with prednisolone (initiated after his kidney transplant) within 30 days of the last surgery for this soft-tissue infection. Tacrolimus, which was initiated at a reduced dosage (1.5 mg 2×/d) earlier in the patient's course of treatment, was then stopped. One year after his septic episode, the patient had no recurrence and had a partially functional lower right limb.

Only 14 cases of invasive *Nannizziopsis* infections in humans have been reported (*1*–*5*). These infections can be acute or chronic and usually occur in immunocompromised patients. Human infections caused by *Nannizziopsis* are generally cutaneous and subcutaneous, but some cases of pulmonary infection have been noted (*6*,*7*). Probabilistic treatment with azoles is recommended in the absence of a definitive diagnosis. Because serum β-D-glucans are typically very high during infections with *Nannizziopsis* spp., detection of a very high serum β-D-glucan level may guide the diagnosis of invasive fungal infection (*8*).

Given the wide variations in patient response and the potential impact of drug interactions, antifungal treatment should include serum drug monitoring to guide drug selection and optimize treatment dosage. Prognosis still largely depends on the underlying immunosuppression of the patient and the outcome of surgical management. This patient reported no recent travel to Africa, no history of cutaneous lesion or infection, and no recent contact with reptiles, which suggests that severe *Nannizziopsis* infection could occur several years after possible exposure among immunosuppressed patients.

This rare case of septic arthritis due to *N. obscura* occurred secondarily to a skin and soft tissue infection. Such severe infections require urgent medicosurgical treatment; the probability of a favorable outcome often diminishes when diagnosis and treatment are delayed. Medical treatment for infections caused by *N. obscura* is based on antifungals from the azole class, and dosages must be carefully monitored.

Acknowledgments

We would like to thank the team of Parasitology laboratory of Hôpital Necker-Enfants Malades for their help in identifying the strain.

About the Author

Hélène Mascitti is Assistant Clinical Fellow, Specialist in Infectious and Tropical Diseases and Dermatology, working at Raymond-Poincaré Hospital, whose research interests include skin and soft tissue infections, especially infections due to emerging tropical infections.

References

1. Baggott A, McGann H, Barton R, Ratner J. Disseminated *Nannizziopsis obscura* infection in a renal transplant patient—the first reported case. Med Mycol Case Rep. 2017;17:20–4. https://doi.org/10.1016/j.mmcr.2017.06.002
2. Nourrisson C, Vidal-Roux M, Cayot S, Jacomet C, Bothorel C, Ledoux-Pilon A, et al. Invasive infections caused by *Nannizziopsis* spp. molds in immunocompromised patients. Emerg Infect Dis. 2018;24:549–52. https://doi.org/10.3201/eid2403.170772
3. Sigler L, Hambleton S, Paré JA. Molecular characterization of reptile pathogens currently known as members of the chrysosporium anamorph of *Nannizziopsis vriesii* complex and relationship with some human-associated isolates. J Clin Microbiol. 2013;51:3338–57. https://doi.org/10.1128/JCM.01465-13
4. Steininger C, van Lunzen J, Sobottka I, Rohde H, Horstkotte MA, Stellbrink HJ. Mycotic brain abscess caused by opportunistic reptile pathogen. Emerg Infect Dis. 2005;11:349–50. https://doi.org/10.3201/eid1102.040915
5. Stillwell WT, Rubin BD, Axelrod JL. Chrysosporium, a new causative agent in osteomyelitis. A case report. Clin Orthop Relat Res. 1984;(184):190–2.
6. Cabañes FJ, Sutton DA, Guarro J. *Chrysosporium-related Fungi and Reptiles: A Fatal Attraction*. Heitman J, editor. PLoS Pathog. 2014;10:e1004367. https://dx.plos.org/10.1371/journal.ppat.1004367
7. Stchigel AM, Sutton DA, Cano-Lira JF, Cabañes FJ, Abarca L, Tintelnot K, et al. Phylogeny of chrysosporia infecting reptiles: proposal of the new family *Nannizziopsiaceae* and

five new species. Persoonia - Mol Phylogeny Evol Fungi. 2013;31:86–100.
8. Garcia-Hermoso D, Hamane S, Fekkar A, Jabet A, Denis B, Siguier M, et al. Invasive infections with *Nannizziopsis obscura* species complex in 9 patients from West Africa, France, 2004–2020. Emerg Infect Dis. 2020;26:2022–30. https://doi.org/10.3201/eid2609.200276

Address for correspondence: Aurélien Dinh, Hôpital Universitaire Raymond-Poincaré, 104 bd Raymond Poincaré 92380 Garches, France; email: aurelien.dinh@aphp.fr

Invasive Meningococcal X Disease during the COVID-19 Pandemic, Brazil

Lucila O. Fukasawa, Bernadete L. Liphaus, Maria Gisele Gonçalves, Fabio T. Higa, Carlos H. Camargo, Telma R.M.P. Carvalhanas, Ana Paula S. Lemos

Author affiliations: Adolfo Lutz Institute, São Paulo, Brazil (L.O. Fukasawa, M.G. Gonçalves, F.T. Higa, C.H. Camargo, A.P.S. Lemos); Epidemiological Surveillance Center "Professor Alexandre Vranjac," São Paulo (B.L. Liphaus, T.R.M.P. Carvalhanas)

DOI: http://doi.org/10.3201/eid2809.220531

Invasive meningococcal disease persists as a fulminant disorder worldwide. Although cases caused by *Neisseria meningitidis* serogroup X (MenX) occur infrequently, outbreaks have been reported in countries in Africa in recent decades. We report 2 cases of MenX invasive meningococcal disease in São Paulo, Brazil, in 2021 and 2022, during the COVID-19 pandemic.

Invasive meningococcal disease (IMD) is a severe disorder that is associated with high rates of morbidity and mortality worldwide (*1*). Although 12 serogroups of *Neisseria meningitidis* have been characterized based on their capsular polysaccharides, most IMD cases are caused by serogroups A, B, C, W, Y, and, more rarely, X (*1*).

N. meningitidis serogroup X (MenX) has been responsible for limited IMD cases in the United States and Europe, but since 1990, MenX isolates have emerged in some countries within the meningitis belt of Africa, causing outbreaks and epidemics in Burkina Faso, Togo, Niger, Kenya, and Uganda (*2*). In Brazil, only 6 cases of MenX IMD cases were reported in the last 15 years; the last one was isolated in the city of São Paulo in 2017 (http://tabnet.datasus.gov.br/cgi/tabcgi.exe?sinannet/cnv/meninbr.def). We report 2 cases of MenX IMD that occurred in São Paulo in 2021 and 2022, during the COVID-19 pandemic. These isolates were identified during routine laboratory-based public health surveillance in the National Reference Laboratory at the Adolfo Lutz Institute in São Paulo.

Case-patient 1 was a 7-month-old boy who, in November 2021, was admitted to a São Paulo emergency department with fever, vomiting, bulging anterior fontanelle, stiff neck, and seizure. Cerebrospinal fluid collected at that time revealed a leukocyte count of 1,440 cells/mm^3 with a 73% proportion of neutrophils; protein level was 263 mg/dL, glucose 19 mg/dL, and lactate 80.5 mg/dL, and results of bacterioscopy and culture were negative. The patient was treated with ceftriaxone (100 mg/kg every 12 h) for 10 days, with a favorable outcome.

Case-patient 2 was a 6-year old boy who, in January 2022, was admitted to a São Paulo City emergency department with fever, headache, and vomiting. A sample of cerebrospinal fluid revealed a leukocyte count of 4920/mm^3 with a 96% proportion of neutrophils; protein level was 207 mg/dL, glucose 48 mg/dL, and lactate 82.3 mg/dL, and results for bacterioscopy and culture were negative. The patient was treated with ceftriaxone (100 mg/kg every 12 h), the recommended antibiotic, with a favorable outcome.

Because both patients were diagnosed with meningitis, chemoprophylaxis with rifampin was administered to all persons characterized as close contacts. Both patients resided in the city of São Paulo but in different regions, 40 km away from each other. Despite the short period between their illnesses, epidemiologic surveillance could not establish an obvious relationship between the 2 patients. Neither patient had traveled to countries with reported MenX disease, nor had they had known contact with other persons diagnosed with meningitis.

We extracted DNA from the cerebrospinal fluid samples obtained from the 2 patients using the Roche MagNa Pure LC 2.0 platform (https://lifescience.roche.com) according to the manufacturer's instructions. Both DNA samples were positive for *N. meningitidis* (*ctrA* gene) by multiplex real-time PCR (*3*), and these results were confirmed using another real-time PCR targeting the meningococcal *sodC* gene (*4*). Both samples were positive for genogroup X (*xcbB* gene)

by multiplex real-time PCR and negative for genogroups A, B, C, W, and Y (*5*).

A previous study demonstrated that the 413 bp fragment of the *rplF* gene, which encodes the 50S ribosomal protein L6, is a suitable genetic target for differentiating species within the genus *Neisseria* (*6*). A sequence analysis of the *rplF* gene of both of our patient samples revealed an *rplF* fragment assigned to allele 1, confirming the genospecies *N. meningitidis* (*6*). We conducted multilocus sequence typing according to standard protocols using the the PubMLST database (http://pubmlst.org/neisseria) and identified Nm400, the isolate from case-patient 2, as sequence type 2888, which is not assigned to a clonal complex. Because of the unavailability of clinical material for Nm111, the isolate from case-patient 1, multilocus sequence typing could not be performed for that isolate.

According to the PubMLST database (as of March 12, 2022), there are 4 records of ST2888: 1 is serogroup X, 2 are serogroup B, and 1 isolate did not have a serogroup recorded. Only 1 case of IMD caused by MenX ST2888 was reported, in Italy in 2009, in a patient who had not traveled abroad and who had a favorable outcome (*7*).

A large study in sub-Saharan Africa showed that the current population structure reveals MenX to be of a predominantly single lineage—ST181 of MenX belongs to a single main lineage, ST181 (clonal complex 181)—which is unlike the diversified MenX population found in Europe (*8*). A recent study in Italy described 4 cases of serogroup X IMD among refugees: 3 were immigrants from Africa, and the other was an immigrant from Bangladesh who had been in contact with refugees from Africa for several months. This highlights the potential threat of new lineages being introduced into vulnerable populations in times of humanitarian crises and conflicts (*9*).

Given the COVID-19 pandemic scenario that has brought an interruption in nonpharmacologic measures to control SARS-CoV-2 transmission, and considering the globally observed reduction of meningococcal vaccination coverage (*10*), a resurgence in cases of IMD will be likely, and cases of non–vaccine-preventable serogroup X should be monitored. Ongoing surveillance of IMD, as well as addition of surveillance initiatives in some regions, will be needed to ensure a successful public health response in terms of both prevention and control.

Acknowledgments

The authors thank the laboratory technicians of Santo André Adolfo Lutz Institute and Hospitals as well as the local epidemiologic surveillance staff.

Our team made use of the Neisseria Multi Locus Sequence Typing website (https://pubmlst.org/ neisseria/), developed by Keith Jolley and sited at the University of Oxford. The development of this site has been funded by the Wellcome Trust and European Union.

About the Author

Dr. Fukasawa is a pharmacist and scientific researcher whose primary research interests include molecular surveillance of bacterial diseases caused by *Neisseria meningitidis*, *Streptococcus pneumoniae*, and *Haemophilus influenzae*.

References

1. Chang Q, Tzeng YL, Stephens DS. Meningococcal disease: changes in epidemiology and prevention. Clin Epidemiol. 2012;4:237–45. https://doi: 10.2147/CLEP.S28410
2. Mustapha MM, Harrison LH. Vaccine prevention of meningococcal disease in Africa: major advances, remaining challenges. Hum Vaccin Immunother. 2018;14:1107–15. https://doi.org/10.1080/21645515.2017.1412020
3. Sacchi CT, Fukasawa LO, Gonçalves MG, Salgado MM, Shutt KA, Carvalhanas TR, et al; São Paulo RT-PCR Surveillance Project Team. Incorporation of real-time PCR into routine public health surveillance of culture negative bacterial meningitis in São Paulo, Brazil. PLoS One. 2011;6:e20675. https://doi.org/10.1371/journal.pone.0020675
4. Dolan Thomas J, Hatcher CP, Satterfield DA, Theodore MJ, Bach MC, Linscott KB, et al. *sodC*-based real-time PCR for detection of *Neisseria meningitidis*. PLoS One. 2011;6:e19361. https://doi.org/10.1371/journal.pone.0019361
5. Wang X, Theodore MJ, Mair R, Trujillo-Lopez E, du Plessis M, Wolter N, et al. Clinical validation of multiplex real-time PCR assays for detection of bacterial meningitis pathogens. J Clin Microbiol. 2012;50:702–8. https://doi.org/10.1128/JCM.06087-11
6. Bennett JS, Watkins ER, Jolley KA, Harrison OB, Maiden MCJ. Identifying *Neisseria* species by use of the 50S ribosomal protein L6 (*rplF*) gene. J Clin Microbiol. 2014;52:1375–81. https://doi.org/10.1128/JCM.03529-13
7. Fazio C, Starnino S, Solda MD, Sofia T, Neri A, Mastrantonio P, et al. *Neisseria meningitidis* serogroup X sequence type 2888, Italy. Emerg Infect Dis. 2010;16:359–60. https://doi.org/10.3201/eid1602.091553
8. Agnememel A, Hong E, Giorgini D, Nuñez-Samudio V, Deghmane AE, Taha MK. *Neisseria meningitidis* serogroup X in sub-Saharan Africa. Emerg Infect Dis. 2016;22:698–702. https://doi.org/10.3201/eid2204.150653
9. Stefanelli P, Neri A, Vacca P, Picicco D, Daprai L, Mainardi G, et al. Meningococci of serogroup X clonal complex 181 in refugee camps, Italy. Emerg Infect Dis. 2017;23:870–2. https://doi.org/10.3201/eid2305.161713
10. Alderson MR, Arkwright PD, Bai X, Black S, Borrow R, Caugant DA, et al. Surveillance and control of meningococcal disease in the COVID-19 era: a Global Meningococcal Initiative review. J Infect. 2022;84:289–96. https://doi.org/10.1016/j.jinf.2021.11.016

Address for correspondence: Ana Paula S. Lemos, Centro de Bacteriologia, Instituto Adolfo Lutz, Avenida Dr Arnaldo, 355, Pacaembu, São Paulo CEP 01246-902, Brazil; email: ana.lemos@ial.sp.gov.br

Feline Panleukopenia Virus in Dogs from Italy and Egypt

Georgia Diakoudi, Costantina Desario, Gianvito Lanave, Stefania Salucci, Linda A. Ndiana, Aya Attia Koraney Zarea, Ehab Ali Fouad, Alessio Lorusso, Flora Alfano, Alessandra Cavalli, Canio Buonavoglia, Vito Martella, Nicola Decaro

Author affiliations: University of Bari Aldo Moro, Bari, Italy (G. Diakoudi, C. Desario, G. Lanave, L.A. Ndiana, A.A. Koraney Zarea, A. Cavalli, C. Buonavoglia, V. Martella, N. Decaro); Istituto Zooprofilattico Sperimentale dell'Abruzzo e Molise G. Caporale, Teramo, Italy (S. Salucci, A. Lorusso); National Research Centre, Giza, Egypt (E.A. Fouad); Istituto Zooprofilattico Sperimentale del Mezzogiorno, Portici, Italy (F. Alfano)

DOI: https://doi.org/10.3201/eid2809.220388

Canine parvovirus and feline panleukopenia virus (FPV) are variants of *Carnivore protoparvovirus 1*. We identified and characterized FPV in dogs from Italy and Egypt using genomic sequencing and phylogenetic analyses. Cost-effective sequencing strategies should be used to monitor interspecies spread, evolution dynamics, and potential host jumping of FPV.

Canine parvovirus (CPV or CPV-2) and feline panleukopenia virus (FPV) are variants of *Carnivore protoparvovirus 1* and major pathogens of domestic and wild carnivores. The linear, single-stranded DNA genome contains 2 open reading frames that encode 2 nonstructural and 2 capsid proteins (*1*).

FPV and CPV are closely related antigenically and genetically (≈98% identity at the nucleotide level) but differ in host range and pathogenicity. These biological differences are determined by amino acid mutations in the VP2 capsid protein (*2*). CPV-2 antigenic variants 2a, 2b, and 2c are able to infect felids and cause FPV-like disease (*2*). FPV is believed to be incapable of infecting dogs but has been shown to replicate in some canine tissues after experimental oronasal infection (*3*). Furthermore, studies have reported the presence of FPV in dogs with CPV-like gastroenteritis (*4*–*8*).

The Infectious Diseases Unit, Department of Veterinary Medicine, University of Bari, Italy, has performed routine screening and characterization of canine samples for CPV and FPV since the mid-1990s and has combined traditional virological and molecular techniques to differentiate between FPV and CPV types 2a/2b and 2b/2c (*9*). During 2019–2021, we screened and typed ≈1,000 *Carnivore protoparvovirus 1* strains from cats and dogs. In 2021, FPV was unexpectedly identified in dogs from epidemiologically unrelated cases. We identified FPV in a blood sample obtained from a 1-year-old dog from Giza, Egypt, that had an unexplained fever (case A) and in fecal samples from 3 dead adult dogs in Teramo, Italy (case series B). The dogs from Italy had severe gastrointestinal symptoms that the attending veterinarian initially suspected were from poisoning.

Because finding FPV in dogs is unusual, we analyzed the samples by using 2 PCR primer sets that differentiated between canine and feline cytochrome b genes (*10*). We confirmed that the FPV samples were of canine origin. Moreover, toxicologic analysis of the 3 dogs in case series B excluded a diagnosis of poisoning, and other enteric canine pathogens were excluded as causes of the gastrointestinal symptoms by using culture and molecular assays. We performed immunofluorescence analyses of tissue from the small intestines of the 3 dogs in case series B and detected parvoviral antigens in epithelial cells (Appendix Figure 1, https://wwwnc.cdc.gov/EID/article/28/9/22-0388-App1.pdf). Attempts to isolate the virus by infecting feline or canine cell lines were unsuccessful, likely because of low viral titers.

To acquire complete viral genome sequences of samples from each case, we performed genomic PCR by using LA Taq polymerase (Takara Bio, http://www.takarabio.com). PCR products were used for library preparation. We performed adaptor ligation of genomic DNA by using the Ligation Sequencing Kit (Oxford Nanopore Technologies, https://nanoporetech.com) according to the manufacturer's guidelines. Sequencing was performed by using the FLO-MIN106D Flow Cell, R9 version, and MinION Mk1C sequencing platform (Oxford Nanopore Technologies).

We obtained complete sequences of coding regions for the virus strains from Italy (ITA/2021/164-1; GenBank accession no. OM638042) and Egypt (EGY/2021/139-188; GenBank accession no. OM638043). The ITA/2021/164-1 and EGY/2021/139-188 strains were characterized as FPV on the basis of sequence and phylogenetic analyses. We aligned amino acid sequences for VP2 from FPV, CPV, and the dog-associated FPV strains from Italy and Egypt to determine biological differences between the variants (Figure). We identified an I101T aa substitution in our cases that is likely associated with host range determination (Figure) (*2*). The FPV strains from Italy and Egypt segregated into different phylogenetic clusters (Appendix Figure 2).

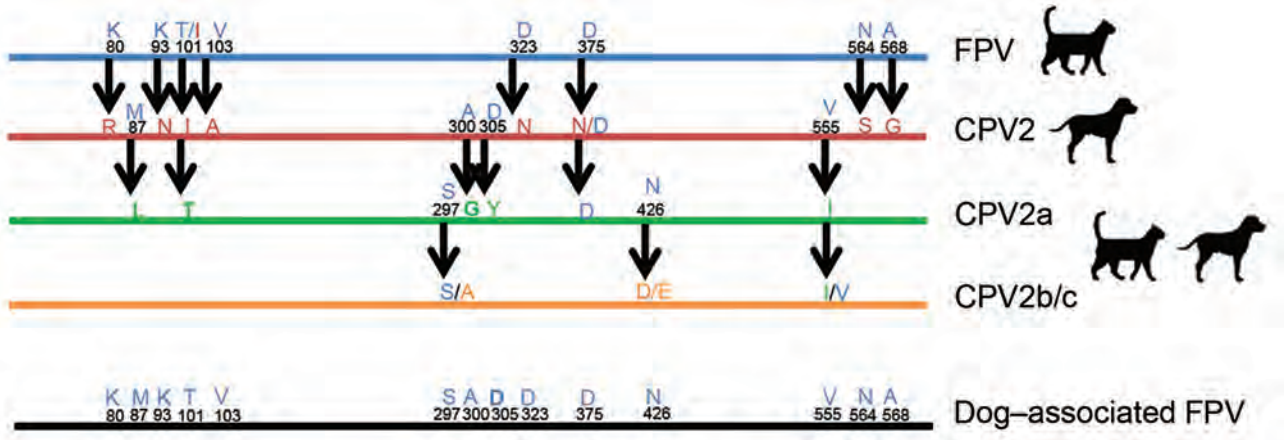

Figure. Genetic differences in feline panleukopenia virus in dogs from Italy and Egypt. Amino acid residues in the capsid protein VP2 differed between FPV, CPV-2, CPV-2a, CPV-2b, and CPV-2c variants of *Carnivore protoparvovirus 1*. Colors indicate variant origins of amino acid residues. We identified an I101T aa substitution mutation in FPV from these dog-associated cases. CPV, canine parvovirus; FPV, feline panleukopenia virus.

FPV has been recently reported in Pakistan, Vietnam, Thailand, and China in dogs that had gastroenteritis (*4*–*8*). These viruses were characterized as FPV after partial or complete sequence analysis of the gene encoding VP2. A unique K93N substitution mutation involved in host range control (*2*) was identified in an FPV strain in Thailand (*4*), and I101T mutations were found in dog-associated FPV strains from Vietnam (*5*) and China (*6*). As noted, the I101T mutation was also found in our dog-associated FPV strains. I101 has been observed in prototypical FPV strains, whereas T101 has been found in recent FPV isolates (*5*). The I101T substitution has also been observed in CPV-2 and its variant CPV-2a and is believed to be a further adaptation of CPV to the canine host (*2*).

In conclusion, we identified FPV from unrelated cases in dogs. In case A, fever was the only clinical sign in a young dog, whereas a fatal systemic syndrome with enteric signs occurred in 3 adult dogs in case series B. However, the role of FPV in these cases remains unclear. Adoption of cost-effective sequencing strategies in recent years has demonstrated that residual circulation of FPV or FPV-like viruses occurs in dogs in some settings. Genomic sequencing and further phylogenetic analyses can be used to monitor the spread, evolution, and potential host jumping of *Carnivore protoparvovirus 1* variants in domestic and wild carnivores.

This study was supported by grants from the Ministry of Health, Italy: Ricerca Corrente 2019 'NGS e diagnostica molecolare in sanità animale' (A.L., N.D.) and Ricerca Corrente 2018 'Nuovi virus gastroenterici di cane e gatto: sviluppo di protocolli NGS per la valutazione del rischio zoonosico' (F.A., N.D.).

The study was approved by the Ethics Committee of the Department of Veterinary Medicine, University of Bari Aldo Moro, Italy (authorization no. 28/2020) and Medical Research Ethics Committee at the National Research Centre, Egypt (authorization no. 6211022021). All experiments were performed in accordance with relevant guidelines and regulations.

About the Author

Dr. Diakoudi is a research scientist at the University of Bari Aldo Moro, Italy. Her research interests focus on virus discovery in animals, particularly viruses with zoonotic potential.

References

1. Cotmore SF, Agbandje-McKenna M, Canuti M, Chiorini JA, Eis-Hubinger AM, Hughes J, et al. Ictv Report Consortium. ICTV virus taxonomy profile: *Parvoviridae*. J Gen Virol. 2019;100:367–8. https://doi.org/10.1099/jgv.0.001212
2. Callaway HM, Welsch K, Weichert W, Allison AB, Hafenstein SL, Huang K, et al. Complex and dynamic interactions between parvovirus capsids, transferrin receptors, and antibodies control cell infection and host range. J Virol. 2018;92:e00460-18 PubMed https://doi.org/10.1128/JVI.00460-18
3. Truyen U, Parrish CR. Canine and feline host ranges of canine parvovirus and feline panleukopenia virus: distinct host cell tropisms of each virus in vitro and in vivo. J Virol. 1992;66:5399–408. https://doi.org/10.1128/jvi.66.9.5399-5408.1992
4. Inthong N, Kaewmongkol S, Meekhanon N, Sirinarumitr K, Sirinarumitr T. Dynamic evolution of canine parvovirus in Thailand. Vet World. 2020;13:245–55. https://doi.org/10.14202/vetworld.2020.245-255
5. Hoang M, Wu CN, Lin CF, Nguyen HTT, Le VP, Chiou MT, et al. Genetic characterization of feline panleukopenia virus from dogs in Vietnam reveals a unique Thr101 mutation in VP2. PeerJ. 2020;8:e9752. https://doi.org/10.7717/peerj.9752

6. Chen B, Zhang X, Zhu J, Liao L, Bao E. Molecular epidemiological survey of canine parvovirus circulating in China from 2014 to 2019. Pathogens. 2021;10:588. https://doi.org/10.3390/pathogens10050588
7. Ahmed N, Riaz A, Zubair Z, Saqib M, Ijaz S, Nawaz-Ul-Rehman MS, et al. Molecular analysis of partial VP-2 gene amplified from rectal swab samples of diarrheic dogs in Pakistan confirms the circulation of canine parvovirus genetic variant CPV-2a and detects sequences of feline panleukopenia virus (FPV). Virol J. 2018;15:45. https://doi.org/10.1186/s12985-018-0958-y
8. Charoenkul K, Tangwangvivat R, Janetanakit T, Boonyapisitsopa S, Bunpapong N, Chaiyawong S, et al. Emergence of canine parvovirus type 2c in domestic dogs and cats from Thailand. Transbound Emerg Dis. 2019;66:1518–28. https://doi.org/10.1111/tbed.13177
9. Ndiana LA, Lanave G, Desario C, Berjaoui S, Alfano F, Puglia I, et al. Circulation of diverse protoparvoviruses in wild carnivores, Italy. Transbound Emerg Dis. 2021;68:2489–502. https://doi.org/10.1111/tbed.13917
10. Abdel-Rahman SM, El-Saadani MA, Ashry KM, Haggag AS. Detection of adulteration and identification of cat's, dog's, donkey's and horse's meat using species-specific PCR and PCR-RFLP techniques. Aust J Basic & Appl Sci. 2009;3:1716–9. http://www.ajbasweb.com/old/ajbas/2009/1716-1719

Address for correspondence: Nicola Decaro, Department of Veterinary Medicine, University of Bari Aldo Moro, Strada Prov. per Casamassima Km 3, 70010 Valenzano, Bari, Italy; email: nicola.decaro@uniba.it

Trichodysplasia Spinulosa Polyomavirus Endothelial Infection, California, USA

Lauren Lawrence,[1] Aihui Wang, Gregory Charville, Angus Toland, Benjamin Pinsky, Yasodha Natkunam, Sheren Younes, Henning Stehr, Dita Gratzinger

Author affiliations: Stanford Healthcare, Palo Alto, California, USA (L. Lawrence, A. Toland); Stanford University School of Medicine, Stanford, California, USA (A. Wang, G. Charville, B. Pinsky, Y. Natkunam, S. Younes, H. Stehr, D. Gratzinger)

DOI: https://doi.org/10.3201/eid2809.220856

[1]Current affiliation: Guardant Health, Redwood City, California, USA.

We describe 3 patients in California, USA, with trichodysplasia spinulosa polyomavirus (TSPyV) infection of endothelium after steroid administration. We detected TSPyV RNA in tissue specimens by in situ hybridization, which revealed localization to endothelial cells. These cases suggest that diseases associated with endothelial inflammation could be associated with TSPyV infection.

Trichodysplasia spinulosa polyomavirus (TSPyV) is an alphapolyomavirus whose primary clinical manifestation in a posttransplant setting is folliculocentric papular cutaneous eruptions, typically involving the face (*1*). Identification of TSPyV nucleic acids in tonsillar tissue has led to the speculation that lymphoid tissue might be a latency site (*2*); however, some disagreement exists in the literature as to whether the clinical diagnosis of trichodysplasia spinulosa reflects primary infection or reactivation of latent virus (*3*,*4*). Although cutaneous disease is the primary clinical manifestation of infection, TSPyV has been identified in blood, urine, cerebrospinal fluid, tonsils, and respiratory specimens by various methods, including nucleic acid detection, immunohistochemistry, and electron microscopy (*2*,*4*–*6*). TSPyV DNA loads can be high, especially in blood (up to 10^8 viral copies/mL), months before the appearance of typical trichodysplasia spinulosa skin lesions (*4*).

This case study was part of a larger project approved by the Stanford Institutional Review Board (approval no. 58311) designed to explore oncogenesis by alphapolyomaviruses. We identified rare cases on our next generation sequencing panel of solid tumors with off-target, high quality reads that aligned to the TSPyV genome. We hypothesized that some of these cases might represent TSPyV-mediated neoplasms. Our cases comprised 1 patient with metastatic lung adenocarcinoma involving the brain (case 1), 1 patient with meningioma (case 2), and 1 patient with a metastatic perivascular epithelial cell tumor involving the liver (Table). It is unclear whether the mental status changes observed in cases 1 and 2 were attributable to viral infection or were secondary to the tumors (Table). All 3 patients received steroids immediately preceding resection. We performed in situ hybridization using a custom RNAScope probe that targeted the complete TSPyV viral genome (GenBank accession no. NC_014361.1) and RNAscope 2.5 HD Reagent Kit-RED (Advanced Cell Diagnostics, https://acdbio.com) to detect TSPyV RNA in cutaneous biopsy specimens. One case of cutaneous trichodysplasia spinulosa was

Table. Case summaries of 3 patients with trichodysplasia spinulosa polyomavirus endothelial infection, California, USA*

Case no.	Histopathologic diagnosis	Immunosuppression	Localization of RNA	Clinical manifestation
1	Metastatic pulmonary adenocarcinoma involving brain	Dexamethasone (4 mg) leading up to resection; rituximab/bendamustine treatment completed 18 mo before resection for follicular lymphoma	Endothelium	Ground level fall, confusion, forgetfulness, ambulatory instability
2	Anaplastic meningioma	Dexamethasone (2 mg × 10 d, then 1 mg × 2 d) leading up to resection	Endothelium	Confusion, headaches, cheek numbness, ambulatory instability
3	Metastatic perivascular epithelial cell tumor involving liver	Gemcitabine/docetaxel completed 1 mo before resection; prednisone (8 mg orally 2×/d) for 1 mo leading up to resection	Endothelium	Abdominal pain, fever, vomiting, hypoxia

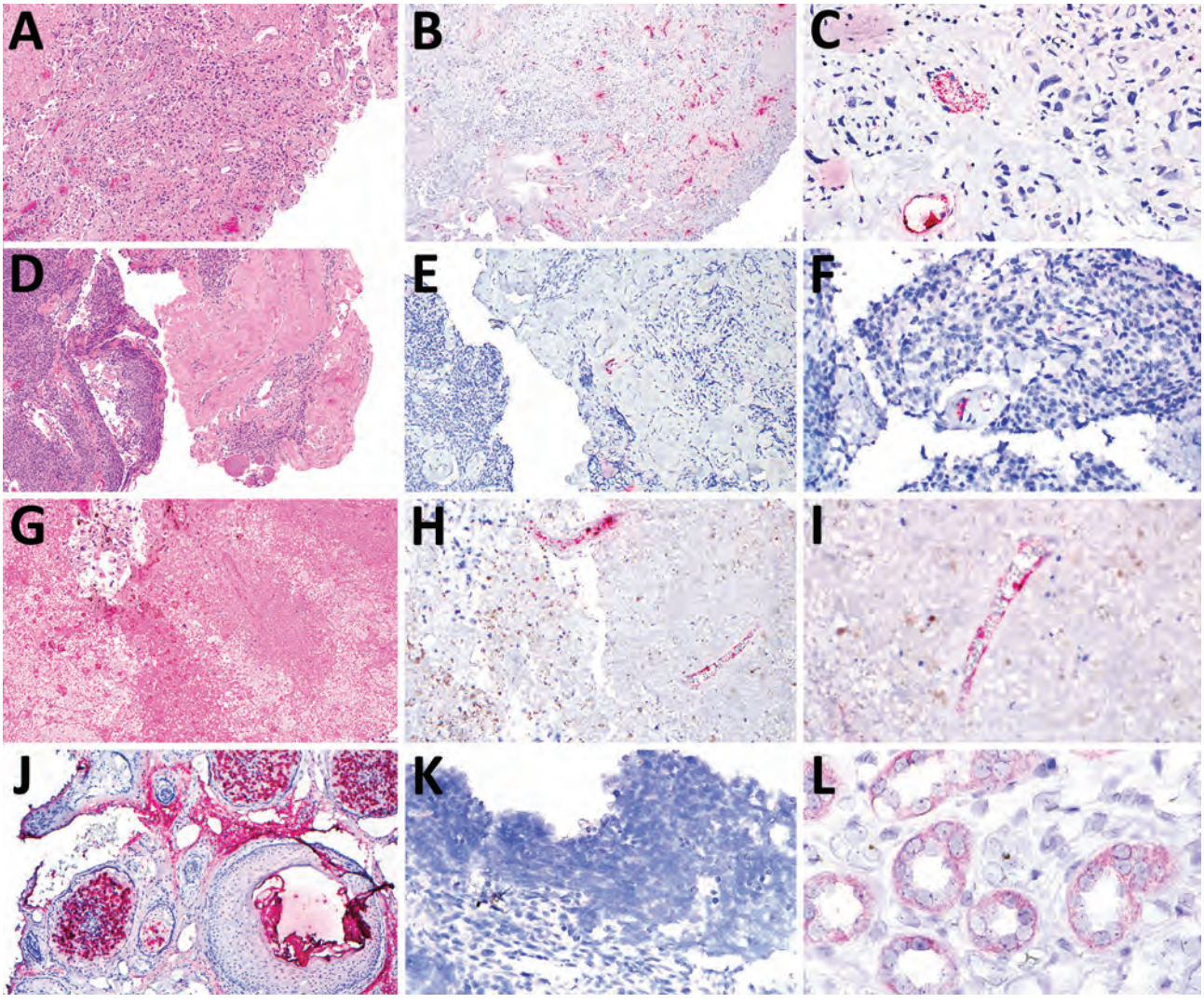

Figure. Tissue samples from 3 patients with trichodysplasia spinulosa polyomavirus endothelial infection, California, USA. We performed hematoxylin and eosin (H&E) staining and RNAScope in situ hybridization (ISH) to detect trichodysplasia spinulosa polyomavirus (TSPyV) in formalin-fixed, paraffin-embedded tissue specimens. Bright red, granular staining in endothelium indicates TSPyV RNA. A) Case 1, H&E staining, original magnification ×10; B) case 1, TSPyV ISH, original magnification ×10; C) case 1, TSPyV ISH, original magnification ×40; D) case 2, H&E staining, original magnification ×5; E) case 2, TSPyV ISH, original magnification ×10; F) case 2, TSPyV ISH, original magnification ×40; G) case 3, H&E staining, original magnification ×5; H) case 3, TSPyV ISH, original magnification ×10; I) case 3, TSPyV ISH, original magnification ×40; J) biopsy from patient with cutaneous trichodysplasia spinulosa (positive control), TSPyV ISH, original magnification ×10; K) cutaneous biopsy from patient with Merkel cell polyomavirus-positive Merkel cell carcinoma (negative control), TSPyV ISH, original magnification ×40; L) renal biopsy from patient with BK polyomavirus nephropathy (negative control), TSPyV ISH, original magnification ×60.

used as a positive control for TSPyV RNA. We used the RNAscope 2.5 LS Probe-Hs-PPIB-sense probe (Advanced Cell Diagnostics), which is specific for peptidylprolyl isomerase B, to demonstrate the presence of intact RNA in the tissue sections. For negative in situ hybridization controls, we used tissue specimens from patients with Merkel cell polyomavirus-positive Merkel cell carcinoma and BK polyomavirus nephropathy and a T-cell lymphoma tissue microarray that included 1 case of Merkel cell polyomavirus-positive T-cell lymphoma.

In contrast to our hypothesis, we found that TSPyV RNA did not localize to neoplastic cells. However, TSPyV RNA localized to the endothelium in all 3 cases (Figure). The BK polyomavirus nephropathy sections showed weak, orange-red discoloration of tubular epithelium (Figure, panel L) that was distinguishable from the bright red, granular staining patterns for TSPyV RNA observed in the positive control and tissue specimens from the 3 patients. This discoloration was interpreted as negative for TSPyV RNA by board-certified pathologists who had experience evaluating RNAScope in situ hybridizations.

TSPyV is a DNA virus, and detection of TSPyV RNA indicates active viral replication and infection. Our in situ hybridization results suggest that TSPyV can infect endothelial cells, likely within various tissues. These cases provide insight into a potential cellular reservoir for TSPyV infection. In addition, these data raise the possibility that other diseases associated with endothelial inflammation could be associated with TSPyV infection. Overall, this small case series improves our knowledge of the scope of human TSPyV infection.

Acknowledgments

We thank Norm Cyr for assistance with the figure layout.

This study was supported by a Mentored Trainee Grant for Personalized Medicine in the Department of Pathology, Stanford University.

About the Author

Dr. Lawrence is a molecular genetic pathology fellow at Stanford Healthcare in the Department of Pathology. Her clinical and research interests focus on molecular diagnostics and hematopathology.

References

1. Narayanan D, Rady PL, Tyring SK. Recent developments in trichodysplasia spinulosa disease. Transpl Infect Dis. 2020;22:e13434. https://doi.org/10.1111/tid.13434
2. Sadeghi M, Aaltonen LM, Hedman L, Chen T, Söderlund-Venermo M, Hedman K. Detection of TS polyomavirus DNA in tonsillar tissues of children and adults: evidence for site of viral latency. J Clin Virol. 2014;59:55–8. https://doi.org/10.1016/j.jcv.2013.11.008
3. Wu JH, Nguyen HP, Rady PL, Tyring SK. Molecular insight into the viral biology and clinical features of trichodysplasia spinulosa. Br J Dermatol. 2016;174:490–8. https://doi.org/10.1111/bjd.14239
4. van der Meijden E, Horváth B, Nijland M, de Vries K, Rácz EK, Diercks GF, et al. Primary polyomavirus infection, not reactivation, as the cause of trichodysplasia spinulosa in immunocompromised patients. J Infect Dis. 2017;215:1080–4. https://doi.org/10.1093/infdis/jiw403
5. Borgogna C, Albertini S, Zavattaro E, Veronese F, Peruzzi L, van der Meijden E, et al. Primary trichodysplasia spinulosa polyomavirus infection in a kidney transplant child displaying virus-infected decoy cells in the urine. J Med Virol. 2019;91:1896–900. https://doi.org/10.1002/jmv.25519
6. Siebrasse EA, Bauer I, Holtz LR, Le BM, Lassa-Claxton S, Canter C, et al. Human polyomaviruses in children undergoing transplantation, United States, 2008–2010. Emerg Infect Dis. 2012;18:1676–9. https://doi.org/10.3201/eid1810.120359

Address for correspondence: Lauren Lawrence, Guardant Health, 505 Penobscot Dr, Redwood City, CA 94063, USA; email: llawrence@guardanthealth.com

Plagues Upon the Earth: Disease and the Course of Human History

Kyle Harper

Princeton University Press, Princeton, NJ, USA, 2021; ISBN: 9780691192123; ISBN-10: 069119212X; ISBN-13: 978-0691192123; Pages: 704; Price: US $35.00

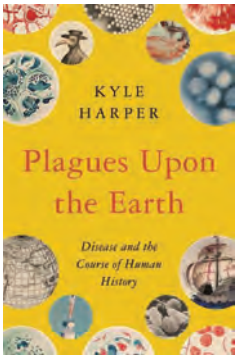

Daniel Defoe's 1722 novel, A Journal of the Plague Year, which chronicles London's 1664–65 bubonic plague, is a superb starting point for books about plagues. Since then, >2,000 books about plagues have been penned. Harper's "claim to novelty rests in part on the effort to draw from a new source of knowledge: genomes," which he boldly states in his 15-page introduction. This goal is marvelously achieved in the next 494 pages. Another 160 pages of notes and references accentuate the detailed nature of this tome.

The work is anchored around 4 transformative energy revolutions: mastery of fire, invention of farming, regular transatlantic crossings, and harnessing fossil fuels. The variations of disease burden and the imprint of endemics and epidemics on human history become the compelling story. The author quotes biologist E.O. Wilson, who favored consilience: harnessing knowledge from multiple domains to arrive at a unified explanation. Plagues Upon the Earth comes as close as possible to consilience to explain the cruel march against humanity engendered by infectious diseases.

The first section, Fire, discusses evolution and genetics in the microbiology world. Mastery of fire "allowed our ancestors to disperse out of Africa and settle from the equator to the Arctic." Creative use of fire promoted human adaptation to various climates and infectious agents contaminating the environment and food sources. The second section, Farms, is informative, especially the chapter Dung and Death. The author's portrayal of the lowly house fly might haunt your next summer picnic. This segment includes Darwin's remarkable description of the kissing bug. Section 3, Frontiers, unpacks a plethora of plague information. The chapter Of Lice and Men artfully depicts John Donne's Devotions upon Emergent Occasions, which Harper considers "one of the most beautiful meditations on sickness ever written," and includes the literary gems "no man is an island" and "never send to know for whom the bell tolls; it tolls for thee."

The amalgamation of humanities and science is refreshing. The last section, Fossils, melds economics, global health, disease, and technology. Harper marvels over what economist Angus Deaton calls the "Great Escape," the ability of humankind to rise above the "doom of poverty and early death." This ability and the enhanced technical capacity to prevent, diagnose, and treat disease are associated with life expectancy elongation. However, Harper's lucid counterstatement is sobering. He states, "The evolution of pathogens is the basic reason we can never entirely escape the risk of global pandemics."

The writing is clear and straightforward in an organized, breezy, digestible style. Scientific and genetic concepts are logically presented. Well-placed metaphors, analogies, and quotations are used effectively to augment the point being made. For example, a 1921 appraisal of mosquitoes by English physician and writer Havelock Ellis asks us, "If you would see all of Nature gathered up at one point, in all her loveliness, and her skill, and her deadliness, and her sex, where would you find a more exquisite symbol than the mosquito?"

Anyone with an interest in science history, microbial genetics, evolution, and understanding plagues will find this a worthy and enlightening read. Molecular biologists and evolutionary geneticists might find certain explanations somewhat simplified, but always well crafted.

W. Clyde Partin

Author affiliations: Emory University, Atlanta, Georgia, USA; Editorial Board member, Emerging Infectious Diseases, Atlanta

DOI: https://doi.org/10.3201/eid2809.220812

Address for correspondence: W. Clyde Partin, Internal Medicine, Emory University, 1365 Clifton Rd NE, Atlanta, GA 30322-1007, USA; email: wpart01@emory.edu

Attributed to the Boreads Painter (active 575–550 BCE), *Black-Figure Kylix with Bellerophon Fighting the Chimaera* (ca. 570 BCE). Terracotta. 4 3/4 in × 7 in × 5 1/2 in/12 cm × 17.8 cm × 14 cm. Public domain image courtesy of the J. Paul Getty Museum, Villa Collection, Malibu, California, USA, 85.AE.121.1.

Agile Thinking Slays the Chimaera

Byron Breedlove

Disease outbreaks caused by high-consequence infectious pathogens can disrupt human lives in myriad ways by causing health, societal, and economic problems that require nimble and creative strategic responses. Similar disruptions can result from mythical monsters running roughshod over imaginary kingdoms.

The Chimaera, originally from Greek mythology, was such a monster. This hybrid creature terrorized the mythical countryside, killing humans and livestock, creating fear and panic. The earliest known description of the Chimaera comes from the 8th century BCE epic poem *The Iliad*, in which the Greek poet Homer described it as "a thing of immortal make, not human, lion fronted and snake behind, a goat in the middle, and snorting out the breath of the terrible flame of bright fire."

Art historian Marilyn Low Schmitt wrote, "The story of Bellerophon and the Chimaera was one of the earliest legends to be represented in Greek art. In the legend Bellerophon traveled from Argos to Tiryns to Lycia, where the Lycian king, Iobates, commanded him to slay the Chimaera." Bellerophon, a young

Author affiliation: Centers for Disease Control and Prevention, Atlanta, Georgia, USA

DOI: https://doi.org/10.3201/eid2809.AC2809

Corinthian warrior who was a son of the Greek god Poseidon, confronted an intimidating challenge in being pitted against this deadly monster. But there was also an element of subterfuge behind King Iobates' motives beyond any desire to rid the land of this scourge.

Iobates' daughter Stheneboea was married to the neighboring king, Proteus. She had falsely accused Bellerophon of sexual impropriety. Unbeknownst to Proteus, Bellerophon had actually snubbed Stheneboea's advances. But believing he had been dishonored, Proteus secretly asked his father-in-law, Iobates, for his complicity in eliminating the warrior whom Proteus dared not challenge directly. Both kings no doubt assumed the Chimaera would slay Bellerophon.

Indeed, had Bellerophon not tamed the flying horse Pegasus, gifted to him by the gods to aid in this endeavor, he would most likely have suffered a grim fate. Mounted on Pegasus, Bellerophon flew above the Chimaera, where he was able to surveil the situation, rather than lunging headfirst into battle. From this vantage point, Bellerophon repeatedly shot arrows into the enraged monster but could not kill it. He delivered the coup de grâce, when, as Schmitt noted, he connived "to drop into the Chimaera's throat a lump of lead which would melt in the fiery breath and sear its organs." How Bellerophon acquired a lump of lead is not revealed, and in other versions of this tale, Bellerophon prevailed by lodging a lead-tipped spear point in the creature's throat, where it melted.

This month's cover image shows the interior of a kylix, a broad-bowled drinking cup, emblazoned with Bellerophon and Pegasus battling the Chimaera. Art historians have attributed many similarly styled works of pottery from this era in Greek history to an artisan known as the Boreads Painter. Although the identity of the Boreads Painter remains unknown, the British Museum observes that "Nevertheless consistent individual characteristics of style suggest the existence of a unique artistic personality." This anonymous artisan, as the British Museum documents, has been given the name of the Boreads Painter for an image he created of the sons of Boreas, Greek god of the North Wind. That image appears on what the British Museum describes as "his masterpiece, a cup in the Villa Giulia in Rome decorated on the tondo with an image of a pair of Boreads pursuing a pair of Harpies."

On the basis of the volume of similarly styled artifacts, historians believe that this artist operated one of the more important and productive pottery studios in Sparta from 575 to 550 BCE. Some of his distinctive stylistic elements include his specific way of drawing eyes, ears, knees, and hips and his practice of encircling images with a band of pomegranates.

The J. Paul Getty Museum, which houses this kylix, describes the cup's interior in this manner: "In his right hand, the hero holds the reins of his winged horse, Pegasus, who rears up to meet the monster. Bellerophon is shown in the kneeling pose used to characterize quick movement in Greek art of the Archaic period (about 700–480 B.C.)." Although this depiction of the battle differs from written descriptions of Bellerophon attacking while mounted on Pegasus, the Getty Museum offers a practical reason for such a departure: "The unique, symmetrical arrangement of the rearing horse and monster framing the hero is the result of the artist's attempt to find creative ways to fill the circular area of the interior of a cup."

Bellerophon's success was predicated on having a reliable ally in Pegasus and from his strategic planning literally on the fly. Those on the front lines of public health efforts to prevent, investigate, and mitigate outbreaks of diseases caused by high-consequence pathogens are also engaged in a high-stakes endeavor. Monkeypox, rabies, Nipah virus infection, and a cluster of hemorrhagic fever diseases (e.g., Ebola virus disease, Marburg hemorrhagic fever, Crimean-Congo hemorrhagic fever, and Rift Valley fever) are among the diseases caused by high-consequence pathogens. Many pathogens are themselves "chimeric," because organisms can combine genetic material to mutate into variants that create challenges for treatment and control, requiring innovative and agile thinking, as demonstrated by Bellerophon while slaying the Chimaera.

Bibliography

1. Belay ED, Monroe SS. Low-incidence, high-consequence pathogens. Emerg Infect Dis. 2014;20:319–21. https://doi.org/10.3201/eid2002.131748
2. British Museum. The Boreads Painter [cited 2022 Jun 9]. https://www.britishmuseum.org/collection/term/BIOG57451
3. Cartwright M. Bellerophon [cited 2022 Jul 23]. https://www.worldhistory.org/Bellerophon
4. Centers for Disease Control and Prevention. Division of High Consequence Pathogens and Pathology [cited 2022 Jul 18]. https://www.cdc.gov/ncezid/dhcpp/index.html
5. Getty Museum. Black-figure kylix [cited 2022 Jul 14]. https://www.getty.edu/art/collection/object/108DSR
6. Getty Museum. Lakonian black-figure kylix; detached fragments [cited 2022 Jul 14]. https://www.getty.edu/art/collection/object/103VPC
7. Homer. The Iliad. Book VI (179−182). Lattimore R, translator. Chicago: The University of Chicago Press; 1951, 2011.
8. Schmitt ML. Bellerophon and the chimaera in archaic Greek art. Am J Archaeol. 1966;70:341–7. https://doi.org/10.2307/502324

Address for correspondence: Byron Breedlove, EID Journal, Centers for Disease Control and Prevention, 1600 Clifton Rd NE, Mailstop H16-2, Atlanta, GA 30329-4027, USA; email: wbb1@cdc.gov

EMERGING INFECTIOUS DISEASES®

Upcoming Issue • Poxviruses

- Systematic Review and Metaanalysis of Foodborne Tickborne Encephalitis, Europe, 1980–2021
- Demographic and Socioeconomic Factors Associated with Hospitalization and Fungal Infection Risk, United States, 2019
- Environmental Persistence of Monkeypox Virus on Surfaces in Household of Person with Travel-Associated Infection, Dallas, Texas, USA, 2021
- Rapid Increase in Suspected SARS-CoV-2 Reinfections, Clark County, Nevada, USA, December 2021
- Novel Zoonotic Avian Influenza Virus
- SARS-CoV-2 Secondary Attack Rates in Vaccinated and Unvaccinated Household Contacts during Replacement of Delta with Omicron Variant, Spain
- *Plasmodium falciparum* Parasites with *pfhrp2* and *pfhrp3* Deletions, Djibouti and Horn of Africa
- Importation and Circulation of Vaccine-Derived Poliovirus Serotype 2, Senegal, 2020–2021
- Nosocomial COVID-19 Incidence and Secondary Attack Rates among Patients of Tertiary Care Center, Zurich, Switzerland
- Human Monkeypox without Viral Prodrome or Sexual Exposure, California, 2022
- Presence of *Ophiodiomyces ophiodiicola*, Etiologic Agent of Snake Fungal Disease, in Europe since the Late 1950s
- Epidemiology of Early Monkeypox Virus Transmission in Sexual Networks of Gay and Bisexual Men, England, 2022
- Contaminated Dialysis Water Supply Faucet as Reservoir for Carbapenemase-Producing Pseudomonas aeruginosa
- Early Estimates of Monkeypox Incubation Period, Generation Time, and Reproduction Number, Italy, May–June 2022
- Emerging Tickborne Bacteria in Cattle from Colombia
- Identifying Contact Risks for SARS-CoV-2 Transmission to Healthcare Workers during Outbreak in COVID-19 Ward
- *Haematospirillum jordaniae* Cellulitis and Bacteremia
- Cluster of Donor-Derived Cryptococcosis after Liver and Kidney Transplantation
- Introduction and Differential Diagnosis of Monkeypox in Argentina, 2022

Complete list of articles in the October issue at https://wwwnc.cdc.gov/eid/#issue-292

Earning CME Credit

To obtain credit, you should first read the journal article. After reading the article, you should be able to answer the following, related, multiple-choice questions. To complete the questions (with a minimum 75% passing score) and earn continuing medical education (CME) credit, please go to http://www.medscape.org/journal/eid. Credit cannot be obtained for tests completed on paper, although you may use the worksheet below to keep a record of your answers.

You must be a registered user on http://www.medscape.org. If you are not registered on http://www.medscape.org, please click on the "Register" link on the right hand side of the website.

Only one answer is correct for each question. Once you successfully answer all post-test questions, you will be able to view and/or print your certificate. For questions regarding this activity, contact the accredited provider, CME@medscape.net. For technical assistance, contact CME@medscape.net. American Medical Association's Physician's Recognition Award (AMA PRA) credits are accepted in the US as evidence of participation in CME activities. For further information on this award, please go to https://www.ama-assn.org. The AMA has determined that physicians not licensed in the US who participate in this CME activity are eligible for AMA PRA Category 1 Credits™. Through agreements that the AMA has made with agencies in some countries, AMA PRA credit may be acceptable as evidence of participation in CME activities. If you are not licensed in the US, please complete the questions online, print the AMA PRA CME credit certificate, and present it to your national medical association for review.

Article Title

Fetal Loss and Preterm Birth Caused by Intraamniotic *Haemophilus influenzae* Infection, New Zealand

CME Questions

1. Your patient is a 29-year-old pregnant woman with suspected chorioamnionitis. On the basis of the 10-year surveillance of pregnancy-associated invasive Haemophilus influenzae infection in Auckland, New Zealand, by Hills and colleagues, which one of the following statements about the epidemiology of pregnancy-associated invasive H. influenzae disease is correct?

A. Among 54 cases of pregnancy-associated invasive *H. influenzae* disease in 52 unique pregnancies, intra-amniotic infection (IAI) occurred in one third
B. Overall incidence of pregnancy-associated invasive *H. influenzae* disease was 19.9/100,000 births
C. Older women and those of Māori ethnicity had higher rates of pregnancy-associated invasive *H. influenzae* disease
D. Of the 54 cases of pregnancy-associated invasive *H. influenzae* disease, 38 (70.4%) were neonatal cases and 16 (29.6%) were maternal cases

2. According to the 10-year surveillance of pregnancy-associated invasive H. influenzae infection in Auckland, New Zealand, by Hills and colleagues, which one of the following statements about clinical and microbiological features of pregnancy-associated invasive H. influenzae disease is correct?

A. Adverse pregnancy outcomes (fetal loss, preterm birth, infant need for neonatal intensive care unit (NICU) or special care baby unit (SCBU) admission occurred in 45 pregnancies (93.8%)
B. Most isolates were Hib and resistant to amoxicillin
C. Approximately one fifth of affected pregnancies resulted in a live birth of an infant not requiring NICU/SCBU care
D. Maternal mortality rate was 13%

3. On the basis of the 10-year surveillance of pregnancy-associated invasive *H. influenzae* infection in Auckland, New Zealand, by Hills and colleagues, which one of the following statements about clinical implications of disease burden and mechanisms of adverse pregnancy outcomes is correct?

A. The findings suggest that IAI is unlikely to be the cause of preterm birth in most women with pregnancy-associated invasive *H. influenzae* disease
B. Outcomes of invasive *H. influenzae* disease for the pregnant woman are generally poor
C. Invasive *H. influenzae* disease should be considered in pregnant women with signs of chorioamnionitis, and appropriate empiric antibiotic treatment should be given
D. Pregnant women are most likely to acquire invasive *H. influenzae* infection from an upper respiratory source

Earning CME Credit

To obtain credit, you should first read the journal article. After reading the article, you should be able to answer the following, related, multiple-choice questions. To complete the questions (with a minimum 75% passing score) and earn continuing medical education (CME) credit, please go to http://www.medscape.org/journal/eid. Credit cannot be obtained for tests completed on paper, although you may use the worksheet below to keep a record of your answers.

You must be a registered user on http://www.medscape.org. If you are not registered on http://www.medscape.org, please click on the "Register" link on the right hand side of the website.

Only one answer is correct for each question. Once you successfully answer all post-test questions, you will be able to view and/or print your certificate. For questions regarding this activity, contact the accredited provider, CME@medscape.net. For technical assistance, contact CME@medscape.net. American Medical Association's Physician's Recognition Award (AMA PRA) credits are accepted in the US as evidence of participation in CME activities. For further information on this award, please go to https://www.ama-assn.org. The AMA has determined that physicians not licensed in the US who participate in this CME activity are eligible for AMA PRA Category 1 Credits™. Through agreements that the AMA has made with agencies in some countries, AMA PRA credit may be acceptable as evidence of participation in CME activities. If you are not licensed in the US, please complete the questions online, print the AMA PRA CME credit certificate, and present it to your national medical association for review.

Article Title

Increasing Incidence of Invasive Group A *Streptococcus* Disease, Idaho, USA, 2008–2019

CME Questions

1. You are advising a public health department about anticipated health care use for and management of invasive group A *Streptococcus* (iGAS). On the basis of the retrospective analytical study by Dunne and colleagues, which one of the following statements about epidemiology and clinical features of iGAS in Idaho during 2008 to 2019 is correct?

A. During 2008 through 2019 iGAS incidence in Idaho increased approximately 75%, whereas streptococcal toxic shock syndrome (STSS) incidence remained stable
B. Case fatality rate was 16.7% for 2008 to 2013 and 10.4% during 2014 to 2019
C. Pneumonia was the most common clinical syndrome
D. Average annual incidence during 2008 to 2019 was highest among Hispanic/Latino persons

2. According to the retrospective analytical study by Dunne and colleagues, which one of the following statements about *emm* typing results and potential risk factors for increased incidence in iGAS between 2014 to 2019 and 2008 to 2013 is correct?

A. *emm* types 1, 12, 28, 11, and 4 were most common in iGAS, and 2 outbreaks and a household cluster were identified
B. In STSS cases, *emm* type 12 was most common
C. Postpartum cases were a significant driver of the observed increase in iGAS cases
D. Skin injuries, drug use, and GAS pharyngitis were significant risk factors for the increase in iGAS from 2008 to 2013 to 2014 to 2019

3. According to the retrospective analytical study by Dunne and colleagues, which one of the following statements about the clinical and public health implications of the epidemiology and clinical features of iGAS in Idaho during 2008 to 2019 is correct?

A. Apparent increases in iGAS incidence in Idaho during 2008 to 2019 were spurious, related to changes in the surveillance system that led to increased case reporting
B. *emm* typing is unlikely to facilitate outbreak detection
C. In Idaho, iGAS is not a significant public health concern
D. Lack of identified risk factors contributing to increasing iGAS incidence in the general population suggests a potential role for vaccination as a preventive strategy

Emerging Infectious Diseases

Spotlight Topics

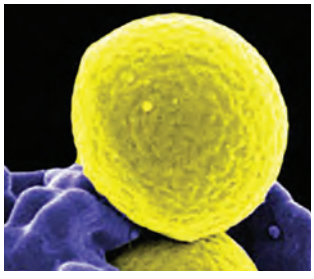


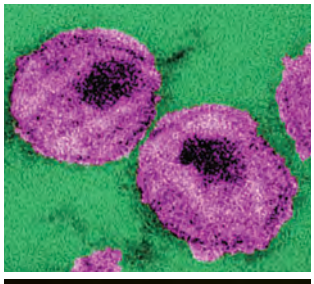

Antimicrobial resistance
Ebola • Etymologia
Food safety • HIV-AIDS
Influenza • Lyme disease
Malaria • MERS • Pneumonia
Rabies • Ticks • Tuberculosis
Coronavirus • Zika

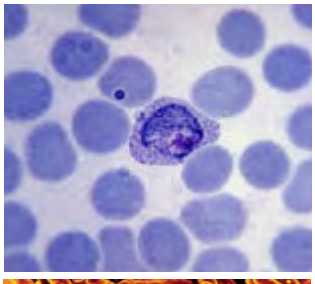
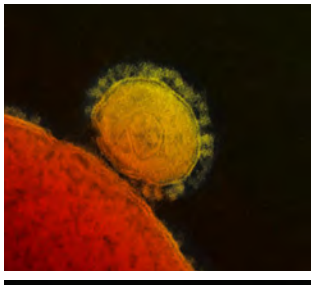
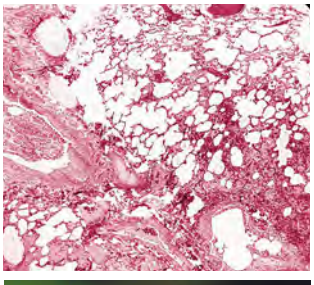
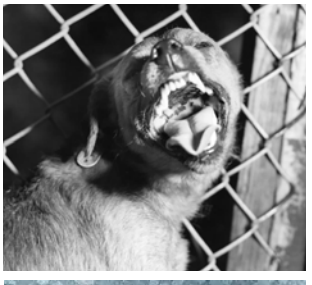



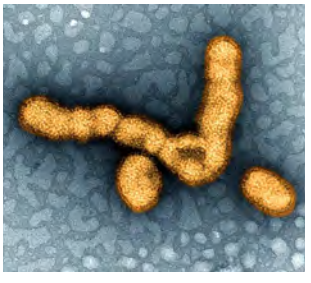
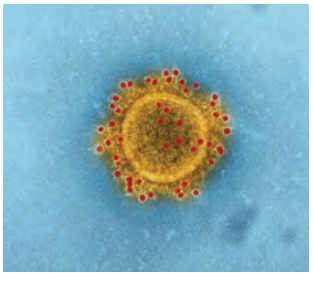

EID's spotlight topics highlight the latest articles and information on emerging infectious disease topics in our global community

https://wwwnc.cdc.gov/eid/page/spotlight-topics